EDUCATIONAL EXHIBITS

384 Lifting the Veil: A Guide to Interpreting Diffusion Tensor Imaging of the Brain for Operative Planning

David Polinger-Hyman
Medical College of Wisconsin, Milwaukee, WI, USA

Summary & Objectives

Provide a guide for interpreting pre operative diffusion tensor imaging (DTI) of the brain. After brief review of physics including sequence acquisition, patient examples will be used to show lesions in different locations to illustrate normal and abnormal white matter tracts. Observers will feel more confident interpreting pre operative DTI exams, and in the process learn key white matter tracts to include those forming the sagittal stratum, passing through the temporal stem, terminating in the inferior frontal gyrus and more.

Purpose

1. Learn to interpret subcortical brain mapping for operative planning.
2. Learn key locations where several tracts are in close proximity and basic functions of major tracts included.

Materials & Methods

Outline:

1. Brief description of multi direction diffusion acquisition and tensor modeling including minimum requirements and limitations (for example, minimum of 6 diffusion directions and crossing fibers). Include brief explanation of fractional anisotropy (FA) and directional FA map which will be used as the backbone of the examples shown. Constrained spherical deconvolution (CSD) based tractography will be used selectively to further illustrate tracts which are partially obscured on the color FA maps, for example frontal aslant tract (FAT) and corticobulbar tract.
2. Anatomy of white matter tracts with brief description of what is known about function. To include clues to see parts of tracts obscured because of crossing fibers or because they run together and in the same direction as other tracts. For example, frontal aslant and corticobulbar fibers terminating in the inferior frontal gyrus and inferolateral pre central gyrus, respectively which pass from medial to lateral through the superior longitudinal fasciculus (SLF). Also vertical portions uncinate fasciculus and arcuate fasciculus which are challenging to see otherwise as their anteroposterior directions travel with the inferior frontal occipital fasciculus (IFOF) and SLF, respectively.
3. Present several patient examples showing white matter tracts displaced, in direct contact with and/or infiltrated by brain masses and/or adjacent edema. Questions will be asked to allow the viewer to test their knowledge. Emphasis will be made on tracts running together and/or terminating in characteristic locations to include temporal stem, occipital lobe and inferior frontal gyrus.
4. Provide a suggested template to use for reporting.

Results & Conclusion

NA

Images/Tables

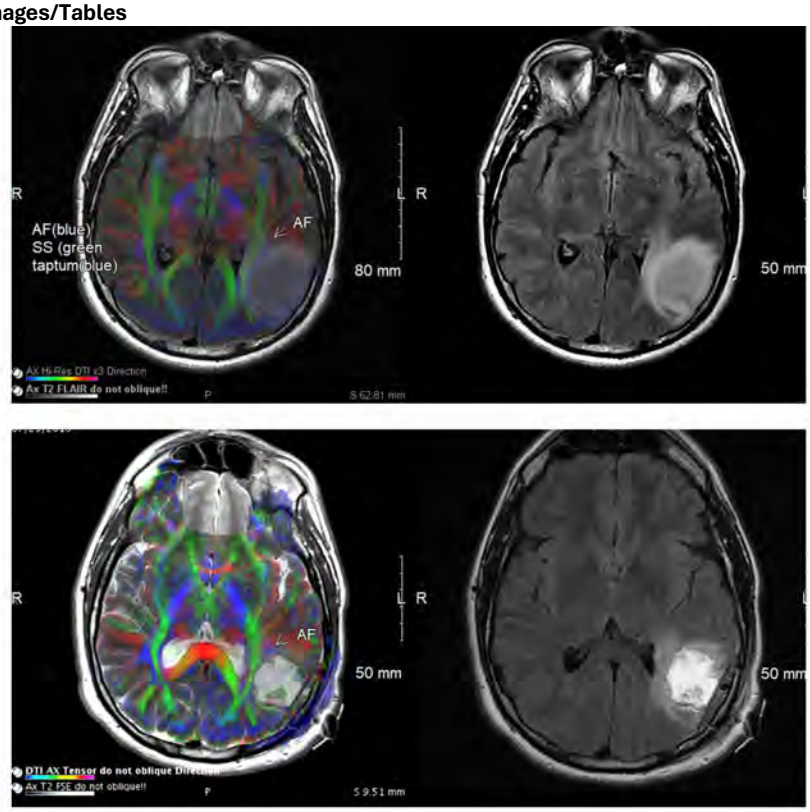

Low grade astrocytoma (top pre op, bottom post op), small amount left behind to preserve vertical portion arcuate fasciculus (AF-language risk) and sagittal stratum(SS-visual risk). Medial margin of lesion contacts/infiltrates SS made up of predominately inferior frontal occipital fasciculus (IFOF), inferior longitudinal fasciculus (ILF), optic radiation (OR) at that level. Notice normal anatomy on the right from lateral to medial (AF, SS, tapetum). No language or visual deficit post op. To review what fiber tracts joint posteriorly to make up the sagittal stratum? (SLF, Middle LF, ILF, anterior commissure(AC), IFOF, OR)

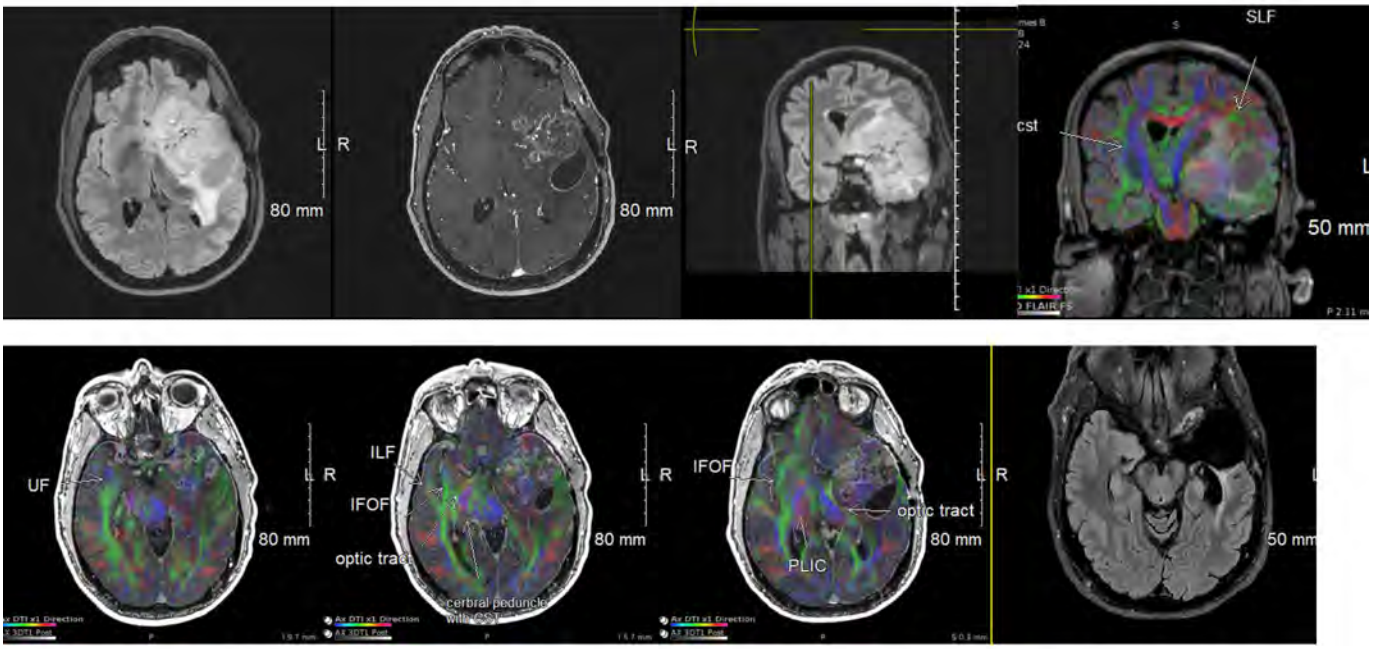

Oligodendroglioma involving frontal lobe, insula and temporal stem. Normal tracts shown on right infiltrated by the tumor on left include uncinate fasciculus (UF), inferior frontal occipital fasciculus (IFOF), inferior longitudinal fasciculus (ILF). CST displaced by and in close proximity to medial margin as it traverses cerebral peduncle and posterior limb internal capsule (PLIC). Mass effect upon adjacent optic tract. Body of SLF is along superior margin of the lesion. What other tracts passing through temporal stem could be involved? (anterior commissure and Meyer loop of optic radiation). Post op (right lower image) patient had word finding difficulty that gradually improved (resected IFOF). No visual complaint despite risk of right superior quadrantanopia.

241 Imaging-Based Updates from Nasopharyngeal Cancer TNM Staging 9th Version

Noor Badrawi MBBS, Pejman Maralani MD
Department of Medical Imaging, University of Toronto, Sunnybrook Health Sciences Centre, Toronto, Ontario, Canada

Summary & Objectives

This exhibit reviews the updates introduced in the 9th edition of the AJCC/UICC TNM staging system for nasopharyngeal carcinoma, with emphasis on key imaging features. As radiologists play a crucial role in tumor staging, familiarity with these revisions is essential for disease evaluation and patient management.

Purpose

To compare and illustrate the imaging definitions and stage groupings for NPC between the 8th and 9th versions. Review will be through real-life case-based examples.

Materials & Methods

A retrospective review was conducted of pathologically confirmed nasopharyngeal carcinoma cases with baseline MRI and CT scans. Each case was staged according to both the 8th and 9th editions of the AJCC/UICC TNM staging system, with comparisons highlighting the changes in overall stage classification. Key modifications are illustrated through educational visual case examples.

Results & Conclusion

The 9th edition of the AJCC/UICC TNM staging system introduces several key imaging-based revisions to the staging of nasopharyngeal carcinoma. Imaging evidence of extranodal extension is now incorporated into the N3 category, underscoring the expanded role of imaging in tumor staging. The M1 category is subdivided into M1a (≤3 metastases) and M1b (>3 metastases). Stages I and II have been merged, while stages III and IVA are downgraded to stages II and III, respectively. Both stage I and stage IV are further divided into substages, and only cases with metastatic disease (M1) are designated as stage IV. Familiarity with these TNM-9 updates enhances staging consistency and supports evidence-based management of patients with nasopharyngeal carcinoma.

Images/Tables

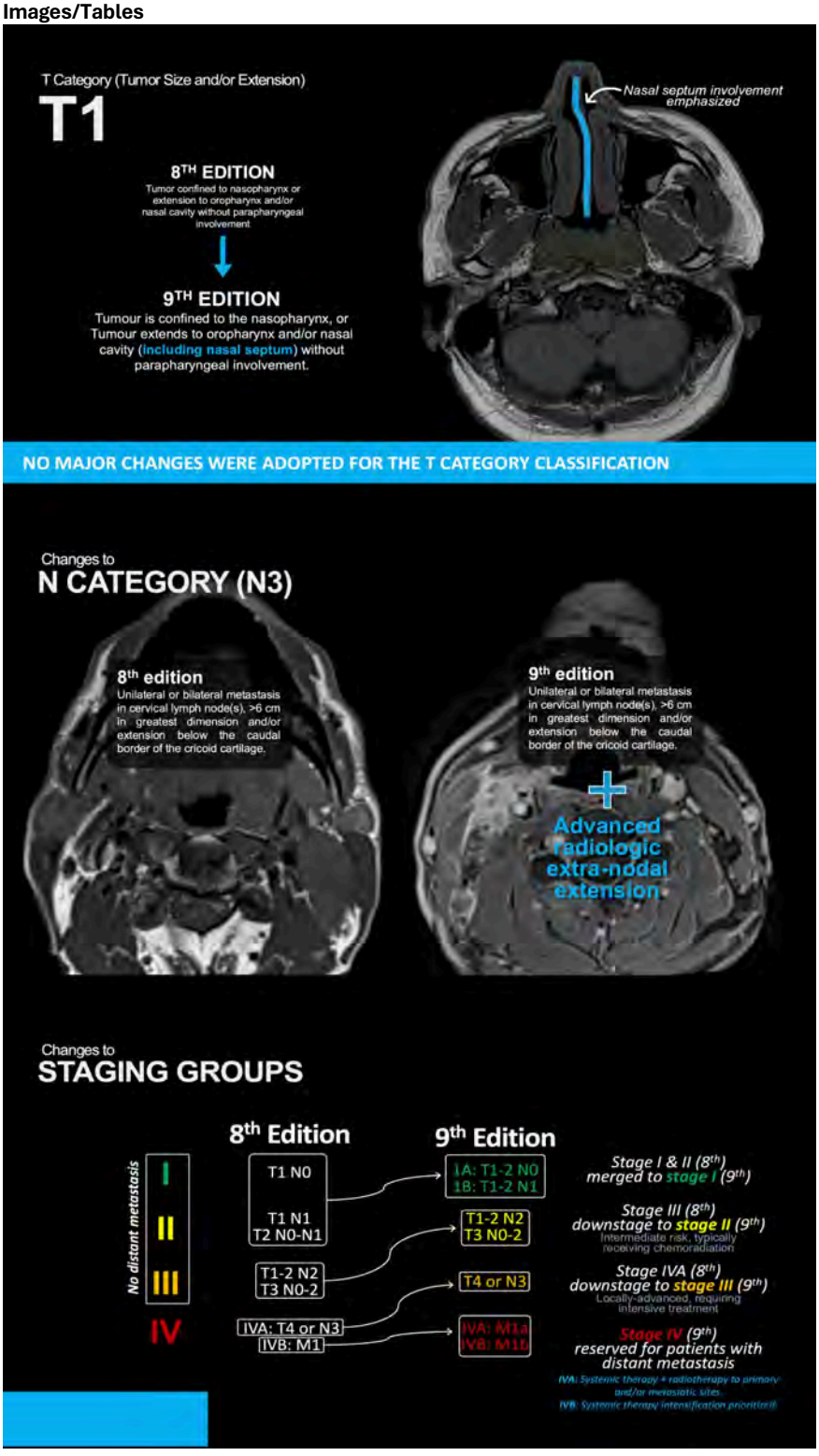

---

450 Decoding Autoimmune Encephalitis: Imaging Patterns and Clinical Vignettes Across Antibody-Mediated Subtypes

Albert D Jiao MD, Luke Odisho MD, Aristides Andres Capizzano MD, MS
University of Michigan, Ann Arbor, MI, USA

Summary & Objectives

Autoimmune encephalitis represents a diverse group of immune-mediated inflammatory disorders of the central nervous system driven by autoantibodies directed against neuronal or glial antigens. Despite increasing recognition, the radiologic manifestations of autoimmune encephalitis remain underappreciated and often overlap with infectious, metabolic, or neoplastic processes. Early identification of characteristic imaging features is crucial for guiding serologic testing and timely initiation of therapy.

This educational exhibit aims to familiarize neuroradiologists with the imaging spectrum of antibody-mediated encephalitides through illustrative clinical vignettes, emphasizing the diagnostic importance of MRI pattern recognition.

Purpose
To demonstrate the characteristic imaging and clinical features of antibody-mediated encephalitides, and to improve radiologists' ability to recognize these subtle yet characteristic imaging findings.
Materials & Methods
Patient cases with a confirmed diagnosis of autoimmune encephalitis supported by cerebrospinal fluid (CSF) or serum antibody testing and corresponding neuroimaging abnormalities were included in this educational exhibit. Antibody subtypes represented in this series include anti-Hu (ANNA-1), CASPR2, anti-GABA B receptor, anti-KLHL11, and anti-GFAP, among others.
For each case, available CT and MRI examinations were reviewed in detail. Imaging features were analyzed with respect to anatomic distribution, signal characteristics, enhancement patterns, and interval evolution. Clinical data including presenting symptoms, associated malignancy or paraneoplastic syndromes, and laboratory results were correlated with imaging findings.
Results & Conclusion
A variety of clinical scenarios and imaging patterns was observed depending on the autoantibody involved in the disease process. For example, in a male patient with a history of small cell lung cancer and anti-GABA b receptor encephalitis, MRI demonstrated characteristic left mesial temporal FLAIR signal hyperintensity with associated reduced diffusivity. In a female pediatric patient with a history of anti-GFAP disease, initial MRI demonstrated mass-like enhancement in the right posterior temporal region with associated exuberant edema, ultimately requiring serum antibody testing and brain biopsy for diagnosis. A brain MRI from a male patient with history of anti-KLHL11 and testicular cancer demonstrated progressive FLAIR signal abnormality in the bilateral thalami and throughout the right temporal lobe, eventually leading to atrophy of the right temporal lobe.
Recognition of these imaging patterns within the appropriate clinical context enables neuroradiologists to raise early suspicion for autoimmune etiology, prompting antibody testing and therapy before irreversible injury occurs. Past medical history of autoimmune disease, recent malignancy diagnosis, or atypical encephalitis with a negative viral workup should prompt the neuroradiologist to consider autoimmune etiology with a high degree of suspicion. Through a visually rich case-based presentation, this exhibit underscores the radiologist's central role in identifying and characterizing autoimmune encephalitis.
Images/Tables

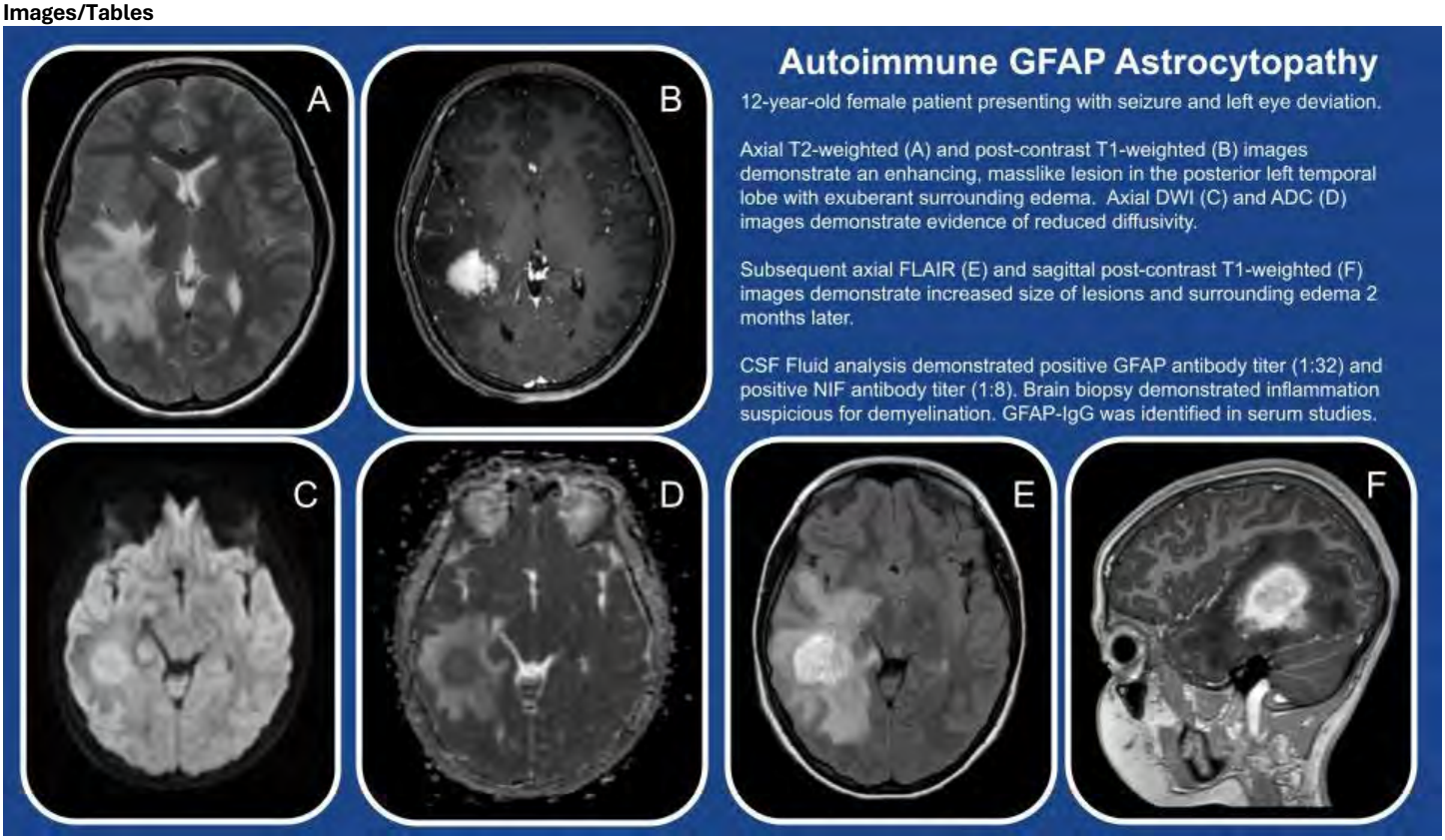

488 The Maxillary Nerve (V2): A Highway for Perineural and Trans-spatial Disease Spread
Elena Greco MD, Lamia Hauter MS2, Jasper Erickson MD, Joshua P. Nickerson M.D., FACR, Jeffrey M. Pollock M.D., FASFNR
Oregon Health and Science University, Portland, Oregon, USA
Summary & Objectives
Owing to its extensive anatomic connections, the maxillary nerve (V2) serves as a critical pathway for perineural and trans-spatial spread of both neoplastic and infectious diseases. V2 is the second division of the trigeminal nerve. It originates from the trigeminal ganglion in Meckel's cave within the middle cranial fossa and courses anteriorly toward the foramen rotundum, through which it exits the cranial cavity and enters the pterygopalatine fossa, a key crossroad of neurovascular transit. Here, it gives rise to several branches oriented in different directions. Medially, two ganglionic branches connect V2 to the pterygopalatine ganglion. Through this ganglion, fibers reach the nasal cavity via the sphenopalatine foramen and the palate via the greater and lesser palatine foramina. Posteriorly, small branches traverse the pterygoid canal and the pharyngeal canal, contributing to nasopharyngeal innervation. Laterally, the zygomatic nerve passes through the inferior orbital fissure into the orbit, where it divides and exits through foramina in the zygomatic bone to supply the cheek and temple. Posterolaterally, the posterior superior alveolar nerve exits through the pterygomaxillary fissure to reach the infratemporal fossa, entering alveolar foramina on the maxilla to innervate the maxillary sinus mucosa and upper

molar teeth. Continuing anteriorly, V2 enters the orbit through the inferior orbital fissure, where it becomes the infraorbital nerve. It courses along the infraorbital groove and infraorbital canal, giving rise to the middle and anterior superior alveolar nerves. Finally, the infraorbital nerve emerges through the infraorbital foramen, dividing into terminal branches that interconnect with the facial nerve and the zygomaticofacial nerve, forming the infraorbital plexus.

Purpose

This exhibit will demonstrate the anatomy of V2 on cross-sectional imaging and then illustrate, through some representative cases, the sequential extracranial-to-intracranial propagation of pathologic processes along the V2 trajectory.

Materials & Methods

Case summary

Case 1 – Melanoma of the lower eyelid with perineural spread from the infraorbital region along V2, traversing the infraorbital canal, pterygopalatine fossa, foramen rotundum, Meckel's cave, and cisternal segment, with secondary involvement of V1 and V3. Figure 1 depicts sequential MR images demonstrating the continuous perineural spread of melanoma along the maxillary nerve segments in this case.

Case 2 – Invasive fungal sinusitis with perineural inflammatory extension from the nasal and paranasal sinuses into the pterygopalatine fossa, extending along V2 through the foramen rotundum to the middle cranial fossa.

Case 3 – Adenoid Cystic Carcinoma with perineural invasion from the hard palate via the greater palatine nerve and foramen, extending into the pterygopalatine fossa and along V2 toward the foramen rotundum to the middle cranial fossa.

Results & Conclusion

These cases collectively highlight how knowing the anatomic routes of spread through V2 is essential for detecting early perineural or trans-spatial spread, underscoring the importance of an anatomy-driven, compartment-based approach to skull base and facial imaging interpretation in patients with neoplastic or infectious pathology.

Images/Tables

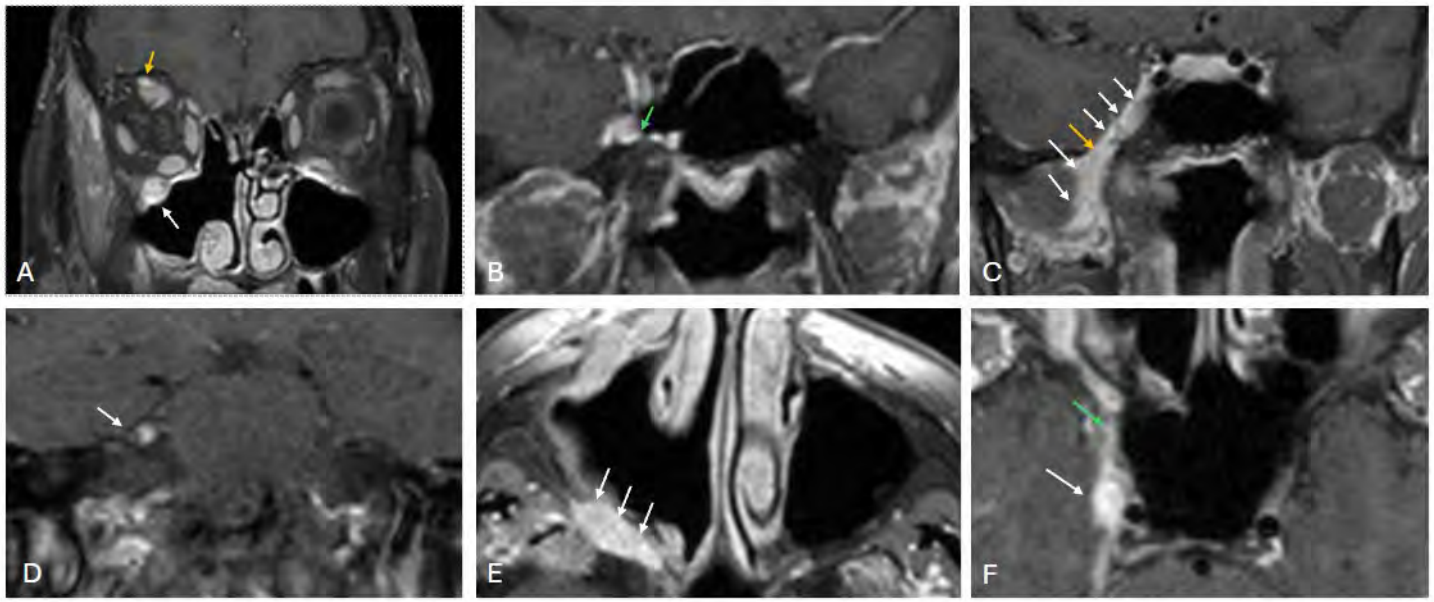

Figure 1. Coronal (A–D) and axial (E–F) contrast-enhanced fat-suppressed T1-weighted MR images demonstrating perineural spread of melanoma along the right maxillary nerve (V2). **(A)** Enlargement and enhancement of the right infraorbital nerve with extension of abnormal signal and soft-tissue infiltration (white arrow). The right supraorbital nerve also shows enhancement, indicating secondary perineural spread along V1 (yellow arrow). **(B)** Enlargement of the right foramen rotundum (green arrow) **(C)** Thickening and enhancement of the V3 segment extending through the foramen ovale (yellow arrow). **(D)** Abnormal enhancement of the cisternal segment of the right trigeminal nerve (white arrow). **(E)** Enhancement of the right pterygopalatine fossa (white arrows) . **(F)** Enlargement and enhancement of Meckel's cave (white arrow) and the foramen rotundum (green arrow).

1185 Dynamic Cross-Sectional Imaging of the Pediatric Cervical Spine: Revealing Pathology with Motion

Johna Joseph Chemistry BA[1], Sarah J Moum MD[2]

[1]Northwestern University Feinberg School of Medicine, Chicago, IL, USA. [2]Ann & Robert H. Lurie Children's Hospital of Chicago Northwestern University Feinberg School of Medicine, Chicago, IL, USA

Summary & Objectives

The developing cervical spine can predispose children to neurologic or vascular pathology with changes in position. When imaging is obtained only in the neutral position, these abnormalities may go unnoticed. Tailoring CT or MRI protocols to include dynamic imaging, such as flexion, extension, head rotation, or arms raised positions, can uncover alterations in spinal alignment and associated effects on adjacent structures, helping to explain a child's symptomatology.

In Hirayama disease, patients develop asymmetric myelomalacia of the distal cervical spinal cord and unilateral forearm muscle wasting and weakness due to discrepant growth between the spinal cord and spinal canal. Imaging during neck flexion reveals forward displacement of the dura with engorgement of the posterior epidural venous plexus, which often looks normal when the neck is in neutral position.

Congenital fusion anomalies between the skull base and cervical vertebrae, such as atlas assimilation, predispose to craniocervical instability, increasing the risk for spinal canal compression and neurologic compromise.

In bow hunter syndrome, neck rotation can result in vertebral artery compression by congenital structural lesions, hyperrotation, or developmentally narrowed foramen, leading to arterial dissection and neurologic symptoms. While imaging at midline may be normal or show mild abnormalities, dynamic imaging helps confirm vascular compression and guide further treatment.
Children can present with thoracic outlet syndrome from dynamic neural or less commonly vascular compression by structural abnormalities, such as cervical ribs or elongated transverse processes. Imaging with arms raised can exacerbate thoracic outlet narrowing, facilitating diagnosis.
By selecting a dynamic imaging protocol tailored to age and safety considerations, neuroradiologists can accurately diagnose clinically significant cervical spine pathology in pediatric patients, helping to avoid further neurovascular injury and direct management decisions.

Educational Objectives

- Review developmental biomechanics that predispose children to dynamic cervical pathology
- Review dynamic imaging protocols tailored to motion, age, and radiation-related risks
- Recognize situations where neutral CT and MR imaging may miss clinically significant findings
- Identify the characteristic flexion MRI features seen in Hirayama disease
- Describe the cross-sectional imaging findings of rotational vertebral artery compromise in bow hunter syndrome
- Evaluate congenital craniocervical fusion anomalies and associated instability risks
- Assess for neuropathic and vascular compression in pediatric thoracic outlet syndrome

Purpose

N/A

Materials & Methods

N/A

Results & Conclusion

N/A

Images/Tables

261 Tackling MRI Artifacts in Head and Neck Imaging: Problems and Solutions

Momin Muzaffar MD, Emily Miller MD, Stephen Sammet MD PhD
University of Chicago, Chicago, IL, USA

Summary & Objectives

As the field of Magnetic Resonance Imaging (MRI) continues to advance and newer pulse sequences and artificial intelligence (AI) in the form of automatic image post-processing algorithms are introduced into routine clinical practice, the number of artifacts that radiologists encounter also continues to increase. While novel imaging sequences and deep learning algorithms continue to push the boundaries of anatomical details that are achievable with MRI, they also bring with them a renewed set of hurdles that radiologists must contend with to maintain diagnostic quality. The anatomy of the head and neck poses a unique challenge in MRI because of the small size of the structures and exquisite anatomic detail required, coupled with the complexity posed by the proximity of soft tissues, bone (skull base, cervical spine, facial bones), and air-tissue interfaces (sinuses, mastoid air cells, pharynx, trachea), frequently on multiple images. In addition, many patients with head and neck cancers suffer from significant discomfort that makes prolonged scan times unfeasible, and therefore, neck protocols must be optimized for both comprehensive detail and speed. This educational exhibit aims to inform readers on the variety of MRI artifacts that can not only tarnish the quality of MR imaging in the head and neck but also lead to misinterpretation by mimicking or masking pathology. This exhibit will review a host of common and uncommon artifacts, elucidate the underpinnings their existence, and highlight solutions to mitigate such issues.

Purpose

The purpose of this educational exhibit is to 1) showcase the spectrum of common and uncommon MRI artifacts that a neuroradiologist should be familiar with when interpreting MR studies of the brain, skull base, maxillofacial skeleton, and neck, and 2) highlight solutions to mitigate these artifacts.

Materials & Methods

In addition to covering common MRI artifacts such as motion (swallowing artifact), poor signal to noise ratio, chemical shift artifact, and susceptibility artifact (such as from dental work or surgical instrumentation), this exhibit will illustrate certain recognizable MRI artifacts in the head and neck including:

- Voxel bleeding/ cross-talk artifact
- Incomplete and incorrect fat suppression
- Electrical coupling
- Aliasing
- Parallel imaging unfolding artifact
- Compressed sensing artifact
- DL algorithm artifacts
- Banding artifact
- B1-field inhomogeneity artifact
- N/2 ghosting
- Herringbone artifact
- Radiofrequency artifact
- Flow artifact on 3D acquisitions
- Free induction decay artifact

Results & Conclusion

Despite advances in MRI hardware and software technology, MR artifacts remain common, and head and neck anatomy poses its own unique challenges when addressing these artifacts. The educational exhibit will equip the reader with a firm understanding of the spectrum of artifacts that can occur in head and neck MR imaging and provide tangible solutions to reduce or eliminate these artifacts.

Images/Tables


Voxel bleeding/Cross-talk artifact


Banding artifact


Compressed sensing artifact

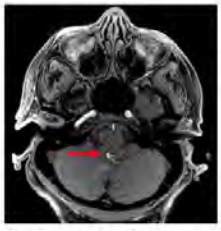
Parallel imaging unfolding artifact


Zipper artifact

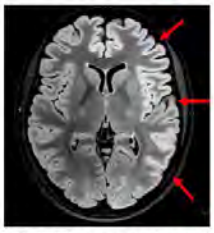
B1-field inhomogeneity artifact

176 A Primer in Nuclear Neuro-Oncology: SSTR Positive Tumors of the Head, Neck, and Spine

Derek Hesse MD, Marlee Crews MD, Rishi Jain BA, Ihsan Tarabichi Sankari MD, Ditte Primdahl MD, Stephen Magill MD, PhD, Ryan Avery MD, Hatice Savas MD, Eric Russell MD
Northwestern University, Chicago, IL, USA

Summary & Objectives

The use of Somatostatin Receptor Positron Emission Tomography (SSTR PET) for the evaluation of neoplasms has markedly increased – including evaluation for primary and metastatic lesions of the head, neck, and spine. Indications for SSTR PET include neuroendocrine tumors of the pancreas and gastrointestinal tract, pheochromocytoma, neuroblastoma, paraganglioma, meningioma, and other etiologies which express somatostatin receptors. This imaging modality is valuable for detecting primary tumors and assessing metastatic disease as well as problem solving in cases that are unclear on MRI or CT, such as meningiomas with complex skull base involvement[1]. SSTR PET provides complementary information in cases where MRI may be limited, owing to its high sensitivity and specificity[2,3]. Beyond qualitative assessment, quantitative analysis in SSTR PET using standardized uptake values is increasingly recognized as valuable; early evidence suggests these measures hold diagnostic and prognostic significance[4,5]. This educational exhibit will review a variety of SSTR positive neoplasms of the head, neck, and spine and includes examples of SSTR-avid normal structures and non-neoplastic entities that radiologists must recognize to avoid diagnostic pitfalls. The clinical implications of SSTR PET findings will be discussed including pertinent results for surgical management, determining the utility of peptide receptor radionuclide therapy, and treatment response monitoring. It is important for radiologists to supplement their evaluation of the head, neck, and spine with knowledge of SSTR PET imaging to arrive at the best diagnosis and management recommendations.

Purpose

The purpose of this exhibit is to raise awareness of SSTR positive tumors that may be seen in the head, neck, and spine. An additional aim is to improve recognition of benign and physiologic etiologies of SSTR uptake in the head, neck, and spine to help radiologists communicate only the pertinent findings to the referring clinician. Furthermore, the role of SSTR PET in surgical management, determining the clinical utility of peptide receptor radionuclide therapy, and treatment response monitoring will be discussed.

Materials & Methods

A cohort of over 1000 unique patients with SSTR PET scans at our institution revealed examples of SSTR positive tumors of the head, neck, and spine and benign and physiologic causes of uptake in these regions.

Results & Conclusion

This educational exhibit gives an overview of SSTR positive tumors of the head, neck, and spine with SSTR PET and CT/MR images of patients with 1) complex skull base meningioma, 2) optic nerve sheath meningioma, 3) spinal canal meningioma, 4) paraganglioma, 5) hemangioblastoma, 6) pineal tumor, 7) esthesioneuroblastoma, 8) pituitary macroadenoma, 9) medullary thyroid carcinoma, and 10) medulloblastoma. Benign and physiologic etiologies which may show uptake on SSTR PET included in the exhibit are a) spinal hemangioma, b) fibrous dysplasia, c) osteoblastic degenerative changes of the spine, and d) physiologic uptake in the pituitary, salivary, and thyroid glands. The clinical implications of SSTR PET are discussed in conjunction with collaborating authors from Neurosurgery and Neuro-oncology. Familiarity with the pathologic and benign etiologies of SSTR PET uptake of the head, neck, and spine improves diagnosis and understanding the clinical implications improves management recommendations.

Images/Tables

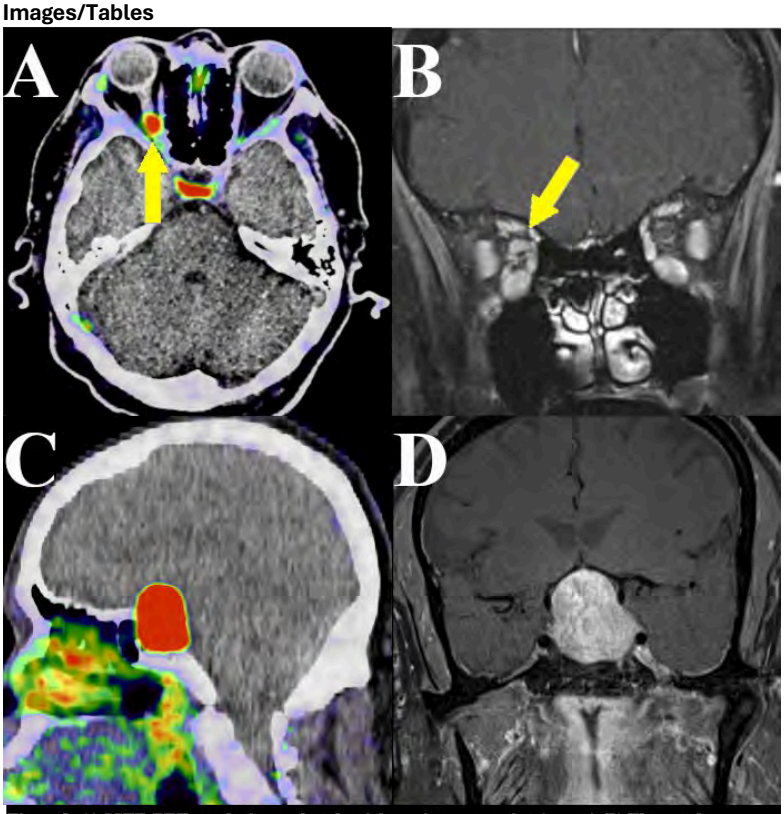

Figure 1: A) SSTR PET uptake is noted at the right optic nerve region (arrow). B) The uptake corresponds to dural based enhancement of the optic nerve sheath on postcontrast T1 MR images, most compatible with an optic nerve sheath meningioma (arrow). C) SSTR PET shows an avid sellar/ suprasellar mass. D) Postcontrast MRI confirms a typical appearance of a pituitary macroadenoma.

321 Reading Between the Lines: Decoding Cerebellar Linear Abnormalities

Myriam Z. Bermudez Allende MD
Cleveland Clinic, Weston, FL, USA

Summary & Objectives

The cerebellum is our coordination system that regulates balance, movement and cognitive functions. It plays a significant role in fine-tuning voluntary movements. Twenty to 30% of ischemic infarcts involve the posterior circulation, presenting with ataxia, tremors, dizziness, unsteady gait and headaches. Frequently, they can be asymptomatic and found incidentally on imaging or present with very minor symptoms.

1. Illustrate the spectrum of linear cerebellar signal abnormalities on MRI, emphasizing characteristic imaging appearance of acute cerebellar infarction.
2. Differentiate true linear cerebellar infarcts from mimics, including normal cerebellar folia variation, developmental venous anomalies, linear chronic demyelinating plaques, linear leptomeningeal metastases, and cerebellar folia subarachnoid hemorrhage.
3. Correlate imaging findings across multiple sequences (DWI, T2, FLAIR, GRE/SWI, and post-contrast T1) and discuss the clues to identify key distinguishing features.
4. Promote diagnostic accuracy and confidence in interpreting posterior fossa imaging by recognizing common pitfalls and applying a systematic approach to linear abnormal signal in the cerebellum.

Purpose

While linear cerebellar infarcts and fissural patterns have been well described in the literature, additional entities can share similar linear signal abnormalities. Highlighting the importance of recognizing the different imaging findings to distinguish lacunar infarct mimics. Awareness of these alternative pathologies, in conjunction with careful evaluation of imaging sequence characteristics and enhancement patterns, is essential to avoid diagnostic pitfalls and ensure accurate interpretation of posterior fossa pathology.

Materials & Methods

Ten cases demonstrating linear cerebellar signal abnormalities were retrospectively selected from our institutional imaging archive. Cases included clinically confirmed examples of acute lacunar cerebellar infarction, normal cerebellar folia fissure, linear developmental venous anomalies, linear leptomeningeal metastases, and cerebellar folia subarachnoid hemorrhage. MRI examinations were reviewed by two neuroradiologists evaluating different MRI sequences. Imaging features were analyzed for location, morphology, enhancement characteristics, and correlation with clinical presentation. Representative cases were compiled to illustrate key imaging distinctions among these cerebellar abnormalities.

Results & Conclusion

Recognizing linear imaging patterns in the posterior fossa is critical to accurately differentiate cerebellar infarction from other similar linear lesion mimics. Linear restricted diffusion is consistent with an acute lacunar infarct which evolves into a linear T2 hyperintense signal abnormality. A linear T2 hyperintense signal involving the cortex in the posterior fossa can also be seen in benign entities such as anatomical variation of the folia architecture. Linear developmental venous anomalies (DVAs) may appear as linear typically branching enhancing structures with associated linear gradient susceptibility artifact and low T2 signal. Patients with linear leptomeningeal carcinomatosis may also exhibit thin areas of irregular enhancement along the cerebellar surface, while linear subarachnoid hemorrhage will present as sulcal or folia FLAIR hyperintense signal with associated gradient susceptibility artifact.

Cerebellar involvement in Multiple Sclerosis is a common clinical finding and chronic demyelinating plaques typically have T2 and FLAIR linear hyperintense signal, although active demyelinating plaques can show restricted diffusion and areas of associated enhancement similar to acute/subacute lacunar infarcts.

Distinguishing these disease entities relies on the diagnostic correlation of multiple sequences, enhancement patterns, and their imaging characteristics, which together prevent misinterpretation, increase diagnostic accuracy and help guide the appropriate clinical management.

Images/Tables

Figure 1

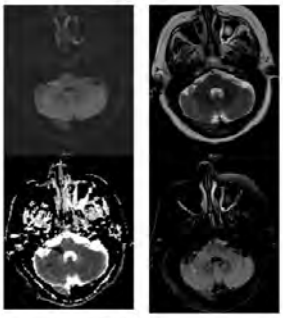

Figure 2

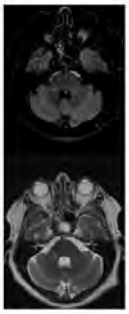

Figure 3

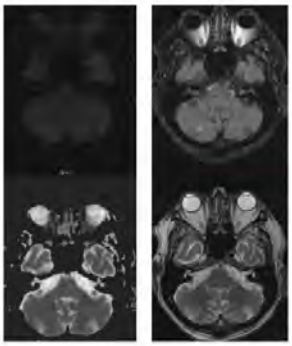

Figure 4

Figure 5

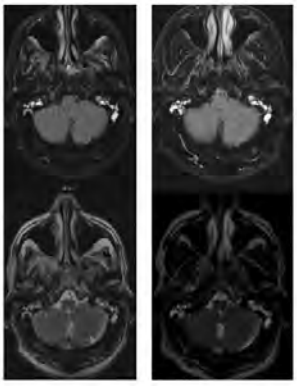

Figure 6

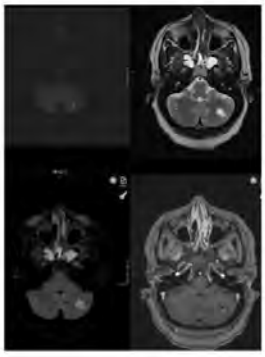

Figure 7

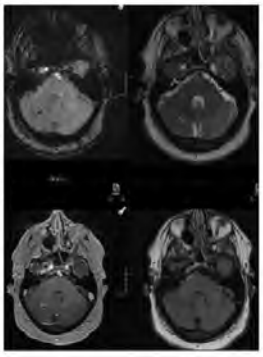

Figure 8

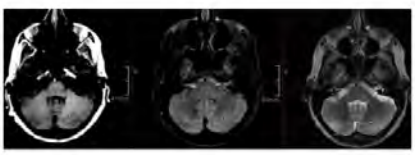

352 Staying on Tract: Central Spinal Cord Myelopathies

Anthony Sanchez MD, Adrian QingYu Xu MD
University of Utah, Salt Lake City, Utah, USA

Summary & Objectives

This will be an educational exhibit focused on differential diagnosis of select central distribution spinal cord myelopathies.

Purpose

The goal of this education exhibit is to teach trainees (medical students, residents, fellows) key imaging findings that will help distinguish central spinal myelopathies from each other and to refresh attending radiologists on key imaging findings that may help narrow their differential diagnosis.

Materials & Methods

We will briefly discussing spinal cord tract and vascular anatomy with diagrams. This will be followed by a discussion of grey matter predominant spinal cord myelopathies and then central white and grey matter involving spinal cord myelopathies which will be shown in a case-based format with the first slide containing clinical presentation and images, second slide containing the diagnosis with labels, and third slide discussing additional details about the diagnosis. The diseases covered will include: NMO, MOGAD, MS, Lupus, Radiation, Acute flaccid myelitis, dAVF, and Ischemia from arterial occlusive and compressive myelopathies.

Results & Conclusion

At the end of each of the two sections, a table will highlight distinguishing imaging features of the discussed myelopathies and associated findings to help separate them from each other.

Images/Tables

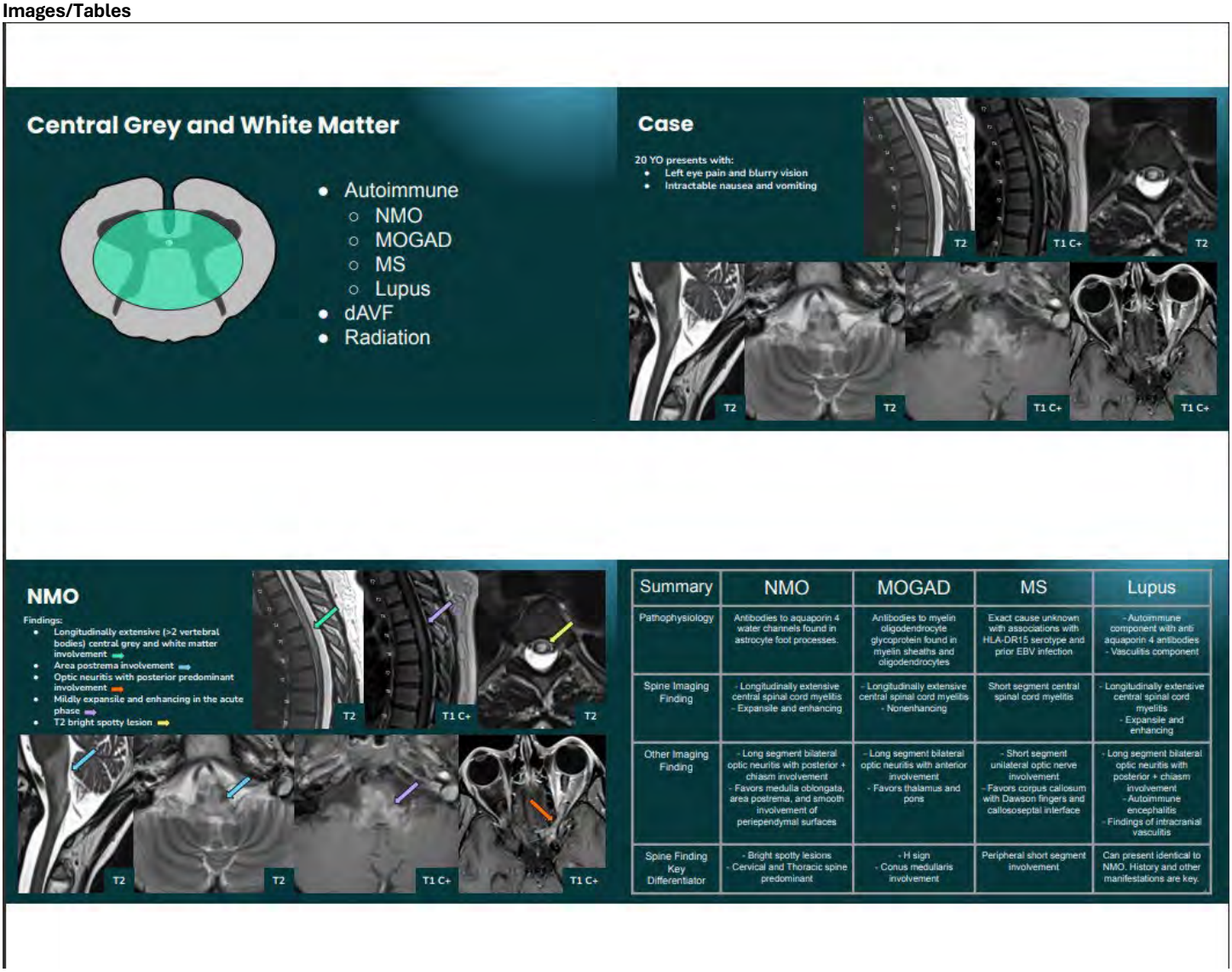

584 Postoperative Imaging of the Temporal Bone

Aditya Duhan MD[1], Fahad Farooq MD[2], Abbas Hamza Abbas[3], Saurav Jha MBBS[4], Swastika Lamture MD[1], Mamta Gupta MD[1], Charanjeet Singh MD[1]
[1]University of Colorado, Aurora, CO, USA. [2]SUNY Upstate Medical University, Syracuse, NY, USA. [3]University of basra collage of medicine, Basra, CO, Iraq. [4]Patan Academy of Health Sciences, Kathmandu, Nepal, Nepal

Summary & Objectives

The surgical evaluation of the temporal bone is most challenging due to complex anatomy, there are variety of surgerical procedures performed (tympanoplasty, mastoidectomy, IAC/CPA approaches, and pre-existing disease. Postoperative imaging is critical for monitoring tumor recurrence,

assessing unexpected surgical outcomes, and diagnosing complications.This exhibit reviews the expected postoperative findings and potential complications following the most common temporal bone surgeries, detailing the optimal imaging modalities for evaluation.

Purpose

- Identify the common surgical procedures related to the temporal bone and understand when to use CT versus MRI.
- Explain the typical CT findings associated with ossicular chain reconstruction (OCR) prostheses and the differences between mastoidectomy cavities (CWU vs. CWD).
- Recognize the CT and MRI signs of major complications, such as prosthesis dislocation, obliterative otosclerosis, pneumolabyrinth (which may indicate a fistula), and recurrent cholesteatoma.
- Distinguish between enhancing scar tissue or tumors and non-enhancing fat grafts by using post-contrast, fat-saturated MRI sequences after IAC/CPA surgery.

Materials & Methods

To showcase the expected postoperative anatomy, we selected representative CT and MRI images. This includes examples like Type 1 tympanoplasty, TORP/PORP placement, and the differences between CWU and CWD mastoidectomy. The images were obtained following our standard institutional protocols: CT scans were done with thin sections (about 0.5 mm) using a bone algorithm, while the MRI protocols featured T1, T2, and fluid-sensitive volumetric sequences (FIESTA/SPACE). We also included contrast-enhanced T1 with fat saturation and non-echo-planar DWI (half-Fourier SS-TSE or PROPELLER).

Results & Conclusion

CT scans have proven to be the best option for assessing the conductive mechanism. Some key takeaways include the strength of the connection between the OCR prosthetic stapes footplate and the condition of the mastoid cavity, whether it has an intact canal wall or an enlarged CWD cavity. The main issues spotted on CT scans were prosthesis dislocation and bone growth due to obliterative otosclerosis. On the other hand, MRI is better suited for monitoring soft tissue and tumors. Non-echo-planar DWI showed impressive accuracy in spotting recurrent cholesteatoma, which appears as a distinct high signal, no matter the type of mastoidectomy performed.[1] After contrast, fat-saturated MRI effectively differentiated between non-enhancing fat grafts (used in IAC closure) and enhancing residual or recurrent tumors. A pneumolabyrinth seen on CT is a specific, albeit less common, finding linked to perilymphatic fistula. In conclusion, when it comes to postoperative imaging of the temporal bone, radiologists need to combine their understanding of surgical anatomy with the best choice of imaging modality. CT is crucial for assessing hardware and bone-related issues, while MRI with non-echo-planar DWI is essential for monitoring cholesteatoma.[2] A systematic approach that focuses on identifying the main pathology and correlating CT and MRI findings with specific surgical objectives is vital for accurate and clinically relevant reporting. Radiologists play a significant role in determining whether patients need revision surgery or can continue with surveillance.

Images/Tables

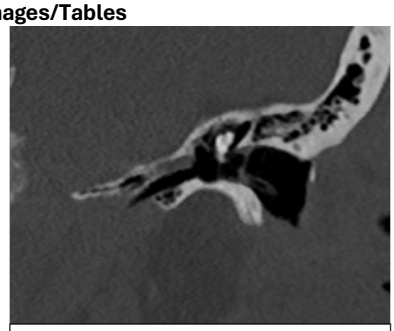

Tympanostomy tubes. Coronal CT image shows left tympanostomy tube (arrows), which are placed in the inferior portion of the tympanic membrane.

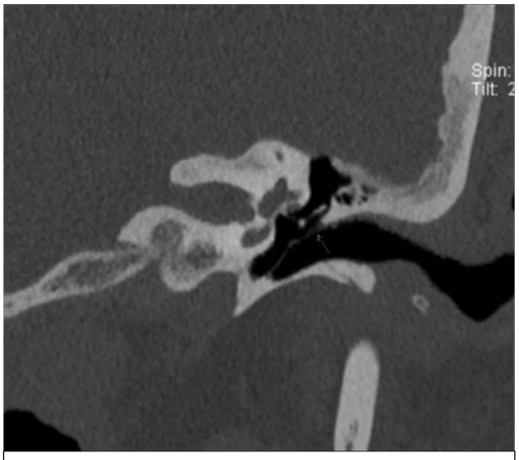

Type 1 tympanoplasty (myringoplasty). Coronal CT image shows expected thickening of the right tympanic membrane (arrow) after repair of its upper portion.

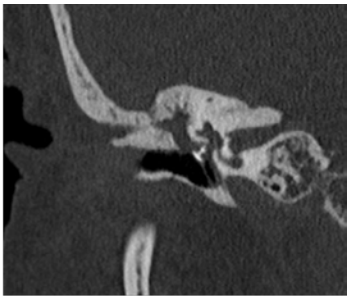

CT images show the intact stapes in contact with a metallic PORP, which is also in contact with the tympanic membrane.

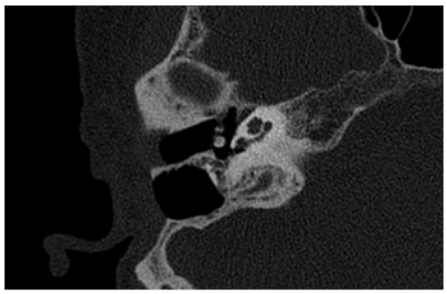

Axial oblique CT image at the level of the oval window shows the contact of the sculpted incus (white arrow) with the stapes (black arrow) and the manubrium of the malleus (arrowhead).

Axial oblique CT image at the level of the oval window shows the loop of the stapes prosthesis attached to the long process of the incus manubrium of the malleus

---

719 High-Stakes Diagnosis: Differentiating Cervicofacial Necrotizing Fasciitis From Its Mimics

Amir M Pirmoazen MD, Sahl Hakim DO, Ruben Ortiz Cordero MD, Oswaldo A Guevara Tirado MD, Peter Fiester MD
University of Florida, Jacksonville, FL, USA

Summary & Objectives

Background:

Necrotizing fasciitis (NF) is a rapidly progressive, life-threatening soft tissue infection, characterized by widespread fascial necrosis and systemic toxicity. It frequently presents with nonspecific clinical pictures that can closely mimic cellulitis, making early recognition challenging. Although NF most commonly involves the torso, extremities, or perineum, the head and neck is affected in a small subset of cases, approximately 1 to 10%.

Cervicofacial necrotizing fasciitis (CFNF) particularly carries a high mobility and morbidity due to potential for rapid spread along the cervical fascial planes, often extending into the mediastinum or skull base.
Prompt diagnosis using contrast-enhanced CT in the emergency setting is crucial, as early identification of fascial gas, non-enhancing fascia, and deep spade fluid collections can be lifesaving. Additionally, CT can delineate the full extent of disease and detect complications, differentiating CFNF from less aggressive infections. MRI serves an important complementary role in follow-up evaluation, particularly in assessing residual infection, soft tissue viability, and postoperative changes.

Summary:

- Cervicofacial necrotizing fasciitis (CFNF) accounts for <10% of all necrotizing fasciitis case and carries significant morbidity and mortality.
- Most cases are odontogenic or pharyngeal in origin with rapid fascial plane spread.
- Early detection of fascial gas, non-enhancing fascia, and cervical deep space fluid tracing is crucial for survival.
- Imaging, most notably contrast-enhanced Computed Tomography (CT) can distinguish CFNF from its mimics, preventing treatment delay.

Objectives:

- Present a series of institutional cases demonstrating variable presentation, imaging pattern, and mimics of CFNF.
- Highlight diagnostic pearls and pitfalls.
- Summarize radiologic algorithms for early diagnosis.
- Reinforce the key message “Prompt Diagnosis Saves Lives.”

Purpose

- To illustrate key CT findings of cervicofacial necrotizing fasciitis, a rare but life-threathening infection.
- To emphasize the importance of early radiologic recognition, given reported mortality rates of up to 70% with delayed diagnosis.
- To differentiate CFNF from its mimics such as odontogenic or pyogenic cellulitis/abscess, extension of pneumomediastinum into cervical fascial planes, post-traumatic or iatrogenic fistulous tracts.
- To provide a visual diagnostic framework for prompt diagnosis.

Materials & Methods

NA

Results & Conclusion

- Early CT diagnosis of CFNF in the emergency setting is essential for survival.
- MRI aids in follow-up and evaulation of residual or recurrent infection.
- Recognizing key imaging findings prevents treatment delay and improves outcomes.
- Radiologists play a central role in guiding timely and life-saving management.

Images/Tables

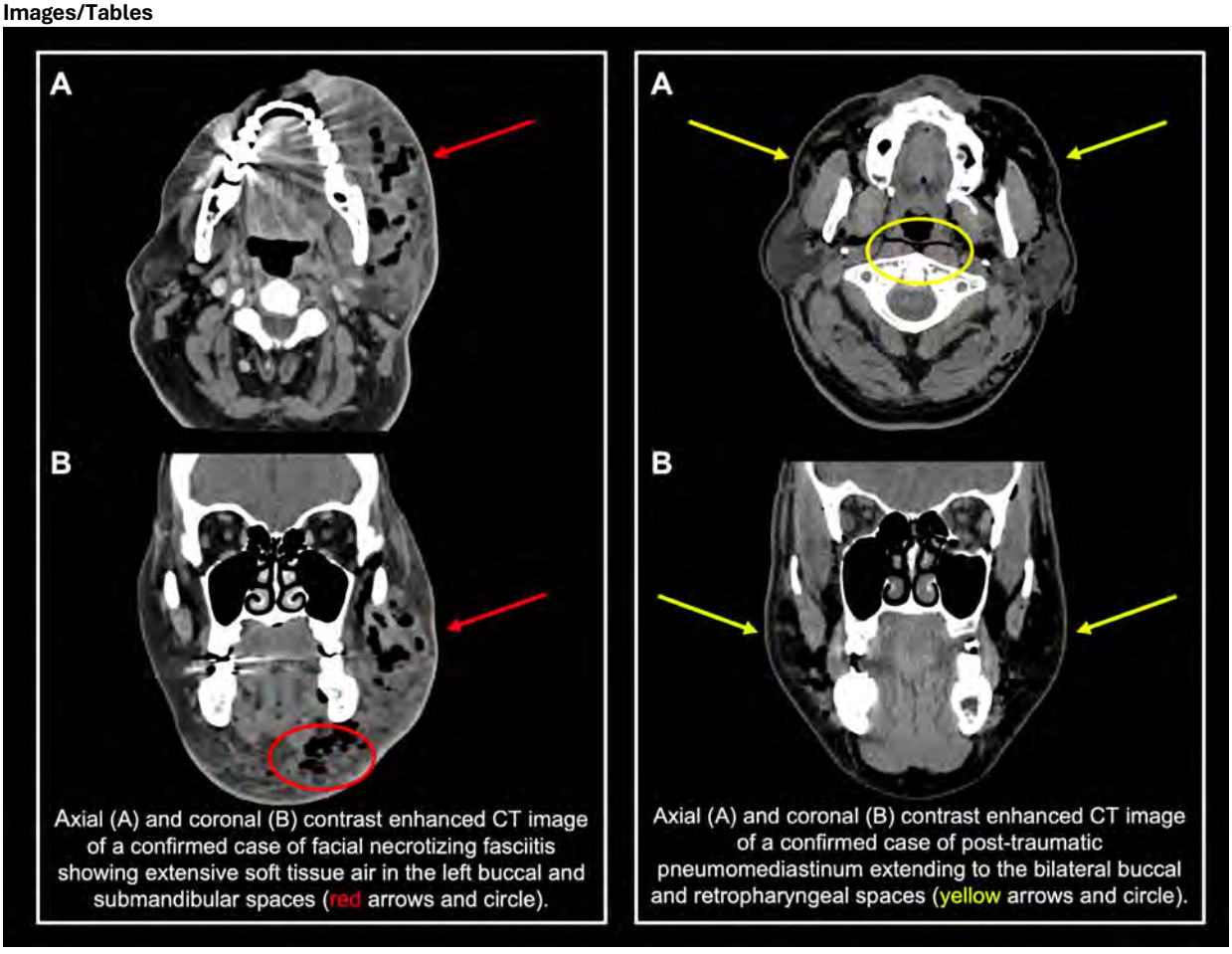

810 It's all in the throat: Unveiling Laryngeal Cancer and the Secrets of the Posterior Paraglottic Space

Tatiana Gillanders MD, Cecilia E Marenco MD, Karla A Borgna MD, Diego A Mongui Moya MD, Manuel Perez Akly MD, Cristina H Besada MD
Hospital Italiano de Buenos Aires, Buenos Aires, Buenos Aires, Argentina

Summary & Objectives

Summary : The posterior paraglottic space (otherwise known as thyro-cricoarytenoid space) is a critical radiological turnpoint for therapeutic decision-making in laryngeal cancer, due to its poor prognosis with conservative treatment. Its involvement directly contraindicates minimally invasive surgery (TORS/TLM) for T1-T3 tumors, forcing a shift to definitive chemoradiation or open resection. We will discuss a variety of cases highlighting the critical need for accurate radiological identification of the posterior paraglottic space to provide indispensable prognostic information and ensure optimal patient care.

Learning Objectives

1. Recognize the key anatomic sites necessary for accurate laryngeal T-staging.
2. Identify the posterior paraglottic space on cross-sectional imaging (CT/MRI).
3. Demonstrate the importance of the posterior paraglottic space in defining candidacy for minimally invasive surgical treatment options.

Purpose

To review the normal radiological anatomy of the posterior paraglottic space (PPS) and to demonstrate how its status on cross-sectional imaging dictates patient eligibility for minimally invasive, larynx-sparing surgical management of T1-T3 laryngeal carcinoma.

Materials & Methods

We present a structured review of the essential laryngeal anatomy required for accurate T-staging (including illustrative CT and MRI examples). Illustrative cases of T1-T4 laryngeal carcinoma are utilized to highlight the precise radiological identification of PPS involvement (versus preservation) and the resulting impact on therapeutic decision-making regarding the feasibility of transoral techniques.

Results & Conclusion

Results: For T1 and T2 stage cancers, treatment is trending toward minimally invasive options like transoral robotic surgery and transoral laser microsurgery. Importantly, these techniques are also now being used for select T3 stage tumors, as long as there is no posterior paraglottic space extension. Accurate staging of this space is therefore vital for determining the most appropriate and effective treatment strategy, which directly impacts patient outcomes.

Conclusion: It is essential for radiologists to prioritize the assessment of the posterior paraglottic space. By doing so, they can provide more accurate prognostic information and optimize treatment strategies, ultimately leading to improved patient outcomes.

Images/Tables

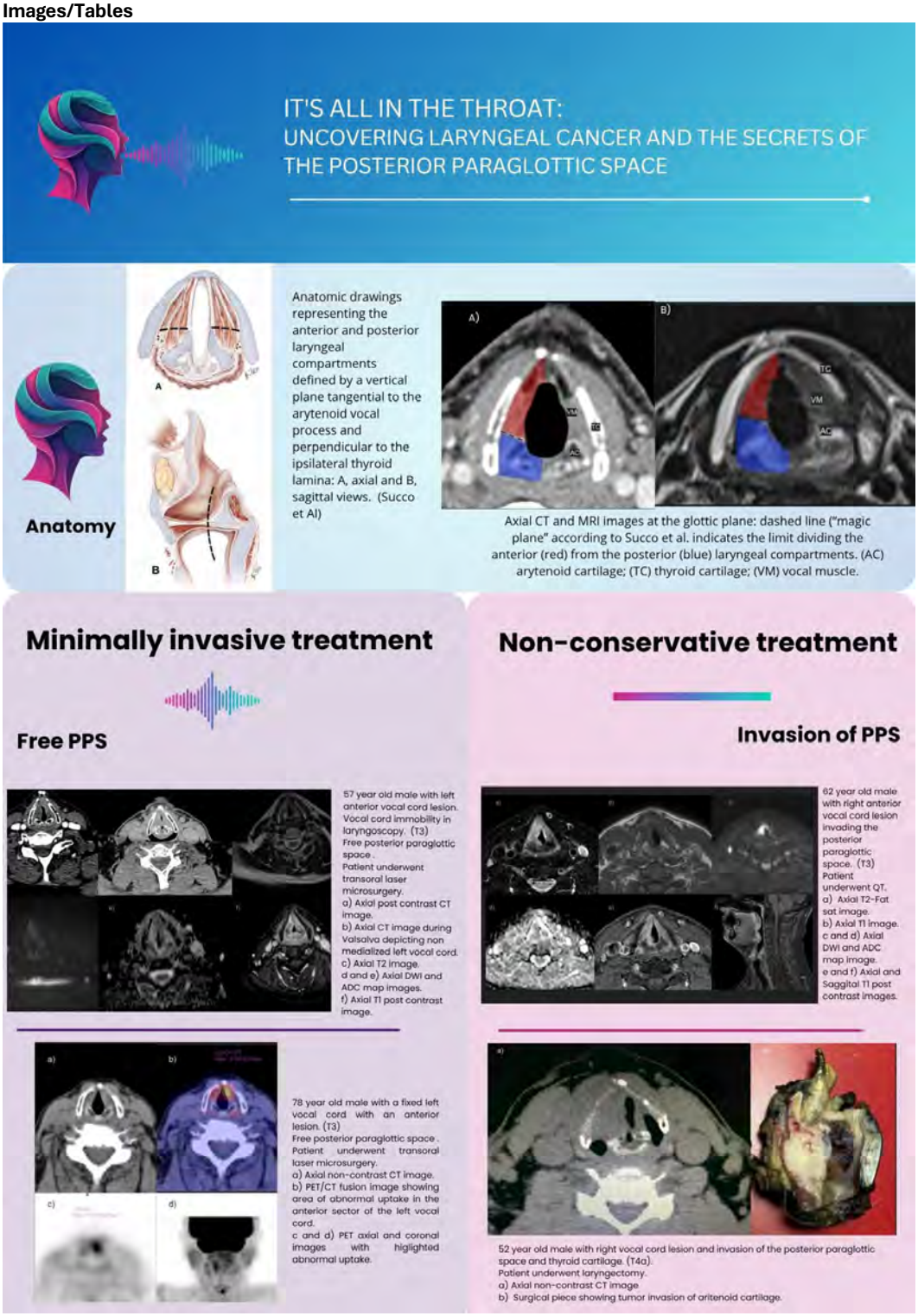

555 Unmasking Neuroinflammatory Adverse Events of Immune Checkpoint Inhibitors

Luke A Odisho MD, Albert Jiao MD, Donna Edwards MD, Mohannad Ibrahim MD, Aristides Capizzano MD
University of Michigan Medical Center, Ann Arbor, Michigan, USA

Summary & Objectives

Immune checkpoint inhibitors such as nivolumab and relatlimab have expanded therapeutic options for advanced malignancies, particularly metastatic melanoma. However, these agents can cause immune-mediated toxicities affecting multiple organ systems, including the nervous system. Neurologic immune-mediated adverse effects remain relatively rare but carry significant morbidity and mortality. They can involve either the central or peripheral nervous systems, with variable imaging and clinical presentations that may mimic metastatic disease.

This educational exhibit reviews various clinical cases of neurologic immune-mediated adverse effects in patients receiving immune checkpoint inhibitors, demonstrating how subtle imaging features can mimic intracranial metastases.

Purpose

To describe the clinical and imaging manifestations of neurologic immune-mediated adverse effects associated with immune checkpoint inhibitors.

Materials & Methods

This educational exhibit presents a series of patients who developed new neurological symptoms during or shortly after treatment with immune checkpoint inhibitors for a range of malignancies. The various cases demonstrate diagnostic workup including detailed neurological examinations, CT and MRI imaging, and cerebrospinal fluid analysis. Imaging characteristics were reviewed with attention to lesion location, patterns of contrast enhancement, and associated parenchymal signal changes. CSF studies included cell counts, protein levels, oligoclonal bands, and IgG index. Clinical features, imaging findings, and laboratory results were carefully integrated to help distinguish immune-mediated neurological complications from disease progression or metastasis. Treatment therapies including modification or discontinuation of immune checkpoint inhibitors and the use of corticosteroids or other immunosuppressive treatments were documented. Follow-up imaging and clinical assessments were analyzed to evaluate response to therapy and overall outcomes.

Results & Conclusion

Across the various cases, patients developed new neurological symptoms within months of initiating immune checkpoint inhibitor therapy. For example, a female patient with a history of melanoma being treated with combination immune checkpoint inhibitors developed symptoms of fluctuating horizontal diplopia with a component of binocular diplopia on far-right gaze, a pattern consistent with right CN VI palsy. Imaging demonstrated multiple new enhancing brain foci originally interpreted as metastases. These involved the pontomedullary sulcus at the origin of the right CN VI and subependymal periventricular white matter with subtle associated T2 hyperintensity. Total spine MRI was negative. CSF analysis revealed mild lymphocytic pleocytosis, elevated protein, and oligoclonal bands, supporting an autoimmune etiology. Following discontinuation of the immune checkpoint inhibitor therapy and initiation of corticosteroids, follow-up MRIs demonstrated complete resolution of all enhancing foci. Awareness of various neurotoxicities related to immune checkpoint inhibitors and their imaging correlate is critical to avoid misdiagnosis and inappropriate oncologic management. This educational exhibit aims to help individuals recognize these characteristic imaging findings allowing for early initiation of appropriate immunosuppressive therapy.

Images/Tables

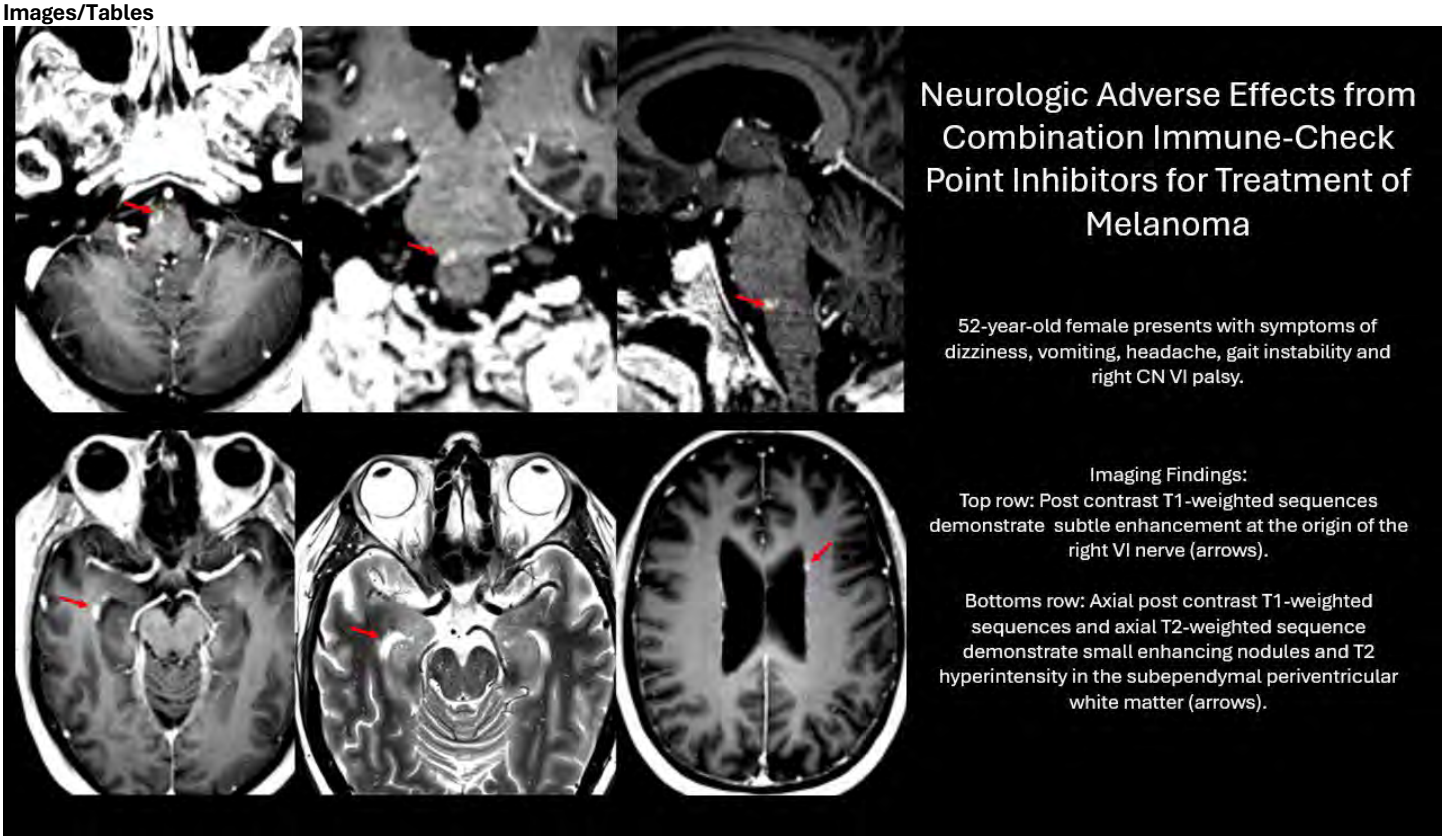

---

227 When Cures Turn Neurotoxic: Radiologic Manifestations of Treatment-Induced CNS Injury

Lamia S Choudhury MD, Kader Karli Oguz MD, Matthew Bobinski MD, PhD
UC Davis, Sacramento, CA, USA

Summary & Objectives

As advanced therapies expand, ranging from chimeric antigen receptor (CAR) T-cell therapy to adeno-associated viral (AAV) gene therapy, neuroradiologists are increasingly encountering unanticipated treatment-related neurotoxicity. This exhibit presents two instructive cases illustrating the neuroimaging spectrum of drug-induced CNS and neuromuscular complications: immune effector cell-associated neurotoxicity syndrome (ICANS) following CAR-T therapy and immune-mediated ocular myositis following AAV gene therapy (Elevidys) for Duchenne muscular dystrophy.

Case 1 involves a patient with relapsed B-cell acute lymphoblastic leukemia who developed progressive encephalopathy following CAR-T cell therapy. Initial MRI demonstrated diffuse bilateral white matter hyperintensity on FLAIR, nonspecific but concerning for treatment-related neurotoxicity given the patient's concurrent clinical decline. Within days, follow-up MRI revealed diffuse cortical edema with restricted diffusion in bilateral cerebral hemispheres, caudate heads, and thalami, suspicious for acute hypoxic/anoxic injury. Subsequent CT demonstrated diffuse cerebral edema with loss of gray-white differentiation, sulcal and ventricular effacement, and tonsillar herniation, representing terminal stage injury from severe immune effector cell-associated neurotoxicity syndrome (ICANS) and cytokine release syndrome. This case underscores the importance of recognizing early nonspecific white matter changes and subtle susceptibility foci as early indicators of catastrophic neurologic progression.

Case 2 shows a child with Duchenne muscular dystrophy and recent Elevidys AAV gene therapy who presented with acute binocular diplopia and transient upper extremity weakness. MRI of the brain and orbits with contrast showed enhancing bilateral temporalis muscles and thickened right lateral rectus and superior rectus muscles, consistent with immune-mediated ocular myositis. Corticosteroid therapy resulted in clinical improvement. This case highlights the role of MRI in identifying localized post-gene therapy inflammatory changes that may otherwise be misattributed to primary neurologic or orbital pathology.
Together, these cases illustrate a variety of therapy-related neurologic and myopathic complications detectable on imaging from diffuse cerebral edema in ICANS to localized extraocular muscle inflammation after gene therapy. Familiarity with these patterns enables radiologists to prompt timely multidisciplinary intervention and avoid irreversible neurologic sequelae.

Educational Objective:

After reviewing this exhibit, participants will be able to:

1. Identify early imaging features of CAR-T–related ICANS, including diffuse bilateral white matter FLAIR hyperintensity and tiny susceptibility foci, and distinguish them from mimics such as PRES, leukemic infiltration, or infectious encephalitis.
2. Recognize the temporal progression of therapy-related neurotoxicity, from subtle white matter changes to restricted diffusion in deep gray structures and ultimately diffuse cerebral edema with herniation.
3. Detect MRI signs of gene therapy–associated immune-mediated myositis, including enhancement and enlargement of extraocular and temporalis muscles.
4. Integrate imaging findings with clinical context and communicate effectively, using structured reporting to alert oncology and neurocritical care teams for timely intervention.

Purpose

N/A

Materials & Methods

N/A

Results & Conclusion

N/A

Images/Tables

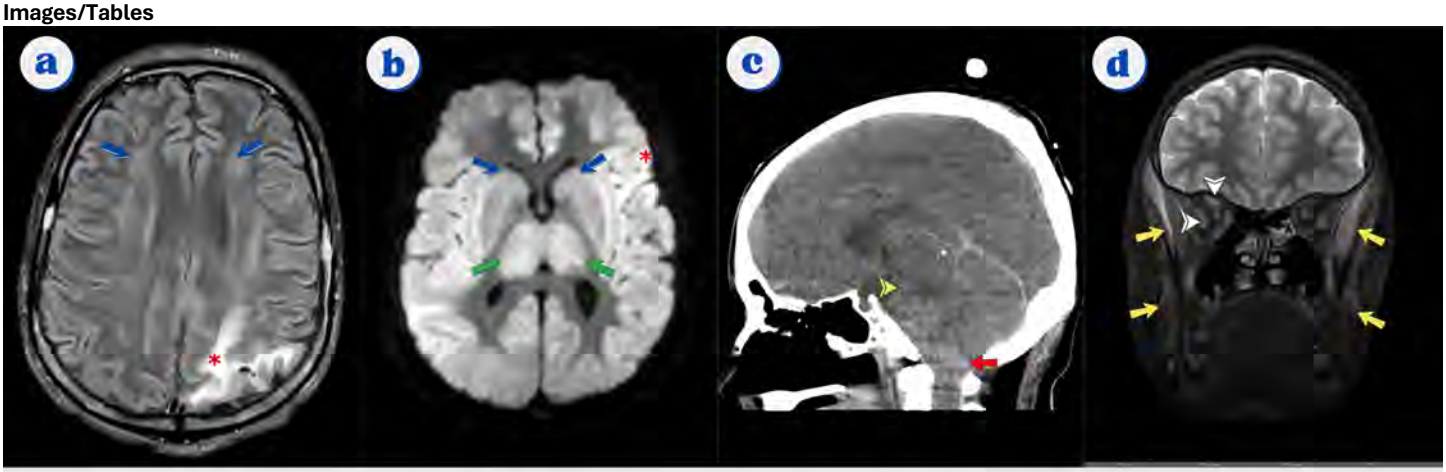

Figure 1. Drug-related neuroimaging findings across two distinct therapeutic toxicities.
(a) Axial FLAIR MR image demonstrates subtle symmetric hyperintensities within the deep cerebral white matter bilaterally (blue arrows), which are nonspecific but, in the appropriate clinical context, are concerning for early treatment-related neurotoxicity (ICANS) following CAR-T therapy. Signal abnormality in the left parietal lobe represents chronic treatment-related changes (red asterisk).
(b) Axial diffusion-weighted MR image demonstrates symmetric restricted diffusion in the thalami (green arrows), bilateral caudate heads (blue arrows), and cortex (red asterisk) consistent with diffuse cytotoxic injury secondary to ICANS following CAR-T therapy.
(c) Sagittal noncontrast CT image of the head shows loss of gray-white matter differentiation, effacement of the basal cisterns (yellow arrowheads), and inferior cerebellar tonsillar herniation (red arrow), findings indicative of global cerebral edema and herniation due to severe ICANS.
(d) Coronal T2-weighted image of the orbits reveals enlarged right lateral and superior rectus muscles (white arrowheads) and edematous bilateral temporalis and masseter muscles (yellow arrows), characteristic of ocular myositis following gene therapy for Duchenne muscular dystrophy (Elevidys).

---

278 **"Back Breakers": an Imaging Review of Spine Instrumentation**

Kevin Jiang MD, Subhash Venigalla MD, Samuel Ivie, Abraham Le, Tyler Chiu, Mary Foster, Jonathan Leary MD, Michael Gaub MD, Bundhit Tantiwongkosi MD, Michael McGinity MD
UT Health San Antonio, San Antonio, TX, USA

Summary & Objectives

Medical advances in the past two decades have allowed for an increased number of spine surgeries which has in turn increased imaging volume for spine instrumentation across multiple modalities. Proper imaging evaluation of spine hardware first requires an understanding of the spectrum of spine pathology requiring instrumentation. There are five main categories of such spine pathology and six main types of spine hardware. Preoperative imaging can assess for severity/extent of disease and surgical planning. Postoperative imaging can assess for hardware integrity and other possible complications.

- Review cervical, thoracic, and lumbar spine anatomy and the three-column model

- Discuss the imaging spectrum of spine pathology requiring spinal instrumentation
- Describe the six main types of spine instrumentation with imaging correlation (XR, CT, MR) and clinical photographs of the hardware
- Illustrate important imaging findings of hardware complications

Purpose

This educational exhibit will illustrate relevant information the radiologist can consider when reporting on spine instrumentation by reviewing the spectrum of spine pathologies requiring instrumentation, the main types of spine hardware, and possible postoperative complications.

Materials & Methods

In collaboration with the neurosurgery department, we have reviewed imaging for a spectrum of spine patients requiring instrumentation in our hospital system, which is a level 1 trauma center and the only academic institution in San Antonio, TX.

Results & Conclusion

The spectrum of spine pathology requiring instrumentation includes trauma, degenerative, infection, neoplasm, and congenital. The main types of spine hardware include pedicle screws and rods, cervical lateral mass screws and rods, corpectomy titanium expandable cage, TLIF static PEEK cage, ACDF plate and screws, and lateral approach interbody fusion cage. Postoperative complications to keep in mind are hardware fracture, malposition, migration, loosening, infection, subsidence, and pseudoarthrosis. It is important for the radiologist to understand these aspects of spine instrumentation as they relate to imaging because they can impact both pre-and post-operative management of spine patients.

Images/Tables

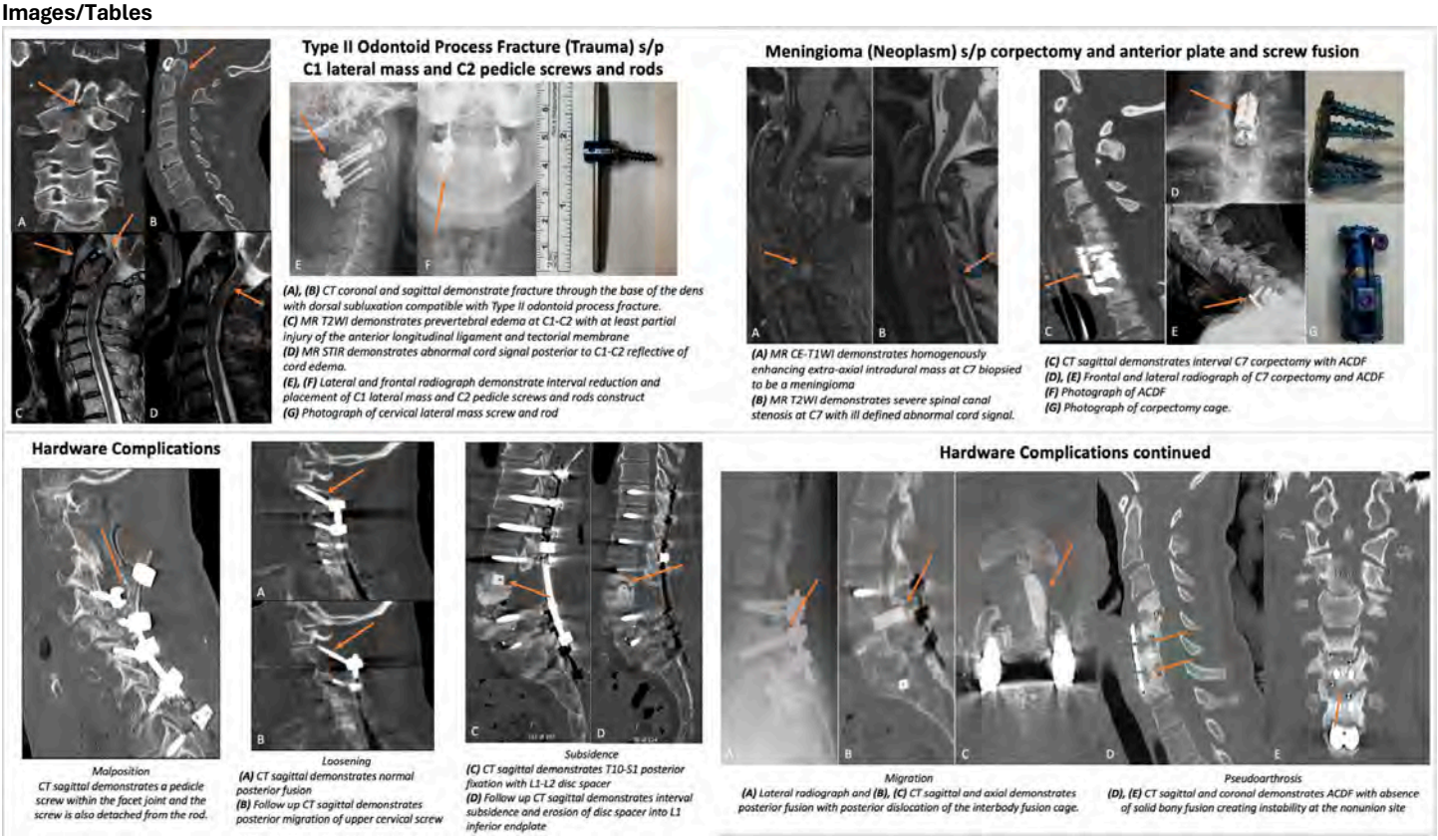

---

312 Prolonged Venous Transit on Perfusion Imaging: An Evolving Marker of Outcomes in Large Vessel Occlusion Stroke

Jay Kakadiya MD[1], Dhairya A. Lakhani MD[2], Hamza A Salim MD[3], Manisha Koneru MD[4], Dylan Wolman MD[5], Shyam Majmundar MD[6], Ferdinand Hui MD[7], Hanzhang Lu MD[8], Adam A Dmytriw MD[9], Adrien Guenego MD[10], Jeremy J. Heit MD[11], Gregory W. Albers MD[12], Tobias D Faizy MD[13], Vivek S. Yedavalli MD[8]

[1]The Russell H. Morgan Department of Radiology and Radiological Science, Johns Hopkins University School of Medicine, Baltimore, MD, USA. [2]Department of Neuroradiology, West Virginia University, Morgantown, WV, USA. [3]Department of Neuroradiology, MD Anderson Medical Center, Houston, TX, USA. [4]Cooper Medical School of Rowan University, Camden, NJ, USA. [5]Department of Radiology, Brown University, Providence, RI, USA. [6]Division of Interventional Neuroradiology, Department of Radiology, University of Maryland Medical Center, Baltimore, MD, USA. [7]Division of Radiology, Queen's Medical Center, University of Hawaii, Hawaii, Hawaii, USA. [8]Division of Neuroradiology, Department of Radiology and Radiological Sciences, Johns Hopkins University, Baltimore, MD, USA. [9]Neuroendovascular Program, Massachusetts General Hospital & Brigham and Women's Hospital, Harvard Medical School, Boston, MA, USA. [10]Department of Interventional Neuroradiology, Erasme University Hospital, Brussels, Brussels, Belgium. [11]Department of Interventional Neuroradiology, Stanford Medical Center, Palo Alto, CA, USA. [12]Stanford Stroke Center, Department of Neurology and Neurological Sciences, Stanford University, Palo Alto, CA, USA. [13]Department of Radiology, Neuroendovascular Program, University Medical Center, Münster, Münster, Germany

Summary & Objectives

Prolonged venous transit (PVT) on CT perfusion imaging represents delayed venous drainage and impaired microvascular function after arterial recanalization in acute ischemic stroke. This educational exhibit aims to (1) review the physiologic basis of PVT as a venous outflow marker, (2) summarize key clinical and imaging correlates from the literature, (3) compare its prognostic value to established arterial perfusion metrics, and (4) illustrate its application through representative imaging examples and a proposed workflow for integration into clinical practice.

Purpose

While arterial parameters such as Tmax, cerebral blood flow (CBF), and cerebral blood volume (CBV) remain central to stroke assessment, they often fail to capture post-reperfusion microvascular dysfunction that contributes to infarct progression and poor clinical outcomes. This exhibit explores PVT as an emerging, reproducible, and easily interpretable imaging biomarker of venous outflow (VO) status, emphasizing its role in predicting outcomes after mechanical thrombectomy (MT) for large vessel occlusion (LVO) stroke.

Materials & Methods

A comprehensive literature review was conducted using PubMed, Scopus, and Embase to identify studies evaluating PVT in acute ischemic stroke up to September 2025. Inclusion criteria comprised studies assessing PVT on CT perfusion using Tmax ≥10 s thresholds at dural sinus levels (superior sagittal sinus or torcula) and correlating findings with clinical and functional outcomes. Parameters including NIHSS, length of stay (LOS), modified Rankin Scale (mRS) at 90 days, and mortality were analyzed. Data from 12 primary studies (n ≈ 1,500 patients) were synthesized and visually summarized with representative cases and comparative ROC analyses.

Results & Conclusion

Across studies, **PVT-positive (PVT$^+$)** status was consistently associated with higher NIHSS at presentation, longer hospital stays, larger Tmax >6 s and mismatch volumes, and poorer 90-day functional outcomes (mRS 3–6). PVT$^+$ independently predicted unfavorable outcomes and mortality despite successful reperfusion, with adjusted odds ratios of 1.22. ROC analyses demonstrated PVT's superior prognostic value compared with conventional perfusion indices, achieving AUC values up to 0.821, further enhanced when combined with CBV index (AUC 0.831). Interobserver and intraobserver agreement was excellent (κ = 0.79–0.87), supporting its reproducibility.

Collectively, these findings establish PVT as a reliable imaging marker linking macrovascular reperfusion with microvascular health. Its assessment is simple, reproducible, and clinically relevant, offering incremental prognostic value for outcome prediction and individualized post-thrombectomy management. Incorporating PVT into standard perfusion analysis may refine risk stratification and improve personalized stroke care.

Images/Tables

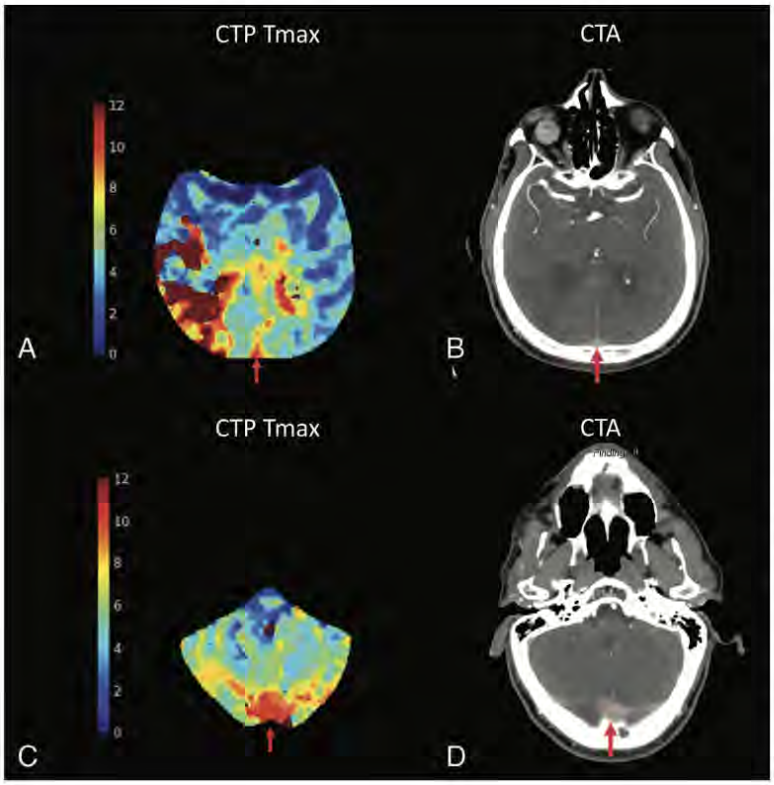

E

Author	Outcome Assessed	Key Findings
Yedavalli et al., 2025[38]	90-day mRS, mortality (mRS 6), poor functional outcome (mRS 4-6 vs 0-3)	PVT+ moderately correlated with 90-day mRS (ρ = 0.35, $p < 0.0001$). Weak to moderately correlated with poor functional outcomes (r = 0.27, $p = 0.002$), and mortality (r = 0.26, $p = 0.002$).
Yedavalli et al., 2025[40]	90 days mortality after successful reperfusion	PVT+ independently predicted higher mortality (OR 1.22, P=0.03) in successfully reperfused AIS – LVO patients.
Mei et al., 2025[37]	Favourable functional outcomes at 90-day (mRS ≤2); include only patient with successful MT	Combinations of PVT, Dichotomized CBV Index (CBV Index ≥0.8), and Dichotomized HIR (HIR<0.4) demonstrated the best predictive performance (AUC = 0.727) for favorable 90-day mRS score, separate analysis revealed PVT as best predictor (AUC = 0.658).
Mei et al., 2025[20]	Favourable functional outcomes at 90-day (mRS ≤2); includes all the patient underwent MT	Combinations of PVT and Dichotomized CBV Index (CBV Index ≥0.8) demonstrated the best predictive performance (AUC = 0.831) for favorable 90-day mRS score, separate analysis revealed PVT as best predictor (AUC = 0.821).
Mei et al., 2025[44]	Dichotomous mRS score at discharge (favorable: mRS 0-2; unfavorable: mRS 3-6)	PVT+ was independently associated with unfavorable mRS (OR = 0.231, p = 0.047) at discharge despite successful reperfusion.
Mei et al., 2025[45]	NIHSS percentage change, dichotomous NIHSS percent change ≥70%	PVT+ was independently associated with lower NIHSS percent change (B = -0.163, p = 0.049); less likely achieve higher than 70% NIHSS improvement (OR = 0.331, p = 0.024).
Salim et al., 2025[47]	Excellent functional recovery (mRS 0–1)	PVT+ was independently associated with lower odds of excellent recovery (aOR = 0.11; p = 0.006) following thrombectomy.
Koneru et al., 2025[43]	Length of hospital stay (LOS)	PVT+ associated with longer LOS and prolonged recovery course (3 days; p = 0.03).
Salim et al., 2025[39]	Functional outcome (mRS 0-2); includes only anterior circulation DMVO	PVT+ was independently associated with unfavorable outcomes in DMVO stroke (aOR = 0.14; p = 0.046), extending utility beyond LVO.
Salim et al., 2025[41]	Interobserver and intraobserver agreement	Demonstrated substantial reliability in PVT assessment; interobserver agreement (κ = 0.79), intraobserver agreement (κ = 0.87).
Salim et al., 2025[42]	Predictors of PVT+ status	Older age (aOR = 1.98, p = 0.043) and higher admission NIHSS (aOR = 1.05, p = 0.028) were independent predictors of PVT+.
Koneru et al., 2025[51]	Total hospital cost for stroke care	PVT+ associated with increased hospitalization costs (~$12,000 higher), indicating both clinical and economic burden. (p = 0.03)

---

437 Pearls and Pitfalls of CSF Leaks and the Use of Photon Counting CT

Joy Li MD, John Kim MD
University of Michigan, Ann Arbor, Michigan, USA

Summary & Objectives

Summary:

Spontaneous intracranial hypotension (SIH) occurs as a result of cerebrospinal fluid (CSF) leak in the absence of prior trauma or intervention such as lumbar puncture. Spontaneous CSF leaks may result from a dural tear or dehiscence (sometimes due to shearing by a nearby osteophyte), dehiscence of a meningeal cyst, or a CSF-venous fistula. SIH is a rare cause of headaches and can often present with subtle imaging findings, thus presenting a diagnostic challenge. This exhibit will review cases of patients who developed spontaneous CSF leaks from various causes to highlight the diagnostic algorithm for CSF leaks utilizing a combination of brain and spine MRI, digital subtraction myelogram (DSM), and CT myelography. Photon counting CT for CT myelography will also be discussed as an aid for detection of subtle CSF leaks.

Educational objectives:

1. Identify the clinical presentations for SIH
2. Identify MRI findings of SIH in the brain and spine
3. Delineate an algorithmic approach for diagnosing SIH, including indications for CT myelography and digital subtraction myelography (DSM)
4. Define a protocol for performing dynamic CT myelography and its benefits versus conventional CT myelography

5. Understand the benefits of using proton counting CT when performing CT myelography
6. Define a protocol for performing DSM, including various patient positioning that may elucidate a source of leak
7. Discuss targeted therapeutic intervention options once source of CSF leak is identified

Purpose

N/A

Materials & Methods

N/A

Results & Conclusion

1. SIH can have a variety of clinical presentations and can be a cause of debilitating symptoms.
2. When the CSF leak is subtle, MRI may be unrevealing. CT myelogram using photon counting CT and lateral decubitus DSM are helpful diagnostic tools for detecting a source of leak.
3. Accurate detection of a source of leak can provide patients with targeted therapeutic options which can provide relief for their symptoms.

Images/Tables

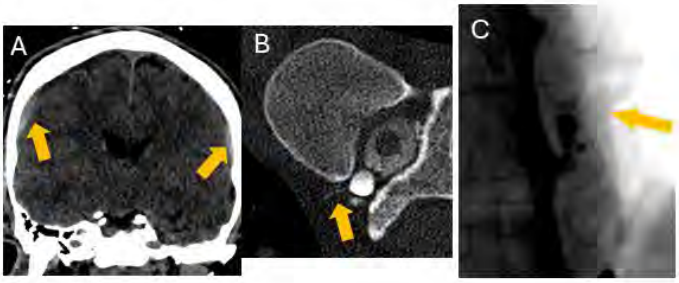

Figure 1. A 56-year-old patient was found down. (A) Coronal head CT demonstrates bilateral subdural hematomas. Brain MRI (not shown) demonstrated prominent brainstem sagging. (B) Right lateral decubitus photon counting CT myelogram demonstrates suspicious curvilinear contrast (arrow) arising from the right T10-T11 neural foramen. (C) Subsequent right lateral decubitus DSM confirms an outpouching of contrast opacifying right paraspinal veins, consistent with a CSF-venous fistula (arrow).

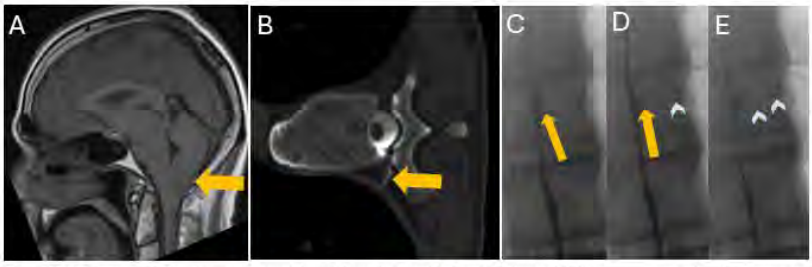

Figure 2. A 50-year-old patient presented with headache. (A) Sagittal brain MRI demonstrates brainstem sagging and inferiorly displaced cerebellar tonsils (arrow). (B) Right lateral decubitus photon counting CT myelography demonstrates curvilinear contrast arising from the thecal sac into right paraspinal soft tissues (arrow). (C-E) Lateral decubitus DSM images demonstrate progressive filling of a contrast outpouching extending from the thecal sac into the right paraspinal soft tissues with subsequent opacifying of right paravertebral veins (arrowheads), consistent with a CSF-venous fistula.

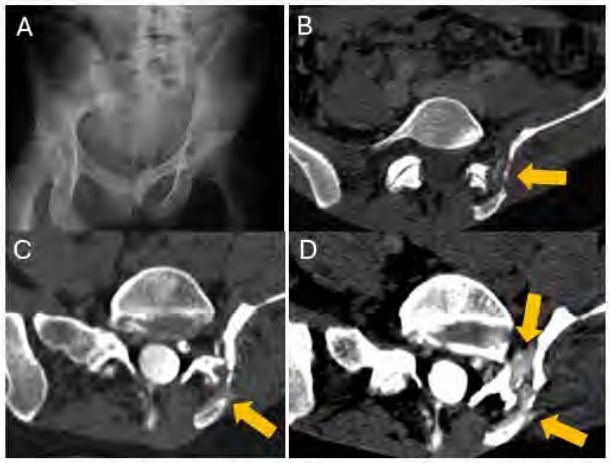

Figure 3. A 36-year-old patient with a history of chronic pelvic pain presented with new positional headaches. (A) AP hip radiograph demonstrates a severely dysplastic left hemipelvis. (B) Axial pelvis CT demonstrates bony fragments from a chronic pelvic fracture (arrow) in the vicinity of the left L5-S1 neural foramen. (C) Left lateral decubitus Axial CT myelogram demonstrates a trace extradural fluid collection or contrast extravasation (arrow). (D) After the patient sat upright for 5 minutes, repeat CT scan was obtained which demonstrates a new hyperdense collection along the lateral aspect of the L5-S1 facet joint and left nerve sheath (arrows).

574 Permeability and Perfusion Applications Utilizing Gadopiclenol in Head and Neck Neuroradiology: It Is All in the Curve

Matthew L White MD, Yan Zhang MD, Sean Kelly MD, Devin A DeLuna MD
University of Nebraska Medical Center, Omaha, NE, USA

Summary & Objectives

Permeability and perfusion imaging are well-established MRI techniques in the evaluation of head and neck pathologies, providing complementary physiologic information about tissue microvasculature and capillary integrity. Recent advances in contrast agent design have introduced gadopiclenol (Bracco Diagnostics, USA), a novel macrocyclic nonionic gadolinium-based agent characterized by exceptionally high relaxivity in human plasma - approximately two to three times greater than that of conventional agents. Despite its promising chemical profile, the published literature on gadopiclenol remains limited, particularly concerning its use for combined permeability and perfusion studies in head and neck imaging. The objective of this work is to demonstrate the feasibility, imaging characteristics, and diagnostic potential of gadopiclenol-enhanced permeability and perfusion MRI in neuroradiologic evaluation of head and neck lesions.

Purpose

This study aims to explore the clinical applicability of gadopiclenol in providing high-quality permeability and perfusion maps for the head and neck region. Specifically, the goal is to assess whether the superior relaxivity of gadopiclenol can optimize dynamic T1- and T2*-weighted acquisitions, yielding reliable physiologic data that enhance lesion characterization. The analysis includes representative cases to illustrate its potential role in differentiating schwannomas, paragangliomas, neurofibromas, varices, hemangiomas, undifferentiated pleomorphic sarcoma, chondrosarcoma and skull base myeloma. Representative analyses were also performed to evaluate the utility of gadopiclenol in differentiating post-radiation changes from tumor recurrence and in assessing lymph node malignancy.

Materials & Methods

All MRI examinations were performed using FDA-approved doses of gadopiclenol. Although permeability and perfusion analysis represent off-label applications, the imaging protocol was optimized to leverage the agent's high relaxivity. A half-dose of gadopiclenol was first administered for permeability imaging, followed by the remaining half for T2* perfusion sequence. Exams were conducted on both 1.5T and 3.0T scanners. Image post-processing was performed using Olea Sphere (Olea Medical, France). Perfusion parameters included corrected relative blood volume (rBV), relative blood flow (rBF), time-to-peak (TTP), time-to-maximum enhancement (TME), leakage correction factor (K2), and mean transit time (MTT). Permeability parameters analyzed were the transfer constant (Ktrans), rate constant (Kep), extravascular extracellular volume fraction (Ve), and plasma volume fraction (Vp).

Results & Conclusion

Results & Conclusion

Gadopiclenol (Vueway, Bracco Diagnostics Inc, USA.) produced excellent image quality with robust signal enhancement, allowing simultaneous evaluation of perfusion and permeability characteristics in a single examination. The resulting maps provided detailed physiologic and hemodynamic information that improved lesion delineation and diagnostic confidence. Distinct differences in vascularity and permeability profiles were observed across various head and neck pathologies, including differentiation of recurrent tumor from post-therapy changes and characterization of complex facial and skull base lesions.

The greater relaxivity of gadopiclenol created optimal dynamic T1 and T2* sequences. These preliminary findings suggest that gadopiclenol-based perfusion and permeability imaging can serve as a powerful adjunct in head and neck neuroradiology. Radiologists proficient in these advanced techniques may significantly enhance diagnostic accuracy and patient care.

Images/Tables

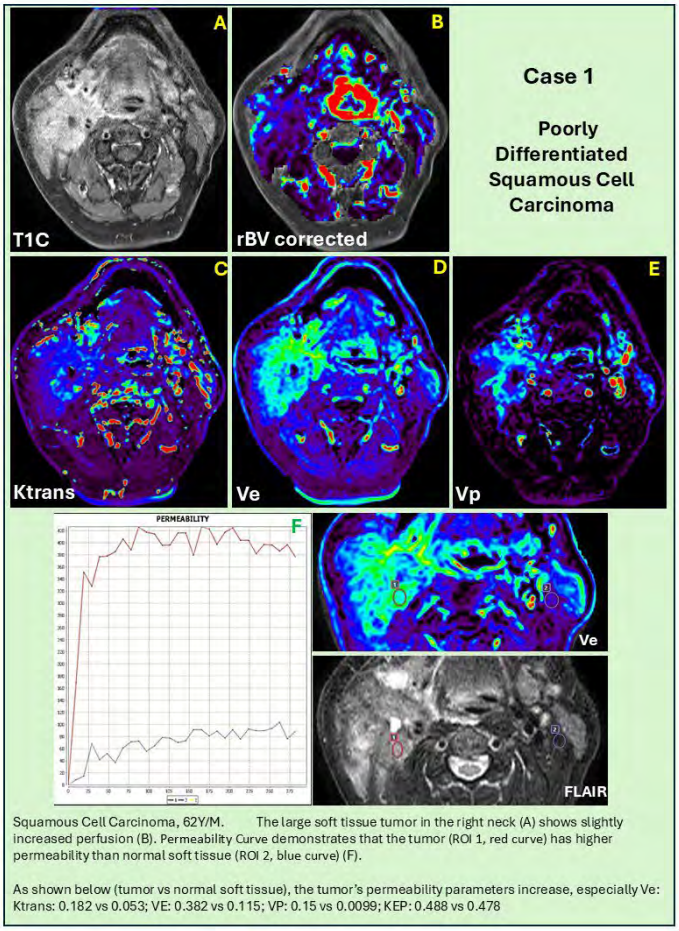

Squamous Cell Carcinoma, 62Y/M. The large soft tissue tumor in the right neck (A) shows slightly increased perfusion (B). Permeability Curve demonstrates that the tumor (ROI 1, red curve) has higher permeability than normal soft tissue (ROI 2, blue curve) (F).

As shown below (tumor vs normal soft tissue), the tumor's permeability parameters increase, especially Ve: Ktrans: 0.182 vs 0.053; VE: 0.382 vs 0.115; VP: 0.15 vs 0.0099; KEP: 0.488 vs 0.478

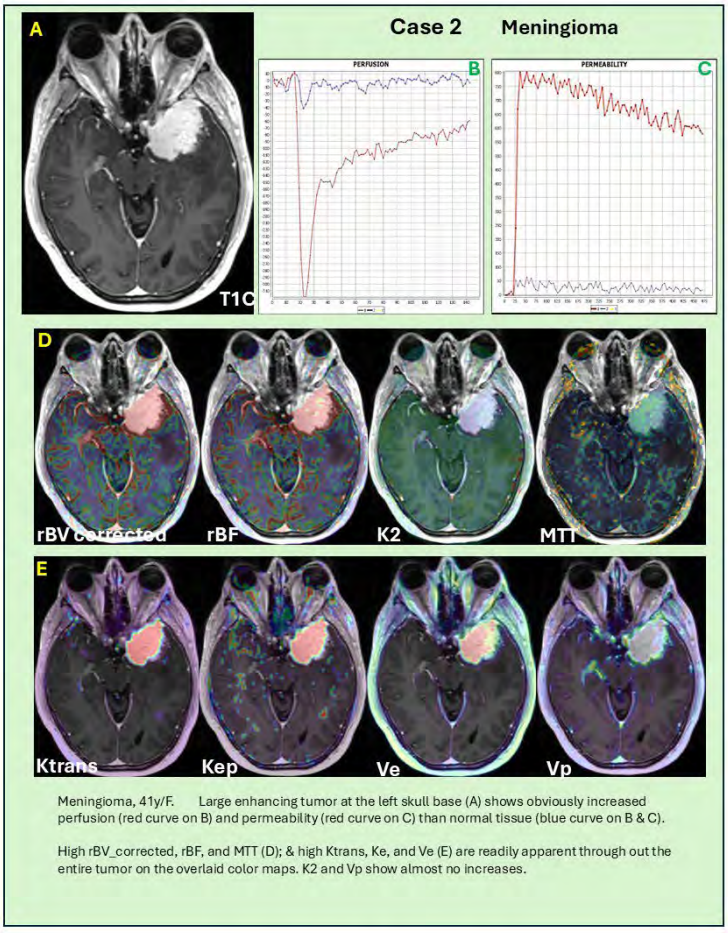

Meningioma, 41y/F. Large enhancing tumor at the left skull base (A) shows obviously increased perfusion (red curve on B) and permeability (red curve on C) than normal tissue (blue curve on B & C).

High rBV_corrected, rBF, and MTT (D); & high Ktrans, Ke, and Ve (E) are readily apparent through out the entire tumor on the overlaid color maps. K2 and Vp show almost no increases.

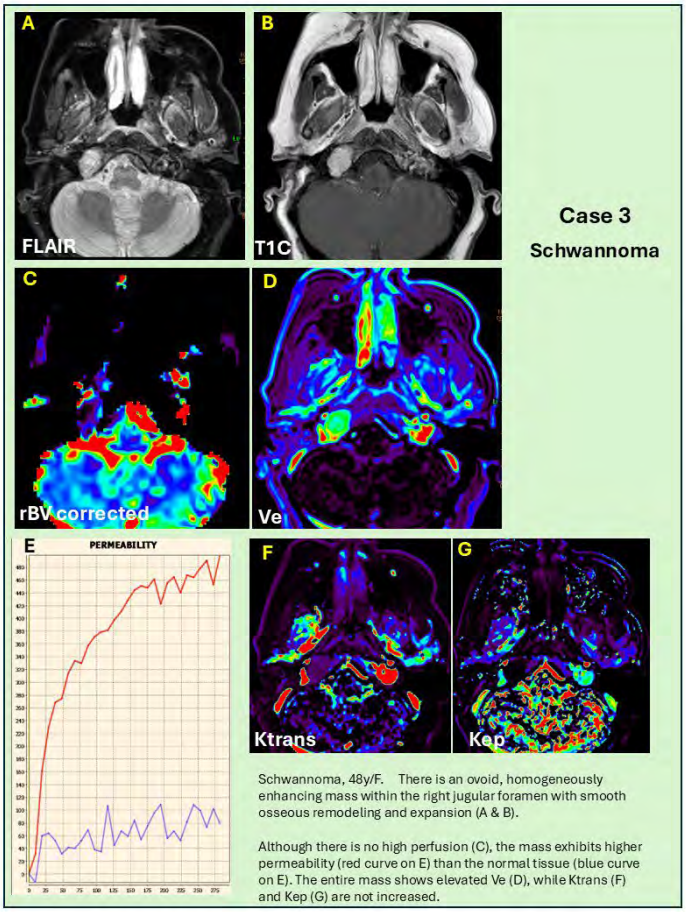

Schwannoma, 48y/F. There is an ovoid, homogeneously enhancing mass within the right jugular foramen with smooth osseous remodeling and expansion (A & B).

Although there is no high perfusion (C), the mass exhibits higher permeability (red curve on E) than the normal tissue (blue curve on E). The entire mass shows elevated Ve (D), while Ktrans (F) and Kep (G) are not increased.

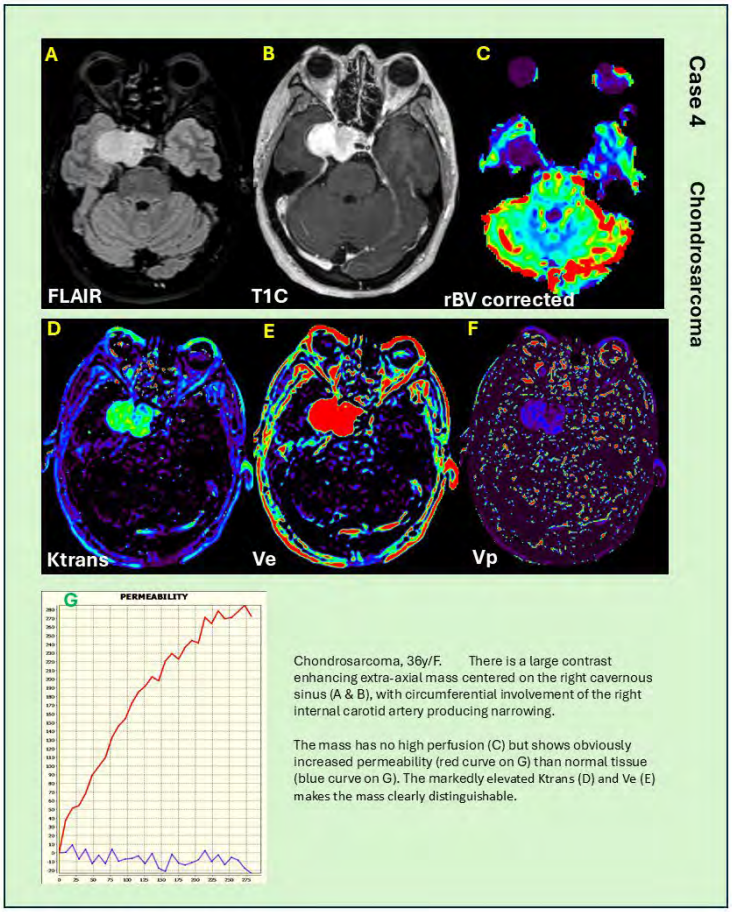

Chondrosarcoma, 36y/F. There is a large contrast enhancing extra-axial mass centered on the right cavernous sinus (A & B), with circumferential involvement of the right internal carotid artery producing narrowing.

The mass has no high perfusion (C) but shows obviously increased permeability (red curve on G) than normal tissue (blue curve on G). The markedly elevated Ktrans (D) and Ve (E) makes the mass clearly distinguishable.

620 Game On! From Jeopardy to AI: Gamification in Radiology Education

Pootipong Wongveerasin MD, Nicholas O V Cunningham MD, Harprit Bedi M.D.
Boston Medical Center, Boston, MA, USA

Summary & Objectives

"Gamification", the use of addictive game mechanics to promote engagement, has become an indispensable tool in radiology education. This exhibits reviews the current landscape of gamified learning in radiology, ranging from the freely available, web-based resources that educators can readily adopt, to the novel emerging AI-integrated platforms, representing the next generation of interactive training. Finally, we present an original prototype radiology card game, developed in Godot engine by a resident for the residents, to illustrate how open-source game development can be leveraged to create a concept-driven game, that foster collaboration, competition and diagnostic reasoning.
Objectives:
1. Summarize current and emerging gamification tools in radiology education.
2. Identify free, accessible platforms that are educators can easily adopt.
3. Demonstrate how custom game design, i.e., a card game can expand diagnostic reasoning, interactive learning and concept retention.

Purpose

Modern radiology trainees thrive on interactivity and collaboration. As radiology transitions toward competency-based assessment and the reintroduced ABR Oral Examination, gamified learning offers a means to foster quick reasoning and communication skills in a safe and engaging environment. Although interest in educational gamification is rising, awareness of the available tool remains limited. This exhibit aims to update the educators on the state of gamified radiology education, pointing them to the resources already available online.

Materials & Methods

A literature review was performed to identify published gamified platforms used in radiology education. Tools are grouped by complexity and availability of access:

- Foundational (Free, web-based, minimal setup): Jeopardy!, Family Feud PowerPoint Templates, Kahoot! interactive quizzes
- Intermediate (Rigid structured platform with feedback and tracking): Kaizen Education app, other institutional-built quiz portal, DDx: Duel of Differentials (Our custom game).
- Advanced (Computationally intensive, e.g., AI-driven, computer vision, 3D interactive virtual environment): RadGame, RADHunters, and other virtual or adaptive systems incorporating computer vision and analytics.

Results & Conclusion

Across the reviewed literature, gamification consistently improved learner engagement, motivation, and satisfaction. Studies of *Kahoot!* and *Jeopardy!* report higher participation and retention; *Kaizen* matches or exceeds traditional assessments while improving teamwork and enjoyment. Games like *RadGame* and *RADHunters* mark the shift towards AI-feedback gamification. Our custom card-game demonstrates a novel way to foster diagnostic reasoning rather than rote memorization. By integrating both existing resources and creative development, educators can transform passive case review into an active, memorable learning experience.

---

831 The 2024 McDonald Criteria for Multiple Sclerosis: Refining MRI Diagnostics with Central Vein Sign and Paramagnetic Rim Lesions

Nasim Batavani MD, Clinical Neuroradiology Fellow, Michelle Pisa Do, Neuroradiology Fellow, Sathish Kumar Dundamadappa MD, Neuroradiologist
UMass Chan Medical School, Worcester, MA, USA

Summary & Objectives

Familiarize radiologists with the 2024 McDonald criteria for Multiple Sclerosis (MS), updates from a radiological perspective.
Outline key differences between the 2017 and 2024 guidelines.
Pictorial representation of suggested criteria for defining central vein sign (CVS) and paramagnetic rim lesions (PRL).
Discuss specific updates for clinically isolated syndrome and older patient populations.

Purpose

To enhance radiologists' understanding of new supportive image markers for the diagnosis of MS, CVS and PRLs.

Materials & Methods

Summary of Key differences between 2017 and 2024 guidelines:

- MRI is essential for diagnosing MS.
- The optic nerve is now the fifth site for dissemination in space.
- Guidelines apply to all ages with some caveats.
- Unified criteria cover both relapsing and progressive disease.
- Central vein sign and paramagnetic rim lesions are added as supportive imaging markers.

Central vein sign:

Depicts perivenular preference for demyelinating plaques.
The perivascular sites are privileged for immune cells to interact with antigen-presenting cells, which can then trigger an inflammatory cascade leading to the formation of lesions around the veins
Criteria:

- Linear or dot-like hypointense focus within the lesion (depicting the medullary vein)
- Should show linear morphology in one plane
- Centrally located
- Less than 2 mm in diameter
- Runs partially or entirely through the lesion

Paramagnetic rim lesions:

Paramagnetic rim is best seen in phase maps of susceptibility weighted imaging.

Initially described with 7T, can be seen with 3T as well as 1.5T
Related to iron-containing proinflammatory macrophages/microglia at the lesion edge, loss of diamagnetic myelin, changes in paramagnetic deoxyhemoglobin, and presence of free radicles.
Highly specific for MS; correlation with chronic active/smoldering lesions; continuous low-grade demyelination, lesion growth, and non-relapsing clinical disease progression
The rim:

- Appears as a discrete paramagnetic border on susceptibility-sensitive MRI, best seen in phase maps; may be dark or bright depending on magnet handedness.
- Covers at least two-thirds of the outer white matter edge of the lesion (excluding cortical or ependymal borders) on the most visible slice.
- Is visible on at least two consecutive slices (2D) or in two orthogonal planes (3D).
- Aligns with part or all of a T2-hyperintense lesion core.

Key considerations:

- Ensure high-quality SWI.
- Phase maps are highly sensitive; review carefully and adjust windowing.
- PRL has high specificity for MS.
- Larger lesions often lead to PRL development.
- Lesions are easier to spot in periventricular and deep white matter than juxtacortical areas.
- Confirm no contrast enhancement or prior lesion presence.

Results & Conclusion
The revised McDonald criteria broaden the scope of previous guidelines by incorporating additional imaging markers. It is essential for radiologists to become well-versed in these updated standards and adhere to recommended protocols for diagnosing central vein signs and paramagnetic rim lesions.
Images/Tables

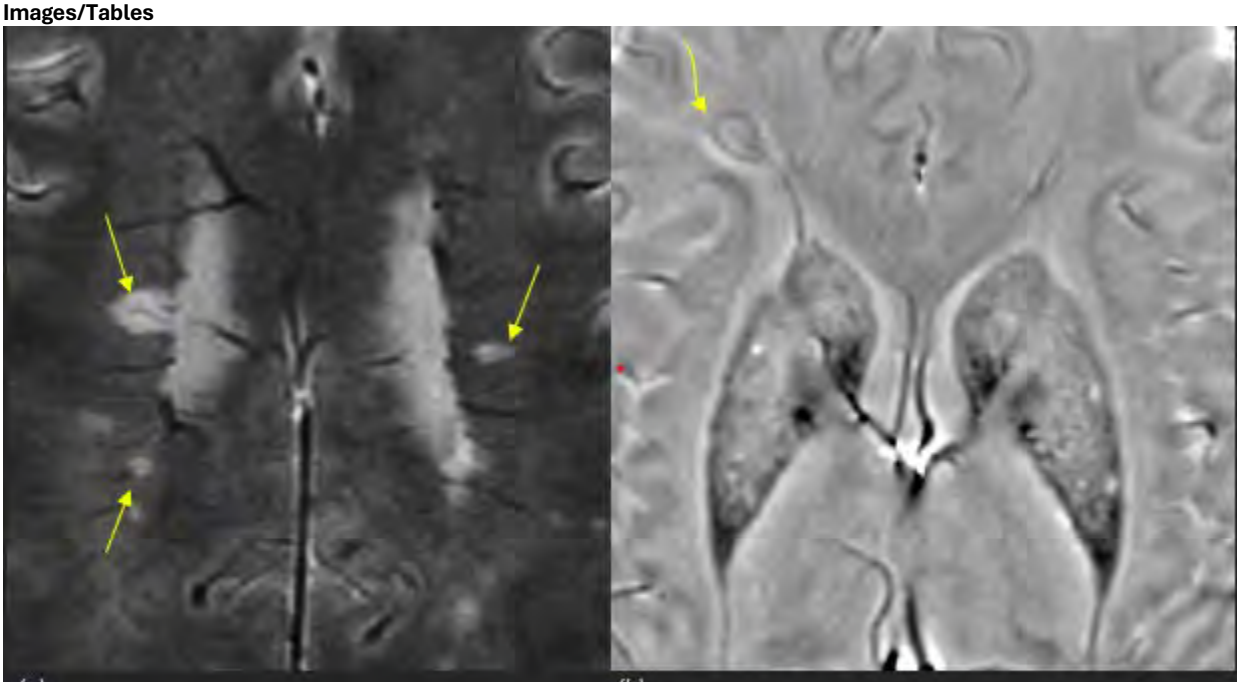

Figure 1. (a)Axial susceptibility-weighted imaging showing multiple periventricular demyelinating plaques with central vein sign (straight arrows). (b) Phase imaging demonstrating paramagnetic rim lesion (curved arrow).

---

868 Enhanced Detection of Focal Cortical Dysplasia Type IIb with Voxel-Based Processing Maps: A Comparative Analysis of Residents and Specialists
Bryann A Cortes Rodriguez MD, Mariana Mercado Flores MD, Haziel Maya Garcia MD, Arturo M Rodriguez Saldivar MD, Andres F Rios Victoria MD
Hospital Universitario Dr. José Eleuterio Gonzalez, Monterrey, Nuevo Leon, Mexico
Summary & Objectives
Focal cortical dysplasia type IIB (FCD IIB) is a frequent cause of drug-resistant partial epilepsy in younger patients. However, many lesions remain undetected on routine MRI due to subtle cortical and subcortical changes. Advanced post-processing techniques such as textures maps, including cortical thickness, gray–white matter gradient, and relative intensity maps, have shown potential to improve lesions detections.
This study aims to evaluate the diagnostic impact of these maps on the detection of FCD IIB by non-expert general radiologists, assessing their ability to identify lesions more accurately and efficiently compared with conventional MRI alone.

Purpose

To propose, design and validate an easy and practical workflow that helps non-expert general radiologists to improve detection of focal cortical dysplasia type IIB through the use of voxel-based post-processing maps. Two radiologists independently reviewed 50 MRI studies of patients with long term drug-resistant epilepsy; 25 with histopathologically confirmed FCD IIB and 25 without structural abnormalities. After an initial evaluation using conventional MRI, the same cases were re-evaluated with cortical thickness, GM–WM gradient, and relative intensity maps. The study assessed diagnostic time, accuracy, and the ability to correctly identify patients with FCD IIB, demonstrating the high value of the texture maps in standard radiological practice.

Materials & Methods

Fifty anonymized MRI studies from patients with pharmacoresistant epilepsy were retrospectively selected. Twenty-five cases had a confirmed diagnosis of focal cortical dysplasia type IIB based on histopathological examination, and twenty-five were control subjects without structural abnormalities. All studies were processed using voxel-based post-processing pipelines (PyNoel) to generate cortical thickness, gray–white matter gradient, and relative intensity maps.

Two general radiologists without prior experience in epilepsy imaging independently reviewed the studies in two phases:

- **Phase 1: Conventional MRI only (T1 and FLAIR in volumetric adquisition).**
- **Phase 2: The same cases supplemented with the three post-processing maps.**

The observers were blinded to diagnosis during both sessions. Diagnostic accuracy, sensitivity, specificity, and interpretation time were recorded and compared between both reading phases.

Results & Conclusion

The incorporation of voxel-based post-processing maps significantly enhanced diagnostic performance across all readers. For general radiologists, sensitivity for detecting focal cortical dysplasia type IIB increased from 52% with conventional MRI to 84% when aided with texture maps ($p < 0.01$). Specificity improved from 76% to 88%, and mean detection time decreased by approximately 25%.

Both radiologists mentioned greater confidence in identifying cortical and subcortical blurring and subtle signal abnormalities when texture maps were available. Visual correlation among the three map types facilitated detection of lesions that were inperceptible on standard MRI images.

These findings support the integration of texture maps post-processing into routine radiological workflows. Even for non-specialist readers, these tools improve diagnostic accuracy, consistency, and efficiency, representing a valuable adjunct for the identification of subtle epileptogenic lesions such as focal cortical dysplasia type IIB.

Images/Tables

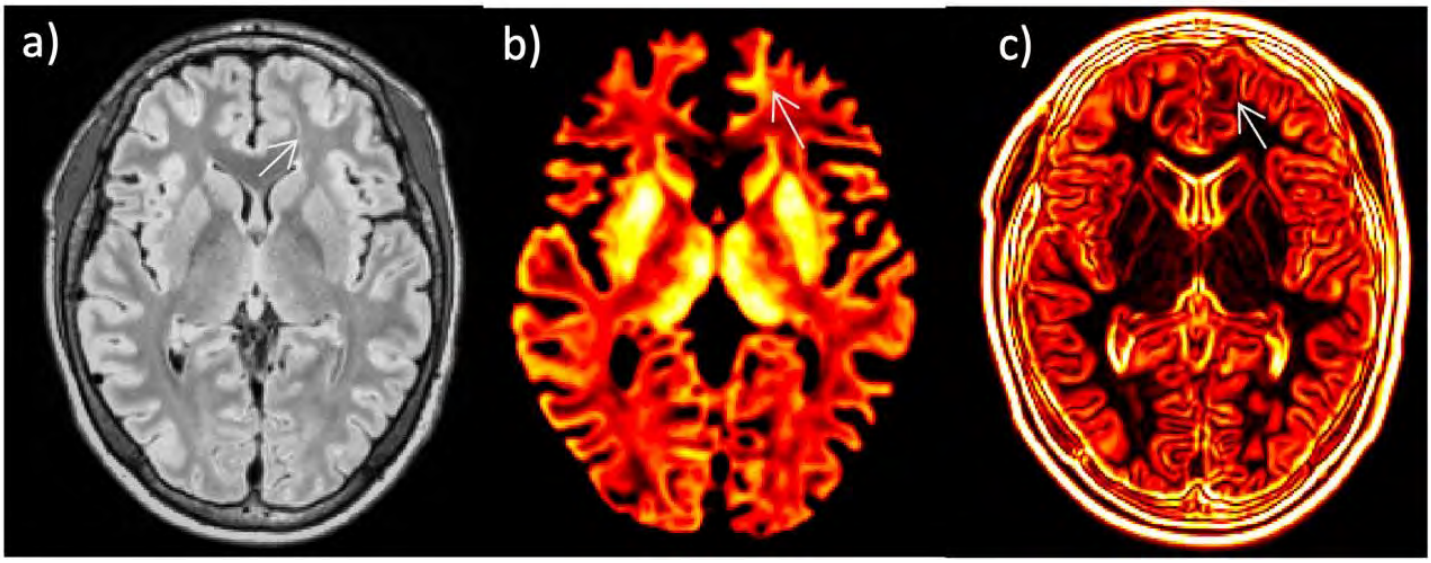

899 Theranostics in Neuro-Oncology: From Molecular Target to Clinical Reality

Michelle Chen MD[1], Marc Benayoun MD, PhD[2], Maria Ponisio MD[3], Vilma Kosovic[4], Ana M Franceschi MD, PhD[1]

[1]Donald and Barbara Zucker School of Medicine at Hofstra/Northwell, New York, NY, USA. [2]Wake Forest University School of Medicine, Winston-Salem, NC, USA. [3]Washington University Medicine Mallinckrodt Institute of Radiology, St. Louis, MO, USA. [4]Dubrovnik General Hospital, Dubrovnik, Dubrovnik, Croatia

Summary & Objectives

Theranostics, the integration of molecular imaging with targeted radionuclide therapy, represents a paradigm shift in neuro-oncology. It offers unprecedented precision for primary brain tumors and metastases, pathologies for which conventional therapies are often limited by anatomical constraints, tumor heterogeneity, and the formidable blood-brain barrier (BBB). This exhibit illustrates how theranostic approaches provide non-invasive, biomarker-driven patient selection, individualized dosimetry, and real-time treatment monitoring.

The objectives of this educational exhibit are to:

(1) review the fundamental theranostic principle and its unique advantages for personalized medicine in the CNS tumor management.

(2) detail the clinically validated and emerging molecular targets, including SSTR, LAT1, NK-1R, GRPR, FAP, and PSMA;

(3) illustrate innovative delivery strategies, such as osmotic disruption and super-selective intra-arterial (ssIA) administration, for overcoming the BBB; and

(4) Compare the distinct roles of beta (ex, ^{177}Lu) and alpha (ex, ^{213}Bi) emitters to complete the clinical picture of how treatment is optimized for neuro-oncologic applications.

Purpose
N/a
Materials & Methods
N/a
Results & Conclusion
Theranostics has moved from concept to clinical reality, with specific applications demonstrating significant, disease-specific success.
Meningioma: SSTR2-targeted therapy with ^{177}Lu-DOTATATE represents a promising investigational approach for meningioma treatment, exemplifying the potential of theranostics in neuro-oncology. While peptide receptor radionuclide therapy (PRRT) with ^{177}Lu-DOTATATE remains investigational rather than standard treatment for meningioma, systemic administration of this beta-emitter has shown promising results in patients with progressive, refractory WHO Grade II tumors.
Glioblastoma (GBM): Several distinct theranostic strategies are showing promise, each addressing a different aspect of the tumor's biology. A systemic approach targeting the LAT1 amino acid transporter with TLX101 (^{131}I-IPA) achieved a median overall survival (OS) of 13 months in recurrent GBM. In parallel, a locoregional strategy using the alpha-emitter ^{213}Bi-Substance P to target the NK-1R has achieved a 10.9-month median OS. A third, anti-vascular approach targets PSMA on tumor neovasculature, where efficacy is dramatically enhanced by ssIA delivery, resulting in 15-fold greater tumor uptake than with IV administration.
Brain Metastases: Theranostic applications extend beyond primary tumors. PSMA-targeted therapy, already standard for prostate cancer, is now being investigated for PSMA-positive brain metastases. Furthermore, fibroblast activation protein (FAP) is emerging as a promising cancer-agnostic target for metastases from various primaries, with therapeutic applications of novel FAPI tracers in early-phase research.
Emerging Applications: The field continues to expand, with GRPR showing 100% expression in gliomas, offering a broad target for future development, and LAT1 PET showing utility in predicting progression in low-grade gliomas.
In conclusion, theranostics is not a single modality but a diverse arsenal of targeted agents. From systemic beta-therapy for meningiomas to locoregional alpha-therapy and anti-vascular strategies for GBM, these applications demonstrate a foundational advancement in neuro-oncology. By tailoring the target, radionuclide, and delivery method to the specific disease, theranostics provides precise, personalized options that are changing the treatment landscape for brain tumor patients.

---

925 After-Hours Approach to Skull Base MRI
Nahyun Jo MD, Francis Deng MD
Johns Hopkins University, Baltimore, MD, USA
Summary & Objectives
- Main objective: Provide the list of indications and differential diagnosis for skull base MRI ordered out of preoperative or elective/outpatient settings
- Provide a quick pictorial overview of cranial nerve and skull base anatomy on skull base MRI
- Example set of protocol, importance, and application of each sequences in a set of skull base MRI protocol to prioritize sequences and tailor to emergent/urgent clinical questions

Purpose
Skull base magnetic resonance imaging (MRI) is used in a variety of clinical contexts, including the evaluation of cranial nerve neuropathies, preoperative surgical planning, and assessment of pathologies affecting adjacent anatomical structures. It employs high-resolution three-dimensional sequences that yield detailed anatomical information. Nevertheless, the examination is frequently lengthy and comprehensive. Moreover, extended acquisition times and reduced slice thickness render the study susceptible to motion-related artifacts. In the context of after-hours imaging, the necessity of employing this prolonged and resource-intensive protocol warrants scrutiny.
This review provides an overview of the utility of skull base MRI in a non-elective setting. It provides an overview of protocol modifications, enabling radiologists to prioritize sequences to address specific pressured clinical questions while minimizing scanner utilization time.
A visual overview of relevant anatomy is provided to facilitate rapid reference, including cranial nerve courses, key anatomical landmarks, and critical adjacent structures.
Following the introductory sections, the presentation adopts a symptom-based approach to differential diagnosis. This organizational structure provides a comprehensive yet quick overview of indications for after-hours skull base MRI indications and related differential diagnoses. The goal is to guide an active search for radiologists in fast-paced environments.
Materials & Methods
Anatomy
- foramen contents with an example on MRI
- CN course and trajectory

Protocol: Each delineated with purpose and example
- Duration of the entire protocol, with roughly the duration of each sequence
- T1
- 2D spin echo
- 3D spoiled GRE
- T2 with fat suppression
- Heavily T2-weighted images
- What does the T2/T1 signal mean?
- DWI/ADC
- EPI

- HASTE/TSE technique and implication
- FLAIR
- Post contrast CISS
- Post contrast T1 fat sat
- 3D spoiled GRE
- 2D spin echo

Indications

- **Cranial neuropathy**
- Optic nerve
- Optic neuritis
- Optic nerve glioma
- Trigeminal nerve
- Schwannoma
- Perineural spread
- Facial nerve palsy
- Bells palsy
- Perineural spread
- Leptomeningeal spread of tumor
- Meningitis
- Vestibular neuritis and labyrinthitis
- Diplopia
- Normal study
- Trochlear nucleus ischemia - Brain stem stroke
- Ataxia/vertigo - Wallenberg syndrome
- Superficial siderosis
- Trigeminal neuralgia
- Postoperative appearance of neurovascular decompression
- Complications of rhizotomy
- Vidian nerve neuralgia / Vasomotor rhinitis
- Occipital nerve neuralgia
- Vocal cord paralysis
- **Bone lesions**
- Chordoma
- Chondrosarcoma
- **Sinus or orbit tumors**
- Esthesioneuroblastoma
- Rhabdomyosarcoma
- Langerhans cell histiocytosis
- Invasive fungal sinusitis
- Meningoencephalocele
- Nasopharyngeal carcinoma
- **Extra-axial lesions**
- Meningioma / Meningioma mimics: Sarcoma, lymphoma, GPA, IGG4, Erdheim-Chester, Tolosa-Hunt.
- Epidermoid cyst / Neurenteric cyst
- **Infectious/inflammatory**
- Osteomyelitis / Petrous apicitis

Results & Conclusion

After reading this presentation, the reader will be able to:

- Understand the application of skull base MRI in after-hours setting and will be able to tailor the protocol.
- Understand expected pathologies and differential diagnosis for each urgent or emergent indication for skull base MRI.
- Provide helpful information in the report for clinicians that can change acute management.

Images/Tables

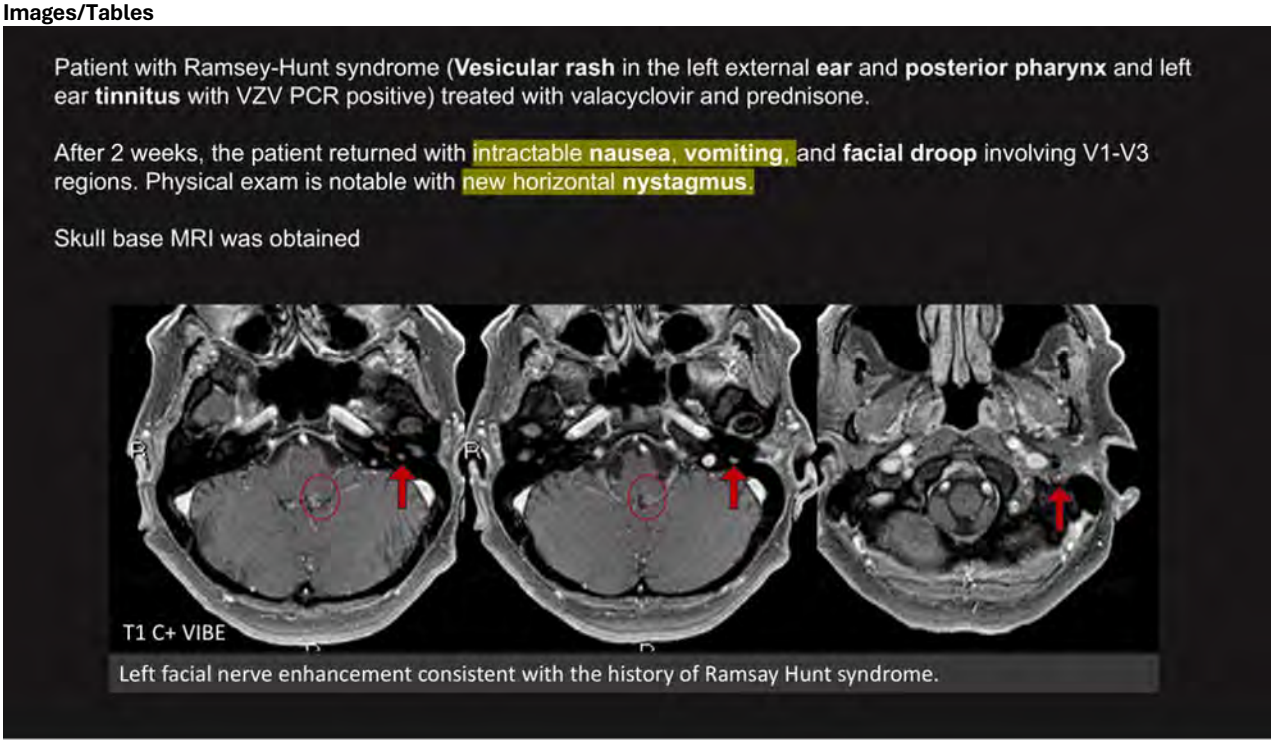

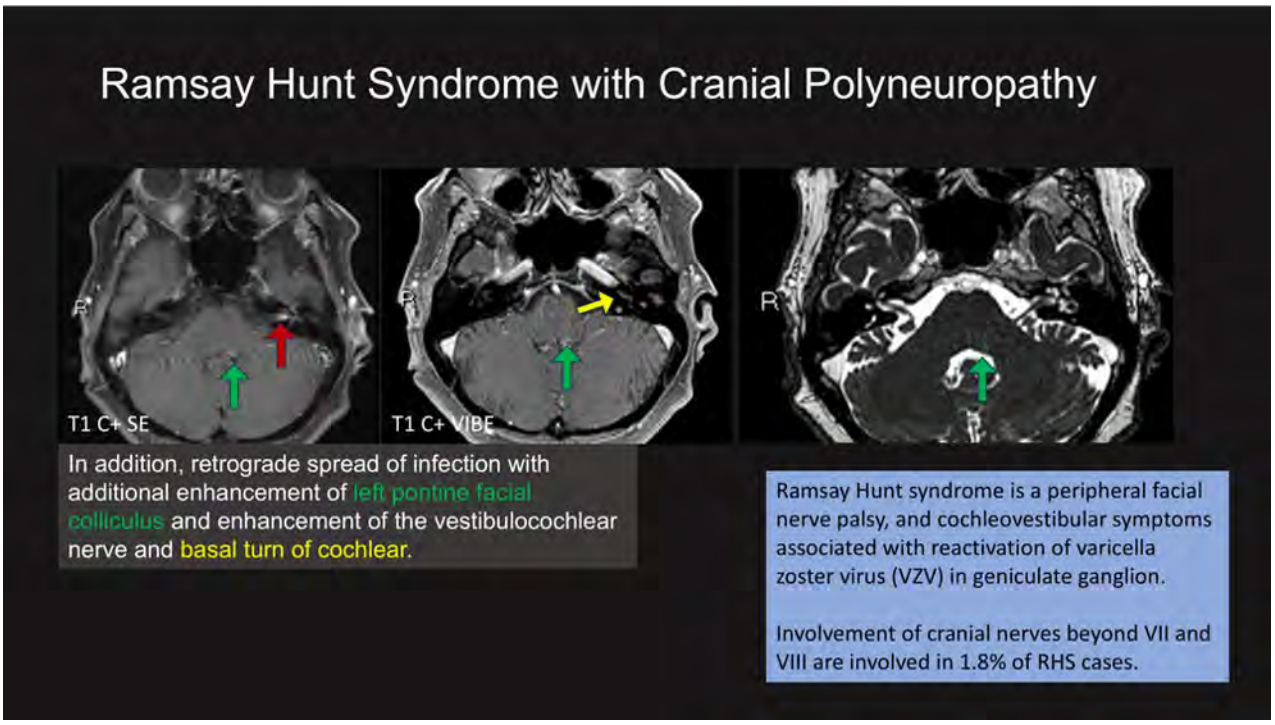

---

930 Central Nervous System Involvement in Multiple Myeloma: Recognition of the Variety of Imaging Patterns in the Current Setting of Multi-agent Treatment and Refractory Disease

Chimatu Sichona MD, Alper Sever MD, Hamza Hashmi MD, Alicia Meng MD, Michael T Starc MD
Memorial Sloan Kettering Cancer Center, New York, NY, USA

Summary & Objectives

Imaging review demonstrating the critical importance of recognizing the increasing variety of central nervous system (CNS) manifestations in multiple myeloma (MM).

Purpose

CNS extramedullary involvement in multiple myeloma is an indicator of advanced disease. Traditionally, leptomeningeal spread has been the predominant pattern described in the literature. In the current era of advanced multi-agent treatment regimens and prolonged survival in patients with refractory MM, neuroradiologists are encountering an increasing variety of patterns of CNS manifestations. These variant imaging patterns are often under-reported and may not be properly identified as disease progression, leading to potential misinterpretation as treatment-related changes, infection or other neoplastic processes.

Materials & Methods

A retrospective review of our institutional imaging database of the past 15 years identified over 50 cases of CNS MM with MRI evidence of involvement. These cases were correlated with input from MM clinicians and corroborated with treatment, pathologic data and outcomes. Patterns were categorized according to anatomic distribution and enhancement characteristics.

Results & Conclusion

Results

A wide variety of CNS myeloma imaging patterns were observed including diffuse leptomeningeal disease, small multifocal leptomeningeal nodules, subependymal disease, discrete parenchymal masses, ill-defined infiltrative parenchymal lesions and new hydrocephalus. Lesions were treated with a variety of regimens including systemic therapy, intrathecal chemotherapy and targeted radiation.

Discussion & Conclusion

CNS involvement in MM represents a diagnostic challenge due to its variable manifestations and overlap with inflammatory, infectious and other neoplastic etiologies. The existing radiology literature has focused on osseous manifestations of MM with lesser reported extramedullary leptomeningeal findings. Recognition of atypical imaging patterns including parenchymal involvement is increasingly important in the context of multi-refractory MM and novel therapeutic agents. Integration of imaging, CSF analysis, and clinical history remains essential for accurate diagnosis. Early detection by the neuroradiologist, even in unusual patterns, allows for timely adjustment of therapy, potentially improving outcomes even in this late disease stage.

Images/Tables

Imaging patterns of CNS MM on T1-weighted post contrast images:
A. Patchy ill-defined parenchymal subcortical enhancement within the right parietal lobe involving the post central gyrus.
B. Solitary well-circumscribed left thalamic mass with mass effect on the third ventricle.
C. Multiple supratentorial and infratentorial leptomeningeal nodules (arrows).
D. Diffuse leptomeningeal enhancement with hydrocephalus.

---

942 Spectrum of Imaging in IgG4 Related Disease (IgG4-RD) of The Head and Neck

Namita Bhagat MD[1], Mihran Ali Khdhir MD[1], Anisa Chowdhary MD[2], Ajay Malhotra MD[1]

[1]Yale New Haven Hospital, New Haven, CT, USA. [2]YNHH-Bridgeport Hospital, Bridgeport, CT, USA

Summary & Objectives

IgG4 disease is a multisystem fibrosclerosing inflammatory disorder. Head and neck is the second most commonly affected region and involves the orbit, salivary glands, thyroid, paranasal sinuses, cervical lymph nodes and primary CNS involvement. Diagnostic criteria for IgG4 disease includes Serum IgG4 concentration > 135 mg/dL and greater than 40% of IgG plasma cells being IgG4 and >10 cells/high-powered field of biopsy sample in any affected organ.

Purpose

This educational exhibit reviews the epidemiology, clinical features and imaging spectrum of IgG4 related disease of head and neck on CT and MRI emphasizing the role of imaging and various differential diagnosis that should be considered.

Materials & Methods

Key Imaging Findings

The salivary glands are most commonly involved in head and neck and have two main patterns of involvement: multigland involvement (Miculicz's disease) and isolated involvement of submandibular gland (Kuttner tumor), which can mimic neoplasm, Sjogren disease, sarcoidosis and lymphoma. Orbital involvement occurs in the form of lacrimal gland involvement, extraocular muscles, orbital fat, eyelid, and cranial nerves including the optic nerve and infraorbital nerve. On MRI, orbital IgG4-RD has hypointense signal on both T1W and T2W images, with marked contrast enhancement. IgG4 related ophthalmopathy should be differentiated from idiopathic orbital inflammation which is often painful and involves the entire musle belly and tendon whereas IgG4 disease spares the tendinous insertions. Compared with orbital lymphoma, IgG4-related orbital disease has a significantly higher apparent diffusion coefficient (ADC), with ADC greater than 1.2. With orbital involvement, reduced ADC value is a helpful differentiator from pleomorphic adenoma or idiopathic orbital inflammation, which show facilitated diffusion. Thyroid gland involvement has two patterns: Riedel's thyroiditis (RT), with extensive fibrosis of the thyroid gland and surrounding tissues and Hashimoto's thyroiditis with no extra-thyroid extension. Primary CNS involvement may affect the meninges, pituitary gland and less commonly the cranial nerves and brain parenchyma. Imaging in IgG4 related pachymeningitis is is nonspecific. Absence of intralesional calcifications within markedly T2-hypointense lesions favors IgG4-related hypertrophic pachymeningitis. Imaging features of IgG4-related hypophysitis are nonspecific and include an enlarged pituitary gland or thickened stalk with homogeneous enhancement mimicking sarcoidosis, LCH and lymphocytic hypophysitis. Parasinus sinus involvement can have two distinct patterns: diffuse mucosal disease and focally destructive mass-like lesion. Diffuse disease mimics chronic rhinosinusitis. Mass-like lesion involves the maxillary sinus and presents as a destructive lesion, with trans-spatial invasion and differentiation from invasive fungal sinusitis (IFS) is particularly crucial. Rarely, the disease can manifest as B/L paravertebral masses which are separate from the spine and often require histopathology for diagnosis.

Results & Conclusion

It is important to recognize and be familiar with imaging manifestations of IgG4 related disease as accurate imaging diagnosis minimizes additional testing. Once the condition is diagnosed at one site, whole-body imaging should be considered to identify other potential sites of disease. Although post treatment follow-up currently relies largely on clinical symptoms, with imaging to delineate disease bulk, the role of imaging in both pre-treatment prognostication and monitoring treatment response are currently being investigated.

Images/Tables

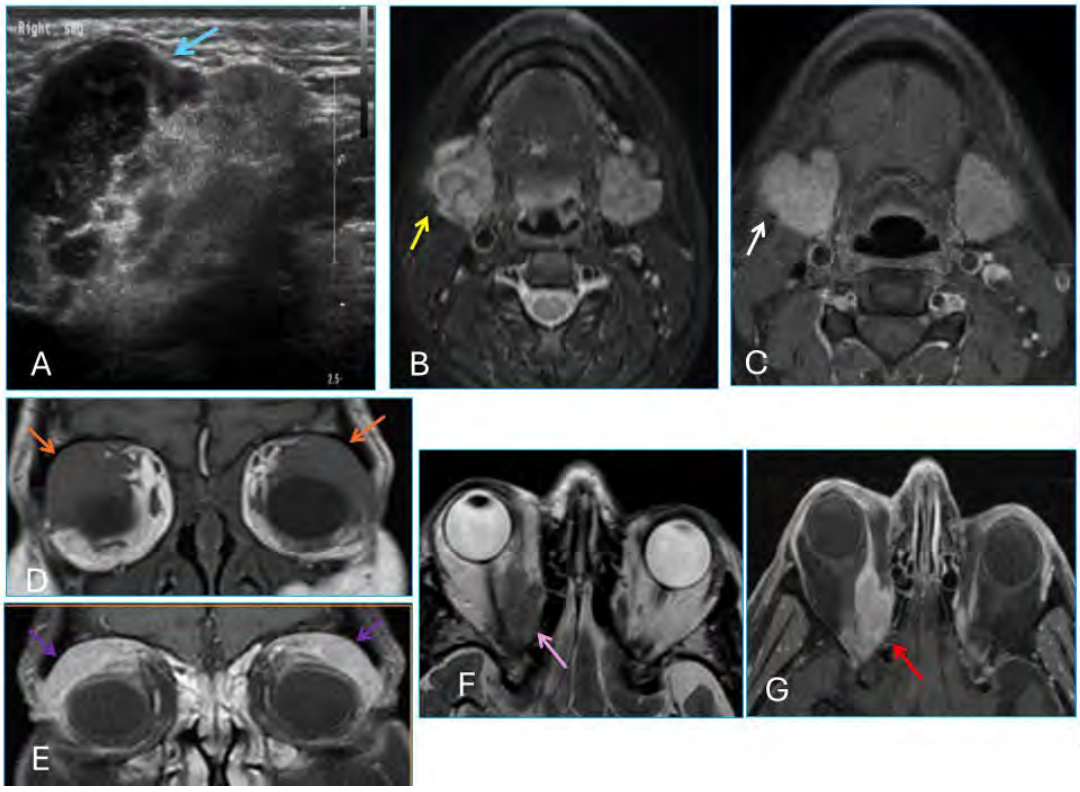

Figure A: US shows well defined geographical hypoechoic appearance of Kuttner tumor in right submandibular gland (blue arrow) with normal surrounding gland parenchyma. Figures B and C demonstrating well defined mixed intensity signal on STIR (yellow arrow) with homogenous contrast enhancement(white arrow). Figures D and E demonstrating symmetrically enlarged T2 hypointense B/L lacrimal glands(orange arrows) with homogenous post contrast enhancement (purple arrows). Figures F and G demonstrate enlargement and T2 hypointensity of right medial rectus muscle (pink arrow) with homogenous contrast enhancement (red arrow).

---

953 Beyond the Basics: Imaging the Full Spectrum of Idiopathic Intracranial Hypertension

Sam Thomas DO, Anthony La Nasa MD, Devin A DeLuna MD, Sean Kelly MD
University of Nebraska Medical Center, Omaha, NE, USA

Summary & Objectives

This electronic educational exhibit is designed to enhance neuroradiology education and training by providing a comprehensive, image-rich review of idiopathic intracranial hypertension (IIH) on MRI, MR venography, and CT. While radiologists are familiar with hallmark findings such as a partially empty sella and optic nerve sheath distension, this exhibit expands the diagnostic perspective by emphasizing less well-known imaging signs and complications. Viewers will learn to recognize both classic and subtle features, understand their diagnostic implications, and identify potential complications and treatment considerations. After reviewing the exhibit, participants will be confident in suggesting IIH by imaging and evaluating associated sequelae.

Purpose

The purpose of this exhibit is to:

1. Review the complete MRI spectrum of IIH, including conventional and emerging signs.

2. Highlight imaging-documented complications of IIH that may be underrecognized in clinical practice.
3. Correlate imaging findings with clinical management, including medical therapy and surgical interventions such as venous sinus stenting.

Materials & Methods

The exhibit incorporates anonymized institutional cases utilizing MRI and CT. The presentation is structured in four sections:

1. Clinical Overview: Brief discussion of IIH epidemiology, pathophysiology, and clinical presentation with emphasis on radiologic correlation.
2. Classic Imaging Findings: Illustration of the well-known MRI features—partially empty sella, optic nerve sheath ectasia and tortuosity, and posterior globe flattening with papilledema.
3. Advanced Imaging Features: Review of less widely recognized findings, including lateral transverse sinus stenosis, Meckel's cave ectasia, calvarial and skull-base thinning with arachnoid pits, and oculomotor cistern prominence.
4. Complications and Treatment: Highlight examples of complications related to IIH from our institution, including meningoencephaloceles, spontaneous CSF leaks, and cranial neuropathies, as well as pre- and post-treatment examples from patients undergoing CSF shunting or venous sinus stenting.

Results & Conclusion

This educational exhibit synthesizes the full neuroradiologic spectrum of IIH, emphasizing both common and advanced MRI findings and their clinical implications. By engaging with a structured, case-based format, viewers will:

- Recognize the comprehensive range of imaging findings that support a diagnosis of IIH.
- Understand the radiologist's diagnostic value of suggesting IIH by recognizing relatively specific imaging patterns.
- Understand complications that may ultimately alter management, including CSF leaks, cranial neuropathies, and meningoencephaloceles.
- Appreciate the role of imaging in guiding therapy, monitoring response, and detecting post-treatment complications, particularly after venous sinus stenting.

In conclusion, this exhibit provides neuroradiologists and trainees with a concise yet advanced review of IIH imaging. By integrating updated imaging markers and complication assessment, radiologists will be better equipped to recognize IIH, communicate findings effectively, and contribute to multidisciplinary patient care.

Images/Tables

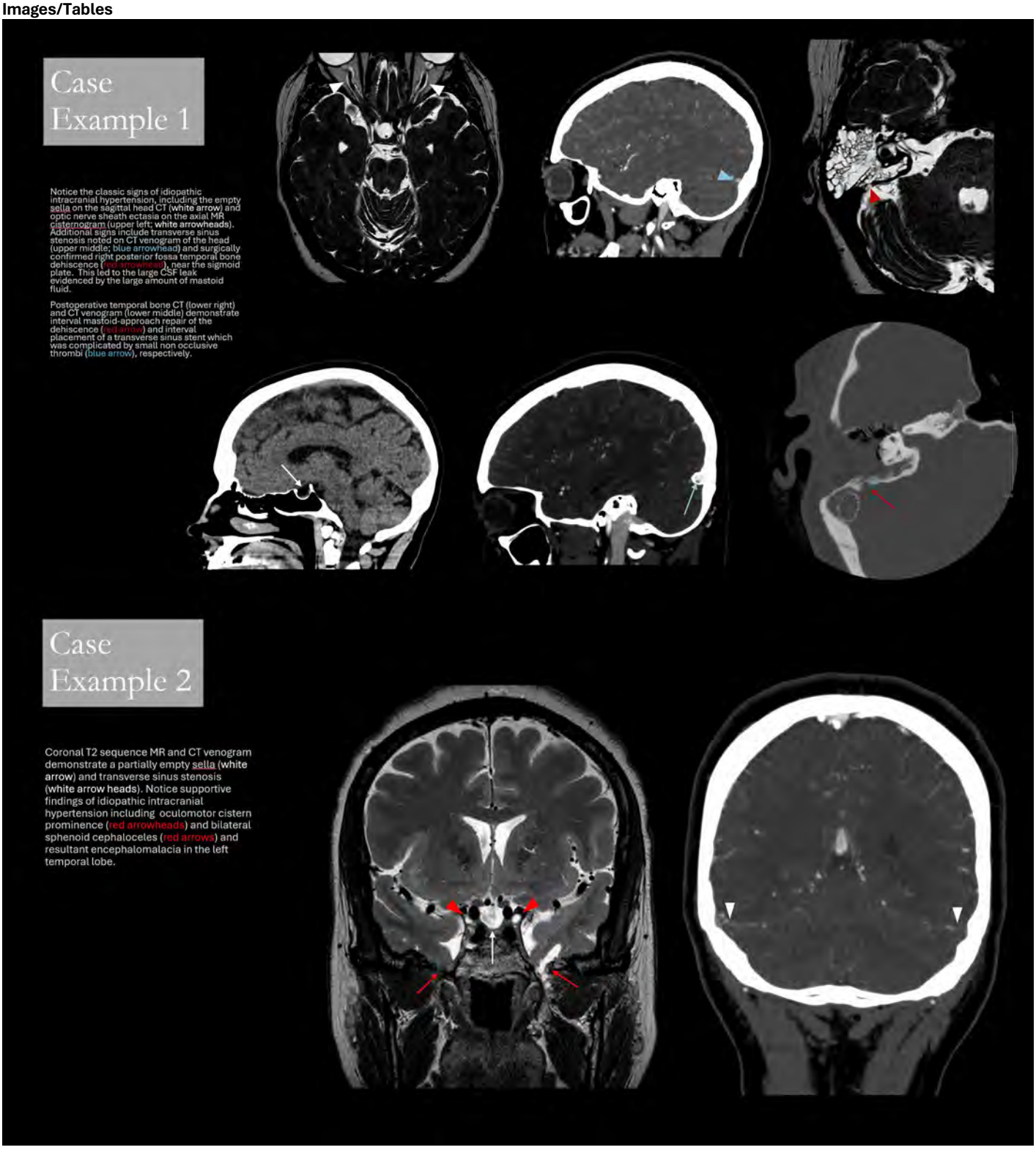

1023 Spotting Musculoskeletal Pathology on Routine Head and Neck Studies: A Case-Based Approach

Grace Wang MD, Amanda Balon MD, Kevin Pham MD, Mickael Tordjman MD, Mark Finkelstein MD, Brian Rigney MD, Amish Doshi MD, Mingqian Huang MD

Mount Sinai Hospital, New York, NY, USA

Summary & Objectives

Routine head and neck imaging frequently captures musculoskeletal structures that may contain clinically significant pathology. These findings, while sometimes incidental, may explain a patient's symptoms or alter management.

This educational exhibit aims to increase radiologist awareness of musculoskeletal abnormalities visible on standard head and neck studies. Through a case-based approach, we illustrate the wide spectrum of pathology that may be encountered within this field of view.

Purpose

The purpose of this exhibit is to highlight how musculoskeletal structures included on routine head and neck computed tomography (CT) and magnetic resonance imaging (MRI) can reveal clinically relevant pathology. Many of these entities—ranging from chronic degenerative to neoplastic or congenital—lie outside the primary area of clinical concern and are often overlooked.

The goal of this exhibit is to help radiologists not only detect but also contextualize these findings, guiding appropriate further evaluation or referral.

Materials & Methods

Representative cases were pulled from routine head and neck CT and MRI examinations that exemplify the diversity of musculoskeletal pathology encountered on head and neck imaging. Each case was correlated with available clinical data and, when applicable, confirmed by surgical or pathologic findings. Imaging modalities included CT and MRI.

Cases were categorized into six groups: (1) mechanical processes, such as chronic rotator cuff tear with acromioclavicular joint cyst formation and basilar invagination from rheumatoid ligamentous laxity; (2) infectious pathology, exemplified by spondylodiscitis with vertebral endplate destruction; (3) inflammatory processes, including rheumatoid pannus with atlantoaxial instability and calcium pyrophosphate deposition in crowned dens syndrome; (4) ischemic myopathies, such as myonecrosis of the sternocleidomastoid; (5) tumoral cases, featuring deep fibrous histiocytoma of the rhomboid muscle and chondrosarcoma of the thyroid cartilage; and (6) congenital and idiopathic myopathies, such as chronic nonbacterial osteomyelitis and congenital hypoplasia of the sternocleidomastoid.

Results & Conclusion

Computed tomography is useful for evaluating osseous erosions, calcifications, joint widening, and cystic tracking, while magnetic resonance imaging is critical for characterizing soft tissue masses, ligamentous pannus, marrow edema, and inflammatory changes.

Head and neck imaging offers an underrecognized opportunity to detect significant musculoskeletal pathology. Awareness of characteristic appearances, relevant anatomy, and clinical correlations enables radiologists to identify these abnormalities, avoid misdiagnosis, and facilitate timely multidisciplinary management.

Images/Tables

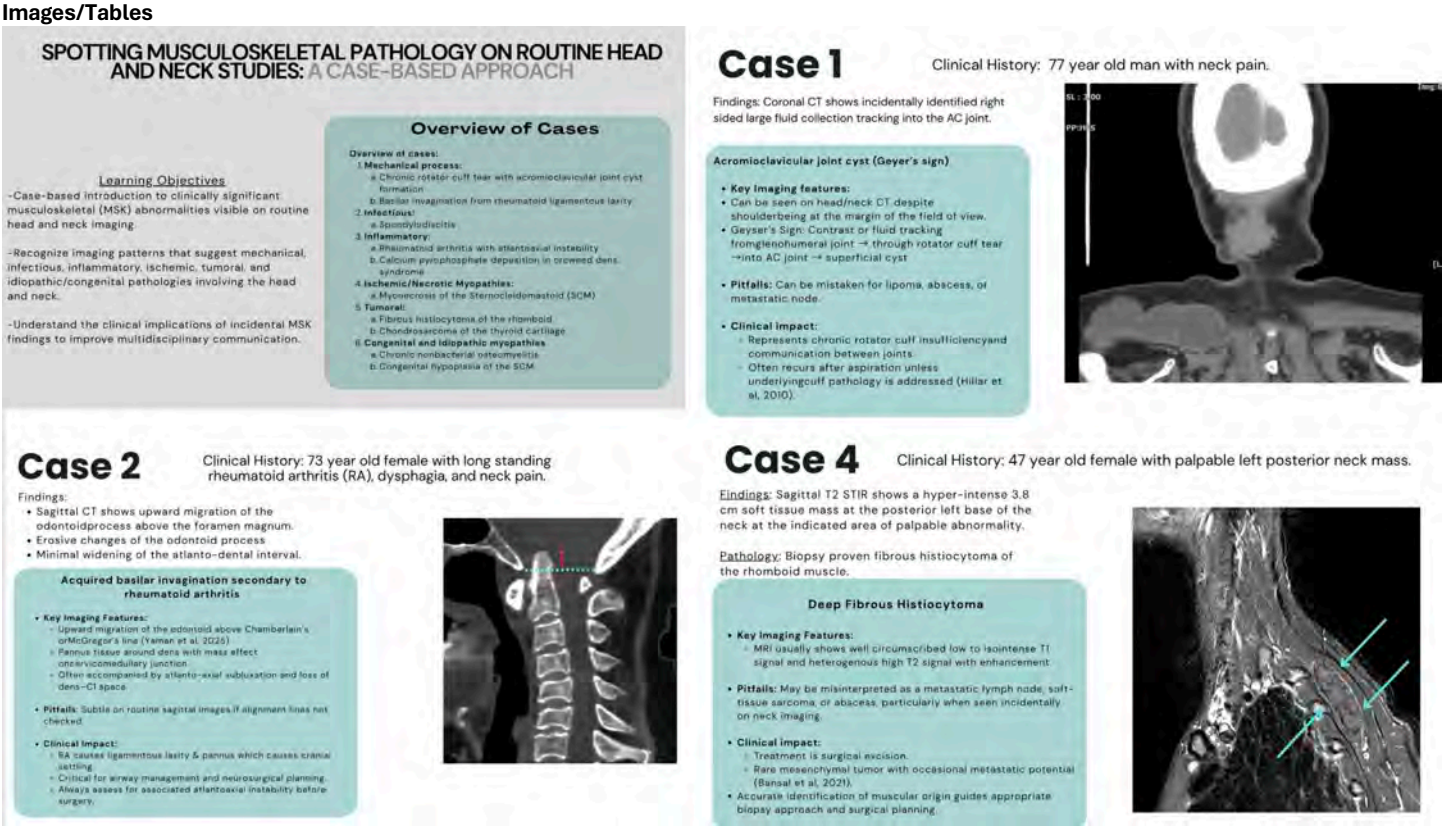

1026 Neurolymphomatosis Imaging: Unveiling the Invisible—A Case-Based Review

Mona Gad, Greg Pommier, Rebecca Choi, Sasicha Manupipatpong, Jacob Schick, Francis Deng, Majid Khan
Department of Radiology and Radiological Science, Johns Hopkins University School of Medicine, Baltimore, MD, USA

Summary & Objectives

Neurolymphomatosis (NL) is a rare but serious manifestation of lymphoma, characterized by infiltration of cranial and/or peripheral nerves by malignant lymphocytes. Clinical presentation is highly variable and may mimic neuropathies or cranial nerve palsies, making diagnosis particularly challenging, especially when NL is the initial manifestation of lymphoma.

Objectives:

1. Understand the definition of neurolymphomatosis, associated pathological subtypes, mechanisms, and subsites of neural involvement.
2. Identify the relevant clinical presentation that may favor neurolymphomatosis over other causes of neuropathy.
3. Appreciate the role of imaging modalities in early recognition of neurolymphomatosis.
4. Describe the imaging differential considerations that can mimic neurolymphomatosis.
5. Recognize the limitations of nerve biopsy and current challenges in diagnosis and treatment.

Purpose

The primary goal of this exhibit is to provide a comprehensive overview of neurolymphomatosis with emphasis on the utility of neuroimaging modalities, particularly MRI and ^{18}F FDG-PET/CT in early diagnosis and guiding therapeutic management in the appropriate clinical context.

Materials & Methods

Illustrative cases of neurolymphomatosis, along with relevant clinical scenarios and imaging differential diagnosis, will be displayed in this exhibit.

1. Definition and epidemiology of NL.
2. Association with non-Hodgkin lymphoma and pathological subtypes implicated in NL.
3. Pathophysiology and disease spectrum, which includes: a. Mechanisms of lymphomatous nerve infiltration. b. Central vs. peripheral nervous system involvement.
4. Variable clinical presentation depending on the involved nerve or neural plexus.
5. Key diagnostic imaging features of NL on MRI and ^{18}F FDG-PET/CT and discrimination from potential radiologic mimics.
6. Diagnostic challenges related to non-neoplastic neuropathy in lymphoma patients, including treatment-related neuropathy (following chemotherapy or radiation), autoimmune or paraneoplastic processes, and compressive neuropathy.
7. Importance of nerve biopsy and its limitations.
8. Management strategies.
9. Clinical implications and future directions, including: a. Importance of early recognition. b. Ongoing research into targeted therapies and biomarkers.

Results & Conclusion

Results: N/A

Conclusion:

Neurolymphomatosis is a rare presentation of lymphoma that represents a diagnostic challenge in clinical practice due to overlapping clinical and imaging features with other causes of neuropathy. Although nerve biopsy is the gold standard for definitive diagnosis, it has significant risks of permanent nerve damage. MRI and ^{18}F FDG-PET/CT are promising imaging alternatives that allow reaching early and precise diagnosis and guiding treatment in the proper clinical setting.

Images/Tables

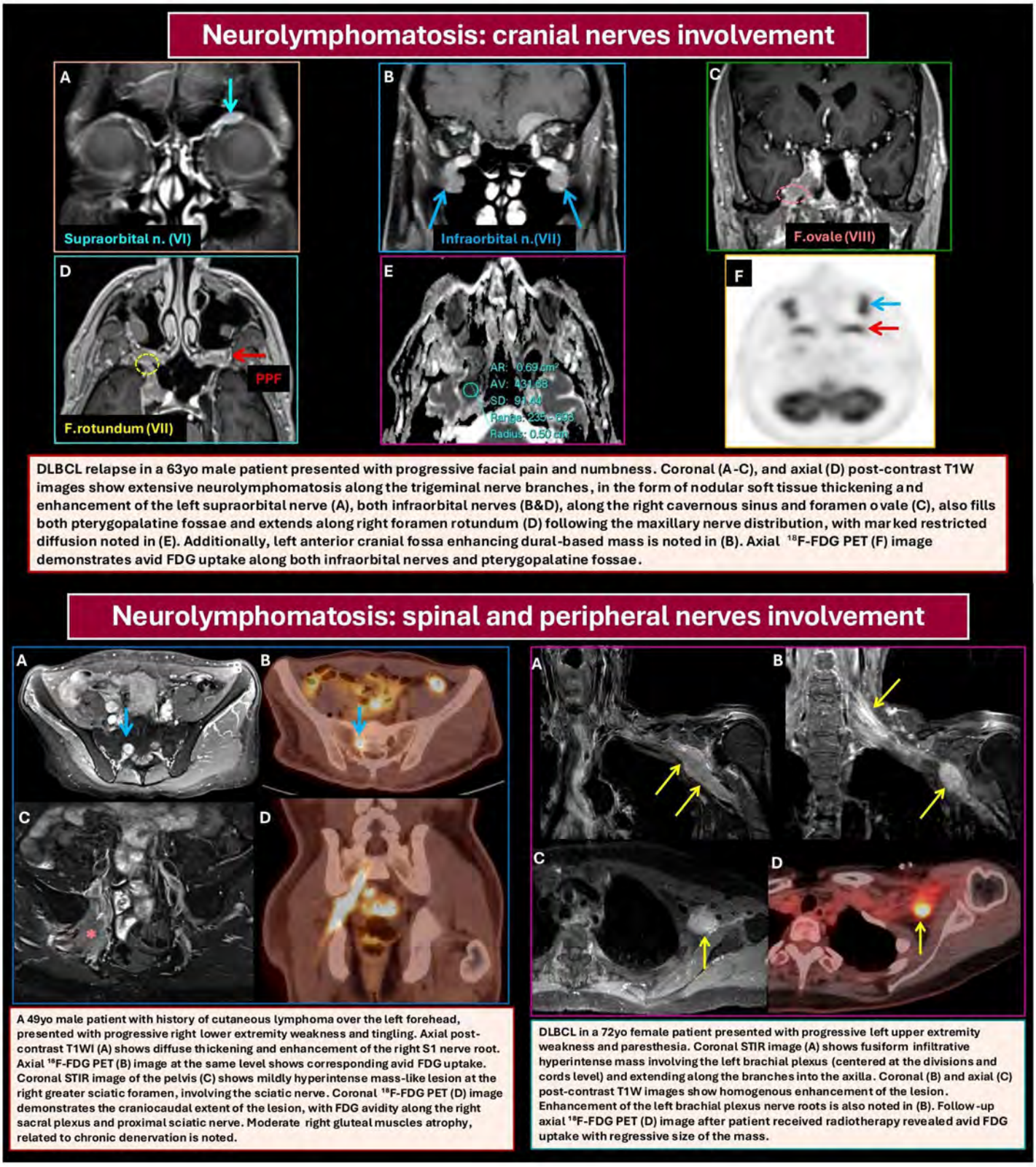

1034 ***From Virtual Dissection to Network Topology*: A Clinician's Guide to Tractography and Graph-Based Connectomics.**

Arturo Maximiliano Rodriguez Saldivar MD, Mariana A Mercado Flores MD, Bryann A Cortés Rodriguez, Haziel Maya Garcia MD, Andres Felipe Rios Victoria

Centro Universitario de Imagen Diagnostica, Monterrey, Nuevo León., Mexico

Summary & Objectives

Diffusion MRI (dMRI) provides a non-invasive window into the brain's white matter architecture. This capability has evolved into two distinct analytical paradigms:

- Fiber tractography, focused on visualizing specific anatomical pathways.
- Graph-based connectomics, which models the brain's global network organization. However, the terms are often used interchangeably, and the quantitative outputs of tractography are frequently misinterpreted as robust measures of "connection strength".

The objective of this review is to clarify the fundamental differences between these two approaches and to delineate their distinct clinical utilities and limitations.

Purpose

1. Contrast the principles of qualitative fiber tractography (i.e., "virtual dissection") with quantitative graph-based connectomics (i.e., "network topology").
2. Identify the specific clinical questions and scenarios best suited for each methodology.
3. Highlight the significant limitations and interpretative pitfalls, particularly regarding tractography-derived quantification, to guide appropriate clinical and research use.

Materials & Methods

Fiber Tractography: This is the process of reconstructing white matter pathways. Based on dMRI's ability to measure the anisotropic diffusion of water molecules , algorithms (either deterministic or probabilistic) integrate local fiber orientations to generate "streamlines". This method models the trajectory of fiber bundles. The resulting visualizations are used for "virtual dissection" to isolate specific tracts (e.g., corticospinal tract, arcuate fasciculus) or for "tractometry," which measures diffusion metrics (like FA or MD) along the path of a tract.

Graph-Based Connectomics: This is a network analysis that uses tractography data as its input. In this framework, the brain is parcellated into a set of "nodes" (representing gray matter regions, often defined by an atlas like AAL). Fiber tractography is then used to map the "edges" (the structural connections) between these nodes. Graph theory is subsequently applied to this network to compute topological properties, such as global and local efficiency, modularity, clustering coefficient, and "hubs". Statistical methods, like the Network-Based Statistic (NBS), can then identify differences in network topology between groups.

Results & Conclusion

- **Clinical Use of Tractography:** The primary strength of tractography is the qualitative visualization of anatomical relationships. It is invaluable for neurosurgical planning, allowing surgeons to see the displacement, infiltration, or proximity of critical pathways (e.g., corticospinal tract, optic radiation) relative to lesions like tumors or cortical tubers.
- **Clinical Use of Graph-Based Connectomics:** This method is not used to visualize individual tracts but to quantify system-level network organization. Its clinical application is primarily in neuroscience research to identify biomarkers for complex neurological and psychiatric disorders. For example, it can detect widespread disruptions in brain network topology, such as identifying altered "subnetworks" in conditions like schizophrenia or Internet Gaming Disorder

Fiber tractography and graph-based connectomics answer different clinical questions. Tractography is the tool of choice for visualizing specific fiber tracts for surgical planning. Graph-based connectomics is the method for quantifying global network organization to understand systemic brain disorders. A critical caveat is that using simple streamline counts from tractography as a quantitative measure of "connection strength" for connectomics is highly unreliable, biased, and prone to a high rate of false positives. Clinicians must select the method based on the question: visualization (tractography) vs. network quantification (graph analysis).

Images/Tables

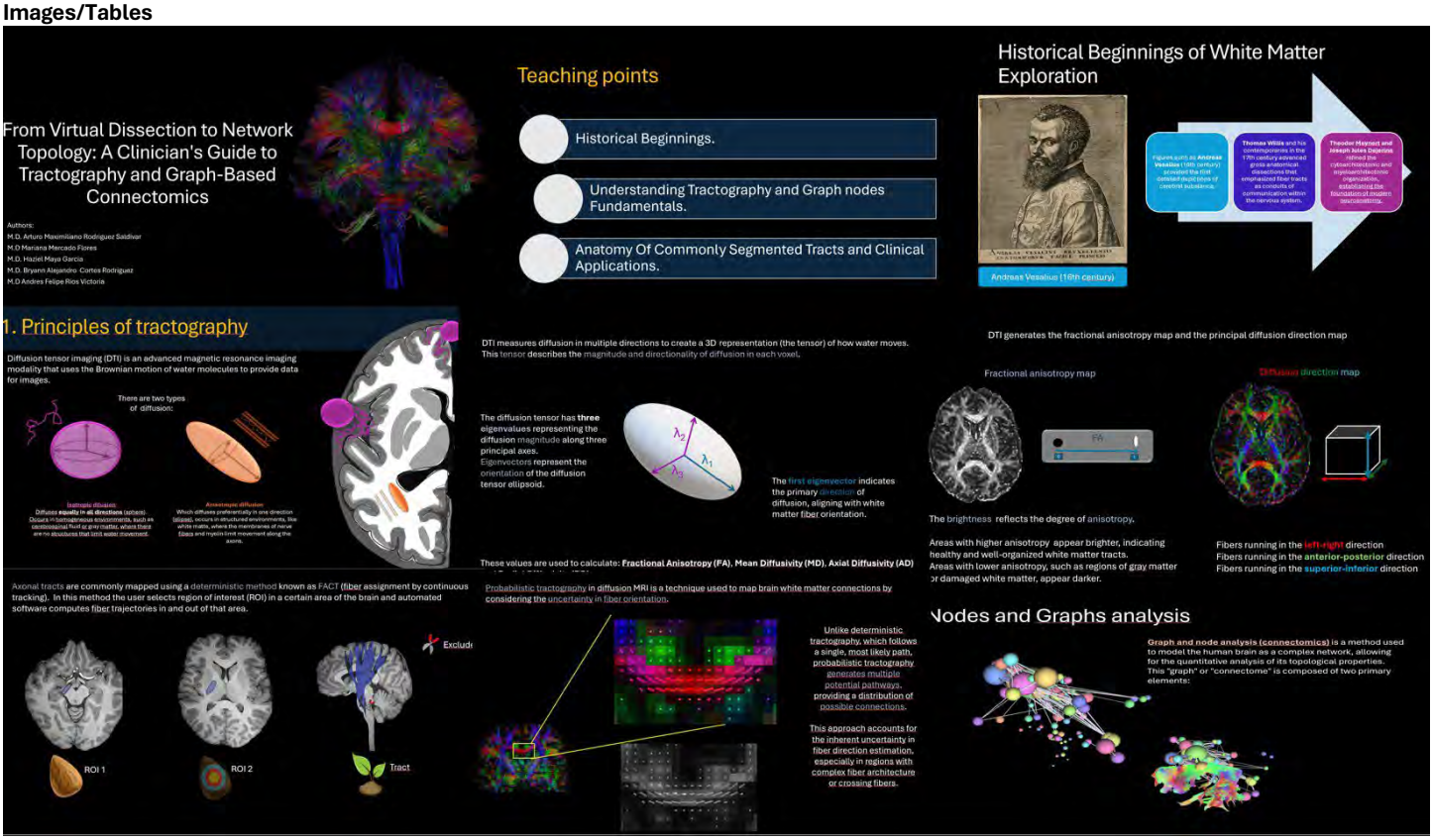

1113 Complications of Kyphoplasty: A Pictorial Overview

Aditya Duhan MD[1], Fahad Farooq MD[2], Swastika Lamture MD[1]
[1]University of Colorado, Aurora, CO, USA. [2]SUNY Upstate Medical University, Syracuse, NY, USA

Summary & Objectives

Kyphoplasty represents an established minimal-invasive method for correction and augmentation of osteoporotic vertebral fractureThe primary objective was to determine the incidence and patterns of perioperative complications to assess the safety of percutaneous kyphoplasty for osteoporotic VCF[1]

Purpose

The purpose of this study was to provide reliable retrospective data on the perioperative and postoperative complications associated with kyphoplasty. Kyphoplasty is well established, minimally-invasive technique for vertebral compression fracture correction and augmentation, but comprehensive data on its associated risks, particularly severe complications, has been lacking in the literature.[1,2] Understanding the true complication profile is crucial for establishing appropriate procedural guidelines and ensuring patient safety.

Materials & Methods

This retrospective study studying clinical and imaging data from 102 consecutive patients (72 women, 30 men; mean age, 69 years) who underwent percutaneous balloon kyphoplasty for osteoporotic vertebral compression fractures between January 2024 and December 2025. A total of 135 vertebral fractures classified as AO Type A1 or A3 were treated.

The indications for kyphoplasty included symptomatic vertebral compression fractures associated with significant pain refractory to conservative management for at least twelve weeks and/or progressive kyphotic deformity on serial imaging. All procedures were performed using percutaneous balloon kyphoplasty with polymethylmethacrylate (PMMA) cement under fluoroscopic guidance. In five cases with A3.1-type fractures, additional internal fixation was performed by spine surgeon later.

Clinical and radiological data were retrospectively collected from the institutional PACS and electronic medical record (Epic) systems. Pain intensity was assessed using the Visual Analogue Scale (VAS). Complications, including cement leakage, new or adjacent-level vertebral fractures, and postoperative sintering, were recorded based on follow-up imaging and clinical documentation.

Results & Conclusion

Mean preoperative pain (VAS 7.6 ± 1.4) was improved significantly to VAS 2.1 ± 1.8 on postoperative Day 1 and to VAS 1.3 ± 1.0 at 6-month follow-up. The overall complication rate was 16.7% (17 patients).

Early Complications:

Cement leakage was detected in 7 patients (6.9%). Most cases were asymptomatic; however, leakage into the neural foramina occurred in 2 patients, with transient radicular pain due to contact with exiting nerve roots which was managed conservatively. Pulmonary or mediastinal cement embolism was identified in 2 patients on postoperative CT scans—both were asymptomatic and treated conservatively with observation and anticoagulation. One patient (1.0%) developed infected spondylitis with epidural abscess and incomplete paraplegia, requiring urgent posterior decompression and anterior corpectomy with 360° fusion. One patient (1.0%) experienced a superficial wound infection, and another (1.0%) required evacuation of a subcutaneous hematoma/pus.

Late Complications:

New adjacent vertebral fractures occurred in 7 patients (6.8%), and progressive reduction in height and secondary canal compromise was observed in 2 patients (2.0%). One patient with pre-existing interstitial lung disease developed postoperative respiratory decompensation, likely exacerbated by procedure-related cement embolism.

Conclusion:

Percutaneous kyphoplasty provides substantial and sustained pain relief in osteoporotic vertebral compression fractures. Nonetheless, potentially serious complications—including cement leakage, pulmonary or mediastinal embolism, and infection—can occur. The procedure should therefore be reserved for experienced intervention neuroradiologist and performed in facilities equipped for prompt recognition and management of acute cardiopulmonary or neurological events.

Images/Tables

Under fluoroscopic guidance methylmethacrylate was injected into the vertebral body cavity through both guide cannulas. A small amount of **cement leakage** is noted

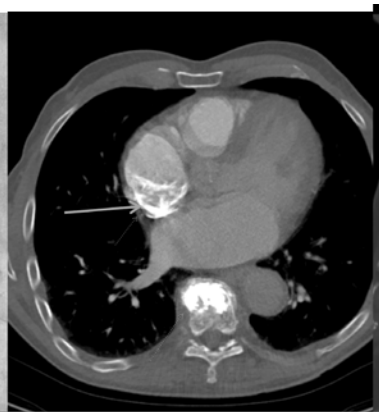

High attenuation foreign material within the right atrium suggestive of cement embolus

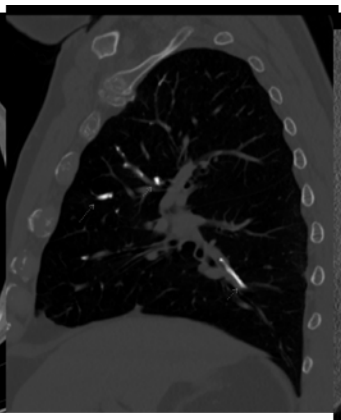

Multiple linear high attenuation foreign material in the segmental branches of the right lung suggestive of pulmonary cement emboli.

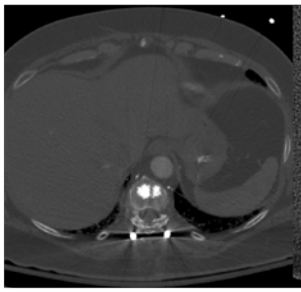

Hyperattenuating content in the paravertebral veins suggestive of cement extravasation

Epidural hyperattenuating cement suggestive of intravasation

Cement leaked out between the cement delivery device and out access cannula. A tube-shaped spike of cement in the pedicle and posterior soft tissue. The cement actually looks almost exactly like the access cannula.

Gas around the cement with non-fusion

---

133 An Introduction to Amyloid-PET Centiloid Values

Houman Sotoudeh MD
UTSouthwestern Medical Center, Dallas, TX, USA

Summary & Objectives

The quantification of β-amyloid plaque burden in the brain is central to Alzheimer's disease (AD) diagnosis and research. However, variability across amyloid PET tracers, acquisition protocols, and image processing pipelines has limited inter-study comparability. The **Centiloid scale**, introduced in 2015, standardizes amyloid PET quantitative data onto a **0–100 continuum**, anchored to young cognitively normal controls (0 Centiloid) and typical AD patients (100 Centiloid), enabling reliable cross-study and cross-tracer comparisons.

Purpose

To provide a practical and educational overview of the Centiloid scale used in amyloid-PET imaging, emphasizing its role in standardizing quantitative measures of amyloid burden across different radiotracers and imaging protocols.

Materials & Methods

This educational exhibit reviews the development, implementation, and interpretation of Centiloid values. Frequently asked questions (FAQs) are addressed, including:

- What Centiloids represent and how they are calculated
- Interpretation of sub-zero and supra-100 values
- Commonly used conversion formulas (e.g., for ^{18}F-florbetapir SUVr)
- Variability and limitations of Centiloid transformations
- Thresholds for amyloid positivity based on visual reads, pathology, and fluid biomarkers (e.g., 24–30 CL for intermediate neuritic plaques)

Additionally, the use of Centiloid values in **clinical trials** is summarized, including their role in **participant selection**, **treatment monitoring**, and **comparison of amyloid clearance across therapies** (e.g., donanemab, aducanumab, lecanemab). Published Centiloid thresholds used in regulatory trials (ranging from ~20 to 50 CL) are highlighted.

Results & Conclusion

Centiloid scaling has emerged as a robust, validated method for standardizing amyloid PET quantitation, improving cross-study consistency and enhancing the interpretability of amyloid burden. As amyloid-targeted therapies enter routine clinical practice, understanding and correctly applying

Centiloid values will be crucial for radiologists and clinicians alike. This exhibit aims to demystify Centiloids and promote their informed use in both research and clinical imaging.

Images/Tables

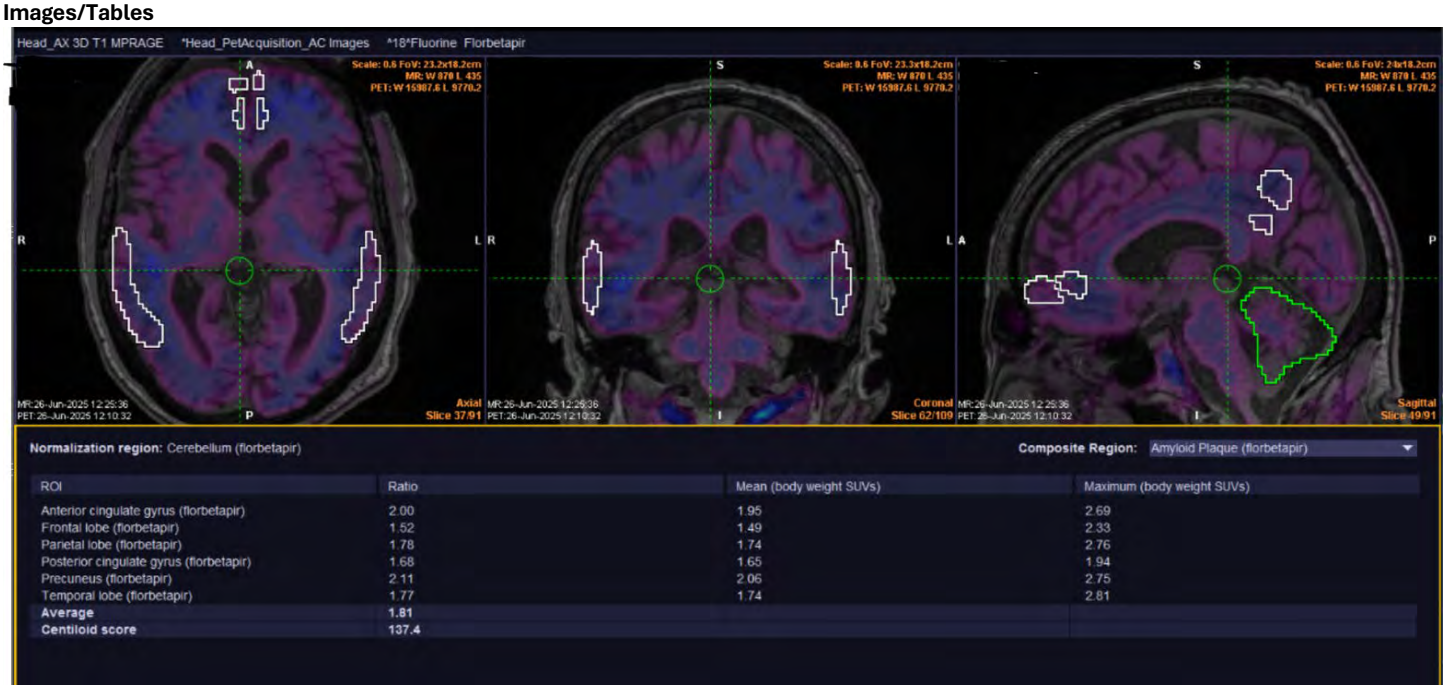

Normalization region: Cerebellum (florbetapir) **Composite Region:** Amyloid Plaque (florbetapir)

ROI	Ratio	Mean (body weight SUVs)	Maximum (body weight SUVs)
Anterior cingulate gyrus (florbetapir)	2.00	1.95	2.69
Frontal lobe (florbetapir)	1.52	1.49	2.33
Parietal lobe (florbetapir)	1.78	1.74	2.76
Posterior cingulate gyrus (florbetapir)	1.68	1.65	1.94
Precuneus (florbetapir)	2.11	2.06	2.75
Temporal lobe (florbetapir)	1.77	1.74	2.81
Average	**1.81**		
Centiloid score	**137.4**		

---

200 Advanced Diffusion MRI and Synthetic MRI for Brain-Tumor Imaging: Practical Metrics and Clinical Impact

Masaaki Hori MD, PhD
Toho University, Ota, Tokyo, Japan

Summary & Objectives

To familiarize trainees and practicing neuroradiologists with advanced diffusion MRI (e.g., diffusional kurtosis imaging with anisotropic and isotropic components) and quantitative synthetic MRI, and to demonstrate how these techniques complement conventional MRI by providing microstructural insight and standardized contrast for brain-tumor assessment.

Purpose

This exhibit equips learners with the essential physics, acquisition choices, and interpretation strategies needed to incorporate advanced diffusion and synthetic MRI into routine neuro-oncologic workflows. By linking quantitative metrics to tissue substrates, attendees will improve diagnostic confidence in staging, treatment-response assessment, and differentiation of progression from treatment-related effects.

Materials & Methods

- Concise review of principles and practical protocols: non-Gaussian diffusion; metrics including mean kurtosis (MK), anisotropic kurtosis (AK), isotropic kurtosis (IK); synthetic MRI–derived T1/T2/PD and synthetic contrasts (e.g., synthetic FLAIR).
- Case-based teaching set covering glioblastoma, metastases, neurinoma, and meningioma with side-by-side conventional MRI, DKI maps, and synthetic contrasts.
- Interpretation framework tying metrics to microstructure (cellularity, alignment, edema necrosis, and infiltrative margins) with suggested reporting phrases and thresholds.

Results & Conclusion

Across representative cases, DKI metrics and synthetic-MRI maps provide complementary information to apparent diffusion coefficient and conventional MR sequences.

Images/Tables

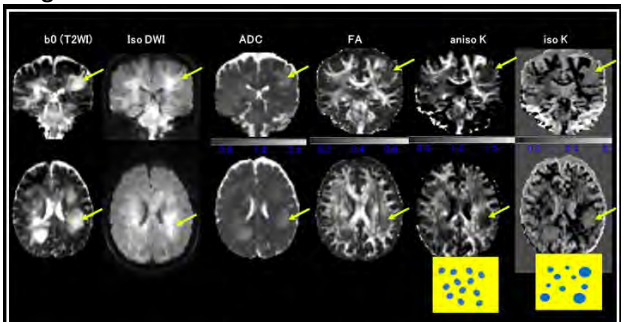

Figure 1. Glioblastoma (IDH wild-type). Mass lesions in the bilateral cerebral white matter appear hyperintense on T2-weighted imaging and diffusion-weighted imaging, with elevated apparent diffusion coefficient values and only mild reduction in fractional anisotropy. Advenced diffusion kurtosis analysis within the tumor demonstrates low anisotropic kurtosis and high isotropic kurtosis, suggesting that the tumor cells are more round than spindle-shaped and that the sizes of individual tumor cells are relatively heterogeneous.

Figure 2. Glioblastoma. Fluid-attenuated inversion-recovery (FLAIR) images synthesized with different inversion times (TI) on synthetic MRI show marked variations in the extent of hyperintense abnormalities. This variability must be recognized when evaluating post-surgical or post-radiation changes.

---

205 **The Post-Treatment Brain – A Comprehensive Guide for Accurate Clinicoradiographic Interpretation in Patients with Glioblastoma**

Daniel P Gewolb MD[1], Joseph Gewolb[2], David Mata MD[1], Ayushi Gupta[3], Umesh Patel MD[1], Ahmet Ilica MD[1], Akarshan Monga MD[1], Michael Hoch MD[4]
[1]University of Miami, Miami, FL, USA. [2]NYCOM, Old Westbury, NY, USA. [3]Miami, FL, USA. [4]Thomas Jefferson University, Philadelphia, PA, USA

Summary & Objectives

There is substantial overlap between treatment-related changes and tumor progression in the post-treatment brain. Only through knowledge of the treatment timeline, effects of specific treatments, tumor and patient factors, pitfalls and specific imaging findings can we provide accurate reports for the patients and clinicians.

- To improve report accuracy in the post-treatment brain
- To learn reporting tips in difficult cases
- To learn the standard treatment pathway including Stupp protocol
- To learn patient and tumor factors which effect survival
- To learn imaging features associated with treatment-change or tumor progression
- To recognize pitfalls to interpretation
- To understand how our reports effect the patient

Purpose

To familiarize radiologists with the standard treatment timeline, tumor and patient factors, imaging findings and pitfalls which are essential to improve interpretive accuracy in post-treatment brain imaging.

Materials & Methods

A thorough review of the literature was performed to understand the treatment timeline and to identify key clinical and imaging features that affect interpretation. The treatment timeline for glioblastoma is typically maximal safe resection followed by concurrent chemoradiation beginning 2-4 weeks following resection and lasting for 6 weeks. After which, the patients are usually started on adjuvant temozolomide for the next 6 months. Imaging is typically performed 24-72 hours following resection, 2-4 weeks following chemoradiation and about every 2 months thereafter. Knowledge of where the patient is along this timeline dramatically affects image interpretation. For instance, true progression in the first 3 months after radiation

can only be determined by imaging if the findings are outside the radiation field as proposed by RANO. Additionally, 85% of radiation necrosis occurs in the first 2 years and new/worsening abnormalities 3 years after the completion of radiation are very unlikely to be due to pure radiation necrosis. Knowledge of patient and tumor factors are also critical. For instance, patients with pseudoprogression are less likely to be symptomatic, and tumors have higher rates of oligo lineage and MGMT methylation in comparison to patients/tumors with true progression. Additionally, clinicians may be more reluctant to change management in a patient that is clinically doing well. Thus, clinical status is important for radiologists to be aware of as it may be best to let the tumor declare itself rather than risk prematurely taking a patient off a clinical trial which may be helping them.
Regarding imaging, there are many features that have an association with either treatment change or tumor progression. Some of which are more specific than others, such as small areas of periventricular enhancement in the radiation field are often treatment related while interval loss of FLAIR suppression in a resection cavity is an early and specific finding for tumor progression. These imaging tips and some pitfalls will be summarized and categorized along the timeline (immediate post operative, initial following chemoradiation, or during surveillance).

Results & Conclusion

The post-treatment brain is one of the most challenging studies to interpret but is of incredible importance. Only through collective knowledge of clinical, tumor and imaging features can radiologists improve the accuracy of their reports.

Images/Tables

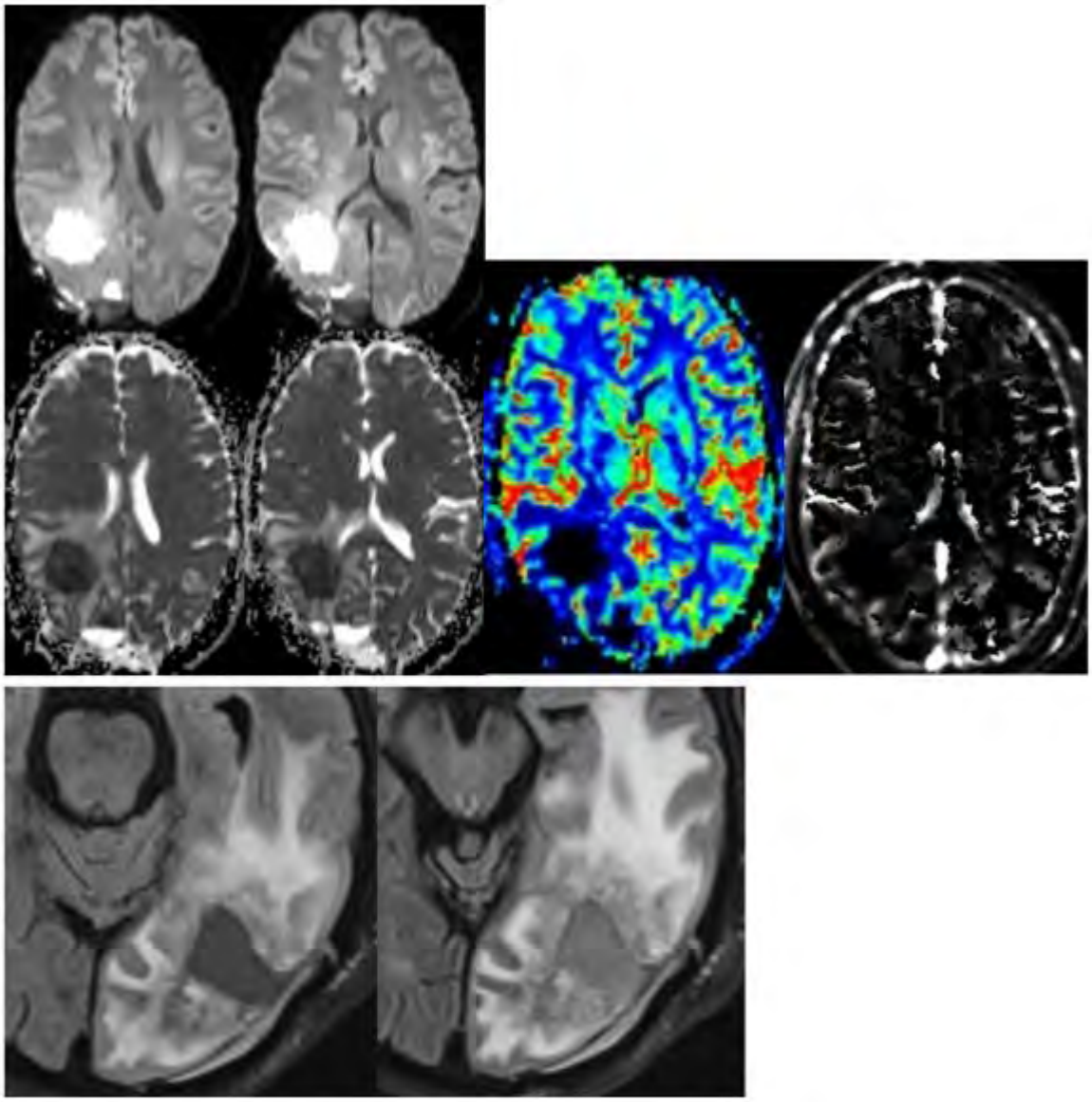

---

288 Neuroimaging of Dementia for Trainees – Puzzle beyond Alzheimer's Disease

Ricardo Paez MD, Jamie Yoon MD, Daniel Kim MD, Talha Shabbir MD, Sarah Ceglar MD
Harbor UCLA Medical Center, Torrance, CA, USA

Summary & Objectives

The diverse spectrum of dementia subtypes presents a significant challenge for radiology trainees in identifying neuroimaging features and providing actionable insights to clinicians. This educational exhibit explores a broad range of dementia types, extending beyond Alzheimer's disease (AD) to include sporadic and inherited vascular dementia such as cerebral autosomal dominant arteriopathy with subcortical infarcts and leukoencephalopathy (CADASIL), cerebral amyloid angiopathy (CAA), frontotemporal dementia (FTD), and Creutzfeldt-Jacob disease (CJD). We

additionally explore Parkinson's disease dementia (PDD), Dementia with Lewy bodies (DLB), as well as Parkinson's plus syndromes including progressive supranuclear palsy (PSP), multisystem atrophy (MSA), and corticobasal degeneration. We introduce search patterns to help trainees systematically evaluate characteristic findings, such as hippocampal atrophy, cortical thinning, and white matter hyperintensities. Recognizing that trainees often have limited experience with advanced imaging modalities, we provide a review of functional MRI (fMRI) for assessing connectivity disruptions, diffusion tensor imaging (DTI) for tractography and microstructural integrity, arterial spin labeling (ASL) for noting alterations in cerebral perfusion, and nuclear medicine techniques (FDG-PET, amyloid PET, hybrid PET-MRI) for metabolic and molecular insights. Additionally, we integrate clinical and laboratory correlates, including established biomarkers (e.g., CSF amyloid-beta and tau levels) and emerging ones (e.g., blood-based neurofilament light chain and plasma p-tau), to guide multidisciplinary collaboration. The exhibit aims to empower trainees with a framework for neurodegenerative disease imaging to contribute to patient management.

Purpose

1. Equip trainees with practical search patterns to differentiate neurodegenerative disease subtypes.
2. Spotlight advanced imaging modalities and their diagnostic utility in dementia evaluation.
3. Outline key reporting elements that inform clinical decision-making and multidisciplinary collaboration.

Materials & Methods

Cases were curated from our institutional PACS and supplemented by illustrative examples from peer-reviewed literature. Selection criteria prioritized multimodal imaging studies demonstrating classic and atypical features of dementia subtypes. All cases adhere to ethical standards, with patient identifiers anonymized in compliance with HIPAA.

Results & Conclusion

Through a series of representative cases, the exhibit demonstrates distinctive neuroimaging patterns as well as cases with mixed types of dementia. For instance, AD shows predominant medial temporal lobe/hippocampal atrophy (A) and posterior cingulate gyrus hypoperfusion on ASL (B). Vascular dementia often reveals multifocal infarcts and white matter hyperintensities on FLAIR MRI, while CAA presents with lobar microhemorrhages on SWI. FTD variants exhibit asymmetric frontal/temporal atrophy with preserved posterior structures. PDD and DLB feature nigrostriatal dopaminergic deficits on DaTscan SPECT (C) often with overlapping cortical involvement. CJD classically demonstrates abnormal FLAIR/DWI signal in the medial thalami bilaterally, although in practice may show nonspecific abnormal diffuse thalamic signal prompting differential diagnoses (D). Conversely, mixed cases may show a combination of these overlapping features (E-H). Advanced modalities can further characterize disease mechanisms: fMRI highlights default mode network disruptions in AD, while DTI quantifies fractional anisotropy reductions in white matter tracts across subtypes. Integration of biomarkers strengthens differentials—for instance, positive amyloid PET supports AD or CAA, whereas negative results steer toward mimics.

Overall, this exhibit serves as a comprehensive toolkit for radiology trainees, fostering confidence in navigating the complexities of dementia neuroimaging.

Images/Tables

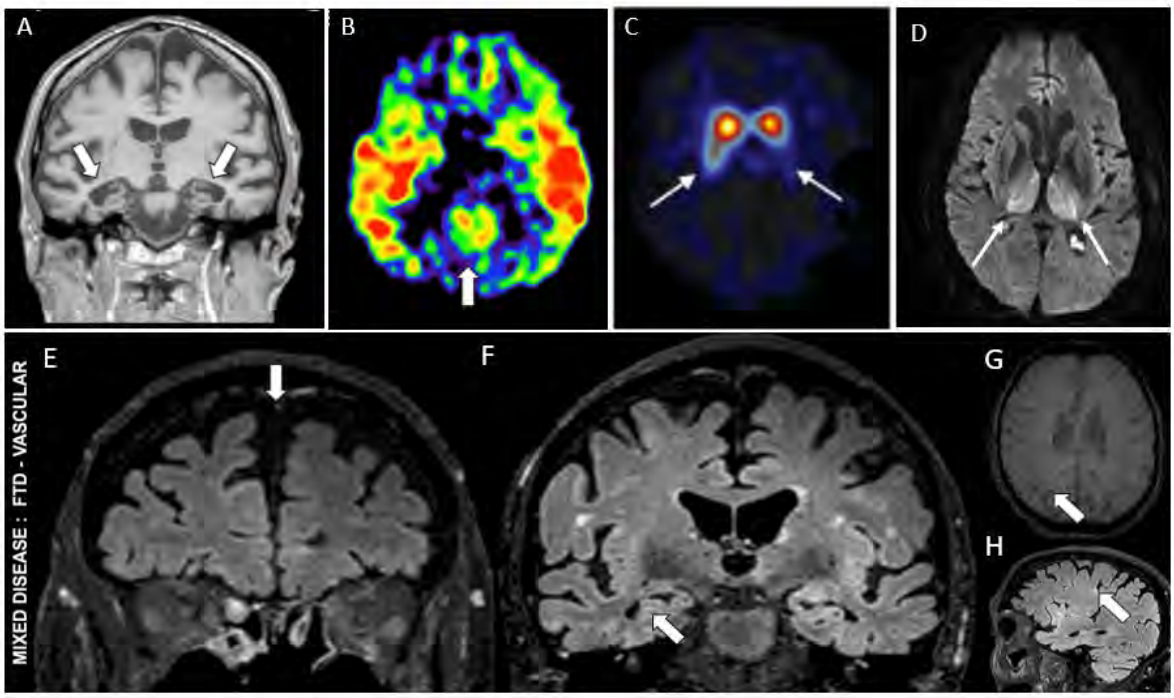

A, B) MRI scans of patient with typical Alzheimer's disease with coronal T1-weighted MRI showing symmetric hippocampal atrophy (two arrows in A) and ASL showing hypoperfusion of the posterior cingulate gyrus (arrow in B) (Adapted from Haller et. al.) C) A DaTscan with I-123 ioflupane showing asymmetric reduced uptake of dopamine in the left striatum as can be seen in PDD/DLB (Adapted from Risacher et. al.). D) MRI scan of patient with erratic behavior and progressive dementia from home institution showing abnormal restriction of diffusion on DWI in the bilateral thalami (white arrows) found to be proven CJD from CSF analysis, although finding nonspecific as can be seen in other toxic-metabolic/inflammatory encephalopathies. E-H) Case showing mixed features with frontotemporal and vascular dementia; coronal FLAIR showing frontal lobe atrophy (arrow in E) and to a lesser degree mesio-temporal atrophy (arrow in F) with few cerebral microbleeds on SWI (arrow in G) and cortical microinfarcts on sagittal FLAIR (arrow in H) (Adapted from Haller et. al.)

351 Primary Bone Lesions of the Spine

Anthony Sanchez MD, Adrian QingYu Xu MD
University of Utah, Salt Lake City, Utah, USA

Summary & Objectives

This educational exhibit will cover a number of primary osseous spine lesions and mimics in a case based format.

Purpose

The goal of this presentation is to teach residents and fellows the key imaging findings differentiating a number of primary osseous spine tumors and to serve as a refresher for attending radiologists.

Materials & Methods

The first slide will contain clinical presentation and images, the second slide will show the diagnosis with imaging labels, and the third slide will discuss additional details about the diagnosis. The diseases that will be covered include: Osteoid osteoma, chordoma, chondrosarcoma, osteochondroma, giant cell tumors, ABC, atypical hemangiomas, lymphoma, and plasmacytoma. Several imaging mimics will also be included.

Results & Conclusion

The last few slides will be a chart summary highlighting key and distinguishing findings.

Images/Tables

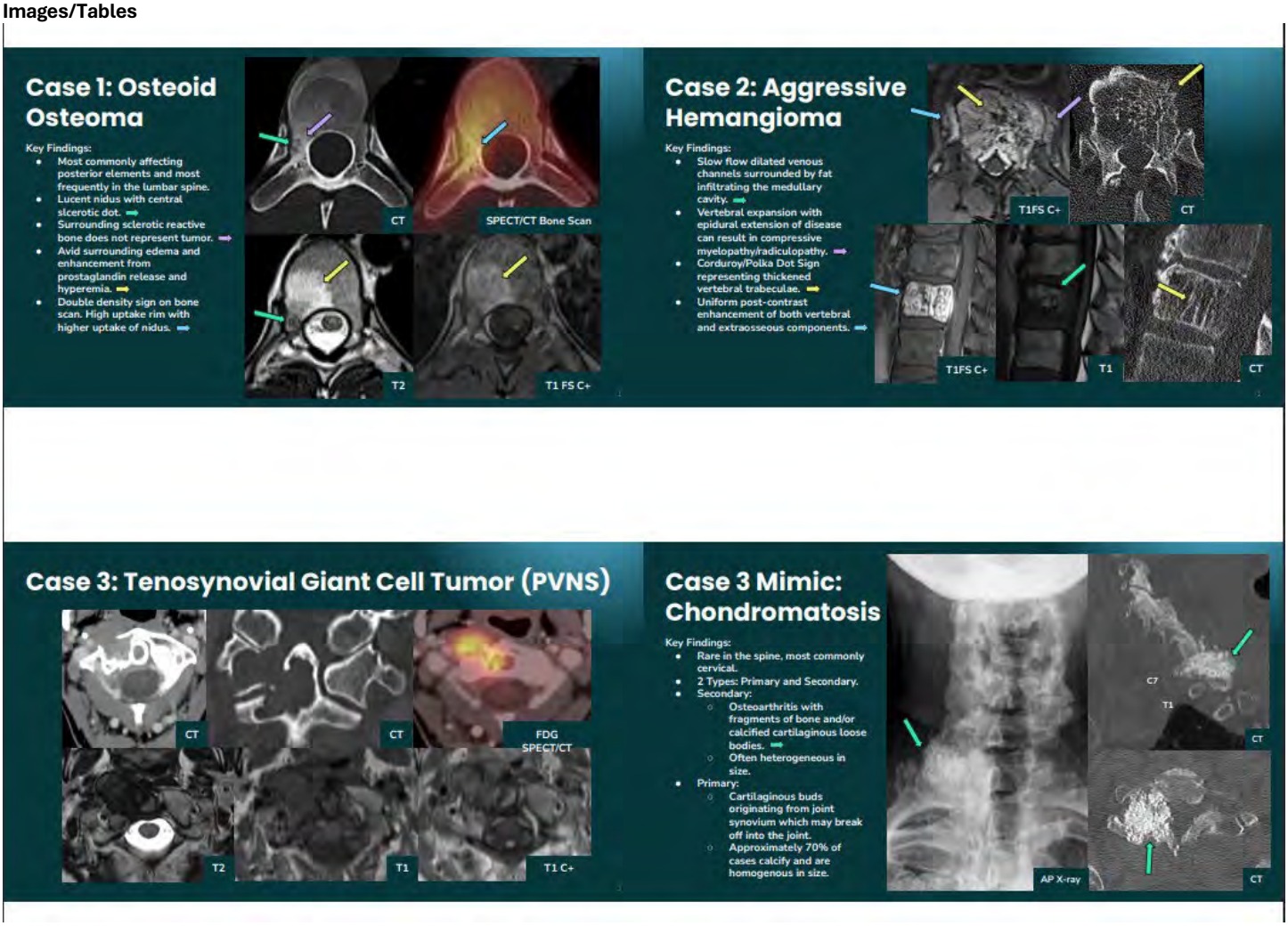

396 Imaging of the Conus Medullaris and Cauda Equina: A Comprehensive Review of Anatomy, Pathology and Key Imaging Findings

Jordan Stafford MD[1], Owais Ahmad Bhat MD[1], Fatemeh Dehghani Firouzabadi MD[1], Rahim Shalash[1], Samuel Thompson[1], Fahim Huda MD[1], M. Reza Taheri MD, PhD[2]
[1]University of Louisville, Louisville, Kentucky, USA. [2]George Washington University, Washington, DC, USA

Summary & Objectives

The conus medullaris and cauda equina are critical neuroanatomic regions susceptible to a wide spectrum of pathologies that often overlap clinically and radiologically. Accurate imaging interpretation is essential given their complex anatomy and diverse etiologies. This educational exhibit provides a comprehensive review of congenital, inflammatory, neoplastic, vascular, and miscellaneous conditions affecting these regions. Emphasis is placed on recognizing hallmark imaging features, correlating them with clinical presentations, and differentiating between conditions with similar appearances. The goal is to provide radiologists with a structured, pattern-based approach to enhance confidence in interpretation and facilitate accurate reporting.

Purpose

This exhibit has three primary objectives. First, it reviews the anatomy and normal MRI appearance of the conus medullaris and cauda equina, establishing a foundation for identifying abnormalities. Second, it illustrates the broad differential diagnosis of pathologies in this region, spanning congenital, inflammatory, neoplastic, vascular, and miscellaneous categories. Third, it emphasizes key imaging characteristics and clinical correlations that help distinguish among etiologies with overlapping presentations, thereby improving diagnostic accuracy and patient care. Additionally, the exhibit highlights the role of advanced imaging techniques in evaluating conus and cauda equina disorders. By combining visual examples with clinical context, the review serves as a practical reference for radiologists ranging from general neuroradiologists to subspecialists managing complex spinal cases.

Materials & Methods

A multimodal imaging review was conducted using MRI cases from institutional archives and published literature. Cases were categorized into five principal groups: (1) **Anatomic/Congenital**; including cystic dilation of the ventriculus terminalis (Figure 1.1), filum terminale lipoma, intradural cysts, diastematomyelia, tethered cord, and neurocutaneous syndromes such as neurofibromatosis type 1; (2) **Inflammatory/Immune-Mediated**; including acute and chronic inflammatory demyelinating polyradiculoneuropathy, neurosarcoidosis (Figure 1.3), paraneoplastic neuropathy, arachnoiditis, and rare infections such as tuberculosis (Figure 1.2), and cytomegalovirus; (3) **Neoplastic**; including myxopapillary ependymoma (Figure 1.4), paraganglioma, peripheral nerve sheath tumors, meningioma, lymphoproliferative disorders, and metastatic CSF seeding; (4) **Vascular**; including arteriovenous malformations, cavernous malformations, infarction, and dural arteriovenous fistulas; and (5) **Miscellaneous**; including degenerative or traumatic cauda equina syndrome, extramedullary hematopoiesis, and epidural lipomatosis. Each case was analyzed for imaging features, lesion localization, enhancement patterns, and clinical presentation, with illustrative MRI examples provided.

Results & Conclusion

Disorders of the conus medullaris and cauda equina encompass a broad spectrum of diseases with overlapping clinical symptoms, such as lower extremity weakness, sensory deficits, and bladder or bowel dysfunction. MRI remains the cornerstone of accurate diagnosis, enabling precise localization and characterization of lesions. A structured approach integrating anatomy, lesion morphology, enhancement patterns, and clinical context is essential. Awareness of uncommon entities, including vascular malformations and rare infections, prevents diagnostic delays and guides appropriate intervention. Through high-quality imaging examples and concise teaching points, this exhibit provides a practical, pattern-based reference, reinforcing the pivotal role of imaging in multidisciplinary care of patients with spinal cord and cauda equina disorders.

Images/Tables

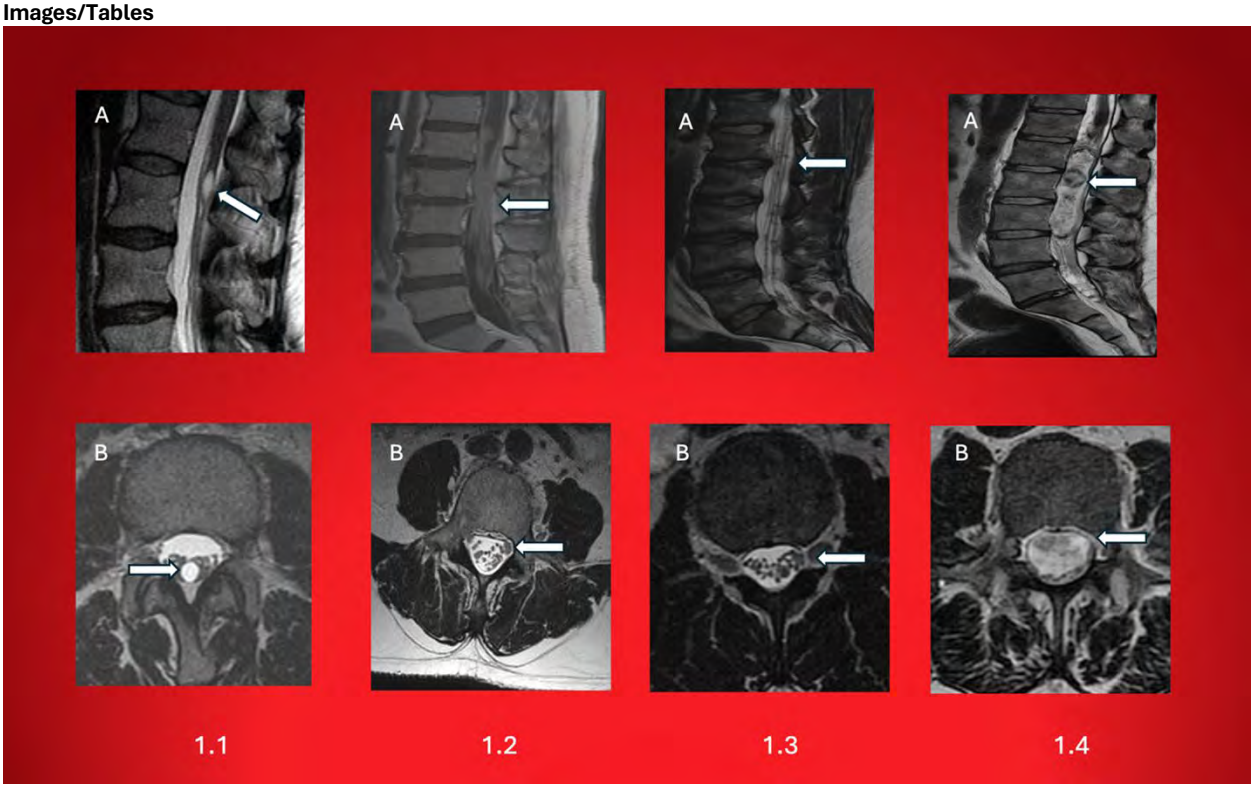

646 Neuroimaging for Patients Presenting with Dizziness in the Emergency Department: Clinical Recommendations and Review of the Literature

Akram Albeer BS[1], Raven Spencer MD[2], Laura Eisenmenger MD[3], WARREN MICHAEL CHANG[2]
[1]Drexel University, Philadelphia, PA, USA. [2]Allegheny Health Network, Pittsburgh, PA, USA. [3]University of Wisconsin, Madison, WI, USA

Summary & Objectives

Learners will be able to:

1. Identify high-yield bedside diagnostic algorithms for dizziness (HINTS, Dix-Hallpike).
2. Identify high-risk clinical features that increase the likelihood of central pathology.
3. Apply timing and trigger-based paradigms according to ACR and SAEM guidelines.
4. Recognize indications for neuroimaging and interpret its diagnostic yield in low- versus high-risk scenarios.

Purpose

Dizziness is a frequent emergency department (ED) presentation, accounting for 2.1–3.6% of annual visits. Increasing neuroimaging utilization—despite low diagnostic yield—drives ED costs and sometimes delays optimal care. While many patients present with dizziness with benign causes

such as dehydration, benign paroxysmal peripheral vertigo, medication interactions, and other causes, a small subset of patients have acute central pathology such as stroke or hemorrhage that can have devastating consequences. Differentiating central and peripheral causes of dizziness has high clinical utility. Evolving guidelines emphasize a diagnostic paradigm based on timing and triggers and distinguishing central from peripheral causes with bedside assessment. Imaging should be reserved for high-risk cases identified by clinical examination.

Materials & Methods

To accomplish the educational objectives, current literature and consensus guidelines from the American College of Radiology (ACR) and Society for Academic Emergency Medicine (SAEM) will be analyzed, focusing on studies of imaging utilization and diagnostic outcomes in ED dizziness. Yield statistics from large cohorts and meta-analyses will be summarized.

Results & Conclusion

Results:

In a large cohort study of 29,510 ED dizziness cases, 21.7% received CT and 9.8% MRI, with pathology identified in only 2% of patients that received CT imaging and only 4% of patients that received MR imaging. Positive findings were found in 12% of patients that received MRI when neurological findings present.

The HINTS exam demonstrates 94% sensitivity and 86.9% specificity for central causes. Performing these examinations on patients with suggestive histories can help triage patients in need of imaging.

SAEM GRACE-3 guidelines recommend against neuroimaging for isolated dizziness at low risk of central pathology with bedside examinations sufficing for most presentations. Using clinical history and provocative testing can help identify those patients in need of imaging.

In a recent study focusing on vertigo in emergency department patients, acute and constant dizziness and vertigo with less than 24 hours of duration and positive cerebellar examinations were strongly associated with acute central pathology. Clinical history and physical exam findings can help prioritize patients more likely to have acute actionable findings and increase diagnostic yield.

Conclusion:

Guideline-driven care prioritizes high-yield clinical algorithms over routine imaging in ED dizziness. Selective imaging improves diagnostic yield and optimizes resource use. Enhanced clinician proficiency with bedside examinations is essential for future practice.

Images/Tables

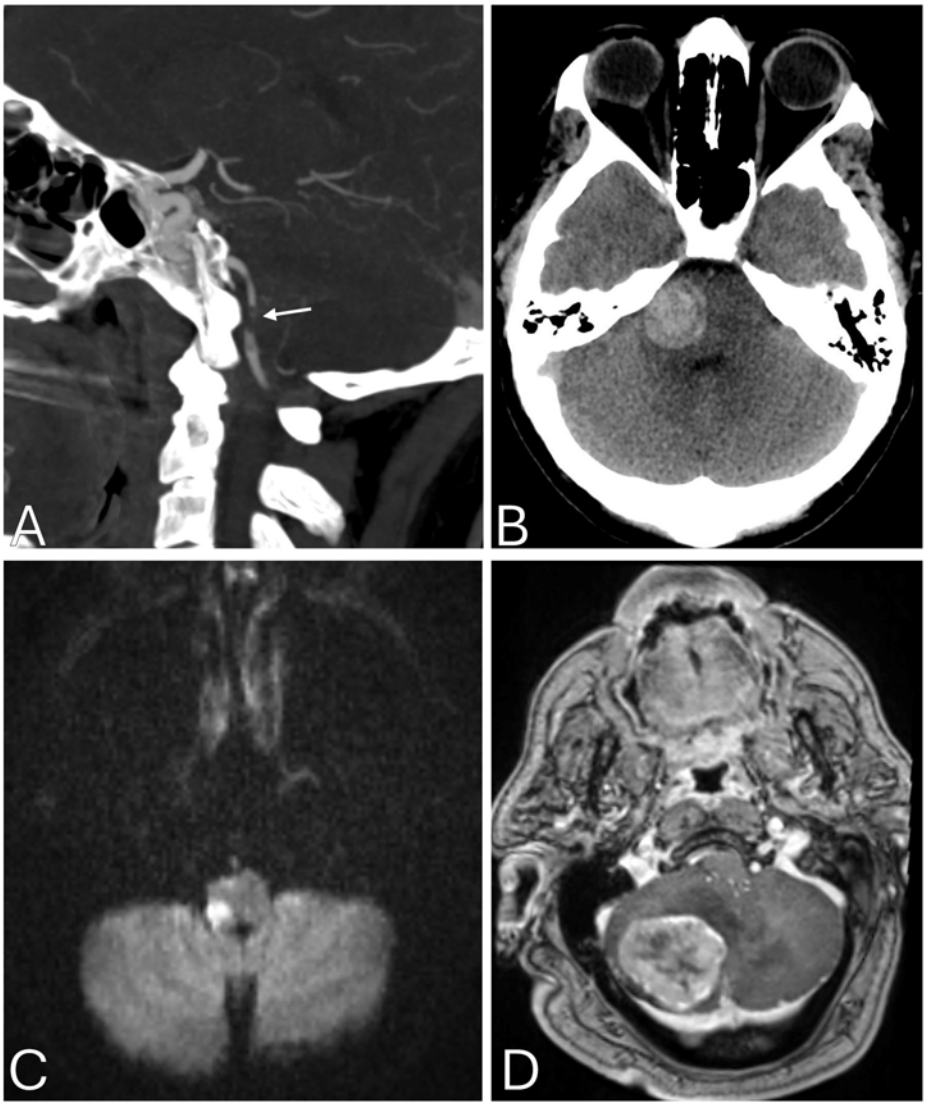

Figure 1. Neuroimaging finding examples in patients who presented with dizziness.
A) Sagittal CTA showing occlusive thrombus in the right V4 vertebral artery. B) Axial non-contrast CT showing right pontine hemorrhagic mass. C) Axial DWI showing a right medulla infarct (Wallenberg Syndrome). D) Axial post-contrast T1 image showing metastatic esophageal adenocarcinoma in the right cerebellum.

729 **Calvarial Tumors and Mimics: Imaging Patterns, Pitfalls, and Pearls**

Bilal Battal MD, Carlos Zamora MD, PhD
University of North Carolina, Department of Radiology, Chapel Hill, NC, USA

Summary & Objectives

Summary: The calvarium consists of the frontal, parietal, temporal, and occipital bones, as well as portions of the zygomatic and sphenoid bones. A wide range of conditions can affect the calvarium, including congenital, traumatic, inflammatory, and neoplastic processes. Calvarial tumors may arise primarily from the calvarium or may represent secondary involvement of systemic processes. These lesions are generally detected incidentally or may present as a palpable mass, local pain or tenderness, or signs of systemic disease. Imaging is essential, along with clinical findings and patient demographics, to narrow the differential diagnosis, guide management, and distinguish neoplastic processes from their mimics.

This educational exhibit provides an overview of both common and uncommon focal calvarial lesions, highlighting a range of conditions that affect the calvarium, with particular emphasis on their CT and MRI features. CT serves as the primary diagnostic tool for evaluating calvarial lesions, offering excellent detail in assessing bone changes such as remodeling, scalloping, erosion, destruction, lytic or sclerotic nature of the lesion, and matrix mineralization. MRI, on the other hand, excels in tissue characterization, allowing more precise assessment of marrow involvement, soft tissue components, and invasion of adjacent structures. Conventional radiographs have a limited role but may serve as the initial modality for lesion detection or be useful for follow-up in well-defined lytic lesions. Catheter angiography may be useful in selected cases for both diagnosis and treatment.

This exhibit will cover a variety of conditions that affect the calvarium, including benign entities such as osteoma, fibrous dysplasia, intraosseous venous vascular malformation/hemangioma, Langerhans cell histiocytosis, intraosseous meningioma, Paget disease, calvarial sarcoidosis, ossifying fibroma, desmoid tumor, and dermoid/epidermoid; malignant lesions such as metastasis, multiple myeloma/plasmacytoma, osteosarcoma, Ewing sarcoma, and lymphoma; and important mimics such as arachnoid granulations, venous lacunae, cephalocele/atretic cephalocele, sinus pericranii,

chronic calcified hematoma, and hyperostosis frontalis interna. Correlation with clinical features and histopathologic findings will be provided in appropriate cases.

Focal calvarial lesions range from incidental, clinically silent findings to aggressive, life-threatening pathologies, encompassing a wide spectrum of benign and malignant neoplasms, as well as tumor mimics. While some lesions have distinctive imaging features that allow a definitive diagnosis, many show overlapping clinical and imaging characteristics. Familiarity with the imaging appearance of calvarial lesions, along with clinical findings and patient demographics, is essential for accurate diagnosis and narrow the differential diagnosis. Imaging also plays a key role in management, including follow-up decisions, assessing resectability, evaluating lesion extent, guiding surgical planning, and identifying potential postoperative complications.

Educational objectives: To illustrate a broad spectrum of benign and malignant calvarial tumors as well as their mimics, highlight characteristic CT and MRI findings that help differentiate neoplastic from non-neoplastic lesions, and emphasize key imaging clues, diagnostic pitfalls, and features that guide accurate diagnosis, appropriate management, and surgical planning.

Purpose

N/A

Materials & Methods

N/A

Results & Conclusion

N/A

Images/Tables

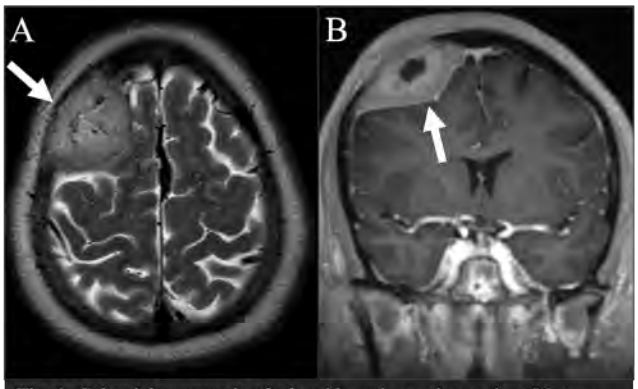

Fig. 1: Calvarial metastasis of adenoid cystic carcinoma in a 56-year-old female. (A) Axial T2WI and (B) coronal post-contrast T1WI show a large enhancing mass (arrows) in the right frontoparietal calvarium with an associated soft tissue component involving the scalp and underlying dura, causing mass effect on the frontal lobe.

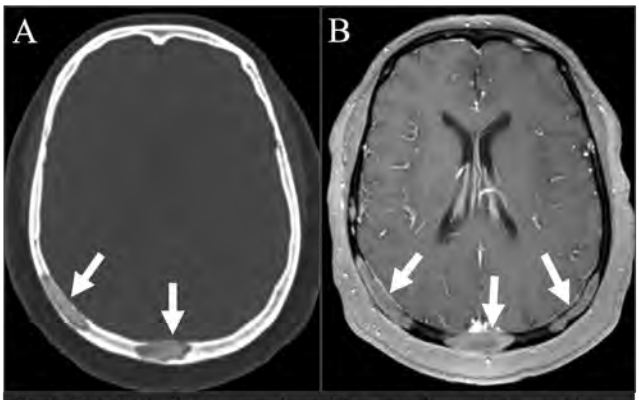

Fig 3: Pathologically proven calvarial bone involvement of sarcoidosis in a 60-year-old female. (A) Axial CT image shows slightly expansile, mixed predominantly lytic calvarial lesions (arrows) with a lace-like internal pattern of calcification. (B) Axial post-contrast T1WI demonstrates homogeneous enhancement of the lesions with underlying smooth pachymeningeal thickening and enhancement (arrows).

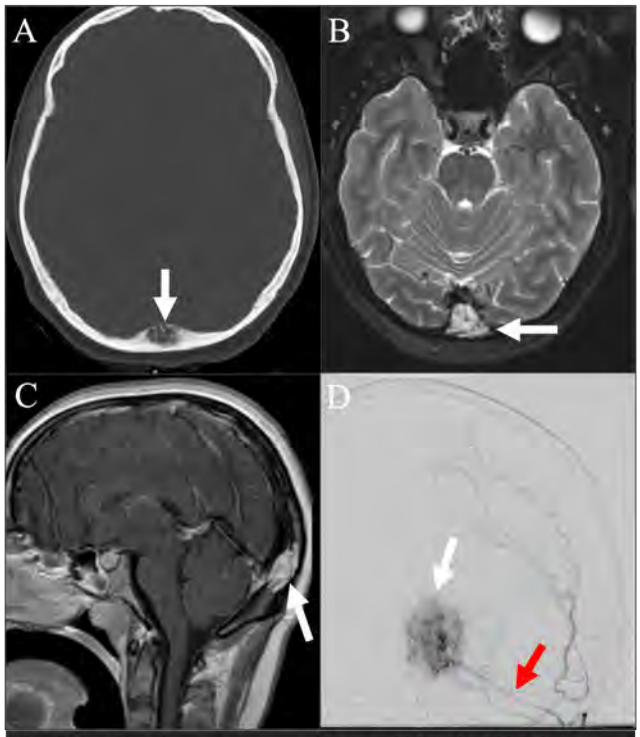

Fig. 2: Capillary hemangioma in a 16-year-old female. (A) CT image shows a well-demarcated, slightly expansile lytic lesion with thickened medullary trabecular spaces in the midline occipital bone (white arrow). (B) Axial FS T2WI demonstrates hyperintense signal within the lesion (white arrow). (C) Sagittal post-contrast T1WI shows avid enhancement and mass effect on the posteroinferior aspect of the superior sagittal sinus and torcula. (D) Selective left occipital artery injection catheter angiography image shows hypervascularity of the lesion (white arrow), supplied by branches of the occipital artery (red arrow).

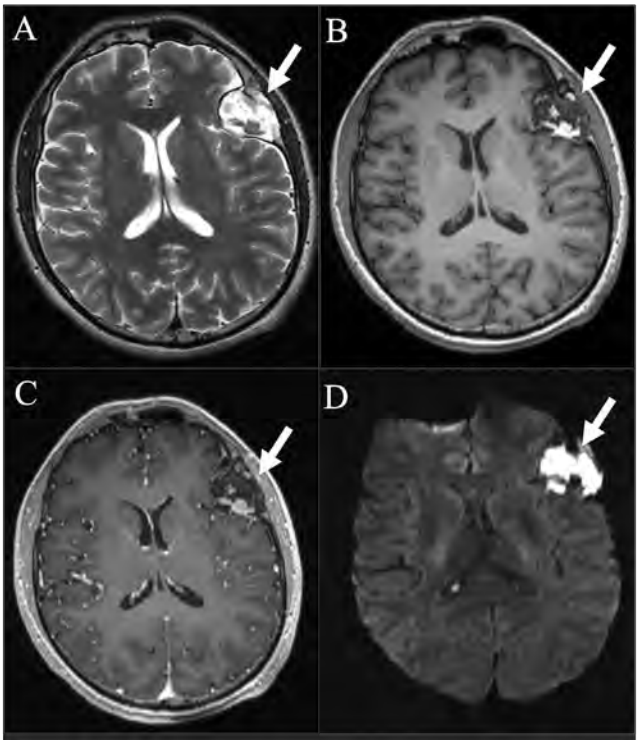

Fig. 4: Pathologically proven epidermoid in a 34-year-old male. (A) Axial T2WI and (B) axial T1WI show a mixed-intensity but predominantly T2 hyperintense and T1 hypointense expansile lesion (arrows) with intrinsic T1 hyperintense and T2 hypointense foci, likely representing high proteinaceous or hemorrhagic content. (C) Post-contrast T1WI shows no appreciable enhancement within the lesion. (D) DWI reveals hyperintense signal within the lesion (arrow), which represents a combination of diffusion restriction and T2 shine-through.

---

898 Imaging Cranial Dural AV Fistulas: Diagnosis, Treatment, and Post-treatment Follow Up

Sanaz Ameli, Mari Hagiwara, Eytan Raz, Charlotte Chung
NYU, New York, NY, USA

Summary & Objectives

Summary
Distinct from other vascular malformations, cranial dural arteriovenous fistulae (dAVFs) are abnormal fistulous connections between dural arteries and veins that comprise 10-15% of cranial vascular malformations. Despite advances in imaging techniques, accurate diagnosis based on non-invasive imaging remains challenging. This is in part due to the heterogeneity of dAVFs in terms of location of the shunt, feeding arteries, venous drainage into cortical veins versus dural venous sinuses, and behavior of the lesion. Improved visualization and understanding of dAVF angioarchitecture and pathophysiology have allowed development of novel treatment strategies, particularly endovascular approaches. Understanding the treatment strategy employed is paramount for appropriate evaluation of dAVFs status post treatment.

Educational objectives:

- Discuss up-to-date understanding of cranial dAVF angioarchitecture, pathophysiology, and relevant anatomy.
- Illustrate multimodal radiographic appearance of cranial dAVFs
- Review current treatment, particularly endovascular, strategies of cranial dAVFs
- Illustrate expected and unexpected radiographic appearance of cranial dAVFs status post endovascular embolization, open surgery, and radiosurgery treatment.

Table of Contents/Outline

1. Cranial dural vascular anatomy
2. Classifying dAVFs based on location, angioarchitecture, and pathophysiology
3. Imaging techniques (CT/MRI, CTA, MRA, DSA) for diagnosing cranial dAVFs
4. Diagnosing cranial dAVFs on non-invasive imaging
5. Treatment strategies of cranial dAVFs
6. Expected appearance of cranial dAVFs status post treatment
7. Pictorial review of unexpected findings in the post-treatment follow up of cranial dAVFs

Purpose

NA

Materials & Methods

NA

Results & Conclusion

NA

Images/Tables

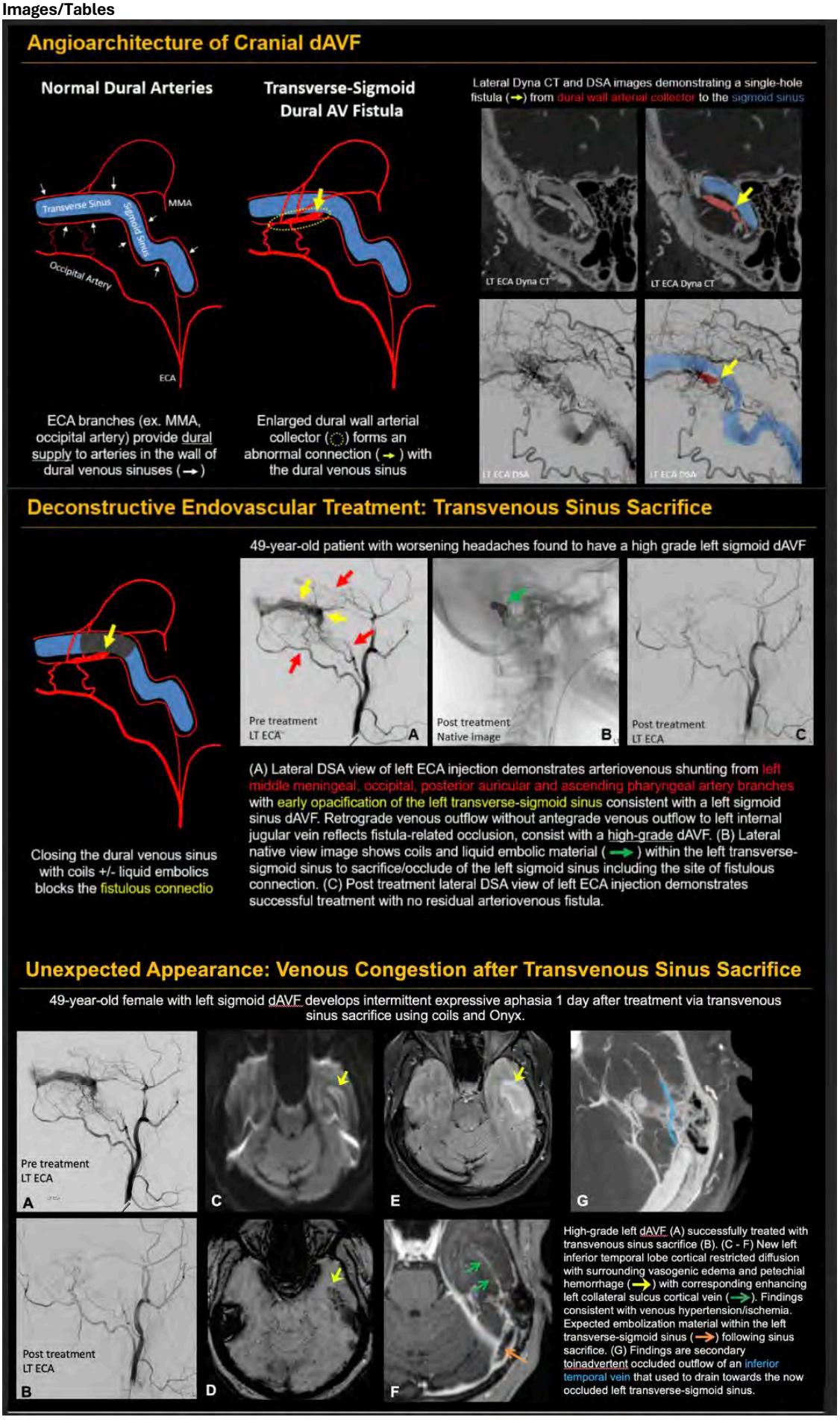

909 Mapping the Dementia Spectrum: A Practical MRI Approach

Ankush Bajaj MD, Salil Soman MD, Andreas Rauschecker MD, PhD, Luke W Bonham MD
UCSF, San Francisco, California, USA

Summary & Objectives

Familiarize learners with key clinical and imaging features of the 10 most common neurodegenerative dementias including amnestic Alzheimer's disease (AD), atypical AD variants, frontotemporal dementia, and other dementia syndromes.

Provide a practical 4-step framework using lobar atrophy patterns, symmetry, subcortical involvement, and coexisting pathology to guide differential diagnosis.

Purpose

Amnestic Alzheimer's disease comprises approximately 50% of neurodegenerative dementia cases, with the remainder including atypical AD variants (15-25%), frontotemporal dementia spectrum (5-15%), vascular dementia (10-20%), and other etiologies.[1] As disease-modifying treatments emerge, radiologists can play an increasingly critical role in narrowing the differential during initial workup and guiding management decisions. This educational exhibit reviews structural MRI features of the 10 most common neurodegenerative dementias and provides a systematic diagnostic framework applicable to daily practice.

Materials & Methods

This exhibit presents representative cases illustrating key clinical, demographic, and MRI features of major neurodegenerative syndromes. A stepwise diagnostic approach is demonstrated: (1) identify the pattern of lobar atrophy, (2) assess symmetry versus asymmetry, (3) evaluate brainstem, striatum, and hippocampal involvement, and (4) integrate coexisting vascular pathology. Visual comparison charts, annotated imaging examples, and diagnostic decision trees provide practical tools for systematic evaluation.

Results & Conclusion

Characteristic MRI atrophy patterns differentiate neurodegenerative syndromes when evaluated systematically. Amnestic AD demonstrates symmetric temporoparietal atrophy with bilateral hippocampal involvement. Atypical AD variants show distinct regional preferences: posterior cortical atrophy (PCA) presents with symmetric severe occipital atrophy,[2] while logopenic variant primary progressive aphasia (lvPPA) exhibits left-lateralized temporoparietal involvement.[3]

Asymmetry distinguishes FTD syndromes from AD variants. Nonfluent/agrammatic variant PPA (navPPA) shows left perisylvian and frontal predominance, while semantic variant PPA (svPPA) demonstrates asymmetric left anterior temporal atrophy.[4] Behavioral variant FTD typically manifests symmetric frontotemporal volume loss.

Subcortical structure evaluation resolves diagnostic ambiguity when lobar patterns overlap. Progressive supranuclear palsy (PSP) shows marked midbrain atrophy beyond expected age-related changes despite only mild frontal involvement. Corticobasal syndrome demonstrates asymmetric perirolandic atrophy with striatal involvement.[5] Conversely, dementia with Lewy bodies (DLB) exhibits posterior-predominant atrophy with characteristic hippocampal sparing.

Vascular dementia displays variable atrophy patterns but is suggested by supportive features including extensive leukoaraiosis and prior infarcts.

This systematic approach enables radiologists to: (1) narrow differential diagnosis using routine structural MRI before advanced imaging, (2) improve diagnostic confidence through stepwise pattern recognition, and (3) guide appropriate subspecialty referral as targeted therapies become available. Understanding these characteristic patterns can enhance the neuroradiologist's role in dementia evaluation and treatment planning.

Images/Tables

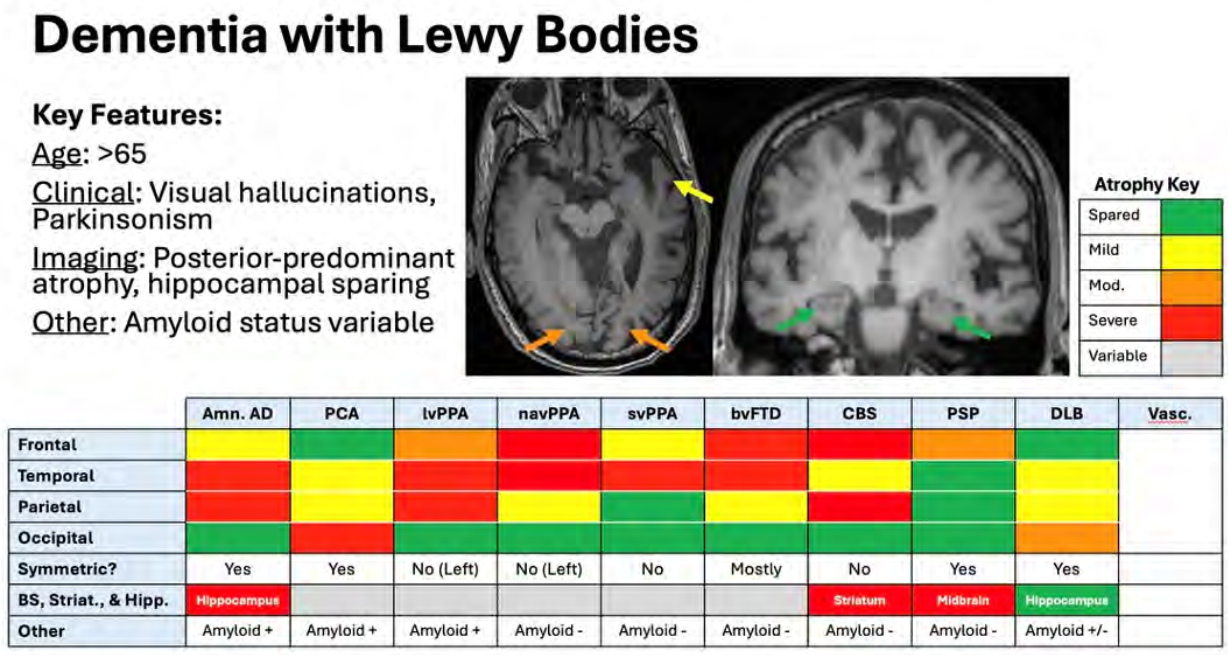

	Amn. AD	PCA	lvPPA	navPPA	svPPA	bvFTD	CBS	PSP	DLB	Vasc.
Frontal										
Temporal										
Parietal										
Occipital										
Symmetric?	Yes	Yes	No (Left)	No (Left)	No	Mostly	No	Yes	Yes	
BS, Striat., & Hipp.	Hippocampus						Striatum	Midbrain	Hippocampus	
Other	Amyloid +	Amyloid +	Amyloid +	Amyloid -	Amyloid -	Amyloid -	Amyloid -	Amyloid -	Amyloid +/-	

Figure 1: Example slide demonstrating structured atrophy review with image examples and interpretation after incorporating clinical data.

1032 A Rare Case of Autoimmune Astrocytopathy: How Tumbling Cytoskeleton Caused a Tumbling Patient

Azwade F Rahman MD, MPH, Sabrina Grondin MD, Avraham Bluestone MD, PhD
Stony Brook University Hospital, Stony Brook, NY, USA

Summary & Objectives

Glial Fibrillary Acidic Protein (GFAP) is an intermediate filament expressed mainly in astrocytes, a type of glial cell found in the central nervous system. Its main role is to provide structural support to the astrocyte and help maintain the blood-brain barrier, support neuronal function, and facilitate the CNS repair processes. Disease states related to this protein involve autoimmune, neoplastic, or genetic processes resulting in astrocytic dysfunction, inflammation, and gliosis. Autoimmune GFAP Astrocytopathy is an autoimmune meningoencephalomyelitis in which IgG antibodies target the intermediate cytoskeletal proteins of CNS astrocytes. These antibodies can be detected within the cerebrospinal fluid. Patients present with headache, fever, altered mental status, neck stiffness, and vision changes. This is a teaching case of a 45-year old male who presented with concern for acute ischemic infarct but imaging showed abnormal features. On magnetic resonance imaging, this disease presents as radial linear perivascular enhancement which extends from the ventricles to the cortical white matter, otherwise known as a radial enhancement pattern. The basal ganglia, thalamus, and brainstem may also be involved. Due to this pattern, it may mimic demyelinating disease such as ADEM, NMOSD, or MOGAD. Within the spine, there can be long-segment fluid signal which extends greater than three vertebral body segments and primarily involves the central cord. There is also leptomeningeal or perivascular enhancement.

Purpose

The following pictorial series will demonstrate the progression of this disease state from its initial presentation to its outpatient follow-up. The goal is to help clinicians consider this in their differential and recognize its distinguishing features from other etiologies that may mimic this pathology.

Materials & Methods

This exhibit was created after careful review and selection of key images on the case from our institutional PACS. The images were anonymized in order to ensure alignment with privacy standards.

Results & Conclusion

The subsequent follow-up and work-up eventually revealed GFAP as the source of the symptoms. The patient underwent significant workup in order to draw this conclusion. Imaging features can likely help sway clinicians towards more effective workup and treatment plans as well as help patients and their families peace of mind with concrete answers.

Images/Tables

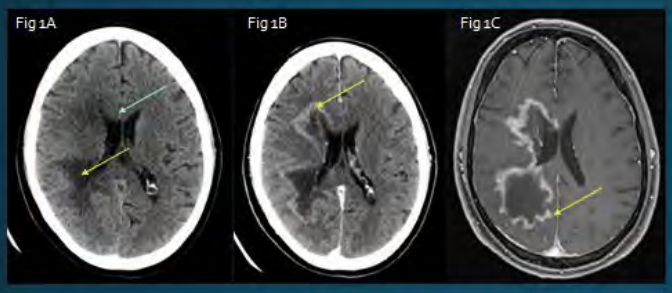

Figure 1. (A) Unenhanced CT of the brain show hypoattenuation of the right cerebral white matter, primarily concentrated within the frontotemporoparietal lobes. There is also evidence of mass effect, presumably from edema as suggested by effacement of the right frontal horn. (B,C) Contrast enhanced CT and MRI, he lesion demonstrated peripheral enhancement in the involved regions.

Figure 2. (A,B) These are the findings of figure one presented in the coronal view at the level of the ventricular atria. (C) T2 FLAIR imaging shows hyperintensity within the periventricular white matter which extending through the intracerebral corticospinal tract.

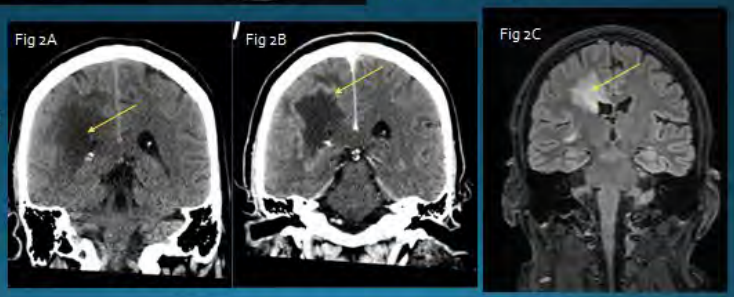

Figure 3. MR spectroscopy demonstrating elevated choline and lactate within the enhancing portions of the lesion. The NAA peak was decreased. The spectroscopy directed at the nonenhancing portions of the lesions shows marked lactate peaks.

Figure 4. MR perfusion applied to the original MRI brain demonstrated elevated relative cerebral blood volume within the enhancing margins of the lesions, up to 4.1.

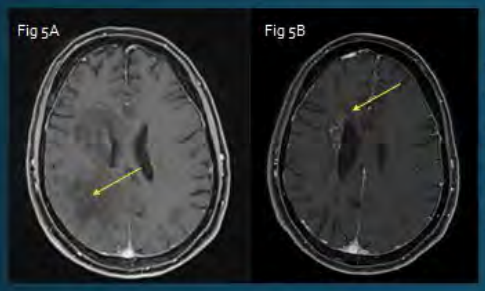

Figure 5. (A) Repeat imaging following corticosteroid therapy showed near complete resolution of peripherally enhancing lesion of the right parietal lobe. There is still evidence of persistent mass effect as suggested by effacement of the right lateral ventricle. (B) Five months of posttreatment, the patients enhancement patterns show curvilinear and nodular enhancement speckled throughout the white matter. It predominates in a perivascular and periventricular distribution.

Figure 6. (A, B) As in Figure 5, these are the findings following treatment within the admission and five months following discharge. (C) Coronal T2 FLAIR showing extension of signal into the cerebral peduncle into the pons which is more extensive than initially presenting.

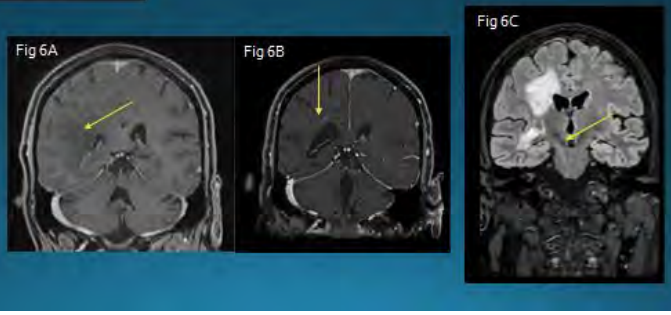

1049 Pediatric Accidental Head Trauma: What the On-Call Resident Must Know

Aldo M Pacheco-Carrillo MD, Alejandra I Castillo-Cervantes MD, Daniel A Chavez-Ruiz MD, Erwin J Nárvaez-Garcia MD
Centro Universitario de Imagen diagnóstica, Monterrey, Nuevo Leon, Mexico

Summary & Objectives

Pediatric head trauma represents a leading cause of morbidity and mortality in children and poses unique diagnostic challenges due to anatomical and biomechanical differences compared with adults.

This educational exhibit illustrates the multimodal imaging spectrum of pediatric head trauma, integrating CT, MRI, and ultrasound findings from real pediatric cases. The objectives are:

1. To review the pathophysiologic basis and age-specific anatomy underlying extra-axial and intra-axial injuries.
2. To highlight key imaging patterns and pitfalls using schematic illustrations and multimodal correlations.
3. To provide a structured, practical approach for on-call neuroradiologists to differentiate normal variants, complications, and mimics such as pseudofractures or non-accidental trauma.

Purpose

The purpose of this exhibit is to provide a comprehensive, case-based review of pediatric head trauma through multimodal correlation, emphasizing how developmental anatomy influences both the mechanism and imaging appearance of traumatic brain injuries.

Special attention is given to differentiating fractures from sutures, identifying mixed-pattern hemorrhages, and recognizing imaging red flags suggestive of abusive or non-accidental trauma.

By consolidating CT, MRI (SWI, DWI, DTI), and ultrasound examples, the exhibit aims to enhance radiologists' confidence and diagnostic accuracy during acute on-call evaluations.

Materials & Methods

This educational exhibit compiles multimodal imaging cases of pediatric head trauma obtained from clinical and teaching archives, organized by anatomical compartment and mechanism of injury.

Extra-axial injuries include epidural, subdural, subarachnoid, and intraventricular hemorrhages, while intra-axial lesions encompass contusions, intraparenchymal hematomas, and diffuse axonal injury.

Uncommon mechanisms such as obstetric trauma, penetrating trauma, and craniocervical junction injuries are also discussed.

CT and MRI were correlated with grayscale and Doppler ultrasound when available.

Each section integrates case images, simplified anatomical diagrams, and cinematic 3D renderings to clarify mechanisms, highlight pitfalls, and emphasize multimodal strengths for diagnosis and prognosis.

Results & Conclusion

The multimodal approach allowed comprehensive depiction of the full spectrum of pediatric head trauma.

CT was the most effective tool for acute diagnosis of fractures and hemorrhage, while MRI provided superior detection of microstructural and subacute injuries, particularly with SWI and DTI sequences.

Ultrasound proved valuable for evaluating neonatal scalp lesions, subgaleal collections, and ventricular hemorrhage.

Recognition of anatomic variants, accessory sutures, and patterns such as leptomeningeal cyst ("growing fracture") prevented misinterpretation and unnecessary intervention.

Understanding age-dependent injury mechanisms and using tailored imaging protocols are essential to distinguish accidental from non-accidental trauma and to guide appropriate management.

A multimodal, anatomy-based evaluation ensures accurate diagnosis, prognosis, and prevention of complications in pediatric traumatic brain injury.

Images/Tables

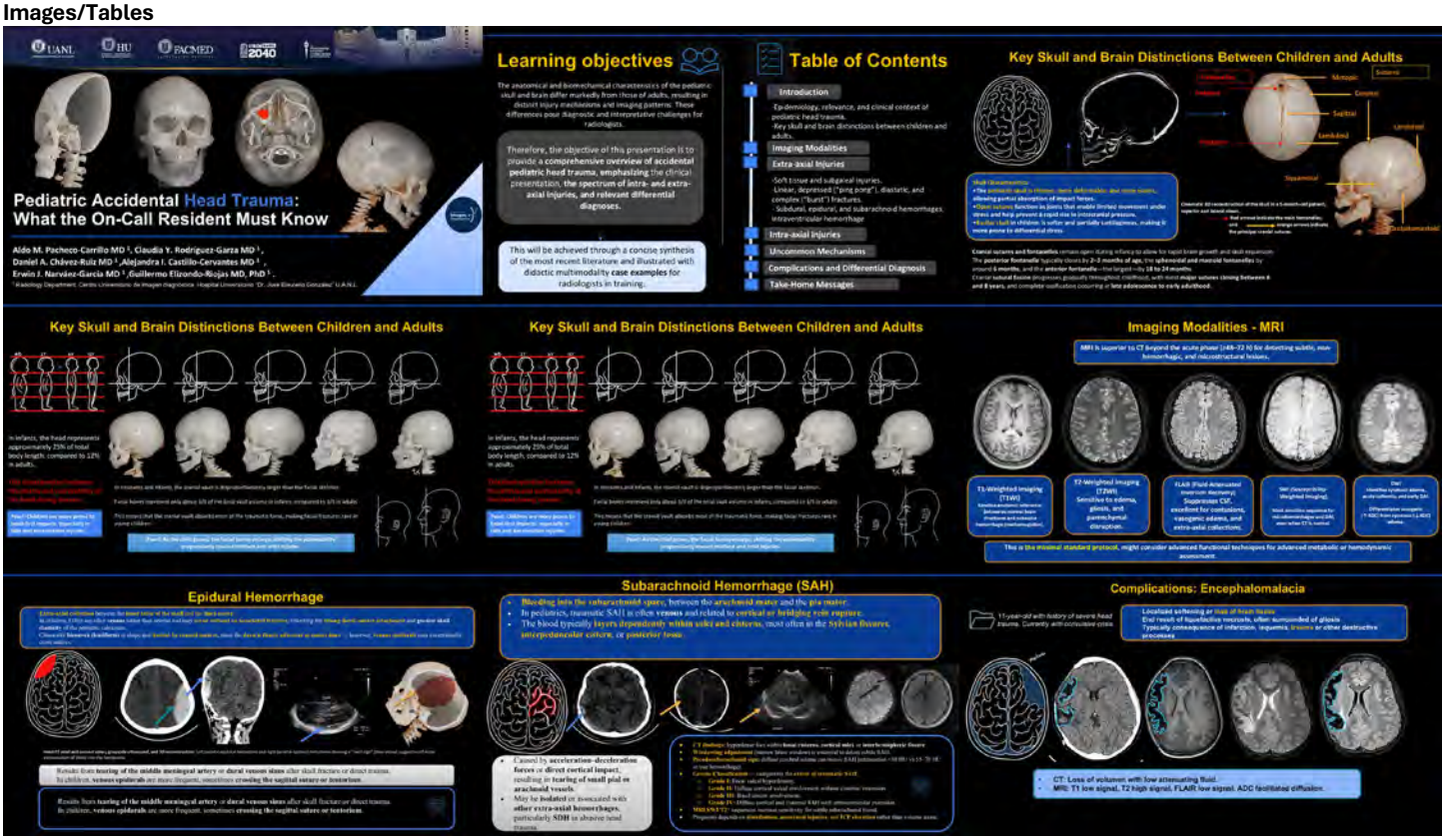

1199 MR Imaging of Acute Dissection in the Vertebrobasilar Artery

Masahiro Ida MD
Mito Medical Center, Mito, Ibaraki, Japan

Summary & Objectives

Acute vertebrobasilar artery dissection (VBD) is a critical cause of posterior circulation stroke, especially in young to middle-aged adults. MR imaging plays a central role in early diagnosis and therapeutic decision-making. Recognition of characteristic findings such as intramural hematoma and intimal flap on high-resolution MR sequences is essential for accurate diagnosis and timely management. We conclude that high-resolution source Gd 3D gradient-echo T1WI may be the most pragmatic and highest-yield modality in acute vertebro-basilar artery dissection.

Purpose

Arterial dissection of the vertebro-basilar system (especially the vertebral artery V4 segment extending to the basilar artery) may lead to posterior-circulation ischemic stroke, subarachnoid hemorrhage or medullary/cerebellar infarction. Accurate and prompt diagnosis is crucial for guiding antithrombotic or endovascular management. Traditional luminal imaging (e.g., TOF-MRA) often shows indirect signs (stenosis, occlusion, “string-and-pearl” morphology), but may fail to depict intramural pathology.

To evaluate and compare multiple MR imaging strategies in the acute phase of vertebro-basilar artery dissection (VBD) — specifically: (1) TOF-MRA, (2) Gd 3D GRE T1WI source images, and (3) high-resolution vessel wall imaging (VWI) — in order to elucidate which technique provides the greatest diagnostic yield in acute VBD. In addition, to discuss the role of diffusion-weighted imaging (DWI) for detecting associated medullary infarction (especially in the acute phase) including its strengths and limitations.

Materials & Methods

1. Diffusion-weighted imaging (DWI)
2. T2-weighted imaging (T2WI)
3. Gd 3D gradient-echo T1-weighted imaging (Gd 3D GRE T1WI)
4. High-resolution vessel wall imaging (HR-VWI)

Results & Conclusion

For acute vertebro-basilar artery dissection, our analysis suggests the following:

- DWI remains crucial for detecting infarction (e.g., medullary infarct) but has limitations in very early posterior-circulation infarction, and thus negative DWI does not exclude infarction in the context of acute VBD.
- Although TOF-MRA is widely available and fast, its sensitivity/specificity for acute VBD mural pathology is limited.
- High-resolution VWI provides excellent visualization of the dissection wall signs (intimal flap, intramural hematoma, mural enhancement) but may be less practical in emergent acute settings due to longer acquisition, motion artefact and variable availability.
- Gd 3D GRE T1WI allow both luminal assessment and wall signal evaluation (source images) with high contrast; they therefore combine luminal and mural information within a clinically reasonable acquisition time. Early VA-dissection studies support the utility of Gd-MRA for detection and follow-up. T2WI and Gd 3D GRE T1WI appears to offer the best combination of luminal and wall assessment in the acute phase, making it the most useful first-line MR technique in acute VBD.
- On balance, given the need for early diagnosis, broad availability and proven utility of Gd 3D GRE T1WI, we reason that high-resolution source Gd 3D GRE T1WI may be the most pragmatic and highest-yield modality in acute vertebro-basilar artery dissection.

- Hence, in the acute diagnostic workflow for suspected vertebro-basilar artery dissection, we recommend prioritising Gd 3D GRE T1WI, supplemented by VWI where available, and always interpreting DWI findings in the broader clinical and vessel-imaging context.

Images/Tables

---

249 Post-Surgical Orbital Imaging: Pitfalls and Pearls

Jamie Yoon MD, Ricardo Paez MD, Daniel Kim MD, Talha Shabbir MD, Sarah Ceglar MD
Harbor-UCLA Medical Center, Torrance, CA, USA

Summary & Objectives

Post-surgical orbital findings are frequently encountered on neuroimaging but can be misinterpreted by trainees unfamiliar with normal postoperative changes. This educational exhibit reviews the spectrum of surgical interventions and their characteristic imaging features. Examples include intraocular lens prostheses following cataract extraction; glaucoma shunts; retinal detachment repair with scleral buckle, intraocular silicone oil, and pneumatic retinopexy; enucleation, exenteration, and orbital implants; and corneal transplantation. For each surgery, representative imaging will demonstrate normal expected findings with descriptions of potential complications such as device migration, extrusion, infection, recurrent detachment, or graft failure. Pearls and pitfalls will be highlighted to help residents avoid common errors, such as mistaking silicone oil for vitreous hemorrhage or prostheses for foreign bodies.

Purpose

To provide radiology residents with a practical framework for recognizing expected imaging appearances and potential mimics of orbital surgeries, emphasizing misinterpretation and timely detection of complications.

Materials & Methods

Representative CT and MRI examples were obtained from our institutional PACS and peer-reviewed literature illustrating postoperative orbital surgeries and potential mimics. All institutional images were de-identified and literature figures were used with citation or open-access permissions. Cases were categorized by surgical type and reviewed for characteristic appearances, pitfalls, and differentiating features. Comparative panels were created to highlight overlapping imaging findings and key distinguishing clues between postsurgical materials and mimics.

Results & Conclusion

Representative CT examples demonstrate similar hyperattenuating appearances of postoperative intraocular and orbital materials and their potential mimics.

A) Vitreous hemorrhage appears as mildly heterogenous hyperattenuating material filling the posterior segment and conforming to the globe contours, typically with lower attenuation than silicone oil. Secondary findings in this case, including retrobulbar hemorrhage, intraconal fat stranding, and mild proptosis further support differentiation from implanted materials.

B) Intraocular silicone oil demonstrates slightly higher uniform hyperattenuation (mean attenuation ~116 HU) that can resemble hemorrhage; however, it typically fills the vitreous cavity and shows a posterior hypoattenuating crescent of residual vitreous due to its lower physical density relative to water.

C) Hydroxyapatite orbital implants appear as dense, stippled, ovoid structures inside of the enucleated socket with attenuation similar to bone and may contain motility peg tracts (arrow).

D) Silicone orbital implants are round hyperattenuating structures which replace the native globe after enucleation/evisceration. Differentiating clues from oil or hemorrhage include the absence of an intact globe, an orbital rather than intraocular location, a smooth spherical contour, and a lack of posterior crescent layering or residual vitreous cavity.

Understanding expected postoperative orbital appearances is essential for radiology residents, particularly during call coverage when prior surgical history may be limited. This exhibit provides a concise case-based review to reduce misinterpretation and support accurate reporting of both normal and abnormal postoperative findings.

Images/Tables

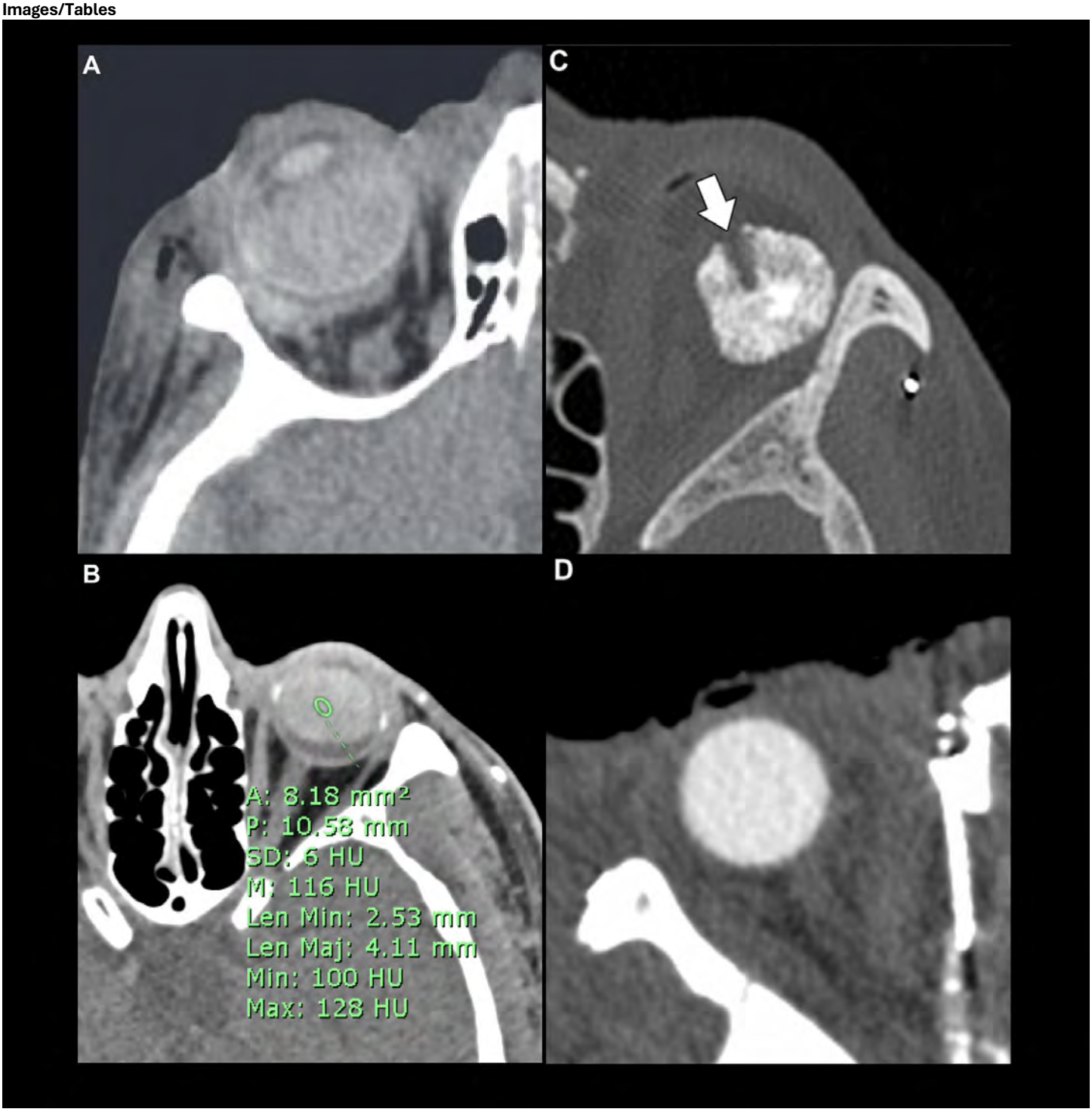

558 Cochlear Implant: What The Radiologist Should Know

Aditya Duhan MD[1], Abbas Hamza Abbas MD[2], Fahad Farooq MD[3], Saurav Jha MBBS[4], Swastika Lamture MD[1], Mamta Gupta MD[1], Charanjeet Singh MD[1]

[1]University of Colorado, Aurora, CO, USA. [2]University of Basra College of medicine, Basra, Basra, Iraq. [3]SUNY Upstate Medical University, Syracuse, NY, USA. [4]Patan Academy of Health Sciences, Kathmandu, Kathmandu, Nepal

Summary & Objectives

Cochlear implants are a vital resource for managing patients with profound sensorineural hearing loss, particularly for those who don't seem to benefit from traditional hearing aids. The success of cochlear implantation hinges on a thorough approach that includes a careful preoperative evaluation. This is where radiology plays a key role, helping to identify any anatomical variations and potential complications. The purpose of this review is to highlight the importance of preoperative radiological assessments for cochlear implantation, especially how imaging protocols can guide the surgical approach and improve outcomes.

Purpose

1. Equip radiologists with a thorough understanding of preoperative imaging for cochlear implantation.

2. Highlight the significance of assessing the anatomy of the temporal bone, ensuring the cochlear nerve is intact, and recognizing any congenital or acquired abnormalities that could affect the surgical method or make electrode placement more challenging.

Materials & Methods

Preoperative imaging for cochlear implantation follows a thorough protocol that combines high-resolution computed tomography (HRCT) and magnetic resonance imaging (MRI) of the temporal bones. The HRCT uses a thin-slice bone algorithm (up to 0.6 mm) and includes axial, coronal, and critical multiplanar reconstructions, featuring the oblique sagittal (Stenvers-like) view. This is crucial for a detailed assessment of the cochlea, the course of the facial nerve, and for spotting any ossification or malformations, such as Mondini dysplasia. On the MRI side, high-resolution T2-weighted sequences (like CISS/FIESTA), typically no thicker than 0.7 mm, are employed to examine the fluid-filled membranous labyrinth. This helps confirm cochlear patency and assess the integrity and size of the cochlear nerve within the internal auditory canal (IAC)[1]. Additionally, three-dimensional volumetric MRI data are collected to aid in precise surgical planning and to help locate the best trajectory for the electrode, ensuring a safe and effective pathway for the implant.

Results & Conclusion

Preoperative imaging for cochlear implantation is all about using a dual-modality approach that combines high-resolution computed tomography (HRCT) and magnetic resonance imaging (MRI) of the temporal bones. HRCT, especially with thin-slice Stenvers views, gives us incredible detail of the bony labyrinth, which is crucial for spotting acquired issues like Labyrinthitis Ossificans (often after meningitis) and congenital problems such as Incomplete Partition Type II (IP-II) and Common Cavity (CC).[1] On the other hand, MRI, particularly with high-resolution T2W sequences like CISS/FIESTA, is key for looking at the soft tissues, checking the cochlear nerve's integrity, and assessing fluid spaces—especially in cases of cystic congenital anomalies like IP-I, where there's a risk of a CSF gusher.[1] The insights we gain from both imaging techniques are vital for pinpointing the exact congenital or acquired reasons behind deafness. This information helps the surgeon choose the right electrode type, insertion method, and prepare for any intraoperative challenges, all aimed at ensuring the implant's success.

Images/Tables

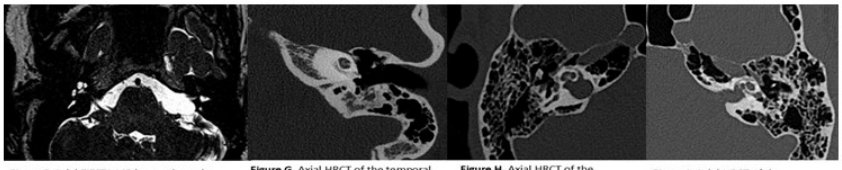

Figure F. Axial FIESTA MR image through the left internal auditory canal in a patient with hearing loss demonstrates **labyrinthitis ossificans**. There is **loss of the normal fluid signal in the middle and apical cochlear turns** (arrowhead), consistent with the **fibrotic phase** of the disease.

Figure G. Axial HRCT of the temporal bone demonstrates **near-complete mineralization/ossification of the basal and likely second cochlear turn**, with distortion of cochlear morphology. There is **sclerosis of the round window niche** and **focal thinning or subtle dehiscence of the superior semicircular canal**

Figure H. Axial HRCT of the temporal bone demonstrates **focal hypoattenuation in the right fissula ante fenestram** (arrowhead), consistent with **fenestral otospongiosis.**

Figure I. Axial HRCT of the temporal bone demonstrates an **extensive hypoattenuating ring around the cochlea**, producing the characteristic **"double-ring" sign**, consistent with **retrofenestral otospongiosis**.

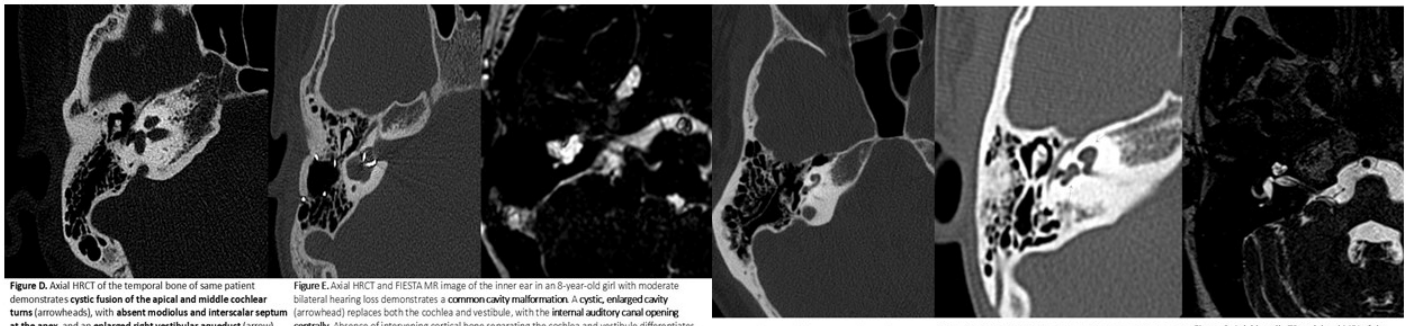

Figure D. Axial HRCT of the temporal bone of same patient demonstrates **cystic fusion of the apical and middle cochlear turns** (arrowheads), with **absent modiolus and interscalar septum at the apex**, and an **enlarged right vestibular aqueduct** (arrow). The **normal interscalar septum indentation** in the medial cochlea is absent.

Figure E. Axial HRCT and FIESTA MR image of the inner ear in an 8-year-old girl with moderate bilateral hearing loss demonstrates a **common cavity malformation**. A **cystic, enlarged cavity** (arrowhead) replaces both the cochlea and vestibule, with the **internal auditory canal opening centrally**. Absence of intervening cortical bone separating the cochlea and vestibule differentiates this malformation from **incomplete partition type I (IP-I)**.

igure A. Axial HRCT of the temporal bone in a 40-year-ld man with bilateral sensorineural hearing loss. The **asal turn of the cochlea appears normal**, whereas the **iddle and apical turns are hypoplastic and nteromedially rotated** (arrowhead), consistent with **ochlear hypoplasia type IV.**

Figure B. Axial HRCT of the temporal bone in a 14-year-old boy with progressive hearing loss demonstrates **cochlear incomplete partition type I (IP-I)**. The **cochlea is cystic and enlarged** (arrowhead C), **lacking a modiolus and interscalar septum**, and is **separated from a dilated vestibule** (arrowhead V) posterior to the internal auditory canal. The cochlea exhibits a **characteristic figure-of-8 appearance**.

Figure C. Axial heavily T2-weighted MRI of the temporal bone in a 33-year-old man with bilateral sensorineural hearing loss demonstrates **cochlear incomplete partition type II (IP-II)**. The **osseous spiral lamina–basilar membrane–neural complex is dysplastic and displaced anteriorly**, with an **increased distance between the osseous spiral lamina and basilar membrane**.

---

577 A review of MRI biomarkers to predict risk of future cognitive impairment and Alzheimer's disease

Samia Sabir BS, Saumya Gurbani MD, PhD, Sarah Dupont MD, MPH, Chadwick Hales MD, PhD
Emory University, Atlanta, GA, USA

Summary & Objectives

Alzheimer's disease (AD) is the most common dementia in the United States, impacting over 6.7 million Americans—a number expected to double by 2060. There is ongoing research in the development and application of biomarkers to identify patients at greatest risk of developing AD. For those at greatest risk there, targeted interventions may delay or prevent onset of the disease. This abstract explores the use of MR techniques as imaging biomarkers for predicting risk for future AD.

Learning Objectives:

1. Describe the natural history of AD from normal cognition to symptomatic disease to dementia.
2. Discuss the differences between pre-clinical risk stratification versus diagnosis of AD.
3. Explore how MRI morphologic changes can be utilized to identify patterns associated with AD diagnosis.
4. Explore quantitative MRI metrics that are potential predictors of future dementia in asymptomatic patients.

Purpose
Dementia is a clinical syndrome of declining mental ability that impacts activities of independent daily living. The most common cause of dementia, Alzheimer's disease (AD), accounts for 60-70% of dementia cases in the United States—affecting more than 6.7 million Americans. As described in the 2024 Lancet Commission's report, many cases of dementia can be prevented with targeted interventions. As pathologic brain changes occur prior to symptom onset in neurodegenerative dementias, there is active research into biomarkers to predict risk of future cognitive decline. These biomarkers include CSF and blood tests for AD-related proteins and radiotracers such as amyloid and tau PET. MRI techniques have also been studied that compare the imaging of healthy subjects and those with varying degrees of cognitive impairment. In this work, we will explore the quantitative MRI metrics that correlate with cognitive impairment and the potential for imaging as a predictive tool for developing AD in cognitively normal patients.
Materials & Methods
This exhibit will first review the natural history of AD neuropathologic changes from no symptoms to symptomatic decline and dementia. This will be followed by a brief review of the difference between using imaging for risk prediction versus diagnosis. Next, results of a literature review of standard and advanced quantitative MR techniques will be presented, with select representative studies described. Imaging studies from a retrospective search of the medical record at our university hospital will be presented where applicable. Examples of techniques discussed include volumetric analyses of cerebral atrophy, cortical thickness, diffusion weighted imaging, quantitative susceptibility mapping, MR spectroscopy, and the use of machine learning models on whole-brain multi-sequence MRI.
Results & Conclusion
Currently, AD is diagnosed once cognitive changes become apparent. Structural and advanced MRI techniques are being explored as tools to predict future cognitive decline. While CSF and blood biomarkers and PET radiotracers have been evaluated for aiding in the diagnosis of symptomatic AD, the studies discussed seek to quantify the risk of developing AD in asymptomatic patients by identifying imaging changes that precede the development of symptoms. With the ongoing development of these techniques, neuroimaging may play a greater role in predicting risk for dementia, which in turn may provide opportunities for prevention or earlier disease-modifying therapies.
Images/Tables

Morphological Metrics	Advanced MRI Biomarkers
Medial temporal lobe atrophy score (MTA)	Diffusion weighted imaging metrics – fractional anisotropy, mean water diffusivity
Entorhinal cortical atrophy (ERICA)	MR spectroscopy - metabolite ratios
White matter hyperintensity volume	Quantitative susceptibility mapping
Structural atrophy maps	Cerebral microbleeds
Machine learning models of brain age	

---

658 The Olive's Uprising (When Degeneration Leads to Hypertrophy): Trace the Pathway, Predict the Side, and Recognize the Pathognomonic Findings
Sophie Y Wong MD, Hoda Shirazian MD, James Y Chen MD
University of California, San Diego, La Jolla, CA, USA
Summary & Objectives
Hypertrophic olivary degeneration represents a unique example of trans-synaptic degeneration in the brain following an acute injury, in which the inferior medullary olive loses its typical inhibitory input and subsequently becomes hypertrophic rather than demonstrating downstream atrophy. Although the olivary hypertrophy and T2 hyperintensity are most pronounced several months after the initial event, characteristic imaging findings typically persist on subsequent imaging studies. Recognition of this entity can be challenging due to the distance between the inferior olivary nucleus and other components of the dentato-rubro-olivary pathway, but findings can be ipsilateral, contralateral, or bilateral, and are pathognomonic once recognized.
After reviewing this educational exhibit, readers should be able to:

- Describe the components of the dentato-rubro-olivary pathway, the locations of the nuclei, their connections, and their primary neurotransmitter effects.
- Use their understanding of lesional pathways to predict the effect of a lesion in each component of the dentato-rubro-olivary pathway: ipsilateral, contralateral, or bilateral medullary olive hypertrophy.
- Recognize examples of various etiologies (for instance: vascular malformation, intracranial mass, ischemic injury) that may result in hypertrophic olivary degeneration and identify the associated clinical symptoms and signs.
- Describe the progression of expected imaging findings on MRI and CT associated with hypertrophic olivary degeneration across the months to years following the initial injury.

Purpose
N/A
Materials & Methods
N/A
Results & Conclusion
N/A

Images/Tables

UC San Diego Health

SELECTED SLIDES: Hypertrophic Olivary Degeneration

Sophie Y. Wong, MD; Hoda Shirazian, MD; James Y. Chen, MD

9/10/2025 Non-contrast head CT

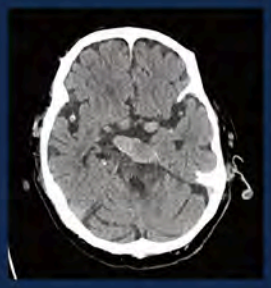

70-year-old male with a history of hypertension, left pontine infarct in 2020 (with residual right hemiparesis, aphasia, and dysphagia), right pontine infarct in January 2024, recurrent brainstem stroke in 1/23/25, now locked-in.

History of seizure activity at home while on Keppra 1500 BID, Valproic Acid 250 QID, and Lacosamide 150 mg BID

Head CT obtained due to concern for breakthrough seizure.

← Axial noncontrast head CT demonstrates vertebrobasilar dolichoectasia with adjacent brainstem atrophy.

1/23/2025 Brain MRI 7/28/2011 Brain MRI

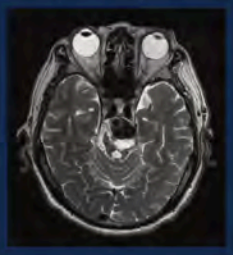

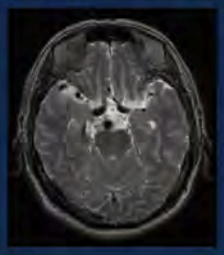

Prior Brain MRI from January 2025 demonstrated a peripheral thrombus and extensive encephalomalacia/ gliosis in the adjacent pons. In comparison, findings were not present on remote prior brain MRI from July 2011.

1/23/2025 Brain MRI

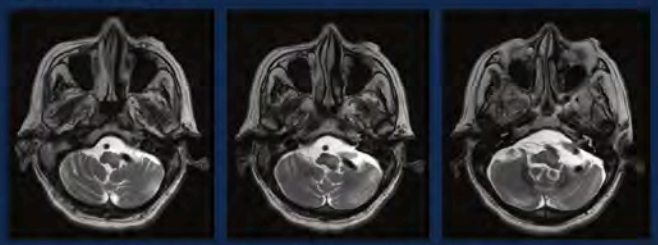

Lower down in the medulla, there is an area of asymmetric hypertrophy and increased T2 signal involving the left medullary olive, suggestive of **hypertrophic olivary degeneration.**

The Dentato-Rubro-Olivary Pathway (Triangle of Guillain-Mollaret)

- Dentatorubral tract (superior cerebellar peduncle):
  - Dentate nucleus → contralateral red nucleus
  - Crosses midline at caudal midbrain (commissure of Wernekinck)
- Central tegmental tract:
  - Red nucleus → ipsilateral inferior olivary nucleus
- Inferior cerebellar peduncle:
  - Efferent fibers from the inferior olivary nucleus
- **INHIBITORY (GABAergic) signal to the inferior olivary nucleus causes HYPERTROPHY with trans-synaptic degeneration**

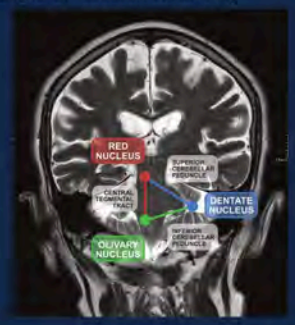

Patterns of Injury

RED: red nucleus
BLUE: dentate nucleus
GREEN: inferior olivary nucleus

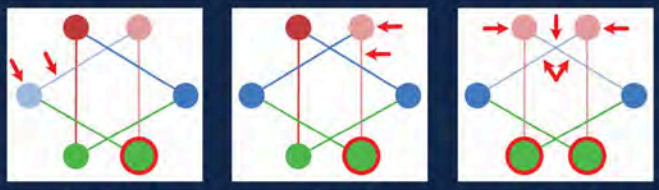

Contralateral
Injury to the contralateral dentate nucleus or superior cerebellar peduncle

Ipsilateral
Injury to the ipsilateral red nucleus or central tegmental tract

Bilateral
Injury to the brainstem affecting the bilateral red nuclei, commissure of Wernekinck, or central tegmental tracts

Findings

- Radiology:
  - Best evaluated on MRI
  - Increased size of the olivary nucleus (depending on time since the initial insult)
  - Hyperintensity on T2-weighted sequences
  - The normal olivary nucleus has a wavy outer border (a white matter capsule called the amiculum) and is located posterior to the preolivary sulcus.
- Pathology: increase in volume due to:
  - Cytoplasmic vacuolar degeneration
  - Neuronal and astrocytic hypertrophy
  - Gliosis

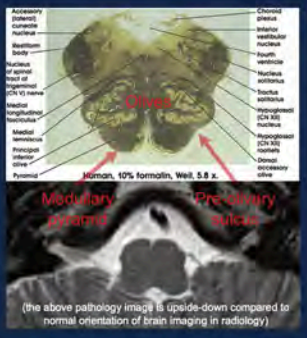

(the above pathology image is upside-down compared to normal orientation of brain imaging in radiology)

Temporal Evolution of Findings

1. First 24 hours: no change
2. 2-7 days: olivary amiculum (the white matter capsule at the periphery) degenerates
3. 3 weeks: progressive olivary hypertrophy
4. 8.5 months: maximum olivary enlargement due to neuronal/astrocytic hypertrophy
5. 9.5 months or later: Pseudohypertrophy due to neuronal degeneration but gemistocytic astrocytes
6. 3-4 years: atrophy of the olivary nucleus

* Increased T2 signal may be seen regardless of whether the hypertrophy is present, and is therefore the most reliable imaging finding.

706 Neuroimaging in ICANS: MRI Patterns and Diagnostic Pitfalls in Immune-Related Encephalopathy Following CAR T-Cell Therapy

SUSHMITHA PUTTAPPA SHIVAGANGE MD, AUGUSTO LIO DA MOTA GONCALVES FILHO MD, Eduardo Portela De Oliveira MD, MARIA LUCIA BRUN VERGARA MD
University of Ottawa, Ottawa, Ontario, Canada

Summary & Objectives

This exhibit reviews the neuroimaging spectrum of Immune Effector Cell-Associated Neurotoxicity Syndrome (ICANS) in patients receiving CAR T-cell therapy, highlighting characteristic and atypical MRI findings.

Purpose

To review the role of neuroimaging in diagnosing and monitoring toxicities related to chimeric antigen receptor (CAR) T-cell therapy, emphasising the diverse MRI patterns of ICANS. This exhibit also highlights atypical imaging patterns that may overlap with other encephalopathic or vascular conditions, underscoring potential diagnostic pitfalls and their implications for accurate interpretation.

Materials & Methods

Acute neurotoxicity following CAR T-cell therapy presents a diagnostic challenge in neuroimaging, with patients often exhibiting a wide spectrum of neurologic symptoms ranging from mild cognitive changes to severe encephalopathy. Early recognition of imaging findings is critical as ICANS is associated with rapid-onset morbidity and mortality[1]. The purpose of this educational exhibit is to provide a review of ICANS-related CNS manifestations, with an emphasis on the varied imaging patterns on brain MRI.

We present a series of patients with hematologic malignancies who developed acute neurologic symptoms following CAR T-cell therapy. Brain MRIs obtained during the acute symptomatic phase and at follow-up were systematically reviewed. Imaging findings illustrate the varied patterns associated with ICANS, highlighting the utility of MRI in detecting early changes and monitoring treatment response.

CASE 1: Diffuse white matter involvement [Figure 1,2]

61-year-old man on CAR-T cell therapy for Stage IV mantle cell lymphoma admitted to ICU with decreased level of consciousness and diffuse limb rigidity suspicious for nonconvulsive status epilepticus. EEG revealed diffuse slowing, no seizures or epileptiform abnormality. Clinically grade 4 ICANS suspected.

MRI Findings: Confluent and patchy T2 and FLAIR white matter hyperintensities in bilateral cerebral hemispheres, most conspicuous in centrum semiovale, along the internal and external/extreme capsules, inferior colliculus and middle cerebellar peduncles.

CASE 2: CLIPPERS Pattern [Figure 3, 4]

72-year-old man on CAR-T Cell therapy for relapsed refractory DLBCL presented with mild confusion, expressive aphasia, tremor and gait difficulties, progressed to severe sensory ataxia, gait instability and falls, clinically suspected as grade 2 ICANS.

MRI Findings: Abnormal increased T2, FLAIR signal in bilateral middle cerebellar peduncles, more conspicous on the left with ill-defined patchy areas of enhancement in these regions.

Case 3: Leptomeningeal and perivascular enhancement [Figure 5-8]

35 year old woman on CAR-T cell therapy for DLBCL developed severe decrease of LOC, rhythmic movements of the feet, eye deviation and generalized tonic-clonic seizure with clinical suspicion of grade 4 ICANS.

MRI Findings: Diffuse leptomeningeal enhancement in bilateral parietooccipital region and subtle linear perivascular enhancement in bilateral cerebral hemispheres. Cortical gyriform DWI hyperintensity in bilateral cerebral hemispheres, conspicuous in bilateral frontal and temporal lobes.

Results & Conclusion

ICANS encompasses a spectrum of neuroimaging manifestations that can overlap with other causes of acute encephalopathy. By showcasing typical and atypical MRI patterns with illustrative cases, this educational exhibit aims to enhance radiologists' diagnostic confidence in distinguishing ICANS from its mimics and to reinforce the role of MRI in early recognition and monitoring of immune-related neurotoxicity in patients undergoing CAR T-cell therapy.

Images/Tables

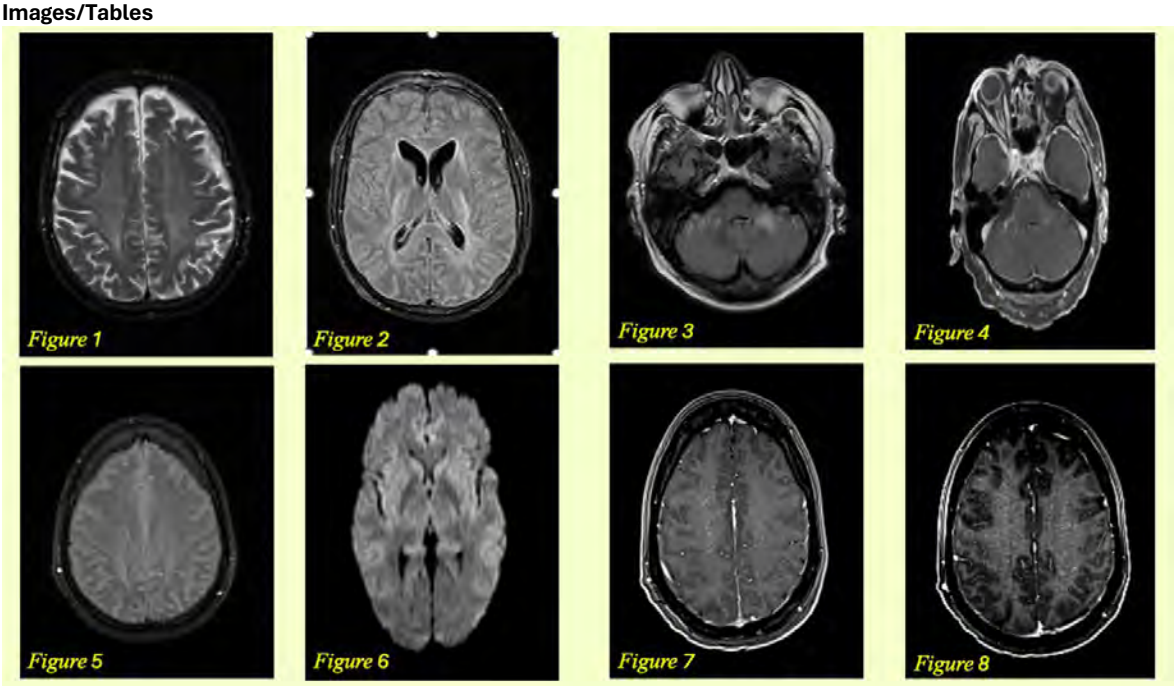

731 Imaging Spectrum and Diagnostic Approach to Orbital Histiocytic Disorders

Alper Sever, Sofia S Haque, Chimatu Sichona, Michael Starc, Alicia Meng, Ira Dunkel, Jasmine Francis, David Abramson, Eli L Diamond
MSKCC, NYC, NY, USA

Summary & Objectives

Orbital histiocytic disorders represent a rare and heterogeneous group of diseases that may closely mimic infection, inflammation, or malignancy. Recognition of their characteristic imaging features is essential for accurate diagnosis and timely management. This exhibit demonstrates multimodality imaging findings of orbital histiocytic disorders including Langerhans Cell Histiocytosis (LCH), Erdheim-Chester Disease (ECD), Rosai-Dorfman Disease (RDD), and Xanthogranuloma (XG), and provides a systematic approach for differential diagnosis.

Purpose

To illustrate characteristic orbital imaging manifestations of histiocytic disorders, identify distinguishing features among subtypes, and highlight radiologic findings that may guide diagnosis and prevent misinterpretation as neoplastic or inflammatory disease.

Materials & Methods

We plan to illustrate approximately 10–20 cases of orbital histiocytosis from an institutional database at a tertiary cancer center, including patients with histopathologic confirmation of LCH, ECD, RDD, and XG. Representative CT and MRI examinations will demonstrate key imaging characteristics, including anatomic location, lesion morphology, bone involvement, enhancement pattern, and symmetry. Correlation with clinical findings and systemic disease manifestations will also be presented.

Results & Conclusion

The following imaging patterns were most commonly observed:

- LCH: Typically manifests as a lytic lesion of the superolateral orbital roof with an enhancing soft-tissue component.
- ECD: Often shows bilateral or symmetric intraconal or retro-orbital infiltration, sometimes extending to the dura or optic nerve sheath.
- RDD: Frequently demonstrates smoothly enhancing soft-tissue thickening, often involving the lacrimal gland or orbital apex without bone destruction.
- XG: Usually presents as a well-defined, enhancing eyelid or lacrimal-gland lesion.

Recognition of characteristic bone, soft-tissue, and systemic imaging features aids in distinguishing histiocytic subtypes. Understanding these imaging patterns enables radiologists to suggest the correct diagnosis, guide biopsy, and initiate appropriate multidisciplinary care.

Images/Tables

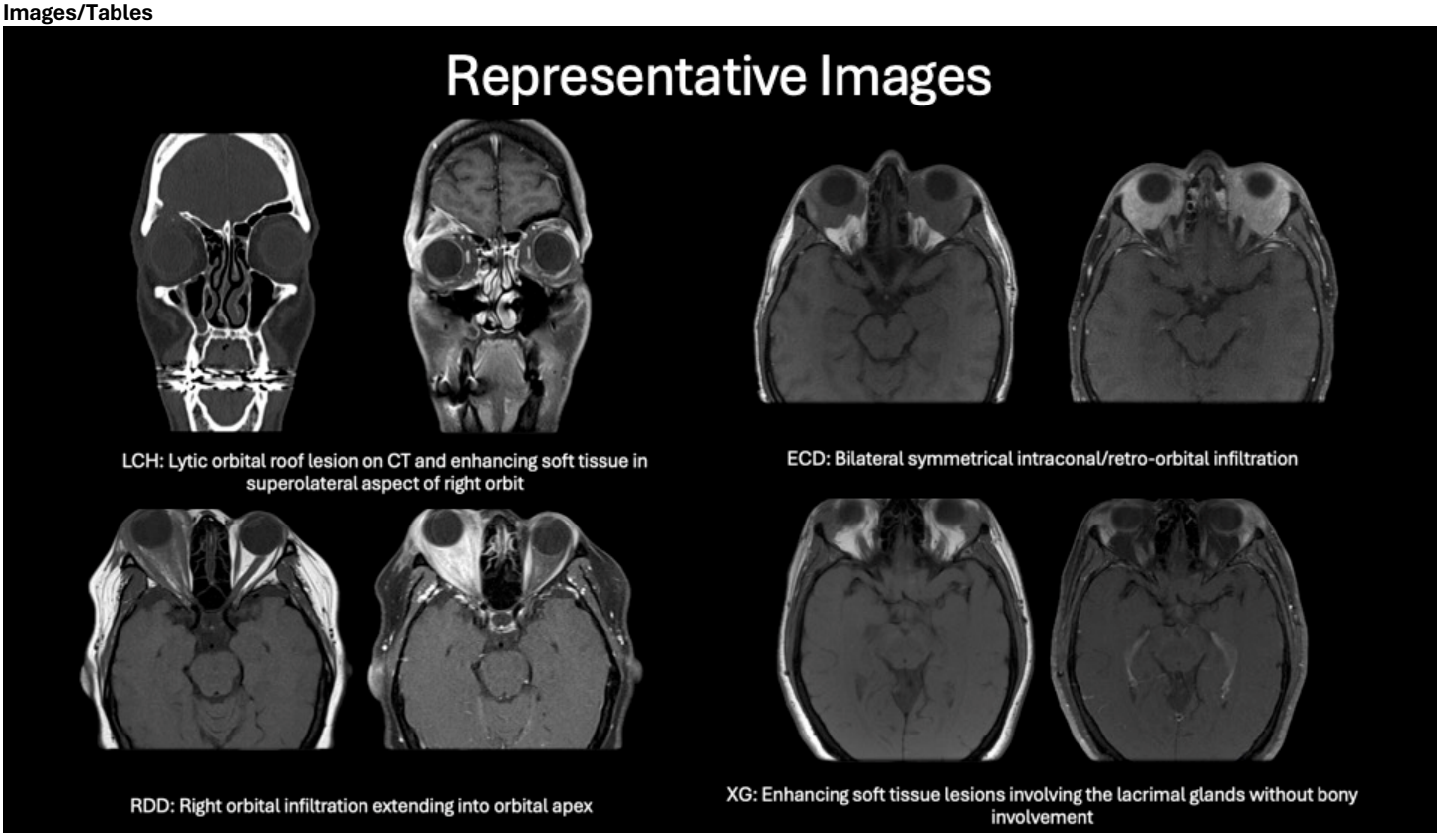

---

888 From "Uh-Oh" to "All Clear": Keeping Away From "CLOSE" Calls in Sinus Surgery

Khalid Kabeel MD, Stephen Little MD
Emory University, Atlanta, Georgia, USA

Summary & Objectives

Summary:

A systematic approach to preoperative sinus evaluation using the **CLOSE** mnemonic provides a comprehensive framework for identifying anatomical hazards. Originally introduced by O'Brien et al. in 2016[1], the CLOSE protocol systematically addresses critical anatomical considerations essential for safe functional endoscopic sinus surgery. The framework encompasses **Cribriform plate** anatomy (Keros classification types I–III), **Lamina papyracea** integrity (including orbital fractures and relationships to ethmoid air cells), **Onodi cells** and their relationship to optic nerves, **sphenoid sinus pneumatization patterns** and carotid canal relationships, and anterior **ethmoidal artery** identification with recognition of supraorbital

pneumatization. This exhibit demonstrates how systematic preoperative imaging analysis using the CLOSE mnemonic transforms potential surgical complications into anticipated anatomical considerations, enabling safer operative planning.

Objectives:

Upon completion of this exhibit, learners will be able to:

1. Apply the CLOSE mnemonic systematically to generate a comprehensive anatomical risk profile on preoperative sinus CT.
2. Differentiate between normal anatomical variants and high-risk features that warrant surgical modification.
3. Classify cribriform plate anatomy using the Keros classification system and recognize asymmetric configurations as preoperative risk factors.
4. Identify lamina papyracea changes, orbital fractures, and their relationship to ethmoid air cells.
5. Recognize anatomical variants including Haller cells, Onodi cells, and uncinate process variations.
6. Classify sphenoid sinus pneumatization patterns and recognize pneumatization into the carotid canal and optic nerve regions.
7. Localize the anterior ethmoidal artery and supraorbital pneumatization on preoperative CT.

Purpose

Please see "Summary and Objectives" section.

Materials & Methods

Please see "Summary and Objectives" section.

Results & Conclusion

Please see "Summary and Objectives" section.

Images/Tables

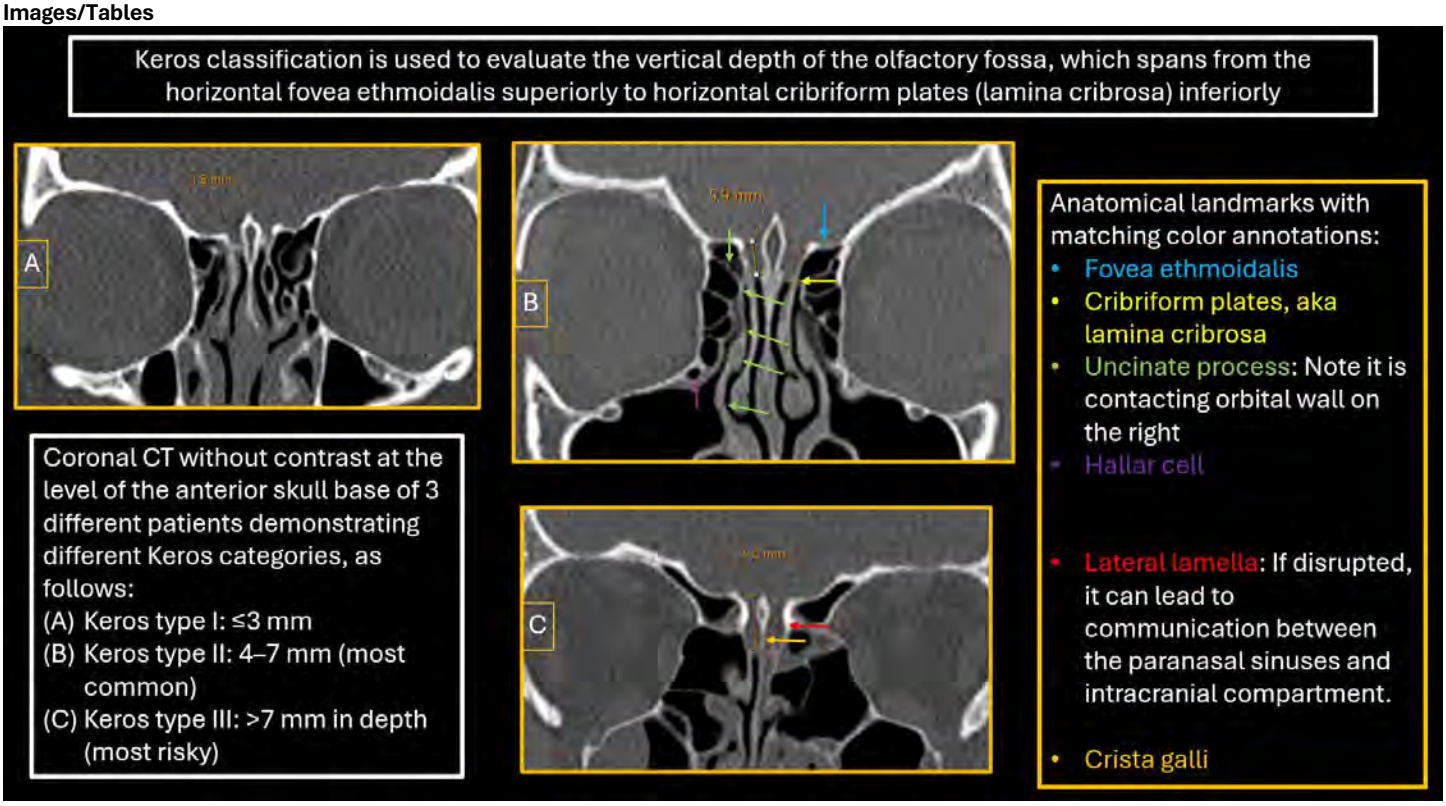

1009 Beyond the Canal: Extra-Spinal Blind Spots on Routine Spine MRI

Hyun Su Kim MD, PhD, Peyman Mirghaderi MD, MPH, Majid Chalian MD
University of Washington, Seattle, Washington, USA

Summary & Objectives

Summary

Spine MRI assessments often extend well beyond the clinically interest region, capturing a wide anatomic field that includes the craniocervical junction, thoracic space, retroperitoneum, pelvis, and extraspinal soft tissues. However, time limitation and a narrow look can lead to systematic "blind spots," where actionable incidental findings are easily overlooked. This exhibit highlights how radiologists can add unique value by deliberately surveying these regions, recognizing subtle abnormalities, and integrating them into clinically meaningful reports.

Using a series of illustrative cases, we demonstrate significant incidental findings detected on spine MRI; such as vascular lesions, deep-seated tumors, infections, insufficiency fractures, and osteonecrosis; and correlate them with CT, contrast-enhanced MRI, and PET-CT when appropriate. For each anatomic zone, we demonstrated typical blind spots, key imaging clues, and common diagnostic pitfalls. Finally, we propose practical, anatomy-based search patterns and reporting tips that can be applied in clinic. By systematically expanding our review beyond the spine itself, radiologists can reduce missed diagnoses, improve patient outcomes, and reinforce their central role in multidisciplinary care.

Educational Objectives

After viewing this exhibit, participants will be able to:

1. Recognize commonly overlooked anatomic regions on routine spine MRI, including the craniocervical junction, thoracic cavity, retroperitoneum, pelvis, and extraspinal soft tissues.

2. Identify the spectrum of clinically significant incidental findings that may arise in these regions, such as vascular lesions, neoplasms, infections, and occult fractures.
3. Apply structured, anatomy-based search patterns to minimize interpretive blind spots in daily spine MRI practice.
4. Incorporate pertinent incidental findings into clear, actionable reports that guide appropriate further imaging, referral, or intervention.
5. Appreciate how vigilance for extra-spinal pathology differentiates radiologists from other clinicians and enhances their diagnostic impact.

Purpose

N/A

Materials & Methods

N/A

Results & Conclusion

N/A

Images/Tables

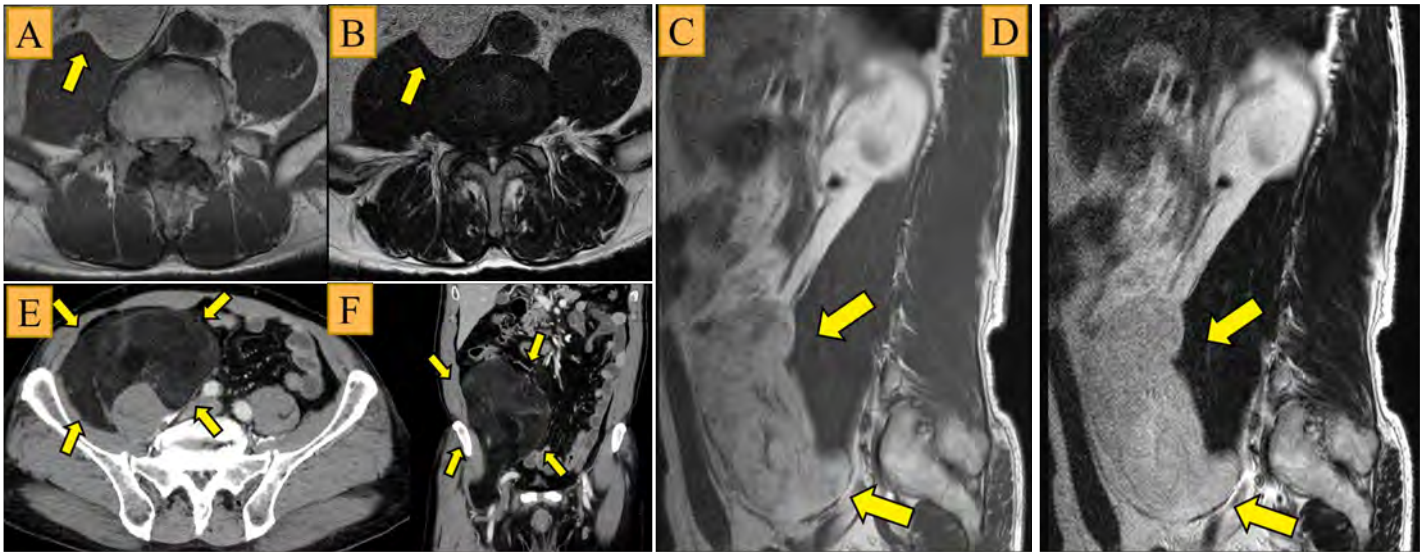

A 77-year-old man with lower back pain.
(A-D) Axial and sagittal T1- and T2-weighted spine MRI of shows a hyperintense mass (arrows) in the retroperitoneum.
(E, F) Contrast-enhanced CT demonstrates a fatty mass with heterogeneous attenuation in the retroperitoneum, extending into the right inguinal region.
Surgical excision was performed, and histopathology confirmed a well-differentiated liposarcoma.

1056 Imaging and intervention in Head and neck vascular anomalies

Shivaprakash B Hiremath DMRD DNB[1], Neetika Gupta MD[2], Gali Shapira-Zaltsberg MD[2], Laila Alshafai[3], Marlise P dos Santos MD FRCPC MSc MPH[4], Ronit Agid MD FRCPC[1], Elka Miller MD FRCPC[5]

[1]Toronto Western Hospital, Toronto, Ontario, Canada. [2]Children's Hospital of Eastern Ontario, Ottawa, Ontario, Canada. [3]Princess Margaret Hospital, Toronto, Ontario, Canada. [4]University of Ottawa, Ottawa, Ontario, Canada. [5]The Hospital for Sick Children, Toronto, Ontario, Canada

Summary & Objectives

Head and neck vascular anomalies represent a heterogeneous group of congenital and acquired disorders with complex anatomy, varying degrees of involvement, and proximity to critical structures, making accurate diagnosis and precise intervention essential. Recent advances in cross-sectional imaging and minimally invasive interventional techniques have greatly enhanced diagnostic accuracy, therapeutic safety, and clinical outcomes.

Purpose

- Understand the classification and pathophysiologic basis of head and neck vascular anomalies.
- Identify key imaging features of vascular neoplasms, malformations and syndromic associations that guide diagnosis and treatment planning.
- Describe interventional strategies, including embolization and sclerotherapy, and their indications.
- Recognize potential complications and appropriate post-treatment imaging surveillance strategies.

Materials & Methods

To evaluate the role of multimodality imaging in the diagnosis and classification of head and neck vascular anomalies, and to assess the safety, efficacy, and outcomes of various image-guided interventional procedures.

Results & Conclusion

The educational exhibit will be based on select patients with vascular anomalies of the Head and neck who underwent imaging and intervention. The study cohort included individuals diagnosed with vascular neoplasms, fast-flow (arteriovenous malformations and fistulas) and slow-flow (venous,

lymphatic, capillary and combined) lesions.
Imaging and intervention in head and neck vascular anomalies demand a comprehensive, multidisciplinary approach. Multimodality imaging ensures accurate classification and guides targeted, image-based therapy. Minimally invasive interventions, particularly embolization and sclerotherapy, offer effective alternatives to surgery with excellent results.

Images/Tables

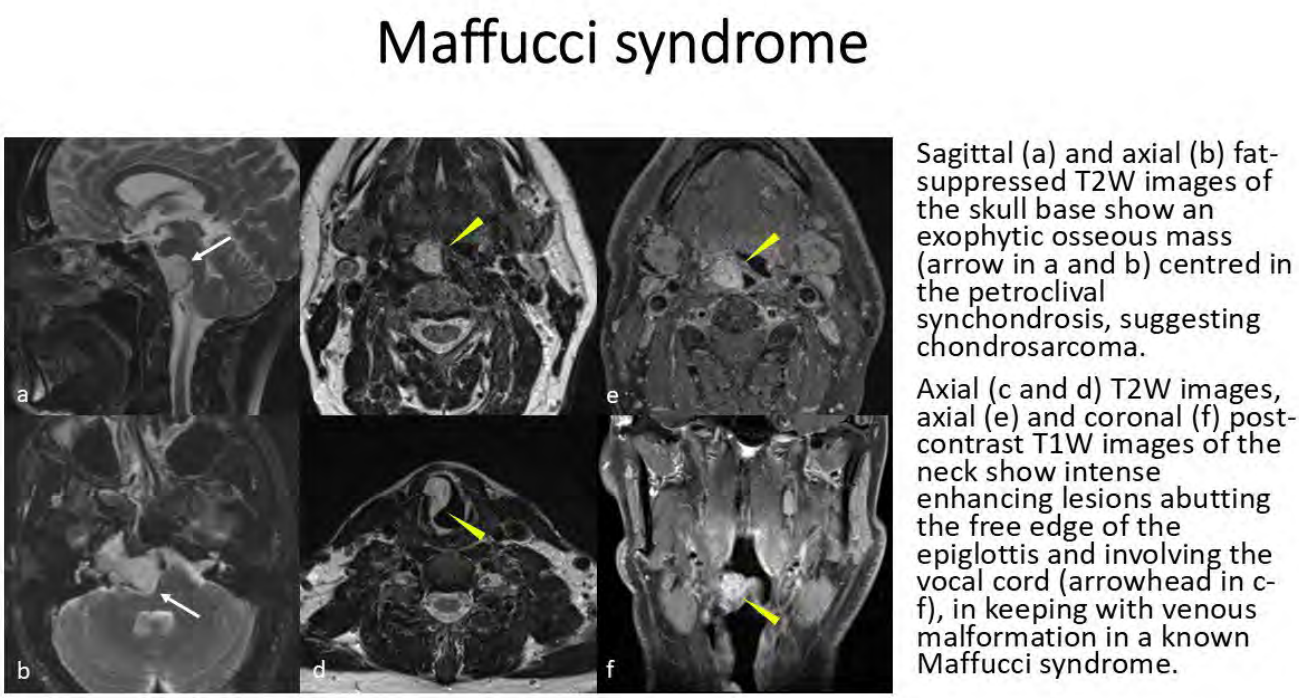

1160 Imaging the Central Nervous System After Radiation Therapy: Changes Beyond Radionecrosis

Omar A Pantoja MD[1], Isaac E Martinez MD[2], Santiago Aristizabal-Ortiz MD[3], Mario Mahecha MD[3], David Timaran-Montenegro M.D., MSCS[4], Susana Calle MD[5], Andres Rodriguez MD[6]

[1]Pontificia Universidad Javeriana, Bogotá, Bogota, Colombia. [2]Universidad Libre, Barranquilla, Barranquilla, Colombia. [3]UT Health Science Center at Houston, Houston, Texas, USA. [4]The University of Texas Health Science Center at Houston, Houston, Texas, USA. [5]The University of Texas MD Anderson Cancer Center, Houston, Texas, USA. [6]The University of Texas Health Science Center,, Hosuton, Texas, USA

Summary & Objectives

1. Describe the mechanisms and temporal classification (acute, early-delayed, late-delayed) of radiation-induced CNS injury.
2. Recognize the imaging characteristics of radiation-induced leukoencephalopathy, pseudoprogression, radiation necrosis, and other major post-RT entities.
3. Differentiate treatment-related changes from tumor recurrence and from infectious, inflammatory, or demyelinating disorders.
4. Apply practical diagnostic strategies using multimodal MRI and advanced techniques to improve accuracy and reduce unnecessary interventions.

Purpose

To provide a comprehensive educational review of CNS imaging findings following radiation therapy, emphasizing the full spectrum of post-treatment effects beyond radionecrosis—including radiation-induced leukoencephalopathy, pseudoprogression, and other non-necrotic entities that may resemble various pathological conditions.

Materials & Methods

A pictorial retrospective review of brain and spine MRI examinations in patients treated with whole-brain radiotherapy (WBRT) or stereotactic radiotherapy/radiosurgery (SRT/SRS). Representative cases were selected to illustrate the range of post-RT manifestations. MRI protocols included T1-weighted pre- and post-contrast, T2/FLAIR, DWI/ADC, GRE/SWI, perfusion, and MR angiography when available. CT and metabolic imaging were reviewed for correlation in selected cases.

Results & Conclusion

Post-radiation CNS changes represent a continuum of tissue injury that varies in timing, distribution, and pathophysiologic substrate. Early and intermediate effects commonly manifest as vasogenic edema or transient alterations in white-matter signal. Late-delayed changes are more complex and encompass radiation-induced leukoencephalopathy, necrotizing leukoencephalopathy, and frank radiation necrosis, which may exhibit variable enhancement, diffusion restriction, or a mass effect and often progress to white matter atrophy. Vascular injury constitutes another important category, including radiation-induced arteritis, moyamoya-like changes, aneurysm formation, and cavernous malformations. Additional patterns include cortical and metabolic syndromes such as SMART, characterized by transient gyriform enhancement and cortical FLAIR hyperintensity, as well as pseudoprogression and pseudoresponse phenomena observed in treated gliomas. Chronic manifestations like mineralizing microangiopathy, hemosiderin deposition, and chronic encapsulated hematoma may appear years after treatment, while spinal cord and cranial nerve injury are less frequent but clinically significant. Secondary neoplasms, though rare, represent a serious late complication. Recognizing the temporal evolution and imaging spectrum of these findings is essential to distinguish post-treatment effects from true progression or other mimicking entities.

Images/Tables

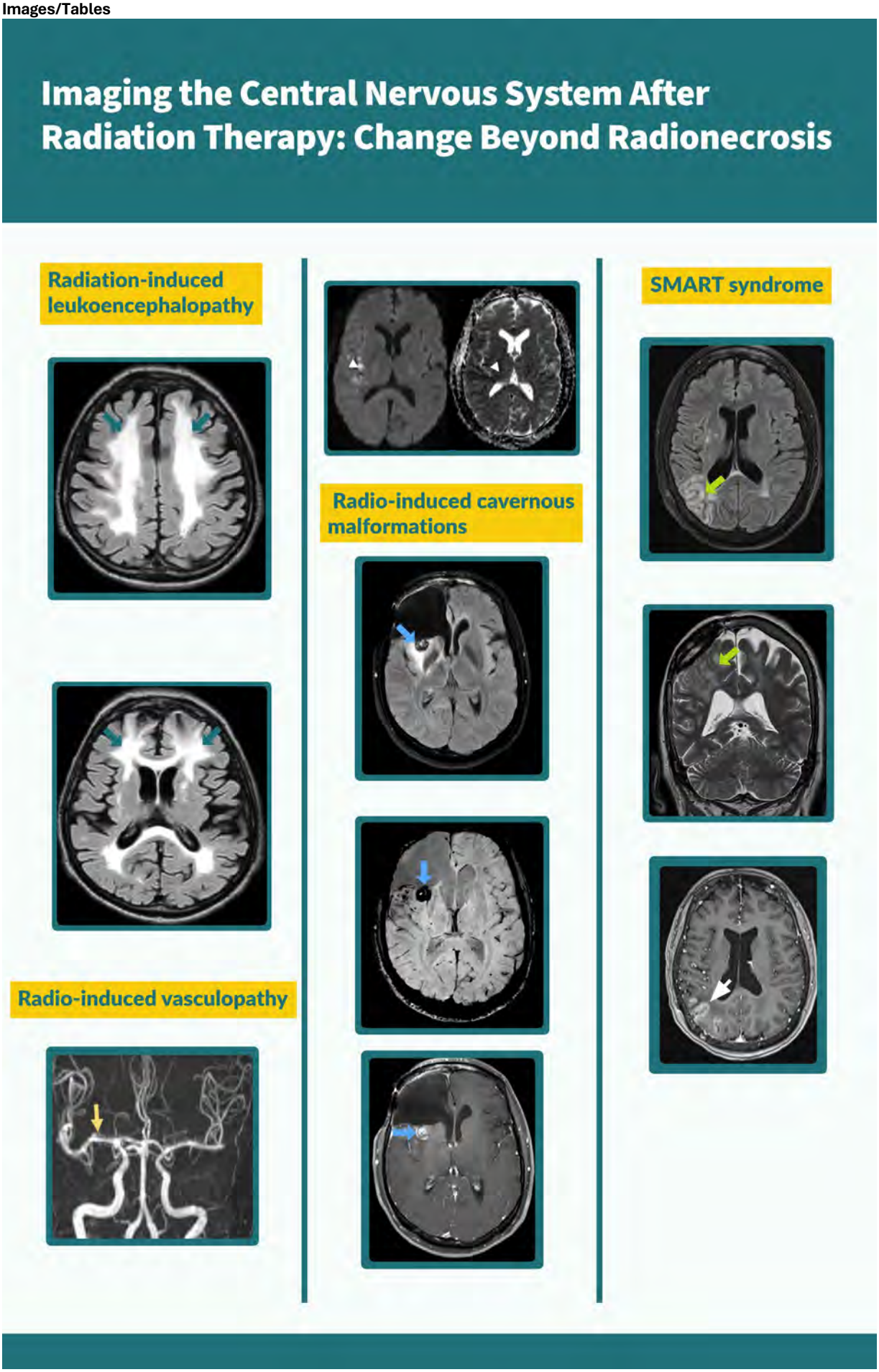

1196 Brachial Plexus MRI: Essential Imaging Insights for Trainees and Radiologists – Case-Based Learning

asif Jamal M.D.
University of Alabama, Birmingham, AL, USA

Summary & Objectives

Summary:
This case-based module provides focused training in brachial plexus MRI interpretation for trainees and practicing radiologists. Using normal anatomy, optimized protocols, and representative pathological cases, learners develop skills for accurate diagnosis. Emphasis is on pattern recognition, systematic evaluation, and clinical correlation.

Objectives:

- Master brachial plexus anatomy (C5–T1 roots to terminal branches)
- Implement standardized, high-resolution MRI protocols
- Develop systematic search patterns for plexus assessment
- Recognize imaging features of common pathologies
- Differentiate traumatic, neoplastic, inflammatory, and compressive etiologies
- Identify normal variants and prevent diagnostic errors
- Correlate imaging findings with clinical management
- Build diagnostic confidence via diverse real-world cases

Purpose

The exhibit addresses the challenges of brachial plexus MRI due to:

- Complex anatomy
- Technical MRI demands
- Wide spectrum of potential pathologies

It highlights the clinical value of:

- Precise surgical planning
- Early intervention for nerve injuries
- Differentiating tumor recurrence from radiation changes
- Predicting functional outcomes via denervation patterns
- Early detection of compressive lesions

Materials & Methods

Case Selection:

- Normal anatomy references and pathological cases from institutional archives
- Selected for diagnostic quality, educational value, and confirmed diagnosis

MRI Protocol:

- **Patient Positioning:** Supine, arms at sides, using neurovascular or phased-array coils
- **Core Sequences:**
    - Coronal STIR (edema, inflammation)
    - Axial T2 Fat-Saturated (nerve morphology)
    - Sagittal T1 (roots and foramina assessment)
    - Post-contrast T1 FS (tumor characterization)
- **Optional Sequences:** 3D STIR/DIXON for isotropic high-resolution imaging
- **Additional as indicated:** DWI, MR myelography, dynamic contrast
- **Scan Time:** ~30–40 minutes
- **Coverage:** Roots → Trunks → Divisions → Cords → Terminal Branches

Pathological Categories:

- Traumatic (avulsion, neuroma)
- Neoplastic (schwannoma, neurofibroma, MPNST)
- Inflammatory (brachial neuritis, post-infectious plexopathy)
- Compressive (thoracic outlet syndrome, cervical rib, Pancoast tumor)
- Radiation-induced and post-surgical/iatrogenic changes
- Each case follows a structured format:
    - **Clinical Vignette:** History, demographics, and symptoms
    - **Imaging Findings:** Annotated key diagnostic features
    - **Systematic Analysis:** Sequential plexus evaluation
    - **Imaging Characteristics:** Signal, morphology, and enhancement patterns
    - **Differential Diagnosis:** Ranked possibilities
    - **Final Diagnosis:** Pathology, clinical decision, follow-up confirmed
    - **Teaching Points:** Core learning objectives.

Results & Conclusion

Results

The standardized protocol provided consistent plexus visualization, high tissue contrast, and reliable pathology detection. Systematic evaluation improved diagnostic confidence, reducing missed findings and false positives. Common pitfalls—inadequate fat suppression, motion artifacts, and subtle T2 changes—were identified and corrected.

The case-based module demonstrated key imaging patterns:

- **Traumatic:** Root avulsion with pseudomeningocele, traction injury (T2 hyperintensity, thickened nerves), muscle denervation.
- **Neoplastic:** Schwannoma (well-defined, T2 bright, homogeneous), neurofibroma ("target sign"), MPNST (irregular, heterogeneous).
- **Inflammatory:** Brachial neuritis with diffuse T2 hyperintensity, nerve enlargement, denervation.
- **Compressive:** Thoracic outlet syndrome showing focal nerve compression and caliber change.
- **Radiation:** Diffuse T2 hyperintensity with minimal enhancement, helping differentiate from recurrence.

Conclusion:

Case-based learning effectively strengthens brachial plexus MRI interpretation by integrating standardized high-resolution protocols with systematic evaluation and pattern recognition. Fat-suppressed sequences provide comprehensive visualization from roots to terminal branches. Recognizing hallmark patterns—pseudomeningocele in avulsion, target sign in neurofibroma, diffuse T2 changes in neuritis—enables accurate etiologic differentiation.

Early diagnosis supports timely intervention, precise localization guides surgery, and distinction between recurrence and radiation effects optimizes oncologic management.

Images/Tables

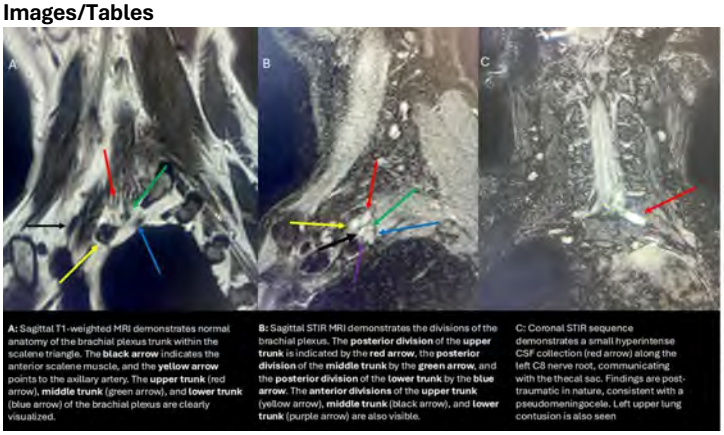

A: Sagittal T1-weighted MRI demonstrates normal anatomy of the brachial plexus trunk within the scalene triangle. The **black arrow** indicates the anterior scalene muscle, and the **yellow arrow** points to the axillary artery. The **upper trunk** (red arrow), **middle trunk** (green arrow), and **lower trunk** (blue arrow) of the brachial plexus are clearly visualized.

B: Sagittal STIR MRI demonstrates the divisions of the brachial plexus. The **posterior division** of the **upper trunk** is indicated by the **red arrow**, the **posterior division** of the **middle trunk** by the **green arrow**, and the **posterior division** of the **lower trunk** by the **blue arrow**. The **anterior divisions** of the **upper trunk** (yellow arrow), **middle trunk** (black arrow), and **lower trunk** (purple arrow) are also visible.

C: Coronal STIR sequence demonstrates a small hyperintense CSF collection (red arrow) along the left C8 nerve root, communicating with the thecal sac. Findings are post-traumatic in nature, consistent with a pseudomeningocele. Left upper lung contusion is also seen

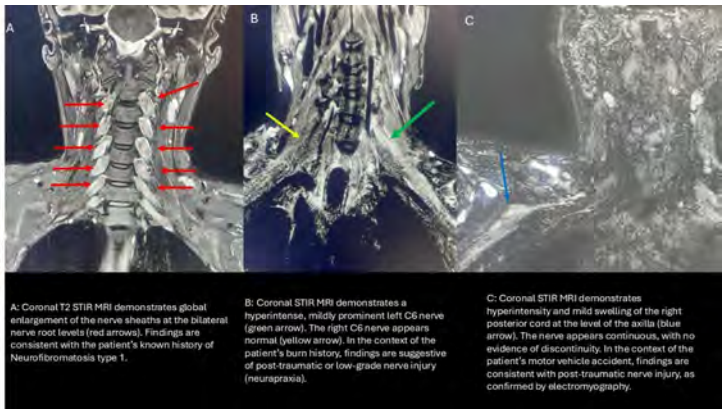

A: Coronal T2 STIR MRI demonstrates global enlargement of the nerve sheaths at the bilateral nerve root levels (red arrows). Findings are consistent with the patient's known history of Neurofibromatosis type 1.

B: Coronal STIR MRI demonstrates a hyperintense, mildly prominent left C6 nerve (green arrow). The right C6 nerve appears normal (yellow arrow). In the context of the patient's burn history, findings are suggestive of post-traumatic or low-grade nerve injury (neurapraxia).

C: Coronal STIR MRI demonstrates hyperintensity and mild swelling of the right posterior cord at the level of the axilla (blue arrow). The nerve appears continuous, with no evidence of discontinuity. In the context of the patient's motor vehicle accident, findings are consistent with post-traumatic nerve injury, as confirmed by electromyography.

1200 Applying RAPNO for Pediatric Brain Tumors: A Reproducible Workflow with RANO Comparison

Mohammad Chaudhry MBBS[1], Fatima Ahmad Qureshy[2], Gagandeep Singh[3]

[1]Columbia University, NY, NY, USA. [2]Sheikh Zayed Hospital, Lahore, Punjab, Pakistan. [3]Columbia University Irving Medical Center (CUIMC), New York, NY, USA

Summary & Objectives

Accurate and consistent assessment of brain tumor response is essential for clinical care, trial enrollment, and longitudinal follow up. The Response Assessment in Neuro-Oncology (RANO) criteria are widely used in adult gliomas, while the Response Assessment in Pediatric Neuro-Oncology (RAPNO) criteria were developed to address the unique behavior and imaging features of childhood tumors. However, practical implementation differs across institutions, and there is limited training material that illustrates how to select measurable lesions, apply criteria, and resolve ambiguous scenarios in real cases.

Objectives:

1. Explain key conceptual differences between RANO and RAPNO.
2. Provide a step-by-step, tumor-specific approach for RAPNO application.
3. Demonstrate reproducible measurement workflows through real MRI examples.
4. Deliver checklists, flowcharts, and case exercises to standardize trainee practice.

Purpose

To create an instructive, case-based exhibit that teaches how to apply RAPNO criteria in pediatric brain tumors while contrasting them with RANO logic in adults. This exhibit aims to equip radiologists, trainees, and researchers with a reproducible and structured approach to lesion selection, measurement, and response categorization, supporting consistency across clinical and research environments.

Materials & Methods

A structured teaching toolkit was developed, consisting of:

- Review of foundational RANO and RAPNO literature.
- Curated de-identified MRI cases representing common pediatric tumor types.
- Side-by-side manual measurement demonstrations (2D products, volumetric notes where applicable).
- Decision flowcharts for choosing measurable disease, confirming progression, and interpreting post treatment changes.
- Interactive worksheets, checklists, and worked examples to simulate real clinical reads.
- Comparison tables illustrating points where RANO and RAPNO diverge in sequence selection, criteria thresholds, and use of longitudinal confirmation scans.

Results & Conclusion

Results:

The educational toolkit provides a step-wise visual method to apply response criteria that improves clarity, supports reproducible measurements, and highlights key differences between adult and pediatric response frameworks. Through real MRI examples and guided exercises, users learn how RAPNO uniquely manages pediatric tumor heterogeneity, non-enhancing disease, and disease confirmation requirements. Participants gain practical skills in consistent lesion selection, tracking, and documentation.

Conclusion:

A standardized, case-rich workflow enhances confidence and consistency in response assessment across trainees and practitioners. This exhibit supports adoption of tumor specific RAPNO criteria in clinical practice and builds a foundation for future quality improvement and AI-assisted measurement initiatives.

---

717 Beyond the Node: Recognizing Imaging Extranodal Extension (iENE) in HPV-Positive Head and Neck Squamous Cell Carcinoma

Karla Anabel Borgna MD, Cecilia Elizabeth Marenco MD, Tatiana Gillanders MD, Manuel Sliman Perez Ackly MD, Cristina Hilda Besada MD
hospital italiano, buenos aires, buenos aires, Argentina

Summary & Objectives

1. Identify key imaging features of extranodal extension (iENE) in HPV-positive head and neck squamous cell carcinoma.
2. Differentiate iENE from other nodal changes
3. Recognize its prognostic and therapeutic implications.
4. Apply a systematic imaging approach to improve detection accuracy and reduce interpretation pitfalls in the evaluation of iENE.

Purpose

To improve neuroradiologists' ability to detect subtle iENE in HPV-positive HNSCC, correlating imaging findings with pathology and outcomes. Promote a systematic nodal evaluation incorporating perinodal changes.

Materials & Methods

This educational exhibit presents selected cases from our institutional experience in the follow-up of head and neck squamous cell carcinoma, focusing on HPV-positive disease.

Cases of patients with HPV-positive squamous cell carcinoma and representative nodal metastases were reviewed using contrast-enhanced MRI and CT studies. Clinical findings, including the surgeon's assessment of nodal fixation or extracapsular spread on palpation, were recorded and correlated with imaging features and histopathology. Findings were classified according to the AOSNHNR–ASHNR–ESHNR Joint Task Force Imaging Guidelines.

Results & Conclusion

The presentation is organized to illustrate the imaging spectrum of imaging extranodal extension (iENE) in HPV-positive nodal metastases, with examples across modalities and correlation with histopathology when available.

MRI and CT findings were categorized according to the AOSNHNR–ASHNR–ESHNR Joint Task Force Imaging Guidelines:

Grade 1: Smooth or minimally irregular nodal margins without evidence of capsular breach.

Grade 2: Focal capsular disruption with minimal perinodal fat stranding.

Grade 3: Gross extranodal extension with invasion of adjacent soft tissues or neurovascular structures.

Representative cases demonstrate how MRI offers superior soft-tissue contrast for detecting early perinodal fat infiltration and subtle capsular irregularities compared to CT.

Examples of false positives (early post-biopsy inflammation, fibrosis, or treatment-related changes) are included to highlight common pitfalls in interpretation.

Key teaching points include:

- HPV-positive tumors may exhibit iENE—do not overlook it.
- iENE impacts staging and adjuvant therapy.
- MRI enhances detection when CT is inconclusive.

Conclusion:

Accurate identification of iENE is crucial in HPV-positive head and neck squamous cell carcinoma, as it directly influences staging, prognosis, and the possibility of adjuvant therapy.

Radiologists should be aware of imaging signs and recognize potential mimickers related to treatment effects.

The integration of a structured approach, combining clinical and morphological findings obtained from pre and post-contrast CT and MRI, improve diagnostic confidence and interobserver consistency.

Ultimately, early and accurate recognition of iENE enhances multidisciplinary decision-making and contributes to a tailored management in HPV-associated head and neck cancer.

Images/Tables

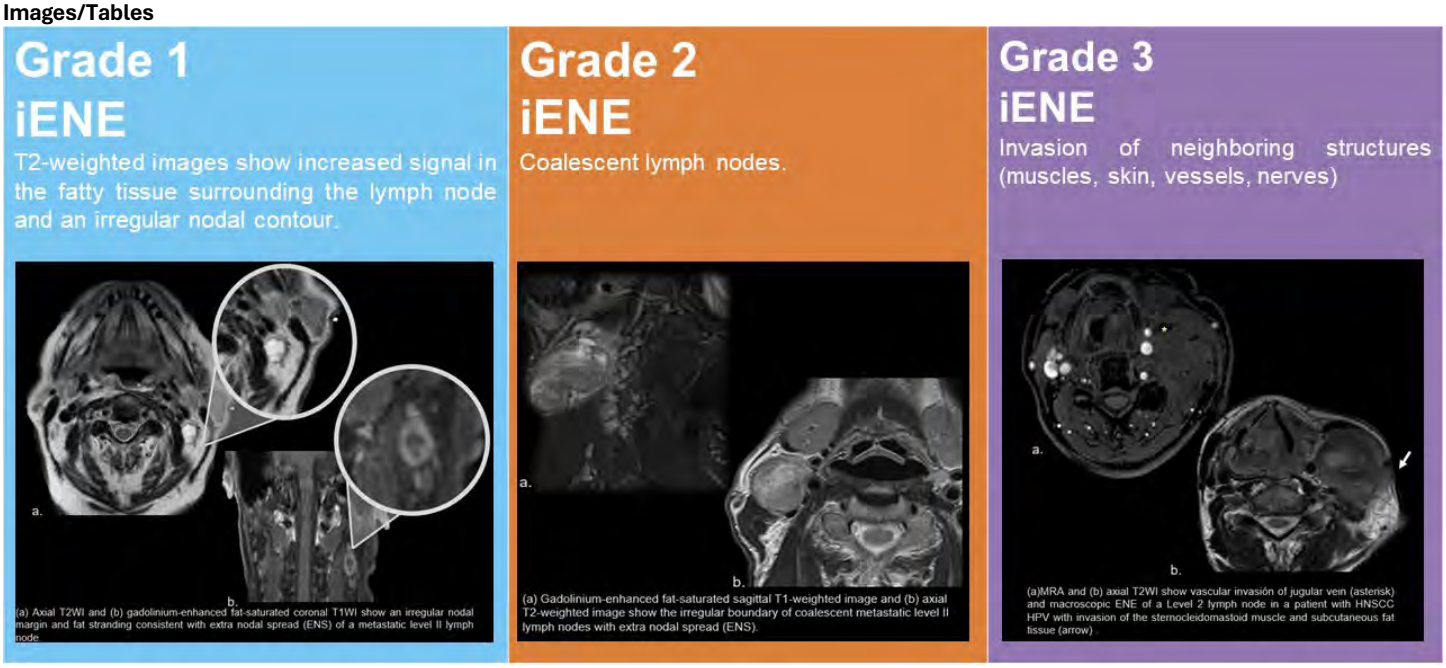

---

910 A Series of Unfortunate Vessels: Central Nervous System Vasculitis, Demystifying the Diagnosis.

Diego J Cebrian Chaustre MD, Derek Grady MD, Scott McNally MD, PhD., Blair A Winegar MD, Karen L Salzman MD
University of Utah Health, Neuroradiology, Salt Lake City, Utah, USA

Summary & Objectives

1. Review the classic imaging features of Central Nervous System (CNS) vasculitis on CT, DSA, MR and vwMRI.
2. Discuss the typical clinical features of vasculitis and treatment options.
3. Review potential mimics of vasculitis with key clinical and imaging features to differentiate from vasculitis.

Purpose

To review the evaluation of CNS vasculitis from an imaging standpoint. This has classically been a somewhat elusive diagnosis to the radiologist. Conventional imaging, such as Digital subtraction angiography (DSA) typically shows alternating stenosis with dilatation primarily involving second and third order branches, and Magnetic Resonance Imaging (MRI) of the brain can present classic features including multifocal infarcts and subarachnoid hemorrhage. However, neither directly images the pathologic process (inflammation of the vessel wall), but rather the downstream effects of it, and often tissue biopsy is required. However, given segmental distribution of inflammation along the vessel length implies the risk for sampling errors and false negatives. Modern imaging techniques like Vessel wall magnetic resonance imaging (vwMRI) may show smooth, concentric, long segment enhancement of the vessels involved. This however corresponds to endothelial dysfunction and leakage of contrast through the Blood-Brain Barrier, rather than inflammation itself. But it can be key to an accurate diagnosis and help identify an adequate target for tissue sampling, increasing its diagnostic yield.

Materials & Methods

Central nervous system (CNS) vasculitis includes a variety of pathologic processes including primary arteritis of the CNS (PACNS) and secondary to systemic vasculitis, including etiologies such as infectious/inflammatory processes, granulomatous disease, collagen vascular disease, drug abuse or radiation therapy.

Over the course of this educational exhibit, we will present several cases of both primary and secondary CNS vasculitis, while discussing its typical imaging findings, as well as potential mimics, including reversible cerebral vasoconstriction syndrome (RCVS), intravascular large B-cell lymphoma, neurosarcoidosis, and cerebral amyloid beta-related angiitis.

Results & Conclusion

CNS vasculitis, both primary and secondary, are important diagnosis for the neuroradiologist. Though rare, early suspicion and identification is key in preventing significant morbidity both from the process and from the diagnostic work up. New imaging techniques (vessel wall MRI) can be key in the diagnosis of the disease, however certain limitations persist, and ultimately, tissue diagnosis might be inevitable. Even more, potential mimics can confound adequate/early diagnosis and/or treatment and should be known by neuroradiologist as well.

Images/Tables

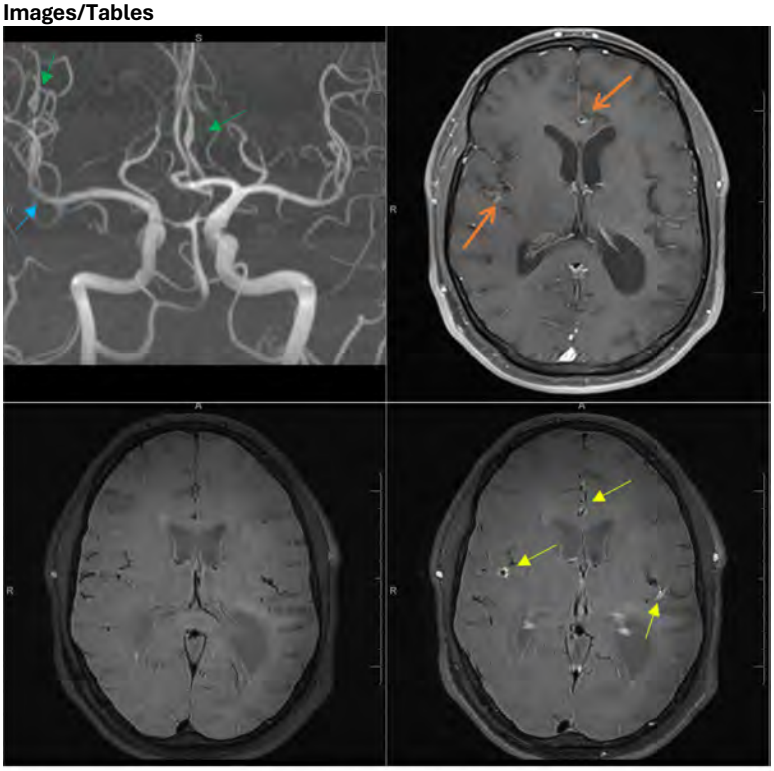

38-year-old male with a PMH of HIV and neurosyphilis, and secondary CNS vasculitis. Multifocal fusiform dilatation of the of the right M2 MCA and left A2 ACA (green arrows in the top left, MRA MIP image), associated with diffuse enhancement in T1 post contrast images (orange arrows). Additionally, luminal irregularity and diffuse narrowing of the right M1 is seen (blue arrow).
On the bottom images (Left to right: Pre and post contrast T1 DANTE sequence), there is diffuse wall enhancement (yellow arrows) of the right MCA and left ACA vessels, predominantly at the area with fusiform aneurismal dilatation.

---

254 Basivertebral Nerve Ablation: A Minimally Invasive Approach to Vertebrogenic Low Back Pain

Kathleen Kilroe B.S[1], Andrew J. Song B.S[1], Jamie E Clarke M.D., M.S.[2], Jay Acharya M.D.[2]
[1]David Geffen School of Medicine at the University of California Los Angeles, Los Angeles, California, USA. [2]Division of Neuroradiology, Department of Diagnostic Radiology, University of California Los Angeles (UCLA), Los Angeles, California, USA

Summary & Objectives

This educational exhibit will summarize the anatomy and pathophysiology of the basivertebral nerve and its role in vertebrogenic low back pain. It will identify imaging findings, including Modic type 1 and type 2 changes on MRI, that correlate with vertebrogenic pain and support the use of basivertebral nerve ablation (BVNA). The exhibit will also describe the technique of image-guided BVNA, including procedural steps, ablation approach, and contraindications. Finally, it will review the clinical evidence supporting the use of BVNA in patients with chronic axial low back pain.

Purpose

Our aim is to review the imaging and procedural technique of basivertebral nerve ablation for vertebrogenic low back pain, focusing on the neuroradiologist's role in diagnosis and treatment.

Materials & Methods

Vertebrogenic pain, a subtype of chronic low back pain, arises from degeneration of the vertebral endplates. The basivertebral nerve, a branch of the sinuvertebral nerve, enters the vertebral body via the basivertebral foramen, most commonly at L3–S1, and bifurcates to innervate the superior and inferior endplates. Degenerated endplates sensitize the BVN, producing chronic axial pain that is often resistant to standard management. Imaging correlates of basivertebral nerve damage include Modic type 1 and 2 changes on Magnetic Resonance Imaging. Type 1 demonstrates T1 hypointensity and T2 hyperintensity, reflecting endplate inflammation, while type 2 appears hyperintense on both sequences, indicating fatty marrow replacement. These findings, combined with clinical assessment, identify vertebral endplate damage and guide patient selection for basivertebral nerve ablation. Basivertebral nerve ablation (BVNA) is a minimally invasive procedure that uses intraosseous radiofrequency energy to disrupt nociceptive fibers of the BVN. It is indicated for patients with chronic vertebrogenic low back pain (≥6 months) unresponsive to conservative therapy and with Modic type 1 or 2 changes on MRI. The procedure is typically performed via a transpedicular or parapedicular approach under fluoroscopic or CT guidance, advancing a trocar into the posterior vertebral body (30–50% anterior to the posterior wall) and ablating the BVN at 85–90°C for 15 minutes. Randomized trials show BVNA yields durable pain and functional improvements, with 64–75% of patients achieving ≥50% pain relief and ≥15-point Oswestry Disability Index improvement at 12 months, maintained up to 5 years. The neuroradiologist plays a key role in identifying imaging findings, selecting appropriate patients, and performing image-guided BVNA safely and effectively.

Results & Conclusion
When combined with the appropriate back pain history, identifying Modic type 1 and 2 changes on MRI can help radiologists confirm endplate damage that may be amendable to treatment via BVNA. BVNA represents an emerging, targeted image-guided therapy offering durable pain relief and functional improvement for patients with chronic vertebrogenic low back pain.
Images/Tables

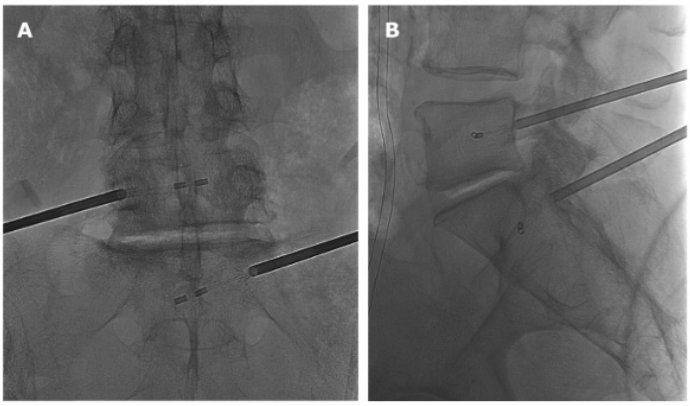

Figure. AP (Panel A) and lateral (Panel B) fluoroscopic views demonstrating bipolar radiofrequency probe placement for basivertebral nerve ablation at the L5–S1 level.

---

340 Mind the Gap: Imaging the Spectrum of Skull Base Cephaloceles
Dhanush Amin MD[1], Raman Deep MD[2]
[1]UAMS, Little Rock, AR, USA. [2]UAB, Birmingham, AL, USA
Summary & Objectives
Skull base cephaloceles are herniations of intracranial contents through congenital, acquired, or spontaneous bony defects of the skull base. These lesions may present with cerebrospinal fluid (CSF) leak, meningitis, or be incidental findings on imaging. Accurate localization and characterization of the defect are crucial for surgical planning and prevention of recurrent CSF leaks.
Objectives:
1. To review the anatomy of the skull base relevant to cephaloceles.
2. To illustrate the imaging features of cephaloceles involving different skull base sites — including the sphenoid sinus, cribriform plate, ethmoid roof, petrous apex, jugular foramen, and occipital bone.
3. To discuss the role of multimodality imaging in diagnosis and preoperative evaluation.
4. To highlight pitfalls and mimics that may lead to misinterpretation.

Purpose
Cephaloceles of the skull base represent an important cause of spontaneous CSF rhinorrhea or otorrhea and may be associated with idiopathic intracranial hypertension, trauma, or prior surgery. Their detection on imaging requires careful assessment of subtle bony and soft tissue findings. The exhibit aims to provide a structured, region-based imaging approach to identifying skull base cephaloceles, emphasizing the role of high-resolution CT and MRI correlation in establishing diagnosis and guiding management.
Materials & Methods
A retrospective review of imaging studies from our neuroradiology database was performed to identify patients with skull base cephaloceles. CT and MRI examinations were analyzed to determine the site, extent, and type of herniated content (meningocele vs. meningoencephalocele). Representative cases were categorized based on anatomic location:
- **Anterior cranial fossa:** Cribriform plate and ethmoid roof defects.
- **Sphenoid bone:** Lateral recess of sphenoid sinus, sphenoid wing, and foramen rotundum.
- **Temporal bone:** Tegmen tympani, petrous apex, and jugular fossa.
- **Posterior fossa:** Occipital and clival cephaloceles.

Each case was correlated with clinical presentation, surgical findings (when available), and etiologic factors (congenital, traumatic, spontaneous, or postoperative).
Results & Conclusion
Skull base cephaloceles encompass a diverse group of defects that may occur at multiple anatomic locations. Recognition of their imaging characteristics on CT and MRI is essential for accurate diagnosis, differentiation from mimics, and optimal surgical planning. A region-based systematic approach ensures comprehensive evaluation and prevents misdiagnosis in this clinically significant entity.

Images/Tables

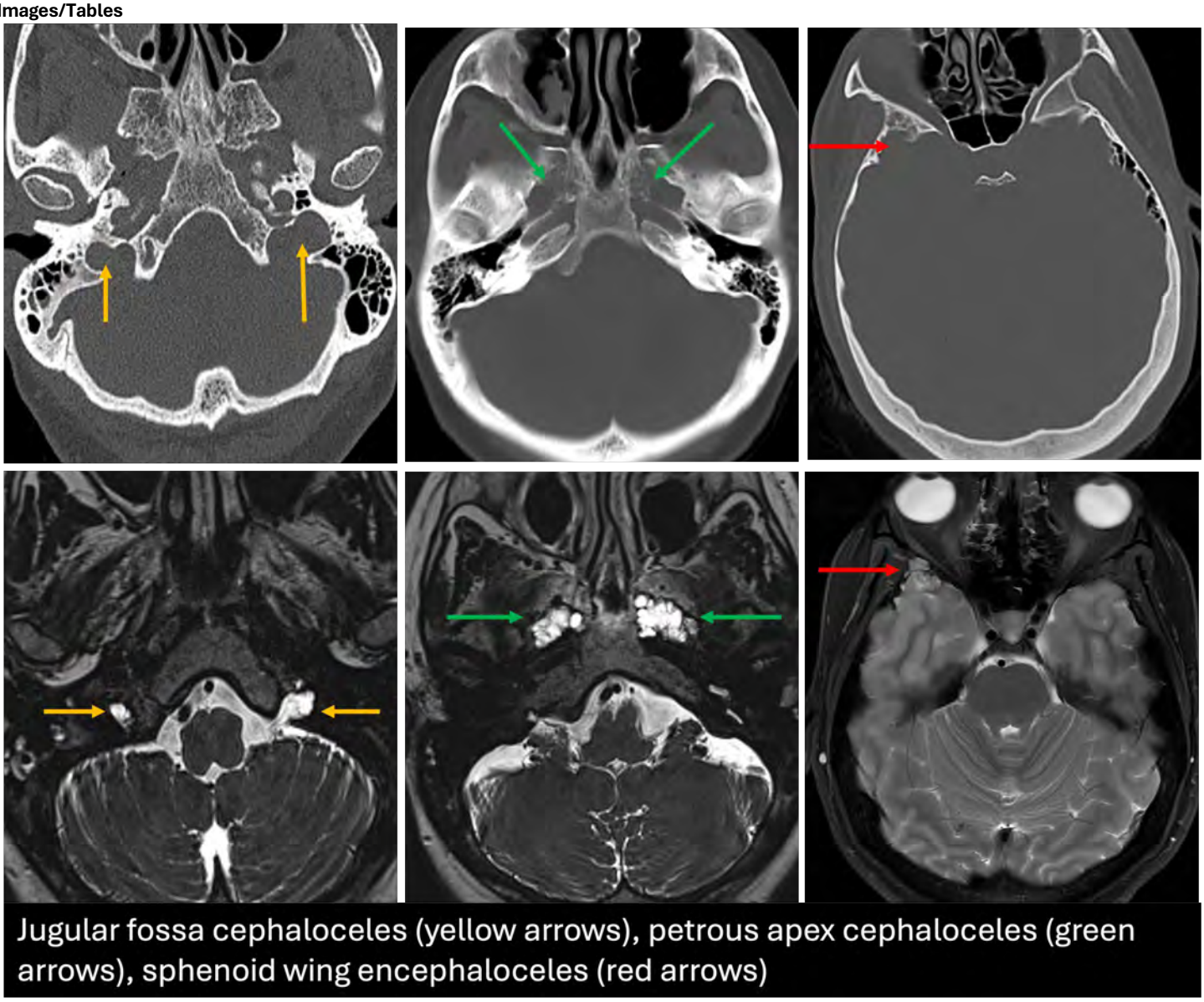

483 Imaging Neurotoxicity in CAR T-Cell Therapy: A Neuroradiologist's Perspective

Rachel Saks MD, Hossein Nejadnik MD
Hospital of the University of Pennsylvania, Philadelphia, PA, USA

Summary & Objectives

As of 2017, chimeric antigen receptor (CAR) T-cell therapies have been FDA approved for the treatment of various hematologic malignancies in children and adults, such as leukemia, lymphoma, and multiple myeloma. Additionally, there are ongoing efforts to apply CAR T-cell therapies for the treatment of solid tumors, including intracranial neoplasms like glioblastoma. Despite this evolving and expanding role of CAR T-cells in cancer treatment, literature regarding CAR T-cell neurotoxicity is scarce. The objective of this investigation was to demonstrate the expected imaging findings associated with CAR T-cell toxicity, in particular immune effector cell–associated neurotoxicity syndrome (ICANS).
This exhibit aims to:
1. Review the clinical symptoms and timing of CAR T-cell therapy related neurotoxicity
2. Illustrate key neuroimaging manifestations of CAR T-cell therapy related neurotoxicity
3. Correlate imaging findings with laboratory markers, clinical parameters, and treatment responses
4. Provide a systematic interpretive framework to help neuroradiologists recognize CAR T-cell related neurotoxicity

Purpose

The purpose of this educational exhibit is to enhance neuroradiologist's understanding of the imaging characteristics, temporal evolution, and diagnostic pitfalls associated with CAR T-cell neurotoxicity, particularly ICANS, in order to provide prompt and comprehensive guidance for clinical management and contribute to safer implementation of cellular immunotherapies in oncologic care.

Materials & Methods

A clinical review of patients who underwent CAR T-cell therapy for hematologic and solid tumors at our institution from 2022-2025 was performed. Subsequently, included patient's brain MRIs were analyzed for characteristic imaging patterns of CAR T-cell therapy related neurotoxicity, including ICANS . Data abstracted from medical records included primary neoplasm/tumor type and prior intervention (surgery or radiation therapy, timing relative to infusion, ICANS grade, and relevant laboratory/immunologic markers. Representative published examples were also reviewed.

Results & Conclusion

A total of 50 patients were reviewed. Neuroimaging abnormalities were most common within 4–14 days post-infusion, coinciding with peak cytokine elevation. MRI demonstrated reversible FLAIR signal abnormality (PRES-like pattern) in mild cases, while severe ICANS showed diffuse cortical edema, deep gray involvement, leptomeningeal enhancement, and occasional hemorrhagic changes.

Approximately 30% of clinically diagnosed cases demonstrated no definitive imaging correlate, emphasizing the need for vigilance for subtle or evolving findings.

Our ongoing work is focused on correlating imaging features with laboratory markers, clinical parameters, and treatment responses, though these data are not yet mature to be included in this abstract.

Neuroimaging findings associated with post CAR T-cell related neurotoxicity presents with a broad imaging spectrum ranging from subtle cortical edema to diffuse encephalopathy, leptomeningeal enhancement, and hemorrhagic changes.

While still a relatively novel therapy, CAR T-cells have the potential to revolutionize cancer treatment. Imaging is integral to monitor not only disease progression and treatment response, but also to evaluate for potential treatment-related adverse events, particularly in severe or atypical presentations, and may inform pathophysiological understanding and management strategies. It is critical that neuroradiologists familiarize themselves with the imaging findings associated with these adverse events to help guide prompt intervention, as the role of CAR T-cell in cancer treatment continues to expand and evolve.

Images/Tables

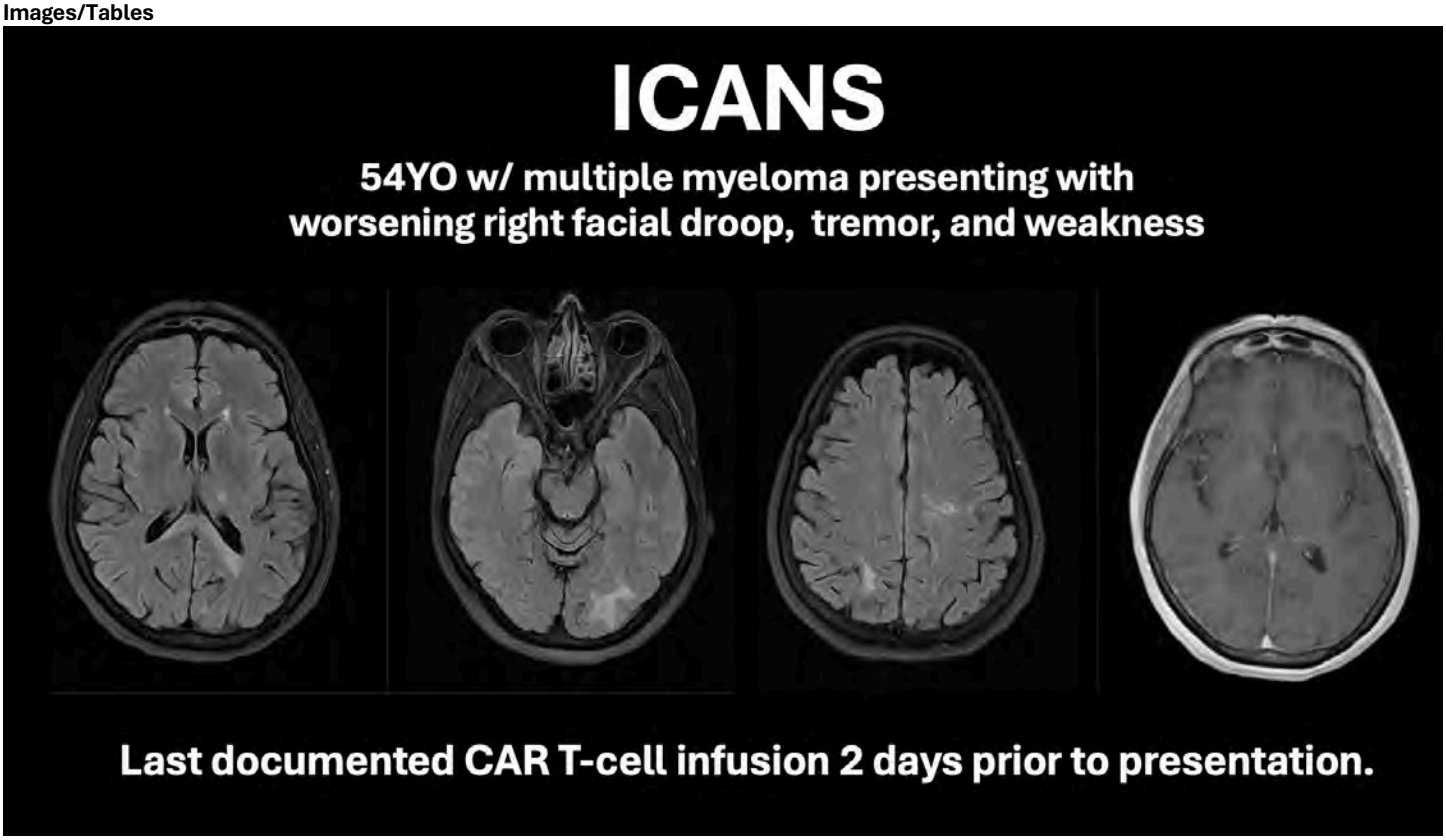

---

566 Lost in Transition: The Importance of Correctly Identifying and Characterizing Lumbosacral Transitional Anatomy

Harrison Lang M.D., Nicholas Koontz M.D., Jeffrey Ross M.D., Tanya Rath M.D.
Mayo Clinic Arizona, Phoenix, Arizona, USA

Summary & Objectives

Despite its relatively high prevalence, lumbosacral transitional anatomy (LSTA) is often underrecognized, underreported, and misunderstood by radiologists and other clinicians which leads to it being a common source of diagnostic error. Correctly identifying and characterizing LSTA is crucial for accurate reporting, surgical planning, and procedural intervention and can help avoid the dreaded complication of wrong-level spinal surgery. Radiologists are often the first clinicians to assess a patient's spinal anatomy when imaging is obtained. This creates an important opportunity for the radiologist to add value to the patient's care by ensuring the radiologist, treatment team, and patient are on the same page regarding patient anatomy. The objectives of this educational exhibit are as follows:

-Highlight the clinical significance of transitional anatomy
-Differentiate "normal" vs. lumbosacral transitional anatomy (LSTA)
-Show the wide range of morphologies that can be seen with LSTA and their imaging appearance across multiple modalities (radiograph, CT, and MRI)
-Share multiple methods ("tips and tricks") to help accurately identify and label LSTA
-Provide a structured approach to accurately characterizing LSTA

Purpose

Lumbosacral transitional anatomy (LSTA) has a high estimated prevalence between 4-30%. Inaccurate characterization of LSTA by the radiologist can lead to incorrect reports, confusion between the radiologist and treatment team/surgeon, and possibly lead to wrong-level spinal surgery. The exhibit will educate radiologists on how to identify and correctly characterize LSTA with the hopes of avoiding these problems. This begins with understanding "normal" vertebral numbering and how LSTA differs from "normal". The exhibit then provides the learner with multiple methods to aid accurate

vertebral numbering (across multiple modalities) including whole-spine imaging, morphologic features of the lumbosacral junction, Castellvi classification, nerve root morphology, amongst others. Finally, the learner is provided with a structured approach so they can immediately implement these methods into clinical practice.

Materials & Methods

N/A

Results & Conclusion

Correctly identifying and characterizing lumbosacral transitional anatomy is important due to its relatively high prevalence and potential to mitigate risk of wrong-level spinal surgery.

Images/Tables

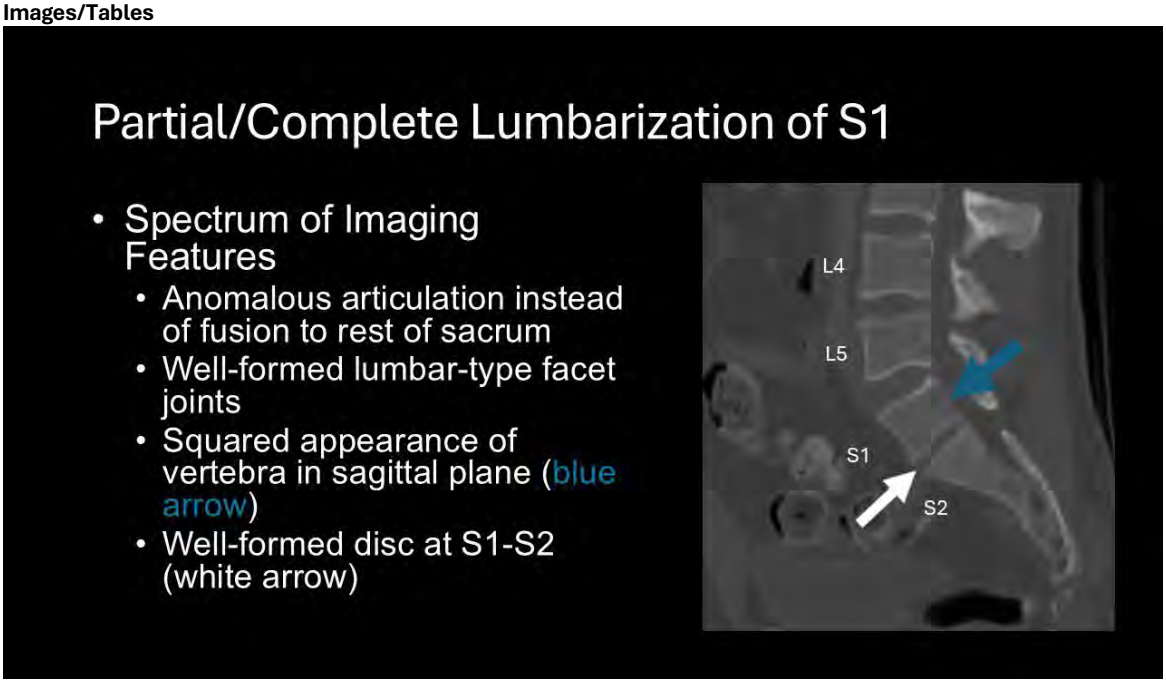

---

797 Multimodal Generative AI Models in Radiology: Foundations, Applications, and Clinical Frontiers

Annie Singh[1], Prabhnoor Kaur[2], Moinak Bhattacharya[3], Angela Lignelli MD[4], Gagandeep Singh MD[4]

[1]Atal Bihari Vajpayee Institute of Medical Sciences, New Delhi, Delhi, India. [2]Guru Gobind Singh Medical College and Hospital, Faridkot, Punjab, India. [3]Department of Computer Science, Stony Brook University, Stony Brook, New york, USA. [4]Neuroradiology Division, Columbia University Irving Medical Center, New York, New York, USA

Summary & Objectives

Learning Objectives:

- Provide radiologists with a concise overview of multimodal and generative AI frameworks in imaging.
- Highlight key model types and their role in image synthesis, reconstruction, and integration.
- Evaluate the clinical utility of generative AI for missing sequence reconstruction, radiogenomic inference, and treatment response simulation using real-world case studies.
- Outline core limitations, including data bias, hallucination risks, and challenges in anatomic fidelity and generalizability.

Summary:

Multimodal AI frameworks are increasingly being recognized as impactful approaches in advancing healthcare analytics due to their ability to interpret and integrate disparate forms of medical data, such as imaging, clinical, and genomic information, much like the daily tasks of radiologists aimed at improving diagnostic accuracy and patient outcomes. Within this ecosystem, generative AI models play a pivotal role by learning underlying data distributions and enabling the creation of new, similar data samples while capturing the underlying information effectively.

Among these, Generative Adversarial Networks (GANs) use a generator and discriminator that compete during training, improving image realism and diagnostic plausibility. In neuroimaging, GANs are used for missing sequence reconstruction, such as generating FLAIR or post-contrast images from existing T1 and T2 scans to complete studies and minimize rescans. Diffusion models learn to add and remove noise, enabling high-fidelity image generation for tissue synthesis and treatment response simulation, accurately depicting subtle tumor or edema changes. Graph Neural Networks (GNNs), meanwhile, represent data in a graph-structured format, making them particularly useful to multimodal imaging where relationships between features (e.g., anatomical structures and genetic markers) are critical. For instance, in oncology, a GNN model was used to predict regional lymph node metastasis in esophageal squamous cell carcinoma. Fusion techniques combine these data streams: early fusion integrates raw features, joint fusion merges intermediate representations, and late fusion aggregates final predictions. Each supports different goals, from radiogenomic mapping to cross-sequence reconstruction and treatment outcome prediction.[1]

Despite their promise, these technologies face major challenges, including limited high-quality datasets and model bias from overfitting on narrow samples. Such issues can produce hallucinations, anatomical inaccuracies, and unstable outputs, reducing clinical reliability. Unmonitored synthetic data generation may also amplify biases or misrepresent pathology, limiting generalizability.[2]

Multimodal generative AI nonetheless marks a transformative advance toward biologically informed, data-driven radiology. Its clinical success will depend on radiologist's active roles in interpreting outputs, validating models, and establishing standards for safety and transparency. This exhibit enables participants to understand these models and their responsible integration to enhance neuroimaging practice.

Purpose

To bridge the knowledge gap among radiologists by elucidating how multimodal generative AI models function and impact clinical imaging, addressing the need for a clear understanding of their mechanisms, reliability, and implications for patient care as these tools begin to influence radiology workflow.

Materials & Methods

Key generative model architectures and their imaging applications were reviewed through illustrative case studies and current literature, emphasizing clinical relevance and potential implementation pathways.

Results & Conclusion

A clear understanding of generative AI principles and limitations enables radiologists to critically evaluate, validate, and responsibly integrate these technologies into clinical practice.

Images/Tables

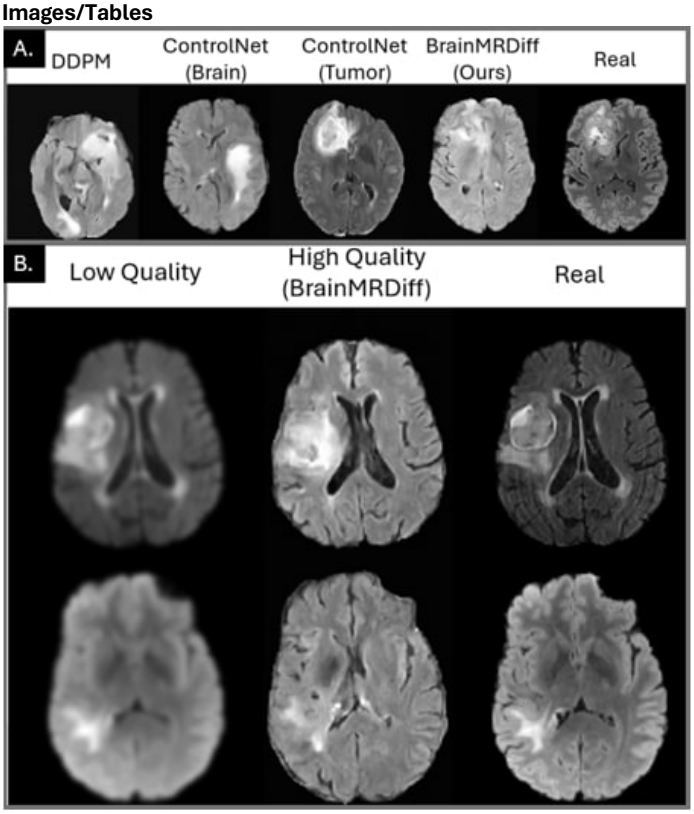

(A) Comparison with existing generative methods: A synthetic MRI generated using BrainMRDiff demonstrates markedly improved anatomical consistency compared to baseline models.

(B) Image quality enhancement: A low-quality or artifact-affected input scan is shown alongside the corresponding high-quality image generated by BrainMRDiff, illustrating its potential utility in restoring diagnostic image quality and preserving clinically relevant features.

---

849 **Duck Versus Squirrel: Recognizing Incomplete Hippocampal Inversion**

Anish Neupane MD[1], Neil Tishkoff MD[2], Kamal Kandel MD[1], Aryan Hemani MD[1], Gaurav Cheraya MD[1], Rowa Mohamed MD[1], Pranita Paudyal MD[1]
[1]YNHH/Bridgeport Hospital, Bridgeport, CT, USA. [2]YNHH/Bridgeport Hospital/Yale University, Bridgeport, CT, USA

Summary & Objectives

Introduction

The Hippocampus is situated in the medial temporal lobe and consists of two abutting gray matter structures: the cornu Ammonis and dentate gyrus. It plays an important role in spatial and episodic memory. Mesial temporal (hippocampal) sclerosis is the most common association with intractable temporal lobe epilepsy. MRI is the optimal imaging modality for hippocampal evaluation with high resolution coronal T2 being the preferred sequence to evaluate the hippocampal anatomy.

Development of hippocampus

The hippocampus is formed by allocortex with gradual in-folding of the dentate gyrus and cornu Ammonis surrounding a hippocampal sulcus by a process called hippocampal inversion. This process occurs between 9-21st week of gestation. Loss of such migration and neurogenesis results in incomplete hippocampal inversion.

Incomplete Hippocampal Inversion (IHI)

IHI is an important finding to recognize epilepsy patients and has a high prevalence of approximately 56%. However, IHI is unusual in patients without seizures. This finding could also point to other areas of brain maldevelopment leading to epilepsy. IHI has also been found to be an independent predictor for temporal lobe epilepsy, extra temporal lobe epilepsy and drug-resistant epilepsy. There have been described associations with complex

prefrontal dysfunction, visual hallucinations, febrile convulsions and sudden unexplained death. IHI is more often unilateral on the left side or bilateral. IHI can be diagnosed with high quality magnetic resonance imaging.
MRI Imaging Appearance of Incomplete Hippocampal Inversion (IHI)
The normal hippocampal body has a transverse orientation with respect to the parahippocampal gyrus and an obliquely oriented collateral sulcus resembling the appearance of a mallard duck. The parahippocampal angle formed by the ascending and descending portion of parahippocampal gyrus is normally obtuse. However, with Incomplete Hippocampal Inversion, the hippocampal body appears globular, is positioned more medially and oriented vertically with respect to the parahippocampal gyrus. There is also vertical orientation of the collateral sulcus which lies lateral to the hippocampus with an acute parahippocampal angle. The subiculum may be bulged rather than flattened. This creates an appearance similar to the standing squirrel with head and body representing the vertically oriented globular hippocampus with its tail representing the vertically oriented collateral sulcus. Loss of internal architecture of hippocampus has also been described.

Purpose

To describe Duck Versus Squirrel appearance as an imaging sign for diagnosing Incomplete Hippocampal Inversion

Materials & Methods

NA

Results & Conclusion

The ability to recognize the Duck versus Squirrel morphologic appearance of the hippocampus on MRI will help radiologists more easily identify the normal hippocampus versus Incomplete Hippocampal Inversion, which is highly associated with epilepsy.

Images/Tables

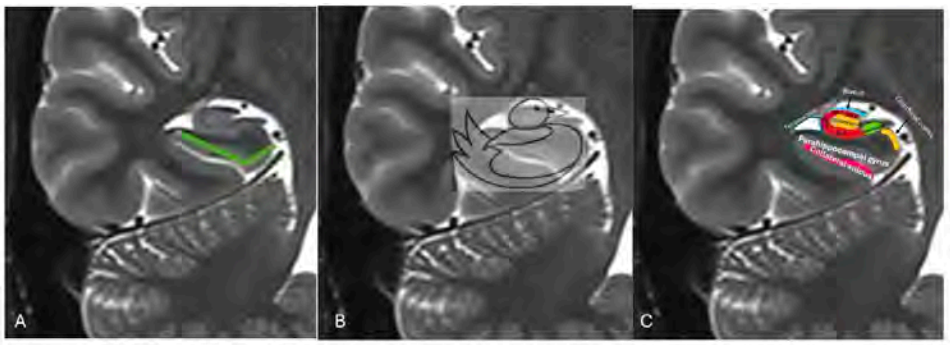

Normal hippocampus: T2 coronal image of right temporal lobe demonstrates hippocampus similar in appearance to a mallard duck(B) with Dentate gyrus and Cornua Ammonis forming the duck's head which is positioned laterally with respect to the duck's breast formed by the subiculum and entorhinal cortex. The collateral sulcus is angled obliquely and superiorly forming the duck's tail. There is normal obtuse parahippocampal angle as outlined in image A.

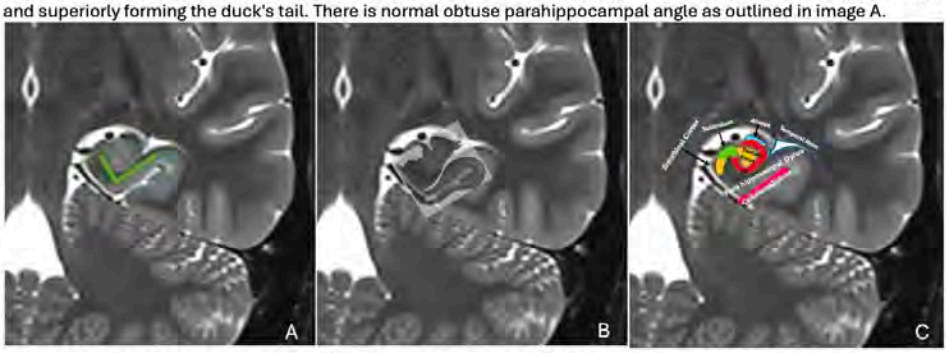

Incomplete hippocampal inversion (IHI): T2 coronal image of the left temporal lobe (A) demonstrates globular appearing left hippocampus(Dentate gyrus and Cornua Ammonis) resembling the squirrel's head and neck(B), bulged subiculum(green) resembling squirrel's hands(B) and vertically oriented collateral sulcus resembling squirrel's tail(B). There is also acute parahippocampal angle as outlined in image A.

---

857 The Great Imitator Revealed: Neuroradiologic Faces of IgG4-Related Disease

Jeya Anandakumar B.Sc[1], Khaleel Atkinson B.Sc[1], Tochukwu M Duru M.B.B.S[2], Erini Makariou MD[2], Earn Chun Christabel Lee MD[2]
[1]Georgetown University School of Medicine, Washington, District of Columbia, USA. [2]Medstar Georgetown University Hospital, Washington, District of Columbia, USA

Summary & Objectives

IgG4-related disease (IgG4-RD) is a rare, immune-mediated condition characterized by elevated serum IgG4 levels and tissue infiltration by IgG4-positive plasma cells. It typically progresses over long periods of time causing chronic inflammation and fibrosis. Patients suffer functional deficits due to mechanical compression of vascular or nerve structures. Imaging wise it is not distinguishable from other forms of hypertrophic pachymeningitis. Several patients were referred to our institution after months, and some, years, before a diagnosis was made, having lost hearing and vision during this time. This educational exhibit aims to increase awareness of this disease, with hope of early diagnosis and treatment.

Purpose

Many patients had delayed diagnosis of IgG4 related disease as they have non specific head and neck imaging findings. However, with the delayed diagnosis, they suffer from progressive disease which lead to loss of important functions such as hearing loss, and vision loss, or suffer progression into severe systemic disease. This exhibit aims to bring awareness to this disease to enable earlier diagnosis and treatment for patients with IgG4 related disease.

Materials & Methods

A retrospective chart review was conducted in our institution with radiologic reports suggesting IgG4-RD between August 2015 and August 2025 . Imaging findings in these reports suggesting the disease include pachymeningitis, pituitary stalk enlargement, nodal disease in the neck and various other criteria. Clinical, radiologic, and pathologic data were collected from the electronic medical record. Pathologic confirmation of IgG4-RD was based on biopsy and histopathologic criteria.

Results & Conclusion

A total of 30 patients were identified with reports suggesting IgG4-related disease involving the brain (n=18) or neck (n=12). Four cases (13%) were biopsy-proven as IgG4-RD with 3 confirmed in the brain and 1 confirmed in the neck. Intracranial findings of proven disease include diffuse pachymeningitis with extension into internal auditory canals and optic canals. Extracranial findings of the head and neck include extensive inflammatory sinusitis, glandular disease such as parotid gland, and lacrimal gland inflammation, as well as lymphadenopathy. In addition, some of these patients have extensive systemic disease including renal, lung and cardiac findings.

Imaging findings of pachymeningitis in the brain, cervical lymphadenopathy and sinus disease are all common non specific findings, often indistinguishable from other common disease. The yield of a true IgG4 related disease is low, yet undiagnosed IgG4 disease can be debilitating, causing patients to lose their vision and hearing, or develop extensive systemic disease. This study is limited as we only identified reports suspicious of IgG4 related disease, which is likely not exhaustive and we probably discounted the missed cases. Of these positive patients, nearly all of them had a delayed diagnosis of months to years, leading them to suffer from important functional deficits. Furthermore, IgG4 related disease responds to high dose glucocorticoids, which early identification potentially can prevent progression of disease. We hope this exhibit will increase awareness of this disease to enable earlier diagnosis and treatment for these patients.

Images/Tables

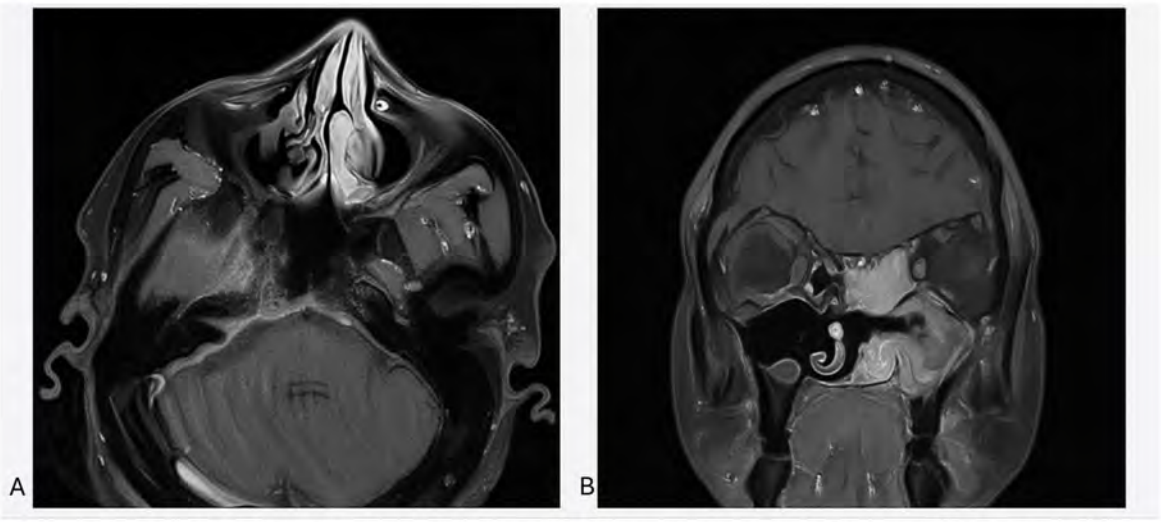

A: Axial T1 post contrast imaging showing dural thickening in the posterior fossa with extension into right internal auditory canal. Biopsy of the dura revealed IgG4 disease.

B: Coronal T1 post contrast imaging showing opacification of the left paranasal sinuses, in the background of prior sinus surgery. Further sinus surgery with biopsy revealed IgG4 disease.

---

871 Between Hemispheres: Stories the Corpus Callosum Tells

Khalid Kabeel MD[1], Mohamed Tantawi MD[2], Abel Abebe MD[2], Joshua Brown MD, PhD[1], Alaha Al Taweel MD[2]

[1]Emory University, Atlanta, Georgia, USA. [2]University of Texas Medical Branch, Galveston, Texas, USA

Summary & Objectives

- Overview:

The corpus callosum, the brain's largest commissural white matter tract, connects the two hemispheres through a vast network of myelinated fibers enabling interhemispheric integration of sensory, motor, and cognitive information.

Anatomically, it is divided into four segments—rostrum, genu, body, and splenium—best visualized on sagittal MRI. This densely myelinated structure follows white matter signal characteristics, appearing hyperintense on T1-weighted and hypointense on T2-weighted sequences.

In our clinical experience, the corpus callosum is often underemphasized in the systematic search pattern of trainees. Yet, its pathologies span a wide spectrum of entities that challenge even experienced radiologists.

This exhibit employs the VINDICATE mnemonic to structure the differential diagnosis of corpus callosal lesions across vascular, infectious, neoplastic, demyelinating, idiopathic, congenital, autoimmune, toxic, and embolic categories. Recognizing these patterns is essential for diagnostic precision and appropriate management.

Through a blend of didactic review and challenging cases, this exhibit will strengthen the participant's ability to confidently interpret corpus callosal pathology.

- Educational Objectives:

Upon completion, participants will be able to:

1. Describe the segmental anatomy of the corpus callosum and recognize selective involvement patterns.
2. Apply the VINDICATE framework to systematically approach corpus callosum pathology.
3. Identify imaging characteristics of CLOCC lesions.
4. Differentiate Susac syndrome from multiple sclerosis based on lesion morphology and location.
5. Distinguish CCIS from neoplastic lesions through clinical and imaging clues.
6. Categorize toxic-metabolic lesions including Marchiafava-Bignami disease.
7. Recognize neoplastic “butterfly” infiltration patterns in glioblastoma and lymphoma.

Purpose

Please see "Summary & Objectives" section.

Materials & Methods

Please see "Summary & Objectives" section.

Results & Conclusion

Please see "Summary & Objectives" section.

Images/Tables

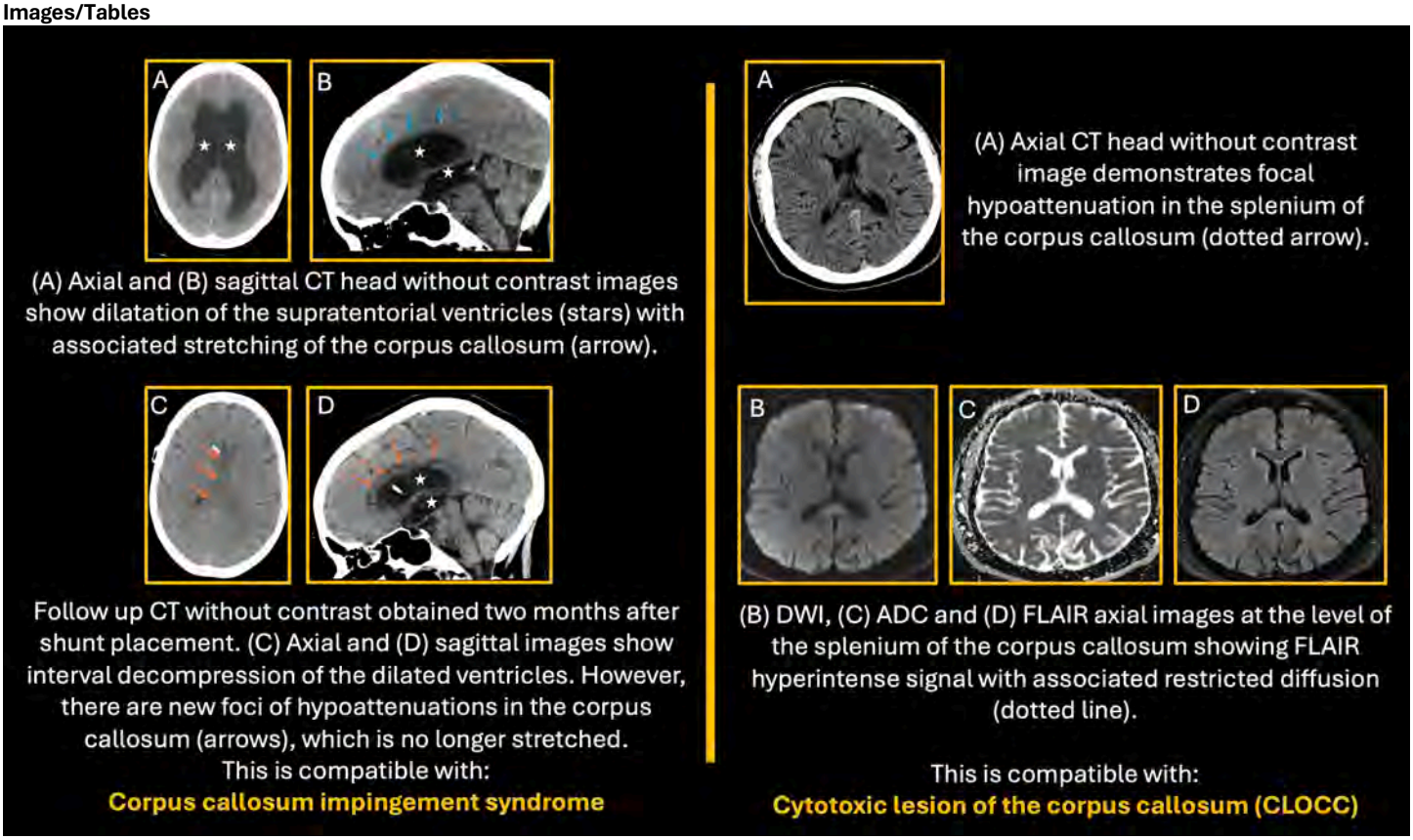

---

954 Overcoming Time and Space: A Successful Short Course for Remote MRI Physics Education

Dyutika Kantamneni MBBS[1], Hong Li MD[2], Nicole Ma MD[3], Qais Iqbal MD[3], Godwin alex mselle MD[4], Jesse Lavtak MD[4], Winland crispin MD[4], Arlene Jamelle Richardson MD[5], Alex Levitt MD[3]

[1]MGM IHS, Navi mumbai, Maharashtra, India. [2]Columbia University Irving Medical Center, Manhattan, New york, USA. [3]Jacobi medical center, Bronx, New york, USA. [4]Kilimanjaro Christian Medical Centre, Moshi, Kilimanjaro, Tanzania, United Republic of. [5]Jackson Park Hospital and Medical Center, Chicago, Illinois, USA

Summary & Objectives

Magnetic Resonance Imaging (MRI) physics remains one of the most conceptually challenging yet foundational areas of radiology education. Despite its central importance, many residents perceive physics as abstract and disconnected from clinical practice. Traditional teaching emphasizes memorization and multiple-choice recall rather than conceptual understanding. To address this, we designed and evaluated a time-efficient, visually oriented MRI physics curriculum paired with interactive polling to enhance engagement and comprehension. The primary objective was to determine whether a concise, image-based didactic delivered remotely via Zoom could produce measurable improvements in MRI physics knowledge among residents with limited prior exposure. This initiative originated through a partnership between RAD-AID and the radiology residency program at Kilimanjaro Christian Medical Center (KCMC) in Tanzania.

Purpose

The goal of this project was to develop and validate a concise, clinically relevant MRI physics curriculum accessible to residents at all levels of training. We sought to overcome barriers identified in prior national surveys insufficient instructional time, lack of physics educators, and limited integration of physics with clinical imaging. Rather than relying on multiple-choice formats, residents were asked to actively describe MRI principles in response to image-based clinical questions. This format aimed to reinforce conceptual reasoning and provide a reproducible framework for evaluating free-response assessments in radiology education.

Materials & Methods

This prospective educational study used a pre- and post-test design across three cohorts of Tanzanian radiology residents (R1–R3). Ninety-four total responses were recorded across three modules; twenty-four residents completed both assessments and were included in the final paired analysis. Each cohort received three hours of instruction divided into modules addressing: (1) signal origin and T1/T2 contrast, (2) inversion recovery, blooming, and diffusion, and (3) flow voids, time-of-flight MRA, and phase-contrast MRV. Grading rubrics were initially generated using structured ChatGPT prompts to outline ideal answers by category, point value, and criteria for full or partial credit, then refined by the authors to improve clarity and eliminate redundancy. Points were awarded for sequence identification (e.g., T2 FLAIR), terminology accuracy (e.g., failed CSF suppression), correct use of MRI physics principles (e.g., inversion time based on CSF T1), and clinical application (e.g., subarachnoid hemorrhage). Statistical analysis was performed in R using paired t-tests and Cohen's *d* effect sizes.

Results & Conclusion

All cohorts demonstrated post-test improvement, with mean score increases of 5–8 percentage points and moderate to large effect sizes (Cohen's *d* = 0.57–0.79). Module 2 (Diffusion/ADC) approached significance ($p = 0.07$). Residents cited the concise format and visual interactivity as key strengths. Even with limited instructional time, participants demonstrated consistent conceptual gains, showing that focused, clinically oriented, image-based instruction can enhance understanding of MRI physics.

This pilot validates a scalable framework for remote MRI physics education that leverages AI-assisted rubric design and clinically integrated teaching. The approach modernizes radiology training and reduces disparities in global access to MRI physics instruction. Future work will expand participation, evaluate knowledge retention, and develop an open-access online platform.

Images/Tables

Paired t-Test Results

Test Case	n	Pre Mean (%)	Post Mean (%)	Mean Δ	SD Δ	SE Δ	t(df)	p-Value	Cohen's d	Effect Size
1	9	36.6	41.4	4.9	8.6	2.9	1.71	0.126	0.57	Moderate
2	9	38.9	46.3	7.4	9.8	3.3	2.09	0.07	0.7	Moderate–Large
3	6	31.2	39.0	7.8	9.9	4.1	1.93	0.112	0.79	Large

---

965 Imaging of Pediatric Head and Neck Masses: A Compartment-Based Diagnostic Approach

Khalid Al-Dasuqi MD[1], Omer Mohammed MD[1], Bulent Aslan MD[2], Cesar Alves MD PhD[3], Sedat G Kandemirli MD[3]

[1]Sidra Medicine, Doha, N/A, Qatar. [2]Beth Israel Deaconess Medical Center, Boston, MA, USA. [3]Boston Children's Hospital, Boston, MA, USA

Summary & Objectives

Pediatric head and neck masses encompass a wide spectrum of congenital, vascular, inflammatory, and neoplastic entities whose imaging evaluation requires a structured, anatomy-based approach. This educational exhibit will illustrate the diagnostic framework for evaluating these lesions by anatomical compartment - skull/scalp, orbit, sinonasal, oral cavity/sublingual space, submandibular space, masticator space, other suprahyoid and infrahyoid spaces - emphasizing key cross-sectional imaging findings, developmental anatomy, and diagnostic pitfalls.

Purpose

To provide a comprehensive, visually driven review of pediatric head and neck masses using a compartmental and pattern-based diagnostic framework, integrating embryologic and contexts. The exhibit aims to enhance interpretive accuracy and provide key pitfalls and pearls pertaining to the various head and neck masses that can be encountered in children.

Materials & Methods

A curated series of pediatric head and neck cases from pediatric tertiary referral centers were reviewed. Lesions were categorized by compartment, composition (cystic, solid, or vascular) and type—congenital or acquired (benign vs malignant). MRI, CT, and ultrasound were analyzed for characteristic imaging signatures. Histopathologic correlation and surgical outcomes were reviewed where available.

Results & Conclusion

Implementation of a compartment-based, multimodality framework improves lesion classification, reduced diagnostic uncertainty, and enhances reporting efficiency in imaging of pediatric head and neck mass.

Structured evaluation using parameters such as midline versus paramedian location, signal intensity, enhancement pattern, diffusion restriction, and relationship to fascial planes is helpful for interpretation. For example, dermoids can be distinguished from thyroglossal duct cysts by their fat content and lack of tract continuity, while cross-compartment spread without bone destruction reliably indicates benign lymphatic or venous malformations.

In conclusion, a structured, compartment-oriented diagnostic paradigm provides a reproducible, evidence-based approach to pediatric head and neck mass evaluation. This framework enhances diagnostic precision, optimizes imaging protocols, and fosters multidisciplinary communication, serving as a practical template for clinical interpretation.

Images/Tables

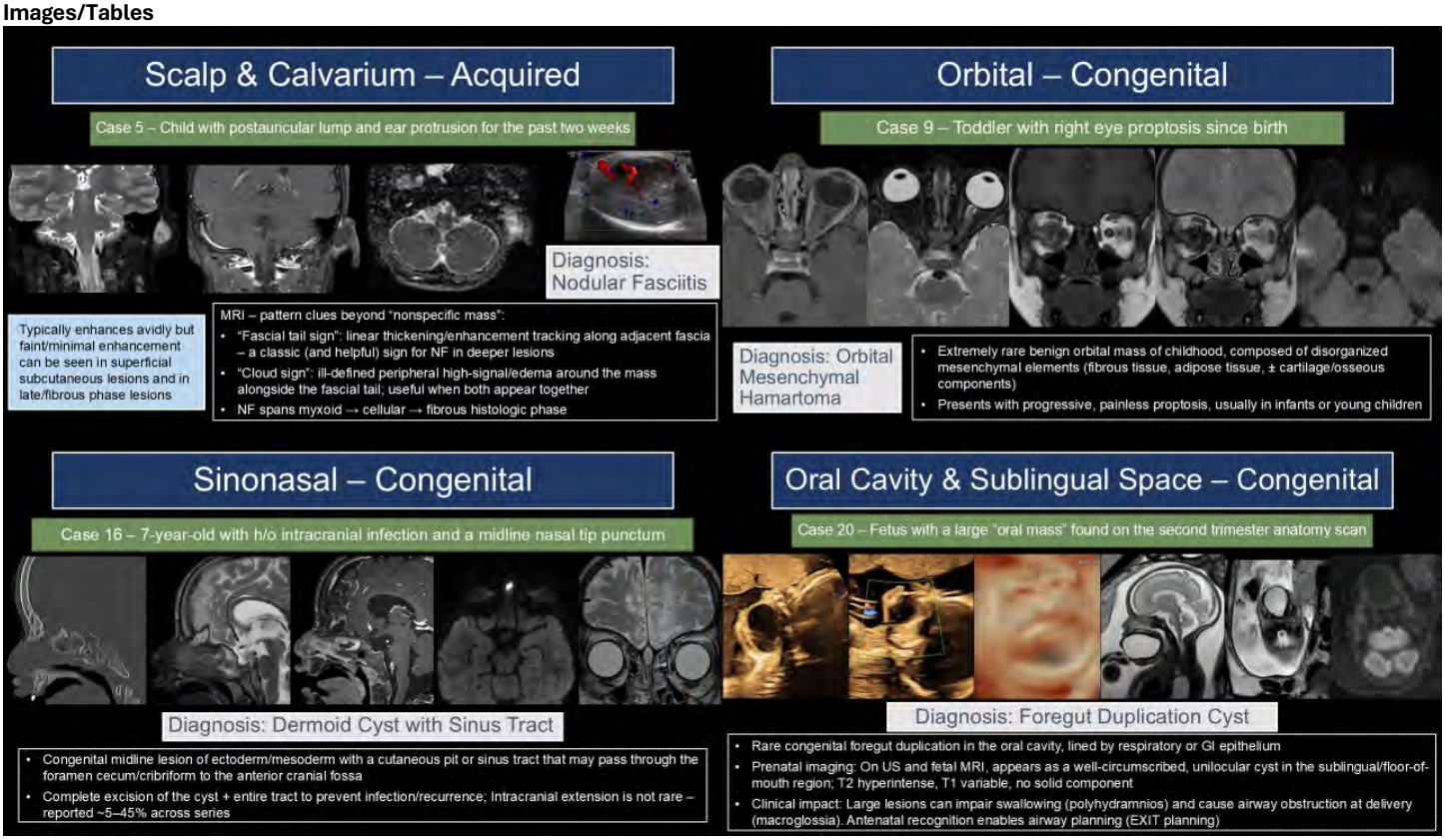

1036 T2 Dark Spinal Lesions: A Pictorial Review

Willem Calderon MD[1], Paul M. Parizel MD, PhD[2], Filip M. Vanhoenacker MD, PhD[3], Alex Rovira MD[4], Carlos Zamora MD, PhD[1]
[1]University of North Carolina, Chapel Hill, North Carolina, USA. [2]Department of Radiology, Royal Perth Hospital, Perth, Western Australia, Australia; The University of Western Australia Medical School, Nedlands, Western Australia, Australia; National Imaging Facility, The Harry Perkins Institute of Medical Research,, Perth, Western Australia, Australia. [3]General Hospital Sint-Maarten, Mechelen, Faculty of Medicine and Health Sciences, Universities, Mechelen, Belgium, Belgium. [4]Hospital Universitari Vall d´Hebron, Barcelona, Spain, Spain

Summary & Objectives

Summary:
T2 dark (hypointense) spinal lesions are relatively uncommon, as most spinal pathologies demonstrate T2 hyperintensity. These lesions usually reflect processes that shorten the T2 relaxation time, such as hemorrhage (hemosiderin deposition), calcification, fibrous tissue, melanin, or vascular flow voids. They can be found in any spinal compartment, including intramedullary, intradural-extramedullary, extradural, or osseous spaces. MRI can provide relevant tissue characterization and precisely delineate the location and extent of disease, while CT is particularly useful for identifying calcification and assessing osseous remodeling, erosion, or destructive patterns.
Because many of these lesions appear similarly hypointense on T2-weighted images, recognizing additional imaging clues is essential for accurate diagnosis. In this exhibit, we classify T2 dark spinal lesions according to their underlying etiology: neoplastic, vascular, inflammatory, infectious, and degenerative. Illustrative pathologies include desmoid tumor, melanocytic schwannoma, meningioma, cavernoma, tuberculoma, pigmented villonodular synovitis, arachnoiditis ossificans, osteoblastoma, osteochondroma, osteosarcoma, extramedullary hematopoiesis, synovial cyst, renal osteodystrophy, arteriovenous malformation, nodular calcification of the alar ligament, hypertrophic pachymeningitis, ossification of the posterior longitudinal ligament, calcified disc extrusion, and vertebral erosion secondary to abdominal aortic aneurysm. The main MRI and CT findings of these entities are reviewed, with emphasis on imaging-pathologic correlation and distinguishing clinical features that aid in narrowing the differential diagnosis.

Educational Objectives:

- List various spinal pathologies that exhibit dark signal intensity on T2-weighted images.
- Review the key MRI features of T2 dark spinal lesions.
- Recognize the utility of CT and MRI in differentiating these entities.

Purpose

N/A

Materials & Methods

N/A

Results & Conclusion

N/A

Images/Tables

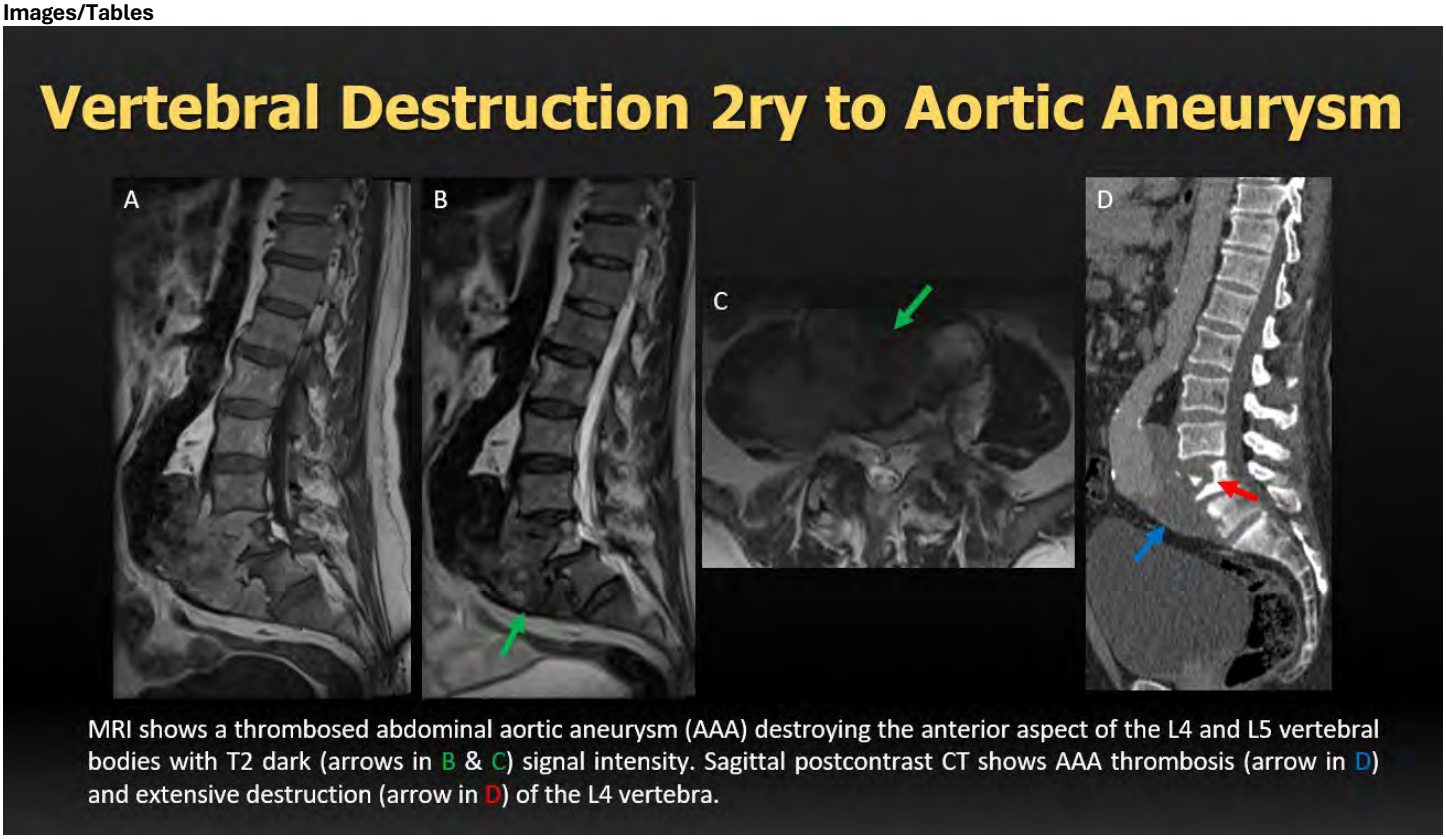

---

169 Maxillo-mandibular Lesions: Gnawing Through the Differentials

Gillean A Cortes DO, Joseph Carbone MD, Charles Li MD, David Fussell MD, David Floriolli MD, Edward Kuoy MD
University of California, Irvine, Orange, CA, USA

Summary & Objectives

Maxillo-mandibular lesions are commonly encountered and usually incidental during head and neck imaging. A wide spectrum of lesions exists but overlapping imaging features often necessitate tissue sampling. Accurate diagnosis guides management and avoids unnecessary procedures.

1. Provide an overview and differential diagnosis for maxillo-mandibular lesions encountered during imaging of the head and neck.
2. Present the multimodal radiologic features with case-based review of maxillo-mandibular lesions.
3. Highlight the approach of maxillo-mandibular lesions including diagnosis and management.

Purpose

To highlight the imaging spectrum of maxillo-mandibular lesions and their clinicopathologic correlations that aid in precise diagnosis.

Materials & Methods

This image-rich educational exhibit showcases the diverse spectrum of maxillo-mandibular lesions through a multimodality, case-based approach. Several key cases presented at our institution will be reviewed such as: periapical cyst, dentigerous cyst, odontogenic keratocyst, non-odontogenic developmental cystic lesions, aneurysmal bone cyst, ameloblastoma, fibrous dysplasia, osteosclerosis, condensing osteitis, cementoblastoma, ossifying fibroma, osteomyelitis, odontogenic carcinoma, invasive squamous cell carcinoma, and osteoradionecrosis.

Results & Conclusion

Maxillo-mandibular lesions are frequently encountered, often as incidental findings during head and neck imaging. There is a broad spectrum of lesions, which may be of odontogenic and non-odontogenic origin and can be further classified by cystic, solid, infectious/inflammatory, benign, and malignant processes. Patient characteristics and location of the lesion may be helpful; however, without pathognomonic imaging features, tissue sampling is frequently required. Accurate diagnosis is essential to prevent further complications, as otherwise treatable lesions with destructive potential may be missed.

Images/Tables

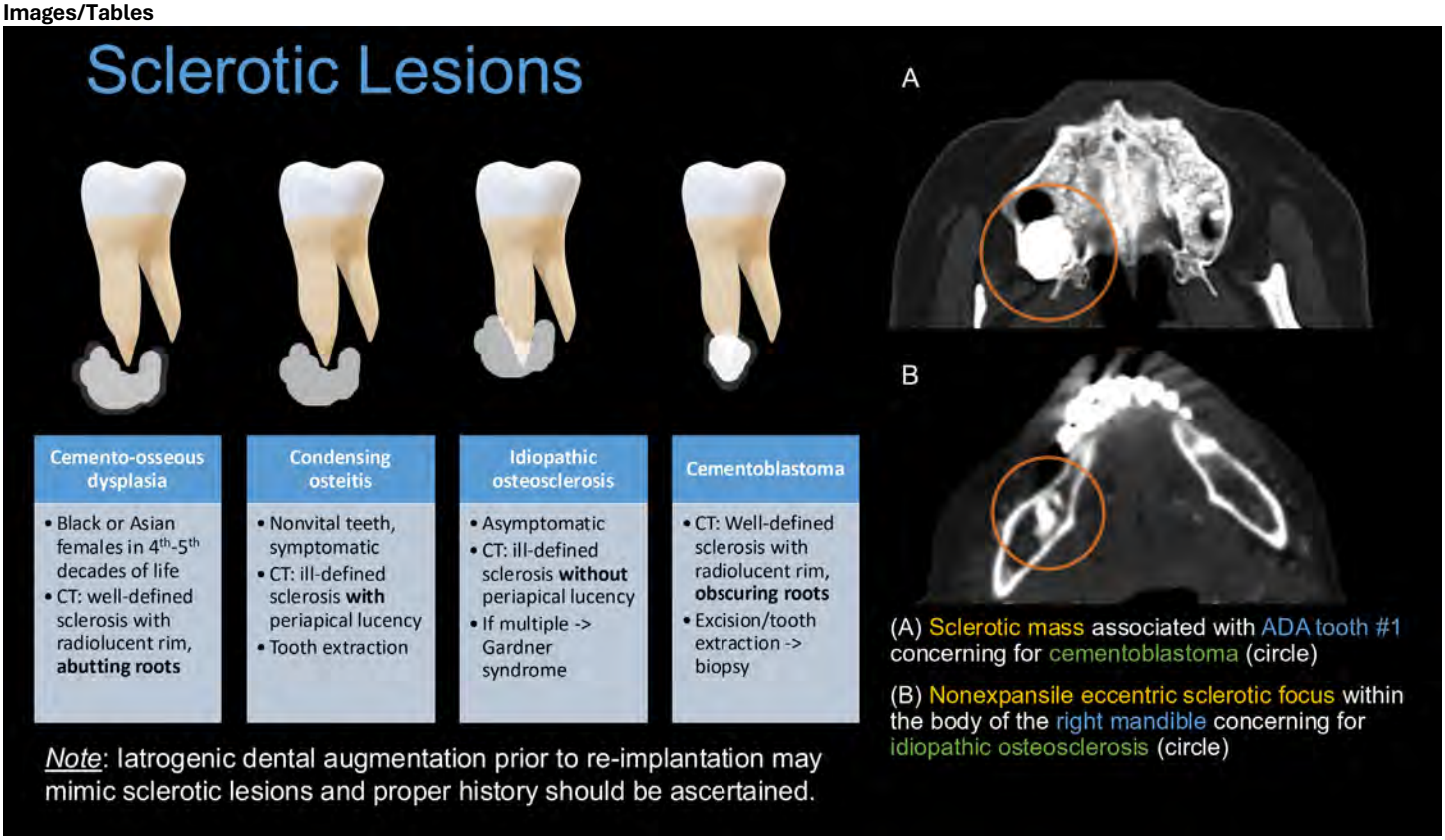

---

195 MRI Imaging And CT Imaging Of Facial Anatomy After Advanced Plastic Surgery And Cosmetic Surgery Procedures.

Anasuya Bhattacharyya M.D., Daniel Ginat M.D.
Chicago, IL, USA

Summary & Objectives

Familiarity with facial anatomy and cosmetic surgery is useful for understanding the consequences of such procedures depicted on imaging. Due to the popularity of plastic and cosmetic aesthetic surgery for medical reasons such as post-traumatic facial disfiguration, as well as non-medical personal beautification to achieve a slimmer face and restoring youthful features reducing sagging and wrinkling, advanced knowledge of deep facial anatomy is crucial for achieving desired outcomes without complications. The procedures generally produce characteristic changes that are readily recognizable on diagnostic imaging, along with potential complications such as filler migration, foreign bodies, edema, abscess, cellulitis, infections, nodules, or complications after removal of fat pads. This article reviews the various CT and MRI imaging findings related to facial anatomy for advanced plastic facial surgery and cosmetic procedures.

Purpose

The face extends from the superior margin of the forehead down to the chin, and across from one ear to the other ear. It is considered the most anterior portion of the head. The underlying facial skeleton, muscles of the face, and subcutaneous tissues make up the appearance, and plays a vital role in the expression of mood and emotions, physical identity, and communication. To enhance the aesthetic appearance, cosmetic surgery is performed on individuals who want to enhance their appearance to improve the ratio of facial harmony, increasing a patient's self confidence levels, but not necessarily for medical or health reasons. Some common targeted procedures include nose reshaping (rhinoplasty), liposuction, eyelid surgery, and facelifts [1]. Targeted procedures such as these are marketed as safe and simple procedures that can be done quickly during a lunch hour, and are attractive alternatives to full facial plastic surgery and facelifts. In general, these procedures are outpatient and are minimally invasive, enhancing a patient's appearance and mental happiness level [1].

Materials & Methods

20 different muscles of facial expression are flat skeletal muscles supplied by the facial nerve. Facial nerve palsy can lead to atrophy of facial muscles and asymmetric expressions [4]. Superficial Musculoaponeurotic System (SMAS) Facelift involves tightening and repositioning deep facial tissue layers of the platysma muscle, parotid fascia, and fibromuscular cheek layers, lifting and rejuvenating the neck and jaw [5].

Results & Conclusion

This article demonstrates the wide variety of facial plastic and cosmetic procedures that can manifest on diagnostic imaging, including both desired outcomes and complications. Due to the affordability and popularity of facial cosmetic procedures, it is imperative radiologists have a deep understanding of the materials used in cosmetic surgery, as well as advanced knowledge of facial anatomy including superficial and deep adipose compartments. Changes are expected from aesthetic surgical modifications and imaging complications, and the speed and accuracy of identifying potential unwanted outcomes is necessary for timely treatment leading to better patient satisfaction. Such cases can be encountered as ancillary findings or can be the specific indication for imaging. Regardless, with what seems to be growing popularity of cosmetic procedures for both medical reasons and personal beautification, it behooves those involved in interpreting the imaging to be familiar with facial anatomy and the resulting surgical alterations.

Images/Tables

MRI Scan Advantages	CT Scan Advantages
Excellent facial contrast visualization detailing soft tissues	Excellent contrast visualization detailing bone
Understands facial filler distribution, fillers, complications	Superior for facial fracture assessment, trauma
Identifies facial inflammation or granulomas	Superior for mapping nasal bone grafts, implants.
Identifies facial nerve, muscle, soft tissue damage	Superior for detailed bone imaging in complex procedures
Uses powerful magnetic field and radio waves	Superior for pre-surgical assessment.
Can detect potential facial tumors and other cancers.	Uses X-rays and ionizing radiation.
Can detect potential facial nerve palsy due to potential future stroke.	High speed results and images in 5-10 minutes.
Provides detailed information about facial trauma	Preferred by patients, no holding breath
Can detect facial inflammatory process or facial tumors	Preferred by patients, quiet machine
Can map abnormal facial growths and potential tumors.	CT scan can be performed with no risk to patients

---

284 **Pattern-Driven Approach to Complex Facial Trauma: A Framework for Structured Evaluation and Reporting**

Colin Wu[1], Edward Pettyjohn MD[2], Srihari Sundararajan MD[3], Sarah Pettyjohn MD[3]
[1]University of the Incarnate Word School of Osteopathic Medicine, San Antonio, TX, USA. [2]University of Illinois College of Medicine at Peoria, Department of Radiology, Peoria, IL, USA. [3]Rutgers Robert Wood Johnson Medical School, New Brunswick, NJ, USA

Summary & Objectives

Complex facial trauma can be challenging to interpret and report. Radiologists—particularly those in training—may be inclined to describe each fracture individually rather than recognize and group them into broader traumatic patterns. Identifying fracture patterns, especially in the midface, promotes a systematic search for associated "do-not-miss" findings that affect surgical, cosmetic, and functional outcomes. Although the anatomy and classification of facial fractures are well described in the literature, their integration into structured, pattern-based reporting has not been widely adopted. This exhibit revisits established principles with a modern framework emphasizing CT workflow efficiency, communication, and educational value for radiologists in training.

Objectives: (1) Review predictable fracture extension along vertical and horizontal buttresses; (2) Recognize characteristic CT patterns of blunt facial trauma; (3) Identify and report visible or suspected complications such as CSF leak, optic-nerve injury, orbital-compartment syndrome, and vascular compromise; (4) Apply structured reporting templates to improve detection, clarity, speed, and consistency.

Purpose

The purpose of this exhibit is to share a practical, CT-based approach for evaluating complex facial fractures that highlights pattern recognition, workflow efficiency, and structured reporting. Rather than focusing solely on anatomic description, this framework translates established principles into a reproducible system that improves day-to-day communication between radiologists and clinicians. It reinforces predictable fracture pathways through the facial buttresses and demonstrates how a structured reporting template can make interpretation faster, clearer, and more consistent. Specific goals include: (1) correlating fracture trajectories with mechanism of injury and potential complications; (2) illustrating practical pearls linking fracture patterns with associated "do-not-miss" findings; and (3) promoting a checklist-style approach that supports completeness, consistency, and quality in acute trauma reporting.

Materials & Methods
This retrospective educational exhibit was developed using representative CT cases of facial trauma from routine clinical practice. All cases were reviewed to highlight characteristic fracture configurations and predictable extensions along facial buttresses. Axial, coronal, and sagittal images, and when available, three-dimensional reconstructions, were used to demonstrate key patterns, including Le Fort, naso-orbito-ethmoidal, zygomaticomaxillary, orbital blowout, and mandibular fractures. Based on these examples, a structured reporting template was designed to function as a checklist for radiologists during live case interpretation, promoting consistency and completeness in trauma reporting. The checklist remains in a pilot phase and will be refined further based on ongoing feedback from trainees and faculty after implementation in clinical workflow.
Results & Conclusion
Initial use of the pattern-based evaluation and checklist-style search pattern has made it easier for learners to approach facial trauma more systematically. Early feedback from trainees suggests that organizing findings by patterns improves confidence and helps reveal subtle, clinically important details that might have otherwise been missed. The checklist has been well received as a quick reference tool during live case interpretation, reinforcing a consistent and thorough search strategy.
Conclusion: A pattern-driven, CT-based framework supported by a structured reporting checklist provides a practical way to make facial trauma interpretation more organized and complete. Although still in the pilot phase, this approach shows promise for improving detection of subtle fracture extensions and promoting clearer, more consistent communication between radiologists and clinical teams.
Images/Tables

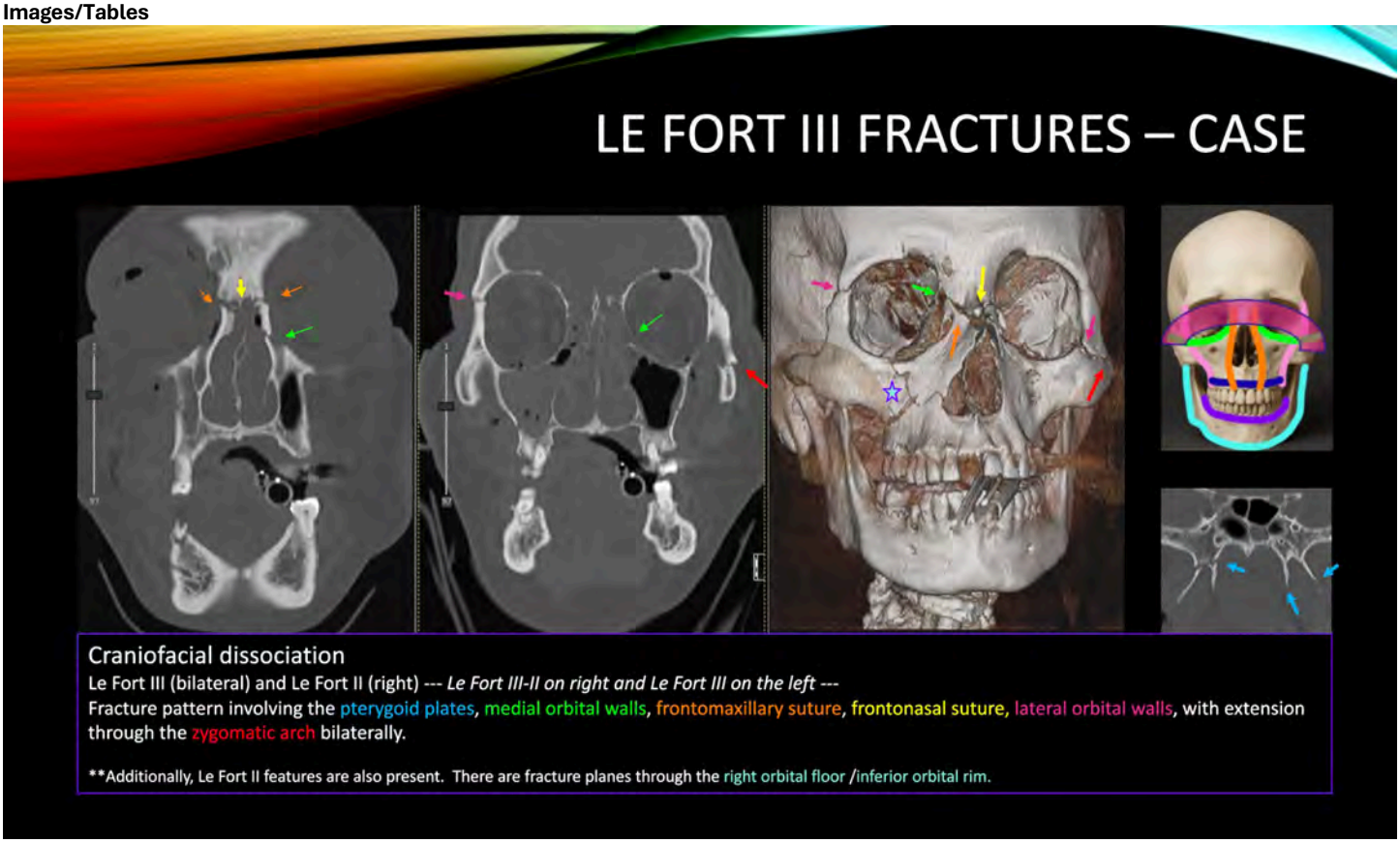

---

370 Radiological Approach to Pontine Lesions
Mona Gad, Francis Deng
Department of Radiology and Radiological Science, Johns Hopkins University School of Medicine, Baltimore, MD, USA
Summary & Objectives
1. Describe the vascular supply and functional neuroanatomy of the pons.
2. List the common pathologies affecting the pons.
3. Recognize the relevant clinical presentation that may guide the neuroradiologist to narrow the differential diagnosis of pontine lesions.
4. Understand the utility of imaging in determining the most probable diagnosis through an imaging-based approach to the most common pontine lesions.

Purpose
The primary goal of this exhibit is to optimize imaging interpretation of pontine pathologies, with a focus on the role of combined clinical and radiological approaches in arriving at the precise diagnosis and guiding clinical decision-making.
Materials & Methods
Illustrative cases of important pontine pathologies, along with relevant clinical scenarios and imaging differential considerations, will be displayed in this exhibit.
1. Blood supply and neuroanatomy of the pons, including the cranial nerve nuclei and pontine tracts.
2. Etiological classification of pontine lesions, including congenital, neurodegenerative, vascular, toxic/metabolic, infectious/inflammatory, and neoplastic.

3. Distinctive imaging features of the lesions involving the pons, with emphasis on disease-specific signs, such as trident sign in osmotic demyelination syndrome.
4. Key clinical history which guides the radiological diagnosis.
5. Important discriminating features of common radiologic mimics, such as medial lemniscus hyperintensity as a marker of small vessel disease.
6. Apply diagnostic criteria during reporting when pontine lesions are encountered in clinical practice, such as Movement Disorder Society criteria for multiple system atrophy.

Results & Conclusion

Results: N/A

Conclusion:

Pontine lesions involve a wide and heterogenous group of diseases. A systematic imaging-based approach in conjunction with proper clinical history can help narrow the differential considerations for such lesions.

Images/Tables

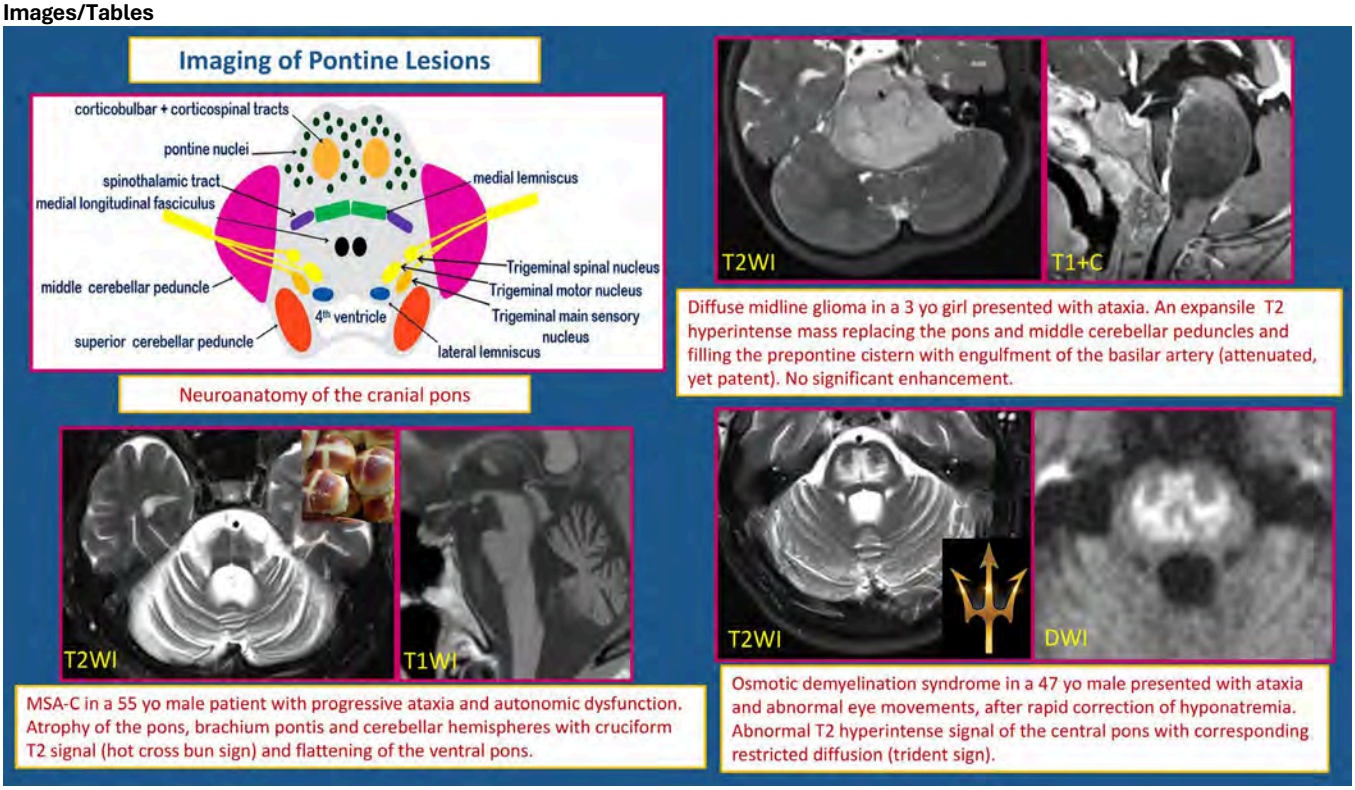

---

678 The Rate Limiting Step: A Walkthrough on Preprocessing Multi-Modal Data for Aneurysm Image Classification

Adriana Ene, Suzanne Amelia Alvernaz, Nipun Velupally, Arvind Draffen, Charles Pierce MD, Michael Tanious MD
UIC, Chicago, Il, USA

Summary & Objectives

The emerging landscape of machine learning offers opportunities in neuroradiology including early detection of malignancies, aneurysms, or hemorrhage, but require robust image datasets for appropriate model training and parameterization. Creation of adequately sized datasets often requires merging images from multiple hospital systems or across different modalities. These merged datasets will have increased variance in image quality and dimensions. Prior to using machine learning approaches for inference of pathologic processes, merged data must undergo careful preprocessing to ensure a consistent, robust dataset.

Purpose

The purpose of this work is to educate radiologic clinicians on the importance and steps in pre-model fitting image preprocessing they can often determine model success. For example, image formats can differ across scanners and institutions when it comes to resolution, voxel spacing, acquisition planes and amount of contrast used (Bloem). Aligning and normalizing multiple modalities or images from multiple sources is necessary to create consistent input dimensions before model inference.

Materials & Methods

In this work, we provide an educational walk through of preprocessing strategies using an aneurysm detection dataset consisting of volumetric CTA and MRI data from multiple institutions, with aneurysms of multiple vascular territories (Rudie). This work walks through the necessary pre-model fitting image processing steps to ensure a robust dataset. We will review and contrast different types of pre-processing steps. A step-by-step workflow for model development, validation, and integration will be demonstrated, with emphasis on how pre-processing steps can improve machine learning outcomes and what steps to be mindful of future implementation of models. This includes a review of DICOM image formatting, volume reconstruction, spatial normalization and resizing, intensity normalization and windowing, and label handling. Such clean preprocessing sets the foundation for flexible downstream inference architectures including convoluted neural networks or large language learning models.

Results & Conclusion

Enhancing radiologists' understanding of the importance and appropriate steps in image preprocessing will help providers review the growing breadth of literature on computational approaches to neuroradiology.

784 Deep Brain Stimulation Decoded: A Radiologist's Guide to Deep Brain Stimulation

Devin A DeLuna MD, Sean Kelly MD
University of Nebraska Medical Center, Omaha, NE, USA

Summary & Objectives

Deep brain stimulation (DBS) is an established surgical therapy for disorders such as Parkinson's disease, essential tremor, dystonia, and more. Accurate electrode placement is critical to clinical efficacy and minimizing adverse effects. Neuroradiologists play a key role in preoperative planning, intraoperative targeting verification, and postoperative assessment.

Purpose

The purpose of this educational exhibit is to familiarize radiologists and trainees with the imaging appearance of DBS systems, highlight key anatomic targets (e.g., subthalamic nucleus, globus pallidus internus, and ventral intermediate nucleus), and review the spectrum of procedure-related complications. Through high-resolution CT and MRI examples, this review enhances confidence in relevant neuroanatomy, recognizing correct lead positioning, identifying normal postoperative appearances, and detecting surgical complications.

Materials & Methods

This pictorial review is based on retrospective analysis of patients who underwent DBS implantation at a tertiary academic hospital. Representative imaging examples were selected to illustrate:

- Relevant neuroanatomy.
- Preoperative planning considerations.
- Normal postoperative appearance of commonly used DBS systems.
- Target verification using MRI and CT.
- Postoperative complications (e.g., hemorrhage, infection, malposition).

Results & Conclusion

Results:

- Multimodal imaging analysis is vital for accurate lead placement.
- CT provides superior visualization of hardware position and is the modality of choice for detecting lead malposition and hemorrhage.
- MRI, performed with DBS-conditional safety protocols, offers superior soft tissue evaluation for perilead edema, infection, and delayed inflammatory changes.
- Illustrative cases emphasize how electrode placement is critical to clinical outcomes.

Conclusions:

Radiologists play a vital role in ensuring safe and effective DBS therapy through accurate imaging interpretation before and after implantation. Familiarity with expected anatomic targets, postoperative appearances, and complications is essential to support neurosurgical teams and optimize patient outcomes. This image-rich exhibit provides a practical visual guide for trainees and practicing neuroradiologists to recognize the successes and pitfalls of DBS therapy.

Images/Tables

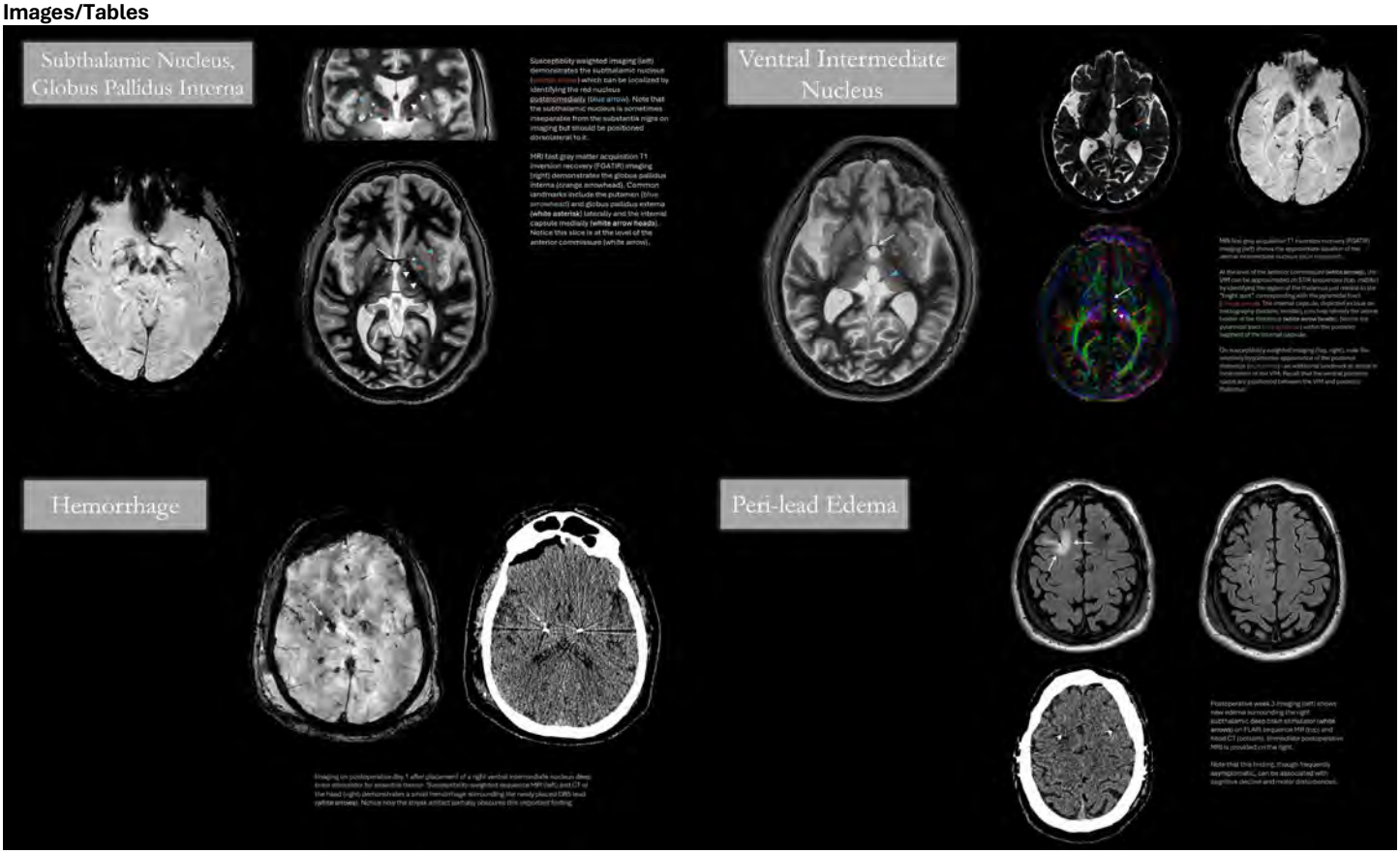

836 What's Your Major Malformation? Current Classification and Imaging Characteristics of Orbital Vascular Malformations

Jon Conatser[1], Mohit Agarwal[1], Ian Rumball[2], Bria Fiebiger[1]
[1]Medical College of Wisconsin, Milwaukee, WI, USA. [2]Medical College of Wisconsi, Milwaukee, WI, USA

Summary & Objectives

Orbital vascular anomalies (OVAs) are broadly categorized as either orbital vascular tumors (OVTs) or orbital vascular malformations (OVMs) by the International Society for the Study of Vascular Anomalies (ISSVA) 2025 edition. OVMs represent a heterogenous group of mostly congenital orbital lesions characterized by non-neoplastic proliferation of vascular tissues. Many different classification systems have been developed over the years in an attempt to
characterize the different types of OVMs. As a result, there are multiple OVMs which are still commonly known by historical misnomers (e.g. orbital cavernous hemangioma, venous varix, lymphangioma) which can lead to diagnostic confusion.

OVMs can broadly be placed into one of three categories according to the 2025 edition of the ISSVA classification system: fast-flow, slow-flow, or developmental anomalies of named vessels. Each category of OVMs have certain imaging characteristics which are helpful clues to differentiate one type of OVM from another. Fast-flow OVMs (e.g. arteriovenous malformation (AVM), arteriovenous fistula (AVM)) demonstrate an abnormal direct connection between the arterial and venous sides of circulation, characterized by prominent arterial feeders and/or enlarged draining veins on imaging. Slow-flow OVMs include capillary, lymphatic, venous, or combined malformations. Orbital capillary vascular malformations are often syndromic and often clinically evident with a cutaneous component. Orbital lymphatic vascular malformations
(formerly known as lymphangiomas) are characterized on imaging by a trans-spatial orbital mass with fluid-fluid levels and no enhancement. The orbital venous vascular malformation formerly known as orbital cavernous hemangioma is the most common orbital vascular lesion in adults and is characterized on imaging by a well-demarcated ovoid intraconal mass showing avid dynamic post-contrast enhancement which progressively fills in on delayed imaging. Another not uncommonly seen orbital venous vascular malformation formerly known as a venous varix is characterized on imaging by an intensely enhancing orbital mass that distends on provocative maneuvers which increase venous pressure. Orbital combined vascular malformations (e.g. venolympathic malformations) demonstrate varying imaging characteristics
depending on the composition of lesion but characteristically show an intra-orbital mass with fluid-fluid levels and varying degrees of enhancement. The educational objective of this exhibit is to explain and review the most current ISSVA classification schema for orbital vascular anomalies with an emphasis on the distinguishing and salient imaging characteristics of common OVMs and to help foster a common diagnostic vocabulary to describe these lesions, in an attempt to help eliminate the use of continued historical misnomers which can lead to diagnostic confusion.

Purpose

Summarize and explain the most current classification of orbital vascular malformations and provide case-based examples of the various orbital vascular malformations.

Materials & Methods

Multiple annotated images in various imaging modalities to highlight the common and characteristic imaging features of the different types of OVMs.

Results & Conclusion

The ISSVA classification schema is the most current and complete classification of vascular malformations that should be used when describing orbital vascular malformations to avoid the use of historical misnomers which can lead to diagnostic confusion. OVMs have distinguishing imaging characteristics.

Images/Tables

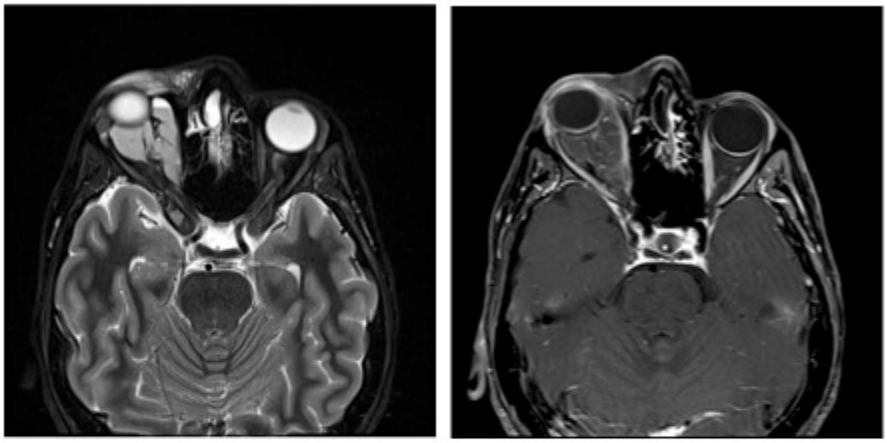

Orbital lymphatic malformation: Right orbital trans-spatial mass with fluid-fluid levels on T2-weighted imaging (left image) demonstrating no enhancement on post-contrast T1-weighted imaging (right image).

Sample of the case-based images to be included in the presentation.

902 Go With the Flow: A Practical Imaging Approach to Head and Neck Vascular Anomalies

Benjamin Spangler M.D., Mason Andrews D.O., Esai Hernandez M.D., Colten Germaine D.O, Shannon Tocchio M.D.
University of New Mexico, Albuquerque, NM, USA

Summary & Objectives

Summary

Vascular anomalies of the head and neck present a complex and heterogeneous group of lesions with overlapping clinical and imaging features. As such, radiologists play a crucial role in diagnosis and characterization, helping to guide management decisions. This educational exhibit provides a practical, imaging-based framework for identifying and differentiating vascular anomalies in the head and neck utilizing a multimodality approach. Through illustrative cases, we review the imaging features of slow-flow and fast-flow vascular malformations, lymphatic malformations, and classic hemangiomas with emphasis on correlating imaging appearance with clinical presentation and hemodynamic behavior to improve diagnostic confidence. The exhibit concludes with a brief overview of the ISSVA classification to align terminology with current international standards.

Objectives

After reviewing this exhibit, participants will be able to:

1. Recognize the spectrum of vascular anomalies that can occur in the head and neck, including slow-flow and fast-flow vascular malformations, lymphatic malformations, and classic hemangiomas.
2. Interpret characteristic imaging findings on ultrasound, CT, MRI, and angiography that define flow dynamics and lesion composition.
3. Apply an imaging-driven approach to classification and reporting that enhances clinical communication and management planning.
4. Understand how the ISSVA classification integrates with radiologic assessment to provide standardized nomenclature and multidisciplinary clarity.

Purpose

The purpose of this educational exhibit is to provide radiologists with a systematic approach to evaluating head and neck vascular anomalies, focusing on identifying flow characteristics and key imaging findings that aid in accurate diagnosis and appropriate treatment selection.

Materials & Methods

Representative cases of head and neck vascular anomalies will be reviewed, encompassing slow-flow and fast-flow vascular malformations, lymphatic malformations, as well as classic hemangiomas. Each case includes multimodality imaging with ultrasound, CT, MRI, and conventional angiography when available. Imaging hallmarks, such as phleboliths, enhancement patterns, flow voids, and diffusion characteristics, will be highlighted. Additionally, schematic diagrams and flowcharts will summarize diagnostic strategies and common pitfalls.

Results & Conclusion

A structured, imaging-based approach focused on flow dynamics allows reliable differentiation between the major categories of vascular anomalies in the head and neck. Recognizing these imaging patterns improves diagnostic accuracy, guides appropriate intervention, and supports clear multidisciplinary communication while incorporating the ISSVA classification further enhances reporting consistency. This exhibit aims to equip radiologists with practical tools and imaging pearls for confident evaluation of these often-challenging lesions.

Images/Tables

ASNR 2026 Images

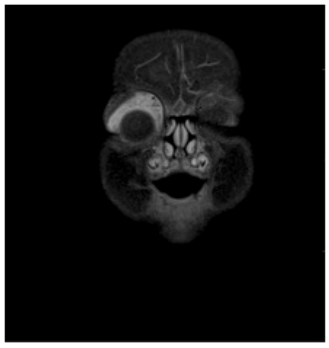

Right Orbital Hemagioma

(Coronal T1 FS Post-Contrast)

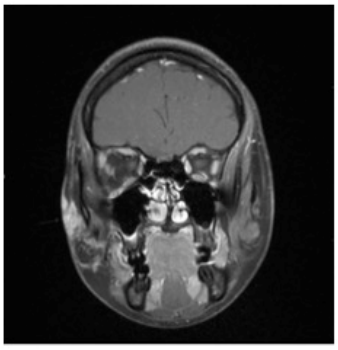

Right Face AVM

(Coronal T1 FS Post-Contrast)

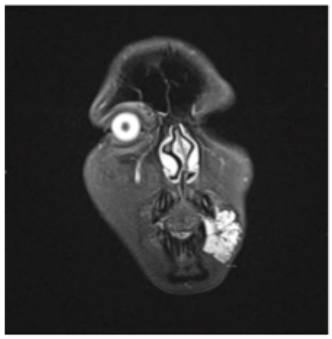

Left Lower Lip Venous Malformation

(Coronal STIR)

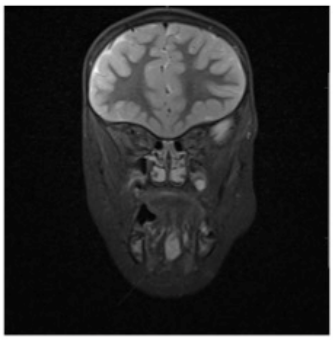

Midline Floor of Mouth Lymphatic Malformation

(Coronal STIR)

947 Post-Radiation Therapy imaging and Related Complications in the Head and Neck: Diagnostic Challenges and Pearls for Radiologists

Haneyeh Shahbazian MD, Benjamin Y Huang MD
University of North Carolina, Chapel Hill, North Carolina, USA

Summary & Objectives

Summary:

RT serves as an essential component of management of head and neck malignancies. However, it is associated with a broad range of complications that can mimic tumor recurrence, infection, or other pathology. Radiologists often play a pivotal role in identifying and differentiating post-radiation therapy complications from disease recurrence, and accurate clinical and radiologic differentiation is imperative for appropriate management and to avoid unnecessary interventions[1].

Common radiation-induced changes occurring across the skull base, face, cranial nerves, and cervical spine can be divided into expected and complicated RT-induced effects[2].

- Expected
- Subcutaneous tissue, muscle, pharyngeal wall, and larynx soft tissue edema
    1. Early symmetric and smooth edema; typically decreases over months
    2. Fat stranding / increased attenuation
- Fat fibrosis:
    1. A late finding; appears as Low T2 signal on MRI
    2. It can be differentiated from local tumor by the lack of mass effect or enhancement.
- Pharyngeal/Laryngeal wall mucosal thickening
    1. Symmetric smooth non enhanced thickening
- Salivary glands:
    1. Early: Edema (enhancement)
    2. Late: Atrophy, fatty replacement, and decreased enhancement
- Lymph nodes:
    1. Decrease in size and loss of central necrosis.
    2. Small enhancing nodes can remain.
- Complications: Common and recognized complications of RT in the HN include osteoradionecrosis, chondronecrosis, osteomyelitis of the cervical spine, soft tissue fibrosis, RT-induced carotid artery stenosis, carotid blowout syndrome, RT-induced cranial neuropathy, RT-induced myelopathy, and secondary neoplasms[2,3].

CECT and fluorodeoxyglucose positron emission tomography (FDG-PET) are the standard imaging modalities for post-RT/CRT surveillance except in the sinonasal cavities and skull base where MRI is preferred. When uncertainty persists after standard imaging evaluation, techniques such as DWI, MR perfusion (etc., etc.) can help in distinguishing expected RT changes and complications of RT from tumor recurrences.

Educational objectives:

1. To be familiar with the spectrum of complications following radiation therapy (RT) for tumors of the head and neck (HN), with an emphasis on radiologic features.
2. To be able to differentiate expected post-RT changes, RT-related complications, and tumor recurrences on surveillance imaging after treatment of HN tumors.
3. To understand how advanced diagnostic imaging tools may assist in distinguishing RT-related complications from tumor recurrences.

Purpose

To delineate common expexted radiologic findings of post radiation therapy of Head and Neck from tumor recurrence and complications

Materials & Methods

NA

Results & Conclusion

NA

Images/Tables

Table1. Radiologic findings of RT-induced changes from tumor recurrence[5-7]

Radiological findings	Post Radiation	Tumor Recurrence
Symmetry	Yes	Often no
Enhancement	Mild/diffusely enhanced	Nodular/mass like/ strong enhancements
Dynamic Contrast–Enhanced MRI (DCE-MRI)	Slow, delayed enhancement	Rapid early enhancement, quick washout
Perfusion CT	Low blood flow (BF) and blood volume (BV)	High BF/BV
Fluorodeoxyglucose (FDG) PET *	Weak uptake with ill-defined linear pattern	Strong focal uptake with nodular/ mass features
Growth pattern	Slow/ stable	Fast/ progressive

*Ideally 12 weeks post RT to reduce false positives

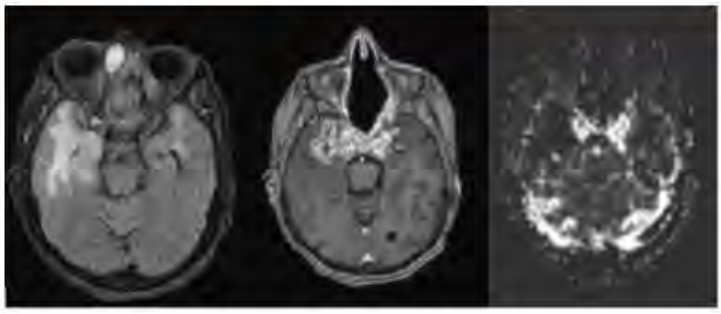

78-year-old female with a history of stage IV T4N0M0 SCC of the left ethmoid, status post-surgical resection and radiotherapy, with recent mental status change. There is a patchy area of T2/FLAIR hyperintensity in the white matter, consistent with moderate chronic small vessel ischemia, accompanied by mild diffuse brain parenchymal loss. No diffusion-weighted signal abnormality is present, which is consistent with delayed radiation necrosis. Extensive postoperative changes from prior sinonasal mass resection. Heterogeneous enhancement with areas of central necrosis in the anteromedial temporal lobes, greater on the right side, and surrounding vasogenic edema and sulci effacement.

1012 A New Look at Metal Artifact

Caleb J Busch, Ulrich Rassner
University of Utah, Salt Lake City, Utah, USA

Summary & Objectives

Metal artifact from implanted medical devices often compromises magnetic resonance imaging (MRI). In this educational exhibit we explain the appearance of different types of metal-induced MRI artifact and instruct how to reduce or resolve them.

Purpose

The degree and appearance of metal artifact can vary greatly between different pulse sequences. Reducing the artifact requires an understanding of the underlying mechanisms of image degradation. The purpose of this exhibit is to explain MRI metal artifacts by considering the alteration of proton resonance frequency and induction of field gradients. This allows one to understand the varied appearances of metal artifacts on gradient echo, spin echo, and echo planar pulse sequences as well as the effect on tissue suppression techniques, but also clarifies the mechanism of action of altering certain scan parameters such as echo time and bandwidths. It also explains why some parameter changes are effective at reducing artifact for some pulse sequences but not others.

Materials & Methods

MRIs elucidating the various metal artifacts and their reduction or resolution by altering scanner technical parameters were collected and compiled at The University of Utah including scans of phantoms and patients.

Results & Conclusion

We demonstrated a simple way of understanding different MRI artifacts induced by metal and how changing scanner technical parameters can reduce or resolve them.

Images/Tables

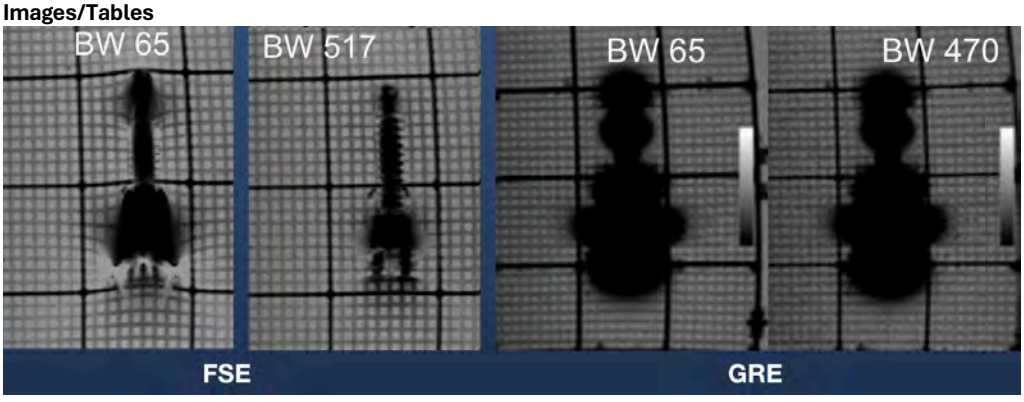

1175 Beyond Parathyroid Adenoma: Expanding the Role of Arterial Phase Imaging in Head and Neck Tumors

Jan A Niec MD, Joseph M Aulino MD, Ryan K Rigsby MD, Simone P Montoya MD, Phillip D Bates MD
Vanderbilt University Medical Center, Nashville, TN, USA

Summary & Objectives

Early arterial phase enhancement can be a key diagnostic feature in select head and neck (H&N) tumors. This finding is distinct from 'hypervascularity', which refers to prominent enhancement irrespective of contrast timing. Arterial phase imaging is an established component of protocols for liver HCCs, pancreatic neuroendocrine tumors, adrenal nodules, renal masses, and parathyroid adenomas; however, it remains underutilized in H&N evaluation.
The educational objectives of this exhibit are to (1) Recognize characteristic arterial phase enhancement patterns across H&N tumors; (2) Differentiate early arterial enhancement from hypervascularity; (3) Identify scenarios where arterial phase timing improves lesion conspicuity and diagnostic confidence; (4) Review practical approaches for optimizing arterial phase acquisition in the H&N.

Purpose

This exhibit demonstrates the broader application of arterial phase imaging to tumors in the H&N beyond parathyroid adenoma.

Materials & Methods

We reviewed clinical and teaching file cases to identify patients with cervical tumors who also underwent arterial phase imaging, i.e. CTA, enhanced MRA, DSA, and 4D MRA.

Results & Conclusion

Multiple tumors demonstrated characteristic early arterial enhancement. Paragangliomas, parathyroid adenomas, endolymphatic sac tumors, medullary thyroid carcinomas, and other neuroendocrine tumors typically display arterial phase enhancement. Other diseases that may enhance with arterial phase imaging include solitary fibrous tumors, alveolar soft part sarcomas, and malignant meningiomas (WHO Grade III).
Knowledge of which hypervascular tumors display arterial phase enhancement may provide a specific tissue diagnosis or help narrow a differential diagnosis. Specifically, arterial phase imaging may help distinguish schwannoma from paraganglioma in the carotid space and jugular foramen.

Images/Tables

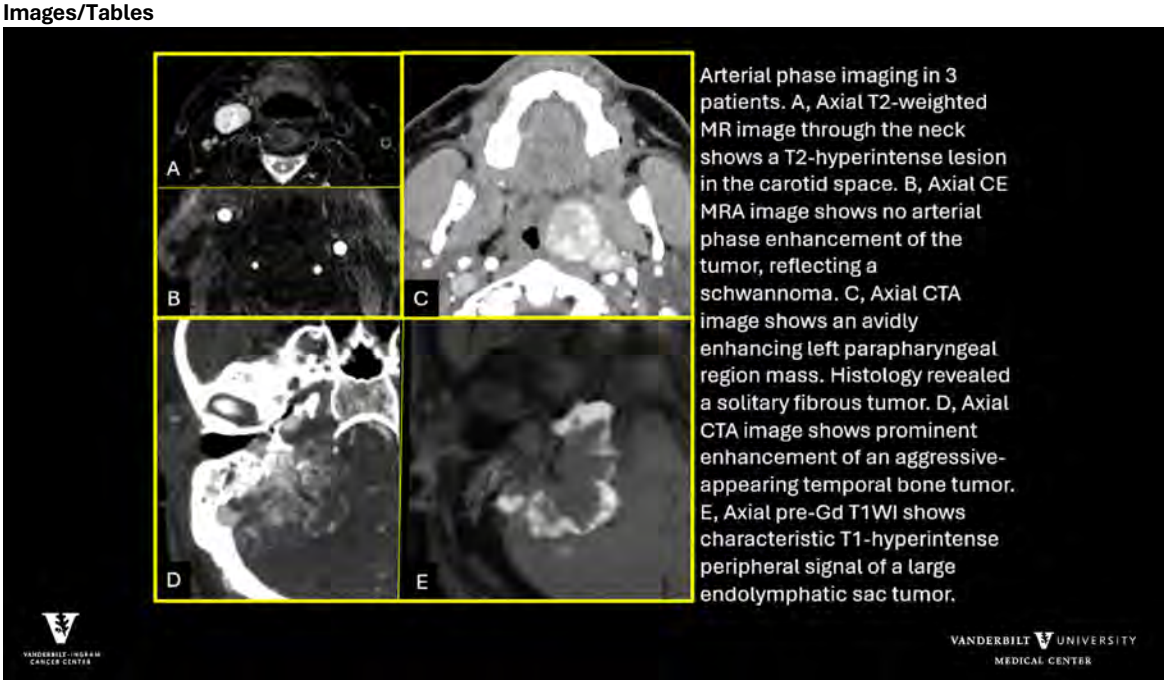

177 Penetrating Traumatic Brain Injuries: What the Neurocritical Care Team Wants to Know. *A structured approach to head CT interpretation in firearm-related penetrating brain injury*.

Olasubomi J Omoleye MD, Ali Mansour MD, Fernando D Goldenberg MD, Olga Pasternak-Wise MD
University of Chicago Medical Center, Chicago, IL, USA

Summary & Objectives

Firearm injuries remain a major public health crisis in the United States, with an estimated 132 firearm-related deaths daily [1]. Penetrating traumatic brain injury (pTBI) from firearm wounds carries a mortality rate between 44% and 55% [2]. Computed tomography (CT) is central to the initial evaluation of patients with pTBI; however, most validated scoring systems used in trauma, such as the Rotterdam and Marshall scores, were derived from blunt traumatic brain injury cohorts and fail to capture the unique imaging features, mechanisms, and prognostic implications of penetrating injuries [3,4].
At the University of Chicago Medical Center, we encounter a disproportionately high number of firearm-related pTBI cases, reflecting the local impact of gun violence in our community. This has allowed us to develop the **UChicago pTBI Imaging Score**, a hierarchical classification system tailored to penetrating brain injury [5]. Despite growing literature on outcomes, there remains no standardized framework to train radiologists on which CT features are most prognostically significant or how to determine which findings are most impactful to managing the neurocritical care treatment decisions. This exhibit aims to bridge that gap by teaching how to systematically analyze initial head CTs in pTBI, emphasizing features most predictive of clinical outcomes and most relevant to neurocritical care decision-making.

Purpose

Educational Objectives:

1. Recognize CT findings of pTBI and their prognostic significance

2. Apply a structured approach “CT Head pTBI Checklist”
3. Understand how imaging findings influence neurocritical care decision-making
4. Strengthen radiology-critical care communication through standardized report frameworks

Materials & Methods

We retrospectively reviewed firearm-related penetrating brain injury cases presenting to our Level 1 trauma center from 2018 to 2023. Imaging features assessed included projectile trajectory, ventricular or cisternal hemorrhage, brainstem or cerebellar injury, and secondary mass effect. Using machine learning-based ensemble modeling, we previously determined the relative contribution of each imaging feature to in-hospital mortality [5].
For this educational exhibit, we curated representative CTs to illustrate key imaging patterns, accompanied by schematic diagrams and a “CT Head pTBI Checklist”. Illustrative materials include annotated CT images, schematic diagrams of projectile trajectories, and a structured “CT Head pTBI Checklist” highlighting features that should be explicitly mentioned in radiology reports.

Results & Conclusion

Features most predictive of mortality included:

1. Transhemispheric projectile trajectory below the level of the third ventricle;
2. Cast (blood-filled) lateral ventricles;
3. Brainstem involvement;
4. (Any) blood in the ambient cisterns;
5. (Any) blood in the lateral ventricles.

These features strongly correlated with in-hospital mortality and are essential for triage, prognostication, and neurocritical care planning. This exhibit translates data-driven insights into practical visual teaching material, providing radiologists with a reproducible interpretive framework for pTBI.
By standardizing how CT findings in pTBI are analyzed and reported, radiologists can better inform the neurocritical care team’s management decisions, ranging from intracranial pressure management to discussions around prognosis and goals of care. Ultimately, this structured educational approach enhances interdisciplinary communication, supports rapid decision-making in the trauma setting, and promotes the adoption of data-informed imaging interpretation for one of neurotrauma’s most devastating injury patterns.

Images/Tables

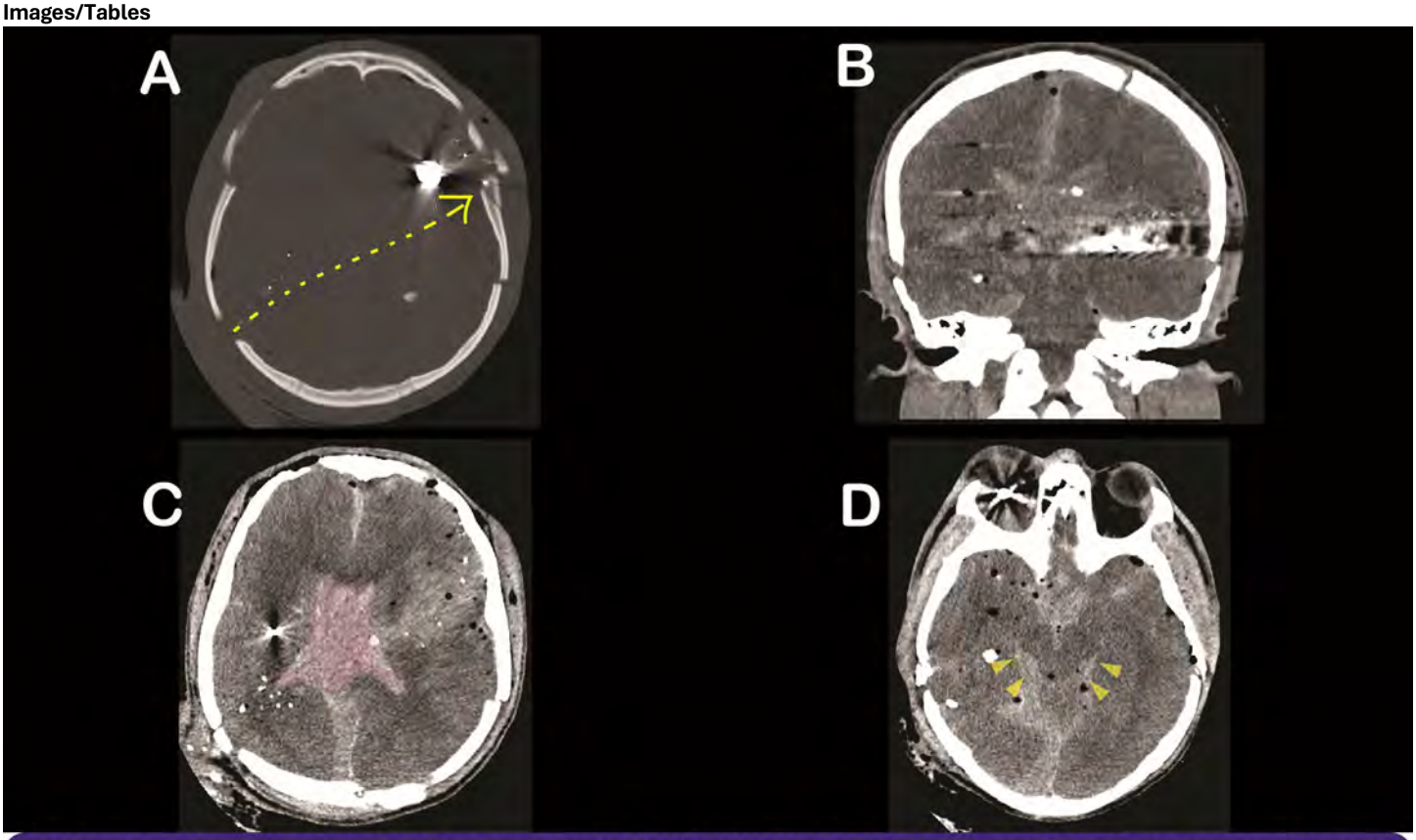

An oblique bullet trajectory extends from the right parietal to left frontal region (dashed arrow) with ballistic and osseous fragments along the path. There are multiple comminuted calvarial fractures (A). The bullet transverses through and below the level of the third ventricle (B). There is extensive intraventricular hemorrhage with cast lateral ventricles (C). There is subarachnoid and subdural hemorrhage. Blood fills the basal cisterns including the ambient cistern (arrow heads). A bullet fragment is also noted in the right orbital cavity just posterior to the globe (D).

---

197 Radiology's ultimate Limbo: Update on imaging of Autoimmune Encephalitis

Meghana Kancharla MD, Siddhanth Suresh MD, Shreyas Reddy K MD
St John's Medical college and Hospital, Bangalore, Karnataka, India

Summary & Objectives

1)-Present a dual classification: Antibody class (intracellular vs extracellular) and anatomic phenotype (limbic; cortical/subcortical; striatal; diencephalic; brainstem/cerebellar; encephalomyelitis; meningoencephalitis).
2)-Specify a core MRI-protocol (T1, T2, FLAIR, DWI) with conditional post-contrast and perfusion when indicated.
3)-Provide an imaging-first differential separating AE from HSV-encephalitis, PRES, toxic-metabolic injury, tumor, and seizure-related change.
4)-Highlight diagnostic-pitfalls (Eg. Phenotypic-overlap) and how MRI mitigates them.

Purpose

Autoimmune encephalitis (AE) is an antibody-mediated inflammatory disorder whose clinical and imaging manifestations depend on the neuroanatomic target of immune-response. Group I (intracellular) is paraneoplastic and less responsive to immunotherapy; Group II (cell-surface) is more treatment-responsive, targeting limbic, striatal, or diencephalic circuits. Mapping symptoms to topology guides interpretation & flags paraneoplastic links.

Materials & Methods

Despite expanded antibody-panels, false-positives and phenotypic-overlap complicate diagnosis, making MRI the first-line tool for pattern-recognition, exclusion of mimics, and triage. This exhibit outlines a topology-driven MR approach integrating pathophysiology, standardized protocols, and pitfalls to hasten treatment.

Imaging Protocol: High-res ax/sag T2/FLAIR to screen mesial temporal region; add DWI for cytotoxic injury; use post-contrast T1 for enhancement patterns; reserve perfusion for equivocal tumefactive lesions & tumor-mimicry.

Results & Conclusion

Canonical imaging patterns:

-Limbic AE: Hippocampal/Amygdala FLAIR hyperintensity ± restricted diffusion, often subtle and unilateral (e.g., LGI1).
-Paraneoplastic AE: Bilateral tumefactive involvement extending beyond limbic regions, necessitating tumor search.
-Extralimbic phenotypes: Striatal, diencephalic, or brainstem signal abnormalities guiding antibody-testing and oncologic work-up.

Differential-guardrails: HSV encephalitis shows asymmetric limbic-insular involvement with diffusion-restriction and hemorrhage; PRES (Posterior-reversible-encephalopathy-syndrome) favors posterior vasogenic-edema; toxic-metabolic and neoplastic lesions show discordant tempo or mass-effect. A pattern-to-antibody-to-work-up checklist standardizes reporting and next steps.

Conclusion:

When antibody-tests mislead, MRI anchors AE diagnosis by linking regional patterns to a focused differential. An anatomic topology-first MR approach—using optimized sequences and awareness of mimics—accelerates immunotherapy, guides cancer-surveillance, and curbs overtreatment.

Images/Tables

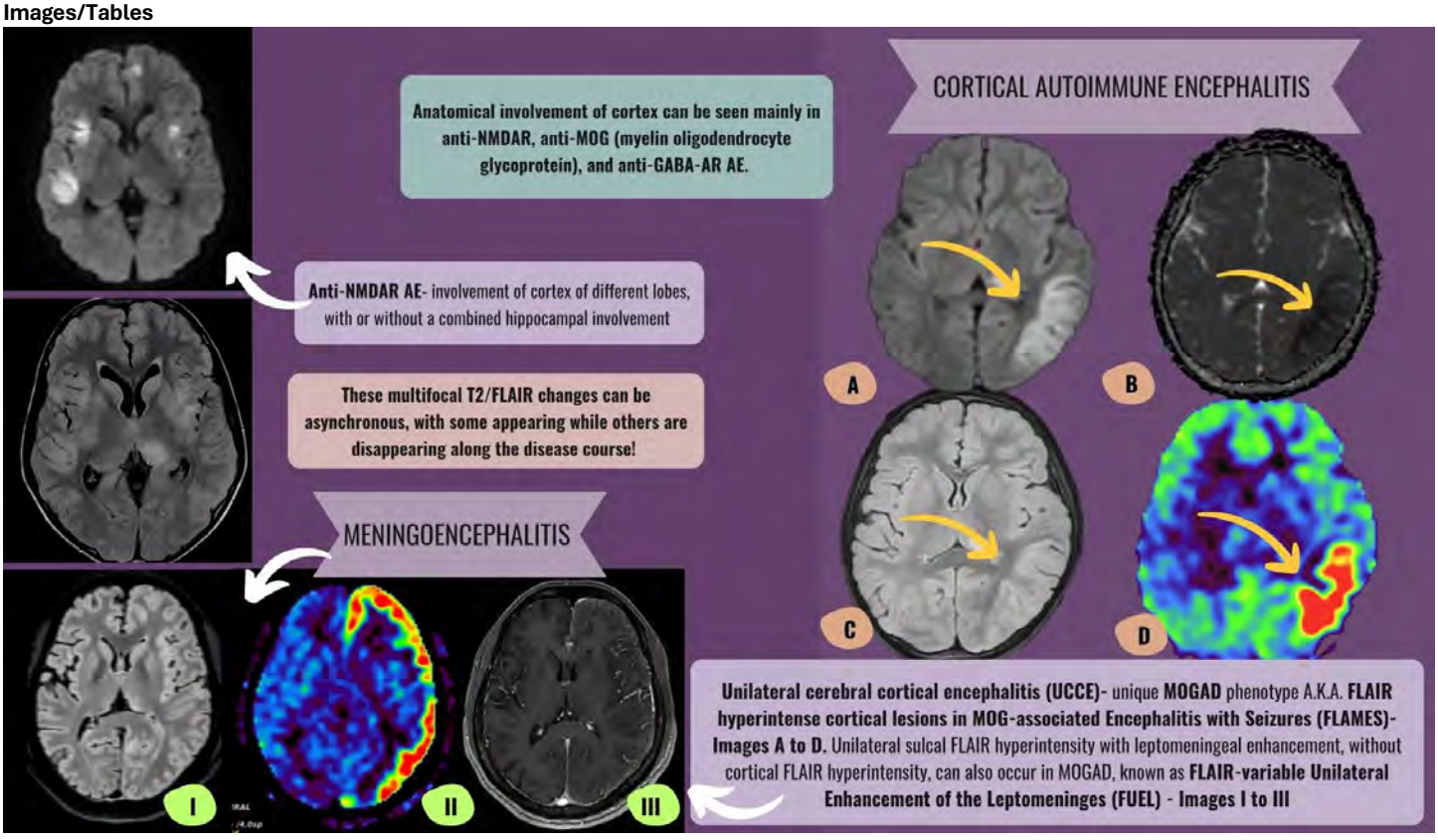

---

243 Beyond the Lumen; Imaging Pediatric arteriopathies

owais Ahmad bhat MD[1], Shumyla Jabeen MD, DM[2]
[1]University of Louisville, Louisville, kentucky, USA. [2]Sher-i-Kashmir institute of medical sciences, srinagar, jammu and kashmir, India

Summary & Objectives

Paediatric arteriopathies are often challenging to diagnose. Besides the well-known signatory puff of smoke appearance in Moyamoya, it is essential to take cognisance of genetic causes and inflammatory arteriopathies which are best characterised by vessel wall imaging. Diagnostic errors with inflammatory arteriopathies are pertinent to occur in absence of optimised vessel wall imaging techniques as distally located, focal abnormalities may easily escape the unwary eye.

The following disease entities will be described:
Moyamoya disease: With involvement of the renal artery, ACTA2 mutation: A genetically determined paediatric vasculopathy mimicking Moyamoya in appearance without basal collaterals associated with structural brain malformations, Focal cerebral arteriopathy (proximal) with concentric enhancement involving the left terminal ICA and MCA extending proximally into the petrous segment of the ICA and distally into the M2 segment of MCA, Focal cerebral arteriopathy (distal) with vessel wall imaging showing focal enhancement in the superior division of the left MCA.

Purpose

To highlight the critical role of imaging including vessel wall imaging in diagnosing and characterising paediatric cerebrovascular (arterial) diseases, particularly those that may be missed or misdiagnosed using conventional vascular imaging alone.

Materials & Methods

The methods and materials used in this study centered on advanced MRI with vessel wall imaging and angiographic evaluation (where deemed necessary) of paediatric cerebrovascular diseases to identify inflammatory, genetic, and structural arterial abnormalities that conventional lumen-based imaging might miss.

Results & Conclusion

Paediatric arteriopathies stem from diverse genetic and acquired causes. Imaging plays an essential role in diagnosis and guides management. Vessel wall imaging is indispensable in the diagnosis of focal cerebral arteriopathy especially the inflammatory variant which is one of the major acquired causes of paediatric stroke. These cases on follow-up may turn out to be transient cerebral arteriopathy, CNS vasculitis, post-infectious vasculitis or even early Moyamoya. Moyamoya disease, besides affecting the cerebral vasculature may also involve systemic arteries such as the renal artery and hence imaging protocols may have to be redesigned in that direction when the clinical presentation so dictates like the presence of uncontrolled hypertension in our case. The characteristic configuration of the cerebral vasculature and structural brain anomalies lead to the diagnosis in genetic vasculopathies like the ACTA2 mutation.

Images/Tables

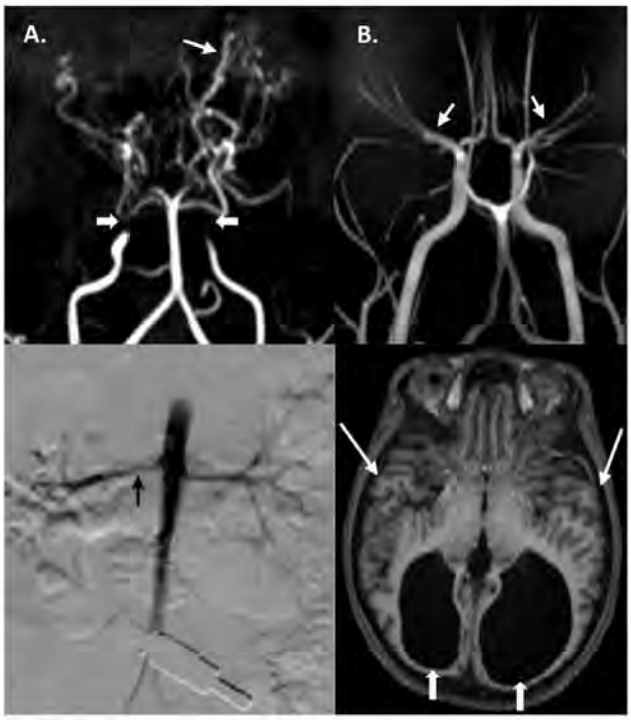

A. TOF-MRA MIP projection (upper image) in a 3 year old with Moyamoya and hypertension shows characteristic appearance with near occlusive changes in both ICAs (block white arrows) and puff-of-smoke appearance(linear white arrow). Digital subtraction angiography (lower image) shows narrowing in the right renal artery(black arrow) distal to the ostium.
B. TOF-MRA MIP projection (upper image) in a case of ACTA2 mutation shows the characteristic abnormal configuration of the cerebral vasculature with radial arrangement of vessels (white arrows). Axial T1 MPRAGE (lower image) shows radial configuration of gyri (linear white arrows) with dilated occipital horns (block white arrows).

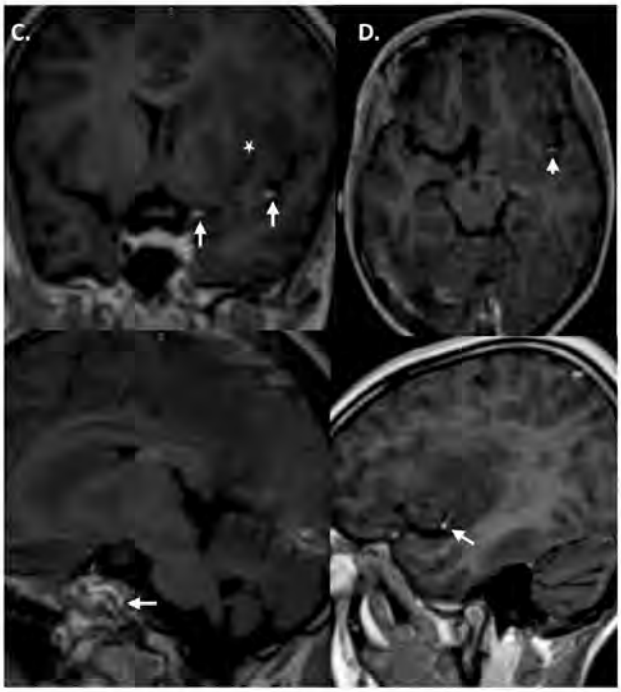

C. Coronal post-contrast T1 SPACE (upper image) in a 12 year old child shows vessel wall enhancement in the terminal ICA and M2 MCA (white arrows). Asterisk shows hypointensity suggestive of infarct in the left gangliocapsular region. Sagittal post-contrast T1 SPACE (lower image) shows enhancement in the cavernous and petrous ICA (white arrow).
D. Axial (upper image) and sagittal (lower image) post-contrast T1 SPACE images in another case of focal cerebral arteriopathy with left MCA cortical infarct shows focal enhancement in the superior division of left MCA (white arrows).

293 Pathology and Imaging of Tauopathies

Sangam Kanekar MD[1], Scott Hwang[2]
[1]Penn State Health, Hershey, PA, USA. [2]Hershey, PA, USA

Summary & Objectives

Tauopathies encompass a distinct spectrum of neurodegenerative disorders characterized by the intracellular aggregation of hyperphosphorylated tau protein forming neurofibrillary tangles (NFTs). These include both primary tauopathies—such as Progressive Supranuclear Palsy (PSP), Corticobasal Degeneration (CBD), and Pick's Disease (PiD)—and secondary forms like Alzheimer's Disease (AD) and Chronic Traumatic Encephalopathy (CTE). The objectives of this work are:
(1) to define the molecular and anatomical correlates underpinning human tauopathies
(2) to evaluate the role of neuroimaging biomarkers in clinical staging, differential diagnosis, and in assessing disease-modifying therapies.

Purpose

A comprehensive understanding of tau pathology and its imaging correlates forms the foundation for developing accurate, pathology-specific diagnostic strategies. The pathological accumulation of tau exhibits a progressive, region-specific propagation that parallels synaptic dysfunction and neuronal network degeneration. Detecting these changes in vivo through non-invasive imaging techniques is pivotal for early diagnosis and the monitoring of disease progression and therapeutic efficacy. This exhibit aims to synthesize the relationship between tau isoform profiles and neuroimaging signatures to bridge neuropathological findings with clinical utility. By correlating histopathological subtypes with advanced imaging biomarkers, we aim to support more refined diagnostic frameworks aligned with underlying molecular pathology.

Materials & Methods

A retrospective review of 101 patients labeled as "tauopathies" in our institutional PACS was performed. All patients underwent 3T MRI encompassing conventional structural imaging, diffusion tensor imaging (DTI), advanced diffusion protocols, and quantitative susceptibility mapping (QSM). Quantitative neuroinflammation imaging metrics—including mean diffusivity (MD), fractional anisotropy (FA), and radial diffusivity (RD)—were analyzed to assess white matter integrity and microstructural changes related to inflammation. Among these, 23 patients also underwent tau positron emission tomography (tau-PET) using radioligands such as Flortaucipir for in vivo quantification of fibrillar tau deposition. Cases were categorized as primary or secondary tauopathies based on pathological mechanisms and isoform predominance.
Primary tauopathies include: 3R tauopathy: Pick's Disease (PiD), characterized by spherical "Pick bodies." 4R tauopathies: Progressive Supranuclear Palsy (PSP), Corticobasal Degeneration (CBD) with "astrocytic plaques," Argyrophilic Grain Disease (AGD), Globular Glial Tauopathy (GGT), and Aging-related Tau Astrogliopathy (ARTAG). Mixed 3R/4R tauopathies: Primary Age-Related Tauopathy (PART) and Frontotemporal Dementia with Parkinsonism linked to chromosome 17 (FTDP-17).
Secondary tauopathies encompass Alzheimer's Disease (AD), Chronic Traumatic Encephalopathy (CTE), and Anti-IgLON5 autoimmune encephalitis, where tau accumulation is secondary to other pathological processes. Structural MRI was analyzed for disease-specific atrophy patterns, such as hippocampal involvement in AD and midbrain atrophy in PSP. DTI and QSM metrics provided insight into axonal degeneration and iron deposition, while tau-PET imaging offered quantitative regional mapping of tau aggregation.

Results & Conclusion

Advanced neuroimaging techniques have become indispensable in understanding tauopathies by enabling the in vivo characterization of molecular pathology, structural alterations, and disease progression. Structural MRI, diffusion metrics, and tau-PET together create a multidimensional biomarker framework that reflects the spatial and temporal dynamics of tau deposition.
Ultimately, neuroimaging serves as the critical interface linking molecular pathology to clinical expression, driving the evolution of precision medicine in the diagnosis and management of tau-related neurodegeneration.

---

369 Idiopathic Intracranial Hypertension Revisited: Pearls and Pitfalls for Radiological Diagnosis and Intervention

Mona Gad, Jee Moon, Vivek Yedavalli, Sachin Gujar, Philippe Gailloud, Francis Deng
Department of Radiology and Radiological Science, Johns Hopkins University School of Medicine, Baltimore, MD, USA

Summary & Objectives

1. Describe the grading scales, quantitative imaging parameters, and optimized protocols for reliable diagnosis of idiopathic intracranial hypertension (IIH).
2. Identify the current imaging pitfalls and remedies to avoid overcalled diagnosis of IIH.
3. Recognize the clinical sequalae and imaging differential considerations for IIH.
4. Understand the role of imaging in determining the degree of venous sinus stenosis and venous outflow patterns and patient selection for endovascular procedures.

Purpose

The primary goal of this exhibit is to provide a comprehensive overview of the role of neuroimaging in diagnosis and guiding therapeutic intervention in the setting of idiopathic intracranial hypertension (IIH), with emphasis on the most reliable diagnostic imaging features and potential pitfalls encountered in clinical practice.

Materials & Methods

The main goal of this exhibit is to optimize image interpretation in the clinical context of possible IIH.

1. Epidemiology, presentation, and sequelae
2. Diagnostic criteria
3. Imaging technique: orbital, brain, and venous structures
4. Skull base: partially empty sella and other spaces
5. Orbits: optic nerve sheath, optic papilla, and posterior globe wall
6. Venous structures: sinus stenosis and collateral pathways
7. Differential diagnosis: secondary intracranial hypertension and radiologic mimics
8. Lumbar puncture: technique and interpretation
9. Treatment: role of venous sinus stenting in medically refractory cases

Results & Conclusion

Results: N/A

Conclusion:

Diagnosing IIH requires a multidisciplinary approach with a combination of clinical history, fundoscopy, neuroimaging, and lumbar puncture. Neuroradiologists should be aware of the most sensitive and specific imaging markers, quantitative metrics, and potential pitfalls relevant to IIH to improve diagnostic confidence in clinical practice, reduce overcalled radiologic diagnosis of IIH, and guide therapeutic intervention for such patients.

Images/Tables

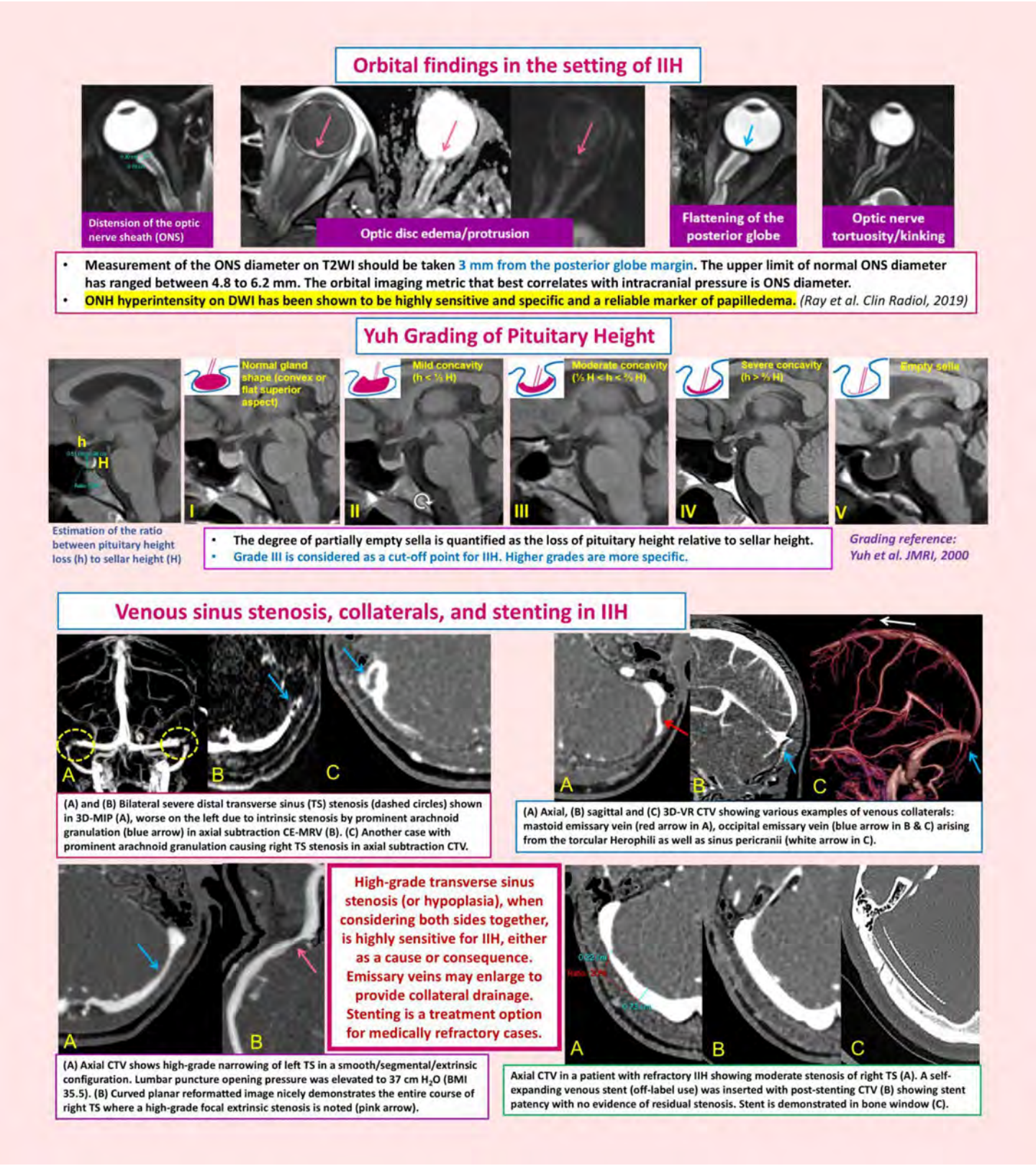

388 Comprehensive Radiologic-Pathologic Correlation in Erdheim-Chester Disease: A Diagnostic Imaging Roadmap

Fatemeh Dehghani Firouzabadi MD[1], Hamid Harandi MD[2], Ali Sheikhy MD[3], Fahimul Huda MD[1]
[1]University of Louisville, Louisville, Kentucky, USA. [2]TUMS, Tehran, Tehran, USA. [3]NIH, Bethesda, Maryland, USA

Summary & Objectives

Erdheim-Chester Disease (ECD) is a rare, multisystemic non-Langerhans cell histiocytosis marked by xanthogranulomatous tissue infiltration. Accurate diagnosis requires integration of imaging findings with histopathologic confirmation. This study highlights the characteristic radiologic and pathologic features of ECD across multiple organ systems.

Purpose

To illustrate and correlate the hallmark radiologic and histopathologic findings of Erdheim-Chester Disease across various organ systems, emphasizing the importance of multidisciplinary evaluation for accurate diagnosis and management.

Materials & Methods

Radiologic imaging from multiple organ systems, including musculoskeletal, central nervous system, soft tissue, abdominal, pulmonary, and cardiovascular structures, was reviewed. Findings were correlated with histopathologic results obtained through biopsy and immunohistochemistry (IHC). Histologic analysis included hematoxylin and eosin (H&E) staining and IHC for CD68 and S100 markers to identify histiocytic infiltration

Results & Conclusion

Radiologic findings involved multiple organ systems. **Uropathy** was characterized by sheathing or narrowing of the proximal ureter, cystomegaly, and hydroureter. **Nephropathy** demonstrated hydronephrosis, cortical thinning, isolated calyceal ectasia, and renal sinus pedicle involvement. **Hepatobiliary** findings included liver and biliary involvement. **Splenic** abnormalities showed spleen involvement. **Vascular** manifestations included periaortic infiltration; sheathing or stenosis of the renal artery; sheathing of aortic branches including the SMA, MA, and celiac artery; and involvement of the coronary, pulmonary, and superior vena cava (SVC) vessels. **Pulmonary** findings consisted of interstitial disease, ground-glass opacities, nodules, honeycombing, parenchymal and pleural involvement, and hilar adenopathy. **Cardiac** manifestations included cardiac involvement with right atrial wall thickening, mediastinal infiltration, and pericardial involvement. **Orbital** findings showed bilateral rectus muscle thickening, retroorbital fat infiltration, and optic nerve involvement. **Central nervous system (CNS)** abnormalities included cortical, basal ganglia, brainstem, cerebellar, pituitary, and peduncular lesions. (Figure 1). **Axial skeletal** findings involved the calvarium (skull), cervical, thoracic, and lumbar spine, as well as the ribs. **Appendicular skeletal** findings included the shoulder girdle (clavicle and scapula), upper limb (humerus, radius, ulna, and hand), pelvic girdle (ilium, ischium, and pubis), and lower limb (femur, tibia, fibula, and feet).

Brain biopsies revealed foamy macrophages on H&E staining with immunohistochemical positivity for CD68, highlighting histiocytic infiltration. Biopsy of the ascending aorta demonstrated a fibrotic background with CD68-positive histiocytic cells and mononuclear inflammation (Figure 1). Core biopsies showed fibrous tissue with plasma cells, lymphocytes, and histiocytes, and CD68 immunostaining confirmed renal histiocytosis. Lung wedge biopsies exhibited histiocytic infiltrates effacing normal architecture, with immunohistochemistry showing CD68 positivity and S100 negativity. These radiologic and pathologic correlations emphasize the diverse organ involvement in ECD and reinforce the need for combined imaging and histopathologic evaluation for accurate diagnosis and effective management.

Images/Tables

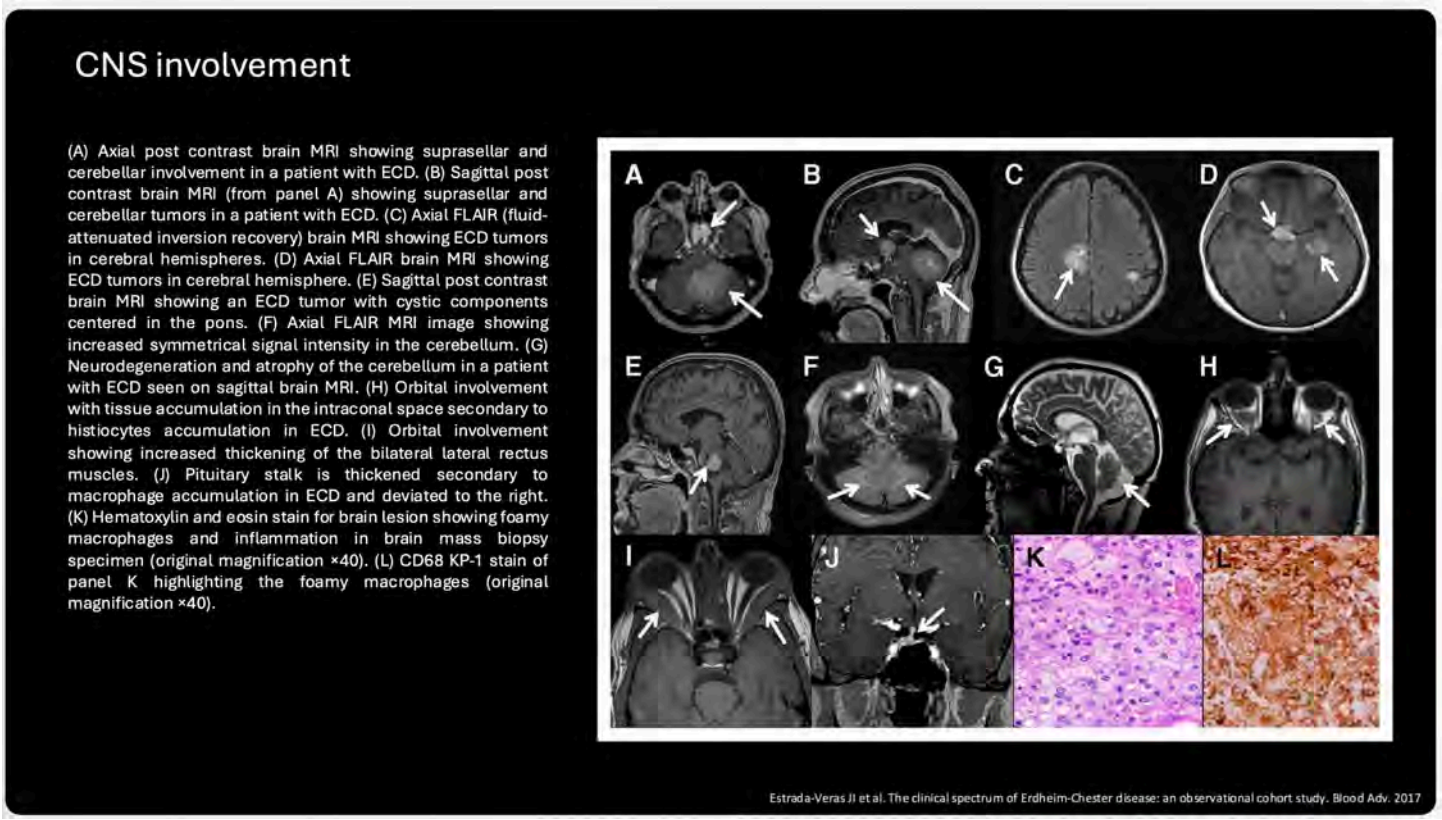

460 Differential Subsampling with Cartesian Ordering (DISCO) of the Pituitary. Maximizing Spatial and Temporal Resolution to Eliminate the "Equivocal Microadenoma".

Cam Kendall MD, Aaron S Field MD PhD, Justin L Brucker MD
UW Madison, Madison, WI, USA

Summary & Objectives

Differential Subsampling with Cartesian Ordering (DISCO, GE HealthCare, Waukesha, WI) is an imaging technique that preferentially oversamples and fills the center of K-space (contrast detail) while the periphery of k-space (edge detail) is filled over time and shared over multiple phases. The stationary anatomy of the pituitary and sella are ideal for image sharing between phases while the oversampling of contrast data with each phase produces excellent T1-weighted contrast. In pituitary microadenoma evaluations, existing methods using spin-echo post-contrast sequences suffer from poor contrast and spatial resolution and are prone to false positives due to volume averaging with the adenohypophysis-neurohypophysis boundary or with the adjacent enhancing cavernous sinus. DISCO has already shown promise in adding value to prostate MRI. The purpose of this exhibit is to explore the feasibility and utility of DISCO imaging of the pituitary.

Purpose

Most dedicated pituitary MRI exams are performed at the request of the clinician after a patient has already presented with an endocrinologic concern or found to have an existing endocrinopathy suspected to be attributed to pituitary pathology. In these patients the dynamic T1 post-contrast imaging is the workhorse for detecting endocrinologically active pituitary masses, most often microadenomas. As above, the challenge of reading pituitary protocol MRI is the small size of the anatomy and therefore limited resolution. The purpose of this exploration was to find a better sequence to dynamically image the pituitary.

Materials & Methods

Out-of-the-box DISCO sequence was employed to image the sellar region (TR/TE 5.9/2.0 ms, FA 12 degrees). Fat saturation on DISCO exams is accomplished with an inversion pulse and so fat saturation was disabled to maximize temporal resolution. Imaging parameters were initially optimized on a 1.5T Signa Artist and 3T Signa Architect (GE HealthCare) scanners. The imaging field of view was progressively reduced to approximately 10x10 cm coronal or axial plane by approximately 4 cm in the Z-plane (axial or coronal through-planes). Axial plane images yielded the highest signal to noise ratio, but coronal plane provided a more familiar presentation of the dynamic sequences. All dynamic phases were multiplanar reformattable.

Results & Conclusion

Differential Subsampling with Cartesian Ordering (DISCO) sequences perform well in the sellar and suprasellar region. We were able to obtain a temporal resolution of 12 seconds per phase with an in-plane resolution of 0.6 x 0.6mm in-plane by 1mm through-plane using a field of view of 10x11cm and matrix of 192x192. This was improved compared to the slightly coarser 0.7x0.7mm in-plane by 2mm through-plane of the conventional spin-echo based technique (TR/TE 500/6.9 FA 111 degrees). T1 contrast was subjectively improved. Notable observations include visualization of the dural margin between the sella and cavernous sinus in the coronal plane, the ability to create multiplanar reformats of each phase, excellent flow-related T1 signal within the circle of Willis, and multiple phases of progressive pituitary enhancement. The feasibility of this technique paves the way for further investigation of DISCO dynamic imaging of the sellar region.

Images/Tables

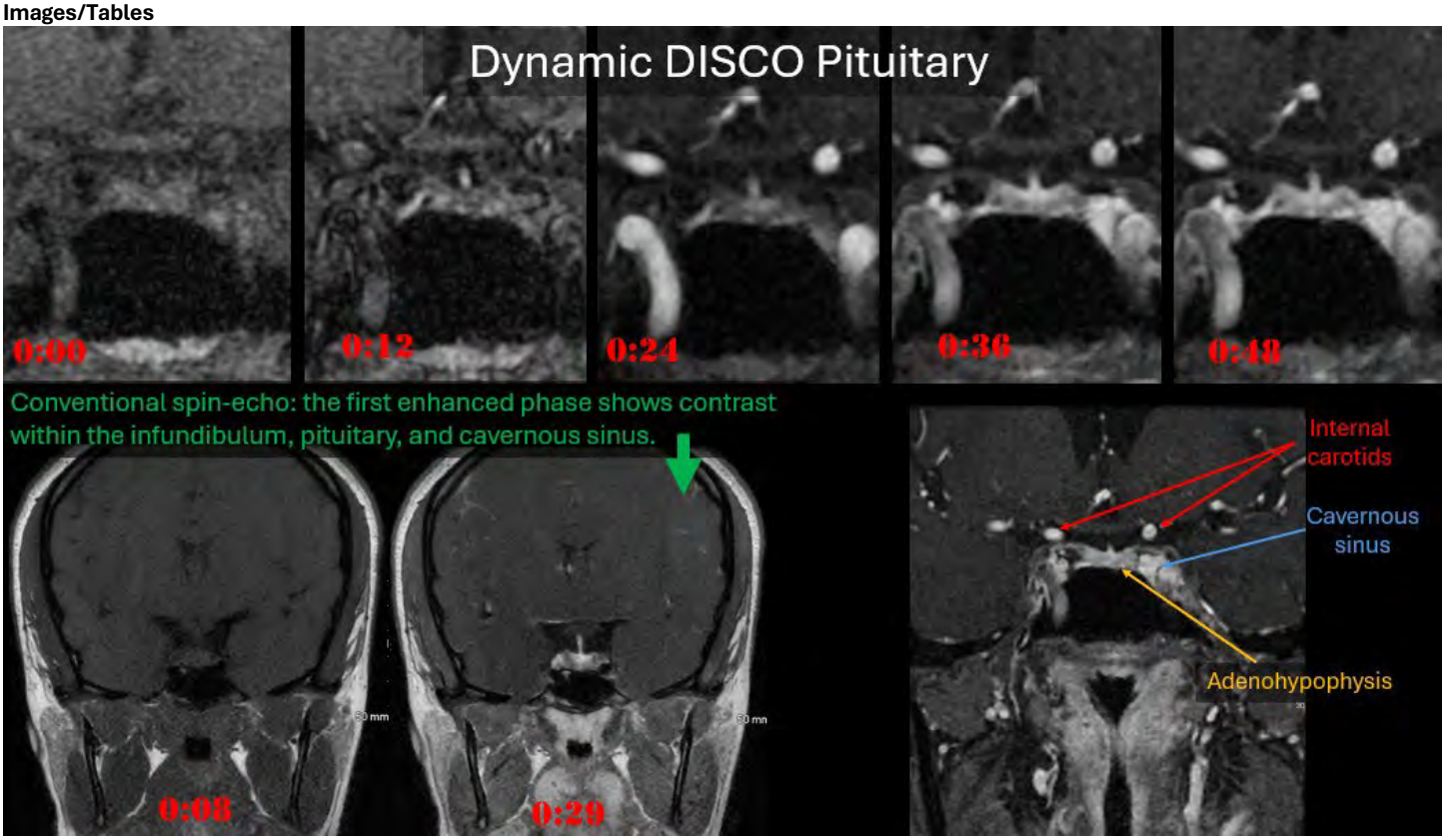

468 "Seeing is Believing": an Imaging Review of Optic Nerve Pathology

Kevin Jiang MD, Brian Yoon MD, Sally Choi MD, Oliver Yu, Rebecca Flores DO, Prabhakar Kesava MD, Manoj Kumar MD, Dhrutiben Maisuri MD, Bundhit Tantiwongkosi MD, Hasanagha Zalov MD, Alireza Paydar MD
UT Health San Antonio, San Antonio, TX, USA

Summary & Objectives

Decreased visual acuity is a common presenting symptom in both the inpatient and outpatient setting and can sometimes point to an underlying optic nerve pathology. While an ophthalmologic examination with fundoscopy is the appropriate first step in management, further imaging may be warranted for a comprehensive evaluation. A proper imaging assessment of the optic nerves requires first an understanding of optic nerve anatomy. Optic nerve pathologies can be categorized into several etiologies. Ultimately, the radiologist can play a role in both initial diagnosis as well as confirmation of clinical exam findings.

- Review optic nerve anatomy
- Showcase several etiologies of optic nerve pathology
- Identify pitfalls in optic nerve imaging

Purpose

This educational exhibit will illustrate a framework for the radiologist to understand the imaging spectrum and considerations of optic nerve pathology.

Materials & Methods

We have reviewed imaging for a variety of patients with optic nerve pathology at a level 1 trauma center/academic institution in San Antonio, TX.

Results & Conclusion

A spectrum of optic nerve pathologies was identified at our institution. Their etiologies include trauma, autoimmune, metabolic, infectious, inflammatory, vascular, neoplastic, and congenital. Understanding optic nerve anatomy can help focus one's search pattern when recognizing an optic nerve disease process. Important imaging considerations include identifying extent of disease as well as paying attention to common blind spots such as the orbital apex for an example.

Images/Tables

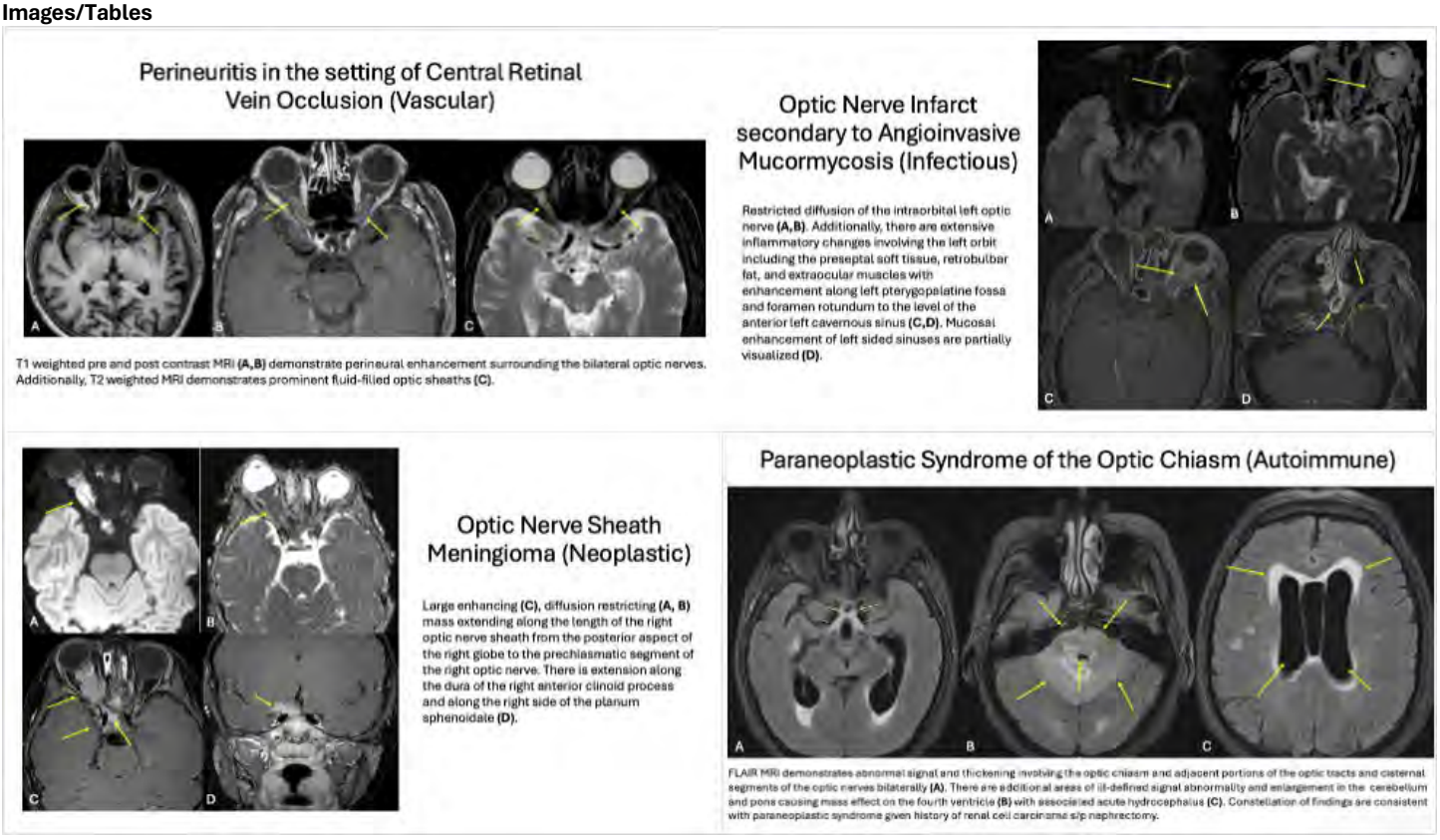

491 Diagnosing Multiple Sclerosis: What the Neuroradiologist Needs to Know About the Updated 2024 McDonald Criteria

James K Sanayei MD, Kyle M Moulton MD
University of Saskatchewan Department of Medical Imaging, Saskatoon, Saskatchewan, Canada

Summary & Objectives

Summary

Multiple sclerosis (MS) is a chronic inflammatory demyelinating disease that affects the central nervous system.[1] Often a challenging clinical diagnosis, multiple attempts have been made over the years to create standardized diagnostic criteria. The Schumacher criteria, published in 1965, focused entirely on clinical findings, incorporating the concepts of dissemination in time and space. In 1983, the Poser criteria incorporated laboratory and paraclinical evidence. The McDonald criteria was the first to incorporate radiological (MRI) evidence into a unified diagnostic schema.[2] Originally published in 2001, it has since been updated several times, with the most recent 2024 revision (published in October 2025) making several key changes to the previous 2017 criteria.[3]

Among the 2024 revisions are several changes that neuroradiologists should be familiar with. First, the optic nerve has been included as the fifth anatomical site to satisfy the dissemination in space requirement (alongside periventricular, cortical/juxtacortical, infratentorial brain, and the spinal cord), with tests such as optical coherence tomography (OCT) and visual evoked potentials (VEPs) allowing diagnosis in lieu of MRI. Second, central vein sign (CVS) and paramagnetic rim lesions (PRLs) have been added as important imaging markers. Third, dissemination in time is no longer considered essential; rather, it is now included as an ancillary criterion (alongside other factors such as CSF positivity, CVS and PRLs). Fourth, patients with radiologically isolated syndrome (incidental imaging findings consistent with MS, but without typical clinical symptoms) can be diagnosed with MS when specific criteria are met. Finally, a single framework can now be used to diagnose both pediatric and adult-onset MS.

Objectives

- Review the historical understanding of multiple sclerosis and how it has evolved in recent years
- Summarize the original McDonald criteria and subsequent revisions
- Define the 2024 revisions and explain their rationale, with a focus on radiological markers
- Apply the revised criteria to a series of cases that emphasize the clinical application of CVS and PRLs

Purpose

N/A

Materials & Methods

N/A

Results & Conclusion

N/A

---

538 Dementias and Degeneration: Demystifying the Imaging Features of Neurodegenerative Disorders

Kevin Pham DO, Nahill Matari MD
Columbia University Irving Medical Center, New York, NY, USA

Summary & Objectives

Neurodegenerative diseases consist of a broad assortment of irreversible and devastating neurologic disorders. There can be considerable overlap in the clinical symptoms for these processes, and while meaningful disease-modifying therapies for many of these diseases may not exist at present, it may provide some sense of peace for patients to have an answer for their cognitive decline. Brain imaging is ubiquitously performed to exclude alternative diagnoses but may uncover certain supportive features that may suggest one of these pathologies. Thus, it would be prudent for radiologists to be able to recognize the imaging features for these disorders in order to help guide clinicians to a diagnosis and unlock any potential treatments that may be available for symptomatic relief.

Educational Objectives:

- Highlight the large array of neurodegenerative disorders and their underlying etiologies
- Review the remarkable imaging findings for each entity
- Discuss typical clinical symptoms associated with each process and existing treatments

Purpose

The primary aim of this educational exhibit is to provide a review of the wide range of neurodegenerative diseases. This will include processes such as Alzheimer disease, Parkinson disease, multiple system atrophy, progressive supranuclear palsy, frontotemporal dementia, amyotrophic lateral sclerosis, multiple sclerosis, cerebral amyloid angiopathy, Creutzfeldt-Jakob disease, and chronic traumatic encephalopathy. The pathologic mechanism, clinical features, any available treatments, and distinguishing imaging findings will be discussed for each entity.

Materials & Methods

The presentation will open with a general discussion of the assortment of neurodegenerative disorders including categorization of their etiologies. This will be followed by a dedicated focus on each disorder which will be accompanied by case-based imaging examples primarily utilizing MRI or CT. The discussion of each disorder will include the current scientific understanding of the underlying pathology, associated clinical symptoms, potential treatments, and a review of the notable imaging findings that can aid in diagnosis.

Results & Conclusion

By the end of this presentation, the viewer should have a better understanding of the different neurodegenerative processes that exist, and they should be able to identify the distinguishing imaging features that would suggest one diagnosis over the other. In doing so, radiologists may better aid their clinicians and patients by helping establish a timely diagnosis. Greater recognition of these entities may also contribute to the ongoing research efforts to slow these neurologically devastating diseases.

Images/Tables

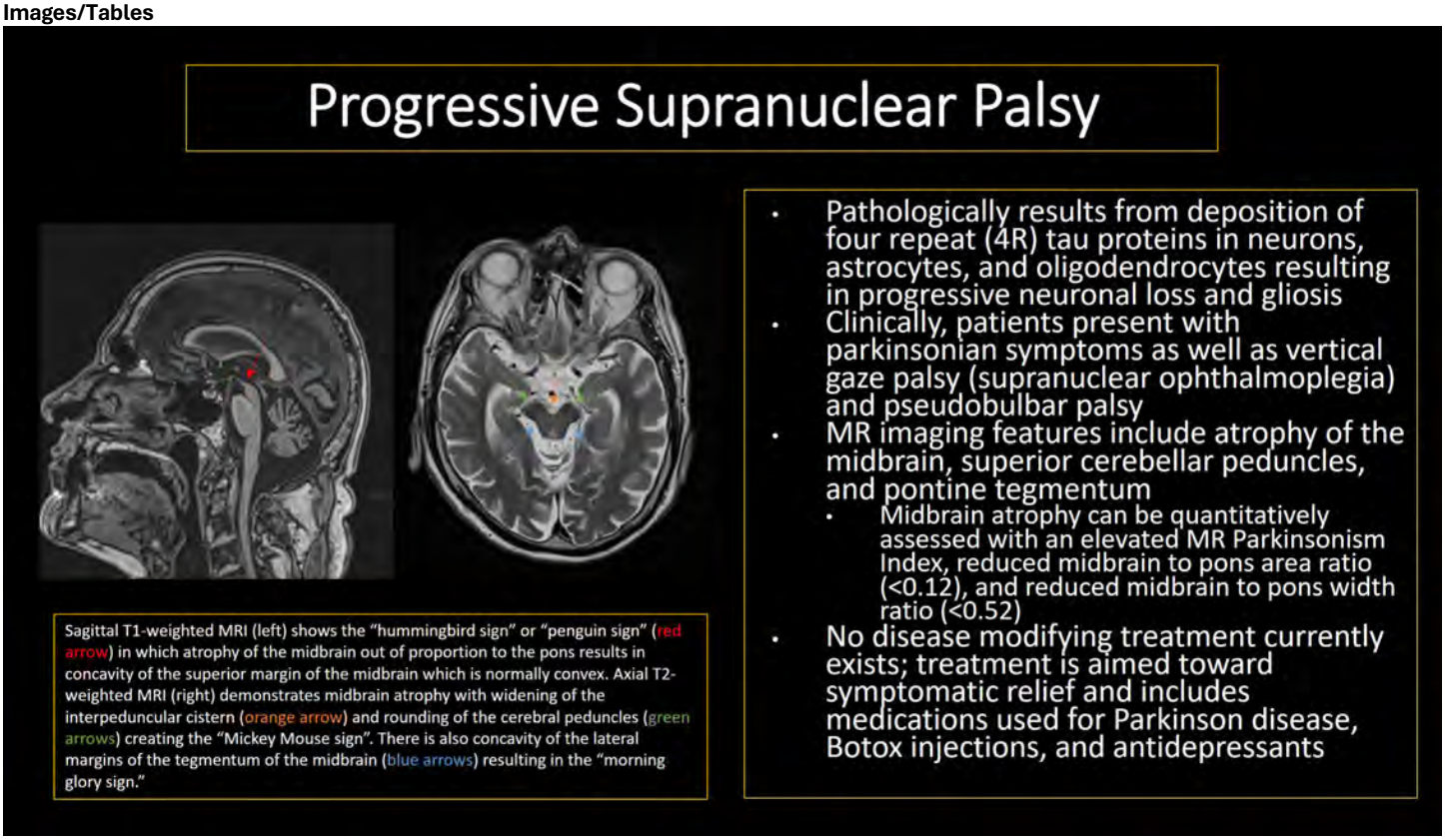

---

559 Foundational Models in Neuroradiology: How General is General Enough

Prabhnoor Kaur MBBS[1], Fatima Ahmad Qureshy[2], Angelica P. Kurtz[3], Moinak Bhattacharya[4], Prateek Prasanna[4], Gagandeep Singh[5]
[1]Guru Gobind Singh Medical College, Faridkot City, Punjab, India. [2]Sheikh Zayed Hospital, Lahore, Punjab, Pakistan. [3]Columbia University Vagelos College of Physicians and Surgeons, New York City, NY, USA. [4]Department of Biomedical Informatics, Stony Brook University, Stony Brook, NY, USA. [5]Department of Radiology, Columbia University Irving Medical Center, New York City, NY, USA

Summary & Objectives

Foundation models (FMs) such as GPT-4, Med-PaLM, RadFM, CLIP, and SAM represent a major leap in artificial intelligence, shifting from single-task tools to flexible, general-purpose systems that can adapt across modalities, anatomical regions, and data domains with minimal retraining.
Their rapid progress has prompted increasing interest in radiology, raising a key translational question: Are general AI systems capable of performing reliably in neuroradiology, where diagnostic precision and multimodal expertise are essential.
Neuroradiology poses unique challenges among imaging fields due to complex tissue microstructure, multimodal inputs, and diagnosis-driven interpretation that depends on both anatomical precision and clinical context. Unlike chest radiography or pathology slides, where visual patterns may be more uniform and standardized, brain imaging demands fine-grained differentiation of subtle abnormalities across time and protocols.
This educational exhibit reviews the capabilities and limitations of general foundation models in neuroradiology, highlighting emerging use cases, safety and reliability considerations, and the importance of specialty-specific refinement.
By the end of this exhibit, attendees will be able to:

- Define foundation models and their role in radiology
- Describe evolution of AI systems from general language models to medical and radiology-specific FMs
- Understand neuroradiology-specific challenges to generalization
- Review current generalist models and "general enough" criteria
- Recognize scenarios where generalist performance is sufficient vs those requiring specialty-tuned models
- Identify key safety, regulatory, and workflow considerations for FM deployment

Purpose

The purpose of this exhibit is to provide neuroradiologists with a clear, practical framework of how foundation models may integrate into brain imaging workflows, and to explore the boundary between "general" capability and "clinically sufficient" performance. While general FMs show impressive flexibility, neuroradiology often requires domain-informed reasoning across subtle findings, physiologic imaging, and serial follow-up.
Key questions addressed include:

- When can a general model safely assist with neuroradiology interpretation?
- Which tasks benefit from neuro-specific training or radiologist supervision?
- How should clinicians evaluate FM tools for everyday practice?

This exhibit aims to support radiologists in critically engaging with emerging AI systems and guiding their safe adoption in clinical care.

Materials & Methods

Conceptual and literature-based analysis of FM performance in neuroradiology across modalities and tasks.

Results & Conclusion

General foundation models have reached a performance threshold where they can meaningfully assist neuroradiologists in triage, structured reporting, and selected imaging tasks. Yet they are not yet “general enough” to autonomously handle the depth, subtlety, and multimodal complexity of neuroradiology.

Progress will require:

- Neuro-specific benchmarking datasets
- Multi-modality validation (CT + MRI + PET)
- Pediatric and rare disease representation
- Longitudinal evaluation frameworks
- Safety guardrails and uncertainty quantification

Neuroradiology remains the proving ground for true generalization in medical AI. Foundation models are the correct foundation but specialty-guided refinement, transparent validation, and radiologist leadership remain essential. The future lies in hybrid models and human-centered AI workflows, where broad foundation intelligence is paired with neuro-specific refinement, rigorous validation, and radiologist oversight. Neuroradiologists will play a central role in guiding safe and effective clinical integration as these technologies continue to mature.

Images/Tables

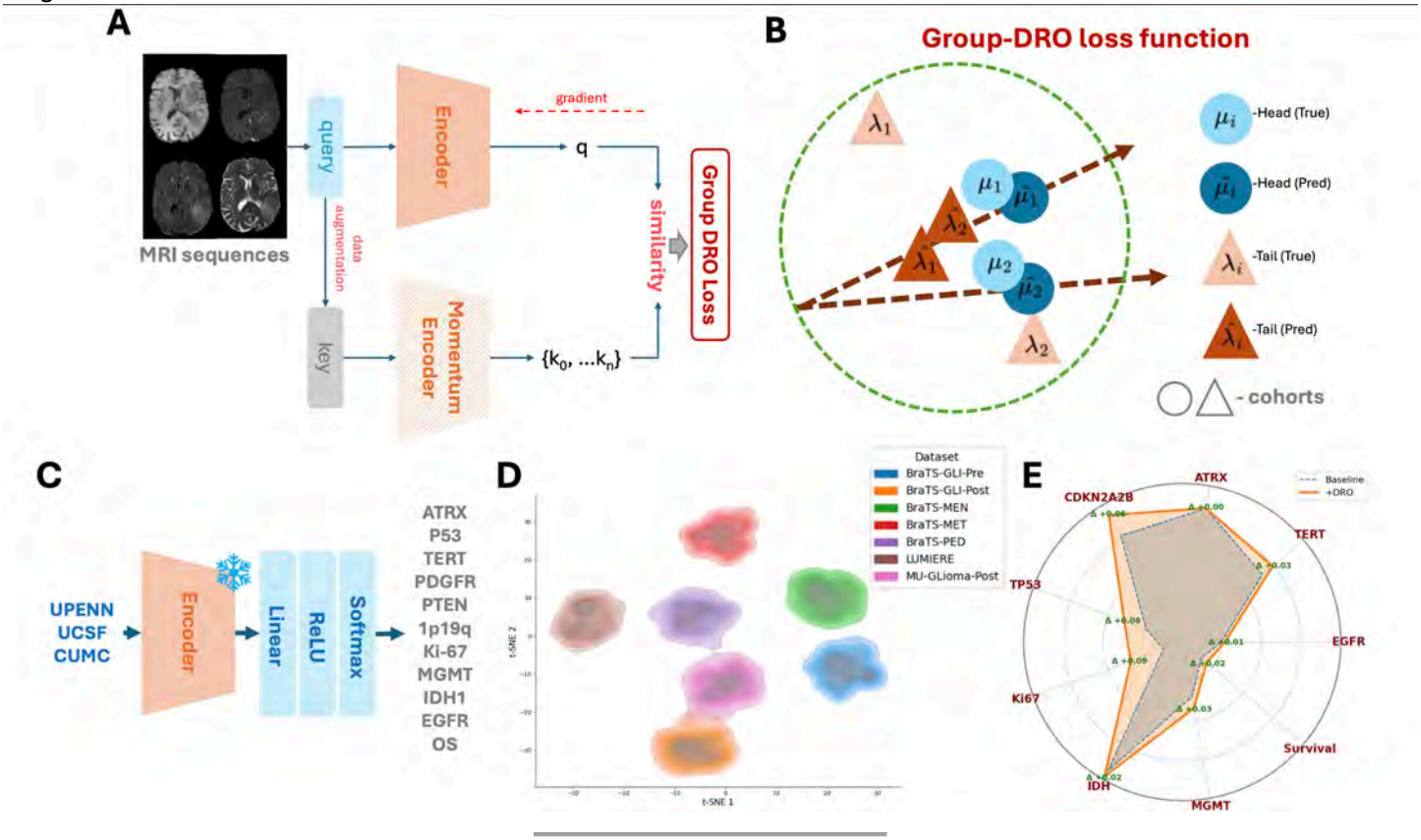

564 To the Dura and Beyond: Imaging Spectrum of Metastatic Meningioma

Armaan Shah MD, Avraham Zlochower MD, John Manov MD, Saeed Asiry MD, Puneet S Pawha MD
Lenox Hill Hospital, New York, NY, USA

Summary & Objectives

Metastatic meningiomas are a rare but clinically significant manifestation of primary intracranial meningioma, occurring in fewer than 1% of cases and most frequently associated with atypical and high-grade (WHO II/III) histology. In our series of five biopsy-confirmed metastatic meningioma cases, three were WHO grade II and two were WHO grade III. This distribution closely matches published data: large systematic reviews report that among metastatic meningiomas, approximately 36% are grade II and 26–40% are grade III, with the remainder being grade I. Most metastatic cases occur after multiple recurrences and are associated with high-grade histology, male sex, and early relapse. The objective of this exhibit is to present five cases of biopsy-confirmed metastatic meningioma via radiologic and pathologic correlation, illustrating a wide spectrum of patterns of metastasis including pulmonary, osseous, leptomeningeal, and soft tissue involvement.

Purpose

The purpose of this educational exhibit is to familiarize radiologists with the under-appreciated phenomenon of meningioma metastasis. By illustrating the diverse radiologic features across multiple imaging modalities, we aim to improve the radiologist’s ability to recognize and potentially distinguish these metastases from other entities.

Materials & Methods

A retrospective search of our institution's radiology report database (Nuance mPOWER™) was conducted using the keywords "malignant meningioma" and "metastatic meningioma" to identify a potential case cohort. From this search, five adult patients with subsequent pathology-confirmed meningiomas were selected. The comprehensive imaging workup for these patients was reviewed, including contrast-enhanced MRI, CT, and functional imaging with both F-18 FDG PET/CT and somatostatin receptor (DOTATATE) PET/CT. Our analysis focused on identifying patterns of

extracranial spread and intracranial dissemination. These radiologic findings were then correlated with the available clinical context, including primary tumor grade and history of recurrence.

Results & Conclusion

Our five cases demonstrated a wide range of metastatic sites, aligning with and expanding upon patterns described in the literature for this rare entity. The most frequent site of metastasis was the thoracic cavity, with findings including multiple FDG-avid parenchymal nodules (SUVmax up to 13.1) and extensive pleural-based masses with associated effusion. Beyond the thorax, confirmed sites were remarkably diverse, including: newly developed lytic osseous lesions in the pelvis; intensely hypermetabolic soft tissue masses (SUVmax up to 17.8) invading the head and neck, including the parotid gland and masticator space; and a rare presentation of leptomeningeal "drop" metastases seen as diffuse enhancement along the conus medullaris and cauda equina.

Metastatic meningiomas, especially those arising from recurrent or high-grade primary tumors, present significant diagnostic challenges. As our cases illustrate, a multimodality imaging approach is indispensable. While MRI and CT define anatomical involvement, functional imaging can be paramount for staging and characterization. FDG-PET/CT effectively identifies widespread metabolically active disease, while DOTATATE PET/CT proves uniquely valuable for confirming the somatostatin receptor-positivity characteristic of meningioma origin and detecting occult lesions. Accurate staging is critical to guide complex, multimodal management, which may include surgery, radiotherapy, and systemic therapies. Given the poor prognosis and the absence of standardized screening protocols, radiologists must maintain a high index of suspicion for these varied and aggressive metastatic patterns.

Images/Tables

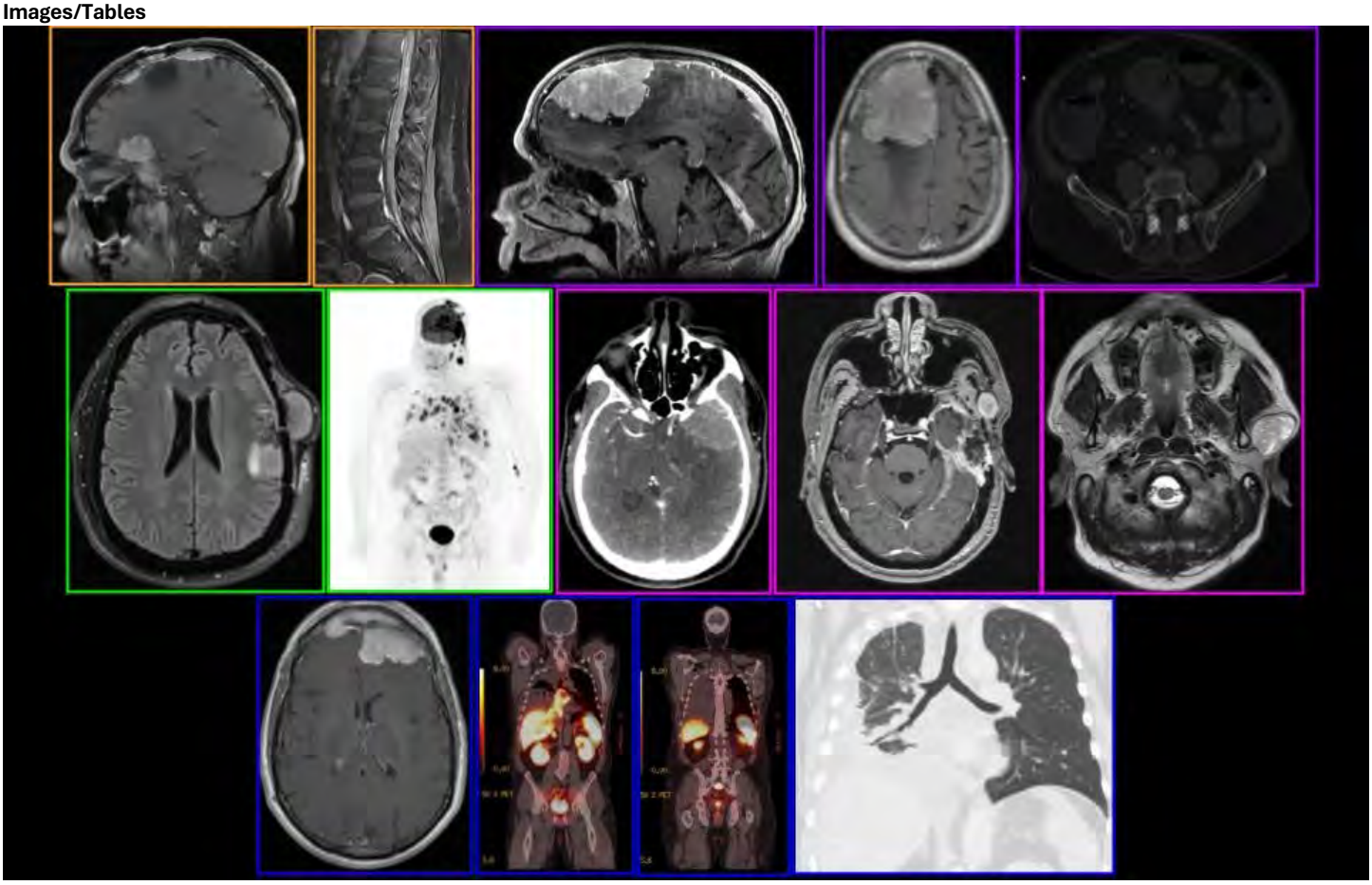

616 **Mind Over Malformations: A Case-Based Guide to Vascular Lesions in the Brain**

Nicholas O V Cunningham MD[1], Pootipong Wongveerasin MD[2], Harprit S Bedi MD[1]

[1]Boston Medical Centerr, Boston, MA, USA. [2]Boston Medical Center, Boston, MA, USA

Summary & Objectives

1. Review common and rare vascular malformations of the CNS such as arteriovenous malformations, arteriovenous fistula, cavernous malformations, vascular conditions, syndromes and other neoplasms.
2. Use cased based with multi-modality imaging such CT, MRI, DSA and Advanced Imaging techniques to illustrate key imaging features for each diagnosis.
3. Review common clinical presentations, relevant differential diagnosis where applicable, classification schema and important considerations specific to each diagnosis, as well as management.

Purpose

1. This exhibit is targeted to radiology trainees.
2. An unknown case showcasing a vascular lesion of the central nervous system will be presented.
3. For each case, the goal is to identify the imaging findings, formulate a differential diagnosis and a suspected diagnosis.
4.Diagnosis, discussion and management considerations will follow.

5. Overall, the purpose of the educational exhibit is to familiarize trainees with the key imaging findings, classification schema, diagnosis, management and key considerations for each diagnosis.
6. The goal is to aid residents in learning to provide accurate, high value radiologic reports which contain important considerations for managing these conditions.

Materials & Methods

1. The exhibit will be in a Microsoft PowerPoint Presentation.
2. The format will be case based.
3. Each case will be divided into three sections with each section showing representative multimodality images pertaining to the diagnosis, as follows:

I: Unknown Case presentation
II: Differentials and Diagnosis
III: Discussion and Management Considerations.

Results & Conclusion

N/A

Images/Tables

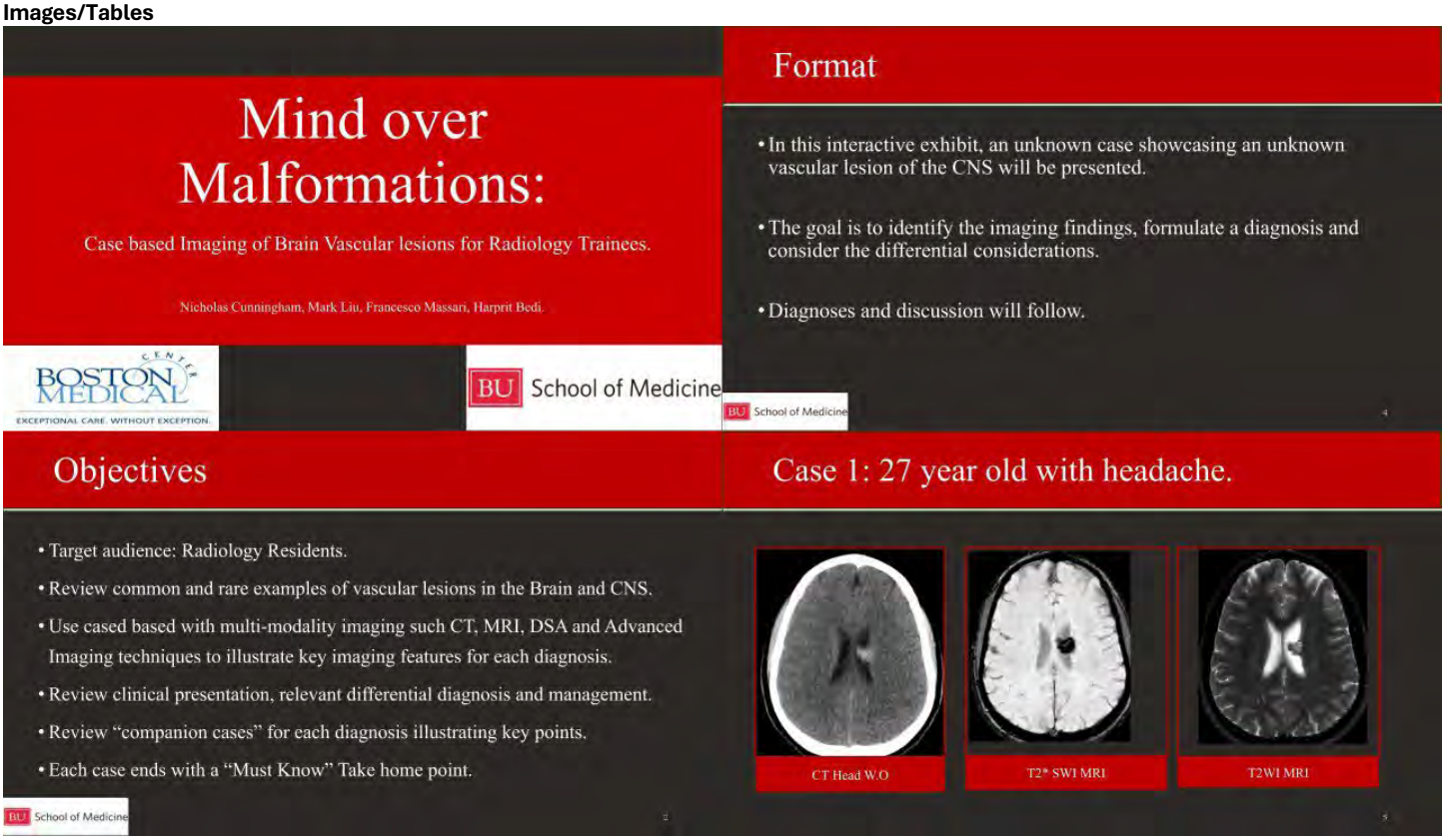

---

671 Chorea-acanthocytosis- mimic of Huntington disease

Amanda R Thadikaran MBBS[1], Bins M John MD[1], Flju Chacko MD[1], Thomas J Eluvathingal Muttikkal MD[2]
[1]Jubilee Mission Medical College and Research Institute, Thrissur, Kerala, India. [2]University of Virginia Health System, Charlottesville, VA, USA

Summary & Objectives

Chorea-acanthocytosis is a subtype of neuro-acanthocytosis-a group of rare heterogeneous neurodegenerative disorders associated with acanthocytosis. Chorea-acanthocytosis is an autosomal recessive disease associated with mutations in VPS13A gene that encodes the protein chorein with imaging and clinical features similar to Huntington disease[1]. Hippocampal sclerosis may occur in chorea-acanthocytosis[2,3] and, when present, can serve as a useful imaging marker to help distinguish it from Huntington disease, guiding further diagnostic workup and appropriate genetic counseling.

Figure A) Axial T1 weighted image shows atrophy of caudate and lentiform nucleus in Chorea-acanthocytosis.
Figure B) Axial T2 weighted image shows atrophy of caudate and lentiform nucleus in Chorea-acanthocytosis.
Figure C) Coronal FLAIR image shows bilateral hippocampal hyperintensity (thick arrow), and increased iron deposition in globus pallidus (thin arrow) in Chorea-acanthocytosis.
Figure D) Coronal PET-CT image shows decreased FDG uptake in bilateral basal ganglia and mesial temporal lobes in Chorea-acanthocytosis.
Figure E) Axial T1 weighted image shows atrophy of caudate and lentiform nucleus in Huntington disease.
Figure F) Axial T2 weighted image shows atrophy of caudate and lentiform nucleus in Huntington disease.
Figure G) Axial FLAIR image shows increased iron deposition in globus pallidus in Huntington disease.

Purpose

The purpose of this educational exhibit is to acquaint radiologists with chorea-acanthocytosis, an imaging mimic of Huntington disease, characterized by basal ganglia atrophy, with the caudate nucleus being more prominently affected than the lentiform nucleus, and also to specifically look for evidence of hippocampal sclerosis which can help differentiate the entities.

Materials & Methods

Retrospective study from PACS

Results & Conclusion

8 cases of Huntington disease were identified including Juvenile variants and a single case of Chorea-acanthocytosis. The imaging appearance where exact mimics on conventional MRI with bilateral basal ganglia atrophy affecting caudate nucleus more than lentiform nucleus, except for bilateral mesial temporal sclerosis which was seen in the case with Chorea-acanthocytosis. Chorea-acanthocytosis had associated mesial temporal sclerosis and seizures which has been described in literature. This can serve as an imaging marker prompting further evaluation to differentiate it from Huntington disease. Clinical features which can help differentiate include orofacial symptoms, dysphagia and seizures, in addition to laboratory evaluation for acanthocytosis, the presence of acanthocytes in peripheral blood.

Images/Tables

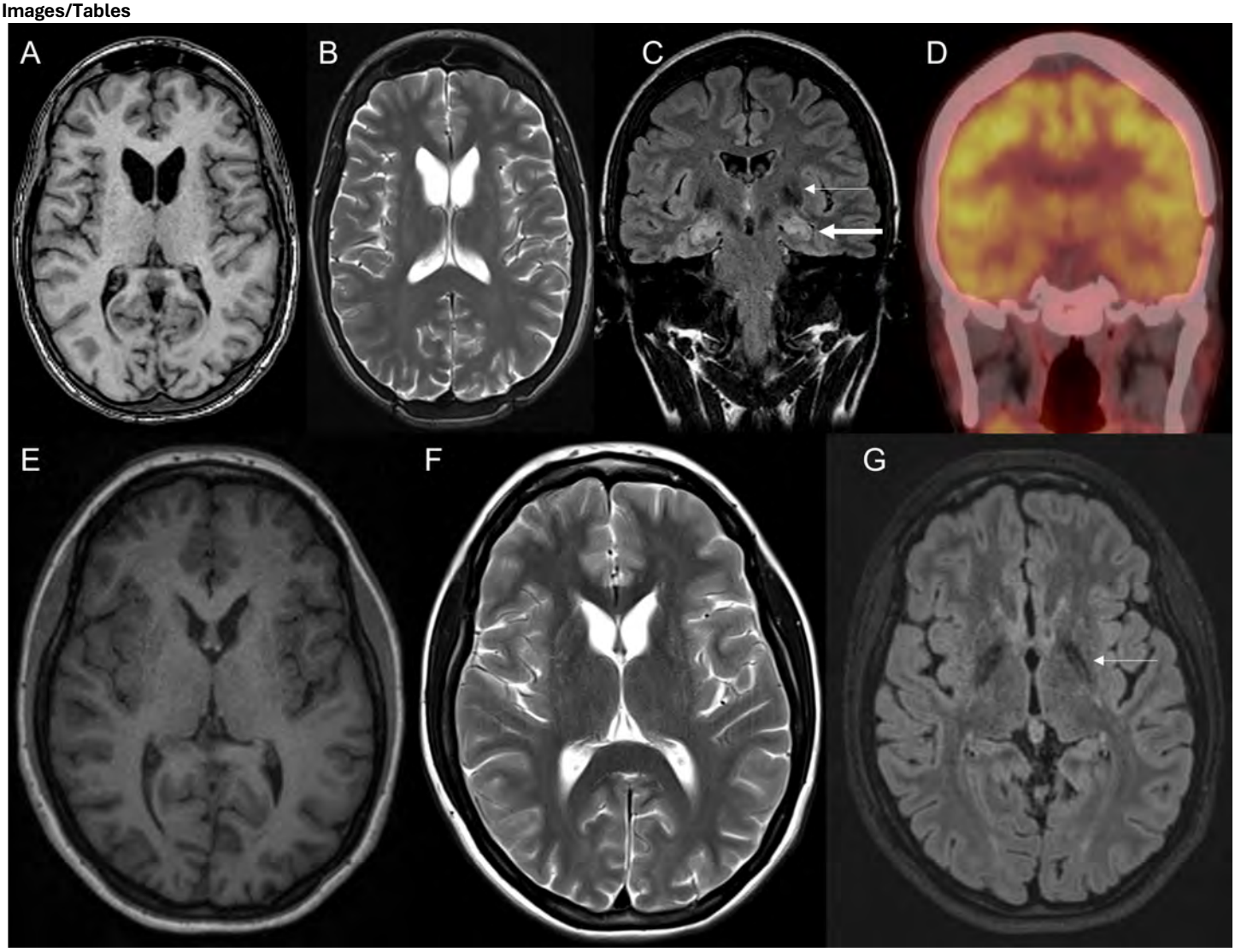

---

728 Following the Glow: Decoding The Perivascular Enhancement in the CNS.

Kamaljeet Singh MBBS, MD, DNB[1], Nerses Nersesyan MD, EDiR, EDiNR[2], Nader Zakhari MD, FRCPC[1], Carlos Torres MD, FRCPC[1]

[1]The University of Ottawa, Ottawa, Ontario, Canada. [2]Sahlgrenska University, Goteborg, Goteborg, Sweden

Summary & Objectives

Perivascular enhancement (PVE) on post-contrast magnetic resonance imaging (MRI) represents pathological alterations within perivascular spaces that are integral to the brain's glymphatic system. Despite growing recognition of its clinical significance, PVE remains underreported in routine radiological interpretation and poses diagnostic challenges. This exhibit aims to illustrate the morphologic patterns of PVE and describe pertinent diagnostic associations to enhance radiological accuracy and clinical recognition.

Purpose

1. To recognise the PVE patterns.
2. To be able to narrow down or arrive to a diagnosis following PVE pattern.
3. How to avoid pitfalls.

Materials & Methods

PVE patterns are classified into four morphologic categories: linear, nodular, curvilinear, and confluent enhancement. Linear PVE predominantly indicated inflammatory and demyelinating processes. Punctate and nodular patterns are associated with neoplastic and infectious etiologies, respectively. Confluent enhancement patterns suggested toxic-metabolic etiologies and post-treatment changes.

Results & Conclusion

Perivascular enhancement exhibits characteristic morphologic patterns that correlate with distinct diagnostic categories. Systematic recognition of these patterns can significantly improve diagnostic accuracy and guide targeted clinical workup, potentially reducing diagnostic delays and improving patient outcomes.

Images/Tables

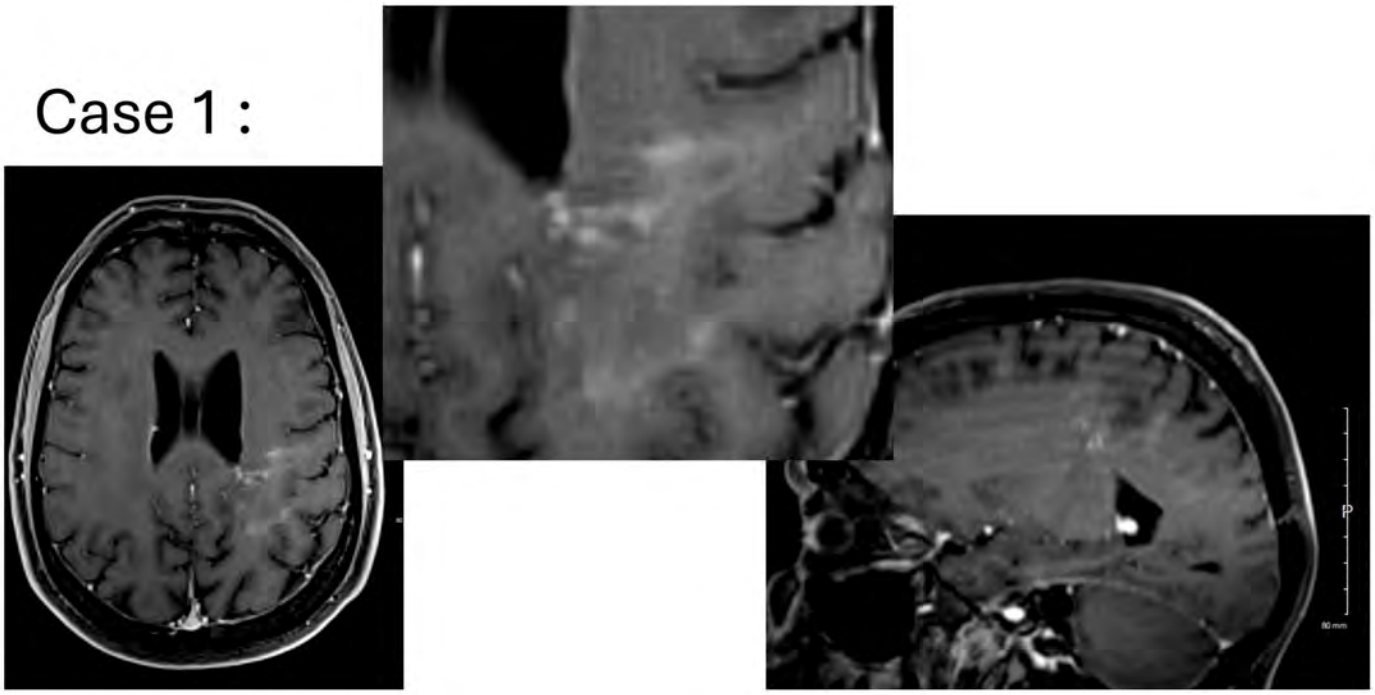

51 yr M with lymphoma.

---

775 **Strategic Multimodality Roadmap for Diagnosing Spinal Vascular Diseases: From Advanced MRA to Photon-Counting Dynamic CTA and Targeted DSA**

Quoc-Anh Nguyen-Duong MD
Can Tho Stroke International Services General Hospital, Can Tho, Can Tho, Vietnam

Summary & Objectives

Spinal vascular diseases (SVDs), including dural arteriovenous fistulas (dAVFs) and arteriovenous malformations (AVMs), remain among the most diagnostically challenging entities in neuroradiology due to their rarity and complex hemodynamics. We propose a comprehensive diagnostic strategy integrating high-resolution MRA, photon-counting dynamic CT angiography (PC-4D-CTA), and targeted digital subtraction angiography (DSA). Since the introduction of photon-counting CT at our institution in December 2023, this workflow has significantly improved pre-angiographic localization, treatment planning, and clinical outcomes.

Educational Objectives

* Review imaging characteristics and classification of major SVD subtypes.
* Describe optimization of MRA and PC-4D-CTA for accurate lesion detection and localization.
* Demonstrate advanced post-processing for generating a DSA roadmap.
* Present a multidisciplinary treatment paradigm informed by dynamic imaging insights.

Purpose

To develop and evaluate a structured imaging workflow combining high-resolution MRI, photon-counting dynamic CTA, and targeted DSA for accurate localization and characterization of spinal vascular lesions, intending to improve pre-angiographic detection and multidisciplinary treatment outcomes.

Materials & Methods

We retrospectively reviewed over 100 patients diagnosed with SVD between 2019 and 2025 at a tertiary referral center. From December 2023 onward, photon-counting CT (NAEOTOM Alpha, Siemens Healthineers) was added to the diagnostic workflow.
All patients underwent:
1. MRI/MRA: 3T MRI with T2WI, 3D SPACE, and time-resolved MRA (TRICKS/TWIST) for screening and localization.
2. PC-4D-CTA: 0.2 mm collimation, 30–40 s dynamic shuttle, 50–60 keV VMI + iodine map to depict arterial inflow, venous drainage, and osseous extension.
3. Post-processing: Curved planar reformats, centerline tracking, and “DSA target maps.”
4. Targeted DSA: Performed based on roadmap findings, minimizing selective injections and fluoroscopy time.

Results & Conclusion

Integration of photon-counting dynamic CTA into the multimodality workflow improved pre-angiographic localization accuracy (> 90%) and reduced fluoroscopy time by 30–40%. Combining MRI, PC-CTA, and DSA transforms spinal vascular diagnosis from exploratory to targeted, offering a reproducible, outcome-driven strategy and an instructive educational model for neuroradiologists.

Transitional Highlight

Even in experienced hands, conventional DSA may fail to reveal the full hemodynamic architecture of spinal shunts. One remarkable case in our series—an intradural AVM with multiple prior unsuccessful DSAs—illustrated this transformation. Dynamic PC-CTA precisely visualized the arterial inflow, venous drainage, and associated osseous invasion, enabling a novel two-stage treatment: targeted vertebroplasty followed by endovascular embolization. The result was dramatic—conversion from wheelchair dependence to independent ambulation. This case exemplifies how dynamic photon-counting angiography turns diagnostic uncertainty into interventional precision.

Images/Tables

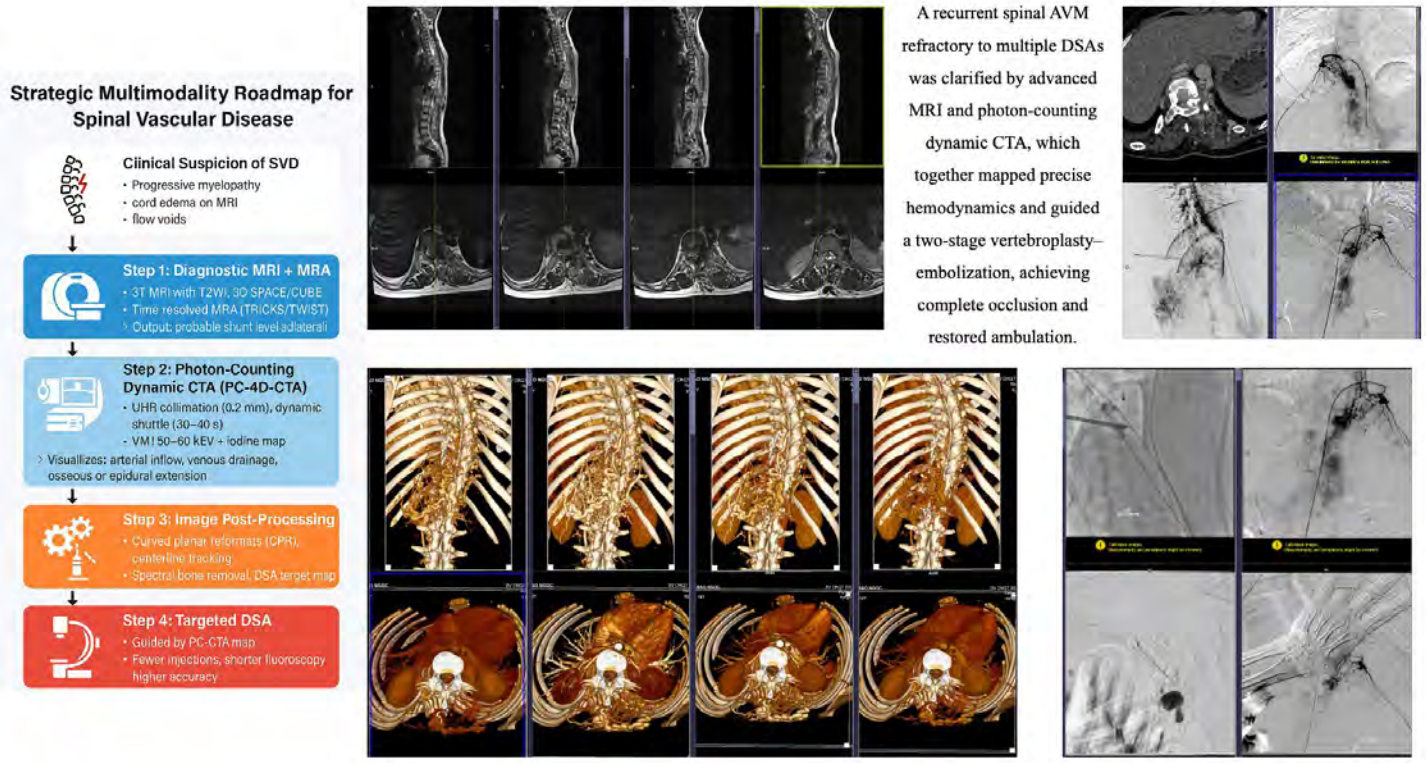

---

887 **Glutamate (Glu)-enhanced CEST: An Improved Selectivity and Sensitivity to Glu by Suppressing Interference from neighboring CEST signals at 3.0 ppm**

Chisato Ando R.T.[1], Mai T Huynh Ph.D.[2], Jihun Kwon Ph.D.[3], Hyuma Ohashi M.S.[4], Zoltan Kovac Ph.D.[5], Masami Yoneyama R.T.[3], A. Dean Sherry Ph.D.[2], Masaya Takahashi Ph.D.[4]

[1]Juntendo University, Bunkyoku, Tokyo, Japan. [2]UT Southwestern Medical Center, Dallas, TX, USA. [3]Philips Japan, Minatoku, Tokyo, Japan. [4]Juntendo University, Bunkyouku, Tokyo, Japan. [5]UT Southwester Medical Center, Dallas, TX, USA

Summary & Objectives

Glutamate (Glu) is the primary excitatory neurotransmitter in the brain and plays essential roles in synaptic communication and energy metabolism. Abnormal Glu levels are implicated in a wide range of neurological and psychiatric disorders. Glu-chemical exchange saturation transfer (Glu-CEST) imaging has been used to map Glu distribution in vivo, but the conventional CEST signal at 3.0 ppm lacks specificity due to contributions from other metabolites. To improve Glu detection reliability, we developed a “Glu-enhanced CEST” method designed to selectively emphasize Glu-related contrast while suppressing contaminating effects. This study aims to evaluate the concentration and pH dependence of Glu-enhanced CEST and assess its feasibility under realistic imaging conditions.

Purpose

Although Glu-CEST has been applied in studies of neurodegenerative and neuropsychiatric disorders [1-2], the conventional CEST contrast at 3.0 ppm is not derived solely from Glu. Our previous results demonstrated that this signal includes substantial contributions from amide protons and guanidinium groups, such as those found in creatine, thereby compromising both specificity and quantitative accuracy [3]. In vivo, where metabolite composition and pH vary regionally, this overlap further complicates interpretation. To address these limitations, we introduce a refined approach termed “Glu-enhanced CEST”, which aims to improve Glu specificity by reducing interference from neighboring resonances.

Materials & Methods

Two phantom studies were conducted.

Study I (Concentration Dependence): Phantoms containing nicotinamide (Nic, 100 mM), Glu (20 mM), and creatine (Cre, 20 mM) were prepared in phosphate buffered saline (PBS). Each metabolite concentration was also adjusted to −50% and +50%, creating nine phantoms at pH 7.0.

Study II (pH Dependence): Constant-concentration phantoms of Nic, Glu, Cre, and glucose, respectively, were adjusted to pH 6.3-7.6, yielding twenty phantoms.

CEST imaging was performed on a 3T MRI system (MR7700, Philips) using saturation amplitudes of 0.5-3.5 μT for 2 s. Glu-enhanced CEST maps were generated by subtracting the CEST map at 1 μT from that at 3 μT. To emulate tissue-like spectral environments, mixed z-spectra were produced by summing the spectra of individual metabolites [3]. Feasibility was confirmed in healthy subjects with external metabolite phantoms positioned near the head during MRI.

Results & Conclusion

Conventional CEST maps obtained at 3.0 ppm showed substantial signal contributions from nicotinamide (Nic) and creatine (Cre) in addition to glutamate (Glu), indicating limited metabolite specificity. In contrast, the Glu-enhanced CEST approach selectively reflected Glu concentration changes in Study I, with minimal influence from Nic or Cre. In Study II, conventional CEST demonstrated variable and non-uniform pH-dependent responses across metabolites, whereas Glu-enhanced CEST exhibited a monotonic pH dependence consistent with Glu alone. Human imaging further confirmed enhanced Glu-selective contrast.

These findings indicate that Glu-enhanced CEST effectively suppresses contaminating metabolite effects and improves both the specificity and sensitivity of Glu detection. This method provides a more reliable means for assessing Glu dynamics in vivo and has strong potential to enhance CEST-based evaluation of neurological disorders involving altered glutamatergic neurotransmission.

Images/Tables

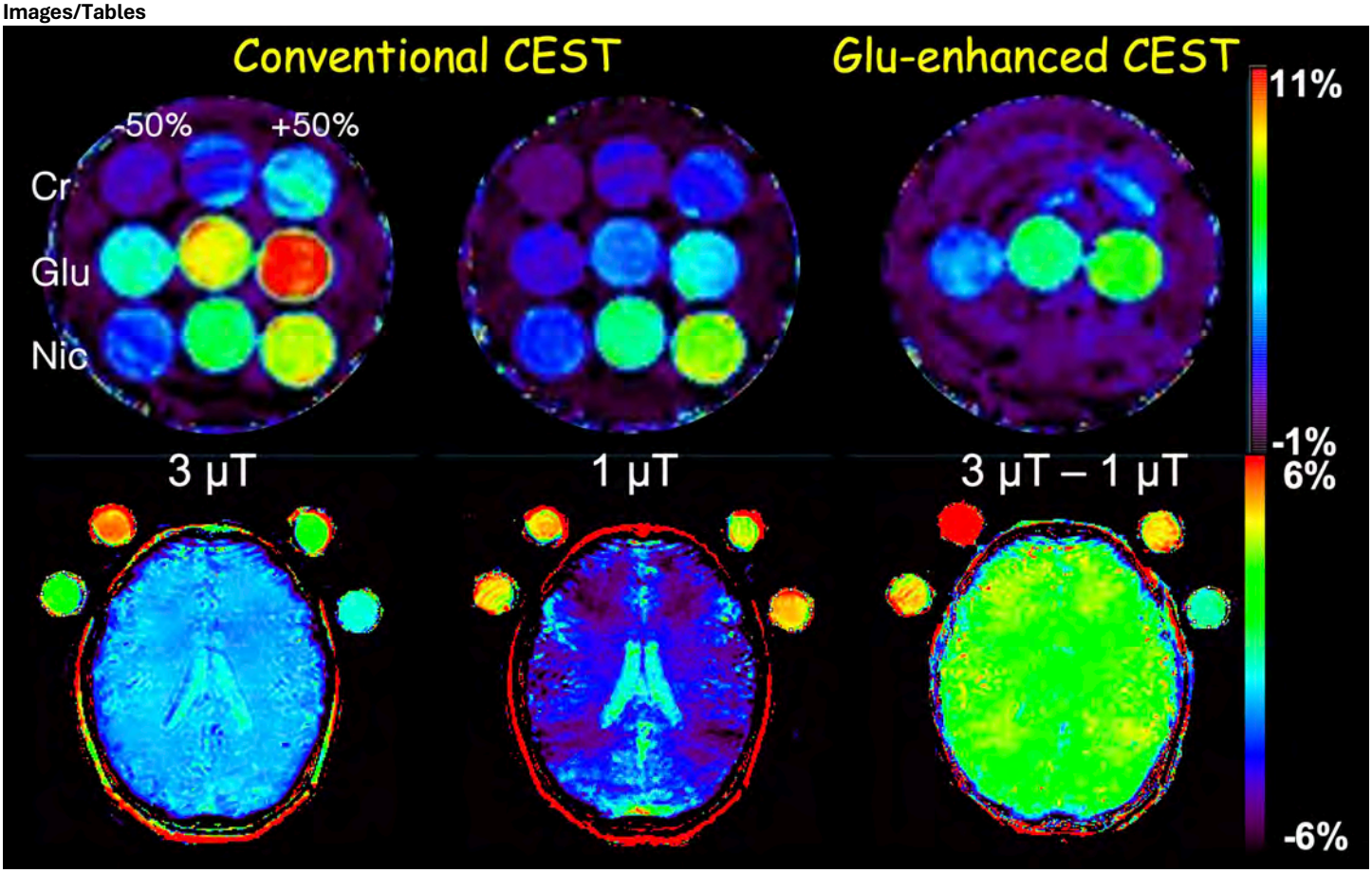

893 Pediatric Telestroke Imaging Toolkit: Standardizing CTA, rapid MRI, and CTP quality checks for resource limited centers with a door-to-decision timeline

Tavia N Hall MS, Anson Dao BS
Medical College of Georgia, Augusta, GA, USA

Summary & Objectives

This exhibit presents a pediatric-aware telestroke imaging toolkit for hub-and-spoke networks, designed for resource-limited centers. Objectives are to: (1) adapt adult telestroke imaging practices to pediatric arterial ischemic stroke (AIS) with dose-conscious parameters [1,2]; (2) provide a usable, no-sedation rapid MRI pathway with a 10–15-minute sequence block and a child-life immobilization playbook [3]; (3) illustrate ultra-early CT perfusion (CTP) pitfalls with arterial/venous input function (AIF/VOF) checks and corrected outputs [4]; and (4) implement a structured STAT report macro and simple timestamps to reduce communication latency [1].

Purpose

This work delivers a practical, ready-to-run framework that sharpens large-vessel occlusion (LVO) detection and streamlines telestroke decision-making for a standard of care in resource-limited environments, while emphasizing radiation stewardship and built-in imaging quality controls [1].

Materials & Methods

This toolkit distills telestroke guidance, pediatric AIS literature, and multicenter workflow data into a concise, spoke-friendly package [1,2,3,5]. The imaging algorithm favors MRI-first when feasible without sedation (DWI/ADC, FLAIR, GRE/SWI ± TOF-MRA ± ASL) [3]; otherwise, it defaults to non-contrast CT followed by arch-to-vertex CTA [1,2]. A rapid, no-sedation MRI pathway targets a 10–15-minute scan, using pediatric adjustments and behavioral support to limit repeats and sustain timely throughput [3].

A CTP quality-assurance module presents two didactic cases: (a) an ultra-early “false core” example highlighting delayed bolus arrival and AIF misplacement, and (b) a motion-contaminated study. Each panel displays raw time-attenuation curves, AIF/VOF validation, reprocessing steps, and revised core/penumbra outputs [4].

A structured STAT macro (hemorrhage yes/no; LVO/dissection; action-oriented impression) is paired with a timestamp checklist—scan end, preliminary read, verbal call—to quantify and shorten communication delays [1]. A unified multi-panel figure integrates before/after CTA adoption,

posterior fossa rapid MRI, CTP pitfalls, and a Door-to-Decision timeline with operational benchmarks: Door-to-CT ≤15 min; CT-to-CTA ≤25 min; preliminary read ≤5 min post-scan; MRI completion ≤30 min; repeat-scan rate <10%; 100% ALARA adherence [1,2].

Results & Conclusion

Published experience links spoke-level NCCT→CTA standardization to improved LVO detection, fewer non-beneficial transfers, and higher endovascular therapy yield [2]. The exhibit adapts these practices for pediatrics using ALARA-driven parameters [3,5]. The no-sedation rapid MRI protocol consolidates high-yield sequences into a short scan and pairs them with a behavioral immobilization guide, improving posterior fossa and subtle cortical infarct detection without delaying care [3].

The CTP QA module demonstrates recognition and correction of overestimated cores and motion artifacts through AIF/VOF validation and reprocessing, promoting CTP as a selective, decision-refining adjunct [4]. The STAT macro and timestamp log center team focus on a 5-minute preliminary-read goal and offer an easy way to document latency improvements [1].

This framework integrates MRI-first imaging (when feasible), NCCT→CTA at the spoke, CTP QA safeguards, and timestamped reporting into a reproducible approach for pediatric telestroke care in resource-limited settings—embedding radiation stewardship, measurable quality control, and efficient tele-decision workflows into everyday neuroradiology practice [1–4].

Images/Tables

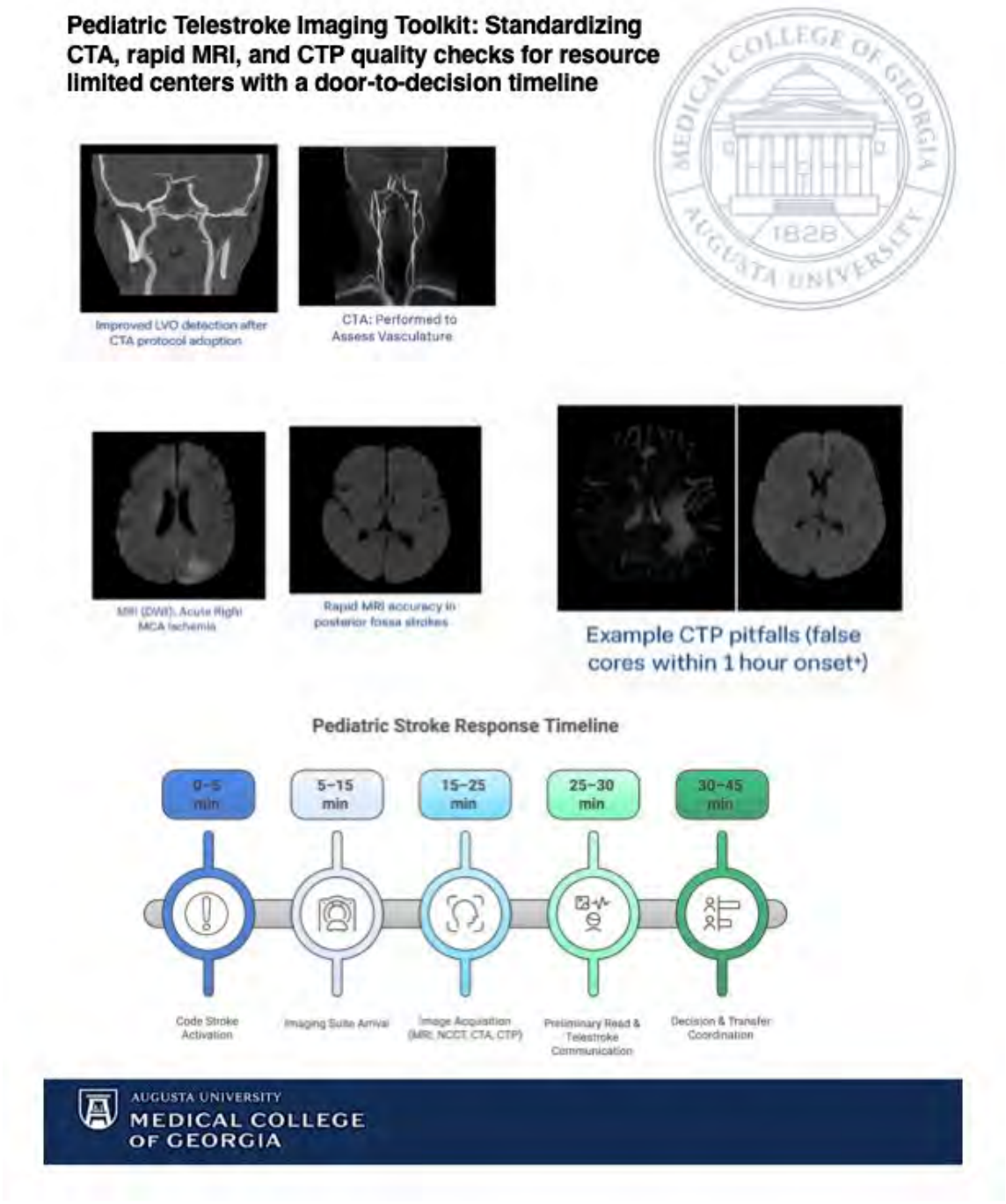

1031 Shedding Light on a Dark Signal: T2 Signal Decrease in Cochlear Fluid as a Marker of Hearing Loss in Vestibular Schwannomas

Mustufa Babar MD, Nahill H Matari MD, MS, MBA
Columbia University Irving Medical Center, New York, NY, USA

Summary & Objectives

Vestibular schwannomas (VS) are benign tumors that commonly arise along the course of the eighth cranial nerve within the internal auditory canal (IAC) and are best identified on MRI of the IAC. These tumors are known to correlate with ipsilateral sensorineural hearing loss on clinical examination; however, an underrecognized imaging correlate is decreased T2 signal intensity within the ipsilateral cochlea, which may portend severe sensorineural hearing loss. This exhibit presents cases of patients with VS and sensorineural hearing loss demonstrating this correlation through decreased cochlear T2 signal on MRI.

Purpose

To demonstrate how decreased T2 signal intensity within the cochlea adjacent to a VS may reflect elevated protein concentration or altered perilymph composition, thereby providing radiologic evidence of a biochemical mechanism underlying hearing loss (1,2). The exhibit aims to review the proposed pathophysiology of cochlear signal alteration in VS, correlate MRI findings with audiometric data, and summarize supporting evidence from recent literature (3,4).

Materials & Methods

MRI studies of the brain and IACs were reviewed in patients with VS. Tumor size, morphology, and cochlear signal characteristics were assessed on each side. Qualitative comparisons of cochlear T2 signal intensity were made between affected and unaffected ears, and findings were correlated with available audiometric data. Relevant literature describing mechanisms linking decreased T2 signal intensity to cochlear dysfunction in VS was reviewed to contextualize imaging findings and infer the underlying pathophysiology, including the roles of cochlear-aperture obstruction, intralabyrinthine protein accumulation, and altered perilymph homeostasis (1–4).

Results & Conclusion

Across the presented series, VS demonstrating decreased cochlear T2 signal intensity consistently correlated with ipsilateral sensorineural hearing loss on audiometric evaluation (Figure 1). In contrast, cases without T2 signal reduction typically showed preserved hearing function. This pattern supports the association between decreased cochlear T2 signal and auditory dysfunction, suggesting that signal alteration reflects underlying cochlear injury (1,3).

The observed T2 signal decrease likely reflects increased protein concentration or altered perilymph composition resulting from cochlear-aperture obstruction or tumor-related disruption of the blood–labyrinthine barrier (1,2). These biochemical alterations shorten T2 relaxation time and appear as decreased signal intensity on MRI (2,4). Such disturbances in perilymphatic homeostasis may impair ionic gradients and hair-cell function, leading to progressive cochlear dysfunction. Although larger tumors may exert additional mass effect or vascular compromise, the presence of cochlear T2 signal changes suggests that hearing loss arises from a combination of mechanical and biochemical mechanisms rather than tumor size alone (1,3,4).

This case series highlights the value of high-resolution T2-weighted MRI as an imaging marker of cochlear integrity in patients with VS. Recognition of decreased cochlear T2 signal may help identify ears at risk for progressive hearing decline and guide surveillance or intervention strategies. Correlating cochlear signal alterations with audiometric data enhances understanding of the pathophysiologic basis of hearing loss in VS and supports the role of MRI as an early marker for hearing preservation (1–4).

Images/Tables

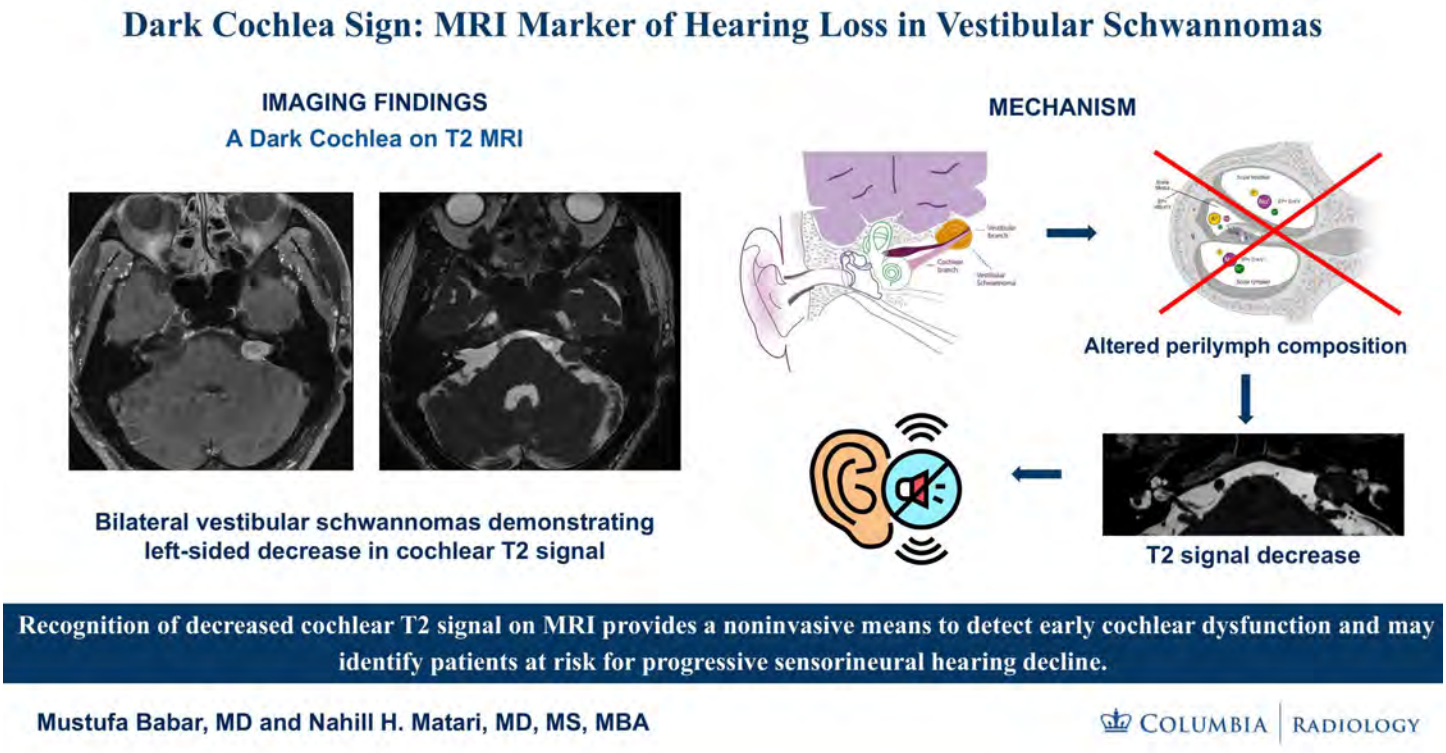

1135 Feeding the Diagnosis: The Neuroradiology of Nutritional Deficiencies

Alina Alam[1], Tristin Latty MD[2], Steven Lev MD[2]
[1]American University of the Caribbean, Miramar, FL, USA. [2]Nassau University Medical Center, East Meadow, NY, USA

Summary & Objectives

Summary

A wide array of nutritional deficiencies and generalized wasting states can affect the brain and spine. These can be easily overlooked on imaging studies due to incomplete histories and overlapping appearances. This exhibit, supported by case challenges and teaching diagrams, provides an algorithmic, pattern-based approach, for confident recognition of often subtle deficiency-related findings.

Educational Objectives

1. Present a pattern-recognition playbook for deficiency-associated abnormalities on MRI/CT of the central nervous system.
2. Integrate clinical risk factors, including alcohol abuse, post-bariatric surgery, and prolonged ICU stay, into the interpretive process.
3. Recognize key mimics (i.e., HIV vacuolar myelopathy; toxic leukoencephalopathy) that can closely resemble deficiency-related brain and spine patterns in routine practice.

Purpose

To present an algorithmic, pattern-based approach to nutritional deficiencies of the brain and spine, emphasizing early recognition and differential diagnosis.

Materials & Methods

We curated representative brain and spine CT/MR cases from our safety-net institution involving patients with deficiency-related disease to emphasize key imaging patterns. To reinforce concepts, we created schematic diagrams and on-image overlays and include an interactive case-challenge to help distinguish nutritional etiologies from close imaging look-alikes. We include a comparison table, a focused literature review, and an algorithmic flowchart to guide the radiologist.

Results & Conclusion

Results

In evaluating deficiency-related disease, the location and symmetry of CT/MR density and signal changes provide early clues. Brain-predominant patterns include symmetric involvement of the medial thalami with extension to the periaqueductal region and mammillary bodies, characteristic of thiamine (vitamin B1) deficiency in Wernicke encephalopathy. Spine-predominant patterns include dorsal column hyperintensity of the cervical cord, with or without lateral corticospinal tract involvement, typical of subacute combined degeneration in cobalamin (vitamin B12) deficiency; copper deficiency can closely mimic this, and vitamin E deficiency may also involve the posterior columns with occasional cerebellar findings. Cortical and subcortical abnormalities in the appropriate clinical context should raise concern for niacin (vitamin B3) deficiency. When both brain and spine are abnormal, or when diffuse white-matter change and/or global atrophy is present, a severe wasting state (e.g., anorexia nervosa or prolonged catabolism) may be contributory, with potential for improvement after refeeding.

Populations at increased risk include individuals with alcohol use disorder, patients after bariatric or other gastrointestinal surgery, those with prolonged ICU stays or limited enteral intake, and oncology patients with catabolic states. Key mimics (i.e., HIV vacuolar myelopathy; toxic leukoencephalopathy) are discussed where distributions overlap to help avoid misclassification.

Advanced modalities, particularly diffusion tensor imaging (DTI), can assist in earlier diagnosis and follow-up.

Conclusion

An algorithmic, pattern-based approach enables timely recognition of malnutrition-related neurologic disease and supports prompt replacement therapy and supportive care.

Images/Tables

Diagnosis	Brain	Spine	DWI / Enhancement	Clinical	Mimics
Thiamine (B1) Wernicke encephalopathy	Bilateral medial thalami, periaqueductal gray, mammillary bodies, tectal plate	Usually normal	Acute DWI hyperintensity; mammillary enhancement	Confusion, ataxia, nystagmus	Osmotic demyelination; hypoxic-ischemic injury
Cobalamin (B12) Subacute combined degeneration (SCD)	Normal or nonspecific WM	Cervical and thoracic; dorsal columns and/or lateral corticospinal tracts	T2 hyperintensity; usually no enhancement	Paresthesias, ataxia	Copper deficiency myelopathy; HIV vacuolar myelopathy
Copper deficiency	Usually normal	Posterior column T2 hyperintensity and/or corticospinal tracts	Typically none	Myelopathy	B12 deficiency SCD
Niacin (B3) Pellagra	Cortical–subcortical	Usually normal	Variable; Diffusion restriction	Dermatitis, diarrhea and cognitive change	Toxic/metabolic encephalopathies
Vitamin E deficiency	Cerebellar vermis/hemisphere	Posterior column T2 hyperintensity	Typically none	Ataxia; fat-malabsorption	Hereditary ataxias; B12 myelopathy
Severe wasting / systemic undernourishment	Diffuse white-matter change and/or global atrophy	Usually normal	Nonspecific	Anorexia nervosa; prolonged catabolic illness; poor intake	Toxic leukoencephalopathy; hypoxic-ischemic injury

136 Evaluating Patients with Acute Dizziness and Vertigo: Continued Use of CT Is Not Sustainable

Cassie Deshong BA[1], Hanul N. Seo BA[1], Clifford Eskey MD,PhD[2], Brian Barnacle MD,JD[2]
[1]Geisel School of Medicine at Dartmouth, Hanover, NH, USA. [2]Dartmouth Health, Lebanon, NH, USA

Summary & Objectives

Review the broad differential diagnosis and imaging approach for acute sustained vertigo.
Understand that CT has low sensitivity for central causes of acute sustained vertigo, with MRI being the appropriate exam.
Recognize that clinicians often obtain a non-contrast CT and CTA of the head and neck to evaluate vertigo in the acute setting due to its speed and accessibility.

Purpose

Acute dizziness or vertigo is a common presentation to emergency departments (ED) in the United States, accounting for up to 3.6% of visits. Clinical evaluation can be challenging because the differential diagnosis is broad, including peripheral and central causes. In the acute setting, clinicians seek to rule out life-threatening brainstem or cerebellar infarcts. The use of non-contrast CT and CTA of the head and neck has been rising in the emergency setting, and a study found 27% of ED patients received a CT. However, CT is not sensitive for detecting central causes of vertigo. The overreliance on CT has made evaluation of vertigo an expensive problem in the emergency setting, with an annual cost of $10 billion. If the history and exam point to a central etiology of vertigo, the appropriate imaging exam should be an MRI. However, a study found that MRI was only performed for 3% of patients presenting with dizziness. This educational exhibit will review the problem of overreliance of CT to evaluate central causes of dizziness.

Materials & Methods

This exhibit will review the differential diagnosis of acute dizziness and vertigo and the methods clinicians employ to distinguish peripheral and central causes. The exhibit will review the evidence that MRI is significantly more sensitive than CT in detecting central causes of vertigo. Through cases, the exhibit will demonstrate examples in which MRI was more sensitive than CT in identifying brainstem and cerebellar infarcts. The exhibit will illustrate the false sense of security when a negative CT leads to delayed diagnosis. Finally, the exhibit will review abbreviated MRI protocols for evaluating central causes of vertigo.

Results & Conclusion

Rapid and accurate diagnosis is critical to optimizing outcomes for patients with vertigo. Clinical tests (e.g.,HINTS test) can distinguish central from peripheral causes of vertigo but require specific clinical training and equipment, which may limit their use and reduce diagnostic accuracy. When imaging is performed, there is an overreliance on CT to identify or exclude a central cause, which is costly and inappropriate. The sensitivity of non-contrast CT for detecting central causes of acute dizziness is approximately 29%, compared to a sensitivity of 80% with MRI. Common hesitations regarding MRI focus on cost, imaging time, and scan availability. However, in the long term, evidence suggests that MRI reduces overall cost by decreasing repeat imaging, lowering re-admission rates, and improving long-term patient outcomes. Concerns about the duration of a conventional MRI can be addressed with an abbreviated MRI protocol. A prior study showed a streamlined protocol using axial DWI, SWI, and FLAIR sequences took 8-12 minutes compared to 22-32 minutes with conventional MRI. The abbreviated protocol also improved turnaround time and reduced patient length of stay.

Images/Tables

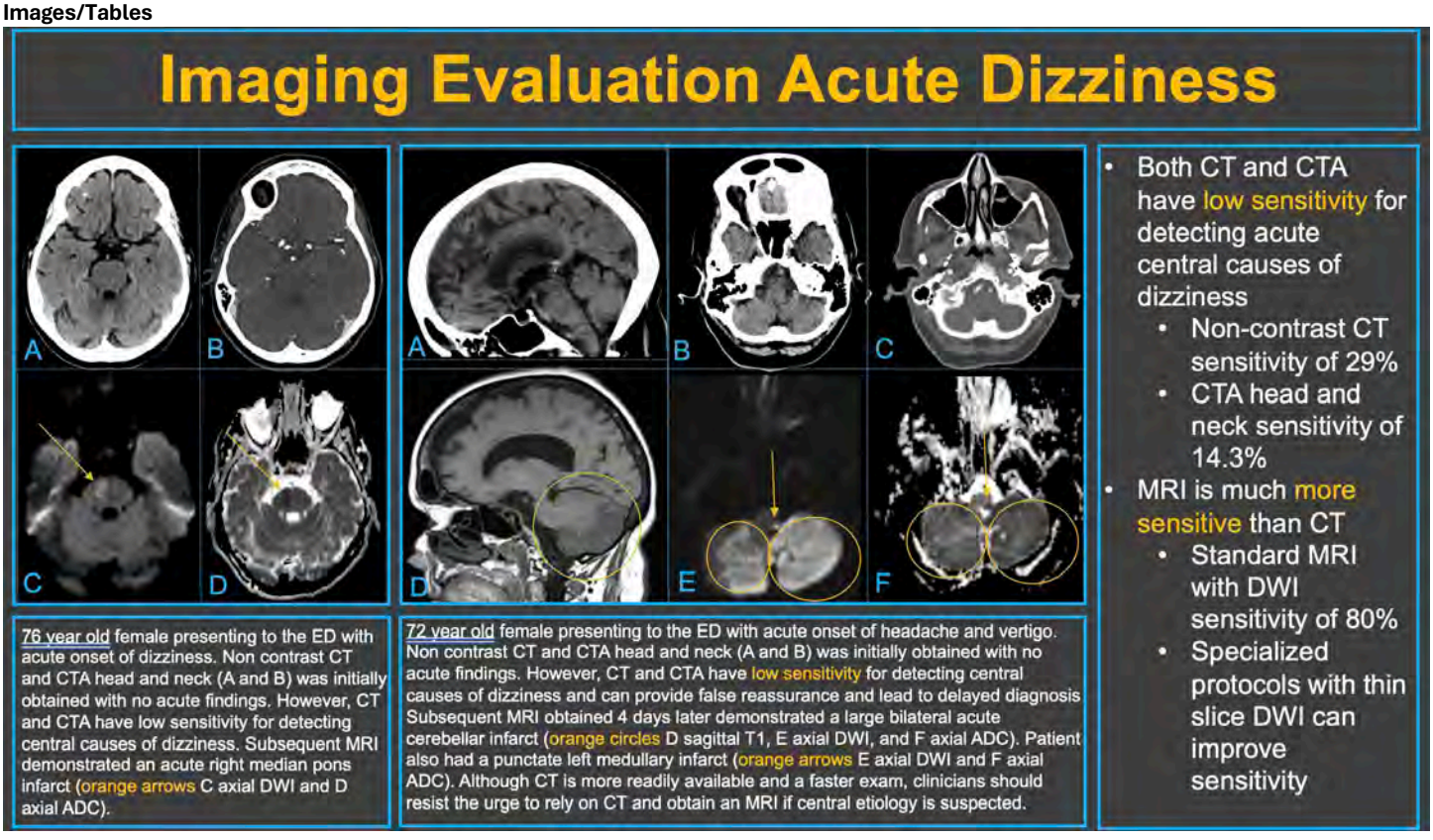

147 Radiologic Evaluation of SLIPPERS: Key Findings and Differential Diagnosis

Sabha Ahmed[1], Shreyas Reddy Kankara[2], Ankit Arora[1], Shravan Reddy K[3], Unnathi Nayak[3]
[1]National Institute for Mental Health and Neuro Sciences, Bengaluru, Karnataka, India. [2]BrainSightAI, Bengaluru, Karnataka, India. [3]St John's Medical College Hospital, Bengaluru, Karnataka, India

Summary & Objectives

SLIPPERS (Supratentorial Lymphocytic Inflammation with Parenchymal Perivascular Enhancement Responsive to Steroids), a rare variant of the CLIPPERS spectrum, is an inflammatory CNS entity involving the supratentorial parenchyma. Clinical presentation of SLIPPERS is usually nonspecific and can present with seizures, focal neurological deficit, headache, cognitive dysfunction, and gait abnormalities. Cerebrospinal fluid (CSF) analysis can show lymphocytic pleocytosis. Biopsy reveals characteristic perivascular lymphocytic inflammation with absence of granulomatous, vasculitic, or malignant changes. Acute episodes are managed with corticosteroids, while long-term therapy involves the use of steroid-sparing immunosuppressive agents. Extensive clinical and laboratory work-up is required to rule out more common infectious/inflammatory and neoplastic mimics of SLIPPERS.
The objective of this pictorial/retrospective review is to summarize hallmark imaging features of SLIPPERS, demonstrate distinguishing imaging clues, and provide an approach to separate SLIPPERS from common mimics to improve diagnostic confidence and guide management.

Purpose

To describe the MRI characteristics of SLIPPERS, correlate imaging with clinical and histopathological data, and delineate imaging features that help differentiate SLIPPERS from its principal mimics (including CLIPPERS, neurosarcoidosis, primary CNS lymphoma, vasculitis, and demyelination).

Materials & Methods

A retrospective review was performed of cases labeled as SLIPPERS at our tertiary neuroimaging center. Imaging datasets were retrieved and systematically reviewed. The following mimics were specifically included for comparison:

- CLIPPERS (chronic lymphocytic inflammation with pontine perivascular enhancement responsive to steroids)
- Neurosarcoidosis
- Autoimmune Glial Fibrillary Astrocytopathy (GFAP)
- Primary CNS lymphoma
- CNS vasculitis
- Demyelinating disease spectrum - Multiple sclerosis and Myelin oligodendrocyte antibody-associated disease (MOGAD)
- Infectious encephalitis (Tuberculosis, Histoplasmosis, Schistosomiasis)
- Metastatic disease and other mass-forming lesions
- Lymphoid Granulomatosis

Results & Conclusion

SLIPPERS represents a distinctive but often under-recognized steroid-responsive inflammatory entity within the CNS. On MRI, it typically demonstrates T2/FLAIR hyperintensities with patchy/nodular or perivascular enhancement. Its imaging patterns can overlap with a broad spectrum of demyelinating, granulomatous, infectious, and neoplastic processes, leading to diagnostic uncertainty.
Awareness of this entity and familiarity with its characteristic distribution and steroid responsiveness allows the radiologist to consider SLIPPERS early in the differential. Raising this possibility prompts appropriate clinical correlation and therapeutic trials, may reduce the need for invasive biopsy, and facilitates timely immunomodulatory treatment. Ultimately, informed radiologic recognition plays a key role in guiding multidisciplinary decision-making and optimizing patient outcomes.

Images/Tables

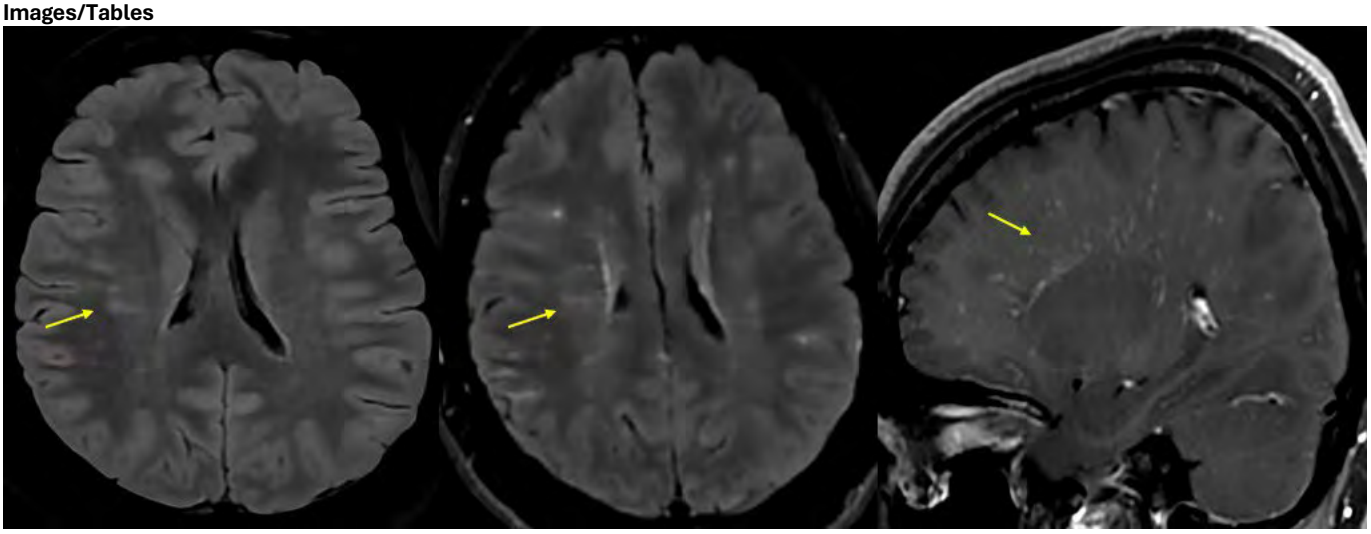

214 Visualizing the Mind: A Multimodal Approach to Neuropsychiatric Diagnosis

fatima mubarak MBBS, dureshahwar kanwar MBBS
aga khan university hospital, karachi, sind, Pakistan

Summary & Objectives

The purpose of this presentation is to highlight the pivotal role of integrated neuroimaging and electroencephalography (EEG) in diagnosing complex neuropsychiatric disorders that often blur the boundaries between neurology and psychiatry. Through a series of illustrative cases—including autoimmune encephalitis, Creutzfeldt-Jakob disease, lymphomatosis cerebri, posterior reversible encephalopathy syndrome, herpes simplex encephalitis, and drug-induced encephalopathy—this session aims to:

1. Demonstrate the complementary value of MRI and EEG in localizing pathology and refining differential diagnoses in neuropsychiatric presentations.
2. Emphasize the importance of correlating clinical features with imaging and electrophysiological findings for accurate and timely diagnosis.
3. Foster multidisciplinary understanding among neurologists, psychiatrists, and radiologists for improved patient outcomes.

Purpose

This case-based approach underscores how multimodal evaluation can transform diagnostic precision and guide effective management in patients presenting with overlapping neuropsychiatric symptoms.

Materials & Methods

This presentation is based on a series of clinically and radiologically confirmed neuropsychiatric cases encountered at The Aga Khan University Hospital. Cases were selected to represent a broad spectrum of neuropsychiatric disorders with overlapping neurological and psychiatric features. Each patient underwent detailed clinical evaluation, neuroimaging with MRI (including conventional and advanced sequences), and electroencephalography (EEG) as part of diagnostic workup. Relevant laboratory and cerebrospinal fluid analyses were incorporated where indicated to support final diagnoses. Imaging and EEG findings were systematically correlated with clinical presentations to highlight characteristic diagnostic patterns and the role of multimodal integration in reaching a definitive diagnosis.

Results & Conclusion

Results:

Across the presented cases, integration of MRI and EEG findings significantly enhanced diagnostic accuracy in patients with complex neuropsychiatric symptoms. Distinct imaging and electrophysiological signatures—such as the delta brush pattern in NMDA receptor encephalitis, pulvinar sign in Creutzfeldt-Jakob disease, diffuse white matter changes in lymphomatosis cerebri, and characteristic PRES and drug-induced encephalopathy patterns—facilitated early differentiation between infectious, autoimmune, neoplastic, vascular, and metabolic etiologies. Correlating these objective findings with detailed clinical assessment allowed for timely diagnosis and appropriate management, often altering patient outcomes.

Conclusion:

Multimodal evaluation combining neuroimaging and EEG is invaluable in unraveling the complex interface between neurology and psychiatry. These cases underscore that early recognition of characteristic radiological and electrophysiological patterns can prevent misdiagnosis, guide targeted therapy, and improve prognostic understanding. Strengthening collaboration among neurologists, radiologists, and psychiatrists is essential for optimizing the care of patients with neuropsychiatric disorders.

Images/Tables

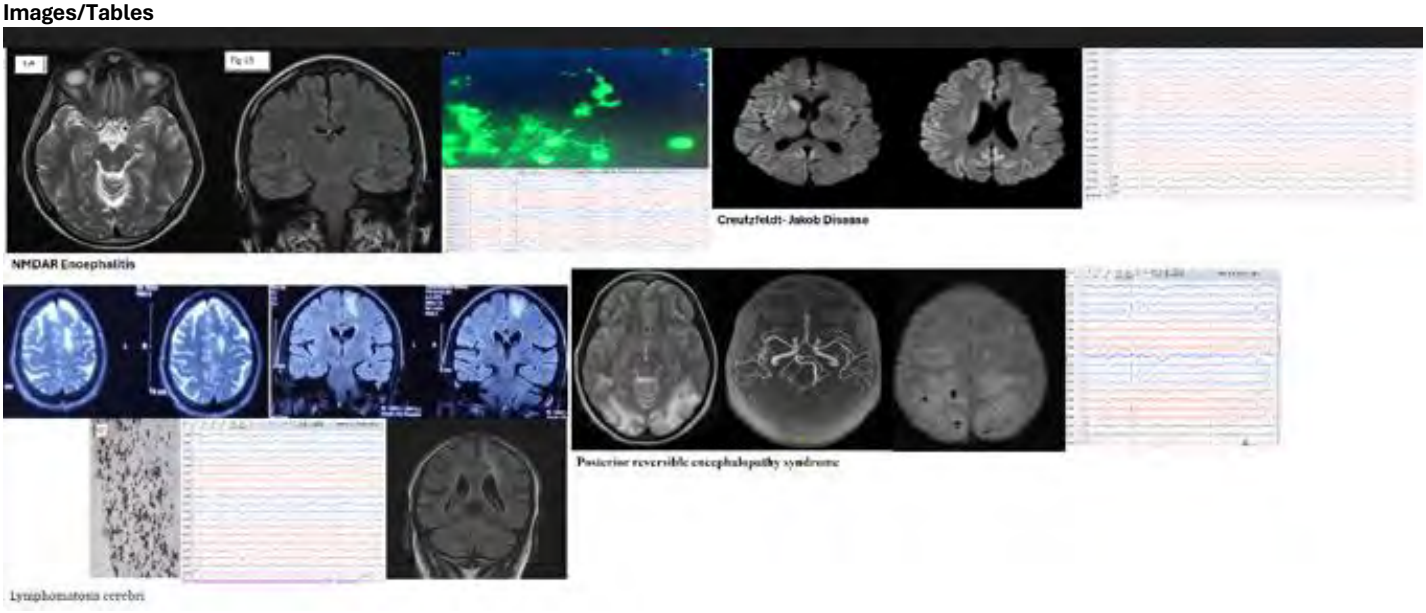

---

393 From Cocaine and Cannabis to Chasing the Dragon: Recognizing the Imaging Spectrum of Street Drug-Induced Brain Injury

Haneyeh Shahbazian MD[1], Edgar Zamora MD[2], Carlos Zamora MD[1]

[1]University Of North Carolina, Department of Radiology, Chapel Hill, NC, USA. [2]Thomas Jefferson Department of Radiology, Philadelphia, PA, USA

Summary & Objectives

Summary:

Substance abuse remains a growing public health concern with profound neurologic implications. Neuroimaging plays a crucial role in detecting and characterizing brain injury resulting from acute and chronic exposure to illicit and toxic substances. According to the United Nations Office on Drugs and Crime, the number of global drug users rose from approximately 240 million a decade ago to 296 million in 2021. These substances lead to neurologic morbidity through various mechanisms, including direct vascular effects (for example, reversible cerebral vasoconstriction syndrome), cardiovascular complications (such as in cardiac arrythmias, hypertensive surges, and myocardial infarction), selective neurologic injury (including “chasing the dragon”, opioid-associated amnesic syndrome, CHANTER syndrome, and POUNCE syndrome), hypoxic injury, and toxic-metabolic injury. Recognizing characteristic imaging patterns associated with different substances is essential for prompt diagnosis, cessation of exposure, appropriate management, and prevention of irreversible injury. This exhibit illustrates the neuroimaging manifestations of commonly encountered substances, including stimulants (cocaine, methamphetamines), opioids, toxic alcohols and inhalants.

Educational Objectives:

- Identify key neuroimaging patterns of vascular, hypoxic, and toxic-metabolic injury related to illicit substance use.

- Recognize characteristic CT and MRI features associated with exposure to cocaine, methamphetamines, opioids, toxic alcohols, and inhalants.
- Discuss the clinical relevance of early radiologic recognition in guiding management and improving patient outcomes.

Purpose

NA

Materials & Methods

NA

Results & Conclusion

NA

Images/Tables

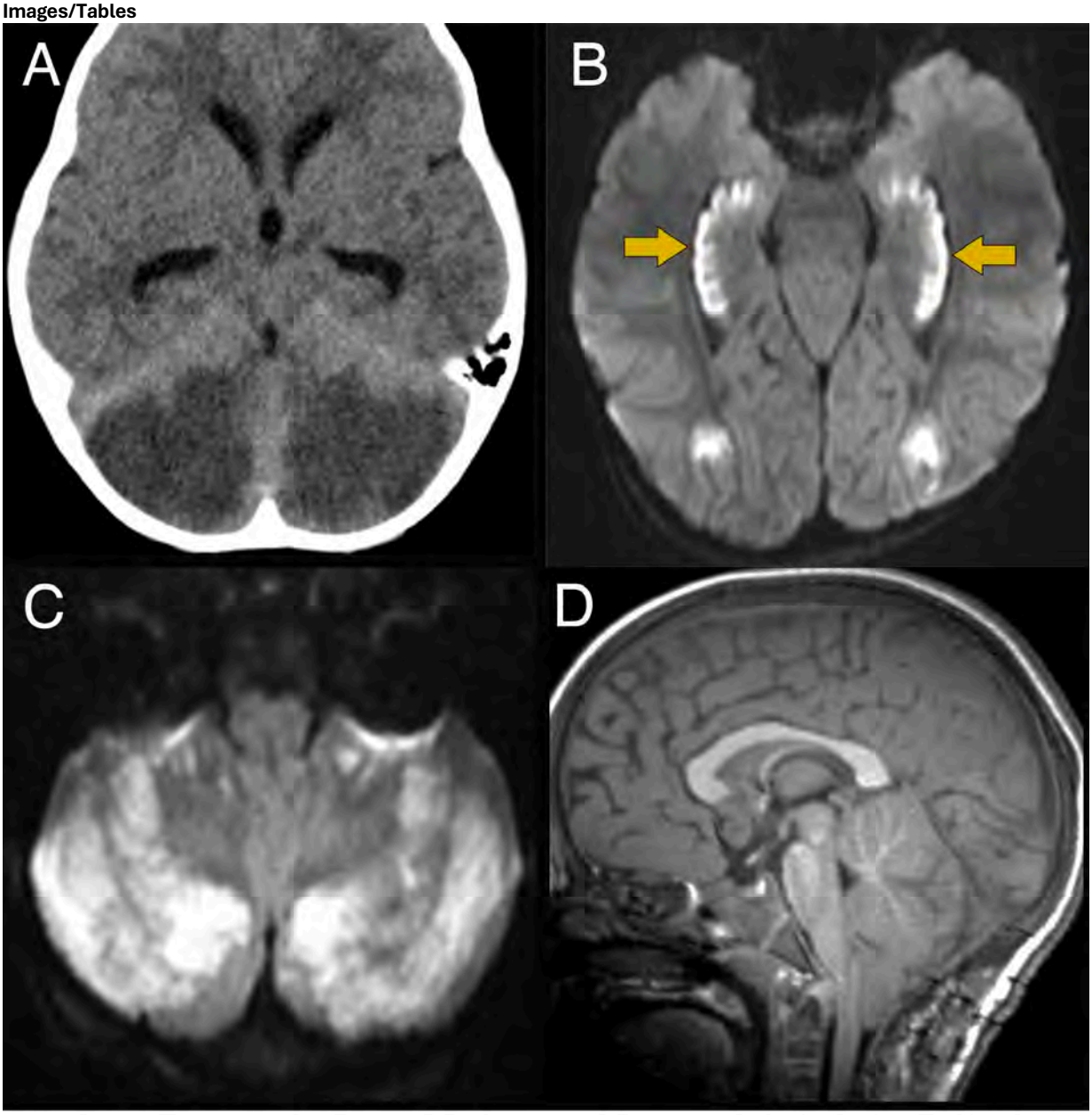

Figure. Pediatric Opioid Use-Associated Neurotoxicity with Cerebellar Edema (POUNCE) in a 2-year-old unresponsive girl with urine toxicology positive for opioids. Axial noncontrast CT **(A)** shows marked cerebellar edema bilaterally, along with mild ventriculomegaly. On MRI, DWI **(B and C)** shows symmetric restricted diffusion in the hippocampi with a curvilinear appearance (arrows), as well as in the suboccipital white matter. There is also prominent restricted diffusion in the cerebellum **(C)**. Sagittal noncontrast T1 demonstrates fulminant cerebellar edema with persistent mass effect in the posterior fossa after suboccipital decompression **(D)**.

436 Mapping the Variants, Understanding vascular Diversity-A Pictorial Review of MRA Brain

Shumaila Arooj
JPMC, Karachi, Sind, Pakistan

Summary & Objectives

The objective of this educational exhibit is to comprehensively review and illustrate key vascular anatomical variants of the intracranial and extracranial circulation as encountered on high-resolution 3.0 Tesla MR angiography (MRA). Recognition of these variants is vital for accurate interpretation, differentiation from pathology, and appropriate clinical correlation.

By systematically demonstrating these variants through representative MRA images, this educational review aims to enhance understanding of their typical appearances, clinical relevance, and potential diagnostic pitfalls. Additionally, it emphasizes the importance of correlating vascular configuration with hemodynamic flow patterns and adjacent anatomic relationships to avoid misinterpretation as aneurysm, stenosis, or dissection.

Purpose

To illustrate the spectrum of normal intracranial and extracranial vascular variants on 3T brain and neck MRA reported via teleradiology. The exhibit aims to highlight their prevalence, characteristic imaging features, and diagnostic significance, enhancing radiologist confidence in distinguishing normal variants from true vascular pathology in daily reporting practice.

Materials & Methods

This retrospective pictorial review includes 776 brain and 485 neck MRA studies performed on a 3.0 Tesla MRI scanner and reported via a structured teleradiology workflow over a two-year period. All studies were acquired using three-dimensional time-of-flight (TOF) and contrast-enhanced MRA sequences optimized for vascular delineation and spatial resolution.

Cases showing motion or susceptibility artifacts were excluded. MRA datasets were analyzed to identify and document anatomical variants involving the anterior, posterior, and extracranial arterial systems. Detected variants included common ACA, azygous ACA, triple ACA, fenestrated ACA, both ACAs from a single CCA, kissing carotids, persistent trigeminal artery, unilateral and bilateral fetal PCA, bovine arch, common CCA origin, and tortuous “corkscrew” or “hairpin-loop” vascular courses.

Each variant was reviewed independently by two neuroradiologists, and discrepancies were resolved by consensus. Representative cases were selected to illustrate key imaging features, emphasizing their normal anatomic basis and characteristic appearances on 3D MRA projections and source images. Clinical data were correlated when available to assess significance or incidental nature.

Results & Conclusion

A wide spectrum of vascular variants was identified, representing both common and rare configurations. Among intracranial variants, common ACA configuration and unilateral fetal-type PCA were most frequent. Azygous and triple ACA patterns were uncommon but distinctly visualized on sagittal MRA reconstructions. Fenestrated ACA and persistent trigeminal artery were rare findings, each observed in less than 1% of cases.

Extracranial arterial variants included bovine arch in approximately 12% of neck MRAs, while a common origin of both CCAs was observed in a smaller subset. Kissing carotids and tortuous “corkscrew” courses of vertebral and carotid arteries were seen incidentally, often associated with advanced age or hypertension. Hairpin-loop configurations were visualized as focal exaggerated curvatures without hemodynamic compromise.

Representative cases highlighted the potential for diagnostic confusion between vascular variants and pathologic entities such as aneurysm, dissection, or vascular malformation. Multiplanar MRA reconstructions provided accurate differentiation through continuity assessment, symmetric flow, and absence of mural irregularity or signal voids. Recognition of these variants improved confidence in reporting and reduced false-positive findings.

Images/Tables

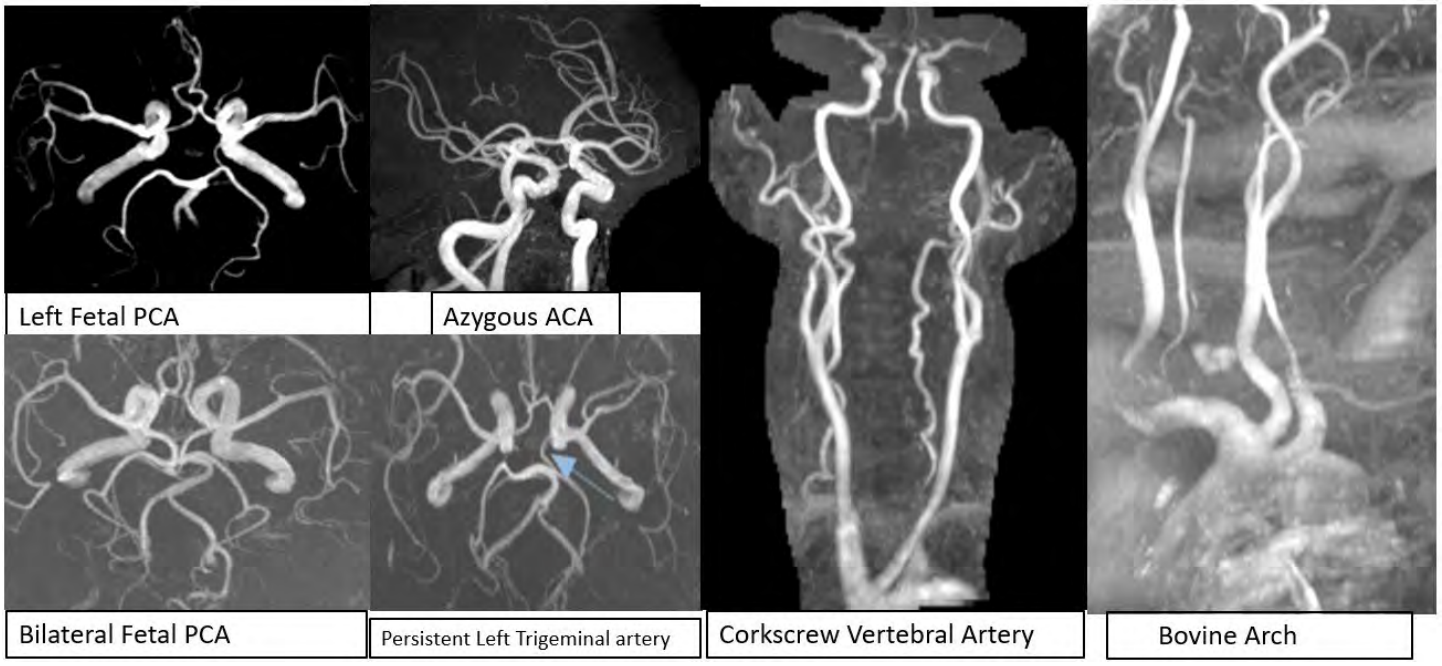

601 Nasopharyngeal Carcinoma: Imaging Evaluation of T4 Disease

Kyle Boudreaux M.D., Katie Bailey
University of South Florida, Tampa, Florida, USA

Summary & Objectives

Nasopharyngeal carcinoma (NPC) arises in the nasopharynx and can become locally invasive before initial diagnosis. Accurate staging of locally invasive NPC is critical for guiding treatment and determining prognosis. Therefore, it is essential for radiologists to recognize the defining features of T4 disease.
T4 NPC is characterized by tumor involvement of any of the following: cranial nerves, intracranial compartment, hypopharynx, parotid gland, orbit, or soft tissues anterolateral the lateral pterygoid muscle.
This educational exhibit illustrates imaging examples of all six structures whose involvement defines T4 nasopharyngeal carcinoma, emphasizing key radiologic findings that facilitate accurate staging and optimal management.

Purpose

The purpose of this exhibit is to provide examples of all six structures whose involvement defines T4 nasopharyngeal carcinoma, as well as, emphasizing key radiologic findings that indicate involvement.

Materials & Methods

A retrospective review of patients with nasopharyngeal carcinoma dating back to 2018 was performed to identify cases demonstrating T4 disease. MRI, CT, and PET studies were reviewed to select representative examples of tumor involvement of each of the six defining structures: cranial nerves, intracranial compartment, hypopharynx, parotid gland, orbit, and soft tissue anterolateral to the lateral pterygoid muscle.
Appropriate images were compiled and annotated to highlight key radiologic features and anatomic landmarks. Relevant literature was reviewed to correlate imaging findings with current AJCC staging criteria.

Results & Conclusion

Representative MRI, CT, and PET cases demonstrated each of the six structures whose involvement defines T4 nasopharyngeal carcinoma: cranial nerves, intracranial compartment, hypopharynx, parotid gland, orbit, and soft tissue anterolateral to the lateral pterygoid muscle.
Familiarity with the imaging appearance of these involved structures is essential to ensuring proper staging and multidisciplinary management to optimize patient outcomes.

Images/Tables

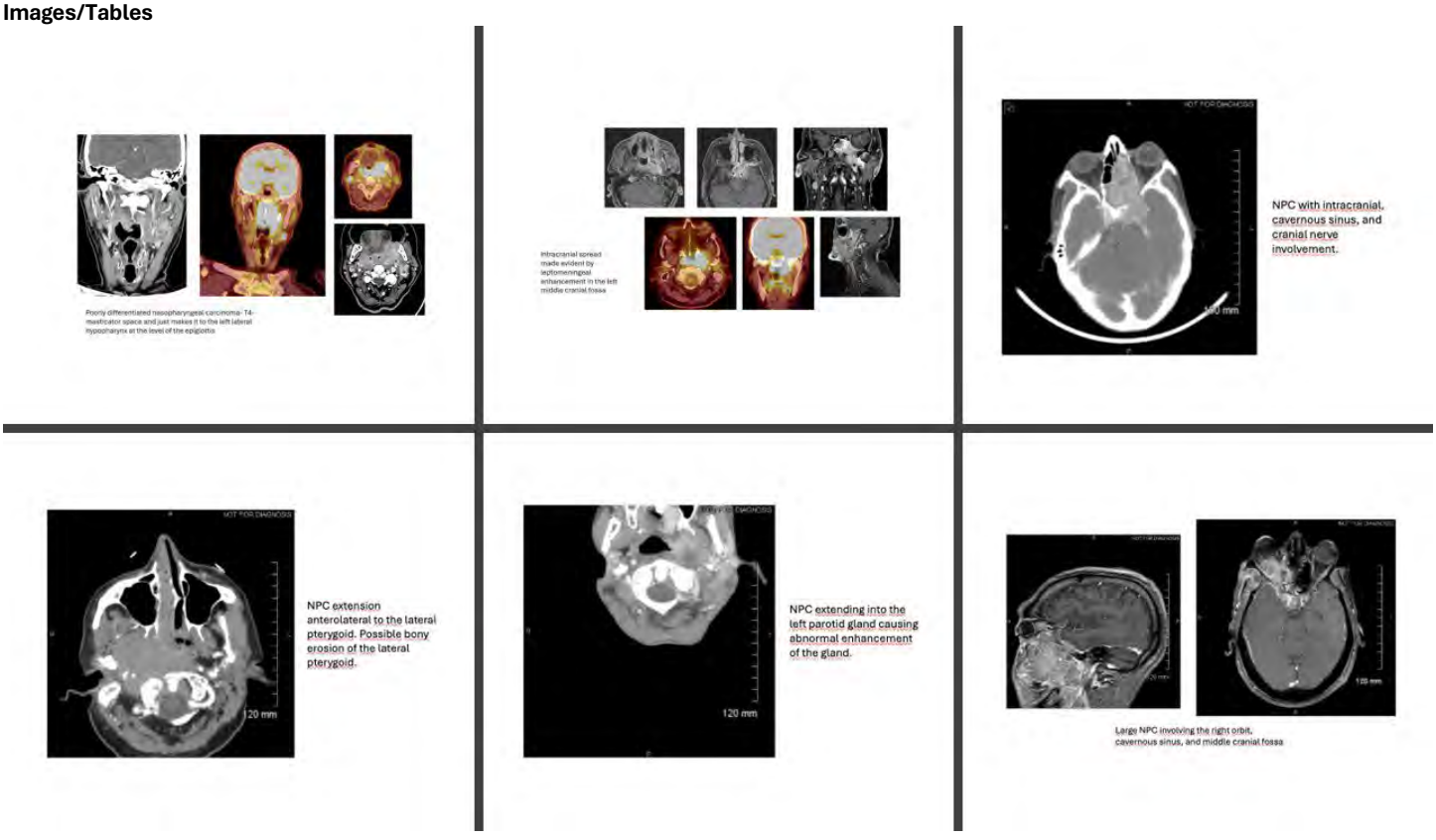

619 Eye Spy: A Case-Based Review of Orbital Pathologies

Peter Wang MD, Charles Li MD, Edward Kuoy MD
University of California, Irvine Medical Center, Orange, California, USA

Summary & Objectives

This educational exhibit reviews the neuroanatomy of the orbit and its compartments as a framework for developing a structured differential diagnosis of orbital lesions. A compartment-based approach will be used to organize common orbital pathologies, including developmental, vascular, infectious, inflammatory, demyelinating, and malignant processes. Characteristic imaging findings will be correlated with ophthalmologic clinical presentations to emphasize interdisciplinary diagnosis and management. Representative cases will include persistent hyperplastic primary vitreous, orbital venolymphatic malformation, carotid–cavernous fistula, central retinal artery occlusion, orbital mucormycosis, giant cell arteritis with bilateral peri-neuritis, anti-MOG antibody optic neuritis, and scirrhous breast cancer metastasis. Through these examples, participants will gain an

understanding of how anatomic localization and imaging patterns integrate with ophthalmologic findings to refine differential diagnoses and improve communication between radiology and ophthalmology.

Purpose

N/A

Materials & Methods

N/A

Results & Conclusion

N/A

Images/Tables

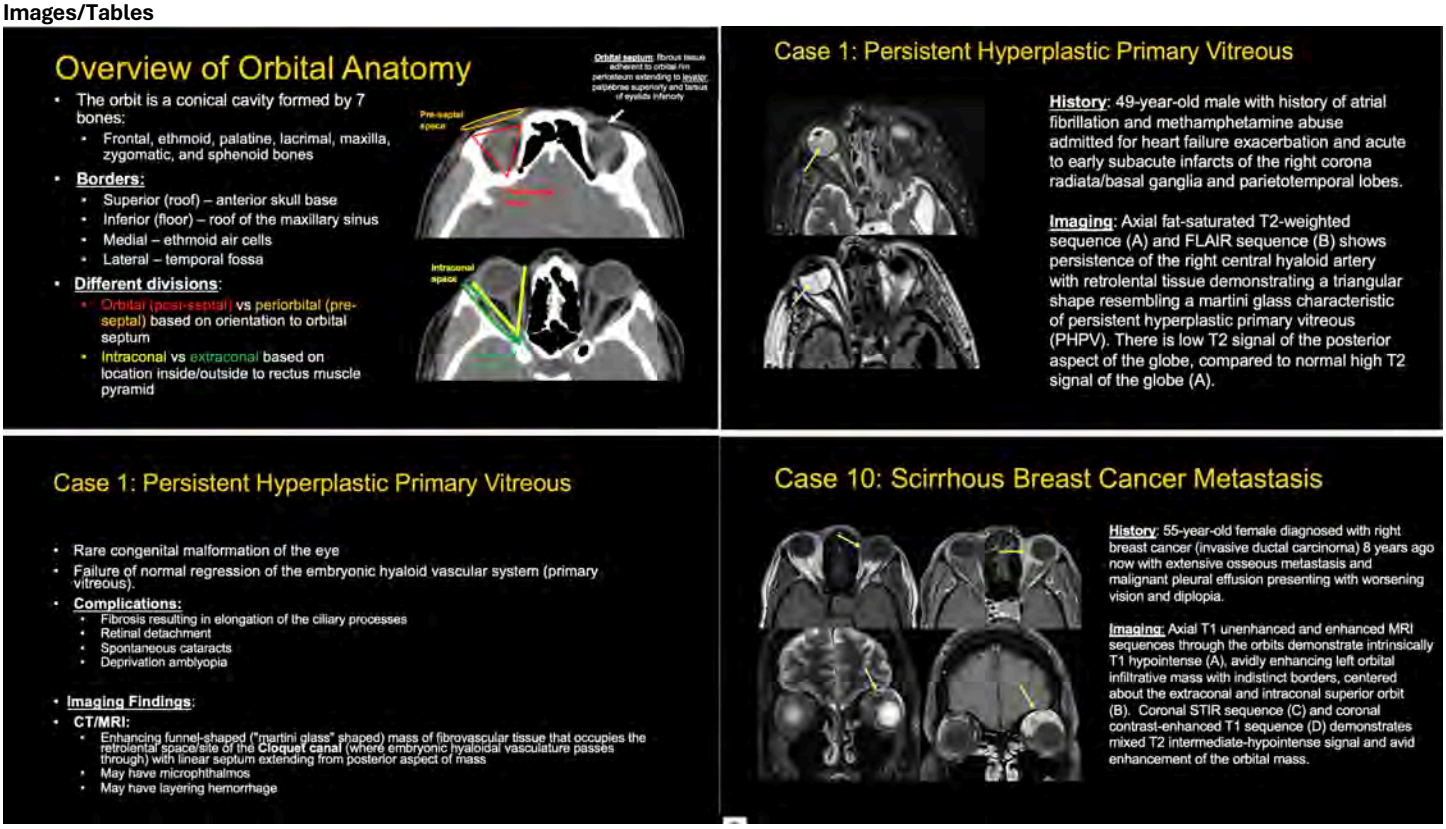

---

762 Treatment of Alzheimer's Disease: From Trajectory Change to Amyloid-Related Imaging Abnormalities

Anthony Peret MD[1], Leonardo Rivera-Rivera PhD[1], Kevin M. Johnson PhD[1], Warren M. Chang MD[2], Aaron S. Field MD PhD[1], Laura B. Eisenmenger MD[1]
[1]University of Wisconsin-Madison, Madison, WI, USA. [2]Allegheny Health Network, Pittsburgh, PA, USA

Summary & Objectives

In this presentation, we aim to review the implications of novel Alzheimer's disease treatments in neuroimaging, including patient selection, evaluation of therapeutic response, and amyloid-related imaging abnormalities (ARIA).

Purpose

The therapeutic landscape of Alzheimer's disease (AD) has evolved significantly over the past decade. While early pharmacological interventions, including cholinesterase inhibitors (such as rivastigmine, donepezil, and galantamine) and NMDA receptor antagonists (such as memantine), provided symptom relief, they offered limited impact on the underlying pathology and disease trajectory. The introduction of monoclonal antibodies targeting amyloid-beta, such as aducanumab, lecanemab, and donanemab, has shifted the focus toward specifically targeting beta-amyloid, the pathological hallmark of AD. This review aims to examine current strategies for evaluating therapeutic response to monoclonal antibodies, with an emphasis on structural and functional imaging biomarkers, and to study the signs of amyloid-related imaging abnormalities (ARIA) associated with monoclonal antibody treatment.

Materials & Methods

Therapeutic response evaluation in AD relies on an integration of clinical assessment and imaging biomarkers. Patient selection is dependent on biological markers, such as CSF amyloid positivity, and imaging criteria, such as amyloid positivity on PET or structural MRI findings, rather than symptom severity, reflecting the early onset of pathology that precedes cognitive impairment. In this educational exhibit, we review the roles of various imaging modalities, including amyloid and tau PET, FDG-PET, and volumetric MRI, in assessing disease burden, progression, and treatment response. Longitudinal imaging allows for comparison of pre- and post-treatment metrics, supporting the evaluation of disease-modifying effects. The exhibit also highlights the monitoring of ARIA, a complication associated with anti-amyloid therapies, emphasizing MRI sequences critical for detection and follow-up.

Results & Conclusion

Imaging studies in clinical trials have demonstrated that monoclonal antibody therapies can reduce amyloid burden in a dose- and time-dependent manner, as indicated by changes in the standardized uptake value ratio on amyloid PET. Similarly, tau-PET and FDG-PET further enable evaluation of neurofibrillary pathology and cerebral metabolism, correlating with disease severity. Structural MRI findings illustrate patterns of brain atrophy, including hippocampal and medial temporal volume loss, ventricular enlargement, and overall cortical thinning, which serve as markers of disease progression and predictors of conversion from mild cognitive impairment to AD dementia. However, paradoxical increases in brain volume losses

have been observed in some anti-amyloid studies, highlighting the complexity of interpreting structural changes. ARIA are MRI-specific pathological conditions attributed to anti-amyloid therapies. They occur in up to 20% of patients treated with monoclonal antibodies. Two forms of ARIA are recognized (Figure): ARIA-E, characterized by parenchymal edema and sulcal effusions on T2 FLAIR imaging, and ARIA-H, characterized by microbleeds and superficial siderosis on susceptibility-weighted imaging. Careful pre-treatment evaluation for cerebral amyloid angiopathy, along with standardized imaging protocols, is essential for risk mitigation and monitoring.
Evaluating therapeutic response in Alzheimer's disease has expanded beyond clinical symptoms to incorporate biomarkers provided by imaging. Structural and functional imaging offers critical insights into the monitoring of amyloid burden, tau pathology, neurodegeneration, and treatment-related complications such as ARIA. Understanding these imaging findings is essential for optimizing patient selection, monitoring therapeutic efficacy, and ensuring safety in clinical practice.

Images/Tables

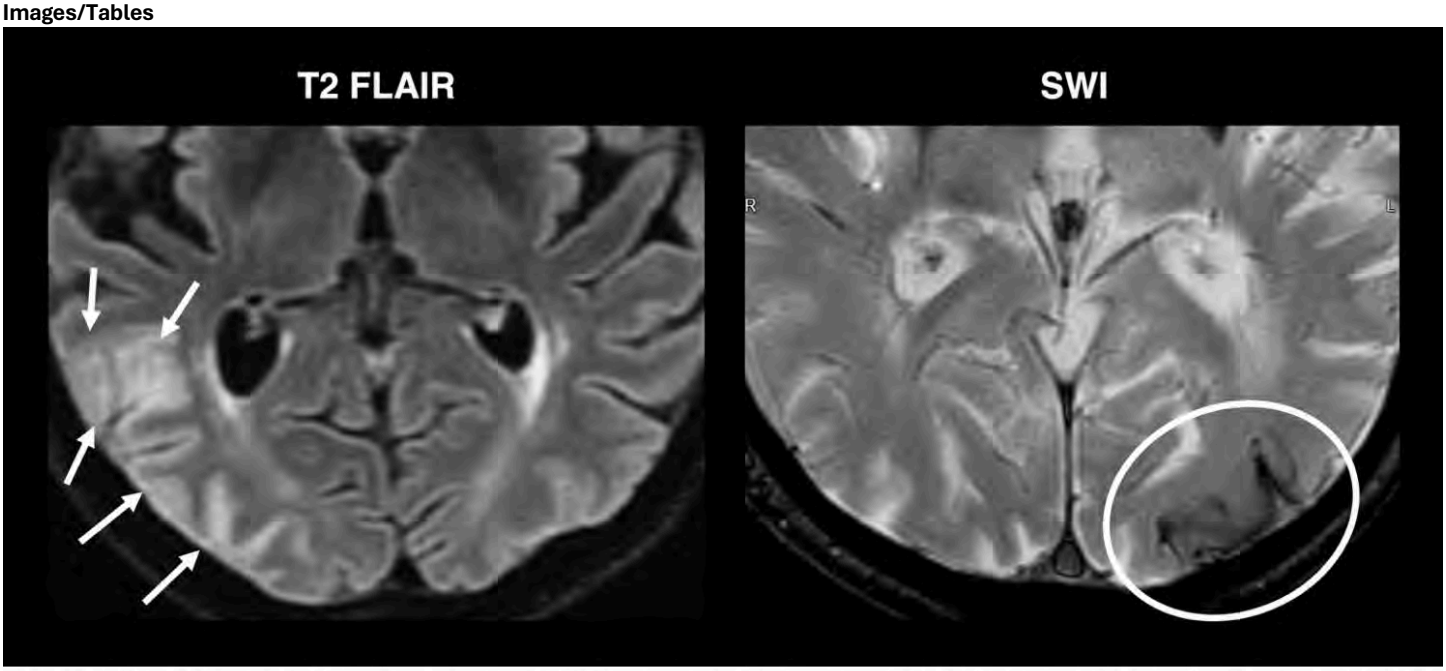

Figure - Amyloid-Related Image Abnormalities (ARIA) type E (edema) and type H (hemorrhage) in two different patients. (Left image) In this patient treated for Alzheimer's disease with aducanumab, an axial view of fluid attenuated inversion recovery (FLAIR) imaging shows extensive cortical and juxtacortical edema in the right occipital lobe (arrows). (Right image) In this patient treated for Alzheimer's disease with lecanemab, an axial view of susceptibility-weighted imaging (SWI) shows lobar hemorrhage with superficial siderosis (circle) along the convexity of the left occipital lobe.

---

143 Through the Fractures: A Sequential Approach to Facial Trauma CT

Valeria Ortega Apraez M.D., Humberto Jose Diaz Silva M.D., Pedro Diaz-Marchan M.D.
Baylor College of medicine, Houston, Texas, USA

Summary & Objectives

This guide provides a systematic approach to evaluating facial fractures on CT. It emphasizes a sequential assessment to prevent missed injuries, organize findings for easier interpretation, and identify features that impact management decisions, based on experience with multiple trauma patients at a Level 1 trauma center. Correct imaging technique, fracture patterns, identify sutures and 3D reconstructions will be shown using CT images, diagrams, and annotated examples, highlighting associated injuries and providing practical insights to support clinical decision-making.

Purpose

To provide a structured approach to facial trauma CT interpretation, helping trainees identify and classify fractures, avoid mistaking sutures for fractures, recognize associated injuries, and understand their implications for surgical planning and management.

Materials & Methods

N/A

Results & Conclusion

This approach encourages a step-back evaluation of facial fractures, following a sequential order that allows thorough assessment, accurate classification, recognition of associated intracranial and orbital injuries, helps prevent overlooked injuries, and improved communication with trauma and surgical teams.

Images/Tables

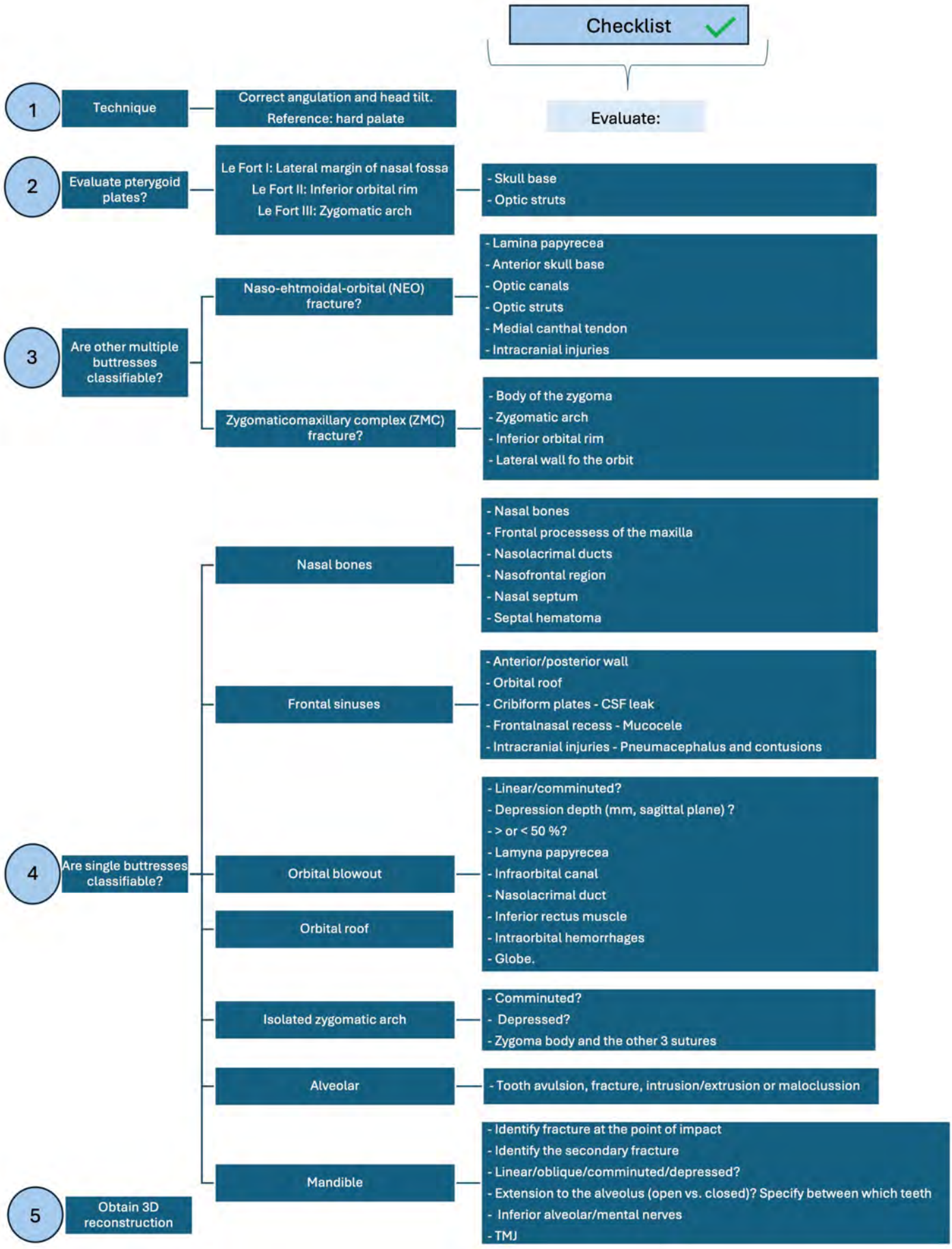

162 "Imaging the Silence: Neuroimaging Patterns in Brain Death"

Heradio Montes Rodríguez MD., Mariana Mercado Flores MD, Juan M Escobedo Gil MD., Cecilia Miranda Garza
Centro Universitario de Imagen diagnóstica, Monterrey, Nuevo León, Mexico

Summary & Objectives

Brain death represents the irreversible cessation of all brain activity and remains a critical diagnosis with profound clinical, ethical, and legal implications. Radiologists play a central role in confirming brain death through neuroimaging, particularly when clinical evaluation is limited or inconclusive.

This educational exhibit aims to review the multimodal imaging findings of brain death across CT, CTA, MR, contrast MRI and ultrasound, emphasizing key diagnostic criteria, technical protocols, and common pitfalls. Through illustrative cases, we provide a structured approach to assist neuroradiologists in confidently identifying imaging features consistent with brain death and differentiating them from reversible conditions.

Purpose

To provide a comprehensive and visually guided overview of the imaging criteria used in the confirmation of brain death, integrating clinical workflow, acquisition techniques, and interpretive pearls that enhance diagnostic accuracy and confidence among neuroradiologists.

Materials & Methods

A retrospective review was performed of confirmed brain death cases evaluated between 2020 and 2024 in a tertiary care center. Imaging modalities included non-contrast CT, CT angiography, CT perfusion, MRI, MR angiography, MR perfusion sequences and ultrasound.

All studies were analyzed for hallmark signs of brain death, including diffuse cerebral edema, loss of gray–white differentiation, effacement of basal cisterns, absence of intracranial blood flow, and lack of perfusion in both CT and MR. Illustrative cases and schematic diagrams were developed for educational visualization.

Results & Conclusion

Imaging findings consistently demonstrated the classical hallmarks of brain death across all modalities, including diffuse cerebral swelling, absent intracranial opacification in CTA, and lack of perfusion signal on CT/MR perfusion. Recognition of these features allows radiologists to support clinical diagnosis and guide multidisciplinary teams in timely certification.

Understanding the technical nuances and limitations of each modality is crucial to avoid false-negative or inconclusive interpretations. A standardized multimodal imaging protocol enhances diagnostic accuracy, reduces uncertainty, and reinforces the radiologist's role in the confirmation of brain death.

---

164 Systemic Approach for Interpreting Trauma Spine MR…Beyond ABCDE

Thotsophon Taechariyakul MD, Tylor D. Connor DO, Graham M. Tooker MD, Brian D. Barnacle MD, Leah A.P. Palifka MD
Dartmouth Hitchcock Medical Center, Lebanon, NH, USA

Summary & Objectives

Summary of Educational Goals:

1. Provide radiologists with a simple, reproducible mnemonic for comprehensive evaluation of spinal trauma.
2. To illustrate through case examples how the "AI" mnemonic structured reporting better encompasses the various types of injuries that may be encountered during spine trauma interpretation beyond the traditional "ABCDE" approach.
3. Encourage adoption of this framework as a teaching tool for trainees and assist practicing radiologists to ensure clinically significant findings are not overlooked.

Purpose

Background & Educational Goals and Objectives:

Interpretation of spinal trauma is challenging due to the wide spectrum of potential soft tissue and osseous injuries, often involving multiple anatomic compartments. Missed injuries may lead to significant morbidity, emphasizing the need for a systematic and reproducible reporting strategy. Traditional trauma evaluation frequently uses the "ABCDE" paradigm, but trauma-specific injuries require a broader framework to encompass both osseous and soft tissue structures.

This educational exhibit aims to illustrate through case examples how the "AI" mnemonic structured reporting better encompasses the various types of injuries that may be encountered during spine trauma interpretation beyond the traditional "ABCDE" approach. This structured sequence is designed to guide radiologists through critical anatomic sites, improve reporting efficiency, and reduce the likelihood of overlooked findings.

Materials & Methods

Mnemonic Breakdown (A → I):

- **A – Alignment:** Assess for traumatic joint subluxation/dislocation and osseous displacement/angulation. Often better assessed on CT.
- **B – Bone:** Evaluate for marrow edema to identify sites of fractures and microtrabecular injuries/osseous contusions (which are often occult on CT). Incidental osseous lesion or marrow pathology.
- **C – Cord:** Identify cord contusion, hemorrhage, compression, or transection.
- **D – Disc:** Examine for traumatic discal injury, disc herniation/bulge, or annular disruption.
- **E – Epidural:** Assess for hematoma or other preexisting abnormal collections or masses.
- **F – Flow Voids:** Assess for evidence of vascular injury such as dissection, pseudoaneurysms, high-grade stenosis/occlusion, or transection.
- **G – liGaments:** Evaluate for ligamentous injury ranging from minor sprain, severe sprain/partial tear, to complete disruption of ligament. A subtle, easily overlooked injury is facet capsular injury.
- **H – Horizontal/Paraspinal Soft Tissues:** Assess paraspinal or prevertebral soft tissues for injury.
- **I – Incidentals:** Recognize clinically relevant but non-traumatic findings that may affect patient management. Examples of important sites include: posterior cranial fossa (cervical spine), visualized lung and posterior chest wall (thoracic), and retroperitoneal and sacral regions (lumbar spine)

Results & Conclusion

Spine trauma interpretation requires careful evaluation of multiple compartments beyond the traditional "ABCDE" approach. The "AI" mnemonic (A → I) expands on traditional approaches to provide a comprehensive, trauma-specific framework in an effort to improve diagnostic accuracy, minimize

reporting variability, and enhance communication with referring clinicians. Integrating this structured method into daily practice may help radiologists streamline their workflow while ensuring clinically significant findings are not overlooked.

Images/Tables

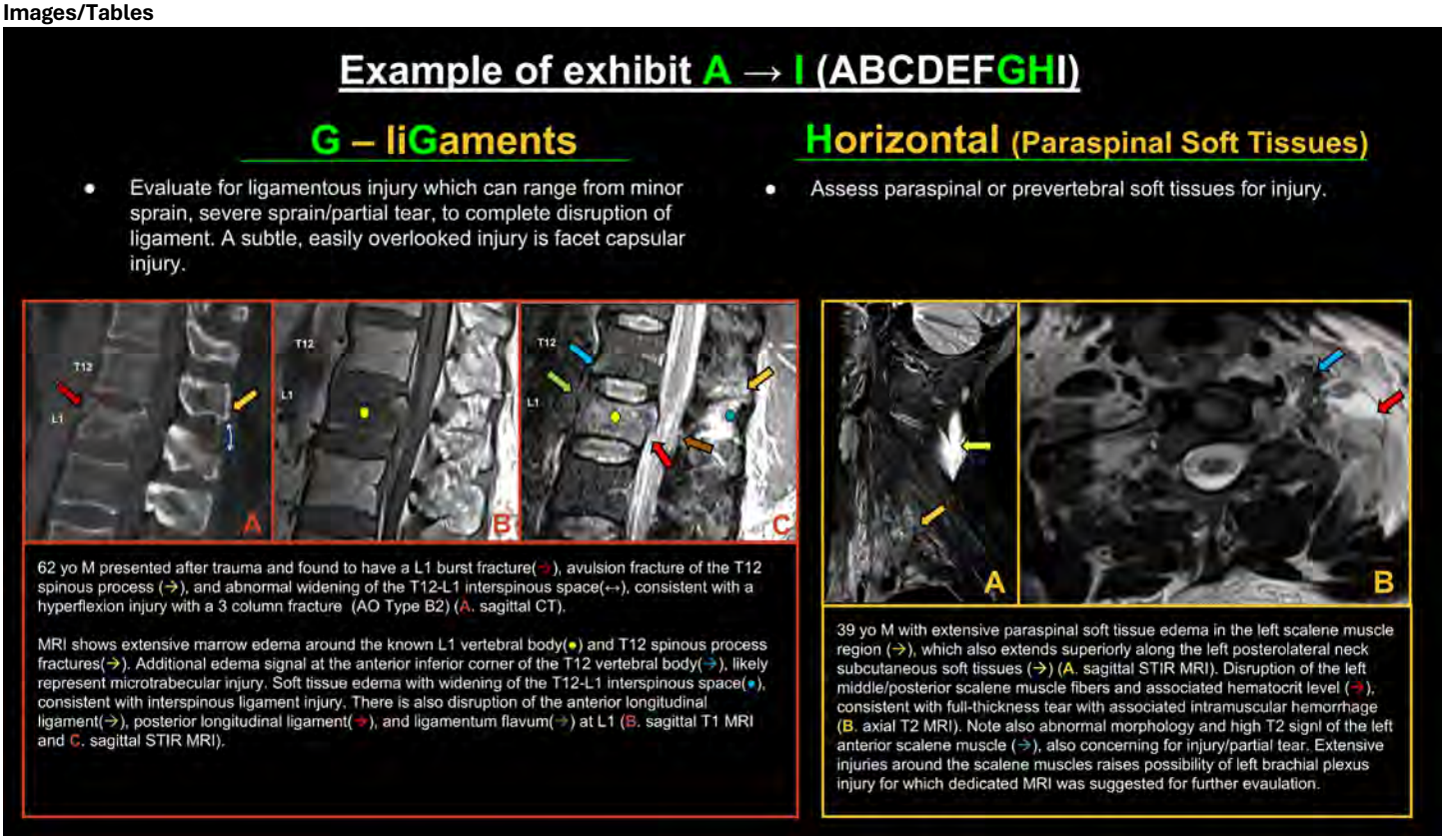

---

170 Better Scan Than Sorry: Stroke Mimics MRI Saved from tPA

RUTH ELIAHOU MD[1], Wael Omar MD[1], Asaf Honig MD[2]
[1]Rabin Medical Center, Petah Tikva, Israel, Israel. [2]Soroka Medical Center, Beer Sheva, Israel, Israel

Summary & Objectives

Up to 30% of patients admitted to the ED with suspected stroke are ultimately diagnosed with stroke mimics based on clinical assessment alone. With multimodal neuroimaging, this rate drops dramatically to 2–4%. Accurate differentiation is critical to avoid unnecessary and potentially harmful treatment with tPA.

Purpose

To highlight common stroke mimics and demonstrate the role of multimodal neuroimaging in improving diagnostic accuracy and patient safety

Materials & Methods

We present a series of cases with acute neurological symptoms mimicking stroke. In many, initial non-contrast CT and CT angiography were unrevealing. Advanced imaging—particularly CT perfusion and/or MRI—proved essential for establishing the correct diagnosis and in some cases spared patients from inappropriate tPA administration.

Results & Conclusion

Our cases include a range of stroke mimics: seizures (ictal and post-ictal), migraines (aura and headache phases), MELAS presenting as subacute infarct, herpes encephalitis, hypoglycemic encephalopathy, contrast media toxicity, transient global amnesia, brainstem cavernous malformation, amyloid spells in cerebral amyloid angiopathy, posterior reversible encephalopathy syndrome (PRES), sinus vein thrombosis, upper cervical cord myelitis, Tumefactive demyelinating lesions, and more.

Key imaging clues for mimics included abnormalities not respecting arterial vascular territories and patterns of generalized hyper perfusion on CT perfusion, which may correlate with the ictal phase of epilepsy or the headache phase of migraine.

Conclusion: Rapid clinical assessment combined with multimodal imaging (CTA, CTP, ±MRI) is essential to accurately identify stroke mimics, improve diagnostic confidence, and prevent unnecessary, potentially harmful treatments.

Images/Tables

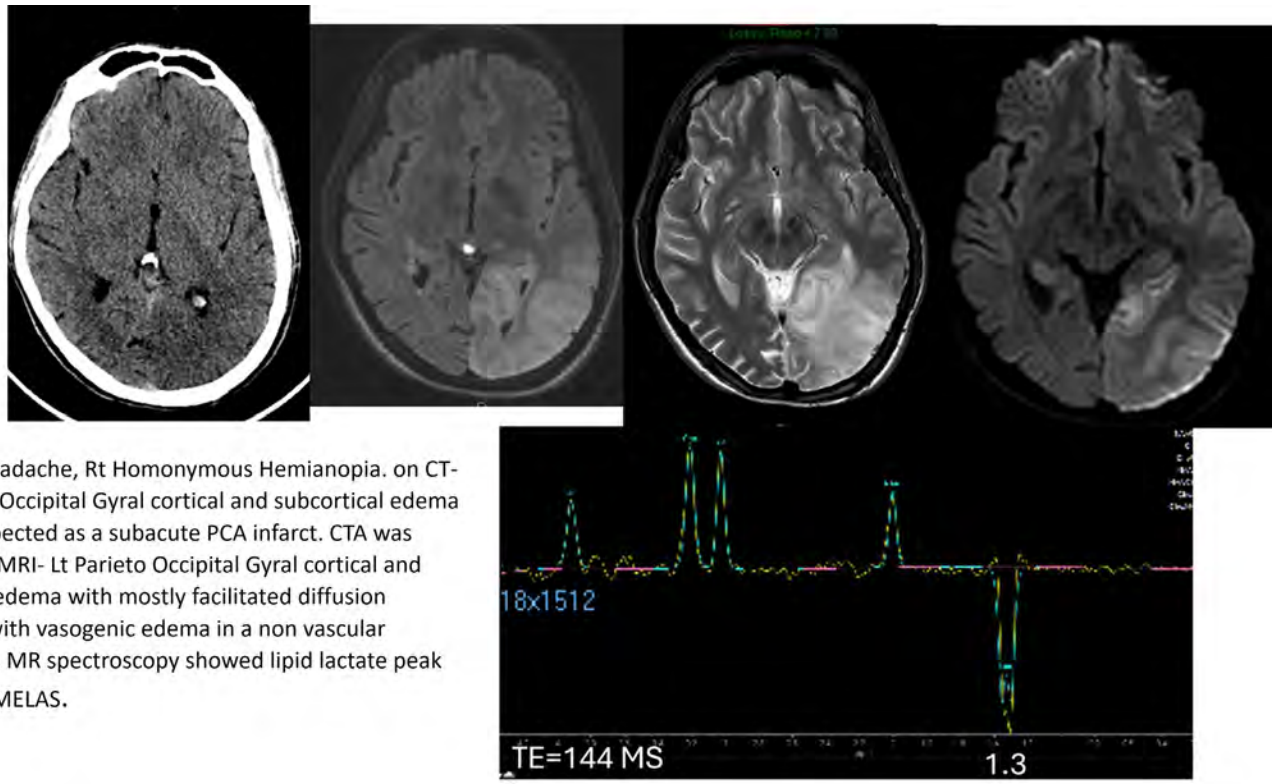

25 YO M, headache, Rt Homonymous Hemianopia. on CT- Left Parieto Occipital Gyral cortical and subcortical edema initially suspected as a subacute PCA infarct. CTA was normal. On MRI- Lt Parieto Occipital Gyral cortical and subcortical edema with mostly facilitated diffusion consistent with vasogenic edema in a non vascular distribution. MR spectroscopy showed lipid lactate peak confirming MELAS.

---

264 The Variable Radiographic Appearance of Craniofacial Langerhans Cell Histiocytosis

Desmond W Chin MD, Lauren Y Peng MD
Kaiser Permanente, Los Angeles, CA, USA

Summary & Objectives

Langerhans cell histiocytosis (LCH) is an uncommon disorder characterized by clonal proliferation of Langerhans-type dendritic cells. In the pediatric population, LCH may present as single-system disease, most commonly involving bone or skin, or as multisystem disease in which the liver, spleen, and bone marrow are also commonly involved.

Craniofacial osseous involvement is common in children but can demonstrate a wide spectrum of imaging appearances. The classic presentation is a sharply marginated lytic calvarial lesion with a “beveled edge” appearance. However, atypical presentations may mimic inflammatory, infectious, or neoplastic entities.

The objective of this educational exhibit is to illustrate the variable imaging appearances of craniofacial LCH using five representative cases, emphasizing the importance of including LCH in the differential diagnosis even when imaging findings are not classic.

Purpose

This educational exhibit aims to:

1. Highlight the variable CT and MRI appearances of craniofacial LCH in children.
2. Demonstrate how atypical imaging features can resemble other disease processes.
3. Reinforce the importance of maintaining a high index of suspicion for LCH when evaluating osseous craniofacial lesions with discordant or mixed imaging features.

Materials & Methods

A retrospective review of five pediatric patients (ages 10–16 years) with biopsy-proven craniofacial LCH was performed. Available imaging studies, including radiographs, CT, and MRI, were reviewed. Lesion location, morphology, and MRI characteristics were analyzed. Representative radiographs, CT, and MRI images were selected for illustrative figures highlighting key imaging features and differential diagnostic considerations.

Results & Conclusion

These five cases demonstrate the variable imaging appearances of LCH with respect to lesion location, definition, enhancement pattern, and diffusion characteristics. While the calvarium is the most common site of involvement, less typical locations such as the temporal bone and pterygopalatine fossa can pose diagnostic challenges.

Temporal bone LCH may mimic other temporal bone masses, including cholesteatoma, rhabdomyosarcoma, or schwannoma arising from cranial nerves. Pterygopalatine fossa involvement may resemble juvenile nasopharyngeal angiofibroma, rhabdomyosarcoma, or trigeminal nerve schwannoma (V2 division). Well-defined lesions can be mistaken for benign or malignant neoplasms, whereas diffusion-restricting lesions may mimic highly cellular tumors or benign entities such as epidermoid cyst or cholesteatoma. Ill-defined or infiltrative LCH lesions can simulate infectious or inflammatory processes, including osteomyelitis or otomastoiditis (if in the temporal bone), while more permeative patterns may raise concern for lymphoma or Ewing sarcoma. Regardless of imaging characteristics, craniofacial LCH can also resemble osseous metastatic disease.

Overall, recognition of this heterogeneity in LCH appearance is important for radiologists to recognize. It is important to consider LCH in the differential diagnoses when evaluating osseous craniofacial lesions in pediatric patients. Awareness of these atypical imaging patterns can prompt appropriate recommendation to pursue tissue diagnosis and prevent unnecessary treatment delay.

Images/Tables

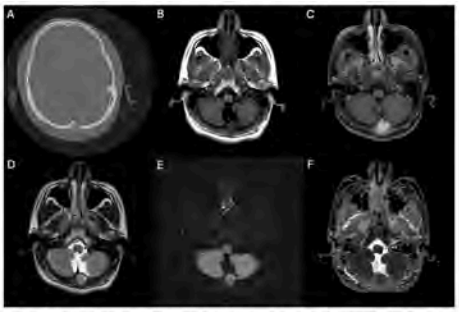

Figure 1. 16-year-old boy with swelling in the occiput. **A.** Axial CT bone shows a lytic lesion in the midline occipital calvarium. **B.** Axial T1 pre-contrast sequence shows a corresponding T1 intermediate signal intensity mass in this region. **C.** Axial T1 fat-saturated post-contrast sequence illustrates corresponding avid enhancement. **D.** Axial T2 sequence shows a circumscribed intermediate signal mass. **E.** DWI sequence reveals no restricted diffusion associated with this mass, confirmed on **F.** ADC map.

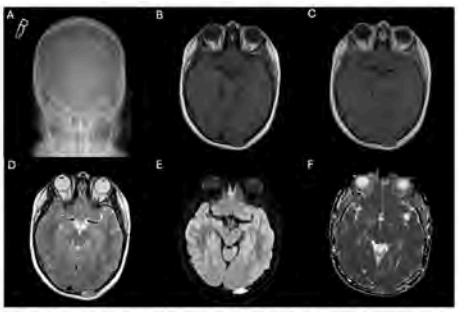

Figure 2. 11-year-old boy with swelling in the left occiput. **A.** Skull radiograph Towne projection demonstrates a circumscribed lytic lesion in the left occipital bone. **B.** Axial T1 pre-contrast sequence shows an expansile intermediate signal intensity mass in the left occipital calvarium. **C.** No associated enhancement of this mass is seen on T1 post-contrast sequence. **D.** Axial T2 sequence shows heterogeneous intermediate to high signal within this mass. **E.** DWI sequence demonstrates restricted diffusion associated with this mass, confirmed on **F.** ADC map.

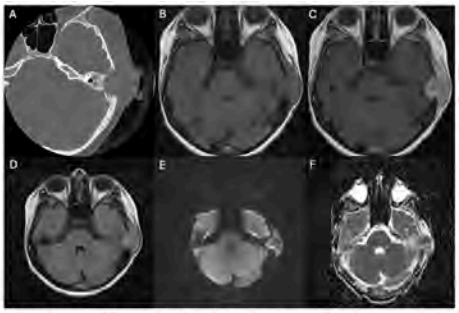

Figure 3. 10-year-old boy with left mastoid pain and swelling. **A.** Axial CT of the left temporal bone shows a well-marginated lucency in the left temporal bone associated with this mass. **B.** Axial T1 pre-contrast shows an intermediate signal intensity mass in the left mastoid region. **C.** Axial T1 post-contrast shows enhancement of this mass. **D.** Axial T2 sequence demonstrates well-circumscribed left temporal bone mass with intermediate T2 signal. **E.** DWI sequence shows no restricted diffusion associated with this mass, confirmed on **F.** ADC map.

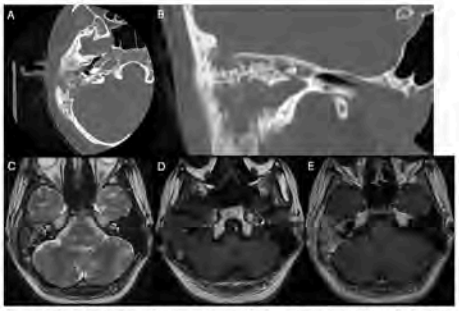

Figure 4. 16-year-old boy with intermittent right ear pain and hearing loss **A.** Axial CT bone through the right temporal bone shows extensive mastoid opacification, osseous erosion, and periosteal reaction. **B.** Stenvers projection CT bone through the right temporal bone again demonstrates mastoid and middle ear opacification, as well as erosion of the tegmen mastoideum. **C.** Axial T2 sequence shows heterogeneous signal throughout the opacified right mastoid and middle ear. Fluid signal within the inner ear structures appears preserved. **D.** Axial T1 pre-contrast sequence illustrates intermediate signal intensity fullness of the right mastoid. Scattered areas of high T1 signal in the right mastoid are suggestive of hemorrhage. **E.** Axial T1 post-contrast sequence demonstrates avid corresponding enhancement throughout the right temporal bone.

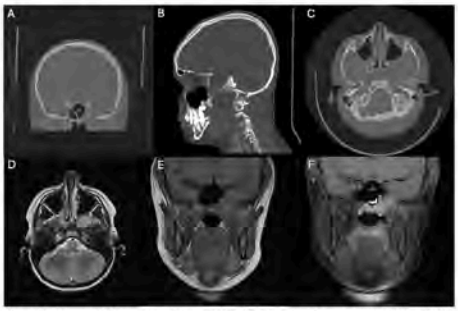

Figure 5. 12-year-old boy with intermittent left facial pain and numbness. **A.** Coronal CT bone, **B.** Sagittal CT bone through the left pterygoid region, and **C.** Axial CT bone all show an expansile mass-like lytic lesion centered at the left pterygoid process. **D.** Axial T2 sequence demonstrates an intermediate signal intensity mass in the left pterygoid region. **E.** Coronal T1 pre-contrast sequence illustrates an ill-defined T1 intermediate signal intensity mass in the left pterygoid region replacing normal marrow signal of the left pterygoid process. **F.** Coronal T1 fat-saturated post-contrast sequence shows corresponding enhancement in this region.

---

404 Mimics of vascular and cardiovascular abnormalities in head and neck imaging

Emily W Avery MD, Bruno P Panzarini MD, James Y Chen MD
UC San Diego, San Diego, CA, USA

Summary & Objectives

While it is critical for the neuroradiologist to diagnose vascular abnormalities quickly and accurately, pitfalls in cross-sectional imaging can pose a challenge to this task. Specifically, normal anatomic variants, technical errors, and other vascular and nonvascular entities can mimic acute vascular pathology. This educational exhibit showcases a series of cases in which such 'vascular mimics' arise. These vascular mimics are crucial to recognize in clinical practice, and we thus aim to showcase the imaging findings, clinical features, and pathophysiology underlying these entities in the interest of improving speedy recognition by neuroradiologists in all stages of training.

Purpose

Vascular abnormalities in the head and neck can be associated with high morbidity and mortality, and quick and accurate diagnosis of acute vascular pathology is a crucial task in neuroradiology. Pitfalls in CT and MRI imaging offer diagnostic challenges to this task. Our aim is to present a wide range of such pitfalls, wherein anatomic variants, technical errors, and other vascular and nonvascular pathologies mimic acute vascular or cardiovascular pathology. This educational exhibit serves to highlight these entities for neuroradiologists in all stages of training, in the interest of facilitating recognition and appropriate management of such 'vascular mimics'.

Materials & Methods

We reviewed CT and MRI studies flagged for discussion on our institution's picture archiving system between January 2020 and June 2025 wherein acute vascular/cardiovascular pathology was initially suspected. We compiled a series of such instances, including:

-Apparent dissection of the internal carotid artery (ICA) due to fenestration of the cervical ICA[1]
-Apparent occlusion of the internal carotid artery due to high-grade proximal stenosis
-Apparent dissection of the internal carotid artery due to back pressure from tandem distal clot[2]
-Artifactual common carotid dissection due to vascular pulsation and rapid CT acquisition
-Pseudo-arteriovenous shunting due to severe venous reflux from increased central venous pressure or stenosis
-Apparent dural arteriovenous fistula due to stenosis of the jugular vein on arterial spin labeling MRI[3]
-Pseudo vertebral artery dissection due to turbulent flow causing apparent intramural hematoma on MRI[4]
-Brain death with diffuse cerebral edema and lack of intracranial vascular opacification, a mimic of poor cardiac output[5]

Results & Conclusion

Our exhibit depicts the imaging findings, clinical features, and pathophysiologic underpinnings of a variety of cases in which anatomic variants, technical errors, and other vascular and nonvascular pathologies mimic acute vascular or cardiovascular injury. These 'vascular mimics' are important to recognize quickly and accurately in the reading room in the interest of timely and appropriate patient care.

Images/Tables

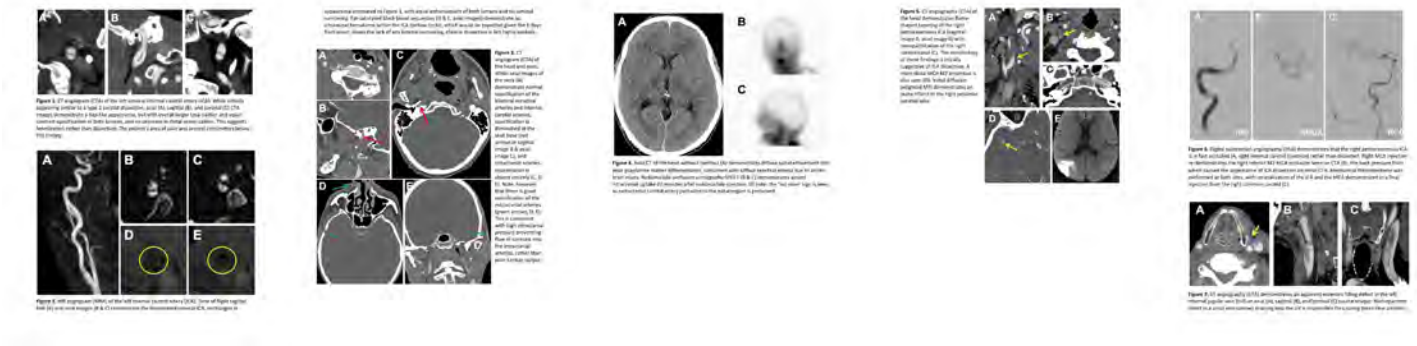

494 **Common, Uncommon, and Pitfalls in Postoperative Spine Imaging Findings**

Azin Aein MD, Noha A. Elghitany, Hadika Mubashir MD, Zahraa Al-Tameemi MD, Alexander S. Oh MD, John Heymann MD, Huda Al Jadiry MD
University of Texas Medical Branch (UTMB), Galveston, TX, USA

Summary & Objectives

We aim to explore the spectrum of postoperative spine imaging findings, highlighting both typical and atypical presentations, as well as the pitfalls and challenges associated with them. It emphasizes common imaging patterns, identifies less frequent but clinically significant features, and discusses potential pitfalls that can lead to misinterpretation. Understanding these features is crucial for radiologists to recognize these presentations, ensuring accurate diagnosis, appropriate management, and avoiding diagnostic errors in postoperative patients.

Purpose

This educational review aims to familiarize radiologists with common and uncommon findings and pitfalls in postsurgical spine patients, thereby improving their ability to distinguish between expected postoperative changes and pathological conditions, and ultimately reducing interpretation errors and guiding appropriate treatment decisions.

Materials & Methods

This study included patients who underwent various spinal procedures, including lumbar puncture, epidural steroid injection, myelogram, spinal fixation (via anterior and posterior approaches), discectomy for herniation, laminectomy, and kyphoplasty. Postoperative imaging studies, primarily MRI and CT scans, were reviewed and analyzed. The imaging studies were analyzed to identify typical and expected postoperative features, detect common implant-related complications, and identify uncommon postoperative changes, as well as potential pitfalls and challenges during interpretation.

Results & Conclusion

Postoperative changes that are common and expected include early fluid collections, inflammatory and edematous changes in the surgical area, and scar formation, which can sometimes mimic recurrent disc herniation. Imaging studies may reveal complications related to the implant, such as hardware failure, misplacement, or loosening, along with progressive degenerative changes in the fused segments or adjacent spinal levels. Less frequent postoperative features encompass pseudomeningocele, CSF leakage, nerve injury or radiculopathy, infection and abscess formation, hematoma, arachnoiditis, radiculitis, pneumorrhachis, recurrent disc herniation, and bone cement leakage during or after kyphoplasty. Some common pitfalls include distinguishing between scar tissue and recurrent disc herniation and recognizing imaging artifacts.

A comprehensive understanding of the spectrum of imaging postsurgical spine changes is essential for precisely identifying and interpreting these findings.

Images/Tables

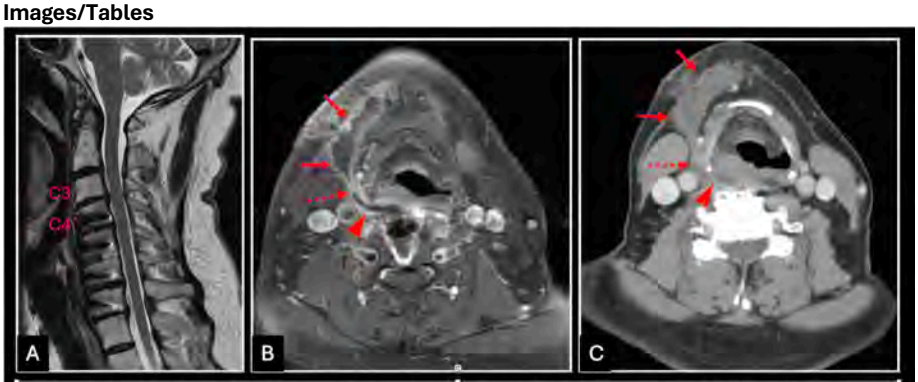

Figure 1: Sagittal T2WI (A) shows anterior cervical discectomy and fixation (ACDF) at C4-C7 with osseous fusion of C5 and C6 vertebral bodies. Moderate spinal canal stenosis at C3-C4 with associated neural foraminal narrowing consistent with adjacent segment disease. Axial T1WI post contrast neck (B) and axial CT soft tissue neck with contrast (C) show new ACDF changes at C3-C4 in the same patient with complication of prevertebral/retropharyngeal abscess formation (arrowheads) with fistulous tract tracking anteriorly into the submandibular region (dashed arrows) and anterior superficial neck phlegmonous changes (arrows). Effacement of the supraglottic larynx is noted.

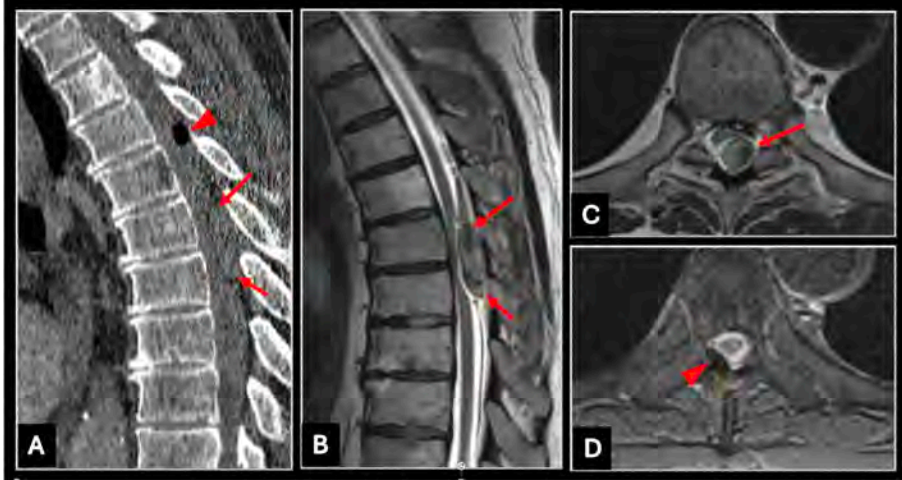

Figure 2: Sagittal NCCT T-spine (A), sagittal T2WI (B), axial T2WI (C) and axial STIR (D) show foci of gas in the posterior epidural space at T4-T5 related to recent epidural injection at T7 (arrowheads). There is a posterior epidural iso-dense collection (arrows) with associated T2 isointense signal extending from T6 to T7 level measures 5.3 cm in CC dimension and 8 mm in maximum thickness.

---

536 **The Many Faces of Trigeminal Neuralgia**

Asma Sulaiman Al Hatmi MD, Shamis Hasan MD
Mcmaster University, Hamilton, Ontario, Canada

Summary & Objectives

The trigeminal nerve (CN V) can be affected by a broad spectrum of pathologies that manifest clinically as trigeminal neuralgia (TN) or neuropathy. Understanding the nerve's complex anatomy, common disease involvement and their imaging appearance across its course—from brainstem to extracranial branches—is essential for accurate diagnosis and management. This educational exhibit presents a comprehensive, case-based radiologic review illustrating the diverse etiologies, characteristic imaging findings, and key diagnostic pearls of trigeminal neuralgia.

Objectives:

1. To review the normal anatomy and imaging appearance of the trigeminal nerve and its divisions.
2. To illustrate the various pathologic processes that may involve the trigeminal nerve along its course.
3. To highlight MRI techniques and key radiologic signs that aid in differentiating the broad spectrum of trigeminal neuralgia etiologies.
4. To provide a structured imaging approach for evaluating patients presenting with trigeminal neuropathy.

Purpose

The purpose of this exhibit is to apply a structured, imaging -based diagnostic approach for evaluating patients with trigeminal pain and to educate radiologists on the imaging evaluation of trigeminal nerve disorders by integrating clinical context, anatomic understanding, and case-based examples.

Materials & Methods

- Representative cases were retrospectively collected from the PACS systems of Hamilton Health Sciences. MRI (including high-resolution T2-weighted CISS/FIESTA and post-contrast sequences) and some CT studies were reviewed to evaluate the trigeminal nerve course,

associated pathology, and secondary findings. Entities were categorized by etiology—**v**ascular, ischemia, inflammatory, demyelinating, infectious, neoplastic, and congenital—with correlation to clinical presentation and surgical or histopathologic outcomes when available. Some rare entities of trigeminal neuralgia were included in our exhibit; like absence of Meckel's cave and postoperative teflon granuloma.

- Annotated images, schematic diagrams, and pearls summary illustrating characteristic imaging findings and differential diagnosis were provided.

Results & Conclusion

Results:

The exhibit encompasses a wide pathologic spectrum that can lead to TN/neuropathy, including:

- **Vascular:** neurovascular compression, Lateral medullary infarction, vascular malformations.
- **Inflammatory/Demyelinating:** Multiple sclerosis plaques, neurosarcoidosis, Tolosa-Hunt syndrome.
- **Neoplastic:** Trigeminal schwannoma, Meckel's cave meningioma, melanoma metastasis, perineural spread of nasopharyngeal or oral carcinoma.
- **Congenital/Developmental:** Absence or hypoplasia of Meckel's cave(a rare entity).
- **Post-surgical:** Teflon granuloma following microvascular decompression (a rare entity).

Conclusion:

Trigeminal neuralgia encompasses a wide pathophysiologic spectrum beyond a vascular compression. Mastery of trigeminal nerve anatomy and its imaging spectrum enables accurate localization and differentiation between benign, inflammatory, vascular, and neoplastic causes. A systematic MRI-based diagnostic approach—from brainstem to extracranial segments—can enhance the diagnostic confidence of trigeminal neuralgia pathology.

Images/Tables

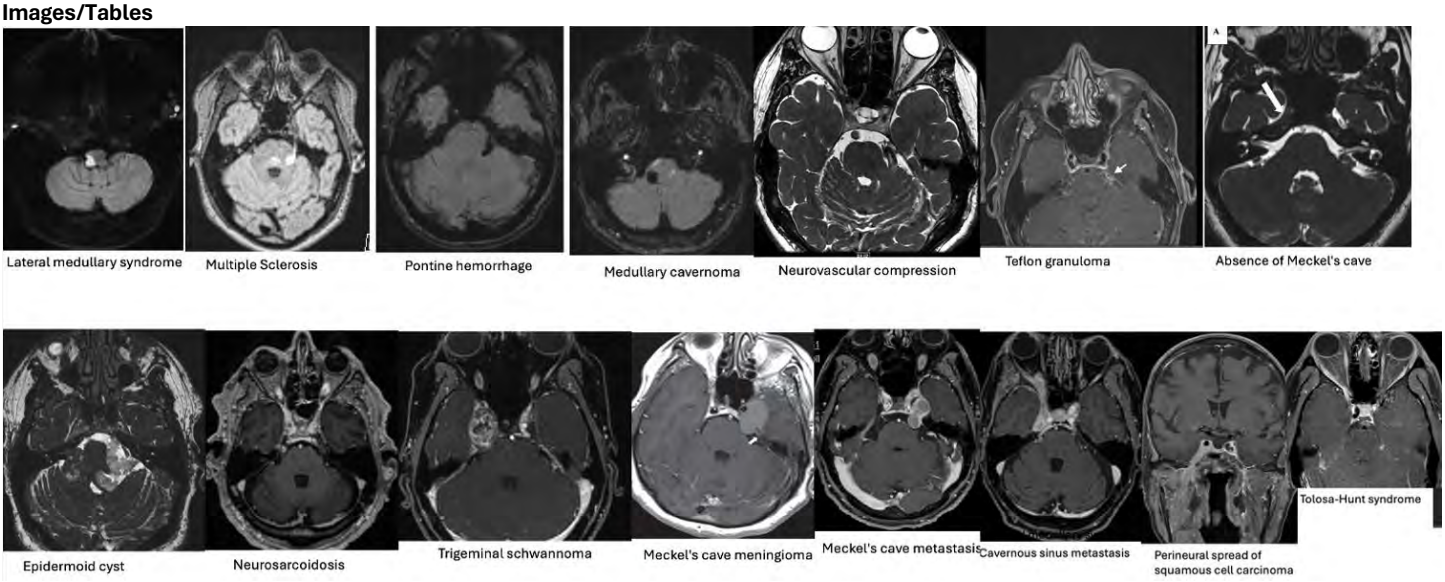

---

581 MRI in Central Nervous System Infections: A Patterned Approach

Aditya Duhan MD[1], Fahad Farooq MD[2], Swastika Lamture MD[1], Saurav Jha MBBS[3], Mamta Gupta MD[1], Charanjeet Singh MD[1]

[1]University of Colorado, Aurora, CO, USA. [2]SUNY Upstate Medical University, Syracuse, NY, USA. [3]Patan Academy of Health Sciences, Kathmandu, Nepal, Nepal

Summary & Objectives

Going beyond simply enumerating possible findings for every infection is the primary objective here. Rather, we want to develop a straightforward and effective diagnosis process for neuroradiologists. In order to classify patterns, we begin by grouping lesions into four primary, clearly recognized imaging patterns: White Matter Hyperintensities, Grey Matter Hyperintensities, Basal Ganglia SOL, and Ring Enhancing Lesions. Standard MRI sequences, such as T1, T2, and enhancement techniques, are used for this classification.In terms of etiological subclassification, we can use sophisticated molecular and functional MRI sequences to rapidly reduce the number of possible diagnoses to a single cause. This is where methods like Susceptibility Weighted Imaging (SWI), Diffusion-Weighted Imaging (DWI), and MR Spectroscopy (MRS) are essential. Important and specific indicators are revealed by these advanced techniques, such as the restricted diffusion that indicates CNS lymphoma or the amino acid peaks on MRS that show bacterial abscesses. This information is essential for identifying the infectious agent and enabling prompt and accurate treatment.

Purpose

1. Create a rational MRI algorithm that can classify CNS infections using conventional sequences like T1, T2, and Enhancement.
2. Learn how to leverage MRI sequences such as DWI and MRS to quickly sub-classify and characterize the underlying cause of CNS infections.

Materials & Methods

Regarding imaging modalities, we focus on studies that use structural MRI methods for initial pattern recognition, such as T1, T2, FLAIR, and Gadoliniu m enhancement.[1,2]

In order to aid in precise differentiation, we next delve into advanced MRI techniques including DWI, MRS, Perfusion, and SWI. Our approach divides le sions into four primary patterns: GM Hyperintensity, WM Hyperintensity, Basal Ganglia SOL, and Ring Enhancing. Next, we identify particular diagnosti c markers, such as metabolic peaks and restricted diffusion, using sophisticated sequences.

Results & Conclusion

Ring Enhancing Lesions: Bacterial abscesses show core **restricted diffusion** and **Amino Acid peaks** on MRS. Fungal abscesses show no core restriction and often a **Trehalose peak**. **Basal Ganglia altered signal intensity** could be secondary to CNS Lymphoma which shows **restricted diffusion** and **high CBV,** differentiating it from Toxoplasmosis (low CBV and hemorrhage). Grey matter **Hyperintensity: Restricted diffusion + Increased Perfusion** suggests infection (encephalitis) over infarction. White matter hyperintensity**.** PML is typically **asymmetrical** with peripheral restriction, while HIV Encephalopathy (HIVE) is **symmetrical** with NAA reduction.

The patterned MRI **approach** is a highly effective diagnostic tool for CNS infections. By combining conventional pattern recognition with the specific data from advanced sequences, it ensures **early, accurate etiological diagnosis**, which is essential for minimizing morbidity and mortality through timely antimicrobial treatment.

Images/Tables

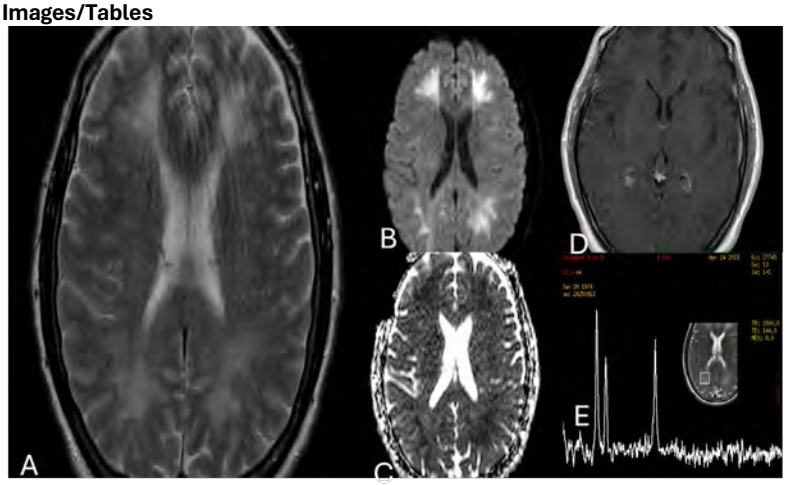

Axial T2(A), DWI (B), ADC (C), post contrast (D) sections of brain and MR spectroscopy at TR: 1500 and TE: 144. Confluent symmetric, non-enhancing ,T2 hyperintensity with diffusion restriction. On single voxel MR spectroscopy, there is elevated Choline/Cr peak and mildly diminished NAA peak. These findings are suggestive of HIV encephalopathy.

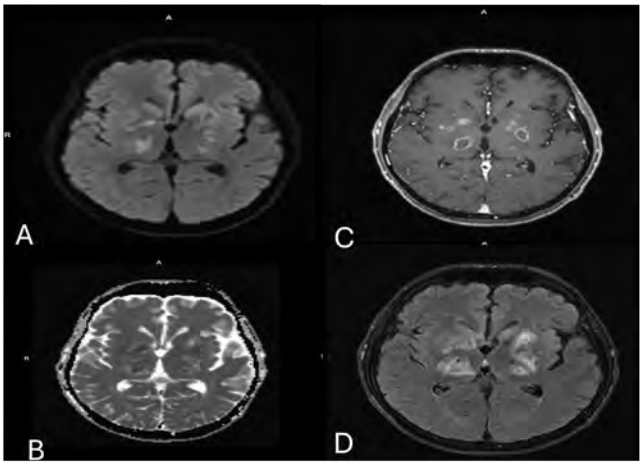

Axial DWI (A), ADC (B), post contrast (C) and FLAIR (D)sections of the brain. Multiple peripherally enhancing lesions (C) in the basal ganglia and thalami with mild hyperintensity on DWI (A) with signal drop on ADC (B). These are heterogeneously hyperintense on FLAIR (D). These turned out to be cerebral toxoplasmosis

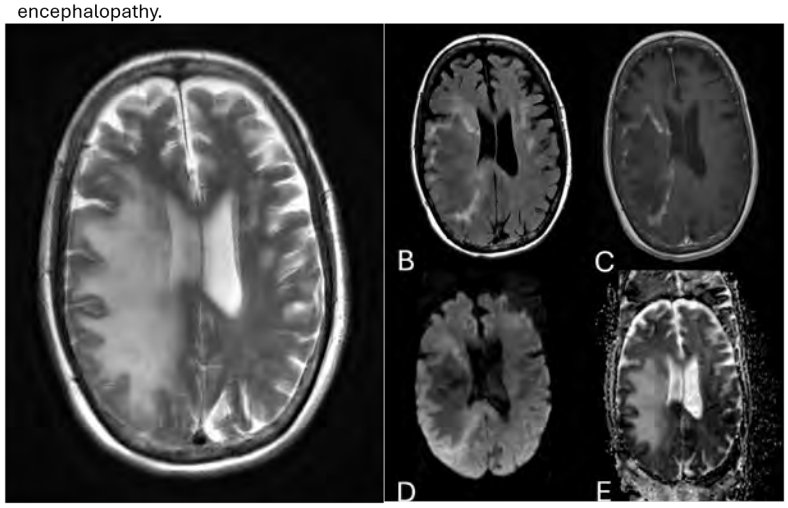

Axial T2 (A), FLAIR (B), post contrast (C), DWI(D) and ADC (E) sections of brain. Ill defined T2 hyperintensity with suppression on FLAIR. Peripheral FLAIR hyperintensity which corresponds to diffusion restriction and rim like enhancement. In the clinical context of HIV, these findings are suggestive of Progressive Multifocal Leukoencephalopathy (PML)

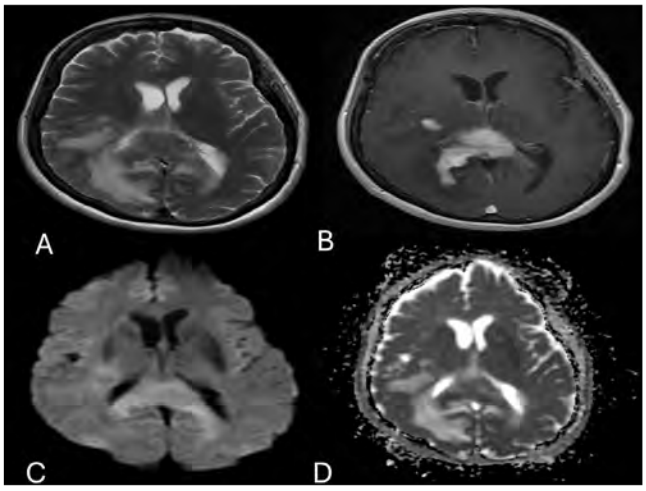

Axial T2(A), post contrast T1(B), DWI (C) and ADC (D) of the brain. T2 hypointense homogeneously enhancing mass in the splenium of corpus callosum crossing the midline with diffusion restriction and moderate surrounding edema suggestive of primary CNS lymphoma

665 Vascular Anomalies of the Spine: An Overview of Anatomy and Imaging Appearances

Miranda Le B.S., Jakob von Morgenland B.S., Jamie E. Clarke M.D., M.S., Jay Acharya M.D.
Division of Neuroradiology, Department of Diagnostic Radiology, University of California Los Angeles (UCLA), Los Angeles, CA, USA

Summary & Objectives

Spinal vascular anomalies represent a diverse group of rare but clinically significant lesions. They may present with progressive myelopathy, acute neurological deficits, or even catastrophic hemorrhage. Since their clinical manifestations often mimic more common spinal cord disorders, diagnostic delays are unfortunately common. This educational exhibit aims to review the imaging spectrum of spinal vascular anomalies, including both high-flow and low-flow lesions, and to highlight the diagnostic strategies that improve detection accuracy. Objectives include: (1) defining the imaging features that distinguish high-flow from low-flow lesions, (2) demonstrating the role of various MRI and CT angiography techniques in their evaluation, and (3) outlining a systematic classification framework to guide diagnosis and clinical management.

Purpose

The purpose of this exhibit is to address the diagnostic challenges posed by spinal vascular anomalies and to emphasize the value of a multimodal imaging approach in improving recognition and characterization. By integrating an array of imaging techniques, radiologists can better identify subtle or occult lesions that may be missed on routine MRI. This exhibit seeks to reduce misclassification and promote more accurate diagnosis to guide intervention and subsequently prevent irreversible neurological injury.

Materials & Methods

We retrospectively reviewed representative cases of spinal vascular anomalies from our institutional database to illustrate the imaging spectrum and diagnostic challenges of these lesions. Cases included both high-flow arteriovenous shunts, such as spinal dural arteriovenous fistulas (SDAVFs), perimedullary arteriovenous fistulas (pmAVFs), and intramedullary arteriovenous malformations (AVMs), and low-flow lesions, including cavernous malformations, hemangioblastomas, and vertebral intraosseous vascular malformations.

The assortment of cases were selected to highlight the use of multimodal imaging techniques. The combination of MRI sequences with volumetric heavily T2-weighted imaging and time-resolved contrast-enhanced MR angiography (TR-MRA) allows for enhanced lesion detection and flow characterization. In some cases, spinal subtraction CT angiography with bone-background fusion was utilized to generate three-dimensional vascular maps for procedural planning and correlation. Cases were analyzed for key imaging features, including flow voids, cord signal changes, and vascular anatomy. A structured classification framework was applied to document lesion type, anatomic compartment, spinal level, feeding arteries, and venous drainage patterns.

Results & Conclusion

Spinal vascular anomalies require a systematic imaging approach combining multiple MR techniques and advanced CT angiography. Early recognition and accurate classification are critical to inform therapy and prevent irreversible neurological damage. This educational exhibit provides a comprehensive framework for assessing, classifying, and reporting these challenging lesions.

Images/Tables

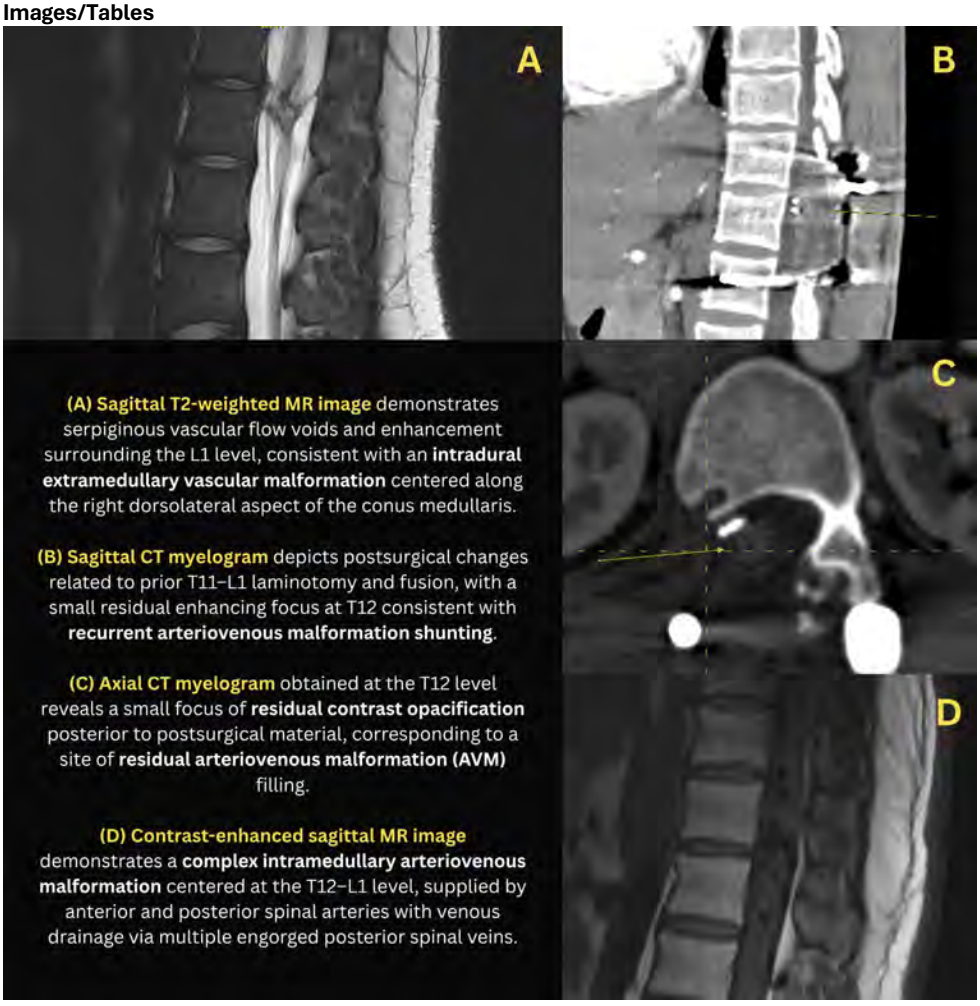

705 Cysts, Syndromes, and Mimicry: A Neuroradiologist's View on Taenia solium Infection.

Arturo Maximiliano Rodriguez Saldivar MD, Andres Felipe Ríos Victoria MD, Bryann Cortés Rodriguez MD, Michel Israel Garcia Gutierrez MD, Mariana Mercado Flores MD, Haziel Maya Garcia MD
Centro Universitario de Imagen Diagnostica, Monterrey, Nuevo León., Mexico

Summary & Objectives

Neurocysticercosis is the most common parasitic infection of the central nervous system and a principal cause of acquired epilepsy worldwide. Its clinical and radiological manifestations are extraordinarily diverse, earning it a reputation as a diagnostic chameleon that can mimic numerous other neurologic diseases. This review summarizes the radiological spectrum of NCC, correlating imaging findings with the parasite's evolutionary stages and varied clinical syndromes. The objectives are to: (1) describe the four distinct stages of parenchymal NCC, (2) differentiate parenchymal disease from the more aggressive extraparenchymal forms , and (3) highlight key clinical presentations, including seizures and Brun's syndrome

Purpose

The purpose of this study is to provide a concise overview of the diverse neuroradiological findings in NCC, correlating illustrative clinical cases from our center with a comprehensive review of published studies**.** We aim to illustrate the typical imaging evolution of parenchymal cysts and contrast these findings with the presentations of extraparenchymal disease, emphasizing the critical role of imaging in diagnosis, staging, and guiding appropriate therapy.

Materials & Methods

A retrospective review of clinical cases diagnosed with neurocysticercosis at the Centro Universitario de Imagen Diagnostica de Monterrey was performed. These cases were analyzed to identify the spectrum of radiological presentations (CT and MR). These institutional findings were then combined with a foundational literature review of published case reports and neuroradiology studies detailing the imaging characteristics and clinical correlations of NCC. The review synthesized data on the pathological stages of the parasite , the imaging features of different anatomical locations (parenchymal, ventricular, and subarachnoid) , and associated clinical syndromes. The diagnostic utility of advanced MR sequences, such as 3D-CISS for intraventricular disease, was also evaluated.

Results & Conclusion

NCC presents as parenchymal or extraparenchymal disease.

Parenchymal NCC evolves in four stages:

Vesicular: A viable, non-enhancing cyst with a pathognomonic scolex.

Colloidal: The cyst degenerates, causing intense inflammation, ring-enhancement, and edema. This stage is highly epileptogenic.

Granular-Nodular: The lesion becomes a smaller, enhancing granulomatous nodule.

Nodular-Calcified: The end-stage is a calcified nodule, which can still trigger seizures due to perilesional inflammation.

Extraparenchymal NCC includes:

Intraventricular: Cysts are often missed by CT but visible on MRI (especially 3D-CISS). Mobility can cause Brun's syndrome—a life-threatening intermittent obstructive hydrocephalus.

Subarachnoid (Racemose): An aggressive form with high mortality. Large, grape-like cysts without scoleces incite severe arachnoiditis, hydrocephalus, and vasculitis.

Conclusion: The radiological spectrum of NCC is vast. Neuroradiology is the cornerstone of diagnosis. MRI is superior for active disease and intraventricular cysts, while CT is definitive for calcifications. A precise understanding of the imaging features corresponding to the parasite's stage and location is essential for diagnosis, risk stratification, and guiding therapy.

Images/Tables

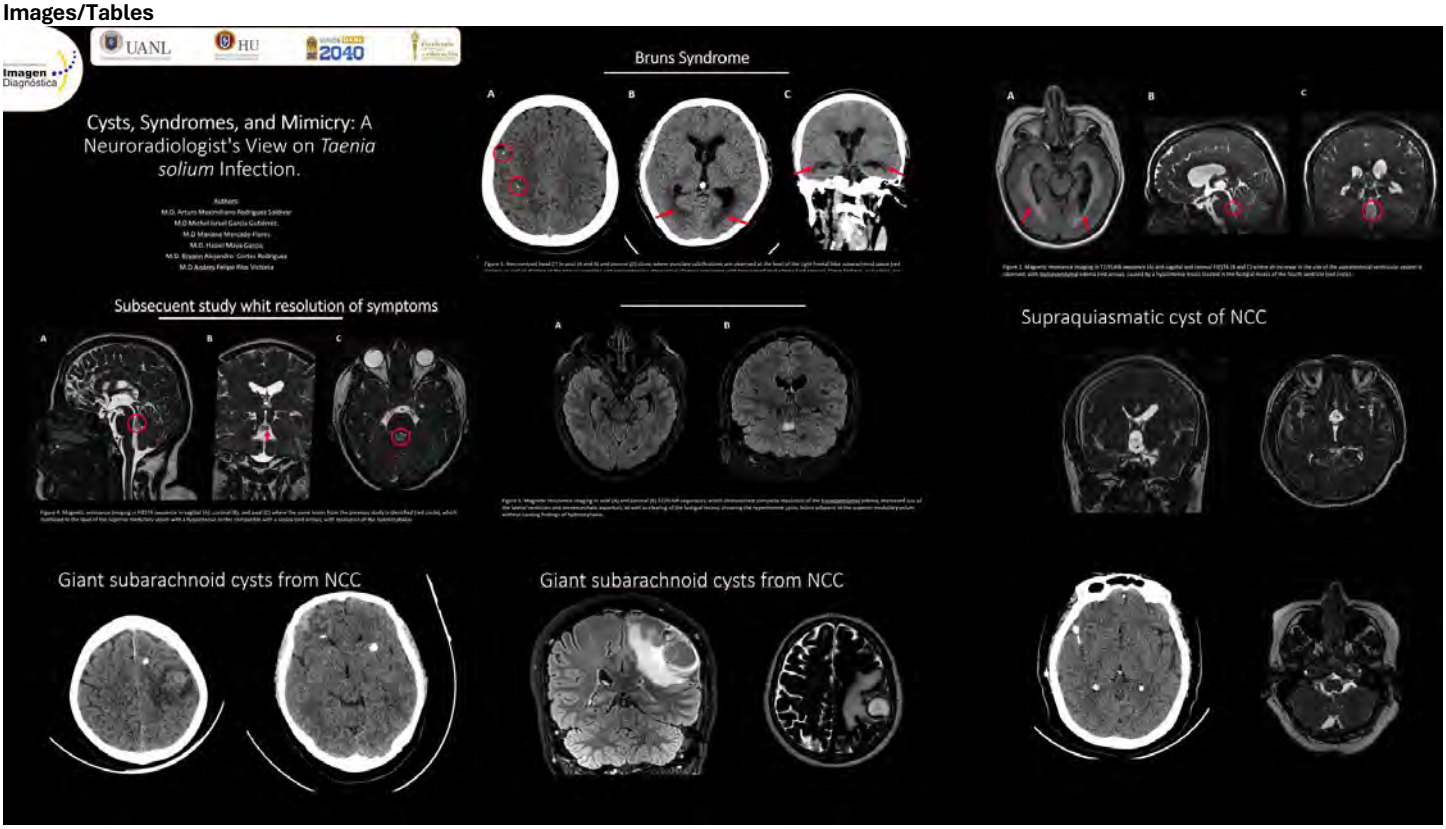

---

760 Spinal Osseous Neoplasms and Mimics

Daniel Kim MD, Ricardo Paez MD, Jamie Yoon MD, Talha Shabbir MD, Sarah Ceglar
Harbor-UCLA Medical Center, Torrance, California, USA

Summary & Objectives

This educational exhibit aims to review the key imaging characteristics and differentiating clinical features of spinal osseous tumors and their mimics. A broad range of neoplastic and non-neoplastic spinal lesions will be presented including primary osseous neoplasms, metastatic disease, lymphoma, plasmacytoma/multiple myeloma, spinal infections, inflammatory processes, metabolic bone disease, degenerative disease, and post-treatment processes. Because mimics can resemble true neoplasms and potentially lead to unnecessary or invasive interventions, recognizing characteristic imaging patterns and correlating with clinical history is essential. Similarly, non-neoplastic processes such as infection require early detection and treatment. This overview aims to guide trainees in differentiating spinal osseous neoplasms from their mimics.

Purpose

To present common spinal osseous neoplasms and their mimics to help radiology residents develop a more comprehensive diagnostic approach to spinal osseous lesions.

Materials & Methods

Representative CT and MRI images were selected from our institutional PACS to illustrate examples of spinal osseous neoplasms and their mimics. These images were de-identified and labeled with corresponding diagnosis and key imaging features. Representative images from peer-reviewed literature sources were also used, where not available on our institutional PACS.

Results & Conclusion

This case series aims to help radiology residents familiarize themselves with common spinal osseous neoplasms and their mimics in order to make systematic and accurate diagnoses and generate clinically meaningful reports. Representative images include:

A) Osseous involvement by lymphoma. Sagittal post-contrast T1 image of the lumbar spine demonstrates an enhancing lesion at L4. Sagittal CT image of the same patient demonstrates an “ivory vertebra” appearance of a thoracic vertebra.

B) Pyogenic discitis/osteomyelitis. Sagittal T1-weighted and post-contrast T1 images demonstrate destructive changes of the L2–L3 endplates and intervertebral disc space with enhancement.

C) Bone marrow necrosis following treatment of breast cancer. Sagittal post-contrast T1-weighted and STIR images show diffuse, curvilinear STIR hyperintense and enhancing lesions throughout the lumbar spine.

D) Disseminated coccidiomycosis. Sagittal T1 post contrast MRI demonstrates multiple enhancing osseous lesions throughout the spine.

Images/Tables

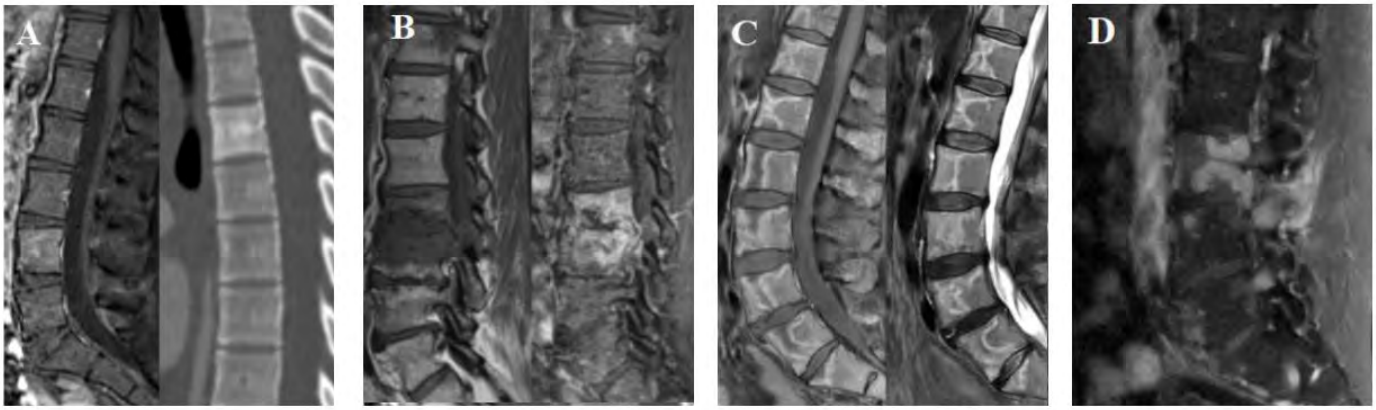

777 Radiographical Features of Adult Sarcomas: Differentiating between Benign from Malignant Paraspinal Masses.

Fatemeh Dehghani Firouzabadi MD[1], Collin Ploeger MD[1], Caroline Ploeger MD[2], Jordan Stafford MD[2], Ramin Hamidi DO, MSc, MBA[2]
[1]University of Louisville, Louisville, kentucky, USA. [2]University of Louisville, Louisville, Kentucky, USA

Summary & Objectives

Adult paraspinal masses represent a diverse group of pathologies that can arise from soft tissue, osseous, neural, or vascular structures adjacent to the spine. Accurate differentiation between benign and malignant paraspinal masses is essential for appropriate management. Moreover, imaging findings of benign and aggressive lesions can overlap.

Purpose

This educational exhibit focuses on the key CT and MRI features that distinguish benign from malignant lesions.

Materials & Methods

This educational exhibit compiles and analyzes representative imaging cases of adult paraspinal masses, focusing on CT and MRI features that differentiate benign from malignant lesions. Comparative analysis emphasized lesion morphology, signal and enhancement patterns, tissue composition (from path proven biopsies), and relationship to adjacent structures.

Results & Conclusion

MRI emerged as the most informative modality for characterizing paraspinal lesions, offering superior soft-tissue contrast and detailed assessment of neurovascular and fascial involvement. Malignant sarcomas, including liposarcoma, rhabdomyosarcoma, and Ewing sarcoma, commonly presented as large, heterogeneous masses with irregular margins, central necrosis, thick or nodular enhancing septa, and diffusion restriction. Evidence of fascial disruption as well as muscular or osseous invasion, further support malignancy (Figure 1A-C).

Conversely, benign lesions such as lipomas or schwannomas demonstrated smooth, well-defined borders, homogeneous internal signal, thin non-enhancing septa (<2 mm), and lack of invasion into adjacent tissues (Figure 1D). CT provided complementary information regarding calcifications and fat composition, while ultrasound aided in assessing vascularity and cystic change.

Recognition of these imaging hallmarks, particularly margin irregularity, internal heterogeneity, and infiltrative behavior, enhances the ability to distinguish malignant sarcomas from benign paraspinal masses noninvasively. Such pattern recognition supports accurate diagnosis, identifying target sites for biopsy, thereby facilitating multidisciplinary management.

Understanding the imaging spectrum of adult sarcomas across modalities, including CT, MRI, and ultrasound, is essential for accurate diagnosis of sarcoma. Recognizing key imaging characteristics can help distinguish benign from malignant lesions, guide biopsy decisions, and optimize patient management.

Images/Tables

A. Contrast-enhanced axial CT reconstruction shows an intramuscular lipomatous tumor invading both the hypaxial and epaxial muscles. The lesion demonstrates areas of fat attenuation (white stars) and soft-tissue nodularity, consistent with malignant lipomatous neoplasm.
B. Axial T1-weighted MRI shows a bilobed lipomatous mass extending across the epaxial and hypaxial compartments (yellow stars) with irregular margins and heterogeneous internal signal.
C. Contrast-enhanced fat-saturated T1-weighted MRI[1] demonstrates a paraspinal liposarcoma invading the epaxial and hypaxial musculature with heterogeneous and thickened areas of enhancement (arrows), characteristic of malignant transformation. Fat content (white stars) presents high signal on T1WI and saturates on fat-saturated T1WI.
D. Contrast-enhanced fat-saturated T1-weighted MRI[1] shows an intramuscular lipoma within the erector spinae muscle, exhibiting homogeneous fat signal intensity, thin non-enhancing septa (< 2 mm), and smooth encapsulated margins, consistent with a benign lesion.

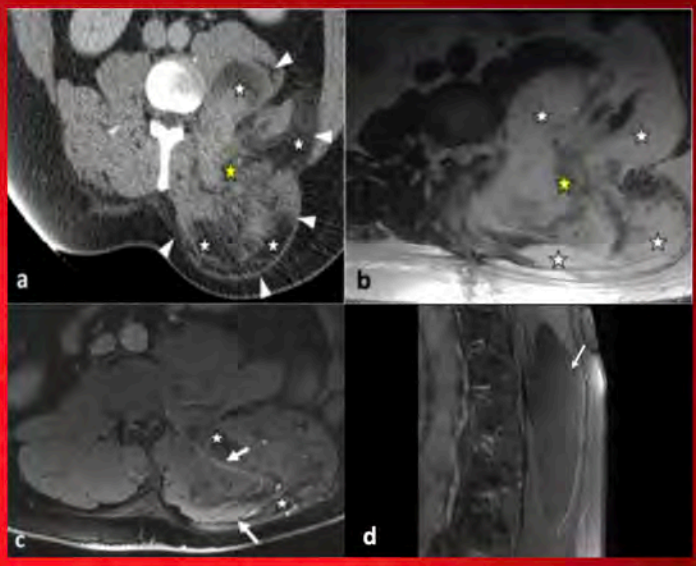

---

779 Blink and You'll Miss It: Subtle Findings in STAT Neuroradiology

Kristian Quevada MD[1], Daniel H Chen MD[1], Grace Ewing DO[1], Christian Fang[2], Amjad Murdos MD[1], Nathan Law MD[1], Khuram Kazmi MD[1]
[1]Cooper University Healthcare, Camden, New Jersey, USA. [2]Rowan-Virtua SOM | School of Osteopathic Medicine, Stratford, New Jersey, United Kingdom

Summary & Objectives

Diagnostic radiology residents traditionally serve as the backbone of preliminary neuroimaging interpretation for urgent and emergent studies performed after hours and on weekends.[1,2] Although overall accuracy is high, a small but meaningful discrepancy rate exists when compared with final attending reports, particularly among junior residents.[2,3] This educational exhibit presents a curated collection of challenging STAT emergency and inpatient neuroradiology cases that highlight subtle findings, some of which were initially overlooked in the high-pressure, real-time clinical environment. Emphasis is placed on key imaging features of Computed Tomography (CT) and Computed Tomography Angiography (CTA) with Magnetic Resonance Imaging (MRI) correlation where applicable.

Objectives

- To illustrate subtle presentations of high-stakes pathologies (e.g., ischemic stroke, fracture, hemorrhage) frequently encountered in emergency and inpatient neuroradiology.
- To provide practical teaching pearls and visual cues that may be helpful for trainees in recognizing these subtle findings with greater confidence.
- To raise awareness of perceptual and cognitive factors contributing to diagnostic misses in the fast-paced on-call environment and promote deliberate search patterns and ultimately reduce diagnostic misinterpretation especially amongst trainees.

Purpose

To demonstrate subtle neuroradiology findings on challenging cases that diagnostic radiology residents, particularly those early in training, may overlook. The exhibit provides targeted educational insights to reduce such errors by highlighting easily missed yet clinically significant findings. Through these examples, we aim to enhance awareness, reinforce systematic search patterns, and promote meticulous attention to subtle imaging cues during neuroimaging interpretation, especially in the high-pressure on-call environment.

Materials & Methods

Cases were retrospectively compiled from the PACS archives of a tertiary academic medical center utilizing a third party database search tool (Nuance mPower). Subsequent curation was performed by three diagnostic radiology residents. Additional cases were contributed by residents from personally maintained collections of prior missed cases. Search criteria was modified via inclusion of final reports with the term 'subtle' and restriction of modality to CT and CTA in the regions of the head, neck, cervical spine, facial bones, and temporal bones. These cases spanned a variety of pathologies including but not limited to traumatic, ischemic, and neoplastic lesions of the brain, cervical spine, and head and neck. Each case was final-signed by a board-certified neuroradiologist.

Results & Conclusion

Fifteen cases were selected following detailed review and consensus. Each case includes annotated images highlighting low-conspicuity findings and corresponding final interpretations by attending neuroradiologists. The final exhibit will display de novo, unedited key images prior to annotation, allowing viewers to challenge their interpretive skills before the findings are unveiled.

This educational exhibit provided an immersive case-based learning experience that highlights subtle findings easily overlooked in neuroradiology, especially in the high pressure setting of on-call interpretation. The exhibit aims to equip trainees with practical tips and strategies to recognize nuanced imaging features and refine their own image review techniques. Reinforcing these principles during residency training can enhance diagnostic accuracy, improve patient outcomes, and promote a culture of continuous learning in the field of neuroradiology.

Images/Tables

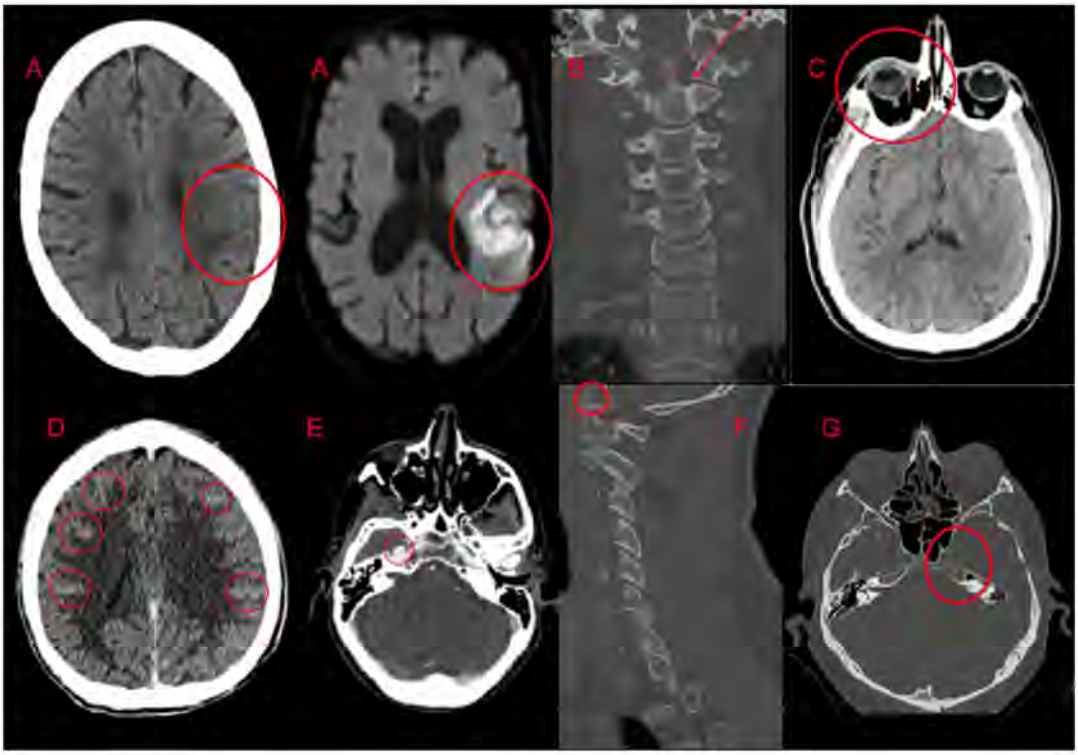

A. Axial CT head shows a subtle wedge-shaped hypodense lesion in the left parietal-temporal region with subtle adjacent sulcal effacement suspicious for acute nonhemorrhagic infarct. Follow-up axial diffusion weighted MRI demonstrates curvilinear restricted diffusion of the area in question, confirming infarct. *Subtle asymmetries such as sulcal effacement may be the only clue to an acute infarct.*
B. Coronal CT cervical spine reveals incomplete acute traumatic type II dens fracture. *Dens fractures are not always complete. This fracture was present on two 2 mm slices; scroll slowly if the study does not provide 0.5 mm slices.*
C. Axial CT head shows right globe crescentic hyperdensity, which on initial review appeared similar to slightly less dense attenuation attributable to volume averaging artifact in the contralateral globe. Follow up fundoscopy confirmed retinal detachment. *Attenuation within the globes should always be carefully considered.*
D. CT head demonstrates tiny multifocal sulcal hyperdensities, suggesting subarachnoid hemorrhage. *Similar findings can be seen in a normal study but tend to be even smaller and more diffuse.*
E. Axial CTA head and neck reveals saccular aneurysm of the right petrous segment internal carotid artery, a rare location for this pathology. *Sagittal imaging (not pictured) was crucial in confirming the finding and is often the optimal initial plane for examining the internal carotid artery.*
F. Axial CT cervical demonstrates an "edge of the film" acute mildly displaced traumatic fracture of the medial left occipital condyle. *The atlanto-occipital joint should be included in one's search pattern.*
G. Maximum intensity projection reformatted axial CT head demonstrates a lytic metastasis of the left petrous apex in a patient with known breast cancer. *Careful side-to-side comparison and meticulous evaluation of not only the cranium but also the skull base on bone windows should be performed, particularly in patients with a history of malignancy known to metastasize to bone.*

892 Quantifying the Invisible: Practical Approaches to Quantify Amyloid Burden Measurement to Guide Clinical Management

Divya Yadav MD[1], Jana Ivanidze[2], John Arrington[1], Robert Gatenby[1]
[1]Moffitt Cancer Center, Tampa, FL, USA. [2]Weill Cornell Medicine, New York, NY, USA

Summary & Objectives

1. Describe the common signs and findings in amyloid PET imaging.
2. Understand different quantitative amyloid assessment methods, and their respective strengths and limitations.
3. Compare qualitative and quantitative amyloid assessment methods, in clinical and research contexts.
4. Integrate amyloid quantification into precision imaging workflows and structured reporting.

Purpose

Amyloid imaging has revolutionized the diagnosis and management of Alzheimer's disease. While qualitative visual reads remain the clinical standard, quantitative approaches—such as standardized uptake value ratios (SUVR), Z-score, and Centiloid scaling—enable objective, reproducible assessment of amyloid burden. This exhibit aims to decipher amyloid quantification techniques, highlight their clinical relevance, and provide practical guidance for implementation in routine neuroimaging workflows.

Materials & Methods

Amyloid PET avidity in cortical gray matter is compared visually with adjacent white matter on PET only images in lateral temporal, frontal, parietal convexities and precuneus. Cerebellum is considered as reference for gray-white differentiation. Amyloid negative images show white matter tracts clearly outlined without any uptake in the cortical gray matter akin to a tree in winter. The described signs in axial and coronal views include a "cartoon hand" in frontal region, "ridge" in the temporal-occipital region, a "diamond" sign in the frontal inter-hemispheric fissure, and a "double convex lens" sign in the parietal region. In contrast, Amyloid positive images show radiotracer uptake throughout the gray matter similar to tree in the summer. The loss of grey-white contrast creates imaging signs such as transitioning into a "plain" surface (temporal-occipital), "kissing hemispheres" appearance (medial occipital, inter-hemispheric fissure).

In addition to visual reads, quantification and three-dimensional visualization can aid in indeterminate cases. These quantification methods enable objective reproducible assessment of amyloid burden across tracers, sites, and time points in clinical and research setting. Centiloid scale quantified by a Centiloid unit (CL) on a 0-100 scale, provides a singular standardized value estimating for the global cortical amyloid load. CL values are scaled to be used across different amyloid PET tracers, offering the potential multi-center comparison of PET results. It can also help in assessing the risk and severity of disease as well as therapeutic response assessment. SUVR and Z-scores comparison to normative database can provide more granular details across specified cortical regions. While the CL provides global threshold value averaged over all cortical regions, the regional Z-scores are more sensitive to subtle changes in regional Aβ burden. Several studies have shown concordance between visual reads and quantification methods.

Results & Conclusion

Implementing a standardized workflow for amyloid PET—integrating both visual interpretation and quantitative metrics such as SUVR and Centiloid scaling—enhances diagnostic consistency, reproducibility, and communication across institutions. Structured reporting templates that incorporate quantitative results alongside qualitative impressions provide a clear, objective framework for longitudinal assessment and therapy monitoring. Standardization not only supports clinical decision-making in the era of disease-modifying treatments but also strengthens the bridge between research and routine patient care.

Images/Tables

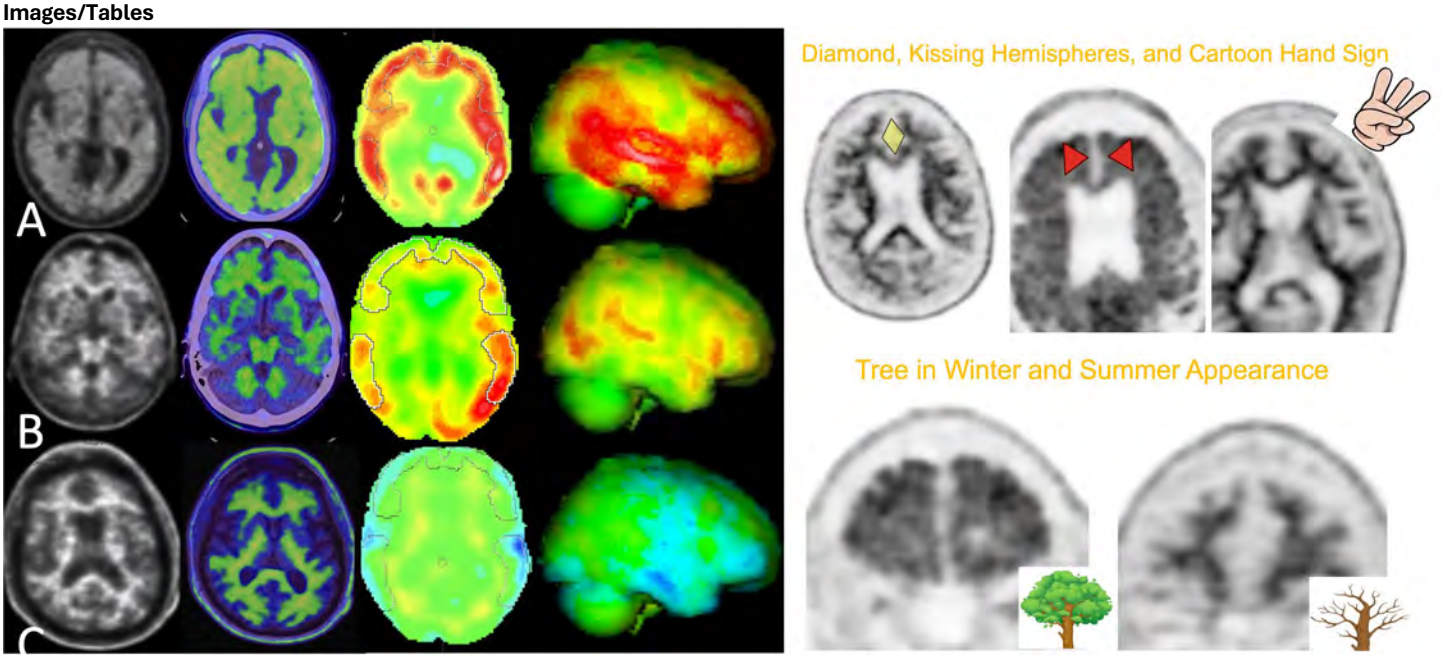

907 The Synaptic Frontier: How SV2A PET is Revolutionizing the Assessment of Neurodegeneration

Michelle Chen MD[1], Faizullah Mashriqi MD[2], Graham Keir MD[3], Ana M. Franceschi MD, PhD[1]
[1]Donald and Barbara Zucker School of Medicine at Hofstra/Northwell, New York, NY, USA. [2]New York University School of Medicine, New York, NY, USA. [3]Piedmont South Imaging, Atlanta, GA, USA

Summary & Objectives

Neurodegenerative diseases present a critical diagnostic challenge, as irreversible pathology often precedes clinical symptoms and detection by conventional imaging. A crucial unmet need exists for biomarkers that capture the earliest stages of neuronal network failure. Synaptic vesicle

glycoprotein 2A (SV2A) PET imaging has emerged as a revolutionary solution, offering non-invasive, quantitative assessment of synaptic density in the living human brain.

This technique utilizes highly selective radiotracers, such as ^{11}C-UCB-J and ^{18}F-SynVesT-1, that bind to SV2A, a protein ubiquitously expressed in presynaptic terminals. This provides a direct, quantifiable measure of synaptic integrity. Unlike traditional biomarkers targeting protein aggregates or metabolic decline, SV2A PET detects synaptic loss before the onset of significant structural atrophy or neuronal death. This offers an unprecedented window into the fundamental pathophysiology driving clinical disease and provides a powerful tool for early and differential diagnosis.

The objectives of this educational exhibit are to: 1) Elucidate the fundamental principles and technical advantages of SV2A PET; 2) Demonstrate its superior diagnostic and prognostic utility across the spectrum of neurodegenerative disorders; and 3) Highlight its transformative potential as a sensitive endpoint for clinical trials and a cornerstone of precision medicine in neurology.

Purpose

N/a

Materials & Methods

N/a

Results & Conclusion

Extensive research demonstrates the robust utility of SV2A PET across diverse neuropathologies, providing insights that surpass traditional imaging. In Alzheimer's disease, SV2A PET reveals significant synaptic loss in the hippocampus and neocortex, which correlates more strongly with cognitive impairment than amyloid or tau burden alone and notably precedes MRI-detectable atrophy. In Parkinson's disease, it quantifies marked synaptic decline in the substantia nigra and other brainstem nuclei, offering a more comprehensive pathological view than dopaminergic imaging.

The technique provides critical diagnostic differentiation. In Frontotemporal Lobar Degeneration (FTLD), synaptic loss is concentrated in regions such as the prefrontal cortex, correlating with behavioral symptoms. In Progressive Supranuclear Palsy (PSP), rapid synaptic decline in the frontal lobe and caudate provide a powerful biomarker for disease progression. Similar distinct patterns are observed in Dementia with Lewy Bodies (DLB) and Huntington's Disease (HD), tying regional synaptic deficits to specific clinical phenotypes.

In conclusion, SV2A PET represents a paradigm shift. By directly quantifying synaptic integrity, the structural correlate of cognitive function, it bridges the gap between molecular pathology and clinical presentation. It serves as an early, sensitive, and objective biomarker for diagnosing neurodegenerative diseases, tracking their progression, and monitoring response to treatment. Additionally, it is proving indispensable as a primary endpoint in clinical trials for synapto-protective and restorative therapies, accelerating the development of disease-modifying treatments. Large-scale validation studies, such as the Parkinson's Progression Markers Initiative (PPMI), are cementing its role as a premier biomarker. SV2A PET is poised to transform clinical practice, enabling earlier intervention, personalized therapeutic strategies, and a profound impact on patient outcomes.

Images/Tables

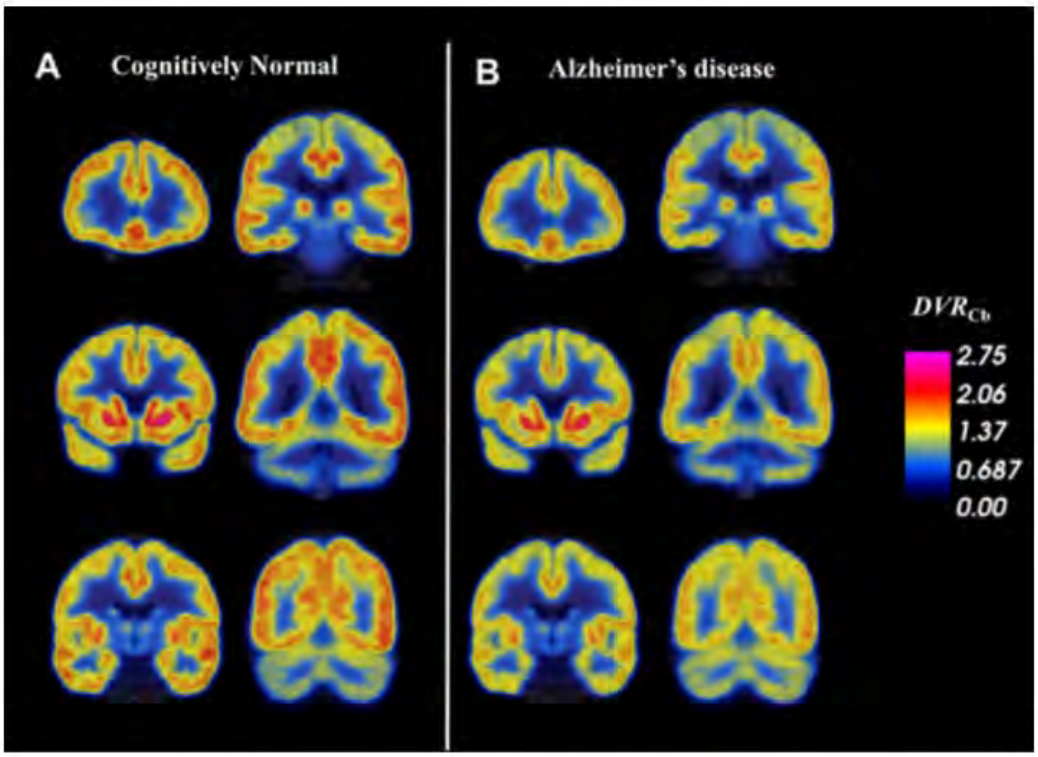

Figure. Synaptic density (DVRCb) in AD and CN groups determined by [^{11}C]UCB-J PET. Coronal sections of average parametric images of DVRCb for (A) 19 CN participants and (B) 34 AD participants. Average images are created after co-registration to a common MNI template. The average parametric PET scans are displayed in pseudo-color representing [^{11}C]UCB-J binding to SV2A (DVRCb) and overlaid on the MNI template T1 MRI. Lower DVRCb in AD compared to CN participants was apparent in the medial temporal lobe and throughout the cortex and subcortex. Image courtesy of Mecca et al, 2020.

1052 Quantitative and qualitative MRI features of cerebral toxoplasmosis: A comprehensive review.

Bryann A Cortés Rodríguez MD, Mariana Mercado Flores MD, Haziel Maya García MD, Lorena Martínez Olvera MD, Andrés F Ríos Victoria MD, Arturo M Rodríguez Saldivar MD
Hospital Universitario Dr. José Eleuterio Gonzalez, Monterrey, Nuevo León, Mexico

Summary & Objectives

Cerebral toxoplasmosis remains one of the major causes of focal brain lesions in immunocompromised patients, including those with advanced HIV infection. MRI is the imaging modality of choice, yet its findings can mimic or overlap with other opportunistic infections, or with brain tumors like primary CNS lymphoma. New techniques such as perfusion, diffusion and spectroscopy can improve diagnostic accuracy with hemodynamic and structural patterns. The main objective of this presentation is to review son of the typical and atypical imaging features of CNS toxoplasmosis and highlight the importance of perfusion imaging in differentiating from other intracranial pathologies.

Purpose

To illustrate some of the characteristic MRI findings of CNS toxoplasmosis across multiple scenarios and cases, emphasizing the role of advanced techniques such as brain perfusion and spectroscopy (MRS) in distinguishing it from the most common differential diagnosis such as CNS lymphoma and other opportunistic infections. The main goal is to provide radiologist with some practical diagnostic clues and some perfusion/spectroscopy-based thresholds that may support and give confidence in the noninvasive diagnosis of toxoplasmosis.

Materials & Methods

We reviewed MRI studies in retrospective of patients with HIV diagnosis with confirmed cerebral toxoplasmosis. Conventional MRI sequences such as T1, T2, FLAIR and DWI, and advanced techniques like DSC brain perfusion and MR spectroscopy were analyzed. Perfusion parameters like relative cerebral blood volume (rCBV) were quantitatively measured in ring enhancing lesions and compared with contralateral healthy white matter; some of these lesions have been postprocessed with a leakage correction pipeline. Some of the characteristic patterns of toxoplasmosis such as the “eccentric target sign”, “concentric target sign”, and ring enhancement appearance were correlated with perfusion findings and some clinical data.

Results & Conclusion

Some of the typical findings included multiple and aleatory ring-enhancing lesions with vasogenic edema, located in basal ganglia and corticomedullary junction. Perfusion analysis demonstrated in some cases hyperperfusion pattern (rCBV < 1.5 compared to contralateral white matter), contrasting with the hyperperfusion pattern observed in neurotoxoplasmosis (rCBV >1.5). Spectroscopy revealed elevated lipid and lactate peaks, with decreased choline and NAA, which is observed in brain infections. In conclusion, combining conventional MRI with advanced techniques helps and enhances diagnostic specificity for CNS toxoplasmosis, giving confidence in differentiating from mimics and guiding therapy in immunocompromised patients.

Images/Tables

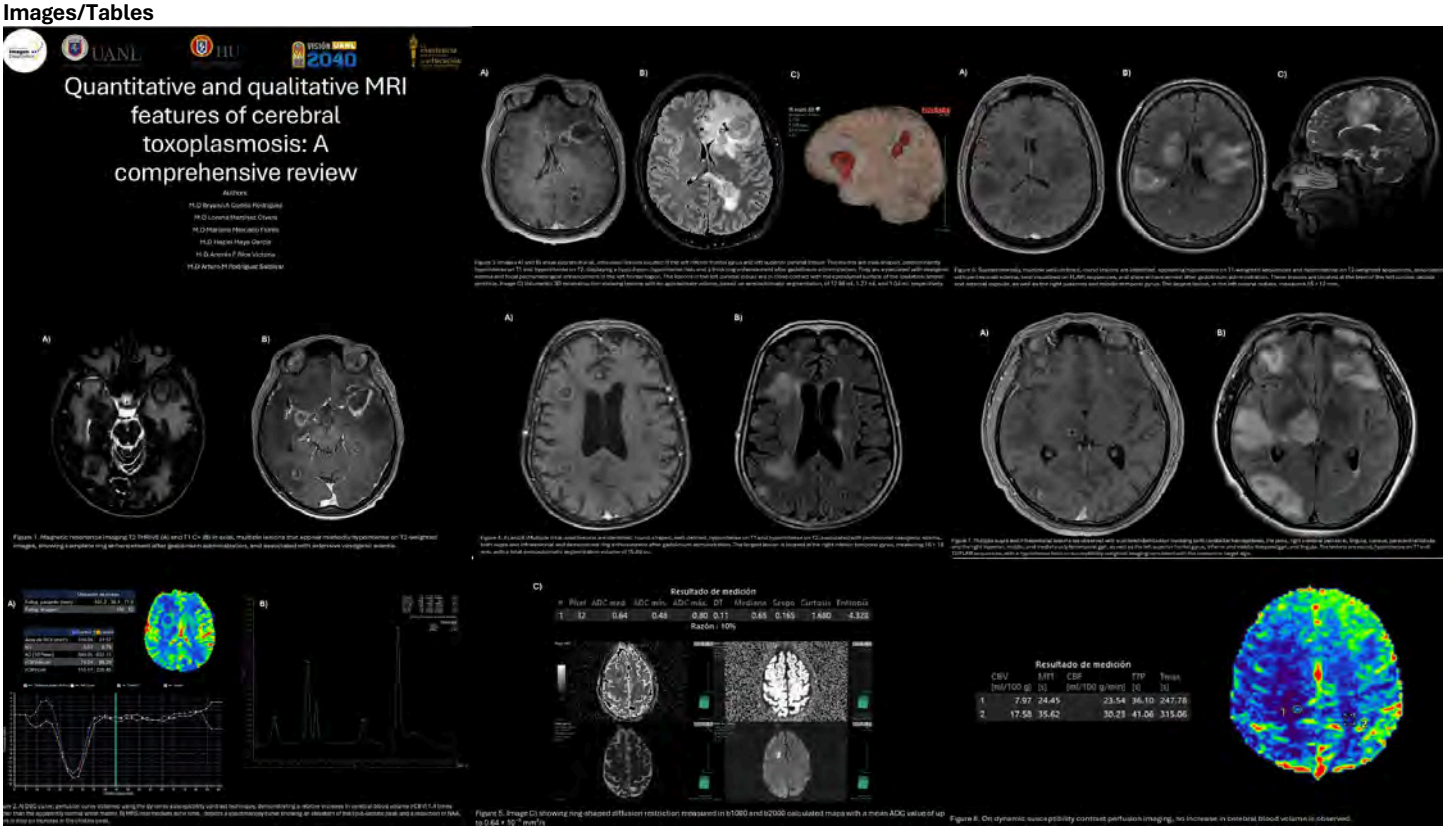

1167 Flow and Motion: A Unified MRI Approach to Chiari I Malformation

Luis T. Ortiz-Figueroa M.D., Susan L. Rebsamen M.D., Justin L. Brucker M.D.
University of Wisconsin School of Medicine and Public Health, Madison, WI, USA

Summary & Objectives

Chiari malformations encompass a spectrum of deformities and malformations that are radiologically defined based on structural criteria. Chiari I malformation is classically defined by caudal displacement of the cerebellar tonsils greater than 3–5 mm below the foramen magnum. However, this structural definition has been questioned, as the degree of tonsillar herniation does not always correlate with symptom severity. Phase-Contrast (PC) MRI and Cine balanced Steady-State Free Precession (bSSFP) sequences have been used to evaluate alterations in cerebrospinal fluid (CSF) flow

dynamics and hyperdynamic motion of the cerebellar tonsils and cervical spinal cord. Despite their growing use, a standardized approach for interpretating PC MRI and Cine bSSFP in Chiari I malformation assessment has yet to be established.

Purpose

The purpose of this educational exhibit is to review the technical aspects of PC MRI and Cine bSSFP, describe the imaging features of Chiari I malformation, and propose a standardized framework for interpreting PC MRI and Cine bSSFP findings in the clinical setting of Chiari I malformation.

Materials & Methods

This exhibit presents case-based reviews demonstrating structural evaluation of Chiari I malformation using sagittal T1- and T2-weighted sequences, and physiologic assessment using PC MRI and Cine bSSFP sequences. We discuss the nuances of altered CSF flow dynamics—such as aliasing and bidirectional flow on PC MRI—and the determinants of hyperdynamic motion of the cerebellar tonsils and cervical spinal cord in Cine bSSFP. Finally, we propose a standardized interpretive approach for PC MRI and Cine bSSFP in the context of Chiari I malformation.

Results & Conclusion

A clearer understanding of PC MRI and Cine bSSFP techniques, together with the structural and physiologic imaging characteristics of Chiari I malformation, may enable the development of a standardized interpretive approach, improving diagnostic consistency and enhancing clinical correlation.

---

231 Comprehensive Overview of Temporal Bone Imaging for the Neuroradiology Trainee

Jamie E Clarke MD, MS, Jay Acharya MD
University of California Los Angeles (UCLA), Los Angeles, CA, USA

Summary & Objectives

Summary & Educational Objectives

The educational objectives of this presentation include (i) reviewing the intricate anatomy of the temporal bone, emphasizing clinically relevant bony, vascular, and neural landmarks, (ii) summarizing the normal variants and common disease processes encountered in temporal bone imaging, and (iii) discussing optimal imaging modalities and protocols for comprehensive temporal bone evaluation with illustrative case examples.

Purpose

Background

The temporal bone, a paired structure at the lateral skull base, plays a critical role in housing the auditory and vestibular apparatus as well as key neurovascular structures. Its complex anatomy and proximity to vital neural and vascular elements make radiologic assessment essential for diagnosing a wide spectrum of pathologies and for surgical planning.

Materials & Methods

Teaching Points

Anatomically, the temporal bone consists of several distinct regions—squamous, mastoid, tympanic, and petrous portions—each with unique radiologic appearances. Key structures include the external auditory canal, ossicles, cochlea, semicircular canals, facial nerve canal, and internal auditory canal. Detailed knowledge of these landmarks is essential for identifying pathology and planning interventions. When imaging the temporal bone, high-resolution CT is the gold standard for evaluating bony anatomy, detecting fractures, ossicular chain disruption, bone erosion from chronic infection or cholesteatoma, and congenital malformations. Ultra-high-resolution and photon-counting detector CT further enhance visualization of minute structures, crucial for surgical mapping. MRI offers superior soft tissue contrast, enabling assessment of the membranous labyrinth, cranial nerves VII and VIII, and the cerebellopontine angle. Heavily T2-weighted sequences are particularly valuable for evaluating fluid-filled spaces, nerve pathology, and distinguishing neoplasms such as vestibular schwannomas or glomus tumors. Clinically, imaging is indicated for unexplained hearing loss, chronic ear infections, congenital anomalies, facial nerve pathology, trauma, and preoperative planning. CT excels in identifying chronic otomastoiditis, cholesteatoma, and complications such as bone erosion. MRI is preferred for soft tissue lesions and nerve involvement. Both modalities are indispensable for surgical planning, including cochlear implantation and tumor resection. Furthermore, postoperative assessment of cochlear implants and other otologic hardware is a growing area of neuroradiology. Imaging modalities, including CT and cone-beam CT, are used to evaluate device position, electrode placement, and complications such as migration, misplacement, magnet dislocation, and infection. Accurate imaging interpretation directly impacts patient outcomes by guiding timely management of hardware-related issues.

Results & Conclusion

Conclusion

A thorough understanding of temporal bone anatomy and pathology, combined with appropriate imaging technique selection, is vital for accurate diagnosis and effective treatment planning. This exhibit provides a comprehensive overview for neuroradiologists and trainees, illustrated with multimodality case examples to enhance diagnostic confidence and clinical decision-making.

---

371 Imaging Patterns of Central Nervous System Histiocytic Diseases

Shreyas Reddy Kankara[1], Sabha Ahmed[2], Shravan Reddy K[3], Ankit Arora[2], Unnathi Nayak[3]
[1]BrainSightAI, Bengaluru, Karnataka, India. [2]National Institute of Mental Health and Neuro Sciences, Bengaluru, Karnataka, India. [3]St John's Medical College Hospital, Bengaluru, Karnataka, India

Summary & Objectives

The histiocytoses are a rare, heterogeneous group of disorders defined by pathologic proliferation of macrophages and dendritic-lineage cells within tissues. They produce a wide and sometimes overlapping spectrum of central nervous system (CNS) and head-and-neck manifestations that may mimic infectious, inflammatory, or neoplastic processes. They can be classified into five groups: a) Langerhans-related histiocytosis, b) Rosai-Dorfman histiocytosis, c) cutaneous and mucocutaneous histiocytosis, d) malignant histiocytosis, and e) hemophagocytic lymphohistiocytosis and macrophage activation syndrome.

This exhibit provides a comprehensive, imaging-focused review of CNS and head & neck histiocytic diseases to improve radiologic recognition and guide targeted diagnostic workup.

Objectives

• To summarize the characteristic neuroimaging appearances of major histiocytic disorders involving the CNS.
• To highlight distinguishing features and common mimics that contribute to diagnostic pitfalls.

Purpose

Histiocytic disorders, notably Langerhans cell histiocytosis [LCH], Erdheim–Chester disease [ECD], Rosai–Dorfman disease [RDD], and Hemophagocytic lymphohistiocytosis [HLH]) can involve any compartment of the neuraxis, producing granulomatous, infiltrative, mass-forming, or neurodegenerative patterns. Accurate radiologic characterisation of lesion distribution, signal characteristics, enhancement pattern, associated bone or systemic findings, and evolution on follow-up aids early suspicion, directs targeted sampling, and prioritises genetic testing. This abstract aims to demonstrate the imaging hallmarks across these entities and to propose a concise framework for differential diagnosis.

Materials & Methods

A retrospective pictorial review of confirmed histiocytic disorder cases evaluated at a tertiary neuroimaging referral center was performed. The series included cases of:

- Langerhans cell histiocytosis (LCH) - Hypothalamo-pituitary involvement, parenchymal abnormalities, dural masses, skull lesions and neurodegenerative changes
- Erdheim–Chester disease (ECD) - It may involve the hypothalamo-pituitary axis, parenchyma, meninges, skull bones, orbits, sinuses, and vessels.
- Rosai–Dorfman disease (RDD) - Usually present as dural-based, homogeneously enhancing masses that can mimic meningiomas. Parenchymal, leptomeningeal, and sellar/suprasellar involvement may also occur but are less common. Cervical lymphadenopathy may be the presenting feature.
- Hemophagocytic lymphohistiocytosis (HLH) - It may present as diffuse cerebral and cerebellar atrophy, diffuse white matter changes, enhancing parenchymal lesions, cerebellitis, cerebral hemorrhage, infarcts, cranial nerve involvement.

Results & Conclusion

CNS histiocytic disorders produce a recognisable yet heterogeneous array of imaging patterns that mirror their inflammatory, infiltrative, or neurodegenerative biology. Awareness of their imaging appearances and a high index of suspicion enables the radiologist to raise the possibility of a histiocytic process. This prompt suggestion directs targeted immunohistochemical and molecular workup by pathology, shortens the diagnostic pathway, and facilitates earlier, disease-specific treatment within a coordinated multidisciplinary team.

Images/Tables

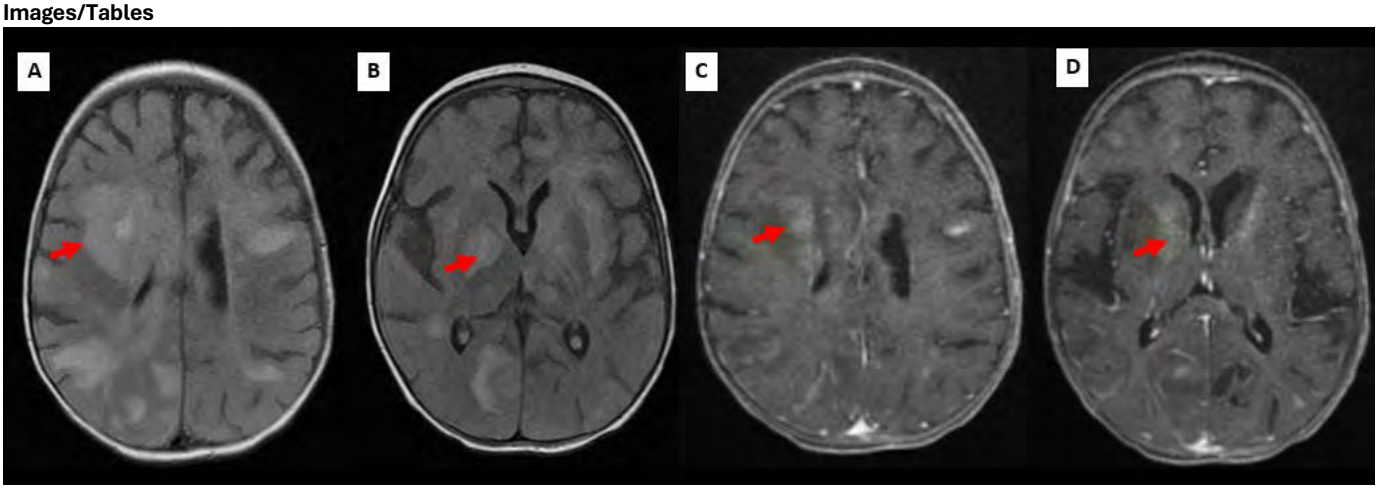

---

452 Cystic Lesions of the Spine: Imaging Spectrum and Diagnostic Approach

Ahmed Abdelmonem MD
UAMS, Little Rock, Arkansas, USA

Summary & Objectives

Cystic spinal lesions represent a diverse group of pathologies that include developmental, degenerative, infectious, and neoplastic entities. Because many of these lesions share overlapping imaging features, accurate characterization relies on a structured approach.

Objectives: To review the imaging characteristics of common cystic spinal lesions on MRI, provide a practical diagnostic algorithm based on location and signal pattern, and discuss key differentiating features and pitfalls.

Purpose

To develop a comprehensive, image-based educational review that enhances recognition and interpretation of cystic lesions within the spinal canal and vertebral column, facilitating accurate differential diagnosis and clinical decision-making.

Materials & Methods

Representative MRI and CT cases were collected from institutional teaching archives, encompassing the full spectrum of cystic spinal lesions:

- **Developmental:** Arachnoid cyst, neurenteric cyst, dermoid/epidermoid cysts.
- **Degenerative:** Synovial and ganglion cysts.
- **Infectious/Inflammatory:** Epidural abscess, cystic tuberculous spondylitis.
- **Neoplastic:** Cystic ependymoma, cystic schwannoma, cystic metastasis.
  Each case was analyzed for lesion location (intradural–extramedullary, intramedullary, extradural), morphology, signal characteristics, enhancement pattern, and associated spinal cord changes. Illustrative figures and diagrams were created to emphasize distinguishing imaging features.

Results & Conclusion
Characteristic imaging appearances and distribution patterns were identified for each lesion type.

- **Arachnoid cysts:** CSF-isointense lesions without enhancement, causing smooth cord displacement.
- **Synovial cysts:** Extradural lesions adjacent to facet joints with variable T1 hyperintensity and peripheral enhancement.
- **Neurenteric cysts:** Ventral to cord, showing T1 hyperintensity from proteinaceous content.
- **Cystic schwannomas:** Well-circumscribed, enhancing mural nodules within an intradural–extramedullary cystic component.
  Common diagnostic pitfalls, such as confusing arachnoid cysts with epidermoid cysts or misidentifying cystic ependymomas, are illustrated with teaching examples.
- **Conclusion:**
  A systematic evaluation of cystic spinal lesions based on **anatomic compartment, signal intensity, and enhancement pattern** allows accurate classification and differentiation among entities. Familiarity with characteristic imaging findings and diagnostic pitfalls improves radiologist confidence and contributes to optimal patient management.

---

455 Imaging of Brain Metastases: Updates on Standard Approaches, Challenges, and Novel Methods
Silvia Arora MD, Raymond Huang MD, PhD
Brigham and Women's Hospital, Boston, MA, USA
Summary & Objectives
Brain metastases are associated with significant morbidity and mortality. An accurate diagnosis of the size and number of metastases is important for determining the best treatment plan for the patient. Earlier detection of brain metastases, and at smaller sizes, also improves patient outcomes. Multiple new and emerging imaging techniques are now available to improve detection of brain metastases, evaluate their response after therapy and to distinguish recurrent metastases from treatment response. Utilization of these techniques can help guide appropriate management and assessment of post-treatment response.
Objectives:

1. Describe the imaging characteristics of brain metastases and strategies to improve sensitivity of detection on MRI, including advanced MRI techniques such as dynamic susceptibility contrast imaging and diffusion tensor imaging.
2. Highlight techniques that can be used to distinguish recurrent metastases from post-treatment changes, such as radiation necrosis, including treatment response assessment maps, dual phase FDG-PET, and novel PET tracers.
3. Discuss diagnostic challenges and dilemmas that can complicate the interpretation of post-treatment imaging, such as radiation necrosis, the use of alternate MRI contrast agents such as ferumoxytol, and the presence of non-enhancing cystic metastases.
4. Describe advancements in radiomics that have improved lesion detection and classification.
5. Discuss leptomeningeal metastases and strategies to enhance detection on MRI.

Purpose
The purpose of this educational exhibit is to highlight how various imaging techniques including conventional MRI, dual phase FDG-PET, and treatment response assessment maps can be used to detect brain metastases and evaluate for recurrence after treatment in order to guide patient management. Using clinical examples, the exhibit will illustrate the unique application of each imaging technique and describe relevant imaging findings to show how they can contribute to patient care.
Materials & Methods
Not applicable
Results & Conclusion
Not applicable
Images/Tables

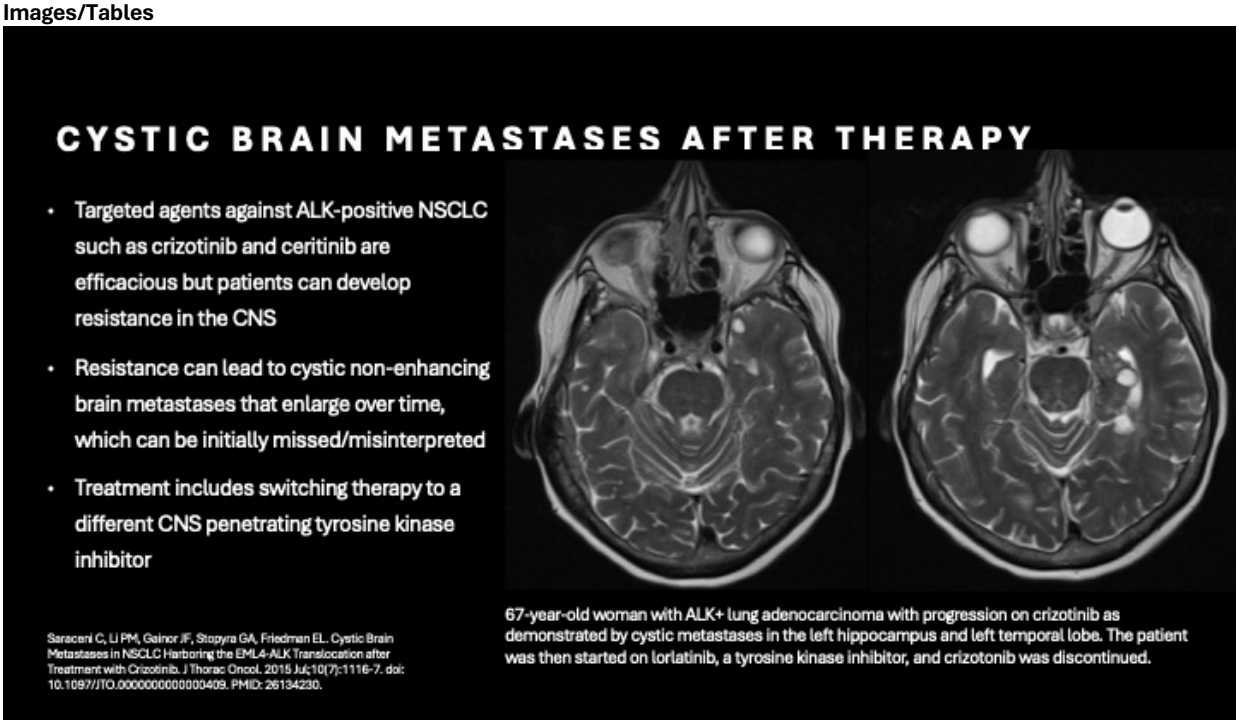

599 Imaging the Spectrum of Hemorrhagic and Acute Vascular Orbital Lesions

Christian Burgos-Sanchez MD[1], Ravi Patel MD[1], Camille Burgos MD[2], Julieta Aristizabal MD[1], Natalya Nagornaya MD[1], Brian C Tse[1], Rita G Bhatia MD[1]
[1]University of Miami Miller School of Medicine, Miami, FL, USA. [2]HCA Aventura Hospital, Miami, FL, USA

Summary & Objectives

Hemorrhagic and vascular orbital lesions encompass a broad spectrum of pathologies that may present with acute or chronic orbital symptoms. Their imaging features often overlap, yet accurate distinction is essential for appropriate management and prognostication. The objective of this educational exhibit is to illustrate the multimodality imaging characteristics, differential considerations, and diagnostic approach to hemorrhagic and vascular orbital lesions, emphasizing key CT and MRI findings that aid confident interpretation.

Purpose

To provide an educational, case-based review of hemorrhagic and vascular orbital lesions, focusing on:
1. The imaging appearance and pathophysiology of hemorrhagic, venous, and arteriovenous orbital lesions.
2. Differentiation between spontaneous, posttraumatic, and secondary hemorrhagic processes.
3. Recognition of vascular entities such as carotid-cavernous fistula, orbital varix, venous thrombosis, and arteriovenous malformations.
4. Common diagnostic pitfalls and structured interpretation strategies.

Materials & Methods

Representative cases were retrospectively reviewed from institutional archives, including patients with confirmed hemorrhagic or vascular orbital lesions. Imaging modalities included contrast-enhanced CT, MRI, MR angiography, and conventional angiography when available. Each case was analyzed for compartmental localization, enhancement pattern, flow characteristics, and associated intracranial findings. Radiologic findings were correlated with clinical and surgical outcomes to highlight diagnostic pearls and pitfalls.

Results & Conclusion

Characteristic imaging patterns were identified across the spectrum of hemorrhagic and vascular orbital pathology:
-Hemorrhagic lesions: Acute hyperdense or T1-hyperintense foci with compartmental mass effect or expansion.
-Venous thrombosis and varices: Dilated, enhancing venous channels with variable flow-related signal loss on MR sequences.
- Carotid-cavernous fistula: Arterialized superior ophthalmic vein, asymmetric cavernous sinus enhancement, and proptosis.
- Vascular malformations: Serpiginous flow voids or enhancing channels reflecting high- versus low-flow dynamics.
Hemorrhagic and vascular orbital lesions present with diverse imaging appearances that require careful multimodality evaluation. Familiarity with their distinguishing features and compartmental anatomy enables accurate diagnosis and guides appropriate management. A systematic, pattern-based approach enhances confidence in differentiating benign from clinically significant vascular and hemorrhagic orbital entities.

Images/Tables

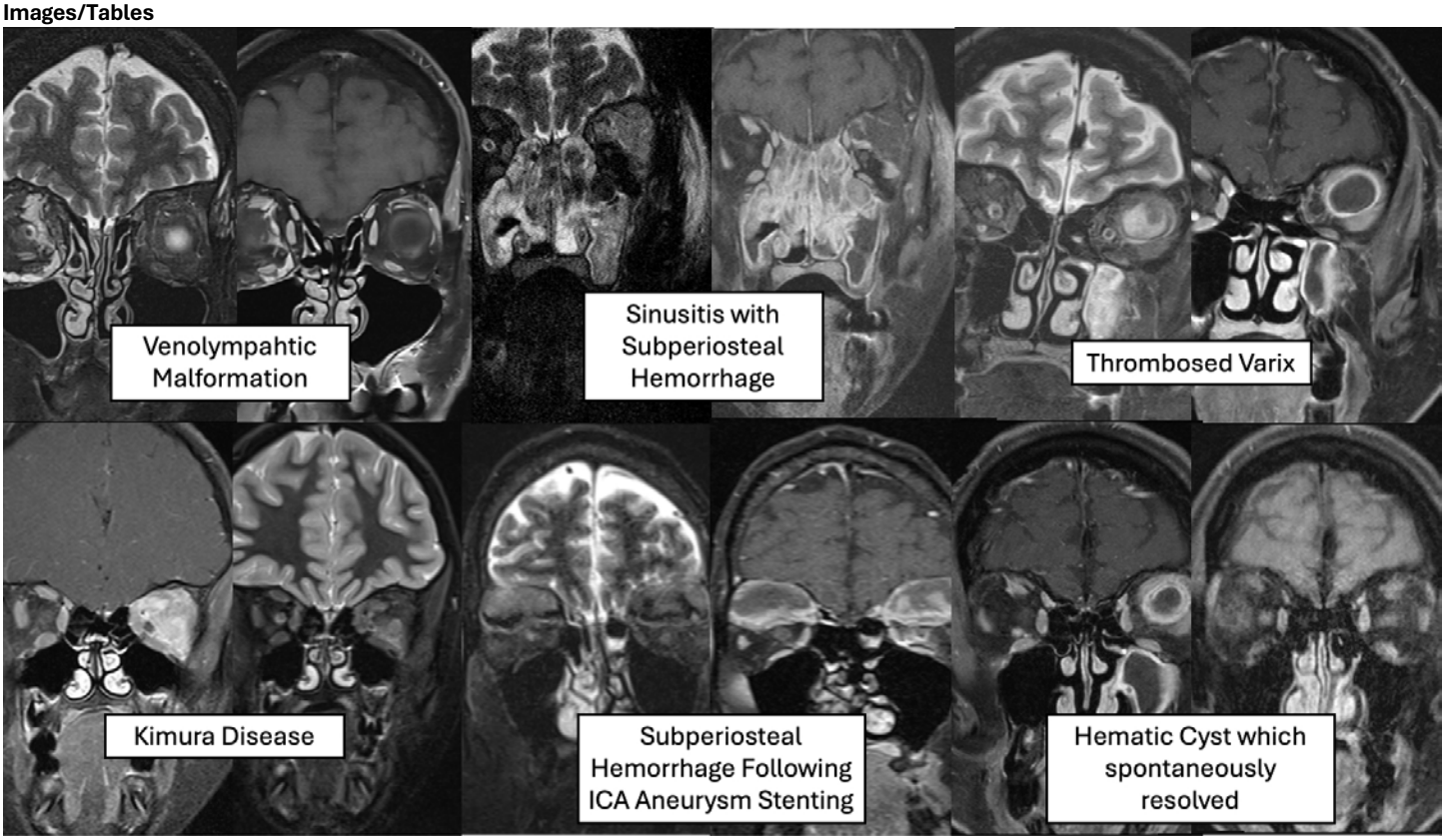

602 When Contrast Crosses Over: A Case Series of Gadolinium Excretion into the Subarachnoid Space

Taylor E Smith MD, MBA, Aline Camargo MD
Emory University, Atlanta, GA, USA

Summary & Objectives

This educational exhibit presents three cases demonstrating hyperintense cerebrospinal fluid (CSF) signal on FLAIR MRI due to gadolinium excretion into the subarachnoid space. These findings, often mistaken for pathology such as subarachnoid hemorrhage or meningitis, underscore the

importance of recognizing post-contrast imaging patterns that mimic disease. Understanding the pathophysiologic mechanisms, imaging characteristics, and clinical context is essential for accurate interpretation and appropriate management.
By the conclusion of this exhibit, participants will be able to:

- **Identify** the MRI characteristics of gadolinium excretion into the subarachnoid space on post-contrast FLAIR imaging.
- **Differentiate** benign gadolinium-related FLAIR hyperintensity from pathologic entities such as subarachnoid hemorrhage, meningitis, or leptomeningeal disease.
- **Explain** the potential mechanisms underlying gadolinium leakage into CSF, including transient blood-brain and blood–CSF barrier disruption.
- **Apply** knowledge of this phenomenon to avoid diagnostic errors and guide multidisciplinary clinical decision-making.

Purpose

To illustrate and educate on the radiologic appearance, diagnostic challenges, and clinical implications of gadolinium excretion into the subarachnoid space (SAS) following contrast administration, with emphasis on recognizing this benign finding to prevent misdiagnosis and unnecessary interventions.

Materials & Methods

A retrospective chart review was conducted over the past year to identify patients who demonstrated abnormal cerebrospinal fluid (CSF) hyperintensity on post-contrast FLAIR MRI sequences. Clinical data, imaging findings, and contrast administration details were reviewed. Cases with confirmed gadolinium excretion into the subarachnoid space were included for analysis, emphasizing radiologic features, clinical presentation, and diagnostic outcomes.

Results & Conclusion

We found cases that demonstrate that gadolinium excretion into the subarachnoid space can closely mimic intracranial pathology on MRI. The most encountered etiologies for hyperintensity of cerebrospinal fluid (CSF) on fluid-attenuated inversion recovery (FLAIR) sequences include hyperoxigenation, subarachnoid hemorrhage, meningitis and leptomeningeal carcinomatosis. In rare cases, it may instead reflect residual contrast agent following recent gadolinium administration. Therefore, recognition of this phenomenon is essential for radiologists to avoid misdiagnosis and unnecessary interventions. The underlying mechanism likely involves transient disruption of the blood–cerebrospinal fluid barrier, altered CSF circulation, or delayed gadolinium clearance, particularly in patients with renal impairment or blood-brain barrier dysfunction.[1,3-6] Although typically benign, the long-term clinical significance of gadolinium deposition in the central nervous system remains uncertain and is the subject of ongoing investigation.
Recognition of gadolinium excretion into the subarachnoid space is vital to prevent diagnostic errors and unnecessary interventions. Radiologists play a pivotal role in differentiating benign contrast-related findings from true pathology. Ongoing research into gadolinium deposition and its potential neurotoxic effects underscores the importance of multidisciplinary awareness and continued vigilance in post-contrast neuroimaging interpretation.

Images/Tables

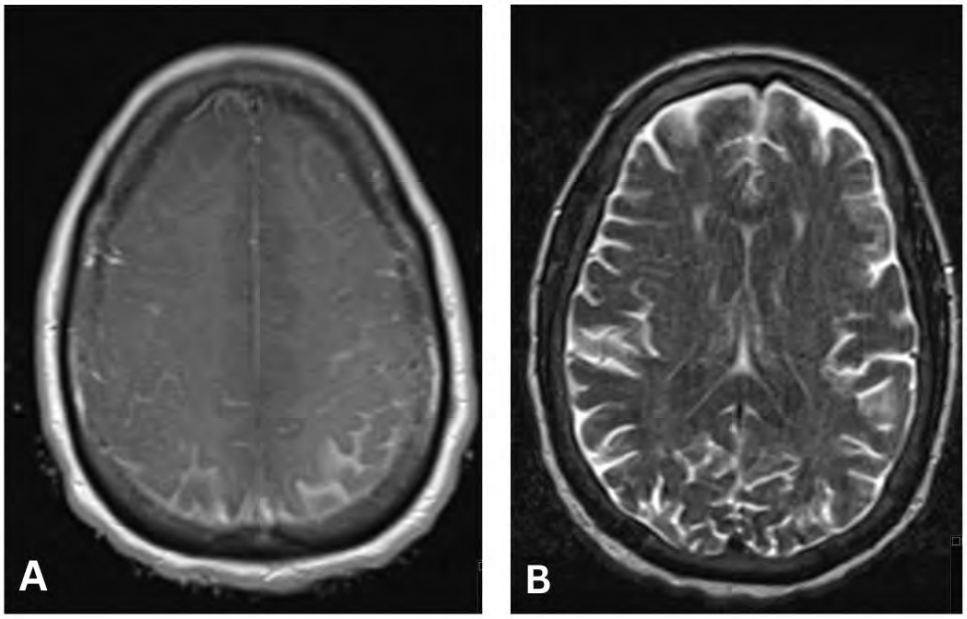

Figure 1. Case of a 58-year-old female with a history of T-spine epidural mass s/p laminectomy and decompression who was admitted for concern for cord edema and dysarthria. A) Axial pre-contrast T1-weighted and B) Axial FLAIR images demonstrate intrinsic T1 hyperintensity involving sulci/subarachnoid spaces with diffuse sulcal CSF FLAIR non-suppression.

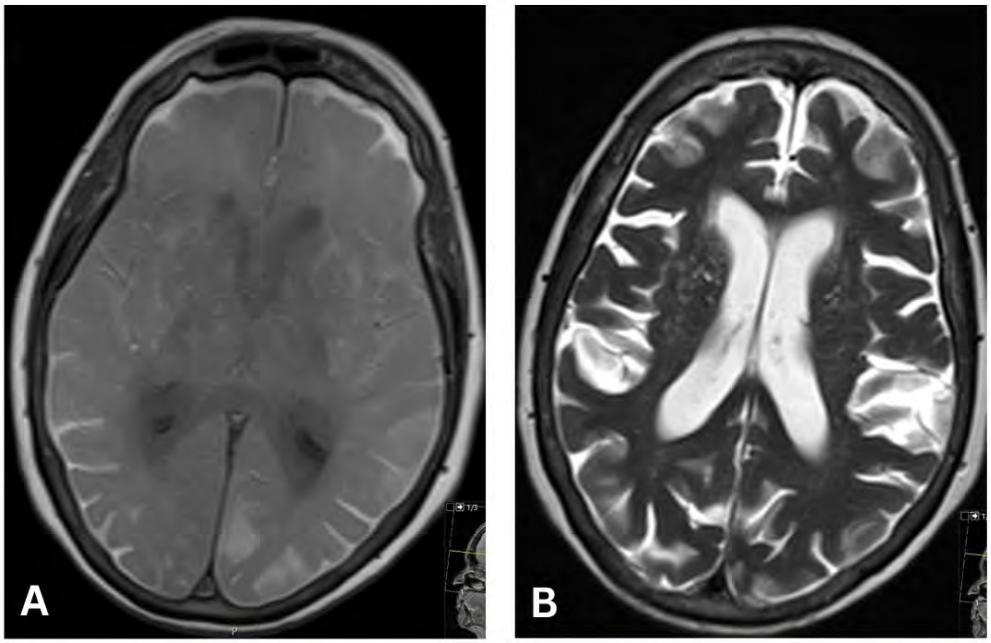

Figure 2. Case of a 86-year-old female who presented after the development of generalized seizures following a cervical epidural steroid injection. A) Axial pre-contrast T1-weighted and B) Axial T2 FLAIR images demonstrate extensive T1 hyperintensity diffusely throughout the extra-axial spaces along both cerebral convexities.

647 Evidence-Based Imaging Pathways for Patients presenting with Headache in the Emergency Department

Ethan Pitney MD[1], Raven Spencer MD[2], Laura Eisenmenger MD[3], WARREN CHANG MD, MBA[2]
[1]Bassett Medical Center, Cooperstown, New York, USA. [2]Allegheny Health Network, Pittsburgh, PA, USA. [3]University of Wisconsin, Madison, WI, USA

Summary & Objectives

Learners will be able to:

1. Distinguish between primary and secondary headache disorders using key history, physical exam findings, and red flag criteria (such as SNOOP10).
2. Apply the ACR Appropriateness Criteria to select optimal neuroimaging modalities for various clinical headache scenarios.
3. Utilize and interpret evidence-based imaging algorithms to guide the initial and subsequent diagnostic approach for different headache types in the ED.
4. Recognize clinical scenarios where lumbar puncture adds diagnostic value for acute headache.

Purpose

Headache is among the most common reasons for emergency department (ED) visits, yet neuroimaging is frequently overused, leading to excess cost and radiation exposure. The diagnosis is challenging because there are many causes of benign headaches that require no additional imaging or follow-up, while secondary causes such as intracranial hemorrhage, neoplasm, aneurysm, or infection can be emergently life threatening.
Current guidelines stress the importance of distinguishing primary headaches from secondary, life-threatening causes by integrating history, examination, and evidence-based imaging pathways. This educational exhibit provides a practical framework for emergency clinicians and radiologists to efficiently triage, evaluate, and manage headache presentations using the latest 2022 ACR Appropriateness Criteria.

Materials & Methods

We conducted a review of the most recent literature as well as the ACR Appropriateness Criteria to identify the most up-to-date guidance on imaging recommendations in the setting of headache.

Results & Conclusion

- Imaging is not routinely indicated for classic primary headaches with normal neurologic exams; reassurance, supportive care and conservative management are emphasized.
- “Thunderclap” headache (worst headache of life) should prompt immediate non-contrast CT; further CTA, MRI/MRV, or lumbar puncture may be warranted if initial imaging is negative yet suspicion for subarachnoid hemorrhage remains high. Clinical and past medical history can be critical, as patients having know aneurysms or vascular malformations should undergo immediate imaging and other factors such as connective tissue disorders, autosomal dominant polycystic kidney disease, or strong family history of aneurysms may warrant further investigation.
- Certain clinical histories, such as positional headaches, may be suggestive of etiology such as intracranial hypotension and may warrant further imaging and/or interventions, while blurred vision and headache in the appropriate patient population may suggest idiopathic intracranial hypotension as a diagnosis with fundoscopic examination as a potential next step in management.
- Specific clinical factors (focal deficit, neck stiffness, papilledema, cancer history, immunocompromised status, age over 50, pregnancy, signs of infection) mandate tailored imaging—MRI/MRV preferred for mass, venous thrombosis, or CNS infection.
- Appropriately applied imaging pathways markedly decrease unnecessary CT/CTA, improve detection of serious causes, and align ED practice with national standards.

Implementing structured, evidence-based imaging algorithms for headache in the ED advances diagnostic accuracy, protects patients from excess imaging, and streamlines care. Enhanced knowledge of headache variants, red flag criteria, and guideline-based selection ensures high-value, patient-centered practice for both radiologists and emergency clinicians.

Images/Tables

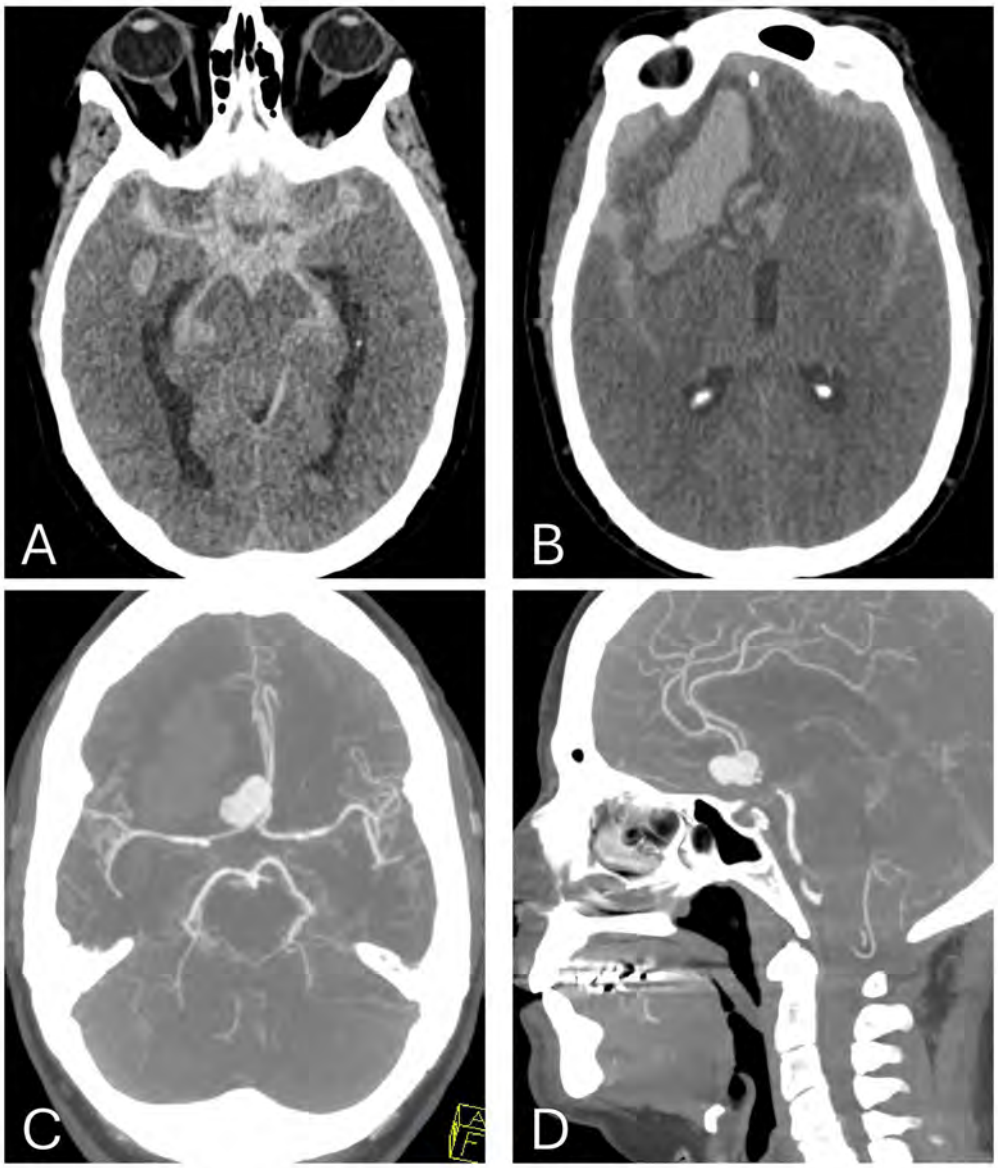

Figure 1. Axial non-contrast head CT (A and B) showing extensive subarachnoid and right frontal parenchymal hemorrhage secondary to ruptured anterior communicating artery aneurysm visualized on axial and sagittal CT angiogram images (C and D).

---

711 4D Parathyroid MRI: A Pictorial Review

Kyle Tegtmeyer MD[1], Allison Peng[1], Mantej Singh[2], Shadman Rahman[3], Carys Kenny-Howell[1], Saeed Rahmani[1], Long H Tu MD PhD[1]

[1]Yale University School of Medicine, New Haven, CT, USA. [2]University of Arizona School of Medicine, Tucson, AZ, USA. [3]Tuoro College of Osteopathic Medicine, New York, NY, USA

Summary & Objectives

Numerous imaging modalities are available for evaluation of the parathyroid glands, with 4D CT being the most common today. Despite the relative ease and speed of 4D CT, this technique is contraindicated in patients with severe allergies to iodinated contrast. 4D parathyroid MRI presents a compelling alternative to 4D CT, with sensitivity for parathyroid adenomas approaching 100% in prior studies [1]. Parathyroid MRI offers similar advantages to 4D CT, including the ability to characterize the typical arterial hyperenhancement pattern of parathyroid adenomas, while offering additional advantages, including evaluating wide anatomic ranges for ectopic parathyroids and the ability to evaluate other nearby anatomic structures for additional or related pathologies [2]. As these examinations tend to be infrequently performed, we believe that there may be value to the neuroradiologist in reviewing parathyroid MRI examination characteristics, imaging prtocols, and associated findings.

Purpose

We seek to provide a comprehensive review of 4D MRI imaging of the parathyroids, including discussion of typical and incidental imaging findings, imaging protocols, exam indications, and limitations. We begin by reviewing the current literature supporting the use of MRI for parathyroid evaluation, and comparison to other imaging modalities. We discuss imaging protocols for exam optimization, as well as possible pitfalls and frequent artifacts.

We then provide a pictorial review of parathyroid MRI findings, including typical imaging findings for cases that are both positive and negative for parathyroid adenomas. Lastly, we seek to characterize a range of possible incidental findings the radiologist may encounter on a dedicated parathyroid MRI examination.

Materials & Methods

We performed a literature review for data on the use and implementation of parathyroid MRI through a comprehensive search of the PubMed database. We review common imaging protocols, including those reported in the literature, as well as protocols used within our institution. We then review a series of high-yield example cases from our institutional database demonstrating examples of parathyroid adenomas and common incidental findings. We additionally demonstrate cases with common artifacts, demonstrating limitations of parathyroid MRI that the neuroradiologist must consider.

Results & Conclusion

4D MRI Parathyroid examinations are an infrequently performed examination that appears to demonstrate a relatively high diagnostic yield for parathyroid adenomas. Review of these typical and incidental imaging findings may assist neuroradiologists in exam interpretation, particularly in practice settings where these examinations are infrequently performed. Review of imaging protocols and pitfalls may also help neuroradiologists to establish protocols for MRI parathyroid examinations where not currently available.

Images/Tables

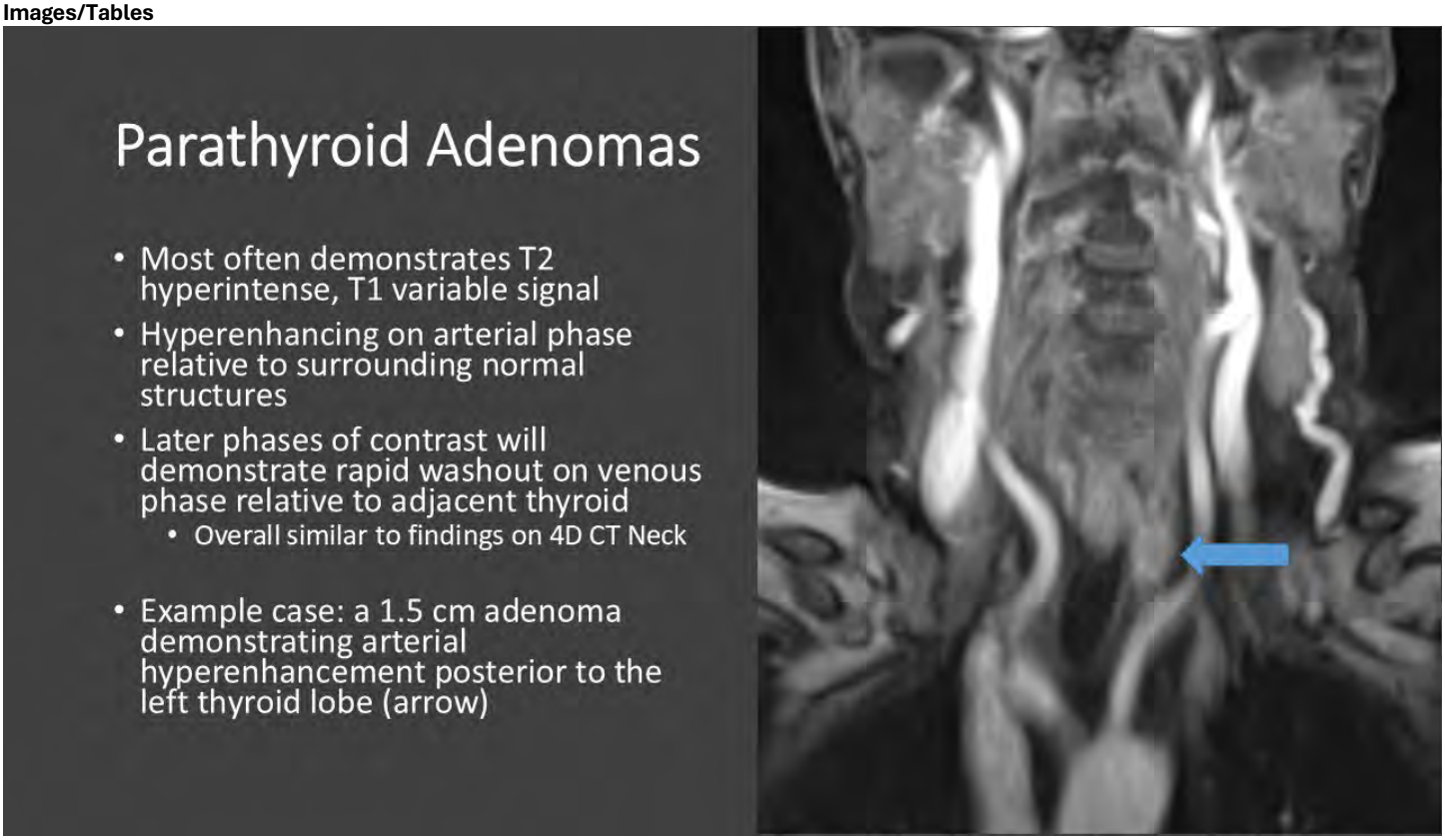

---

726 Everything CT, but the "A": Non-Arterial Findings on CTA Head and Neck

Mohammed Shilleh D.O., David Rusinak M.D.
Northwestern, Chicago, IL, USA

Summary & Objectives

CT angiography (CTA) of the head and neck is routinely performed to evaluate vascular pathology such as stenosis, dissection, occlusion, or aneurysm. However, these examinations also encompass a broad anatomic field that includes the brain, bones, oral cavity and pharynx, salivary glands, and sometimes the venous system. Within these regions lie clinically relevant findings that are frequently overlooked when attention is confined to the arterial vasculature.

This educational exhibit presents six real cases of missed and nearly missed incidental findings unrelated to arterial pathology. Each case illustrates how narrow diagnostic focus and incomplete search patterns can obscure important pathology. Through these examples, the exhibit demonstrates how subtle modifications to a radiologist's interpretive routine—such as utilizing adequate windowing levels to delineate non-arterial structures can substantially reduce oversight.

After viewing this exhibit, participants will be able to:

1. Recognize the spectrum of non-arterial incidental findings encountered on CTA head and neck studies.
2. Apply structured search patterns that systematically incorporate non-arterial regions.
3. Consider practical strategies, such as template reporting as a failsafe.

Purpose

Head and neck CTA remains the standard for vascular evaluation but frequently reveals non-arterial pathology with clinical consequence[1]. Findings in the brain, bones, oral cavity and pharynx, salivary glands, and sometimes the venous system may be missed if the reader's search pattern focuses solely on arteries[2,3]. The purpose of this exhibit is to highlight, through six real-world cases, how non-arterial findings are commonly overlooked and how small, deliberate refinements to a radiologist's visual search pattern—such as structured sweep across bone and soft tissue after vascular

assessment—can prevent such misses. By emphasizing comprehensive review techniques, this work promotes more complete interpretation of CTA studies and positive clincal impact[4,5].

Materials & Methods

A retrospective review of head and neck CTA studies was performed to identify cases where incidental findings unrelated to arterial vasculature were missed or nearly missed. Six representative cases were selected based on clinical relevance and anatomic diversity. For each case, imaging features, diagnostic trajectory, and clinical outcomes were documented. Each case was re-evaluated using a revised interpretive approach emphasizing a structured review sequence: first evaluating arteries, soft tissues, lung apices, brain, face, and finally the spine utilizing the appropriate window levels to adequately assess all structures.

Results & Conclusion

Across the six featured cases, missed or nearly missed non-arterial findings included spine osteomyelitis, brain tumor, salary gland pathology, cervical discitis, venous thrombosis, and oropharyngeal neoplasm. Most oversights stemmed from cognitive anchoring on vascular pathology and failure to review non-arterial compartments in multiplanar reconstructions and/or appropriate window leveling.

Implementing a refined search pattern proved effective: a systematic sweep (evaluating arteries, soft tissues, lung apices, brain, face, and finally the spine) markedly improved detection on second review. Integrating this method with template reporting can prevent deviance from standard search pattern.

In conclusion, these six cases demonstrate that critical pathology may reside just beyond the vessels. Subtle yet deliberate adjustments to the radiologist's search pattern, reinforced through templates, can significantly reduce diagnostic error and ensure comprehensive evaluation of CTA head and neck studies.

Images/Tables

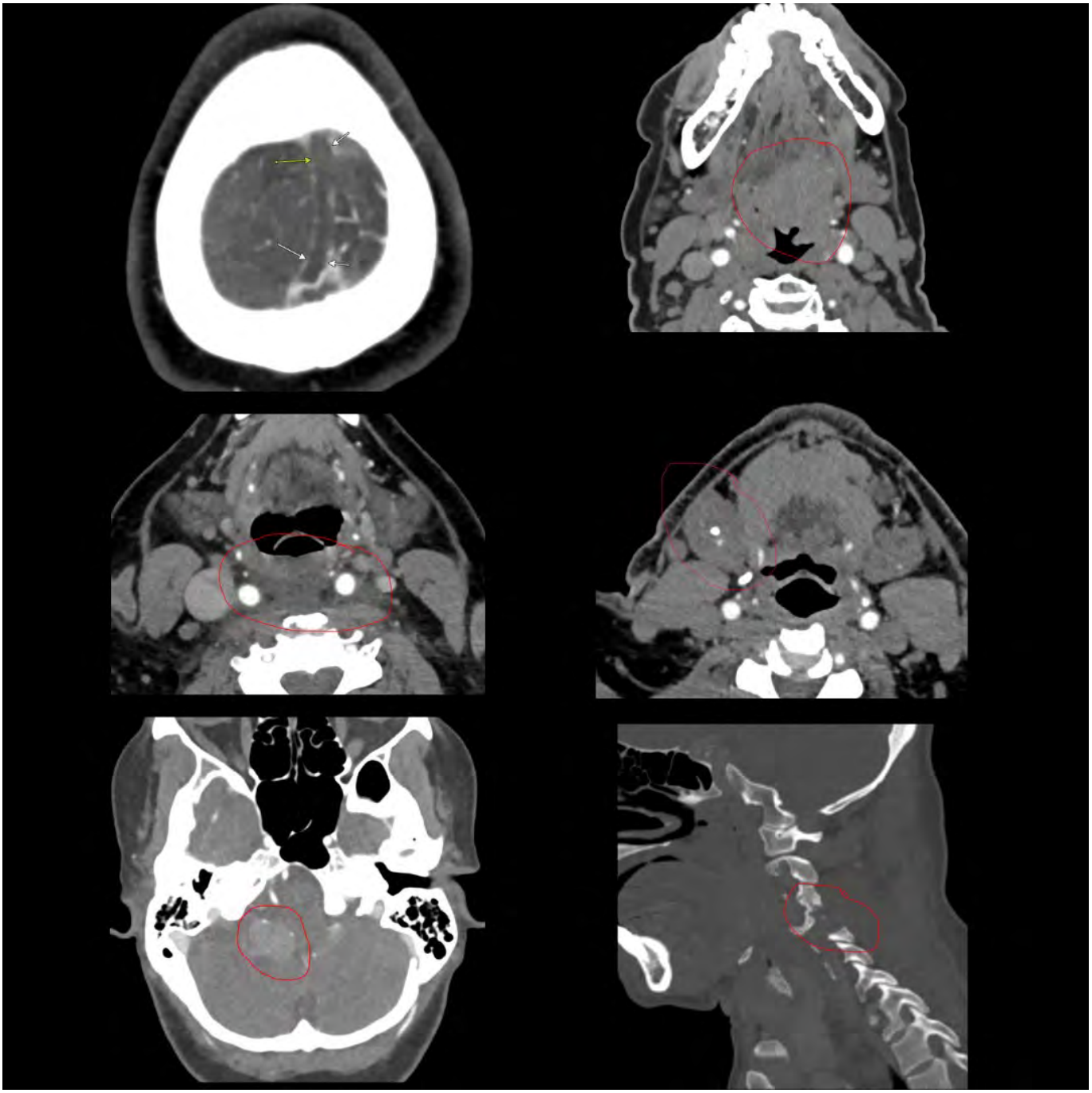

759 **Cytotoxic Lesions of the Corpus Callosum (CLOCCs)**

Varun S Taruvai MD, Akm A Rahman MD, DO
University of Rochester Medical Center, Rochester, NY, USA

Summary & Objectives

1. Understand the pertinent clinical and imaging features of CLOCCs on MRI as well as how to distinguish them from other etiologies of callosal lesions.
2. Present a representative case of clinically confirmed CLOCC.

Purpose

The purpose of this educational exhibit is to present a case of CLOCC, discuss key clinical and imaging features of the diagnosis, and discuss potential differentials for callosal lesions.

Materials & Methods

In this educational exhibit, pertinent MRI images of a representative case of CLOCC are presented. A discussion of clinical presentation, imaging features, and pertinent differentials will be covered.

Results & Conclusion

Cytotoxic Lesions of the Corpus Callosum (CLOCCs), formerly known as Transient Lesions of the Splenium of the Corpus Callosum or Reversible Splenial Lesion Syndrome, are a collection of clinical entities which result in cytotoxic edema and signal change within the corpus callosum.

CLOCCs are associated with a broad range of etiologies, including seizure disorders, metabolic disturbances, infection, or drug-induced (particularly recent cessation of antiepileptics or chemotherapy). Clinical features tend to be nonspecific, typically presenting as new encephalopathy in the setting of one of the above etiologies. Notably, symptoms of hemispheric disconnection such as hemineglect, alien hand syndrome, or agraphia are rarely seen despite direct involvement of the corpus callosum. Although the precise pathophysiologic mechanism is not fully understood, CLOCCs are thought to be a result of T-cell mediated inflammatory pathways causing glutamate excitotoxicity and cytotoxic edema.
MRI is the imaging modality of choice. CLOCCs typically present as a well-circumscribed, ovoid lesion in the midline splenium of the corpus callosum with classic features of cytotoxic edema including T2/FLAIR hyperintensity and diffusion restriction. The predilection for the splenium is thought to be due to the increased glutamate receptor expression in splenial oligodendrocytes. Less commonly, extension may be observed into the lateral splenial substance resulting in the "boomerang sign". Extension into the callosal body is extremely rare. Contrast enhancement and mass effect are typically not seen. Another key feature is transiency; the majority of CLOCCs resolve spontaneously within 1 week to 3 months without residual gliosis or atrophic change. The presence of contrast enhancement, mass effect, persistence beyond 3 months, or callosal atrophy should prompt consideration of other etiologies.
Although CLOCCs typically carry a positive prognosis, it is important to distinguish them from more insidious callosal lesions such as infarction, neoplasm, inflammatory demyelination, or toxin/drug induced damage which may require direct management. Isolated callosal infarcts are rare and demonstrate subacute enhancement with persistent FLAIR hyperintensity and volume loss. Malignancies such as lymphoma demonstrate diffusion restriction but typically enhance avidly, with larger lesions exerting mass effect. Inflammatory demyelination, such as Multiple Sclerosis or ADEM, demonstrates enhancement during active demyelination with persistent FLAIR hyperintensities. Larger regions of demyelination may demonstrate diffusion restriction, but this is typically peripherally distributed. Of these differentials, toxin/drug induced callosal damage such as Marchiafava-Bignami disease or metronidazole toxicity are the most likely to directly involve the corpus callosum and may not enhance. However, Marchiafava-Bignami disease typically precipitates atrophic callosal changes while metronidazole toxicity classically demonstrates concurrent cerebellar involvement.

Images/Tables

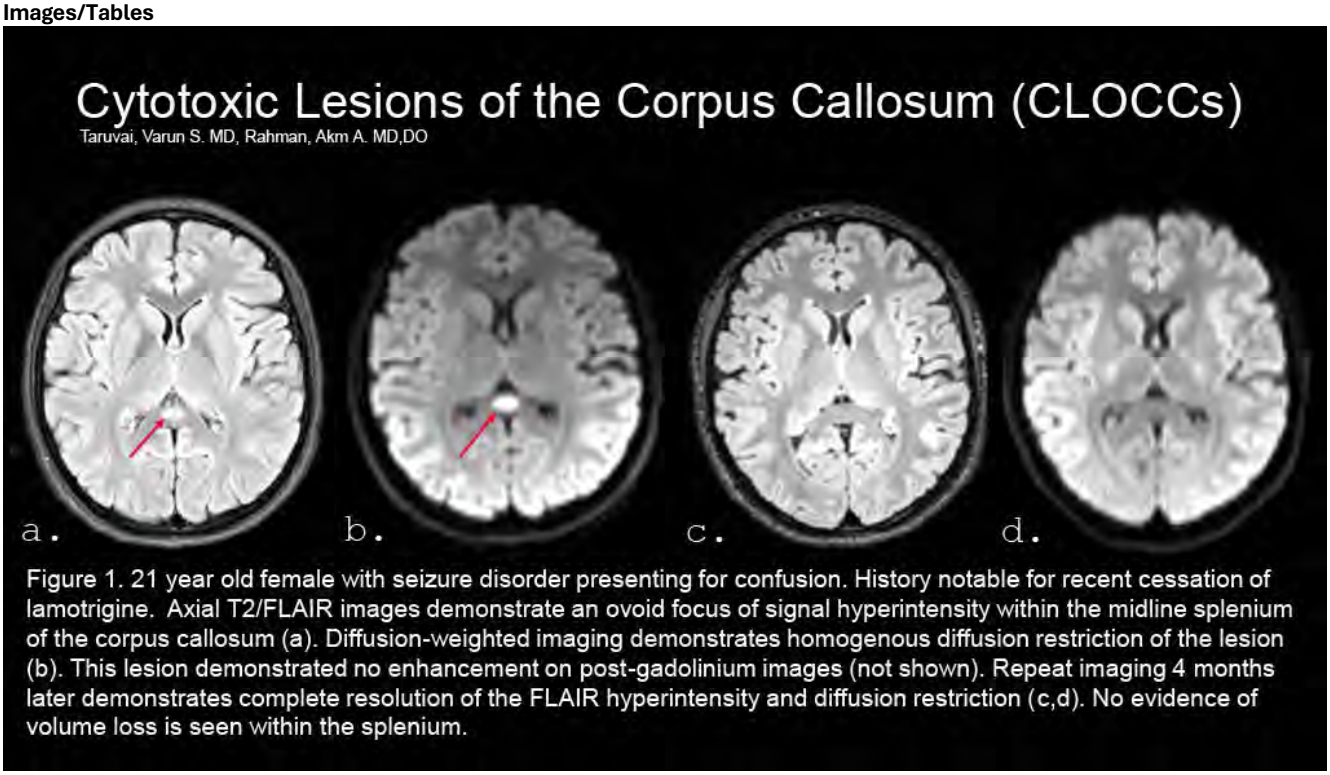

Figure 1. 21 year old female with seizure disorder presenting for confusion. History notable for recent cessation of lamotrigine. Axial T2/FLAIR images demonstrate an ovoid focus of signal hyperintensity within the midline splenium of the corpus callosum (a). Diffusion-weighted imaging demonstrates homogenous diffusion restriction of the lesion (b). This lesion demonstrated no enhancement on post-gadolinium images (not shown). Repeat imaging 4 months later demonstrates complete resolution of the FLAIR hyperintensity and diffusion restriction (c,d). No evidence of volume loss is seen within the splenium.

---

823 Pilocytic Astrocytoma Beyond the Posterior Fossa: A Spectrum of Unusual Appearances

Raman Deep MD[1], Alexander J Mullen MD[1], Dhanush Jayananda Amin MD[2], Siddhartha Gaddamanugu MD[1]
[1]University of Alabama, Birmingham, Alabama, USA. [2]University of Arkansas for Medical Sciences, Little Rock, Arkansas, USA

Summary & Objectives

Pilocytic astrocytoma (PA) is a World Health Organization grade I glioma commonly seen in the posterior fossa especially the cerebellum in children and young adults. The characteristic imaging appearance is a cystic mass with an enhancing mural nodule. However, PAs can also arise in atypical intracranial and spinal locations and may exhibit unconventional imaging features which mimic other high grade neoplasms. Recognizing these unusual appearances is essential for accurate radiologic diagnosis and appropriate clinical management.

Purpose

The purpose of this educational review is to enhance awareness of the diverse imaging characteristics of PA occurring outside its classic posterior fossa location. Recognizing these variations is critical for correct diagnosis, avoiding over-grading, and ensuring optimal therapeutic decision making in pediatric and young adult populations.

Materials & Methods

A comprehensive review of imaging findings of PAs across atypical intracranial and spinal locations was performed, emphasizing MRI and CT characteristics. Lesions were categorized according to their site and imaging morphology. Key features such as enhancement pattern, presence of hemorrhage, edema, and leptomeningeal dissemination were analyzed. Representative cases demonstrating both typical and atypical imaging appearances were included to illustrate the spectrum of findings and their diagnostic challenges.

Results & Conclusion

1. Atypical Anatomical Locations:

- **Cerebral hemispheres***:* Supratentorial masses, frequently solid or solid-cystic. Rarely cortical-based and may be associated with seizures.
- **Intraventricular***:* Arising from choroid plexus or ventricular wall mimicking central neurocytoma or ependymoma.
- **Gangliothalamic***:* Deep-seated lesions demonstrating unusual solid or heterogeneous enhancement.
- **Brainstem***:* Focal or exophytic masses occasionally with an infiltrative pattern may resemble a glioma.
- **Pineal region***:* Solid or heterogeneous solid-cystic masses that can resemble pineal parenchymal or germ cell tumors.
- **Spinal cord***:* Intramedullary, expansile lesions, often with polar cysts or heterogeneous enhancement, resembling ependymoma or astrocytoma.

2. Atypical Imaging Features:

- **Solid enhancement***:* Homogeneous or heterogeneous enhancement mimicking high grade glioma.
- **Hemorrhage***:* Rare but reported, particularly in supratentorial or deep-seated lesions, sometimes leading to misinterpretation as high grade vascular or metastatic lesions.
- **Perilesional edema***:* Usually absent or minimal in classic PA but when present imparting an infiltrative / high grade appearance.
- **Leptomeningeal dissemination***:* Rare but possible at presentation or recurrence; awareness is essential for proper staging and follow-up imaging.

3. Diagnostic Pearls:

- Despite these atypical imaging appearances, the majority of PAs maintain benign imaging features like smooth margins and mild mass effect.
- Patient age, lesion site, and growth pattern remain key contextual indicators of a low-grade process.
- Awareness of atypical presentations helps avoid over grading and unnecessary aggressive management.

Conclusion

Pilocytic astrocytoma, although classically a posterior fossa tumor with cystic and mural nodule morphology, can occur in diverse anatomical locations with atypical imaging appearances that may mimic high-grade neoplasms. Recognizing these uncommon presentations broadens the diagnostic perspective, strengthens radiologic interpretation, and supports timely, appropriate patient management.

Learning Objectives

1. **Recognize** the spectrum of atypical anatomical locations of pilocytic astrocytoma beyond the posterior fossa.
2. **Identify** unusual imaging features that may simulate other tumors, including high-grade neoplasms.
3. **Apply** practical diagnostic clues on routine MRI and CT to improve diagnostic confidence and guide management.

Images/Tables

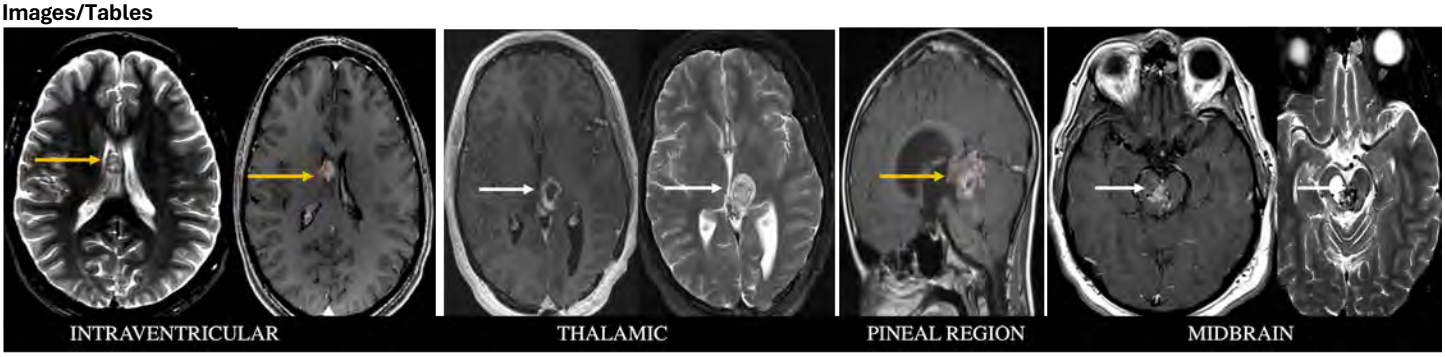

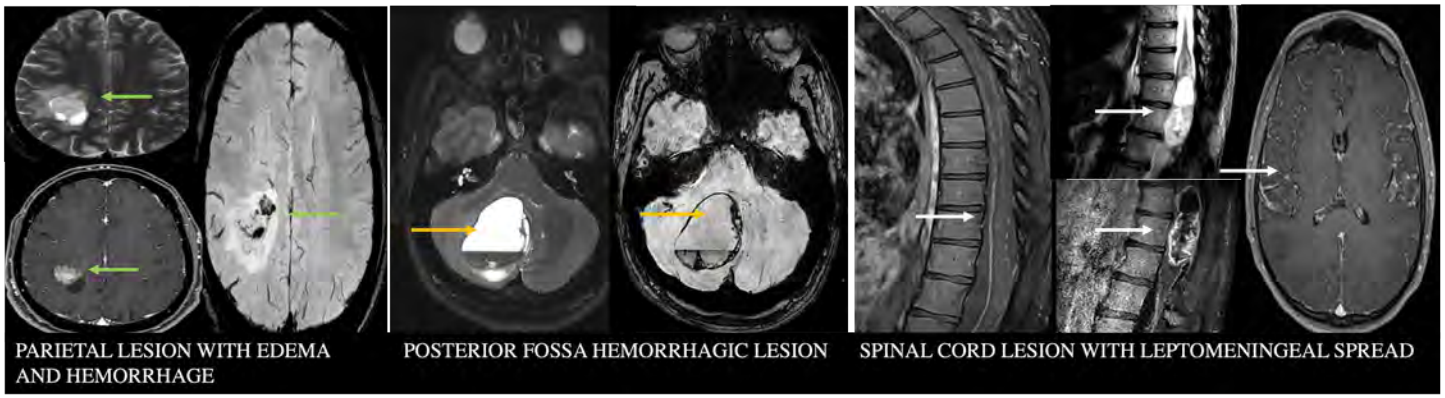

---

943 Imaging based approach to hypomyelinating leukodystrophies

Omer Simitcioglu MD[1], Sedat G Kandemirli MD[2], Khalid Al-Dasuqi MD[3], Bulent Aslan MD[1], Cesar Alves MD[2]

[1]Beth Israel Deaconess Medical Center, Boston, MA, USA. [2]Boston Children's Hospital, Boston, MA, USA. [3]Sidra Medicine, Doha, NA, Qatar

Summary & Objectives

Hypomyelinating leukodystrophies are a clinically and genetically heterogeneous group of disorders characterized by global developmental delay with prominent motor dysfunction, spasticity, nystagmus, and ataxia. Certain specific clinical features may be seen in a few HLDs, which may be quite helpful in diagnosis in corroboration with neuroimaging features.

Hypomyelinating leukodystrophies can be broadly classified as:

- Primary: Directly associated with deficient myelin deposition, Pelizaeus Merzbacher Disease (PMD) is the protype.
- Secondary: Early-onset neuronal disorders with disruption of axon-myelin interactions and secondary myelination failure. Storage disorders: Neuronal ceroid lipofuscinosis, infantile onset GM1/GM2 gangliosidosis, Sialic acid storage diseases, Fucosidosis are some of the disorders.

Despite whole exome sequencing, approximately 10-15% of hypomyelinating leukodystrophies don't have a known genetic diagnosis. Some of the challenges with genetics are copy number variations may not detected with all WES approaches, (meaning that PLP1 duplications can be overlooked) and deep intronic PLP1 variants associated with HEMS are missed by WES, as can be promoter variants in GJC2 (Cx47).

On imaging, hypomyelinating diseases are generally characterized by:

- Mildly hyperintense WM signal on T2-WI
    - T2 hypointensity milder compared to demyelination
    - Diffuse involvement of white matter and absence of myelination in the later myelinating structures (suggesting an absence or arrest at an early stage rather than involvement of already formed myelin)
- Variable signal on T1-WI: Usually iso or hypointense, can be hyperintense depending on amount of myelin deposited
    - In demyelination, T1 signal is invariably low

Purpose

The purpose of this study is to present an imaging based approach on narrowing down the differential diagnosis for hypomyelinating leukodystrophies based on several features like pattern of brainstem involvement, cerebellar atrophy, basal ganglia and thalamic signal changes and calcification.

Materials & Methods

A retrospective review of hypomyelinating leukodystrophies at a single center was performed to illustrate the different types of leukodystrophies. Main imaging patterns are

1. Diffuse hypomyelination: Pelizaeus Merzbacher Disease (PMD), Pelizaeus Merzbacher Like Disease (PMLD), SOX10 Associated PCWH
2. Selective white matter involvement: Hypomyelination with brain stem and spinal cord involvement and leg spasticity (HBSL), Leukoencephalopathy with brain stem and spinal cord involvement and elevated lactate (LBSL), Salla disease
3. Cerebellar atrophy: PolR3 related leukodystrophies (4H syndrome), 18q deletion syndrome, Hypomyelination with atrophy of the basal ganglia and cerebellum (HABC), STAG2 related hypomyelination
4. Basal ganglia abnormalities: Fucosidosis, Gangliosidosis, Neuronal Ceroid Lipofuscinosis (NCL)
5. Calcification: Cockayne syndrome,Trichothiodystrophy, Cerebral folate deficiency

Results & Conclusion

Hypomyelinating leukodystrophies can be challenging to come up with a differential list due to rapidly expanding field, variable and overlapping imaging phenotypes in addition to mimickers like early-onset neuronal disorders that disrupt of axon-myelin interactions. This exhibit will try to cover the main imaging phenotypes in addition to rarer entities.

Images/Tables

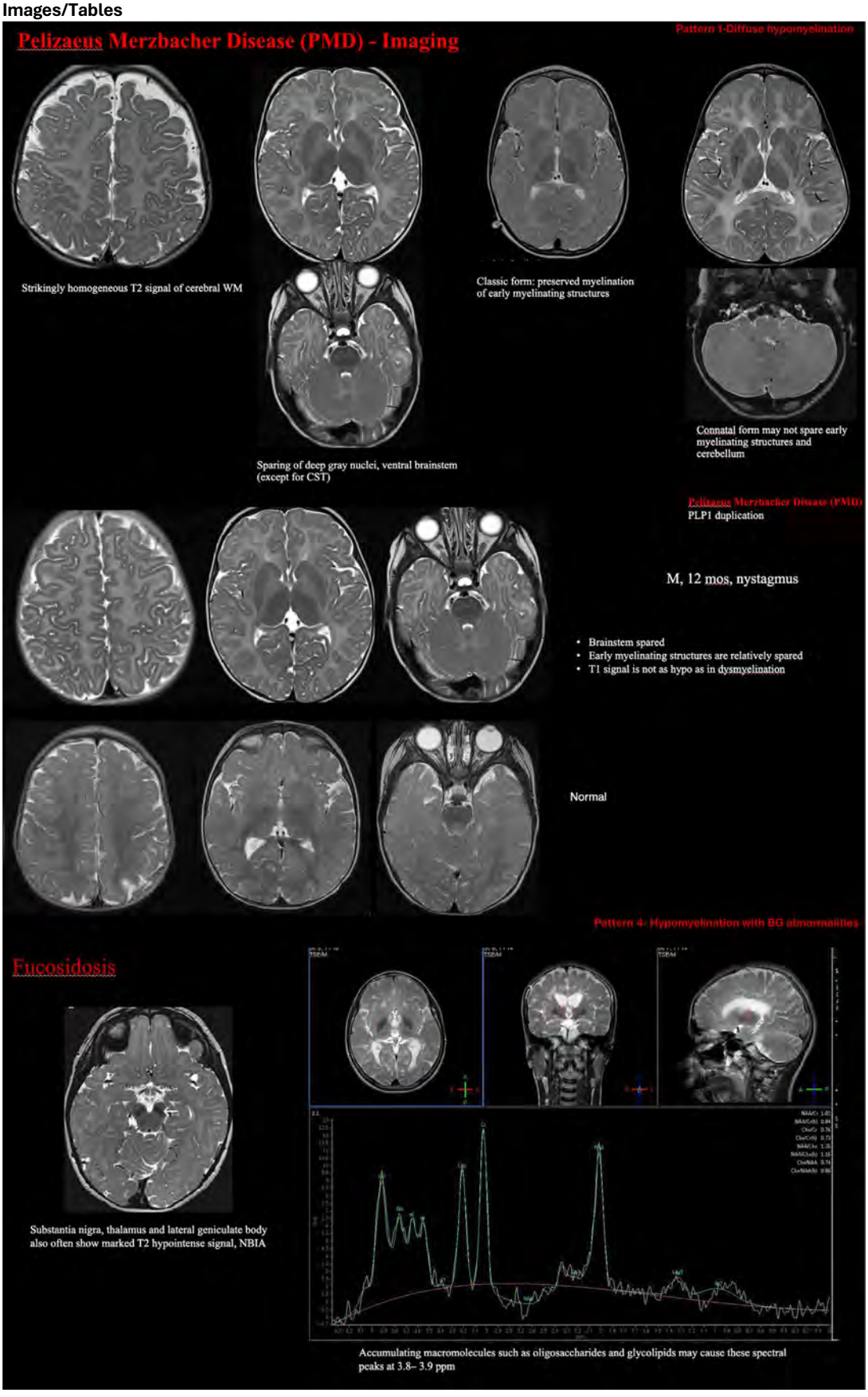

1066 Many Faces of the Facial Nerve: MRI Findings of Common Facial Nerve Pathologies from Pons to Periphery

Kamal Kandel MD[1], Anish Neupane MD[1], Aryan Hemani MD[1], Neil Tishkoff MD[2]

[1]Yale New Haven Health - Bridgeport Hospital, Bridgeport, CT, USA. [2]Yale University School of Medicine, New Haven, CT, USA

Summary & Objectives

Objective: To familiarize the readers the normal segmental anatomy of facial nerve and common pathologies across each segment using Magnetic resonance Imaging (MRI).

Summary:

The facial nerve (CN VII) follows a complex six-segment course from its origin at the pontomedullary junction through the cerebellar pontine angle cistern, internal auditory canal, petrous temporal bone, and extracranial parotid segment beyond the stylomastoid foramen.[1] Temporal bone segments include the labyrinthine, tympanic and mastoid segments. The intricate anatomy of facial nerve and small caliber makes MRI evaluation challenging, highlighting the importance of segmental anatomy for accurate localization of pathology.

The facial nerve exhibits distinct MRI appearances along its anatomical course; each segment associated with characteristic pathologies. The pontomedullary cisternal segment, extending from the pontomedullary junction to the internal auditory canal (IAC), lies anteromedial to the vestibulocochlear nerve. Lesions such as pontine demyelination, ischemic or inflammatory neuropathies, cerebellopontine angle (CPA) masses and vascular compression may occur here. The intracanalicular segment, within the IAC, is affected by facial or vestibular schwannomas and labyrinthitis. The labyrinthine segment, the shortest and narrowest portion extending to the geniculate ganglion, is most vulnerable to facial neuronitis including Bell's palsy, Ramsay Hunt syndrome, Lyme disease and ischemic neuropathy. Tympanic and mastoid segments are susceptible to otitis media, cholesteatoma, or traumatic injury. Beyond the stylomastoid foramen, the extracranial segment may be involved by perineural tumor spread or parotid neoplasms. Some pathologies such as perineural spread, nerve sheath tumors can involve multiple contiguous segments.

MRI plays a vital role in differentiating these pathologies: smooth, linear, or continuous enhancement typically indicates benign inflammatory processes, whereas irregular, nodular, or mass like enhancement suggests neoplastic or infiltrative disease. High-resolution T2-weighted sequences (such as CISS or FIESTA) delineate the nerve's anatomy within the cerebellar pontine angle cistern and IAC, while post-contrast T1-weighted imaging highlights enhancement patterns crucial for diagnosis. This exhibit provides a pictorial roadmap of the facial nerve from brainstem origin to peripheral termination with key MRI findings across common pathologies to enhance understanding of segmental disease patterns and guide accurate interpretation of cranial neuropathies.

Purpose

N/A

Materials & Methods

N/A

Results & Conclusion

N/A

Images/Tables

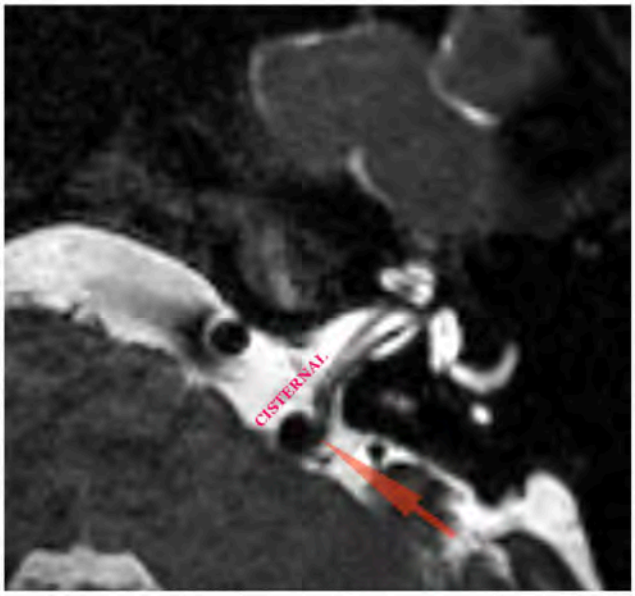

Axial T2WI image showing cisternal segment of facial nerve with vertebral artery (V4) segment abutting the root entry zone.

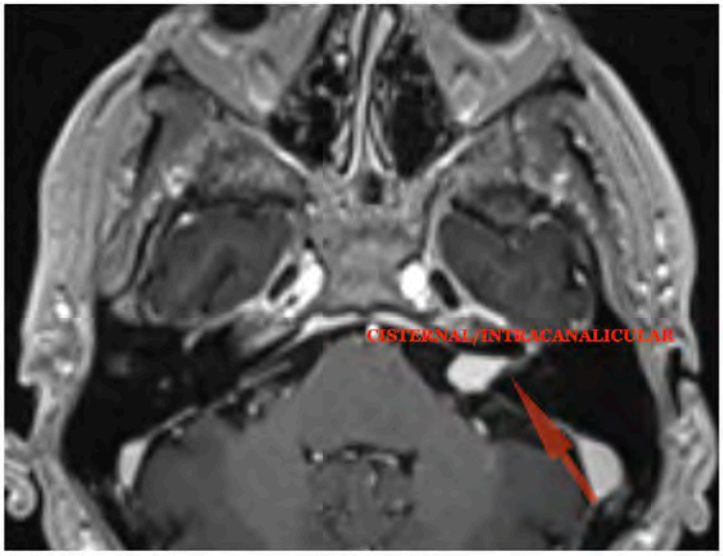

Axial T1WI C+ showing homogeneously enhancing lesion with linear enhancement tracking along the left facial nerve ganglion: A case of vestibular schwannoma with perineural tracking of tumor into the cisternal/intracanalicular segment of facial nerve.

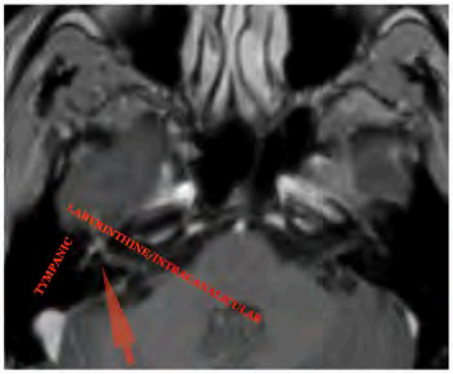

Axial post contrast T1WI C+ image showing linear enhancement of intracanalicular, labyrinthine and tympanic segment of facial nerve: A case of bell's palsy.

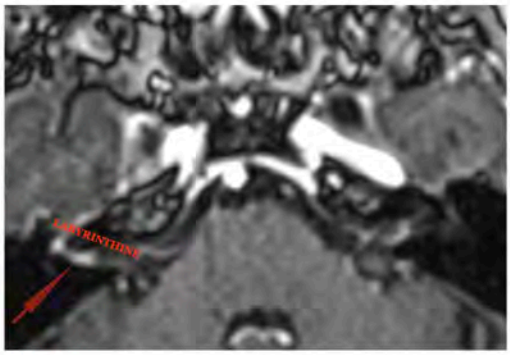

Axial T1WI C+ Image showing linear enhancement of labyrinthine segment and geniculate ganglion of facial nerve: A case of bell's palsy.

Axial T1WI C+ image showing enhancement of lesion of left geniculate ganglion: A case of facial nerve schwannoma.

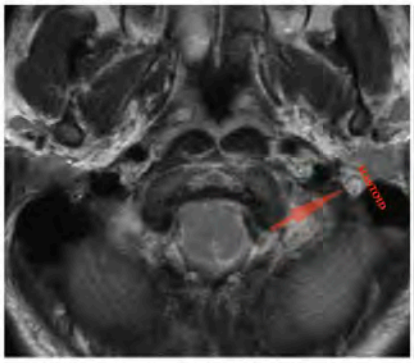

Axial T2WI image showing hyper intense lesion involving the left mastoid segment of facial nerve: A case of facial neurofibroma in a patient with known neurofibromatosis.

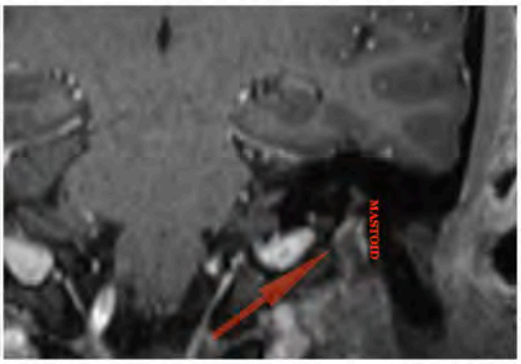

Axial T1WI C+ image showing peripheral enhancement of lesion at mastoid segment of left facial nerve: A case of facial nerve schwannoma.

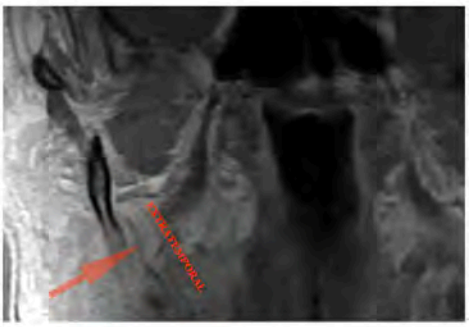

Coronal T1WI C+ image showing enhancement of extra temporal segment right facial nerve: A case of perineural spread of parotid neoplasm.

---

185 Hypoattenuating Dural Venous Sinus Thrombosis on Noncontrast CT

Ben C Smith MD, Derek G Hesse MD, David J Rusinak MD, Alexander J Nemeth MD
Northwestern University, Chicago, IL, USA

Summary & Objectives

Dural venous sinus thrombosis (DVST) is a challenging diagnosis on non-contrast CT. Acute dural venous sinus thrombosis is typically hyperdense compared to the blood pool in the unaffected dural venous sinuses and major intracranial arteries, although the sensitivity of detecting DVST on non-contrast CT is limited.[1] Factors such as variable hematocrit between patients alters the density of the dural venous sinuses in both thrombosed and patent vessels at baseline, which creates diagnostic pitfalls in the absence of secondary findings, such as hemorrhagic venous infarcts. Measuring the Hounsfield units in the dural venous sinuses with normalization to the patient's hematocrit level has been shown to improve diagnostic certainty in a small cohort of patients but was shown to miss 1 in 4 venous thromboses when similar quantitative criteria were applied to a larger group of

patients.[1,2] The timing of the patient's presentation and evaluation with non-contrast CT may further confound the diagnosis as acute, hyperdense clot will subsequently recanalize resulting in lowered density.[3] Education on clinical presentation and comorbid conditions that should raise suspicion for dural venous sinus thrombosis and the direct and indirect signs on non-contrast CT will prepare neuroradiologists to make this challenging diagnosis. We aim to review challenging cases of dural venous sinus thrombosis on non-contrast CT, including cases of hypodense dural venous sinus thrombus, which may be under-recognized by diagnostic radiologists if they are expecting the noncontrast CT appearance of thrombus to be hyperdense.

Purpose

Acute dural venous sinus thrombosis (DVST) is classically hyperdense on non-contrast CT of the brain. However, there are less common cases where confirmed dural venous sinus thrombosis has a hypodense appearance on initial non-contrast CT, including at least seven examples in the past four years at our institution. We propose to review classic cases and manifestations of dural venous sinus thrombosis on noncontrast CT as well as challenging, less common presentations of dural venous sinus thrombosis on noncontrast CT that we have encountered in our practice.

Materials & Methods

Within a large academic institution, seven examples of hypoattenuating dural venous sinus thrombosis were noted over a period of approximately four years at the time of initial diagnosis. Chart review of the patients with hypoattenuating dural venous sinus thrombosis was conducted to elucidate possible etiologies of this less common appearance. Our exhibit aims to review clinical factors that should raise suspicion for dural venous sinus thrombosis and demonstrate the manifestations on non-contrast CT, including hypodense cases. A review of supporting evidence of dural venous sinus thrombosis will be included.

Results & Conclusion

Acute dural venous sinus thrombosis (DVST) often has a hyperdense appearance on non-contrast CT of the brain, but examples of hypodense DVST can be seen. We aim to demonstrate classic examples of acute dural venous sinus thrombosis and examples of less common, hypoattenuating thrombus which may be under-recognized by diagnostic radiologists. The exhibit will explore how to differentiate hypoattenuating thrombus from other etiologies, as well as a review of supporting evidence of dural venous sinus thrombosis on NCCT.

Images/Tables

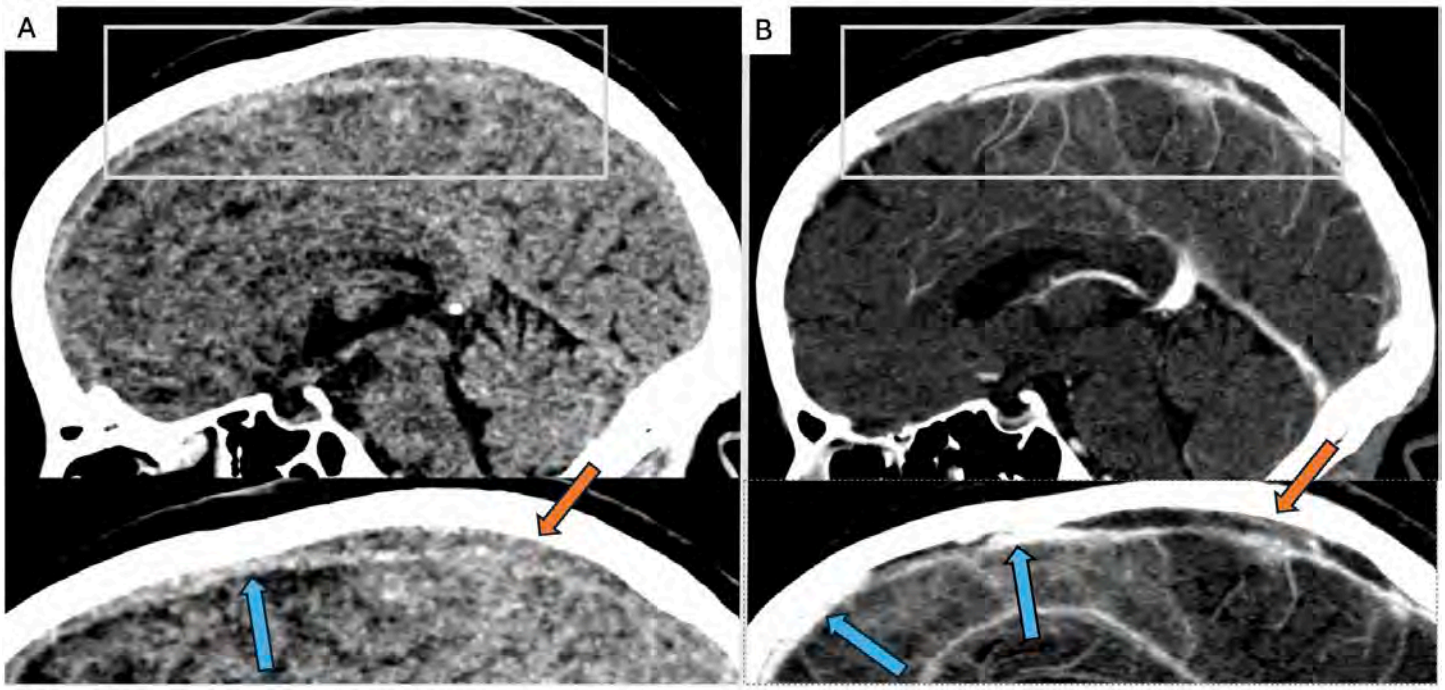

A: Sagittal and magnified views of the initial non-contrast CT of the brain at the time of presentation demonstrating hypoattenuation within the superior sagittal sinus (orange arrow). The more anterior aspect of the superior sagittal sinus demonstrates expected attenuation (blue arrow).
B: Sagittal and magnified views of the CT Venogram obtained one day later. The area of hypoattenuation on the non-contrast CT corresponds to occlusive thrombus within the superior sagittal sinus (orange arrow). The more anterior aspect of the superior sagittal sinus is patent without filling defect (blue arrows).

---

189 The Cortico-cortical and Cortico-subcortical Circuits of the Human Brain Language Centers Including the Dual Limbic and Language Working Fiber Tracts

Nithya P Narayana BS[1], Anusha Gandhi MD[1], Anastasia Loiko[2], Arash Kamali MD[1]
[1]McGovern Medical School at UTHealth Houston, Houston, TX, USA. [2]Rice University, Houston, Texas, USA

Summary & Objectives

The objectives of the exhibit are:

1. Expanding beyond the dual-stream model of language processing as advances in fMRI and DTI have revealed a more interconnected system.
2. Presenting a seven language center based approach to illustrate the integration of language and cognitive processing.
3. Understanding how the dual function of the association tracts in connecting language with the limbic system may explain language disorders with emotional comorbidities.

4. Bridging cognitive and emotional dysregulations in conditions like schizophrenia and PTSD through insights gained from white matter connectivities.
5. Proposing the use of DTI to diagnose and guide therapy for language disorders. Visualizing neural connections highlights the importance of integrating language, executive function, and emotion in creating effective treatments for patients.

Purpose

The current model of language processing, the dual-stream model, divides the brain's language network into a dorsal stream, involved in mapping sound to articulation, and a ventral stream, responsible for mapping sound to meaning. Advances in neuroimaging techniques such as functional magnetic resonance imaging (fMRI) and diffusion tensor imaging (DTI) have led to an increase in neuroscientific research yielding detailed anatomical and functional data on the white matter tracts of the human brain and their connectivities between the different language centers. Through the synthesis of existing knowledge in the literature, this review builds upon the foundation of the dual-stream model and offers a new perspective of focusing on seven key language centers (Broca's area, Wernicke's area, dorsolateral prefrontal cortex (DLPFC), supplementary motor area (SMA), visual word form area (VWFA), superior parietal lobule (SPL), and inferior parietal lobule (IPL)) to delineate the language network.

Materials & Methods

The exploration of language processing in the brain by each language center enhances our understanding of how the different regions integrate various sensory inputs to process language, moving beyond the dichotomy of the dual stream model. We analyzed each of these regions in terms of anatomical location, connectivities through specific white matter fiber tracts, and functional contributions to language processing. A DTI brain imaging technique was used to generate brain scans depicting the white matter fiber tracts involved in connecting language centers, and a comprehensive schematic view was generated incorporating the various tracts connecting the seven language centers. Through a review of the literature, we have found that many of the white matter fiber tracts (uncinate fasciculus (UF), inferior longitudinal fasciculus (ILF), inferior fronto-occipital fasciculus (IFOF), cingulum bundle (CB), prefronto-caudo-thalamic tract (PFCT), and arcuate fasciculus (AF)) associated with language processing also play significant roles in the limbic system. Understanding the intricate connections these tracts provide reveals the integration of language-associated cognitive functions and emotional processings in the human brain.

Results & Conclusion

The theoretical and clinical implications of this research are profound. By better understanding the specific roles and connections of each language center, we can deepen our knowledge of language disorders and may develop more targeted clinical interventions. Furthermore, understanding the language and limbic dual functionality of these specific white matter tracts could lead to improved diagnosis and treatment of language disorders with comorbid emotional impairments.

Images/Tables

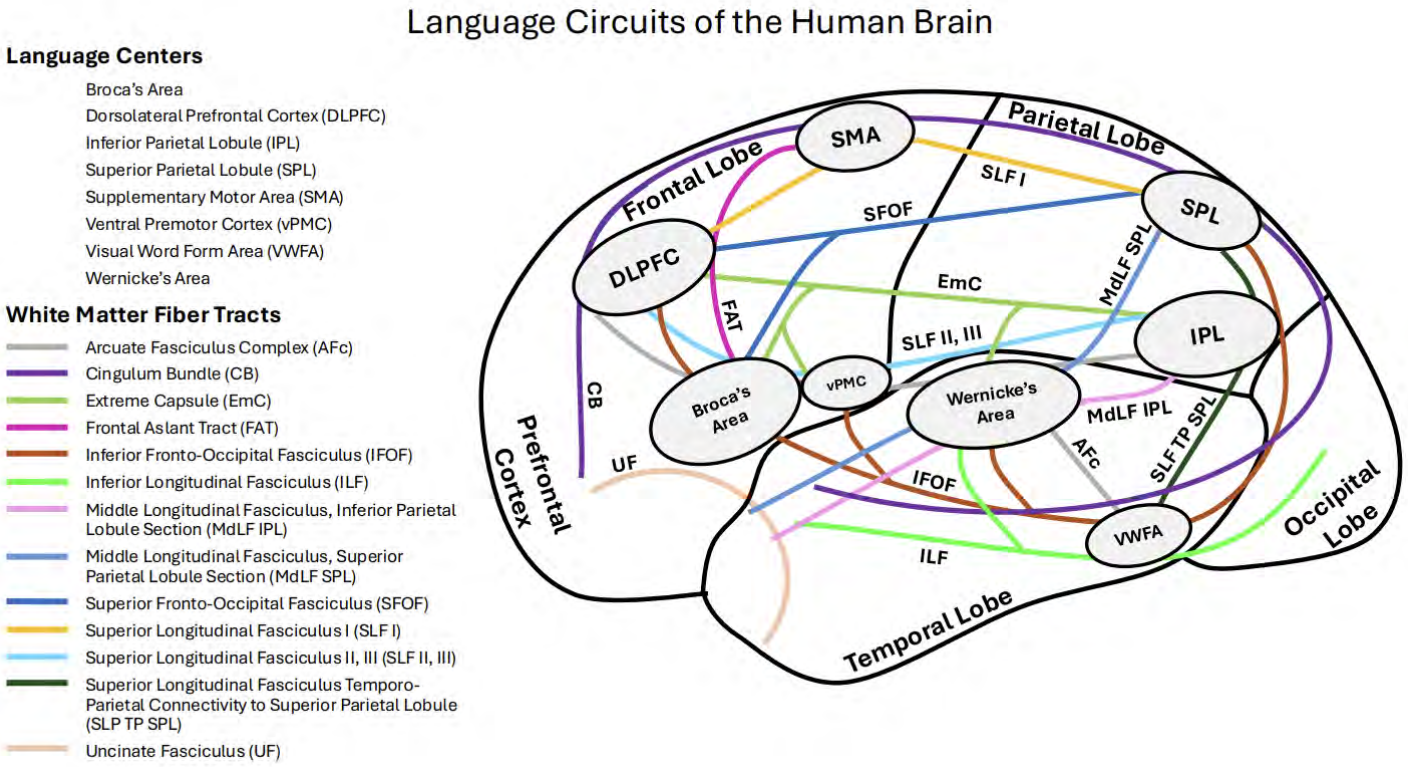

---

199 Brain PET/CT in the Evaluation of Central Nervous System Infections, Inflammatory Disorders, and Neoplasms.

Pedro Daniel Soto Vargas MD

Instituto Nacional de Ciencias Medicas y Nutricion Salvado Zubiran, Mexico City, Mexico City, Mexico

Summary & Objectives

While MRI remains the cornerstone for structural CNS evaluation, PET/CT provides unique metabolic and receptor-based information that aids in differentiating infection, inflammation, and malignancy.

The objectives are to:

- Illustrate the characteristic metabolic patterns of these CNS conditions using PET/CT.
- Highlight the complementary role of PET/CT to MRI in differential diagnosis.

- Review the diagnostic and clinical utility of various molecular radiotracers.
- Discuss common pitfalls and challenges in image interpretation.

Purpose

This educational exhibit aims to provide an overview of the clinical and imaging spectrum of central nervous system (CNS) infections, inflammatory disorders, and neoplasms evaluated with positron emission tomography/computed tomography (PET/CT).

Materials & Methods

A comprehensive review of literature was conducted using Web of Science, PubMed, and Google Scholar. A retrospective review of PET/CT studies performed between 2012 and 2024 was conducted, including patients with confirmed or clinically suspected central nervous system (CNS) infection, inflammatory disorder, or neoplastic disease.

Results & Conclusion

This review presents representative cases and characteristic imaging patterns that highlight the role of PET/CT in three major diagnostic categories:

• Infectious Diseases:

Increased FDG uptake aids in the localization of abscesses, encephalitis and meningitis, allowing distinction between active infection and necrotic or treated lesions. Illustrative examples include bacterial brain abscess, tuberculous meningitis, and fungal infections.

• Inflammatory and Autoimmune Disorders:

FDG PET/CT demonstrates distinctive metabolic patterns in autoimmune encephalitis. Limbic system hypometabolism may support an autoimmune etiology.

• Neoplastic Conditions:

PET/CT plays a pivotal role in differentiating high-grade gliomas from inflammatory pseudotumors, distinguishing tumor recurrence from post-radiation necrosis, and assessing CNS lymphoma.

^{18}F-FDOPA and ^{18}F-FET PET/CT: Provide high sensitivity for glioma detection and grading, especially in cases where FDG demonstrates nonspecific uptake. ^{18}F-FDOPA PET/CT is effective in differentiating tumor recurrence from treatment-related inflammatory changes.

^{18}F-DOTATATE PET/CT: Accurately identifies meningiomas, pituitary tumors, and inflammatory lesions owing to their somatostatin receptor expression, offering functional information complementary to MRI.

^{18}F-FLT PET: Reflects tumor proliferative activity and assists in distinguishing recurrent tumor from post-therapeutic inflammation or radiation necrosis.

Conclusion:

PET/CT is a valuable adjunct in the evaluation of CNS diseases, providing essential metabolic information that aids in differentiating infection, inflammation, and malignancy. Understanding the characteristic uptake patterns and correlating them with MRI and clinical findings can significantly improve diagnostic confidence and guide patient management.

---

255 Shining Light on Vessel Wall Enhancement: A Team Based Approach to Vessel Wall Imaging

Paul Harrie MD, Gustavo Mendez MD
University of Colorado - Anschutz Medical Campus, Aurora, CO, USA

Summary & Objectives

Magnetic Resonance (MR) Intracranial Vessel Wall Imaging (VWI) has become an important adjunct to traditional luminal assessment for characterizing intracranial vascular pathology[1]. Interpretation of VWI within the isolation of the reading room, however, is limited by overlapping imaging features of different processes including atherosclerosis, inflammatory/infectious vasculopathies, RCVS and vasospasm[2]. Furthermore, these imaging features are dependent on high spatial resolution and optimal signal-to-noise ratios which can be compromised by artifact[2,3]. Accurate interpretation of VWI requires the complete clinical context, ideally including multiple imaging time points, awareness of potential pitfalls, and open communication with referring physicians. The objective of this exhibit is to present several cases underscoring the necessity of a multidisciplinary approach to ensure accurate diagnosis and timely treatment.

Purpose

The interpretation of VWI is inherently challenging given how small the area of investigation is. VWI can be susceptible to dogmatic interpretations, sometimes leading to inaccuracies from misconstruing presence, degree or pattern of vessel wall enhancement. this exhibit underscores the importance of a multidisciplinary approach to the interpretation of intracranial MR VWI in the face of these challenges.

Materials & Methods

This retrospective analysis includes several cases from our institution in which the presumptive diagnosis suggested by MR intracranial VWI evolved as more clinical information and lab data was acquired. Conversations with referring physicians, informally in the reading room as well as during monthly stroke education conferences, also helped inform more nuanced interpretation of challenging cases and allowed for consensus diagnoses.

Results & Conclusion

Accurate interpretation of intracranial MR VWI cannot happen in a vacuum and requires open communication with referring physicians to formulate a complete clinical picture. Discussion with referring clinical teams both informally in the reading room and more formally in multidisciplinary conferences is critical to reach a best consensus for diagnosis.

Images/Tables

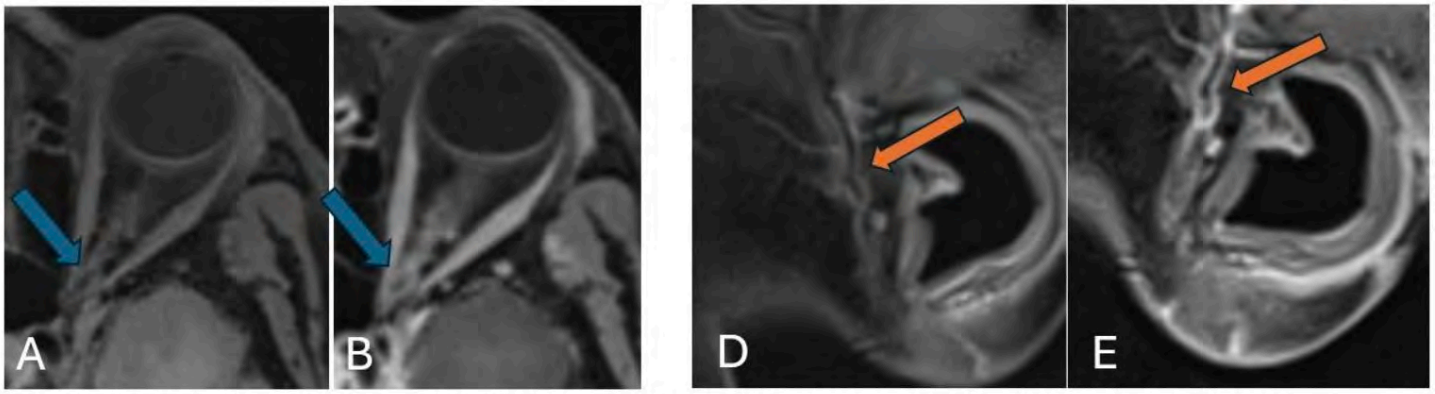

Figure 1: Axial MRA VWI T1 cube pre-contrast **(A)** and post-contrast **(B,C)** images show mild wall enhancement of the left ophthalmic artery. Sagittal MRA VWI T1 cube pre-contrast **(D)** and post-contrast **(E)** images show wall enhancement of the left superficial temporal artery.

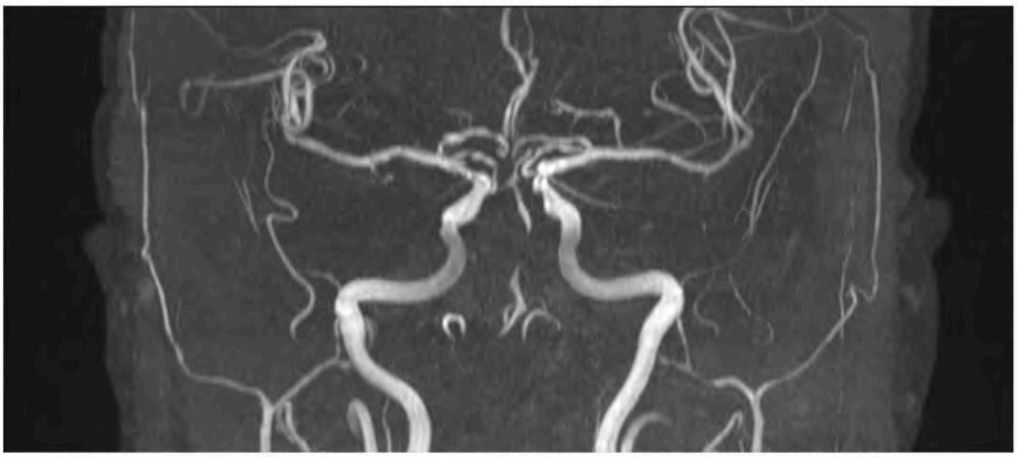

Figure 2: Coronal MRA COW shows irregularity with multifocal stenoses of both the anterior and posterior intracranial vasculature.

---

320 **Cerebral Amyloid Angiopathy- Related Inflammation: An Imaging Overview for the Neuroradiologist**

Kelsey Casano MD[1], Timothy Goyette MD[1], Phaethon Philbrook MD[2], Joseph Tarsia MD[1], Andrew Steven MD[1]
[1]Ochsner Clinic, New Orleans, LA, USA. [2]Emory University, Atlanta, GA, USA

Summary & Objectives

Cerebral amyloid angiopathy–related inflammation (CAA-RI) represents an uncommon but increasingly recognized subset of cerebral amyloid angiopathy (CAA). CAA results from amyloid-β deposition in cortical vessels and is a major cause of intracranial hemorrhage and cognitive decline in the elderly. CAA-RI occurs in a subset of patients with CAA and is characterized by an autoimmune inflammatory response to amyloid deposits. Patient presentation is variable. Clinical features incorporated in the diagnostic criteria include acute to subacute cognitive decline, behavioral changes, headaches, focal neurological deficits, seizures, and encephalopathy.

While CAA is a progressive condition not typically responsive to disease modifying therapy, patients with CAA-RI can have significant clinical improvement with immunosuppressive agents, underscoring the need for prompt diagnosis and treatment. Unfortunately, diagnosis may be difficult as clinical and imaging features often overlap with other entities including PML, meningoencephalitis, CNS vasculitis, PRES, or neoplasm. Additionally, CAA-RI is relatively uncommon and only recently well-described, and some clinicians and radiologists may be unfamiliar with this disease.

Through this exhibit, we review the clinical presentation and spectrum of neuroimaging findings in CAA-RI, which may improve diagnostic accuracy and help expedite appropriate treatment. We also highlight differential considerations and diagnostic pitfalls in the neuroimaging of these patients.

Purpose

Through this exhibit, we review the spectrum of neuroimaging and clinical findings seen in CAA-RI through a case series from our institution in hopes of increasing familiarity with this uncommon, but potentially treatable disease.

Materials & Methods

A literature review was conducted by searching the PubMed database for studies focused on the imaging and treatment of CAA and CAA-RI. CT, MRI, and amyloid PET-CT studies from 18 patients from our institution with clinically diagnosed CAA-RI were reviewed. Patients with neuroimaging findings most characteristic of CAA-RI were selected.

Results & Conclusion

Clinical and imaging diagnosis of CAA-RI is often challenging, but identification of certain MRI findings may strongly suggest the diagnosis. Diagnostic criteria were recently developed to identify patients with either “possible” or “probable” CAA-RI without the need for a brain biopsy. Clinical diagnostic criteria include the presence of typical presenting symptoms (discussed in the introduction section) in patients over the age of 40. Diagnostic imaging criteria relies on identification of typical MRI features. The neuroimaging hallmark includes asymmetric, subcortical white matter

vasogenic lesions with gyral swelling and adjacent sulcal effusions. These vasogenic lesions most often involve the posterior cerebral hemispheres and may correspond to areas of microhemorrhage. Leptomeningeal enhancement overlying white matter lesions may also suggest diagnosis. At least one hemorrhagic finding is required for diagnosis of CAA-RI. These hemorrhagic lesions are also characteristic of non-inflammatory CAA and include lobar hemorrhage, microhemorrhage, and cortical superficial siderosis. Hemorrhagic findings tend to be more profound in patients with CAA-RI compared to those with non-inflammatory CAA. These key imaging features are highlighted through our case series.
Early imaging diagnosis is critical for prompt treatment, which can lead to substantial clinical and radiologic recovery. Neuroradiologists play a central role in differentiating CAA-RI from mimics and guiding management in this severe yet treatable neuroinflammatory condition.
Images/Tables

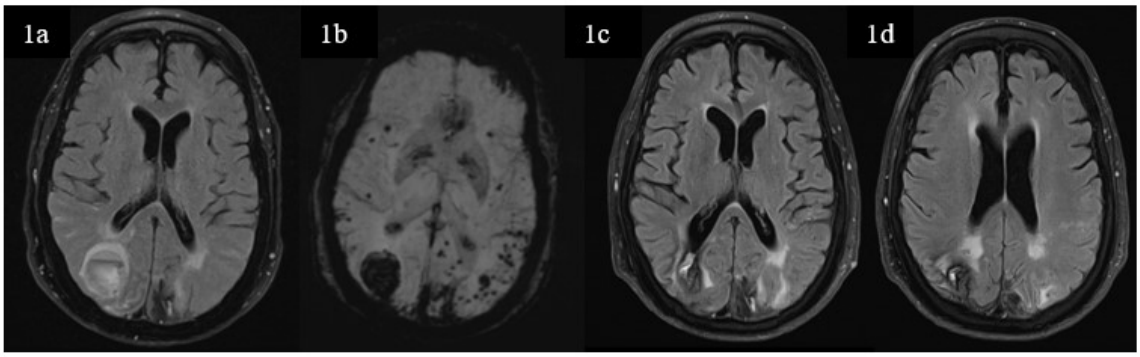

T2 FLAIR (1a) and SWI (1b) images from a 76-year-old male patient with CAA-RI demonstrate acute parenchymal hemorrhage in the right occipital lobe with adjacent subarachnoid blood products. Background parenchyma shows multifocal microhemorrhage with corresponding areas of gyral swelling in the bilateral temporooccipital lobes.

5-month follow up T2 FLAIR images (1c,1d) show remote right occipital hemorrhage and new areas of signal hyperintensity involving the subcortical white matter through the left occipital lobe at site of prior gyral swelling.

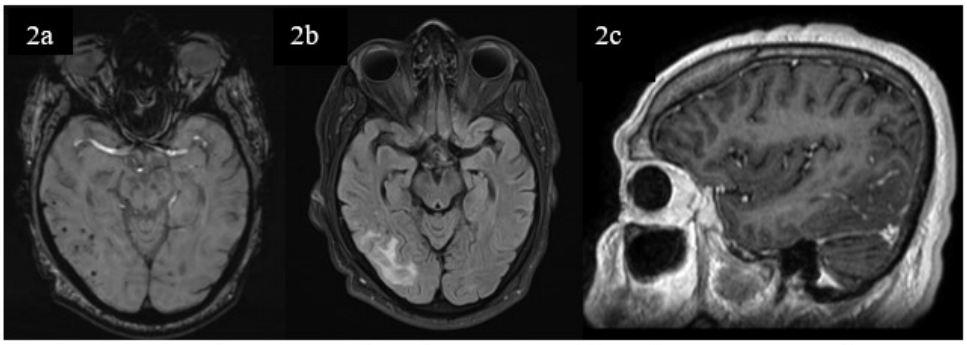

SWI (2a) from a separate patient shows multiple microhemorrhages in the right temporal lobe with corresponding T2 FLAIR (2b) subcortical white matter hyperintensity. Post-contrast T1 images (2c) show leptomeningeal enhancement involving the right temporal lobe.

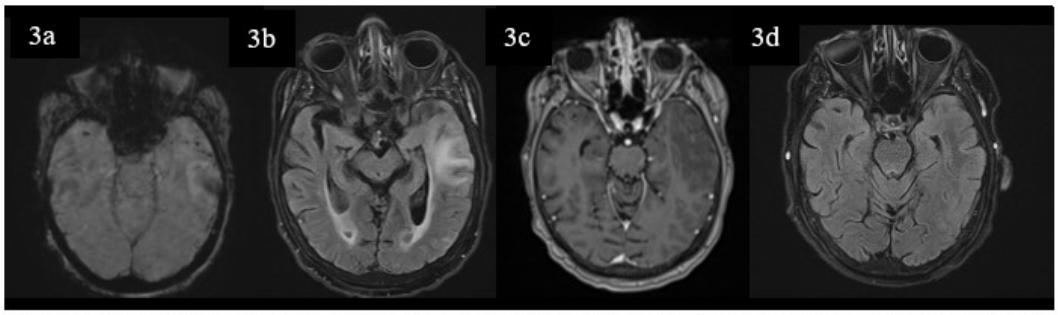

SWI (3a) from a 77-year-old female patient shows few microhemorrhages in the left temporal lobe with corresponding T2 FLAIR (3b) subcortical white matter hyperintensity and subtle leptomeningeal enhancement (3c). There is a sulcal effusion overlying the posterior left temporal lobe (3b).

3-month post-treatment MRI (3d) demonstrates a positive treatment response with resolution of white matter changes, gyral swelling, and sulcal effusions.

606 Mapping Cerebral Microbleeds: Etiologies, Patterns, and the future of Automated Detection.

Gabriel Virador MD, Donna Parizadeh MD, Abiel Habtezghi MD, Adam Averbuch, Christian Pedersen
MCMC-Trinity Health MidAtlantic, Darby, PA, USA

Summary & Objectives

- **Definition & Imaging Features:** Cerebral microbleeds (CMBs) are small, generally 2-10 mm, focal hemosiderin/chronic blood product deposits, seen as hypointense round foci on GRE T2*-weighted or susceptibility-weighted (SWI) MRI.
- **Epidemiology & Common Causes:** CMBs occur in up to 17% of healthy elderly subjects and even more frequently in stroke or dementia patients. Typical etiologies include hypertensive arteriopathy and cerebral amyloid angiopathy, with demographic and genetic factors influencing their prevalence.
- **Uncommon Etiologies:** Less common causes of CMBs include embolic events, genetic vasculopathies, vascular malformations, coagulopathies, trauma, and even obstructive sleep apnea (OSA). Notably, recent prospective data suggest that moderate-to-severe OSA independently doubles the long-term risk of developing new CMBs.
- **Imaging Patterns:** CMB distribution provides diagnostic clues: strictly lobar (cortical) microbleeds often indicate amyloid angiopathy, whereas deep white matter/basal ganglia/brainstem CMBs are usually associated with hypertensive small-vessel disease. In the cerebellum, strictly superficial (cortical/vermal) microbleeds strongly associate with amyloid pathology.

Purpose

Cerebral microbleeds (CMBs) are increasingly recognized neuroimaging markers of small-vessel brain disease. This educational review is designed to aid in identifying and interpreting CMBs based off their distribution and appropriate clinical context. We will summarize MRI detection techniques and lesion appearance, outline epidemiology and etiologies, and illustrate representative cases. We will also highlight atypical etiologies, such as emerging evidence that moderate-to-severe OSA may increase incident CMB risk. Finally, we will review recent AI-driven efforts to detect and quantify CMBs.

Materials & Methods

Representative cases of CMBs were chosen to illustrate a range of CMB distributions (lobar, deep, cerebellar), predominantly from our institution's imaging archive. In parallel, we performed a narrative literature review of CMB prevalence, risk factors, etiologies, emerging associations and strategies for detection automation.

Results & Conclusion

We provide illustrative examples of common CMB patterns consistent with known etiologies such as amyloid angiopathy, hypertension, and embolic events. These examples reinforce that CMB distribution suggests underlying small-vessel pathology, but can also be secondary to other atypical causes. For instance, recent data show moderate-to-severe OSA roughly doubles the 8-year risk of new CMBs, implying sleep apnea may contribute to microvascular brain injury. Clinically, a higher CMB burden predicts stroke recurrence, so identifying CMBs on MRI has prognostic and management implications. Recent efforts are underway by multiple groups to automate the detection of CMBs, including across longitudinal scans and identifying the anatomic location. Educating radiologists about CMB imaging features and etiologies is essential for accurate diagnosis, appropriate clinical care and guiding future research.

Images/Tables

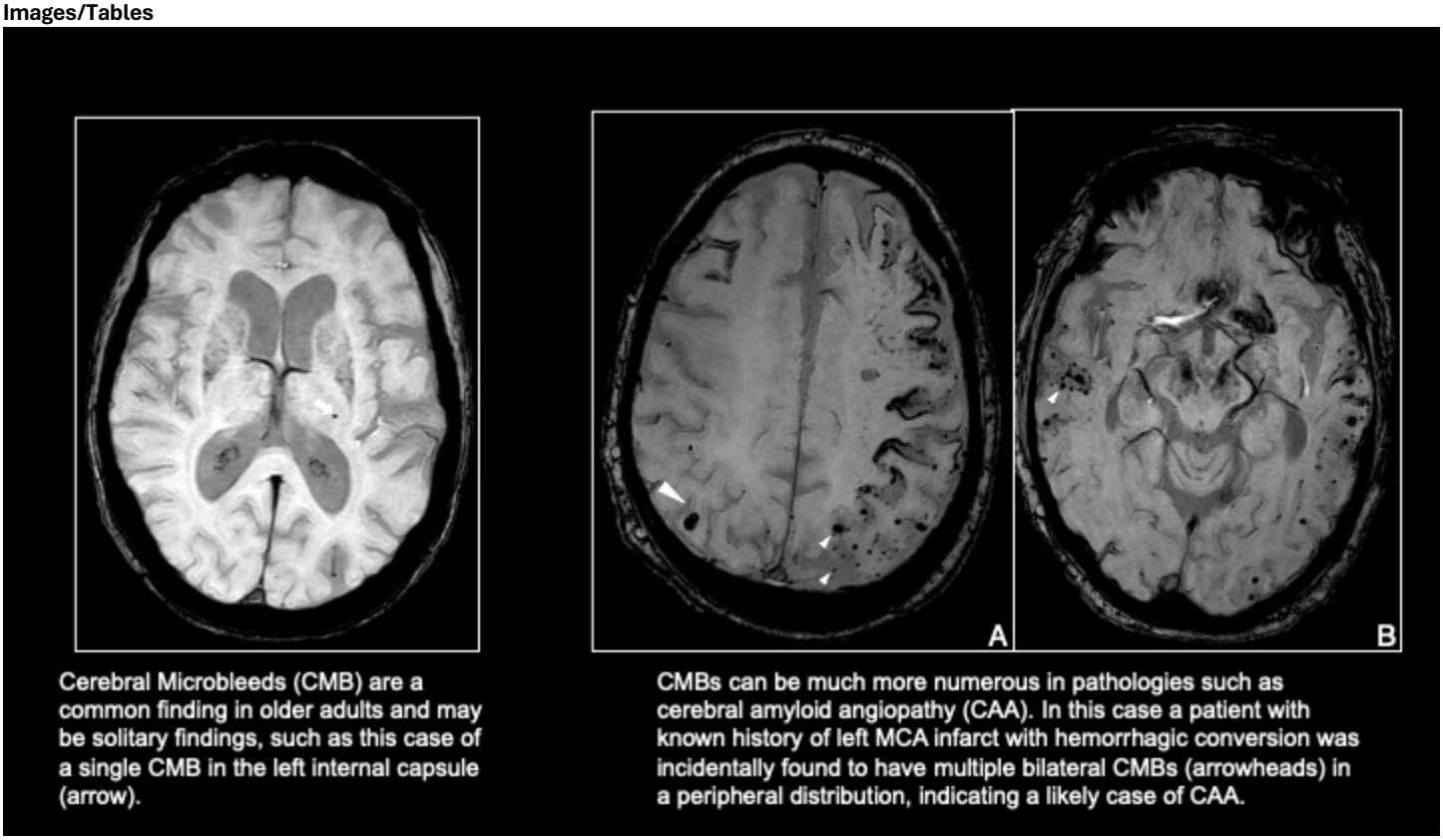

Cerebral Microbleeds (CMB) are a common finding in older adults and may be solitary findings, such as this case of a single CMB in the left internal capsule (arrow).

CMBs can be much more numerous in pathologies such as cerebral amyloid angiopathy (CAA). In this case a patient with known history of left MCA infarct with hemorrhagic conversion was incidentally found to have multiple bilateral CMBs (arrowheads) in a peripheral distribution, indicating a likely case of CAA.

674 A Primer on Laser Interstitial Thermal Therapy and Radiological Findings in Pediatric Patients

Bryan Chan MD, Alan Johnson MD
Northwell Health, Manhasset, New York, USA

Summary & Objectives

Educational Objectives:
* Introduce laser interstitial thermal therapy (LITT) and its application in various intracranial pathologies in pediatric patients
* Describe the sequences obtained during MRI real-time guidance of LITT
* Utilize case examples to review imaging findings pre-treatment, during treatment, and post treatment
* Highlight the evolution of post-treatment changes over time after LITT

Summary:

Laser interstitial thermal therapy (LITT) is a minimally invasive method which utilizes lasers and thermal energy for treatment of intracranial tumors and other pathologies. With the aid of real-time MRI imaging as guidance, this allows for a less invasive approach for lesions that are not surgically accessible or associated with high surgical risk. Retrospective studies have shown LITT to be an effective option for treatment of multiple pathologies including primary tumors, radiation necrosis, and metastasis.[1] In the pediatric population specifically, LITT has shown success in treatment of seizures in cases of hypothalamic hamartomas and has recently started gaining popularity in treatment of intracranial tumors.[2,3] With on-going research to evaluate long-term morbidity and effects and continued increase in clinical practice, knowledge of the imaging findings of a patient on LITT is important to help guide follow-up and ensure successful treatment. This education exhibit aims to introduce LITT, its applications, imaging sequences, and imaging findings throughout treatment with a focus on pediatric applications.

MRI plays a critical role for LITT and serves as the foundation for guidance throughout treatment. Both pre-ablation and post-ablation images are obtained, with specific sequences respectively. Initially, T1 sequences are obtained for localization and positioning of the laser device. Immediately after ablation, typically, post-contrast MRI is performed with additional sequences including T2 Flair and diffusion-weighted sequences. Commonly, there is enhancement and increased diffusion signal within the treatment region after ablation.[4] In addition, susceptibility weighted images demonstrate blooming artifact, suggestive of hemorrhagic products. Regular follow-up imaging with MRI status post LITT is also essential as the post-ablation treatment changes evolve over time. There are expected changes in the lesion cavity, enhancement pattern, and surrounding edema, with enhancement persisting months after treatment.[2]

Although still limited, LITT continues to increase in usage in recent years. Knowledge and understanding of this treatment option and associated radiological findings is essential as research and use of LITT continues to expand.

Purpose

This educational exhibit aims to review the application of laser interstitial thermal therapy in pediatric patients for multiple intracranial pathologies and illustrate imaging findings throughout treatment.

Materials & Methods

Using Northwell Health case database, multiple cases will be used for this exhibit. Pre-treatment, during treatment, and post-treatment follow-up scans will be utilized as teaching points to discuss expected and unexpected findings and changes over time.

Results & Conclusion

Laser Interstitial Thermal Therapy is an emerging treatment option in the pediatric population for various intracranial pathologies including tumors, hypothalamic harmatomas, and seizure foci. Post-ablation images demonstrate expected enhancement, diffusion restriction, and edema which slowly resolves over time. Recognizing both expected and unexpected imaging findings as a radiologist provides useful clinical information to notice early suspicion for recurrent disease and help guide proper follow-up management.

Images/Tables

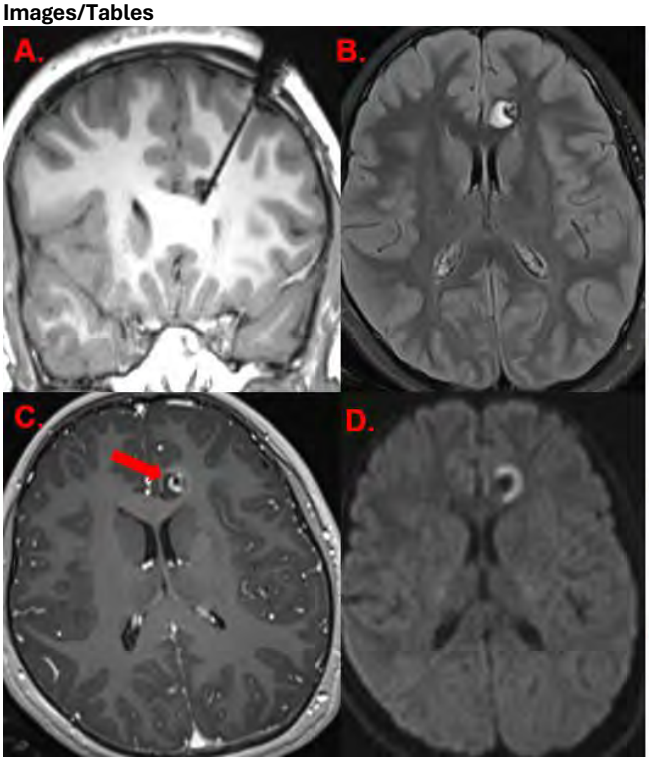

Case example of Laser Interstitial Thermal Therapy for a left frontal lobe lesion.

A. Coronal T1 Image demonstrates the laser device probe within a T1 hypointense lesion in the left frontal lobe.
B. Axial T2 Flair post ablation images shows hyperintense signal surrounding the lesion, suggestive of edema.
C. Axial T1 Post contrast images shows enhancement within the lesion cavitary and peripherally.
D. DWI sequences post ablation demonstrates a ring of increased diffusion signal

689 Imaging Evaluation of Congenital Paraspinal Masses: Differentiating Benign from Malignant Lesions

Julia Brown MD, Fatemeh Dehghani Firouzabadi MD, Ramin Hamidi DO, MSc, MBA
University of Louisville, Louisville, Kentucky, USA

Summary & Objectives

Congenital paraspinal malignancies are extremely rare, with an estimated incidence of 1.7 to 13.4 cases per 100,000 live births. Early detection is challenging because these lesions often resemble benign congenital masses or malformations, making accurate diagnosis difficult.

Purpose

The purpose of this educational exhibit is to review our institutional experience with congenital paraspinal masses and to highlight imaging features that help differentiate benign from malignant lesions.

Materials & Methods

This retrospective review of congenital paraspinal masses was obtained using multiple imaging modalities. Ultrasound was used to assess echotexture, calcifications, and lesion characteristics, while MRI evaluated diffusion restriction, fibrous signal patterns, lesion homogeneity, and local invasion. Multimodality correlation was employed to enhance diagnostic accuracy. Lesions were categorized as benign, including teratomas, lipomas, hemangiomas, neurenteric cysts, neurofibromas, and myofibromas, vs malignant lesions, such as neuroblastomas, sarcomas, and atypical teratoid/rhabdoid tumors, based on imaging features and clinical data. (Figure 1)

Results & Conclusion

The review demonstrated distinct imaging patterns between benign and malignant lesions. Benign masses typically exhibited well-defined margins, homogeneous composition, and minimal local extention. Malignant lesions, in contrast, often presented with heterogeneous signal characteristics, calcifications, restricted diffusion, and demonstrated evidence of surrounding tissue invasion. Multimodality imaging proved particularly useful in detecting and characterizing lesions, even in complex or atypical cases, allowing differentiation that was germane in guiding clinical management. Congenital paraspinal masses require a systematic, multimodality imaging approach to accurately distinguish benign from malignant lesions. Recognizing malignant features early enables timely referral and treatment, improving outcomes for affected neonates. Combining ultrasound, MRI, and clinical context provides practical guidance for diagnosis, informs treatment planning, and ensures optimal care in this rare but clinically significant patient population.

Images/Tables

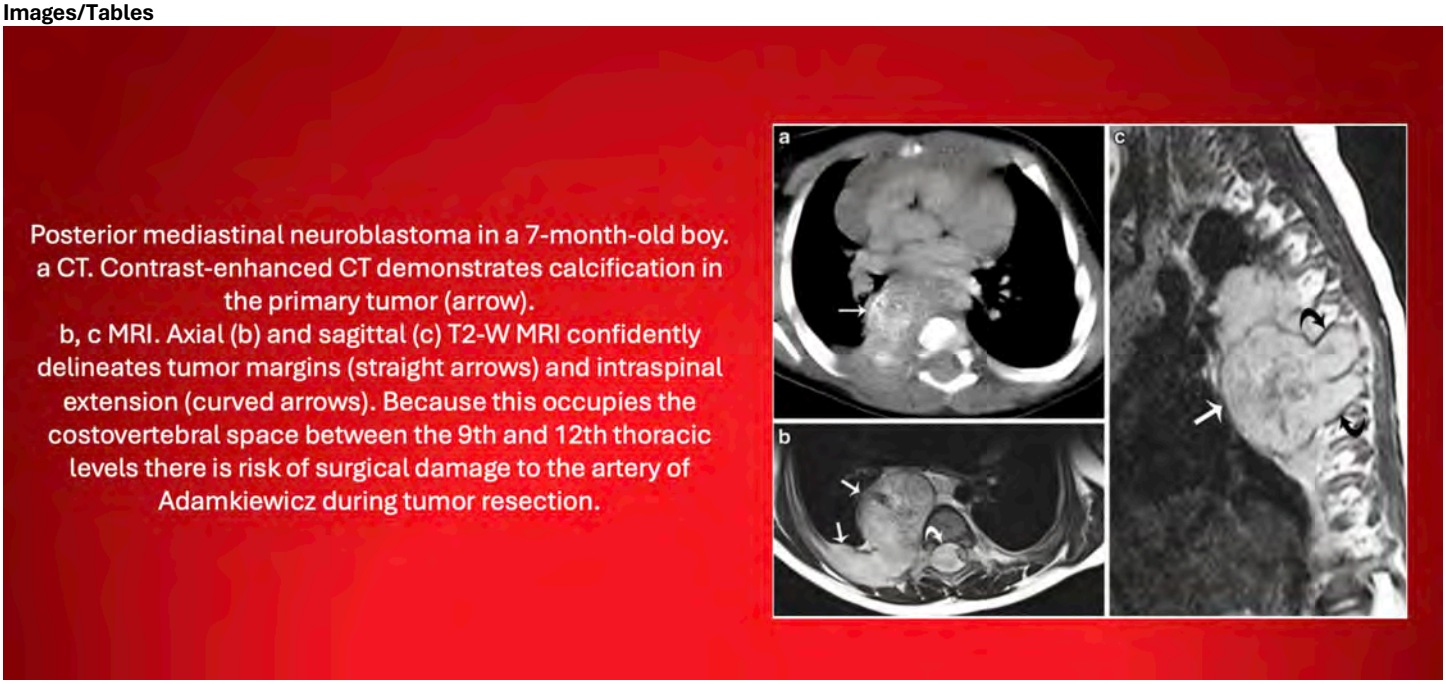

695 Uncommon and Under-recognized Appearances of Glioblastoma Multiforme

Michelle M. Basha MD, Siddhartha Gaddamanugu MD, Aparna Singhal MD
University of Alabama, Birmingham, AL, USA

Summary & Objectives

Glioblastoma multiforme (GBM) is the most common primary malignant intracranial neoplasm in adults. The most characteristic imaging appearance of GBM is a necrotic mass in the cerebral hemispheres with surrounding edema. The differential diagnosis is relatively narrow in cases with typical appearances of glioblastoma multiforme (GBM) mainly metastatic disease and abscess formation. However, the differential diagnosis expands considerably with atypical appearances. Therefore, it is important to recognize uncommon and atypical imaging appearances of GBM and consider it in the differential when appropriate to help patients receive prompt treatment. Delays in diagnosis and treatment can result in significant morbidity and mortality, as GBM is a rapidly growing tumor. This can result in irreversible neurologic damage depending on the area of the brain affected. Diagnosis is ultimately confirmed with biopsy and tissue sampling.

Atypical imaging appearances include non-enhancing mass, non-enhancing infiltrative pattern, focal cortical thickening and absence of surrounding edema. Atypical locations of GBM include basal ganglia, hippocampus. intraventricular, posterior fossa and extra-axial spaces. Differential diagnosis for atypical presentations of GBM is broad and includes cerebral metastasis, CNS lymphoma, cerebral abscess, lower grade astrocytoma, oligodendroglioma, non-tumefactive demyelination, encephalitis and toxoplasmosis (Bruce 2024). Medulloblastoma, ependymoma, and hemangioblastoma are additional tumors to consider in posterior fossa lesions.

Purpose

1. Provide a brief review of molecular and histopathological diagnosis of GBM based on 2021 World health organization (WHO) central nervous system tumor classification.
2. Demonstrate the atypical imaging presentations of biopsy proven GBM in order to help readers understand the wide array of imaging features GBM may demonstrate.
3. Provide a brief synopsis of treatment and management of the tumors presenting with atypical imaging.

Materials & Methods

N/A

Results & Conclusion

Recognition of atypical imaging features of GBM is critical and should be included in the differential diagnosis when appropriate. GBM is the most malignant of all intracranial tumors and prognosis is improved when detected early and treated. Consideration of these features, along with the integration of genetics and pathology, play a critical role in the treatment and prognosis for affected patients.

Images/Tables

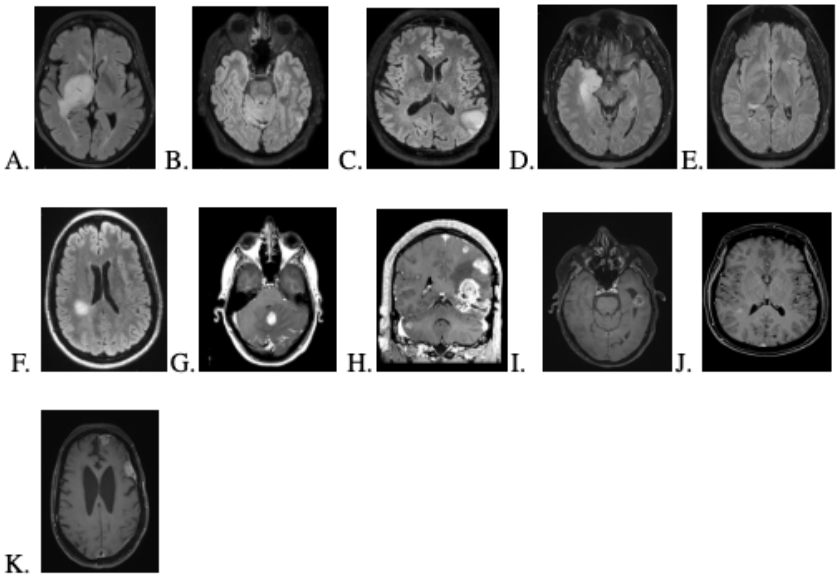

The following are atypical imaging presentations of GBM:

A. Axial FLAIR images reveal well-defined mass which is nonenhancing (not shown) resulting in mild mass effect. Differentials include other low-grade astrocytoma and encephalitis.

B and C. Axial FLAIR images of the brain show slightly expansile lesion within the left temporal lobe with faint peripheral enhancement (not shown). Differential diagnosis includes low-grade cortical tumor, low-grade astrocytoma and encephalitis.

D and E: Axial FLAIR images of the brain demonstrate slightly expansile lesion involving the right amygdala and hippocampus. Differentials include herpes simplex encephalitis, low-grade encephalitis and cortical tumors.

F and J: Axial FLAIR images demonstrate an area of signal abnormality within the corona radiata with no mass effect. Postcontrast images reveal mild enhancement. Differentials include demyelination and CNS lymphoma.

G: Enhancing lesion in the vermis with surrounding edema and mass effect. Differentials include hemangioblastoma and metastasis.

H: Multiple enhancing lesions scattered throughout multiple cerebral lobes and within the posterior fossa. Differentials include primary CNS lymphoma and metastasis.

I and K: Enhancing nodule in the left temporal lobe extending intraventricularly and accompanying multiple dural based enhancing nodules. Differentials include primary CNS lymphoma, metastasis and histiocytosis.

733 Neuroimaging Spectrum of CAR-T Cell Therapy–Associated Neurotoxicity/Complications.

Kamaljeet Singh MBBS, MD, DNB, Carlos Torres MD, FRCPC
The University of Ottawa, Ottawa, Ontario, Canada

Summary & Objectives

Chimeric antigen receptor T-cell (CAR-T) therapy is a novel treatment in refractory B-cell malignancies, yet up to 60 % of patients develop immune effector cell–associated neurotoxicity syndrome (ICANS). Early recognition of imaging and clinical features is critical for prompt management and prevention of irreversible injury.

Purpose

To review the neuroimaging manifestations of ICANS.

Materials & Methods

ICANS arises from cytokine-driven endothelial activation, capillary leak, and blood–brain-barrier dysfunction rather than direct CNS infiltration. MRI findings are often subtle or transient, including diffuse T2/FLAIR cortical–subcortical hyperintensity, thalamic signal alteration, splenial lesions, and leptomeningeal or microhemorrhagic changes on susceptibility imaging. Diffusion restriction in posterior white matter and reversible cytotoxic lesions of the corpus callosum may mimic acute encephalopathies. While conventional CT is usually normal, advanced modalities—SWI, perfusion MRI can reveal microvascular injury and hypometabolic patterns correlating with clinical severity. Timely radiological diagnosis of neurological manifestations of ICANS is important as severe complications can lead to diffuse brain edema, leading to brain herniation and ultimately even death.

Results & Conclusion

Recognition of the radiologic spectrum of CAR-T–related neurotoxicity is crucial for differentiation from infectious, metabolic, or leukemic causes and guiding appropriate therapies.

Images/Tables

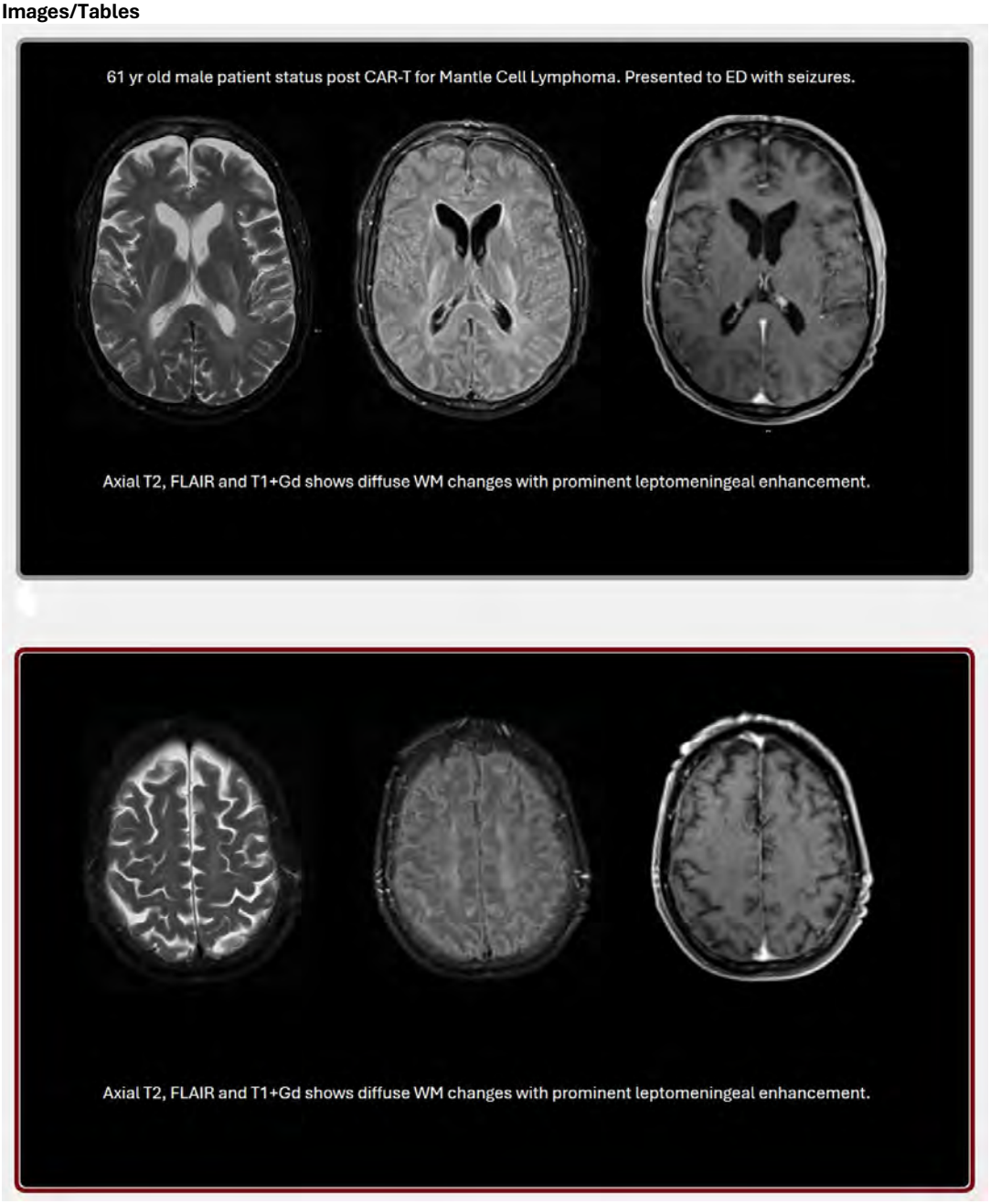

739 A Cortex in Transition: The Imaging Spectrum of Polymicrogyria.

owais ahmad bhat MD[1], Shumyla Jabeen MD,DM[2], Sohaib Mohiuddin MD[1]

[1]University of Louisville, Louisville, Kentucky, USA. [2]Sher-i-Kashmir institute of medical sciences, Srinagar, Jammu AND KASHMIR, India

Summary & Objectives

Polymicrogyria (PMG) is one of the most common malformations of cortical development, often associated with seizures. It may occur in isolation or along schizencephalic clefts, reflecting a continuum of disordered late cortical organisation. The imaging appearance of PMG evolves with myelination, from fine, thin undulations in infants to thickened, irregular cortex in older children and adults. Recognising these patterns is critical for accurate diagnosis and understanding the pathophysiologic spectrum between PMG and schizencephaly.

Purpose

To illustrate the spectrum of imaging appearances of polymicrogyria and its association with schizencephaly across different developmental stages, emphasising how cortical maturation influences imaging morphology.

Materials & Methods

Three patients presenting with seizures were evaluated on MRI.

- **Case A:** Unilateral perisylvian and frontoparietal PMG in an 18-year-old.
- **Case B:** Bilateral open-lip schizencephaly in a 15-month-old.
- **Case C:** Polymicrogyria lining an open-lip cleft in the same patient as B.
- **Case D:** Closed-lip schizencephaly with adjacent PMG and hemiatrophy.

MRI findings were analysed for cortical pattern, cleft configuration, gray–white matter interface, and associated hemispheric volume loss.

Results & Conclusion

Across cases, PMG displayed two imaging patterns:

1. Fine undulating cortex of near-normal thickness (infant pattern).
2. Thickened, irregular cortex with indistinct gray–white junction (mature pattern).

Both patterns were associated with seizures, and schizencephalic clefts were consistently lined by polymicrogyric cortex.

Conclusion:Polymicrogyria and schizencephaly represent a developmental continuum of cortical malformation related to late perinatal insult. The imaging appearance of PMG evolves with cortical myelination, transitioning from fine undulating to thickened irregular morphology. Recognizing these age-related patterns and their coexistence with schizencephalic clefts is essential for accurate diagnosis and understanding of cortical maturation in seizure disorders.

Images/Tables

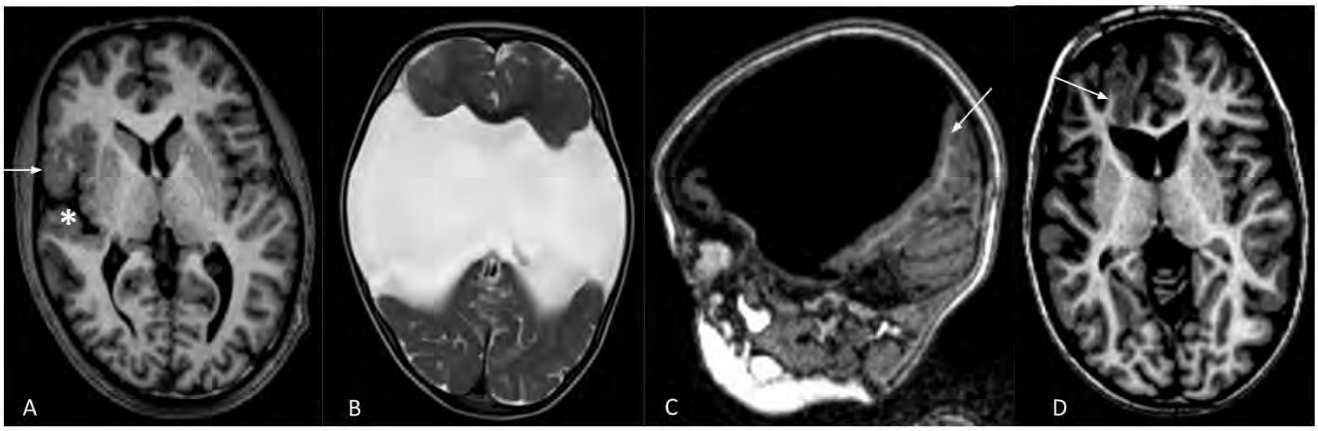

A. **Unilateral perisylvian and frontoparietal polymicrogyria**: Axial T1 MPRAGE in an 18 year old with seizures shows unilateral polymicrogyria along the sylvian fissure (white arrow) extending anteriorly into the frontal cortex. Note the relatively open configuration of the right sylvian fissure (asterisk) on the right compared to the left.

B. **Open lip schizencephaly**: Axial T2 weighted image in a 15 month old female shows bilateral open lip schizencephaly.Note the inconspicuous cortical lining of the cleft on the T2 weighted image.

C. **Polymicrogyria along open lip schizencephaly with normal cortical thickness**: Sagittal T1 MPRAGE in the same patient as B shows thin polymicrogyric gray matter lining the cleft (white arrow).

D. **Polymicrogyria along closed lip schizencephaly with hemiatrophy**: Axial T1 MPRAGE shows polymicrogyric cortex along a cleft with apposed lips extending up to the ventricular margin suggestive of closed lip schizencephaly (white arrow). Surrounding heterotopic gray matter was seen (not shown). Also, note the right hemiatrophy.

992 Prognostic Significance of Nonfunctional Transverse Sinus in Cerebral Sinus Venous Thrombosis

RUTH ELIAHOU MD[1], Jeremy Molad MD[2], Asaf Honig MD[3]

[1]Rabin Medical Center, Petah Tikva, Israel, Israel. [2]Tel Aviv Medical Center, Tel Aviv, Israel, Israel. [3]Soroka Medical Center, Beer Sheva, Israel, Israel

Summary & Objectives

Nonfunctional transverse sinus (NTFS), resulting from marked hypoplasia or atresia, is generally regarded as a normal anatomical variant. Its impact on the clinical course and outcomes of cerebral venous sinus thrombosis (CSVT), however, remains unclear.

Purpose

This study aimed to evaluate the prevalence and prognostic significance of NFTS among patients with CVST.

Materials & Methods

Data from consecutively enrolled patients with CSVT database was retrospectively analyzed. NFTS was defined as a non-thrombosed transverse sinus with severe reduction of the lumen compared to the contralateral side. CSVT Patients with and without NFTS were compared.

Results & Conclusion

Among 443 CSVT patients (mean age 41.4 ± 18.2 years; 64.3% female), 49 (11.1%) had NFTS. NFTS patients had more papilledema compared to non NTFS patients (50.0% vs. 23.0%, p<0.001) and multiple cerebral vein involvement (43.0% vs. 22.0%, p=0.002), with a trend toward fewer excellent outcomes at 90 days (78.0% vs. 87.0%, p=0.067).

In 299 patients with transverse sinus thrombosis (TST), contralateral NFTS (n=29) was associated with higher rates of papilledema (51.3% vs. 24.3%, p<0.001), multiple cerebral vein involvement (51.3% vs. 31.9%, p=0.017), and superior sagittal sinus thrombosis (48.7% vs. 28.9%, p=0.013). NFTS patients with TST had lower rates of excellent outcome (74.4% vs. 89.7%, p=0.006). On multivariable analysis, NFTS independently predicted non-excellent outcome (OR 4.37, 95% CI 1.50–13.0)."

Conclusion: NFTS may impair cerebral venous drainage in CSVT, predisposing to more extensive thrombosis, higher rates of papilledema, and independently predicting poorer functional outcomes in patients with TST.

Images/Tables

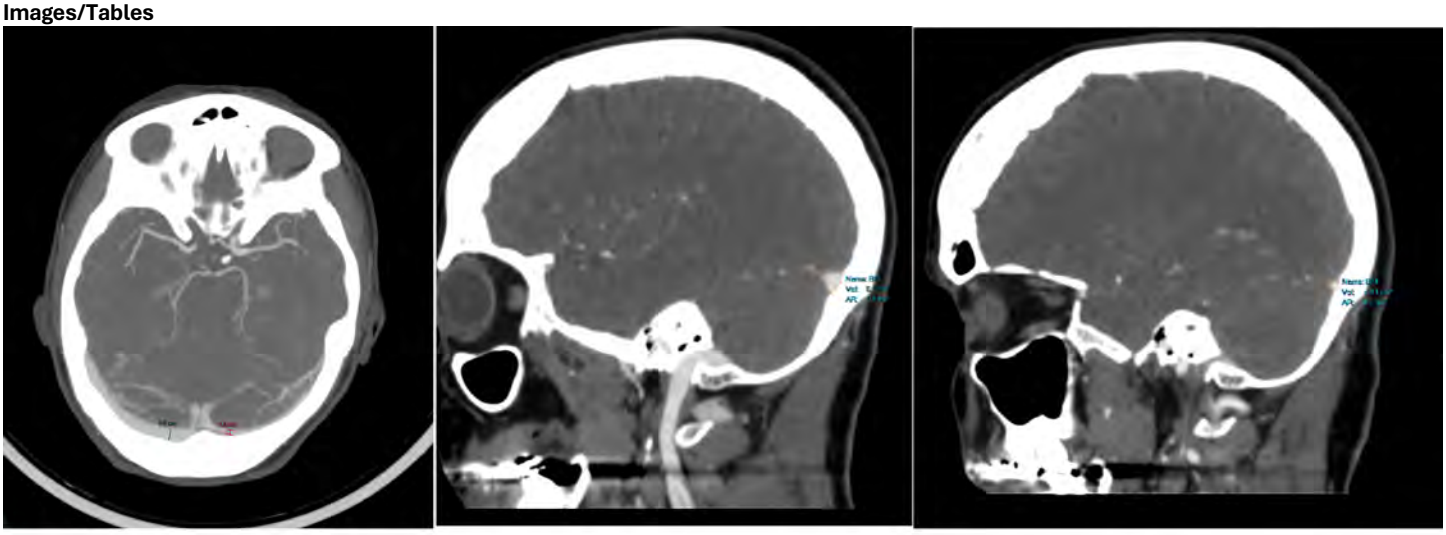

Figure 1- Sagittal post contrast CT angiography image of right and left transverse sinuses: Transverse sinuses are outlined in orange – (A) on the dominant right side- measuring cross-sectional area of 40 mm2 compared to (B) 10 mm2 of the left hypoplastic side. The asymmetry ratio of the hypoplastic to dominant cross-sectional area is 0.25 indicating severe hypoplasia (<0.5).

Figure 2- Axial 3D MIP reconstruction of the hypoplastic left TS measuring 2 mm divided by 6 mm of the dominant sinus – resulting in a diameter ratio of 0.33, indicating marked asymmetry (< 0.5 threshold).

1037 Secondary lymphoma of the central nervous system: an interesting overview

Matheus Carlota, Fernanda Pereira, Barbara Pfluck

Campinas, São Paulo, Brazil

Summary & Objectives

Lymphoproliferative diseases comprise a heterogeneous group of disorders characterized by abnormal proliferation of B and T lymphocytes, encompassing hematologic malignancies such as lymphomas and lymphocytic leukemias, as well as benign and premalignant entities. In the central nervous system (CNS), lymphomas represent about 4% of brain tumors, with higher incidence in men and individuals over 60 years old. Their development is linked to genetic mutations, infections, immunosuppression, and environmental exposures. Clinical presentation varies from asymptomatic cases to systemic and neurological manifestations. Radiological findings differ according to immune status, origin, and disease dissemination pattern. Primary CNS lymphomas typically show single or multiple homogeneous parenchymal lesions, hyperdense on CT, with low T2 signal and restricted diffusion. Secondary CNS lymphomas arise from hematogenous or contiguous spread of systemic neoplasms, exhibiting expansive lesions with mass effect, vasogenic edema, variable contrast enhancement, and diffusion restriction.

Objective: To provide a structured overview of the main radiological patterns of secondary lymphoproliferative diseases involving the CNS and to support radiologists in recognizing their imaging characteristics for earlier diagnosis and better patient outcomes.

Purpose

This study aims to develop an educational and diagnostic reference summarizing the principal imaging findings of secondary lymphoproliferative diseases involving the CNS. The goal is to enhance radiologists' ability to differentiate these lesions from other neoplastic, infectious, or inflammatory processes. Emphasis is placed on the impact of immune status on imaging appearance, the mechanisms of CNS dissemination, and the identification of distinctive MRI and CT patterns. By consolidating radiologic criteria and clinical context, the study seeks to promote early recognition of CNS involvement in patients with systemic lymphoproliferative disorders and to highlight its prognostic relevance.

Materials & Methods

A retrospective descriptive review was conducted using MRI and CT studies from patients with confirmed systemic lymphoproliferative diseases showing secondary CNS involvement. Lesions were evaluated for number, location, morphology, signal characteristics, diffusion patterns, and contrast enhancement. The relationship between imaging findings and clinical variables, such as immune status and disease stage, was analyzed.

Results & Conclusion

Secondary CNS lymphoproliferative diseases most commonly presented as multiple enhancing lesions with mass effect, surrounding vasogenic edema, and restricted diffusion. Enhancement was frequent in periventricular, subependymal, or leptomeningeal regions. Immunosuppressed patients showed more diffuse, infiltrative lesions, while immunocompetent individuals tended to present well-defined masses. Recognition of these imaging features, integrated with clinical and immunological data, proved fundamental for distinguishing secondary lymphomas from other CNS pathologies.

Conclusion: Understanding the radiologic spectrum of secondary lymphoproliferative diseases in the CNS is crucial for accurate and early diagnosis. Familiarity with their imaging characteristics enables more confident interpretation, supports timely therapeutic decisions, and ultimately contributes to improved patient prognosis.

Images/Tables

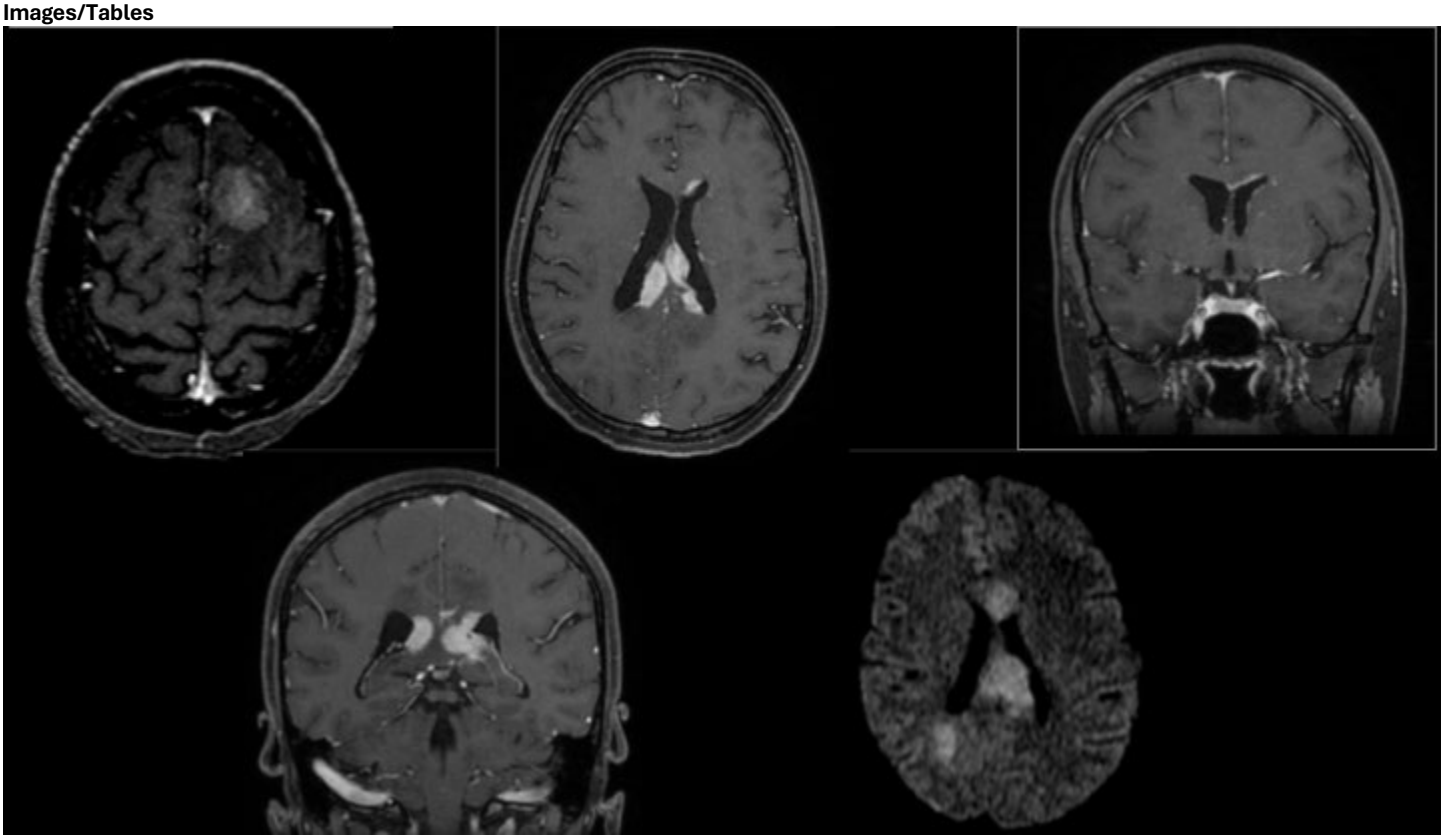

1072 Beyond Evans Index: Quantitative Imaging Biomarkers and a Novel Distance for Ventricular Volume Estimation

Mario Mahecha MD[1], Santiago Aristizabal-Ortiz MD[1], Laura Ocasio MD[2], Winston Zingg[1], David Timaran MD, MSCS[1], Andres Rodriguez MD[1], Andres Felipe Mejia MD[3], Juan Camilo Ricardo MD[4], Valeria Ortega MD[5], Roy Riascos[1]

[1]The University of Texas Health Science Center at Houston, Houston, Texas, USA. [2]Memorial Herman Hospital, Houston, Texas, USA. [3]Fundación Cardioinfantil, Bogota, Bogota, Colombia. [4]Universidad del Rosario, Bogota, Bogota, Colombia. [5]Baylor College of Medicine, Houston, Texas, USA

Summary & Objectives

Summary:

Accurate assessment of ventricular size is essential in disorders such as hydrocephalus, idiopathic normal-pressure hydrocephalus (iNPH), and neurodegenerative disease. Although full volumetric analysis remains the reference standard, it is often impractical for routine use due to time and resource demands. Consequently, radiologists rely on surrogate imaging biomarkers, ranging from simple linear indices to advanced morphological and volumetric ratios to estimate ventricular volume efficiently and reproducibly. This educational exhibit introduces a novel linear measurement, the Calloso-Forniceal Distance (CFD), designed to complement existing indices and provide a theoretically grounded surrogate for ventricular volume.

Objectives:

- To review surrogate imaging biomarkers used for estimating ventricular size.
- To summarize both linear and advanced imaging approaches, emphasizing their radiologic basis and correlation with volumetric standards.
- To evaluate their reproducibility, efficiency, and diagnostic value in clinical practice.

Purpose

This exhibit review radiologic evidence on linear and advanced biomarkers that serve as surrogate measures of ventricular volume in adults, introducing the Calloso-Forniceal Distance as a practical addition to existing measurements. It highlights how combining classic indices with AI-enhanced volumetry can streamline ventricular assessment and improve diagnostic confidence in everyday radiology practice.

Materials & Methods

A narrative review of PubMed-indexed, English-language studies (2013-2025, plus foundational works) was conducted to identify validated surrogate imaging biomarkers of ventricular volume. Included studies proposed or compared indices such as the Evans Index, Bicaudate Index, Frontal-Occipital Horn Ratio, Callosal Angle, z-Evans Index, and ventricular-to-intracranial volume ratios against volumetric benchmarks. The novel Calloso-Forniceal Distance was conceptually analyzed and illustrated as a complementary measure within this framework.

Results & Conclusion

Linear indices such as the Evans and Bicaudate ratios remain the most widely used surrogates, demonstrating strong correlations and high reproducibility on both CT and MRI. Advanced biomarkers, including the Callosal Angle and z-Evans Index, captures three-dimensional ventricular morphology and aid in distinguishing hydrocephalus from atrophy. The Calloso-Forniceal Distance suggests that it reflects vertical expansion patterns of the lateral ventricles features underrepresented by anterior-posterior indices. Volumetric ratios are a alternative, while emerging AI tools promise automated, rapid volumetric estimation. Together, these surrogate biomarkers provide efficient, reliable, and scalable alternatives to full volumetry without compromising diagnostic precision.

Images/Tables

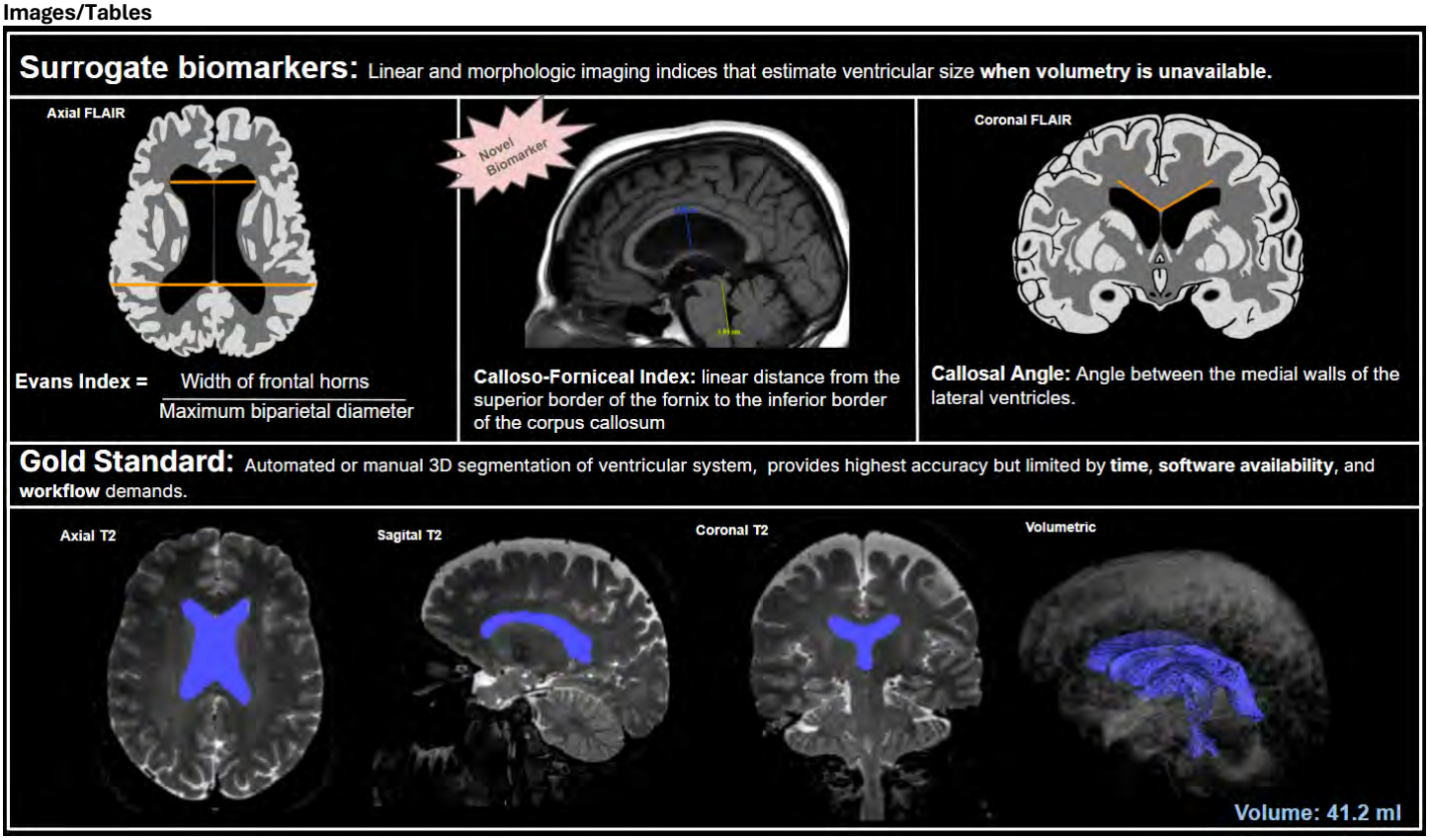

1145 Simplified Imaging Based Approach to Updated 2021 WHO Classification of CNS Tumors of the Pediatric Age Group: What Neuroradiologists Must Know

Adam L Stroh DO[1], Rajan Patel MD[2]

[1]Neuroradiology Fellow, UTHealth Houston, Houston, Texas, USA. [2]Staff Pediatric Neuroradiologist, Associate Professor of Radiology,Texas Children's Hospital, Baylor College of Medicine, Houston, Texas, USA

Summary & Objectives

Summary:

The 4th Edition of the 2016 WHO Central Nervous System (CNS) tumor classification marked a significant shift by beginning to incorporate molecular features into tumor assessment. This edition introduced an integrated approach of layered tumor reports that combined both histological and molecular data for more precise diagnosis.

Building on these advancements, the 5th Edition WHO CNS tumor update released in 2021 presents a more refined and sophisticated classification system. This update enables clinicians to group CNS tumors into more biologically and molecularly defined entities.

This refined classification has important implications for clinical research, as it may impact subject enrollment, treatment assignment, and outcome stratification in clinical trials. Neuroradiologists must familiarize themselves with the updated 2021 WHO Classification of CNS neoplasms, especially for the pediatric age group, to function appropriately as part of the multidisciplinary neuro-oncology clinical team.

Objectives:

1. We aim to emphasize the major changes of the 2021 WHO Classification of CNS Tumors that mainly affect the children and young adults age group.
2. To present the clinical and molecular characteristics of these tumors.
3. To demonstrate the neuroimaging features on multidisciplinary basic as well as advanced MRI modalities.

Purpose

N/A

Materials & Methods

N/A

Results & Conclusion

N/A

Images/Tables

Tumor Type	Major Molecular Designations in WHO CNS5
Diffuse astrocytoma	MYB-altered; MYBL1-altered
Diffuse low-grade glioma (LGG)	MAPK pathway-altered
Diffuse midline glioma	H3 K27-Altered
Diffuse hemispheric glioma	H3 G34-mutant
Diffuse pediatric-type high-grade glioma (HGG)	H3 wildtype and IDH wildtype
Astroblastoma	MN1-altered
Supratentorial ependymoma	ZFTA fusion+; YAP1 fusion+
Posterior fossa ependymoma	Group PFA; Group PFB
Spinal ependymoma	MYCN-amplified
Medulloblastoma	WNT activated; SHH activated and TP53-wildtype; SHH-activated and TP53-mutant; non-WNT/non-SHH
Atypical teratoid/rhabdoid tumor (AT/RT)	ATRT-TYR; ATRT-SHH; ATRT-MYC
Embryonal tumor with multilayered rosettes (ETMR)	C19MC-altered; DICER1-mutant
CNS neuroblastoma	FOXR2-activated
CNS tumor with BCOR internal tandem duplication	BCOR internal tandem duplication
Intracranial mesenchymal tumor	FET-CREB fusion+
CIC-rearranged sarcoma	CIC-rearranged
Primary intracranial sarcoma	DICER1-mutant

---

110 MRI Fingerprints of Gliomas: The Power of T2/FLAIR Mismatch and VASARI Criteria- The First study from low middle income country

fatima mubarak MBBS, Sheheryar Ahmed MBBS
Aga Khan university hospital, karachi, sind, Pakistan

Summary & Objectives

Low-grade gliomas (LGGs, WHO grade I–II) are biologically heterogeneous, with IDH mutation status serving as a key prognostic marker. While histopathology is the gold standard, its invasive nature and limited availability highlight the need for non-invasive imaging biomarkers. The T2/FLAIR mismatch sign has emerged as a radiogenomic marker for IDH-mutant astrocytomas, and structured tools like the VASARI criteria may enhance reproducibility in imaging assessment.

Purpose

To evaluate the diagnostic accuracy of the T2/FLAIR mismatch sign and conventional MRI features for predicting IDH mutations in low grade gliomas, and to assess tumor spread patterns using VASARI criteria.

Materials & Methods

Fifty-two patients with histologically confirmed gliomas (2022–2024) at Aga Khan University Hospital underwent preoperative 1.5T/3T MRI. Two neuroradiologists independently assessed T2/FLAIR mismatch, necrosis, margins, enhancement, and VASARI-defined spread features. Molecular profiling (IDH1/2, ATRX, p53) followed WHO 2021 guidelines. Diagnostic performance was compared against molecular testing.

Results & Conclusion

Results: IDH-mutant gliomas more frequently demonstrated T2/FLAIR mismatch (58.3% vs 10.7%, p<0.001), smooth margins (75% vs 32.1%, p=0.012), and less necrosis (20.8% vs 53.6%, p=0.02). The multivariate imaging model achieved excellent diagnostic accuracy (AUC=0.892; sensitivity 86.2%; specificity 88.9%). VASARI-based analysis showed IDH-mutant tumors had less aggressive spread, with lower rates of midline crossing (14.3% vs 47.6%, p=0.03) and ependymal extension (11.9% vs 38.1%, p=0.041).

Conclusion: T2/FLAIR mismatch, complemented by VASARI criteria, provides a robust, non-invasive strategy for predicting IDH mutation in LGGs. This approach supports prognostication, guides treatment planning, and offers a cost-effective surrogate for molecular testing, particularly valuable in resource-limited settings.

Images/Tables

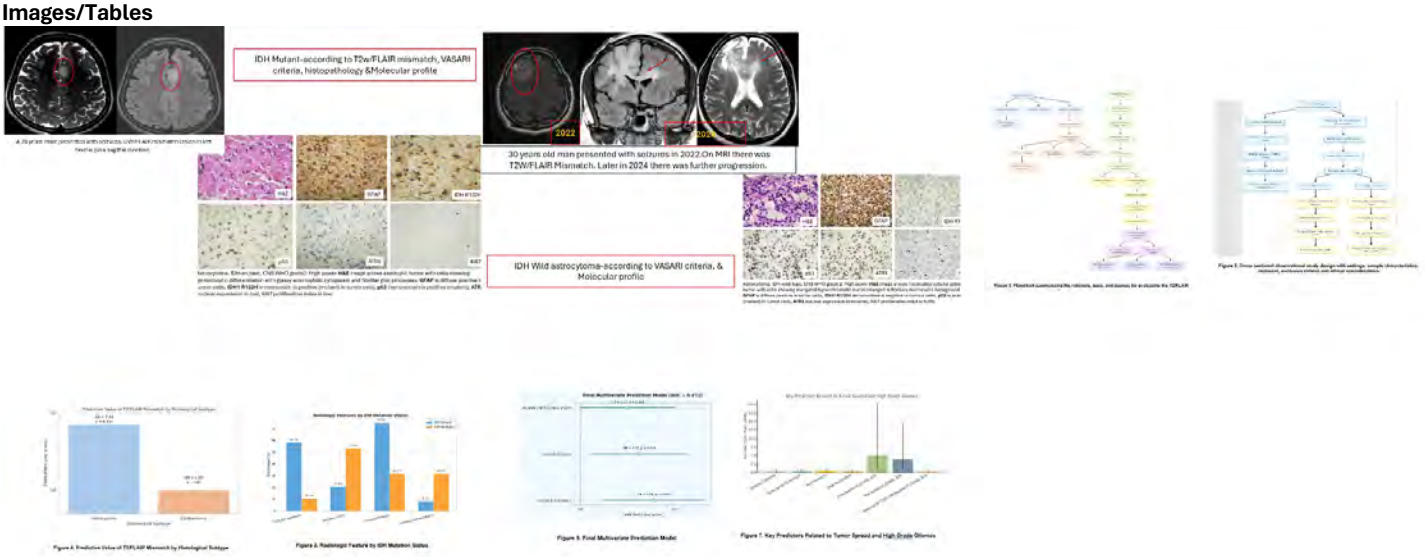

---

114 Stratification of Brain Tumours: Glioma vs Non-Glioma Using a Lightweight ResNet-Based Approach on 3D MRI Data

fatima mubarak MBBS
aga khan university hospital, karachi, sind, Pakistan

Summary & Objectives

Advances in medical imaging have increased the need for efficient analysis of large-scale brain tumour data. The World Health Organisation classifies glioma tumours as low grade (LGG) or high grade (HGG), which pose extra hurdles due to their unique features. To approach each patient with the best plan possible for a better outcome post-surgery, specifically for the accurate classification of glioma and non-glioma tumours. The challenge is compounded by the limited availability of publicly accessible 3D MRI datasets for non-glioma cases and the complexities involved in preprocessing high-dimensional MRI data.

Purpose

This study aims to develop a pipeline for classifying glioma and non-glioma tumors using 3D brain MRI scans. The approach utilizes a lightweight modified ResNet model to enhance diagnostic accuracy and address existing gaps in current research.

Materials & Methods

This study introduces a comprehensive pipeline that includes preprocessing steps such as standardisation, co-registration, skull stripping, and removal of extracranial elements, utilizing techniques like N4ITK bias correction and the SRI-124 template. A lightweight modified ResNet model was developed for classifying glioma vs non-glioma tumours, trained on a private dataset that combines high-field MRI scans. The approach emphasises model efficiency with fewer trainable parameters while maintaining high classification performance.

Results & Conclusion

The proposed model achieved an overall accuracy of 81.45%, with a test loss of 0.9178, a recall of 1.0000, a precision of 0.8287, an F1 score of 0.9063, and an ROC-AUC of 0.6000. These results indicate strong performance, particularly in identifying glioma tumours, demonstrating the effectiveness of the preprocessing pipeline and the lightweight model in brain tumour classification. This research underscores the importance of robust preprocessing and efficient model design in brain tumour classification. The lightweight modified ResNet provides a promising direction for accurate and resource-effective diagnosis, addressing current gaps in available datasets and model complexity. The pipeline lays a foundation for further automation and clinical application in early brain tumour detection.

Images/Tables

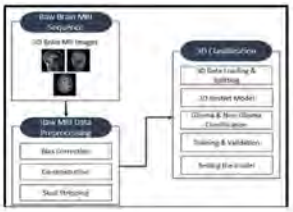

FIG 1: Proposed 3D Model: Illustrates the process of 3D brain MRI classification

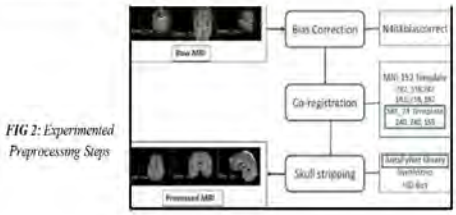

FIG 2: Experimented Preprocessing Steps

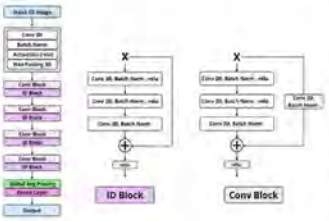

FIG 3: ResNet Architecture: 3D CNN. 3D images pass through layers of convolution, batch normalization, and ReLU activation, finishing with global average pooling and a dense layer for the final output.

FIG 4: Comparison of test losses across Our Model, 3D CNN, and Dilated CNN

Model	Trainable Parameters	Random state=42, lr_rate, Epochs	Samples (GliomaVsNonGlioma)	Metrics on Best Model
Our Model: ResNet (Modified)	347,553	Yes , 0.0002 , 40	275 vs 88 Flair and T1ce both	Val_Accuracy: 1.000 Validation_Loss: 0.0757 Test_Accuracy: 1.000 Test_Recall: 1.000 Test_Precision: 1.000. Test_F1 Score: 1.000 Test_ROC-AUC: 1.000
Our Model: ResNet (Modified)	347,121	Yes , 0.0002 , 40	257 vs 157	Val_Accuracy: 0.8145 Test_Loss: 0.9178 Test_Accuracy: 0.7143 Test_Recall: 1.0000 Test_Precision: 0.8287 Test_F1 Score: 0.9063 Test_ROC-AUC: 0.6000
3D CNN [17]	3,689,986	Yes , 0.0003 , 40	257 vs 157	Val_Accuracy: 0.9016 Test_Loss: 17.7457 Test_Accuracy: 0.6190 Test_Recall: 0.6190 Test_Precision: 0.6593 Test_F1 Score: 0.6156Test_ROC-AUC: 0.6296
Dilated 3D CNN [4]	27,336,310	Yes / 0.00001 / 40	257 vs 157	Val_Accuracy: 0.8307 Test_Loss: 3.7358 Test_Accuracy: 0.7143 Test_Recall: 0.7143 Test_Precision: 0.6984Test_F1 Score: 0.7056Test_ROC-AUC: 0.7143

***Table 1:** Validation test scores*

---

192 **Diagnostic Performance of DWI and ADC parameter in Differentiating Brain Abscess from Malignant Ring-Enhancing Brain Lesions: A Systematic Review and Meta-Analysis**

Saeed Mohammadzadeh[1], Zahra Moradi[1], Alisa Mohebbi[1], Houman Sotoudeh[2]
[1]Tehran University of Medical Science, Tehran, Tehran, Iran, Islamic Republic of. [2]The University of Texas Southwestern Medical Center, Dallas, Texas, USA

Summary & Objectives
Despite the critical need for accurate diagnosis, conventional MRI often fails to reliably distinguish brain abscesses (BA) from malignant ring-enhancing lesions (REBL). Consequently, advanced MRI techniques like Diffusion-Weighted Imaging (DWI) and its quantitative biomarker, the Apparent Diffusion Coefficient (ADC), have emerged as essential tools for improving diagnostic confidence.
Purpose
In this systematic review and meta-analysis we aimed to assess the performance of DWI and ADC in the differentiation of BA from malignant REBL.
Materials & Methods
The protocol was pre-registered at (https://osf.io/mjwek/). We conducted a comprehensive search in PubMed, Embase, and Web of Science until April 5, 2025, for studies that used DWI for differentiation of malignant REBLs from BAs. The risk of bias in the included studies was evaluated using QUADAS-2. ADC were compared between malignant REBLs and BAs using a random-effects model. Diagnostic values of area under the curve (AUC), sensitivity, and specificity were calculated. Sensitivity analysis, publication bias tests, and subgroup analysis were performed.
Results & Conclusion
Thirty-four studies were included with 1382 malignant REBL and 1061 abscesses. The pooled ADC values of malignant REBL and BA were 1797.17×10^{-6} mm^2/s (95% CI: 1446.55–2147.80) and 852.07×10^{-6} mm^2/s (95% CI: 786.52–917.61). Malignant REBLs had 116% higher ADCs than BAs with a significant pooled standardized mean difference of 3.12 (95% CI: 2.32–3.91, I2 = 96.8%, $p < 0.001$). The results of the ADC analysis also demonstrated overall considerable heterogeneity, which was not resolved with subgrouping based on the type of malignancy tumors, type of abscess, b-value, magnitude of strength, type of study (retrospective, prospective), and QUADAS-2. Qualitative assessment of DWI and ADC parameter demonstrated a pooled sensitivity of 92% (95% CI: 89%–95%), specificity of 92% (95% CI: 89%–94%), and AUC of 0.97 (95% CI: 0.95–0.98) for differentiating BAs from malignant REBLs. With caution to high heterogeneity, DWI provides a valuable diagnostic tool for differentiating BAs from malignant REBLs, demonstrating high sensitivity, specificity, and significant ADC difference between the two groups.

---

196 **The white fog of the White Ghost: Unraveling the various facets and mimics of CNS lymphoma**

Meghana Kancharla MD, Clyde Richard Menezes MD
St John's Medical College and Hospital, Bangalore, Karnataka, India

Summary & Objectives
This pictorial review aims to:
1) Review classical and atypical imaging features of CNS Lymphoma in both immunocompetent and immunocompromised patients, including rare variants such as Intravascular lymphoma.
2) Describe MRI surrogate signs that can aid radiologists in suspecting CNS Lymphoma.
3) Highlight the role of advanced-imaging in diagnosis.
4) Outline a practical imaging-based framework for distinguishing CNS Lymphoma from its mimics.
Purpose
Primary CNS lymphoma (PCNSL) - typically intra-axial and exhibits an angiocentric growth pattern. Contrast-enhanced MRI, remains the cornerstone of diagnosis, staging, and treatment response evaluation. Conventional sequences supplemented with diffusion-weighted imaging, dynamic susceptibility contrast perfusion, MR spectroscopy, and susceptibility-weighted imaging improve sensitivity and specificity, acting as a surrogate for histopathology in defining cellularity, vascularity, and tumor environment.

Materials & Methods

Several **surrogate radiologic signs** help identify PCNSL, including:

1) T2/ADC Decreased Indices Sign
2) Snowball/Snowmass Sign
3) Incision/Notch Sign
4) Fist Sign
5) Reef Sign
6) T2 Pseudonecrosis Sign
7) Peritumoral Leukomalacia Sign
8) Sharp Angle/Angular Sign
9) Hard Ring Sign
10) Belly Button Sign
11) Butterfly/Mirror image Sign
12) Perilesional Streak-Like Edema

Atypical features: Patchy/streaky, open ring or gyral-like enhancement, non-enhancing lesions, intraventricular or ependymal spread, hemorrhage or calcification.

Advanced Imaging: Contrast-enhanced MRI with DWI/ADC, DSC perfusion, MR spectroscopy, SWI act as a surrogate for histopathology by assessing cellularity, vascularity, tumor microenvironment.

This review highlights imaging clues to differentiate PCNSL from special subtypes: Primary Dural Lymphoma, Secondary CNS Lymphoma, and Intravascular Lymphoma and imaging mimics- Glioblastoma, metastases, demyelination, abscesses, Toxoplasmosis.

Results & Conclusion

Clinical Relevance and Prognostic Role of Imaging:

-Early imaging-based diagnosis is essential due to the tumor's high sensitivity to chemoradiation.
-Imaging aids in treatment monitoring and detection of recurrence, which often occurs at distant sites.
-Steroid administration before biopsy may obscure characteristic imaging features.
-Low ADC and rCBV values are associated with poor prognosis and aggressive disease.
-Typical findings include periventricular location and contact with CSF surfaces.
-Spinal cord, brainstem, and posterior fossa involvement, though uncommon, should be considered.

Conclusion: CNS lymphoma presents with a wide radiologic spectrum, often overlapping with high-grade tumors and infections. Awareness of classical surrogate signs and atypical features, in conjunction with advanced imaging, facilitates navigating complex differentials, early diagnosis and appropriate management. Accurate radiologic identification directly impacts treatment planning and prognosis. Given its variable appearance and aggressive nature, CNS lymphoma truly remains a master of disguise in neuro-oncology.

Images/Tables

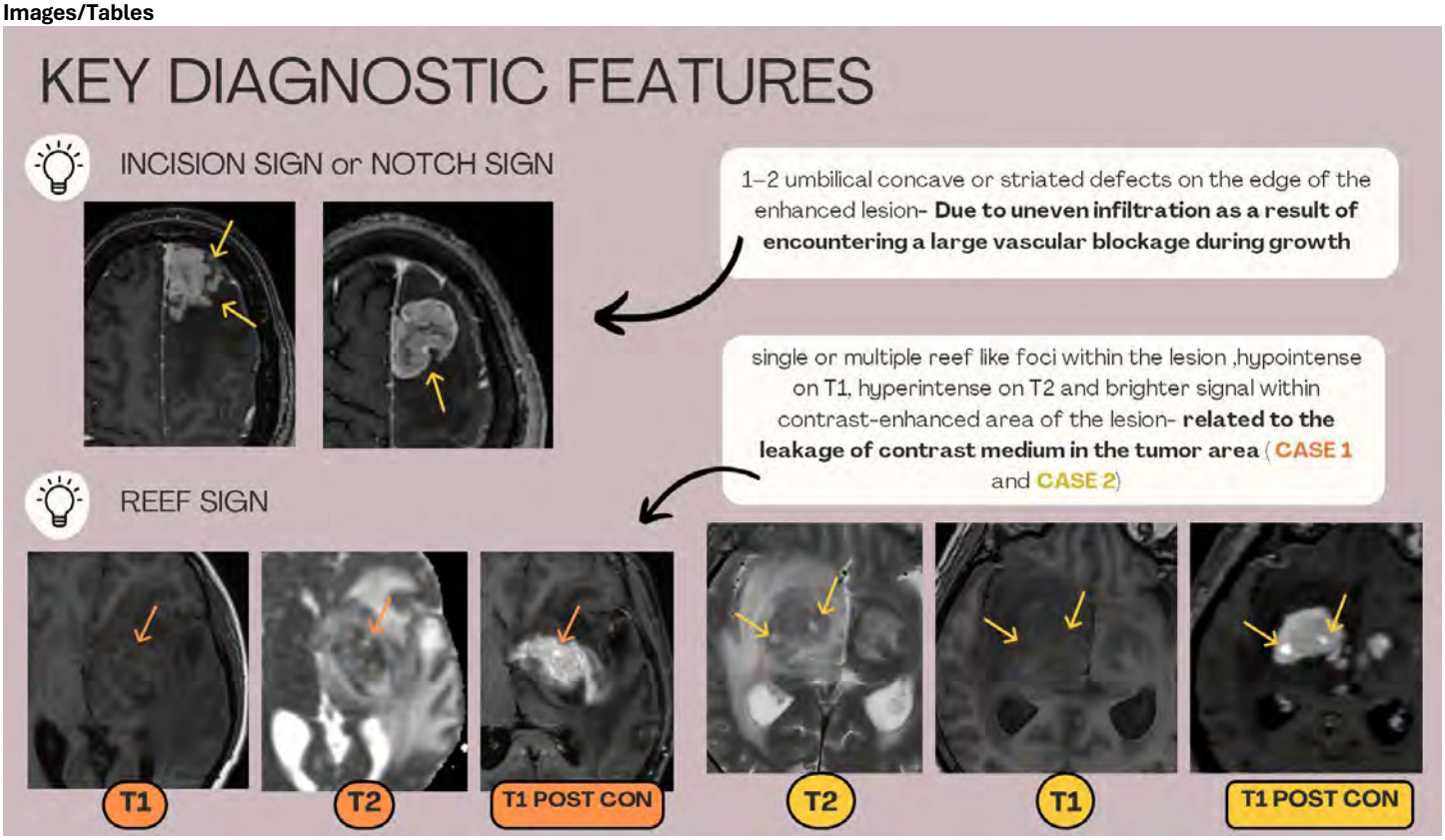

325 Pattern-Based Pediatric Viral Encephalitis: Imaging Clues for West Nile, HIV, HHV-6, Rabies, and Zika

Sawsan O Tabaza MD[1], Karen Moeller MD[2], Nilesh Desai MD[2], Thierry Huisman MD[2], Stephen Kralik MD[1], Lamson Tran[3], Huy B Tran MD[2]
[1]UTHealth Houston, Houston, Texas, USA. [2]Baylor College of Medicine, Houston, Texas, USA. [3]Texas A&M, College Station, Texas, USA

Summary & Objectives

Children with viral encephalitis often look similar at the bedside—fever, seizures, altered mentation—but their MRIs tell distinct stories. This exhibit teaches a practical, memorable way to read those stories by focusing on where the brain is involved and who the child is (age, immune/transplant status, exposure vectors, and maternal infection timing).

Purpose

Objectives:

(1) Highlight hallmark MRI patterns for West Nile, pediatric HIV encephalopathy, post-transplant HHV-6 limbic encephalitis, rabies, and congenital Zika.

(2) Use a distribution-first approach (temporal/limbic, deep gray, brainstem, diffuse white matter/atrophy, congenital malformations) to rapidly narrow the differential.

(3) Link imaging to targeted tests and timely management while avoiding key mimics (autoimmune encephalitis, ADEM, and leukodystrophies).

Purpose:

Provide a clear mental map that pairs dominant lesion distribution with likely viral etiologies so less-common pediatric pathogens are recognized quickly and confidently.

Materials & Methods

Representative pediatric cases and high-quality literature were synthesized across five entities. For each, we extracted the typical host profile, dominant MRI distribution on FLAIR/DWI (± contrast), and high-yield pearls/pitfalls. These informed:

• A one-page pattern flowchart (distribution → likely virus → suggested test).

• Five mini case cards with arrow-labeled images and one-line teaching points for trainees.

Results & Conclusion

Key imaging patterns

• West Nile virus (arbovirus): Deep gray nuclei—especially thalami—with possible basal ganglia and substantia nigra involvement; can parallel anterior horn motor neuron disease.

• Pediatric HIV encephalopathy: Progressive atrophy with symmetric periventricular/deep white-matter T2 hyperintensity and delayed/disordered myelination; opportunistic infections may overlay additional findings.

• HHV-6 (post-transplant): Limbic/mesial temporal predominance (hippocampi, amygdalae); FLAIR/DWI changes often outpace enhancement.

• Rabies: Brainstem with hippocampal/diencephalic involvement (including hypothalamus); T2/FLAIR > contrast; aligns with exposure history (bat/dog).

• Zika (congenital): Microcephaly, cortical malformations, ventriculomegaly, callosal hypogenesis, and calcifications favoring the cortical–subcortical junction (± periventricular/basal ganglia), reflecting antenatal injury.

Workstation use:

1. First, make a distribution: temporal/limbic à HHV-6, deep gray à West Nile, brainstem ± hippocampi à rabies, diffuse WM/atrophy à HIV, and congenital malformations + calcifications à Zika.
2. Then put in host factors: age, immune/transplant status, exposure vector, and maternal infection timing.
3. Next, order tests for the target: HHV-6 PCR, West Nile IgM/PCR, HIV viral load, rabies protocols, and Zika PCR/serology.
4. Finally, think about the mimics: autoimmune encephalitis, demyelinating diseases, leukodystrophies, and HSV for limbic disease.

Conclusions:

A distribution-anchored, context-aware approach turns a long list of rare pediatric encephalitides into a fast, workable differential, guiding the right tests sooner and supporting timely treatment and public-health actions.

Images/Tables

WEST NILE ENCEPHALITIS

- 8-year-old boy with history of AML, post allogenic bone marrow transplant presenting with fevers and changes in speech.

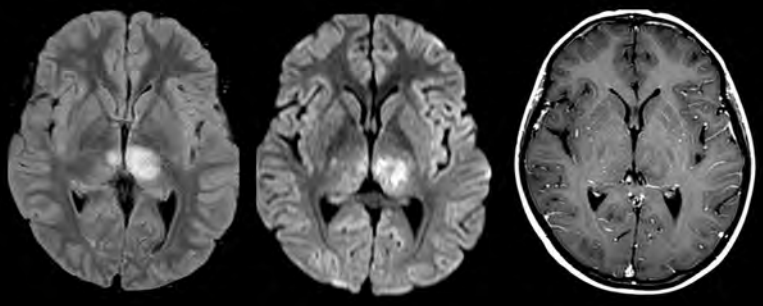

HHV6 ENCEPHALITIS

- 10-year-old boy presented with dilated unresponsive pupils.

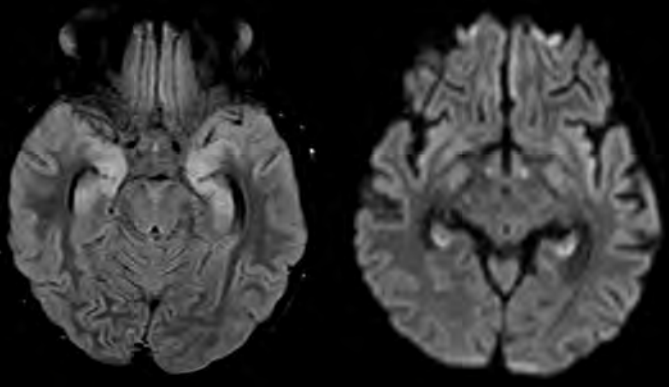

CONGENITAL ZIKA ENCEPHALITIS

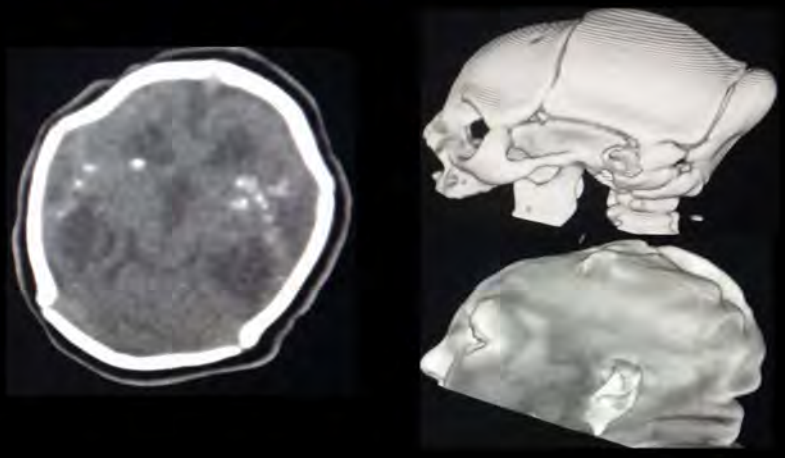

328 Beyond Contact: MRI Evaluation of Trigeminal Neurovascular Conflict — Imaging Predictors and Pitfalls

Srinidhi Srinivasan MBBS MD
Alluri Sitarama Raju Academy of Medical Sciences, Eluru west Godavari, Andhra Pradesh, India

Summary & Objectives

Trigeminal neuralgia is a notably debilitating cranial nerve disorder most often caused by neurovascular conflict (NVC) at the root entry zone of the trigeminal nerve. MRI plays a central role in detecting this conflict and differentiating clinically significant compression from incidental vascular contact.

This educational exhibit aims to:

1. Review the normal anatomy of the trigeminal nerve and its neurovascular relationships.
2. Illustrate the MRI spectrum of trigeminal neurovascular conflict using high-resolution conventional sequences.
3. Emphasize key imaging predictors of symptomatic compression and highlight common diagnostic pitfalls.
   By presenting a series of representative cases, this exhibit provides a structured imaging approach that improves diagnostic confidence and supports surgical planning.

Purpose

To educate radiologists on recognizing clinically significant trigeminal neurovascular conflict on MRI and to differentiate true neurovascular compression from incidental contact. The exhibit focuses on the practical application of routine high-resolution T2-weighted and 3D-CISS sequences for evaluating the trigeminal nerve, particularly in centers where angiographic sequences may not be available.

Materials & Methods

High-resolution MRI studies of 20 patients with clinically diagnosed trigeminal neuralgia were retrospectively reviewed. All scans were performed on a 1.5 T system using 3D-CISS and T2-weighted sequences. Each case was analyzed for:

- Site of vessel contact (root entry zone vs distal segment)
- Type of vessel (arterial vs venous, inferred from morphology and signal void)
- Degree of compression (contact only, indentation, or displacement)
- Nerve morphology (thinning or atrophy)
  Images were anonymized and selected to represent the full range of findings—from asymptomatic contact to severe nerve deformation. Post-operative imaging was included in one case to demonstrate decompression results. All information is presented for educational purposes only, with institutional and patient approval.

Results & Conclusion

MRI reliably demonstrates the relationship between the trigeminal nerve and adjacent vessels.

Findings:

- Contact at the root entry zone, especially by an arterial loop, strongly correlated with clinical symptoms.
- Nerve indentation, displacement, or atrophy were imaging markers of symptomatic compression.
- Venous or distal contacts without deformation were frequently incidental.
- SAMPLE CASES:
- Case 1: Grade I neurovascular conflict-High-resolution 3D-CISS axial image shows mild vascular contact along the cisternal segment of the right trigeminal nerve without visible indentation or displacement.
  Case 2: Grade II neurovascular conflict- Axial and coronal 3D-CISS images demonstrate a vascular loop of the superior cerebellar artery compressing and laterally displacing the right trigeminal nerve at the root entry zone.
  Case 3 — Grade III neurovascular conflict — severe nerve deformation and displacement consistent with clinically significant compression. High-resolution T2-weighted image shows marked deviation and distortion of the left trigeminal nerve with focal atrophy at the root entry zone.
  Case 4 — Follow-up MRI demonstrates contour irregularity and mild scarring along the left trigeminal nerve.
  Interpretation: Adequate nerve–vessel separation with residual fibrosis.
  Conclusion:
- A focused, structured evaluation of the trigeminal nerve using high-resolution T2-weighted sequences is sufficient to identify clinically relevant neurovascular conflict. Recognizing key predictors—location, vessel type, and nerve deformation—allows differentiation between incidental contact and true compression, improving diagnostic accuracy and guiding surgical referral. Even without MRA, conventional MRI provides valuable information for the management of trigeminal neuralgia.

Images/Tables

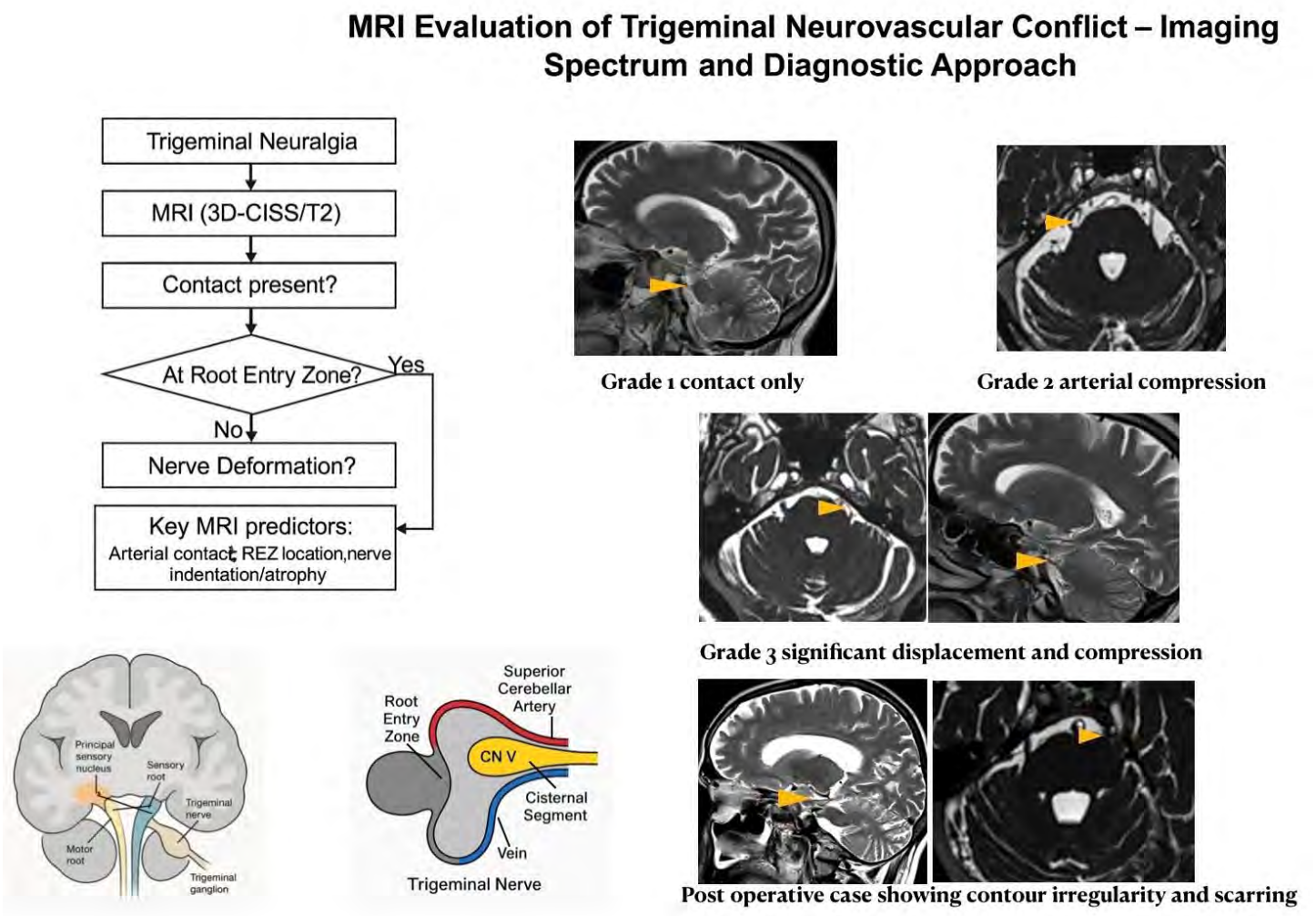

---

379 Neuroimaging of Phakomatoses: Revealing the Unseen Manifestations

Tylor Connor DO, Thotsophon Taechariyakul MD, Graham Tooker MD, Brian Barnacle MD, Leah Palifka MD
Dartmouth Hitchcock Medical Center, Hanover, NH, USA

Summary:

This educational exhibit reviews the neuroradiologic features of four major phakomatoses—Neurofibromatosis Type 1, Von Hippel-Lindau syndrome, PHACES syndrome, and Tuberous Sclerosis Complex—emphasizing their distinct and overlapping imaging patterns across pediatric and young adult populations. Neuroradiology plays a central role in diagnosis, monitoring, and multidisciplinary management through the identification of hallmark CNS and systemic manifestations.

Objectives:

1. Appreciate the characteristic neuroradiologic findings associated with NF1, VHL, PHACES, and TSC.
2. Understand the role of advanced MRI in early detection and longitudinal assessment of neurocutaneous disease.
3. Highlight the importance of imaging in multidisciplinary care and prognosis of patients with phakomatoses.

Purpose:

Neurocutaneous syndromes represent a heterogeneous group of disorders involving structures derived from the embryonic ectoderm, including the brain, skin, and eyes. This educational exhibit reviews the pediatric and young adult neuroradiologic manifestations of common phakomatoses—Neurofibromatosis Type 1 (NF1), Von Hippel-Lindau syndrome (VHL), PHACES syndrome, and Tuberous Sclerosis Complex (TSC)—highlighting hallmark imaging findings and emphasizing neuroradiology's central role in diagnosis, surveillance, and multidisciplinary care.

Materials & Methods:

NF1 features multifocal T2 hyperintense lesions ("unidentified bright objects") commonly seen within the basal ganglia, thalami, and cerebellum, along with optic pathway gliomas, cortical dysplasias, and plexiform neurofibromas.

PHACES syndrome commonly includes posterior fossa anomalies, cerebrovascular dysgenesis, and large segmental facial hemangiomas, often with cardiothoracic or ocular abnormalities.

Tuberous Sclerosis is characterized by cortical tubers, subependymal nodules, and subependymal giant cell astrocytomas near the foramen of Monro, with further systemic involvement such as renal and cardiac lesions.

Von Hippel-Lindau syndrome features cerebellar and spinal hemangioblastomas with enhancing mural nodules, endolymphatic sac tumors, and supratentorial lesions, often coexisting with renal cell carcinoma, pancreatic cysts, or pheochromocytomas.

Collectively, these syndromes exhibited overlapping yet distinct imaging phenotypes that enable precise diagnosis and monitoring.

Results & Conclusion:

Neuroradiology is crucial in the evaluation and management of the phakomatoses. Imaging facilitates diagnosis by identifying the distinct CNS features of NF1, PHACES, TSC, and VHL while supporting ongoing assessment for progression and systemic involvement. Advanced MRI enhances sensitivity for subtle or clinically silent lesions, guiding multidisciplinary care. Early and accurate neuroradiologic recognition of these syndromes enables timely intervention and underscores imaging's essential role in optimizing outcomes for patients with neurocutaneous disease.

Images/Tables

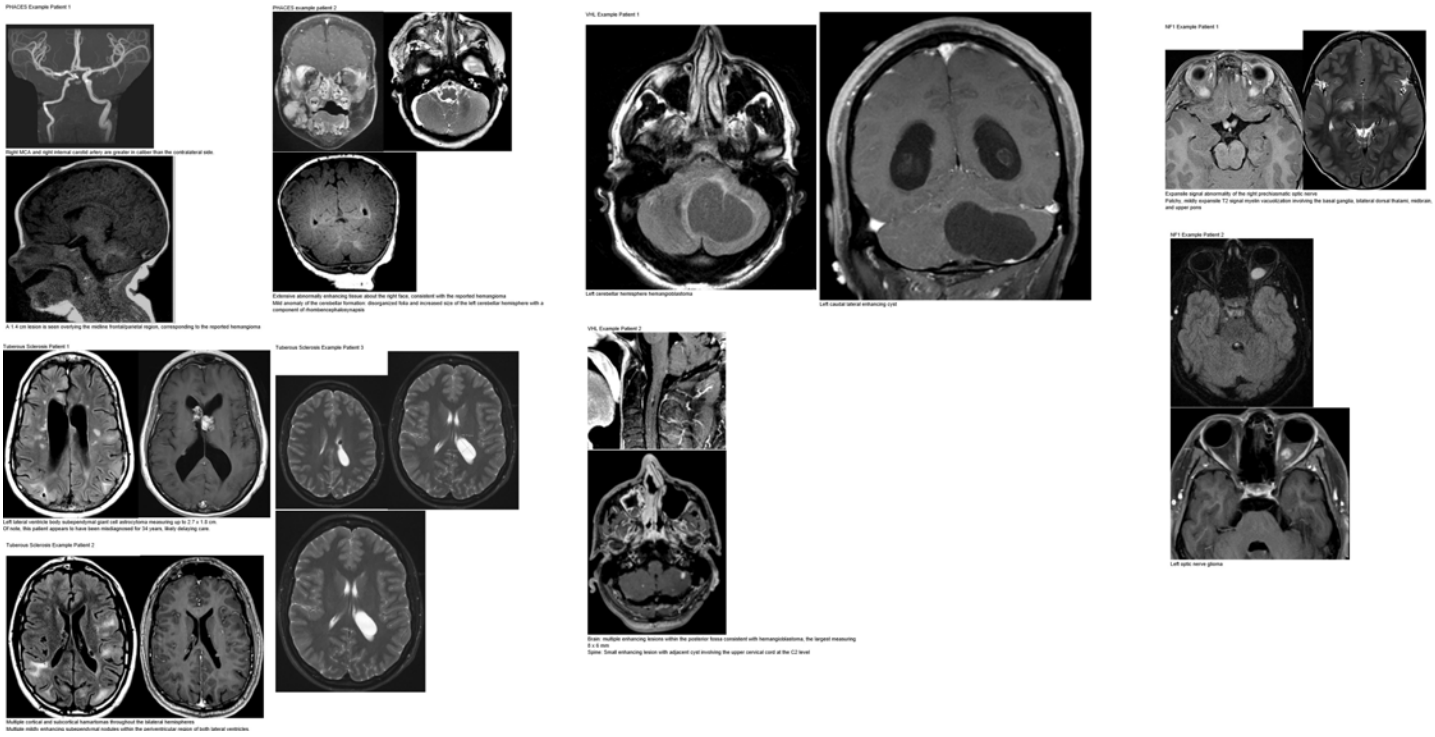

---

380 CHARGE: Imaging Clues to a Complex Congenital Syndrome

Tylor Connor DO, Thotsophon Taechariyakul MD, Graham Tooker MD, Brian Barnacle MD, Leah Palifka MD
Dartmouth Hitchcock Medical Center, Hanover, NH, USA

Summary & Objectives

Summary:

This educational exhibit reviews the characteristic neuroradiologic and craniofacial imaging features of CHARGE syndrome, a complex congenital disorder defined by a constellation of multisystem anomalies. Emphasizing multimodality imaging, this exhibit highlights diagnostic patterns that support early recognition, multidisciplinary management, and genetic confirmation.

Objectives:

1. Understand the key neuroradiologic and craniofacial imaging findings associated with CHARGE syndrome across multiple modalities.
2. Appreciate how imaging contributes to the diagnosis and management of patients with incomplete or atypical CHARGE presentations.
3. Recognize the value of a comprehensive, multidisciplinary approach in correlating imaging features with clinical and genetic findings.

Purpose

CHARGE syndrome is a rare congenital disorder characterized by a constellation of anatomic anomalies, impaired growth milestones, and complex, multidisciplinary care requirements. Early recognition of imaging findings is critical for guiding diagnosis and patient management. This educational exhibit reviews the radiologic features of patients with suspected CHARGE syndrome, highlighting diagnostic patterns that may aid radiologists in clinical practice.

Materials & Methods

Common findings in CHARGE syndrome included semicircular canal hypoplasia/aplasia, coloboma, and choanal atresia. Central nervous system anomalies include olfactory bulb hypoplasia and midline brain malformations. Additional craniofacial findings, such as external ear malformations and cranial nerve anomalies, may also be seen. When present, cardiovascular findings may reveal conotruncal defects in a subset of cases, consistent with known associations. Correlating imaging findings with established diagnostic criteria reinforces the utility of imaging in supporting syndromic diagnosis.

Results & Conclusion

Radiologic evaluation plays a vital role in the recognition of CHARGE syndrome, particularly in patients with incomplete or atypical clinical presentations. This educational exhibit demonstrates key imaging findings across neuroimaging and craniofacial assessment, underscoring the importance of a comprehensive, multimodality approach. By identifying patterns consistent with CHARGE syndrome, radiologists can contribute to earlier diagnosis, guide genetic testing, and facilitate multidisciplinary care planning.

Images/Tables

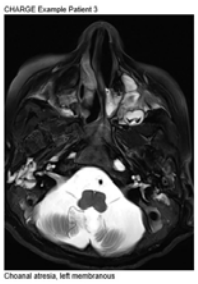

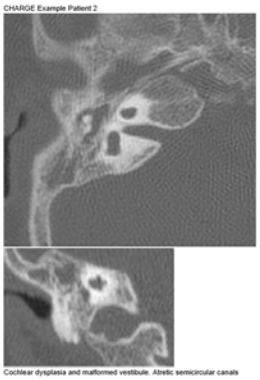

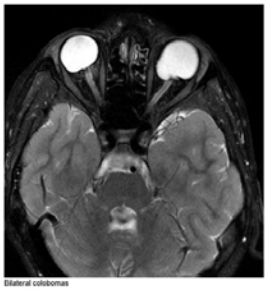

---

451 Photon-Counting CT of the Pterygopalatine Fossa: Enhanced Visualization and Diagnostic Confidence

Raul FP Barbieri MD, Adrienn Toth MD, Maria V Spampinato MD, Albert D Gonzalez MD, Daniella K Zanoni MD, Maria G Matheus MD
MUSC, Charleston, SC, USA

Summary & Objectives

The pterygopalatine fossa (PPF) is a small inverted pyramidal space that serves as a major neurovascular crossroads connecting the oral and nasal cavities, nasopharynx, orbit, masticator space, and middle cranial fossa. It can act as a conduit for the spread of infectious and neoplastic disease across the deep facial spaces. Photon-counting detector CT (PCD-CT), with its higher spatial resolution, reduces image noise, decreases artifacts, lower radiation dose compared with energy-integrating detector (EID) CT, and offers the potential for improved visualization of this anatomically complex region.

Purpose

This educational exhibit reviews the anatomy of the PPF and demonstrates how PCD-CT can enhance the depiction of key anatomic structures, thereby increasing diagnostic accuracy with significant therapeutic implications. Additionally, selected cases of PPF pathology are illustrated to highlight the advantages of PCD-CT in clinical practice.

Materials & Methods

A total of 20 participants (median age 66 years [range, 29–86years]; 15 females) were enrolled. Each underwent an EID CT head and/or neck CT angiogram followed by the same examination using PCD-CT technology. The anatomic evaluation of the PPF region included the palatine canals (greater and lesser), pterygomaxillary fissure, foramen lacerum, Vidian canal, sphenopalatine foramen (SPF), inferior and superior orbital fissures (IOF/SOF), orbital apex, foramen ovale, and foramen rotundum. Using clinical examples, this exhibit illustrates differences in image quality, structural delineation, and the visibility of subtle anatomic structures between EID-CT and PCD-CT.

Results & Conclusion

PCD-CT provided higher image quality and superior delineation of fine and critical structures, allowing better visibility of subtle anatomic details compared with EID CT. This may improve radiologists' accuracy in identifying normal anatomy as well as clinically relevant pathology, including infection involvement and perineural tumor spread.

PCD-CT is an innovative imaging technology that combines high spatial resolution with dose efficiency, revealing anatomic detail beyond the reach of EID CT. Its ability to clearly depict the intricate anatomy of the PPF enhances diagnostic performance and holds expanding clinical potential in head and neck imaging.

Images/Tables

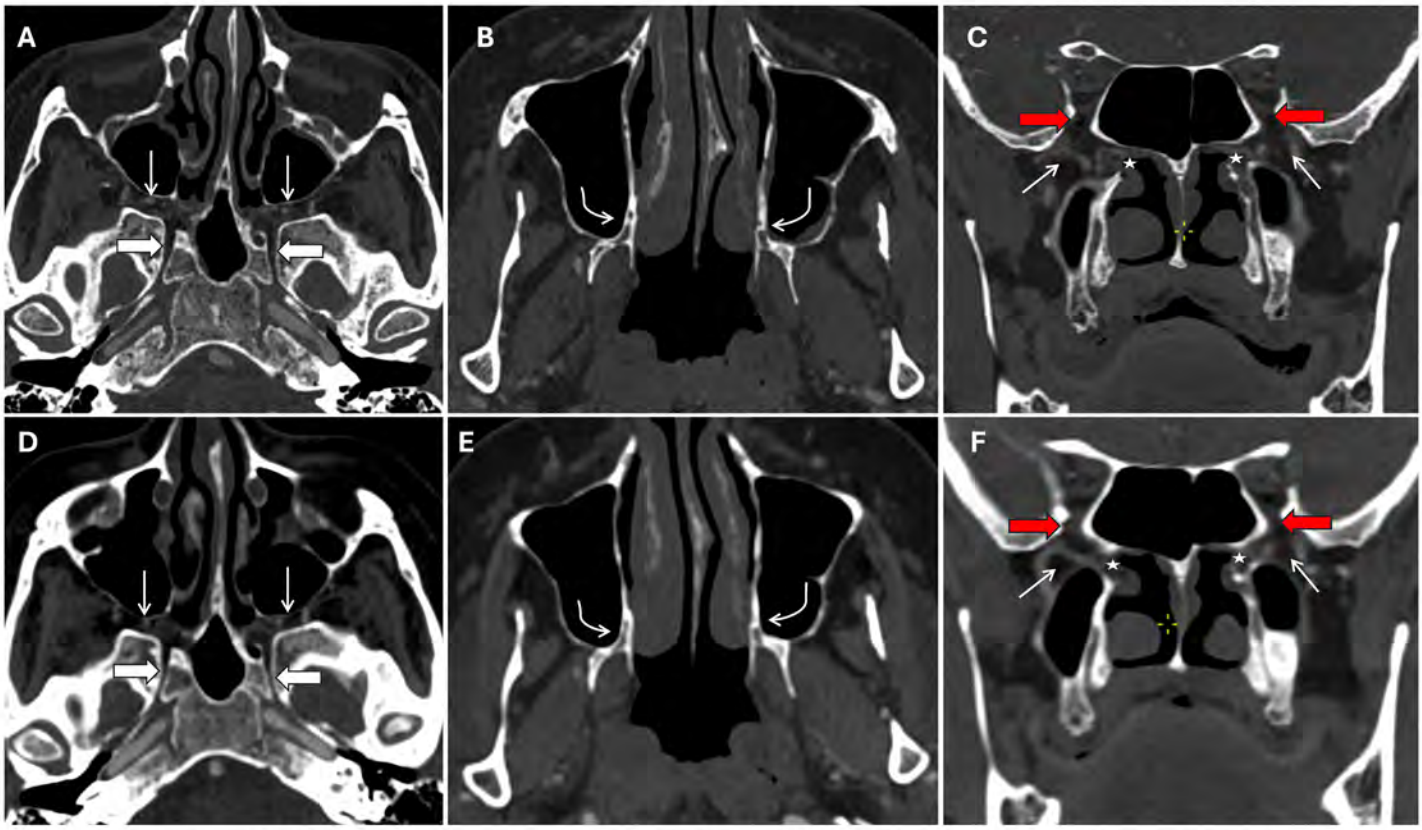

A–C: 0.2 mm axial and coronal PCD-CT images. D–F: Corresponding energy-integrating detector (EID) CT images with 0.6 mm thickness demonstrate poorer delineation of the anatomical structures in the same patient . Pterygopalatine fossa (PPF): thin arrows. Vidian canal: thick arrows. Palatine canals: curved arrows. Inferior orbital fissure (IOF): red arrows. Sphenopalatine foramen (SPF): asterisk.

---

524 **Radiologic Findings in Fahr Syndrome**

Fatemeh Dehghani Firouzabadi MD[1], Ali Jahanshahi MD[1], Jordan Stafford MD[1], Ali Sheikhy MD[2], Robert Bert MD[1], Ramin Hamidi DO, MSc, MBA[1]
[1]University of Louisville, Louisville, Kentucky, USA. [2]National Institutes of Health, Bethesda, Maryland, USA

Summary & Objectives

Fahr's disease and Fahr's syndrome are manifest by unenhanced CT of the head with symmetric bilateral calcifications involving the basal ganglia, thalami, dentate nuclei, juxtacortical white matter as well as the cerebellum. While Fahr's syndrome is caused by an underlying pathology, Fahr's disease is a genetic condition with no known secondary cause.

Clinically, patients may present with movement disorders (parkinsonism, chorea, dystonia), seizures, cognitive decline, psychiatric manifestations. Prevalence is estimated at <1 per million, with a male predominance (2:1) and onset typically in mid-adulthood. Because of its heterogeneous and nonspecific symptoms, diagnosis is frequently delayed, especially in endocrine-related cases.

Educational Objectives:

Participants will learn to:

1. Identify hallmark CT and MRI patterns of Fahr syndrome.
2. Correlate imaging features with neurological and psychiatric manifestations.
3. Understand metabolic, genetic, and toxic mechanisms driving calcification.

Purpose

To provide an educational overview of Fahr's with characteristic imaging findings, clinical spectrum, and metabolic associations. We present a case series to explore correlations between radiologic, biochemical, and clinical parameters. The goal is to enhance diagnostic accuracy and multidisciplinary management of this rare disorder.

Materials & Methods

Imaging Features:

Non-contrast CT (NCCT) is the diagnostic gold standard, revealing dense symmetric calcifications in the basal ganglia, thalami, dentate nuclei, and cerebellum. MRI helps in assessing ischemic changes, vascular narrowing, or demyelination; calcifications appear hypointense on SWI or T2* sequences. Symmetrical, widespread calcifications suggest metabolic or genetic causes, while asymmetric or patchy patterns may indicate infectious or vascular etiologies.

Key Decision Making:

Considerations include hypo/hyperparathyroidism, post-thyroidectomy changes, calcified infarcts, toxoplasmosis, neurocysticercosis, HIV, and we suggest toxic exposures such as lead. Idiopathic or familial forms are often linked to SLC20A2, PDGFB, and PDGFRB gene mutations.

Case Highlights:

1. Hypoparathyroidism-related Fahr syndrome: Severe hypocalcemia and hyperphosphatemia leading to progressive calcifications; correction of calcium and vitamin D levels halts deterioration.

2. Idiopathic Fahr syndrome: Acute seizures and altered mental status without metabolic abnormality; imaging critical for diagnosis and supportive recovery.
3. Ischemic stroke in Fahr's syndrome: Rare presentation due to vascular calcifications causing luminal compromise and microinfarcts.

Management:

There is no curative therapy for Fahr's disease. Treatment for Fahr's syndrome focuses on metabolic correction (maintaining calcium in low-normal range, treating vitamin D deficiency) and symptom control. Levetiracetam is preferred for seizures; dopaminergic agents and physical therapy for movement disorders; and cautious antipsychotic use for psychiatric symptoms. Standard stroke protocols apply when ischemic events occur. Family screening and genetic counseling are advised in familial cases.

Results & Conclusion

Fahr syndrome is a rare but clinically significant entity requiring high radiologic awareness. Integrating imaging with metabolic and clinical data enables early recognition and tailored management. The proposed case series will further delineate imaging-biochemical correlations and support multidisciplinary strategies to improve patient outcomes.

Images/Tables

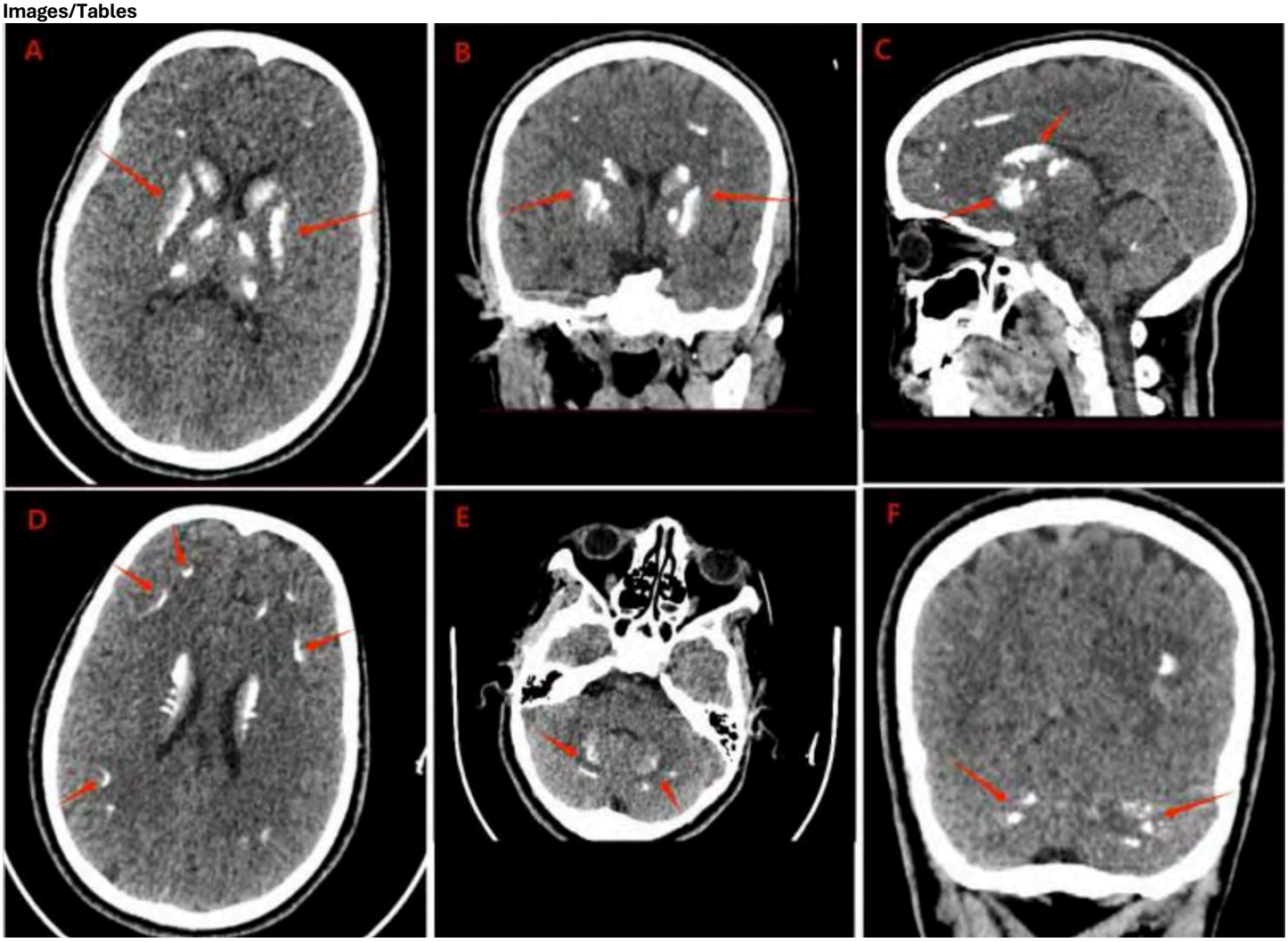

---

597 **Evaluating the CSF SPACE: Using 3D T2 Weighted Imaging (T2WI) in the Workup of CSF Flow Disturbances**

Christopher Chin MD[1], Camilo Aguilar MD[2], Kunal M Patel MD[1], Vinay K Bhatia MD[1]

[1]Mount Sinai Medical Center, Miami Beach, FL, USA. [2]Mount Sinai Medical Center, Miami Beach, Florida, USA

Summary & Objectives

Phase-contrast MRI (PC-MRI) can accurately quantify Cerebrospinal fluid (CSF) flow through a given region, within limitations of velocity encoding (VENC) selection, low-signal-to-noise (SNR), and complex flow dynamics/complex flow regions. High-resolution 3D T2WI offers detailed visualization of complex anatomical locations and identification of CSF motion artifact, indicating flow. Adjunctive integration of these protocols can serve to improve sensitivity for analysis of CSF flow pathology by enhancing anatomic and functional analysis.

This exhibit reviews the principles, limitations, and adjunctive capabilities of PC-MRI and 3D T2WI for analysis of CSF dynamics.

Purpose

To demonstrate how high-resolution 3D T2WI can serve as an adjunct to PC-MRI when evaluating CSF flow dynamics.

Materials & Methods

Pathological states that cause disturbances in the normal CSF flow, such as normal pressure hydrocephalus (NPH) and Chiari malformations, typically rely on PC-MRI for analysis. PC-MRI allows for analysis based on the presence or absence of CSF flow, as well as the quantification of CSF flow velocities and volume in a targeted area, a helpful tool in patients being worked up for NPH.[1] However, because of the low SNR and precision needed in location and degree of flow, PC-MRI may not be able to evaluate subtle low-velocity or spatially complex flow patterns.

3D T2WI is primarily used to provide high resolution imaging (i.e. structural analysis), particularly for anatomically complex regions such as the brain or inner ear. Additionally, it provides good contrast between the CSF spaces and adjacent soft tissues.[2]

Results & Conclusion

Phase-Contrast MRI (with Velocity Encoding): PC-MRI employs phase shifts to quantify flow velocity within a targeted region. This high specificity is limited by the preselected velocity encoding parameter. To quantify CSF flow, a VENC parameter must be set for a targeted region of CSF flow and the VENC setting must include the range of flow velocity at the region of interest with a small margin of error. If a VENC setting is too high, a decreased signal to noise ratio will result; if the VENC is too low, there will be introduction of phase aliasing artifact.[3]

3D T2WI creates clear images of CSF spaces, neural structures, and vasculature. Additionally, CSF flow voids are visible on high resolution T2WI sequences.

Complementary Role of 3D T2WI: We propose incorporating 3D T2WI as an adjunct to PC-MRI, which will combine the high spatial resolution for anatomic detail with functional assessment based on the presence or absence of the expected CSF flow void. By doing so, users can be less specific in predetermined parameters (VENC) and will increase sensitivity for anatomically complex areas and for areas with subtle flow that PC-MRI will not well visualize.

3D T2WI can be used as an adjunct to further increase diagnostic sensitivity for low flow or complex flow areas within the CSF space that are currently not well evaluated by PC-MRI. This approach can be easily integrated into current practice and can aid in evaluation for CSF flow pathology.

Images/Tables

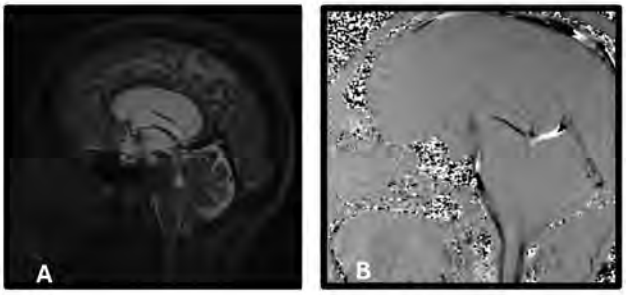

Figure 1.
Sagittal T2 space (**A**) demonstrates obstructing mass at the level of the Aqueduct of Sylvius with CSF flow artifact along the floor of the third ventricle, interpeduncular cistern, and pre-pontine cistern with corresponding phase shift on phase contrast imaging (**B**), reflecting spontaneous third ventriculostomy.

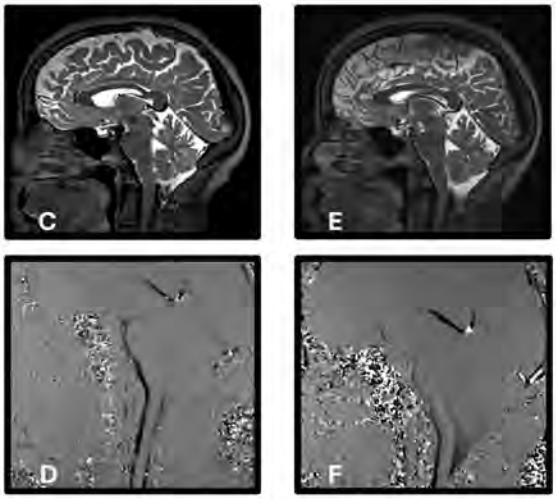

Figure 2.
Patient with history of remote Chiari decompression presented with interval development of cervical spinal cord syrinx and bilateral lower extremity stiffness and instability. Sagittal T2 space (**C**) demonstrates a dorsal arachnoid membrane at the level of the foramen magnum with corresponding absence of phase shift on phase contrast imaging (**D**). Post-operative arachnoid membrane fenestration sagittal T2 space (**E**) demonstrates normal CSF flow/motion artifact at the operated level with corresponding phase shift on the phase sequence (**F**).

---

660 Imaging Spectrum of Horner's Syndrome: A Neuroradiologic Perspective

Mackenna Senti MD, Karthik Rayasam MBBS, Hasan Ozgur MD
University of Arizona, Tucson, Arizona, USA

Summary & Objectives

Patients seldom display the full Horner Syndrome triad of ptosis, miosis, and facial anhidrosis, often making immediate diagnosis difficult. This project develops a practical anatomy-guided framework that uses targeted imaging to rapidly and accurately localize lesions along the oculosympathetic pathway, allowing for timely and effective management across diverse clinical settings.

Purpose

The purpose of this project is to enable quick and safe diagnosis of patients demonstrating suspected signs and symptoms of Horner Syndrome by standardizing evaluation and prioritizing early detection of life-threatening or neoplastic etiologies. This framework is designed for ease of use across a wide range of clinical settings.

Materials & Methods

This protocol combines both clinical examination with a standardized imaging approach aligned to lesion level: high-resolution brain and cervicomedullary MRI (centered around DWI and FLAIR sequences) for central lesions; contrast-enhanced CT or MRI of the neck and thoracic inlet for preganglionic lesions; and vessel-wall MRI, MRA, or CTA for postganglionic lesions. This approach utilizes widely available modalities and allows for rapid triage of acute etiologies, while not sacrificing ability to detect subtle findings.

Results & Conclusion

Horner's syndrome, defined by ipislateral ptosis, miosis, and facial anhidrosis, results from the disruption of the oculosympathetic pathway, which extends from the hypothalamus to the orbit. Accurate lesion localization is essential for timely diagnosis and management, as underlying causes range from benign demyelinating plaques to life-threatening vascular or neoplastic conditions.

Neuroradiologic evaluation focuses on identifying characteristic imaging findings along the three-neuron sympathetic chain:

1. Central (first-order) lesions involve the hypothalamospinal tract and are best visualized with high-resolution brain and cervicomedullary MRI.
2. Preganglionic (second-order) lesions affect the lower cervical and upper thoracic sympathetic chain, often detected via CT or MRI of the neck and thoracic inlet, especially in cases of Pancoast tumors or postsurgical fibrosis.
3. Postganglionic (third-order) lesions follow the internal carotid artery into the cavernous sinus and orbit, where vessel-wall MRI, MRA, and CTA are critical for identifying carotid dissection, cavernous sinus pathology, or orbital apex involvement.

A structured, anatomy-based imaging algorithm, integrating diffusion-weighted imaging, FLAIR, and angiographic sequences, enables precise topographic diagnosis, guides emergent intervention, and highlights the vital role of neuroradiologists in detecting subtle radiologic clues across this complex pathway.

Images/Tables

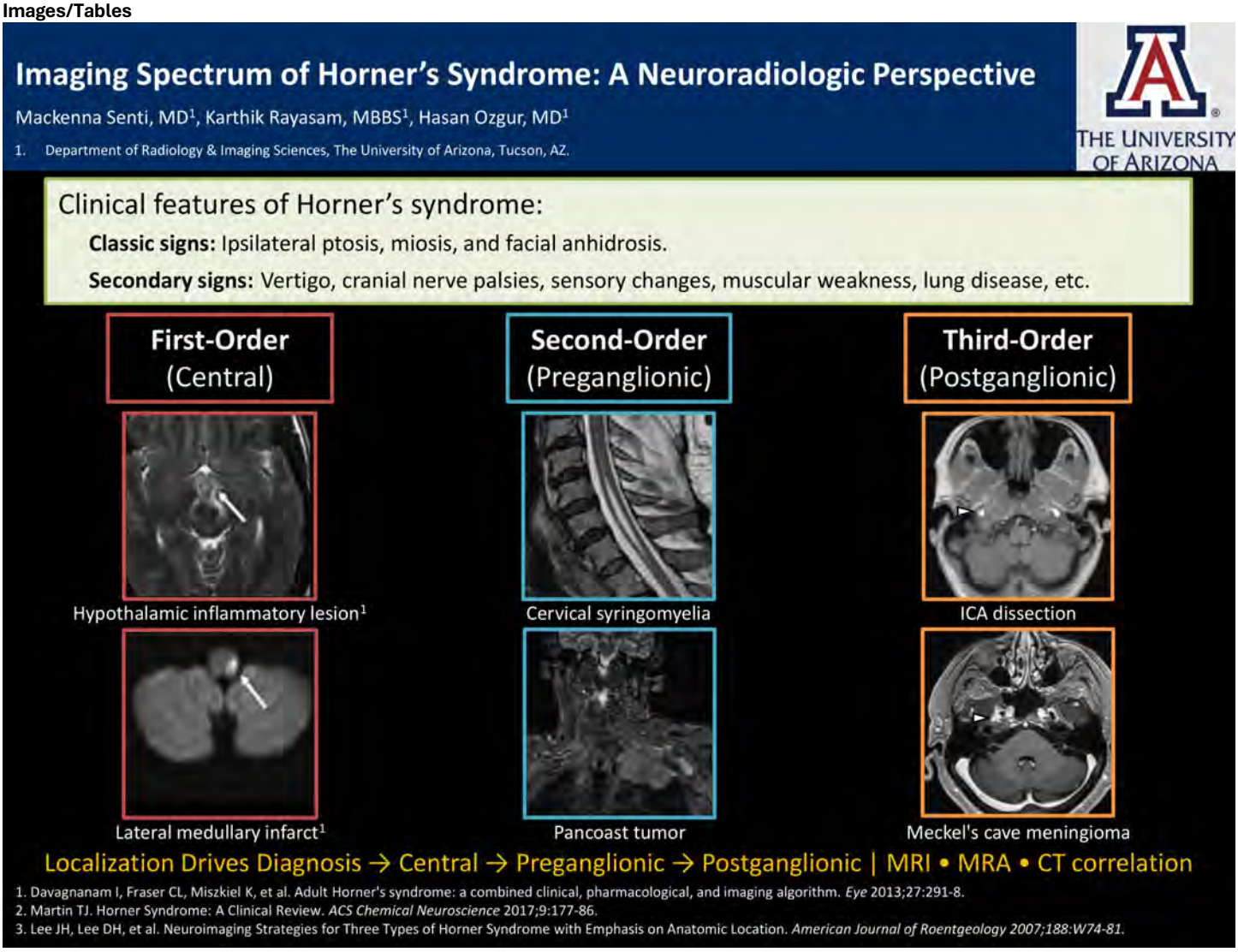

---

704 What the Neuroradiologist Needs to Know about Cerebral Venous Sinus Thrombosis (CVST)

Maha Ahmed MD[1], Bindu Setty MD[1], Kayra Cengiz[2], Asim Mian MD[1], Mohamad Abdalkader MD[1], Umer Ahmed MD[1]
[1]Boston University, Boston, MA, USA. [2]Boston University Chobabian and Avedisian School of Medicine, Boston, MA, USA

Summary & Objectives

Cerebral venous sinus thrombosis (CVST) is an uncommon but potentially reversible cause of intracranial hypertension, venous infarction, or hemorrhage with a high predilection for young people and particularly women [1,2]. Given its variable and often nonspecific clinical presentation, imaging plays a central role in timely and accurate diagnosis to prevent morbidity and mortality [1]. This exhibit aims to (1) review characteristic imaging findings of DVST across CT and MR modalities, (2) highlight common pitfalls and mimics that may lead to misinterpretation, and (3) discuss best practices for imaging protocols to improve detection and confidence in diagnosis.

Purpose

To review the imaging evaluation of cerebral venous sinus thrombosis (CVST) with an emphasis on optimizing protocols and recognizing characteristic findings. The exhibit aims to help radiologists distinguish true thrombosis from normal variants and common mimics, supporting timely and accurate diagnosis, and describe a few case scenarios of missed diagnosis of CSVT.

Materials & Methods

Representative cases of CVST and its imaging mimics were identified using the Philips Performance Bridge radiology analytics platform at Boston Medical Center over a ten year period. Radiology reports were queried using key terms including *"venous sinus thrombosis"* and *"dural sinus*

thrombosis." Relevant CT, CT venography (CTV), MRI, and MR venography (MRV) studies were reviewed to select illustrative examples demonstrating classic imaging findings of CVST and common mimics such as arachnoid granulations, sinus hypoplasia, and flow-related artifacts. All cases were de-identified prior to inclusion. This retrospective review was conducted for educational purposes and did not require IRB approval.

Results & Conclusion

Review of representative cases demonstrates the spectrum of CVST appearances on noncontract CT, CTV, MRI, and MRV, along with mimics that can simulate thrombosis. CTV provides rapid, reliable assessment in the acute setting, whereas MRI and MRV offers superior sensitivity for subacute or chronic thrombus and evaluation of associated parenchymal changes [1]. Figure 1 illustrates a thrombus on post contrast T1 MP RAGE, a 3D sequence with high resolution. Familiarity with normal sinus variants—particularly asymmetric transverse sinuses, hypoplasia, and arachnoid granulations—is essential to avoid overcalling thrombosis [3].

An effective triage approach incorporates clinical features such as new-onset headache, papilledema, focal neurologic deficits, or unexplained intracranial hemorrhage [2]. Protocol optimization, including MRV, DWI, T1 MPRAGE with and without contrast, and susceptibility-weighted sequences, enhance diagnostic accuracy.

Timely identification of CVST depends on awareness of its varied imaging manifestations and potential mimics. A structured, protocol-driven imaging approach allows radiologists to confidently distinguish true thrombosis from benign variants, improving diagnostic precision and patient outcomes.

Images/Tables

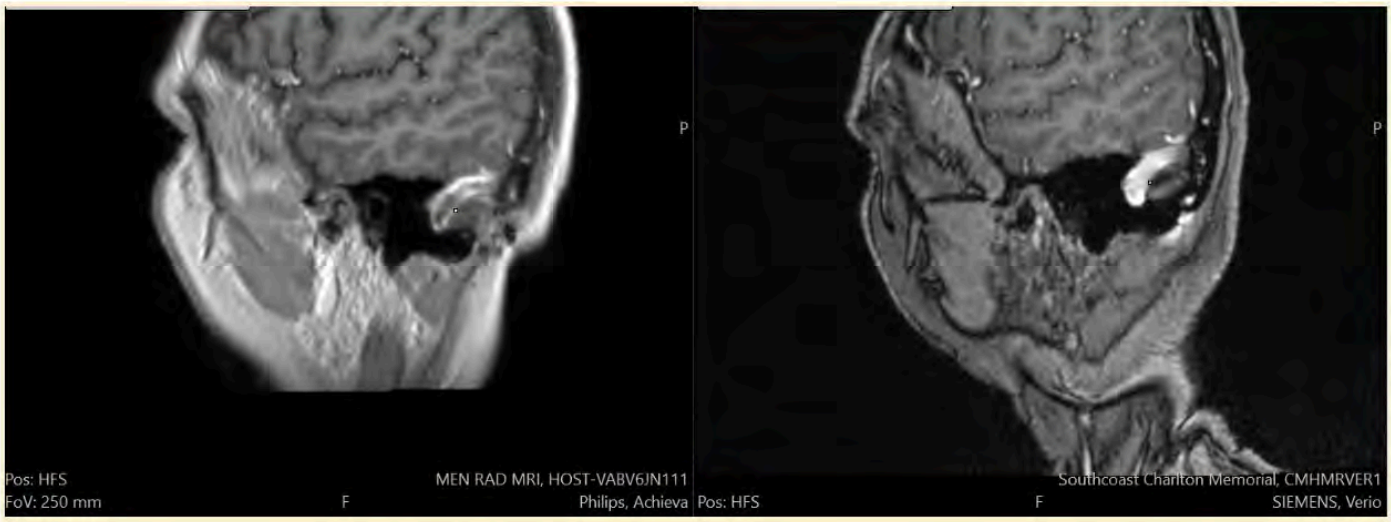

Figure 1: MR of the Brain T1 Post-Contrast Sequence on Sagittal View Showing Dural Venous Sinus Thrombosis Extending from the Transverse Sinus to the Sigmoid Sinus

---

709 Traumatic Meningeal Enhancement: Imaging, Mechanisms, and Clinical Relevance

Alejandro Arbona-Lampaya BS[1], Alejandro Odeh-Couvertier BS[1], Arelys A Angueira-Laureano BS[1], Ricardo G Blanco-Ortiz BS[1], Ricardo Sánchez Jiménez MD[2], Joaquin F Ruiz Lopez MD[2], Eduardo J Labat Álvarez MD[2]

[1]School of Medicine, University of Puerto Rico Medical Sciences Campus, San Juan, PR, USA. [2]Department of Radiology, School of Medicine, University of Puerto Rico Medical Sciences, San Juan, PR, USA

Summary & Objectives

Traumatic Meningeal Enhancement (TME), an MRI finding increasingly recognized in patients with Traumatic Brain Injury (TBI) refers to the observable enhancement of the meninges that can be observed on post-contrast fluid-attenuated inversion recovery (FLAIR), even when head CT is negative. TME reflects disruption of the blood-meningeal barrier (BMB), allowing contrast agents to leak into the meningeal layers following trauma. This phenomenon is thought to represent a spectrum of vascular and inflammatory injury, ranging from subtle meningeal irritation to more extensive meningeal and cortical vascular compromise.

Emerging evidence suggests that TME may serve as a promising biomarker of traumatic vascular injury, with potential diagnostic and prognostic applications. Studies have reported that TME can persist over time and is associated with incomplete clinical recovery, supporting its role as an indicator of ongoing pathophysiological processes after TBI. Given its detection even when CT and conventional MRI sequences are negative, recognition of TME is particularly valuable for identifying subtle or occult injury.

This exhibit will fulfill the following objectives:

- Review the imaging characteristics of TME, with emphasis on contrast-enhanced FLAIR as the most sensitive sequence.
- Summarize the proposed pathophysiologic mechanisms underlying TME, including blood-meningeal barrier disruption, vascular permeability, and inflammation.
- Illustrate the associations between TME and extraaxial hemorrhage, particularly subdural hematoma (SDH), using case-based examples.
- Discuss the clinical implications of TME, including its role as a potential imaging biomarker for injury severity and predictor of clinical recovery.

Purpose

The purpose of this exhibit is to provide a comprehensive overview of TME as an emerging imaging marker in TBI.

Materials & Methods

A retrospective review of head trauma patients from October 2024 to October 2025 was conducted from our institution's PACS search engine. The imaging was reviewed for extra-axial hemorrhages, parenchymal hemorrhages, and the presence of TME on post-contrast FLAIR.

Results & Conclusion

We identified 85 cases of head trauma in our PACS search engine. Of these, 39 patients underwent contrast-enhanced MRI scans. In those patients, we identified 18 representative cases of TME. Of these, 6 had concurrent SDH, 2 had both concurrent subarachnoid hemorrhage (SAH) and SDH, 2 showed evidence of parenchymal hemorrhage with no extraaxial hemorrhage, and 8 showed no evidence of hemorrhage.

---

738 CT Imaging Features of Parathyroid Carcinoma: Case Series and Review of Diagnostic Clues

Pablo Palacios[1], John Manov[2], Puneet Pawha[2]

[1]New York, NY, USA. [2]New York, New York, USA

Summary & Objectives

Parathyroid carcinoma is a rare endocrine malignancy, representing less than 1% of cases of primary hyperparathyroidism. Its clinical presentation can overlap with that of benign parathyroid adenomas, making preoperative diagnosis challenging. Imaging, particularly computed tomography (CT), can play a crucial role in localization, characterization, and surgical planning. There have been few studies describing CT features of parathyroid carcinoma.

Purpose

1. Review clinical and biochemical features that should prompt consideration of parathyroid carcinoma.
2. Describe key CT imaging characteristics associated with parathyroid carcinoma.
3. Suggest possible distinguishing features of parathyroid carcinoma from benign parathyroid lesions on CT imaging.
4. Discuss the importance of CT in evaluating local invasion and regional spread for surgical planning

Materials & Methods

We present a series of 5 patients with histologically confirmed parathyroid carcinoma seen at a multicenter health system from 2014-2025, describing key CT imaging features and presenting correlative clinical, laboratory, and pathological findings. Multiphasic CT imaging (4D-CT) was reviewed for 4 initial or recurrent primary lesions and 1recurrent nodal mass. Through illustrative CT images, this exhibit highlights imaging characteristics that can suggest the diagnosis.

Results & Conclusion

Results

Imaging features of parathyroid carcinoma included heterogeneous enhancement, arterial phase enhancement less than thyroid, cystic/necrotic change, larger lesion size, and irregular margins. Evidence of local invasion was seen in two case. Two patients had regional nodal metastases, and two patients had distant metastases. Correlative ultrasound and sestamibi findings are depicted. This exhibit also explores challenges and tips in differentiating carcinoma from benign parathyroid adenomas, and the role of imaging in surgical mapping and staging.

Concordant with other investigators, our small series of parathyroid carcinomas showed 4D-CT findings of heterogeneous enhancement, arterial hypoenhancement relative to the thyroid gland, large short-to-long axis ratio, larger size (>2cm), and irregular margins.

Conclusion

While parathyroid carcinoma may present clinically in a manner indistinguishable from benign causes of hyperparathyroidism, profound hypercalcemia and certain imaging features may suggest malignancy.

In addition to suggesting malignant histology, 4D-CT is useful to assess for locoregional nodal spread and local extent of disease.

Images/Tables

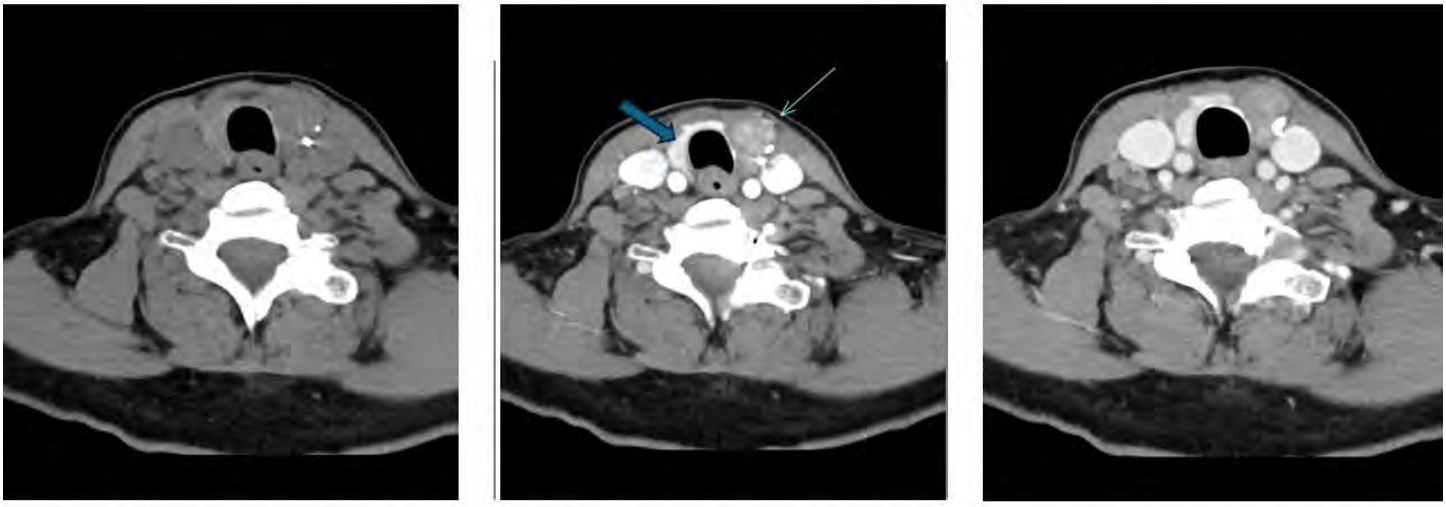

4D-CT demonstrates clips in the left thyroid bed. On the arterial phase, there is heterogeneous enhancement of the mass (thin arrow,) which is less than that of the thyroid gland (thick arrow.) Effacement and possible invasion of the strap muscles is noted.

Final Pathology: Recurrent parathyroid carcinoma, with infiltration of striated muscle.

746 AO Spine Classification for Osteoporotic Vertebral Fractures: A Concise Pictorial Primer for the Radiologist

Kevin Wu, Amit Mahajan
Yale, New Haven, CT, USA

Summary & Objectives

Osteoporosis is a major cause of vertebral fractures in older adults, often leading to pain, spinal deformity, and functional decline. These fractures may be subtle on imaging and are frequently under-recognized. Traditional classification systems, such as the AO Spine Trauma Classification, were designed for high-energy injuries and do not adequately describe osteoporotic fracture morphology.

This educational exhibit aims to provide a pictorial review of osteoporotic vertebral fracture patterns using the **AO Spine–DGOU Osteoporotic Fracture (OF) classification**. Through a series of cross-sectional imaging examples, viewers will gain a clear understanding of the OF1–OF5 fracture types and learn when and how to apply the AO Spine–DGOU system in daily radiologic practice.

Purpose

The exhibit seeks to provide a practical framework for recognizing and classifying osteoporotic vertebral fractures. By integrating the traditional AO Spine Classification (A1–A3) with the AO Spine–DGOU OF subtypes (OF1–OF5), the presentation highlights how fracture morphology relates to osteoporosis severity, kyphotic deformity, and risk of neurologic compromise. Viewers will learn to identify characteristic imaging patterns and understand the clinical significance of each OF subtype and its implication on management.

Materials & Methods

The exhibit presents high-resolution CT and MRI images of osteoporotic vertebral fractures. Fractures are categorized according to:

- **AO Spine Classification:** A1–A3 compression fractures, stability, and neurologic involvement.
- **AO Spine–DGOU OF Classification:**
    - OF1: Edema without deformation
    - OF2: Deformation of one endplate
    - OF3: One endplate with disc involvement
    - OF4: Both endplates involved
    - OF5: Injuries with anterior or posterior tension band failure

Multiple pictorial examples demonstrate each OF subtype, emphasizing morphology, vertebral collapse, endplate and disc involvement, kyphotic deformity, and potential neurologic findings. Additional slides review common pitfalls that may lead to missed or misclassified fractures.

Results & Conclusion

Most osteoporotic fractures correspond to OF2–OF3 subtypes, reflecting partial endplate involvement and often minimal neurologic symptoms. OF4–OF5 fractures demonstrate higher risk of kyphosis and instability. Integrating the AO Spine and OF systems allows a nuanced understanding of fracture morphology in both non-osteoporotic and osteoporotic patients, improving accuracy of diagnosis, communication, and treatment planning. By providing a cross sectional pictorial review, highlighting characteristic imaging features, and identifying potential pitfalls, this exhibit equips clinicians and radiologists with a guide to identify, classify, and manage osteoporotic vertebral fractures effectively, enhancing patient care and educational value.

Images/Tables

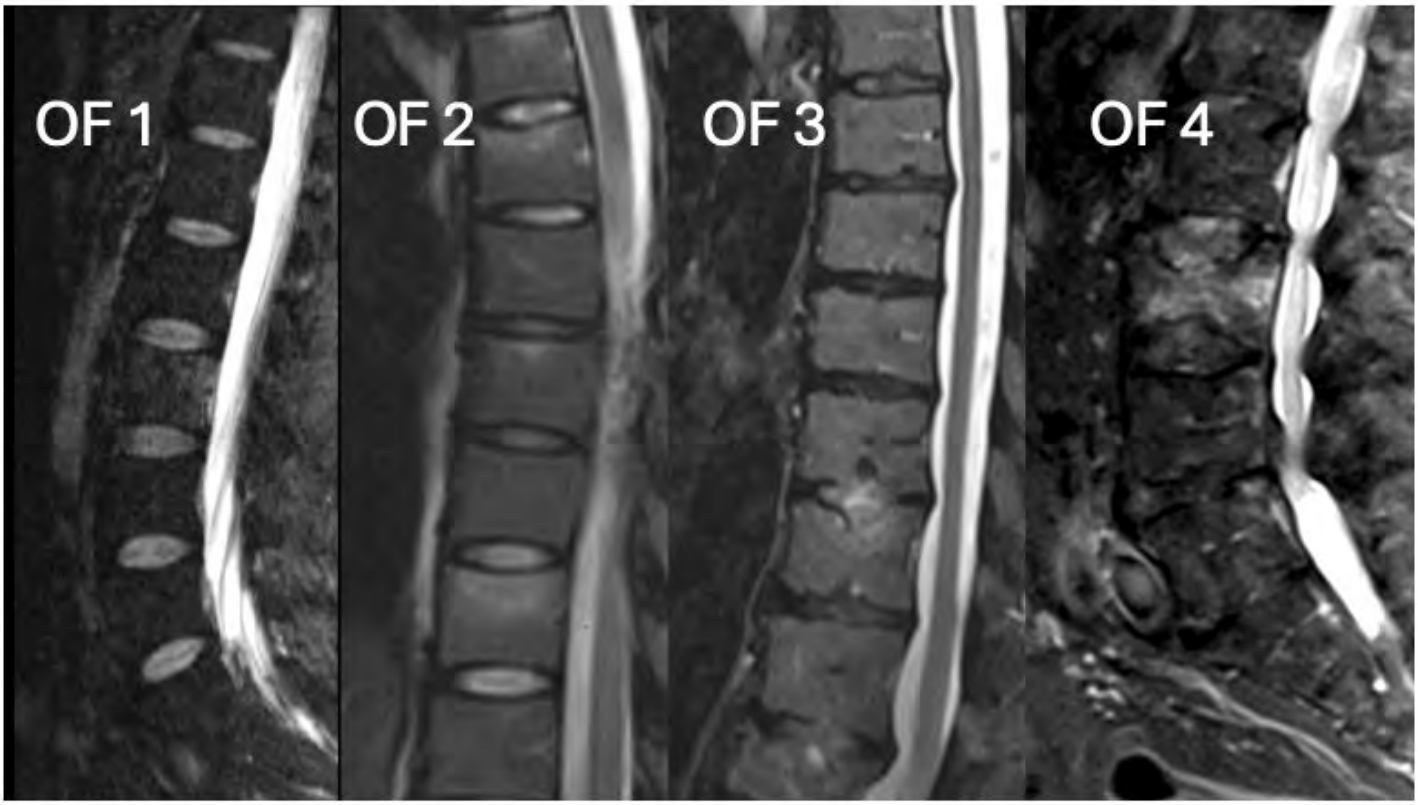

788 Anatomy, Common and Uncommon Pathologies Involving Lumbar Paraspinal Musculature: A Case Based Review

Sraavya Pinjala BS-Biology[1], Robert Koenigsberg DO, FAOCR[2]
[1]Lewis Katz School of Medicine, Philadelphia, PA, USA. [2]Lewis Katz School of Medicine/Temple University, Philadelphia, PA, USA

Summary & Objectives
Despite their clinical relevance, the imaging characteristics of normal and pathological lumbar musculature remain underrepresented in radiology education and literature. This gap contributes to incomplete recognition and limits diagnostic use of lumbar muscle imaging. The goal of this project is to demonstrate that systematic visual comparison of normal and abnormal lumbar musculature will enhance recognition of muscle pathology on imaging, improve diagnostic accuracy, and serve as an effective educational tool for radiology trainees and clinicians.

Purpose
Back pain is one of the most prevalent and disabling conditions worldwide, with over 65 million Americans reporting a recent episode of back pain and 16 million adults reporting that persistent pain limits daily activities. Spinal imaging is typically the initial mode of evaluation for back pain, in which bony and disc pathology often take precedence, while lumbar musculature abnormalities remain overlooked. Paraspinal muscle changes can provide essential clues that can solidify diagnoses and expedite treatment.

Materials & Methods
MRI and CT images of normal musculature were retrospectively reviewed. Images were analyzed from axial, sagittal and coronal planes utilizing STIR, FRFSE, FSE, and STACK sequences. The multifidus, quadratus lumborum, psoas major, and erector spinae muscles were evaluated bilaterally for changes in volume, symmetry, signal intensity, and enhancement pattern across sequences. Cases of abnormal lumbar musculature were identified using the Mpower database through key words such as “multifidus”, “paraspinal”, etc. This produced a diverse case library comprising intramuscular hemangiomas, ganglioneuromas, cystic lesions, fibrous tumors, and paraspinal masses. Each case was reviewed with emphasis on distinguishing imaging features relative to normal anatomical landmarks.

Results & Conclusion
This ongoing project represents an important step towards addressing a significant gap in musculoskeletal imaging. By compiling and characterizing a diverse range of lumbar muscle pathologies in comparison with normal anatomy, this work will serve as a valuable resource for medical students and radiology trainees. Ultimately, this will aid patient outcomes through earlier and more consistent integration of muscle evaluation into spinal imaging.

---

793 Brain stem encephalitis: imaging review

Yang Tang MD PhD
Virginia Commonwealth University, Richmond, VA, USA

Summary & Objectives
Review the imaging appearance of brain stem encephalitis

Purpose
Brain stem encephalitis is a group of rare CNS disorders that can lead to severe neurological compromises. The clinical presentation is often nonspecific.

Materials & Methods
The purpose of this exhibit is to use a case-based approach to illustrate imaging features of various brain stem infection and inflammatory disorders.

Results & Conclusion
Cases of brain stem encephalitis are collected by searching the neuroradiology teaching file and medical records from a tertiary academic institution and are presented in a case-based format.
The following entities will be discussed:

1. Infection: Listeria rhombencephalitis, Lyme disease, brain stem bacterial abscess, tuberculosis
2. Demyelinating diseases: multiple sclerosis, Neuromyelitis optica, MOG antibody associated disease, progressive multifocal encephalopathy.
3. Inflammation: neurosarcoidosis, Bechet’s disease, CLIPPERS.
4. Autoimmune brain stem encephalitis: Bickerstaff encephalitis, GFAP astrocytopathy.

Images/Tables

---

804 Imaging of penetrating injuries of the head and neck in the pediatric population

Umer Ahmed MD, Clara Kerwin MD, Bindu Setty MD
Boston Medical Center, Boston, MA, USA

Summary & Objectives
Penetrating trauma among pediatric patients, while less common than among adult patients, carries significant morbidity and mortality. In the pediatric population, penetrating trauma to the head and neck may be due to accidental injuries with sharp objects, animal bites, and, increasingly,

gunshot wounds. Given the vital nature of the structures of the head and neck, prompt recognition of injury through imaging plays a critical role in the preventing life-threatening complications, guiding timely surgical intervention, and optimizing functional and cosmetic outcomes.
The mainstay of imaging evaluation of penetrating trauma to the head and neck centers on non-contrast CT often with CT angiography. These modalities enable the radiologist to assess the trajectory of penetration, the presence of retained foreign bodies, and any signs of active bleeding or vascular compromise. Given the relative rarity of penetrating trauma among children, pediatric radiologists play a pivotal role in promptly identifying injury extent, recognizing subtle patterns of aeordigestive, vascular, ocular, and neurological involvement, and informing appropriate surgical management.
The objectives of this educational exhibit are as follows:

1. To review the demographic risk factorsassociated with pediatric penetrating trauma to thehead and neckas may be seen at an urban Level 1 trauma center.
2. To detail the common causes of penetrating trauma (e.g. gunshot wounds) and characterize how injury patterns among children are affected by pediatric anatomy.
3. To provide radiologists with pediatric-specific imaging protocol recommendations that can ensure comprehensive evaluation of injury and help guide further management.

Purpose
The exhibit aims to help radiologists identify the range of injuries that can result from penetrating trauma in the pediatric population.
Materials & Methods
Cases of pediatric penetrating trauma were identified using the Philips Performance Bridge radiology analytics platform at Boston Medical Center over a ten-year period. Radiology reports were queried using key terms including “gunshot wound” and “penetrating injury” Relevant CT, CTA, and MRI studies were reviewed to select illustrative examples demonstrating examples of aerodigestive, vascular, and neurological injuries. All cases were de-identified prior to inclusion. This retrospective review was conducted for educational purposes and did not require IRB approval.
Results & Conclusion
Penetrating injuries of the pediatric head and neck, though uncommon, carry substantial risk of morbidity and mortality. Awareness of pediatric-specific anatomical considerations, tailored imaging protocols, and characteristic injury patterns enables radiologists to guide timely surgical and multidisciplinary management. The cases presented within this exhibit demonstrate how radiologists play a critical role in improving diagnostic accuracy, treatment planning, and outcomes for this vulnerable population.

---

852 Inside the Ventricles: A Radiologic Journey Through Intraventricular Lesions.
Luis Gerardo Garcia Armas[1], Nagore Siles[2], Jose Gavito-Higuera[3]
[1]Hospital General Regional No.1 IMSS Tijuana, Tijuana, Baja California, Mexico. [2]San Pedro University hospital, Logrono, La Rioja, Spain. [3]UTHealth Houston medical center, Houston, Texas, USA
Summary & Objectives
Summary
Intraventricular lesions comprise a broad spectrum of neoplastic and non-neoplastic entities that can arise from the ventricular wall, septum pellucidum, or choroid plexus. Because many share overlapping imaging appearances, a systematic and methodical approach is important to get an accurate non-invasive diagnosis and guide management decisions.
This educational exhibit begins with a brief anatomic review of the ventricular system, with key landmarks to provide proper knowledge for lesion localization and interpretation.
A comprehensive image-based review is then presented, focusing on MRI and CT features that assist in narrowing the differential diagnosis. Lesions are classified into neoplastic (primary and secondary) and non-neoplastic (infectious, vascular, and mimickers) categories. The diagnostic approach integrates key imaging clues based on ventricular location, patient demographics, lesion composition, signal intensity, diffusion characteristics, size, calcification or hemorrhage, enhancement pattern, and relationship to the ventricular wall, all these factors can substantially narrow the differential. Representative cases illustrate both neoplastic and non-neoplastic lesions: ependymoma, central neurocytoma, subependymoma, choroid plexus tumors, intraventricular meningioma, colloid cyst, and metastatic lesions, as well as arachnoid and ependymal cysts, xanthogranulomas, and infectious processes. For each entity, key differentiating features and common pitfalls are discussed, highlighting how a methodical evaluation combining radiologic features and clinical context can distinguish benign from malignant entities, optimize management, and prevent misinterpretation and/or unnecessary interventions. MRI remains the cornerstone modality, complemented by CT for assessing calcification and hemorrhage.
Through illustrative examples, diagnostic algorithms, and summary teaching points, the educational focus is on recognizing imaging patterns that drive accurate diagnosis, streamline differential consideration, and enhance diagnostic confidence. Ultimately, this exhibit reinforces the diagnostic value of a pattern- and location-based approach to intraventricular lesions, promoting a consistent and methodical interpretation framework for radiologists in training and in practice.
Purpose

- Educational Objectives

Describe the imaging anatomy of the ventricular system and identify key anatomic landmarks relevant to intraventricular lesions.
Identify key CT and MRI features of intraventricular lesions in adults.
Apply a methodical and systematic imaging approach to the evaluation of intraventricular lesions narrowing the differential diagnosis.
Recognize characteristic imaging features of common neoplastic (ependymoma, neurocytoma, subependymoma, choroid plexus tumors, meningioma) and non-neoplastic (colloid cysts, cystic, infectious, and vascular) intraventricular entities.
Identify common diagnostic pitfalls and key imaging clues that guide accurate diagnosis and proper management.
Materials & Methods
This educational exhibit was developed as a pictorial review of representative MRI and CT cases of intraventricular lesions in adults. Cases were selected from institutional archives and supplemented with examples from the literature to illustrate the imaging spectrum of neoplastic and non-neoplastic entities.

Results & Conclusion

The exhibit summarizes the imaging spectrum of intraventricular lesions and proposes a structured, location- and pattern-based diagnostic approach.

Images/Tables

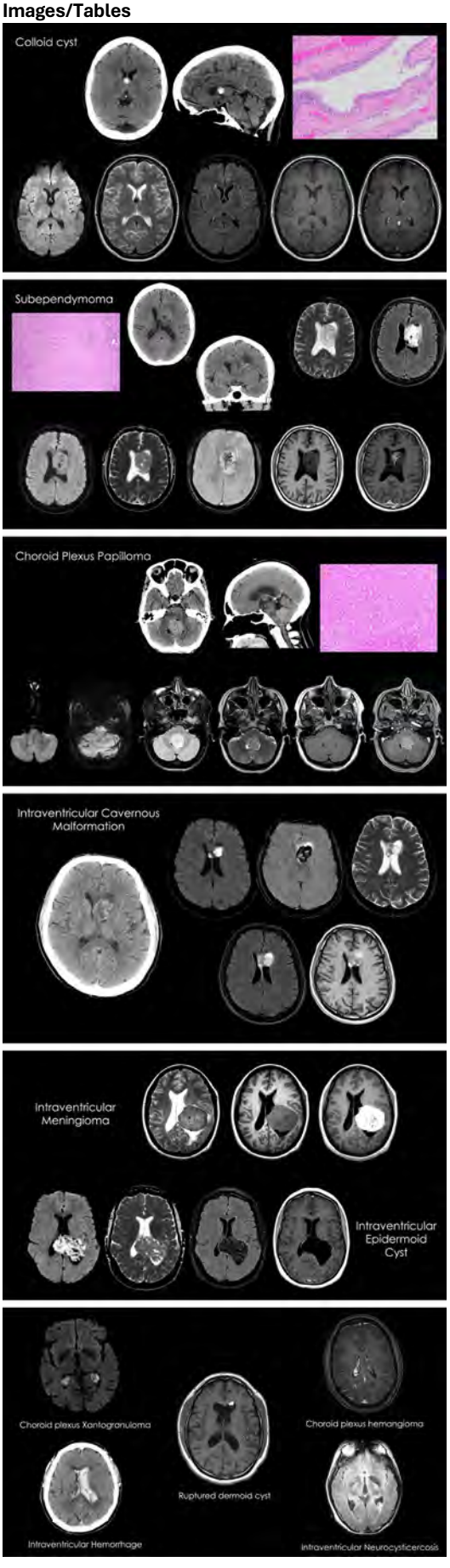

904 Practical Neurovascular Embryology: Minimizing Errors in Code Stroke CTA Interpretation

Sanaz Ameli, Mari Hagiwara, Eytan Raz, Charlotte Chung
NYU, New York, NY, USA

Summary & Objectives

Summary
Anatomic variants in the cerebral arterial circulation are well recognized. Our classical understanding of these variants evolved from classifying commonly seen variants as distinct entities according to their location and morphology. While helpful from a descriptive standpoint, this perspective suggests the existence of only a finite number of variants – a concept that is flawed from both a developmental and functional standpoint. Familiarity with the overarching processes of neurovascular development allows one to view cerebrovascular territories as systems fed by multiple vessels in balance with one another, and appreciate that anatomical variants in fact exist on a spectrum with respect to branching pattern and location; relative vessel size and dominance; territory supplied; and fusion pattern. In the face of the vast spectrum of cerebrovascular variants, abnormal findings on head and neck CT angiogram for acute stroke evaluation can easily be misinterpreted: benign congenitally hypoplastic or absent vessels may be overcalled as occlusions, while occlusions of normal or variant vessels may be missed or misinterpreted as benign variants. Understanding key concepts of neurovascular development, the resultant spectrum of cerebral arterial variants, and accompanying imaging clues can aid accurate interpretation of code stroke CTAs and minimize potentially clinical devastating diagnostic errors.

Educational Objective

- Outline key concepts and processes of neurovascular embryologic development
- Highlight the nature of cerebral arterial variants as a spectrum
- Illustrate occlusions that can be missed or misinterpreted as congenitally hypoplastic/absent vessels
- Illustrate congenitally hypoplastic/absent vessels and other variants that mimic occlusions

Outline:

- Key Neurovascular Development Concepts:
    1. Fusion and regression of longitudinal and transverse vasculature in the embryonic carotid (anterior) and vertebrobasilar (posterior) circulation
    2. Fusion and annexation of embryonic vascular supply from carotid to vertebrobasilar circulation
    3. Evolution in balance between and relative dominance of arterial suppliers of each cerebrovascular territory
- Imaging clues distinguishing congenital hypoplasia/absence from pathologic occlusions
- Case-based illustrations highlighting missed/misinterpreted or mimics of occlusions:
    1. Related to variants in branching pattern and location (ex. MCA bifurcation versus trifurcation, early MCA branching)
    2. Related to variants in vessel size/relative dominance (ex. hypoplastic vertebral artery, AICA-PICA complex vs PICA occlusion, fetal-type PCA versus P1 occlusion)
    3. Related to variants in fusion pattern (ex. basilar nonfusion, azygous or bi-hemispheric ACA, fenestration)

Purpose

NA

Materials & Methods

NA

Results & Conclusion

NA

Images/Tables

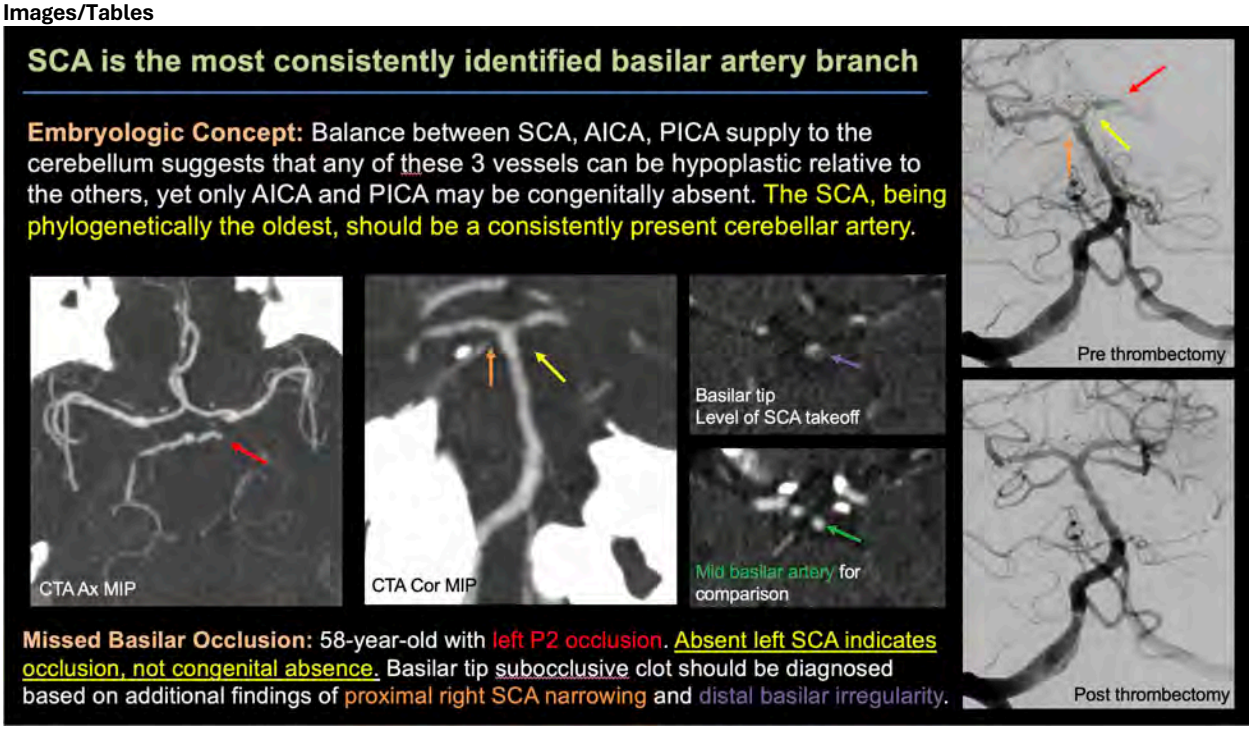

940 Benign/developmental extra-axial cystic lesions of the central nervous system- and beyond! Review of arachnoid, epidermoid, and dermoid cysts.

Azwade F. Rahman MD, MPH, Sabrina Grondin MD, Sanket Desai MD, Giuseppe Cruciata MD
Stony Brook University Hospital, Stony Brook, NY, USA

Summary & Objectives

Cystic lesions within the central nervous system have a broad set of possible etiologies including congenital variation, malformations, perinatal injury, vascular pathology, hemorrhagic sequalae, and infection. Attentiveness to the features of these lesions, including their location, size, and morphology, can help cut down on the expansive list. Arachnoid, epidermoid, and dermoid cysts are congenital lesions that are frequently seen on radiographic evaluations throughout the head, neck, and spinal imaging. This educational review will provide guidance in consistent and accurate diagnosis.

Purpose

The goal of this exhibit is to help illuminate on the key features, diagnostic approaches, and progression of these conditions.

Materials & Methods

The authors engaged in careful reviews of relevant cases on their institutional PACS which is presented in the following submission. Key images from the cases were obtained, which were anonymized, for the purposes of academic presentation.

Results & Conclusion

Differentiation of these lesions are important in distinguishing benign or pathological lineage. Also, despite being considered benign lesions, there are also negative consequences associated with the lesions. Arachnoid cysts can be associated with seizure focus, hydrocephalous, and neurological defects. Dermoid rupture is an example which can result in chemical meningitis, vasospasms, stroke, and may even be fatal. They may also be present in areas of the brain which cause symptomology. Treatment, when warranted, runs the risk of incomplete resection and late recurrence. Other benign cystic lesions can also be present within the neck and spine, which will also be featured in the following exhibit. The suspicion can also vary with age group, clinical history, and metabolic processes. Following this review, participants are expected to be able to help guide clinicians towards the correct clinical approach.

Images/Tables

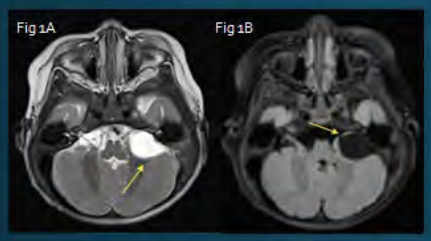

Figure 1. (A) T2 weighted imaging at the level of the posterior fossa demonstrates a left cerebellopontine angle hyperintense lesion. There is mass effect on the adjacent structure. (B) Corresponding FLAIR sequences shows the lesions anteriorly displacing the facial and vestibulocochlear nerves as they exit through the internal auditory canal. The lesions suppresses on FLAIR, which supports the diagnosis of an arachnoid cyst.

Figure 2. (A) Proton density weighted imaging shows a lobulation lesions in the expected location of the right frontal horn (yellow arrow), isointense to the contralateral frontal horn (blue arrow). (B) T1 weighted imaging shows the hypointense lesion extending through the tentorium incisura. The signal of the lesions is somewhat heterogenous which is more conspicuous on image (C), the corresponding FLAIR sequence. The heterogeneity concludes that rather than an arachnoid cyst, this is an epidermoid cyst.

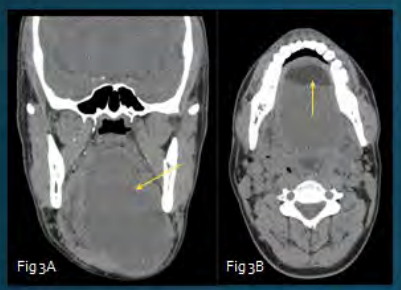

Figure 3. (A) Coronal CT at the level of the mandibular body shows an isodense cystic lesions which extends from the floor of the mouth well below the mandible. It has a thick, irregular rim. (B) The axial image shows a fat-fluid level within the lesion, not conspicuous on coronal views. There is mass effect on the adjacent structures. These findings indicate the layer cellular debris and proteinaceous material found in an extracranial epidermoid cyst.

Figure 4. (A) T1 weighted imaging shows a hyperintense, ovoid, lesion at the location of the optic chiasm. (B) T2 FLAIR sequence imaging shows a focal area of fat saturation, indicating intrinsic fat content. Of note, there is also a fat-fluid level as suggest by the circumferential fluid signal. These imaging findings correspond with a suprasellar dermoid cyst.

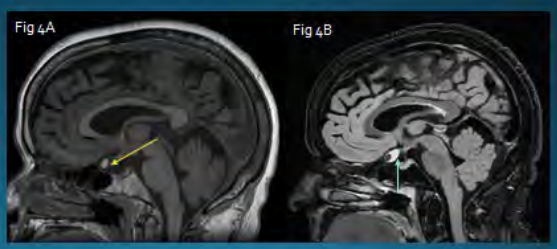

981 What Are You Looking At?! Imaging of Conditions that Present with Proptosis

Adrian Chung-Hei Lee MS[1], Shehbaz Ahmad MD[2], Rahul Hegde MBBS, MD, FRCR[2]
[1]Frank H. Netter MD School of Medicine at Quinnipiac University, North Haven, CT, USA. [2]Yale School of Medicine, New Haven, CT, USA

Summary & Objectives

This educational exhibit aims to review the various abnormalities involving the extra-ocular muscles, intraconal and extraconal compartments of the orbits that may present with proptosis. The exhibit reviews some common and uncommon conditions underlying proptosis, guiding viewers in reviewing their understanding of these conditions and image interpretation in these studies. Key findings and structures in CT and MRI images are discussed to offer insights in differentiating certain etiologies.

Purpose

The purpose of this educational exhibit is to:

1. Understanding the clinical presentation and varied etiologies that can present with proptosis.
2. Detection of proptosis/exophthalmos on CT/MRI
3. Review of imaging abnormalities involving extra-ocular muscles, intraconal and extraconal compartments of the orbits. Understand key imaging findings associated with different disorders that present as proptosis.

Materials & Methods

1. Definition of proptosis/exophthalmos. Incidence and clinical presentation. Initial clinical/lab assessment. Differential considerations based on clinical features - unilateral/bilateral, age, duration, pain, etc.
2. Role of CT and MRI orbits and protocol.
3. Review of common and uncommon pathologies that present with proptosis, including A. Thyroid eye disease B. Idiopathic orbital inflammation C. Orbital cellulitis D. Orbital masses- cavernous malformation, lymphoma, metastatic disease E. Vascular conditions - carotid cavernous fistula, orbital varix. F. Trauma.

Results & Conclusion

The abstract provides a pictorial review of common and a few uncommon conditions that can be detected with CT/MRI that present with proptosis.

Images/Tables

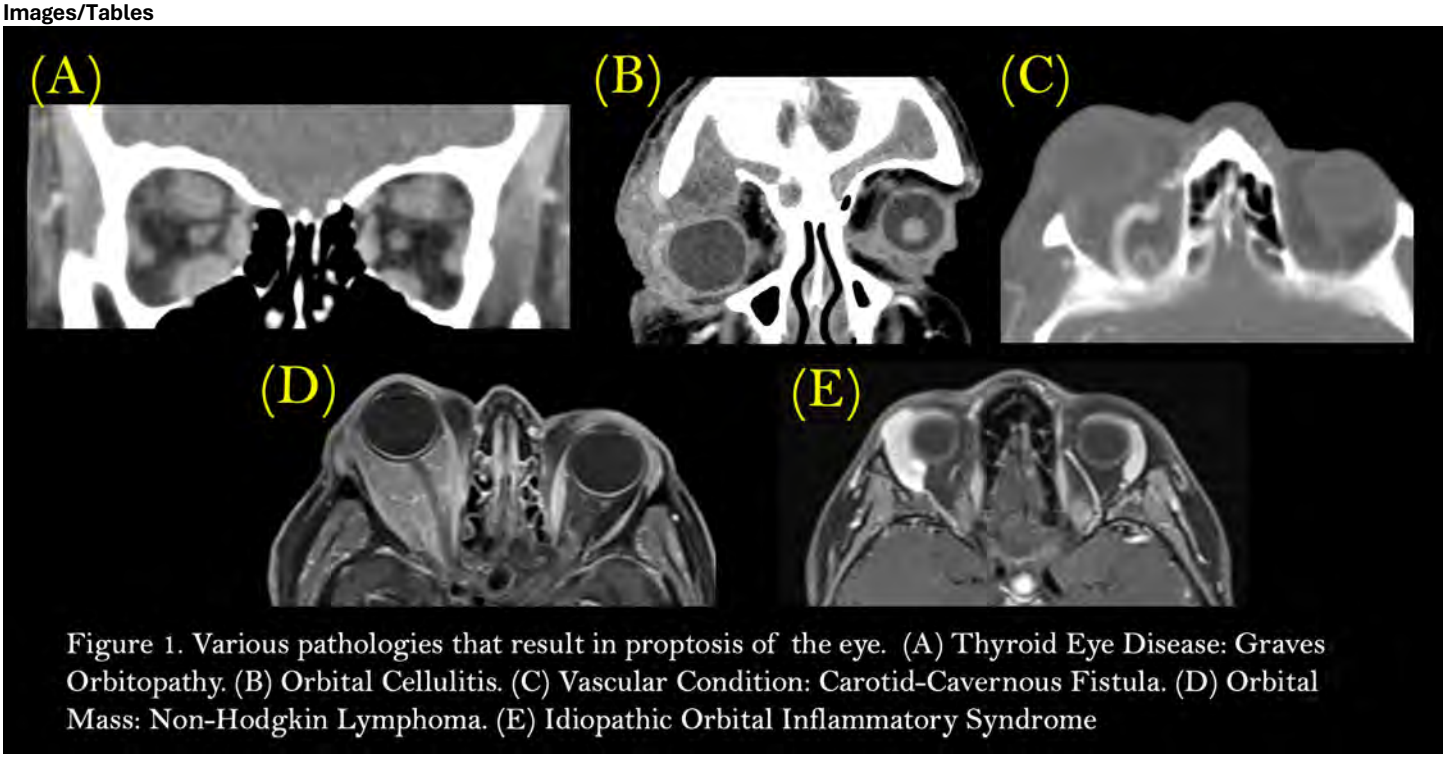

Figure 1. Various pathologies that result in proptosis of the eye. (A) Thyroid Eye Disease: Graves Orbitopathy. (B) Orbital Cellulitis. (C) Vascular Condition: Carotid-Cavernous Fistula. (D) Orbital Mass: Non-Hodgkin Lymphoma. (E) Idiopathic Orbital Inflammatory Syndrome

1083 Unmasking the Pituitary Abscess: Multimodality Imaging Clues to a Hidden Diagnosis

Sriya B Parchuri BSA[1], Santiago Aristizabal-Ortiz MD[1], Mario Mahecha MD[1], Andrés Felipe Mejía MD[2], Eliana Bonfante MD[1]
[1]UTHealth Houston, Houston, TX, USA. [2]Fundación Cardioinfantil – LaCardio, Bogotá, Bogotá D.C., Colombia

Summary & Objectives

Summary:

This educational exhibit illustrates the multimodality imaging spectrum of pituitary abscess, emphasizing its distinguishing MRI and CT features and their correlation with clinical presentation and outcomes. Through representative case examples, it highlights key radiologic clues for early recognition and differentiation from other cystic sellar lesions, as well as common diagnostic pitfalls that can delay treatment.

Objectives:

1. Identify the characteristic MRI and CT findings of pituitary abscess and understand how these features evolve across imaging modalities.
2. Contrast the characteristics that differentiate pituitary abscess from other cysticsellarlesions, including adenoma, Rathke cleft cyst, and craniopharyngioma, based on imaging and clinical context.
3. Recognize the diagnostic value of diffusion-weighted imaging and rim enhancement patterns in establishing an early and accurate diagnosis.

Purpose

The purpose of this exhibit is to illustrate the multimodality imaging characteristics of pituitary abscess on MRI and CT, correlating these radiologic findings with the underlying pathophysiologic mechanisms and clinical outcomes. It further aims to identify the key differentiating features that distinguish pituitary abscess from other cystic sellar lesions such as adenoma, Rathke cleft cyst, and craniopharyngioma, while emphasizing the critical role of diffusion-weighted imaging and contrast enhancement patterns in achieving early and accurate diagnosis.

Materials & Methods

A retrospective review of institutional cases of confirmed pituitary abscesses was performed.

Each case was evaluated for:

- **MRI features:** signal characteristics on T1-, T2-weighted, and diffusion-weighted sequences; rim-enhancement morphology; and sellar/suprasellar extension.
- **CT features:** attenuation, calcification, and bone remodeling.
- **Ancillary data:** clinical presentation and surgical or microbiological confirmation.

  All imaging was reviewed by experienced neuroradiologists to identify consistent patterns and define diagnostic imaging criteria.

Results & Conclusion

Results: Pituitary abscesses typically occur in women and may arise either primarily (in normal pituitary tissue) or secondarily (in pre-existing lesions).

Common causative organisms include Staphylococcus aureus and Aspergillus species in immunocompromised patients.

Imaging characteristics:

- MRI: T1 hypointense, T2 hyperintense central cavity with a peripheral rim-enhancing capsule after contrast administration.
- CT: Sellar/suprasellar hypoattenuating lesion with rim enhancement.

Management: Prompt transsphenoidal drainage and targeted antimicrobial therapy are essential to prevent irreversible pituitary dysfunction or visual deficits.

Conclusion: Pituitary abscess should be considered when a cystic sellar lesion exhibits rim enhancement with central restricted diffusion, especially in postoperative or inflammatory settings. Recognition of this pattern on MRI enables early surgical drainage and prevents irreversible endocrine or visual deficits.

Radiologists play a decisive role, as diffusion-weighted imaging findings often represent the earliest and most specific diagnostic clue.

Teaching point:

Early recognition of a rim-enhancing sellar lesion with central restricted diffusion is key to diagnosing pituitary abscess, a rare but potentially life-threatening infection that can closely mimic more common cystic sellar masses. Awareness of this imaging pattern enables radiologists to prompt timely surgical drainage and antimicrobial therapy, directly influencing patient outcomes by preventing irreversible endocrine dysfunction and visual compromise.

Images/Tables

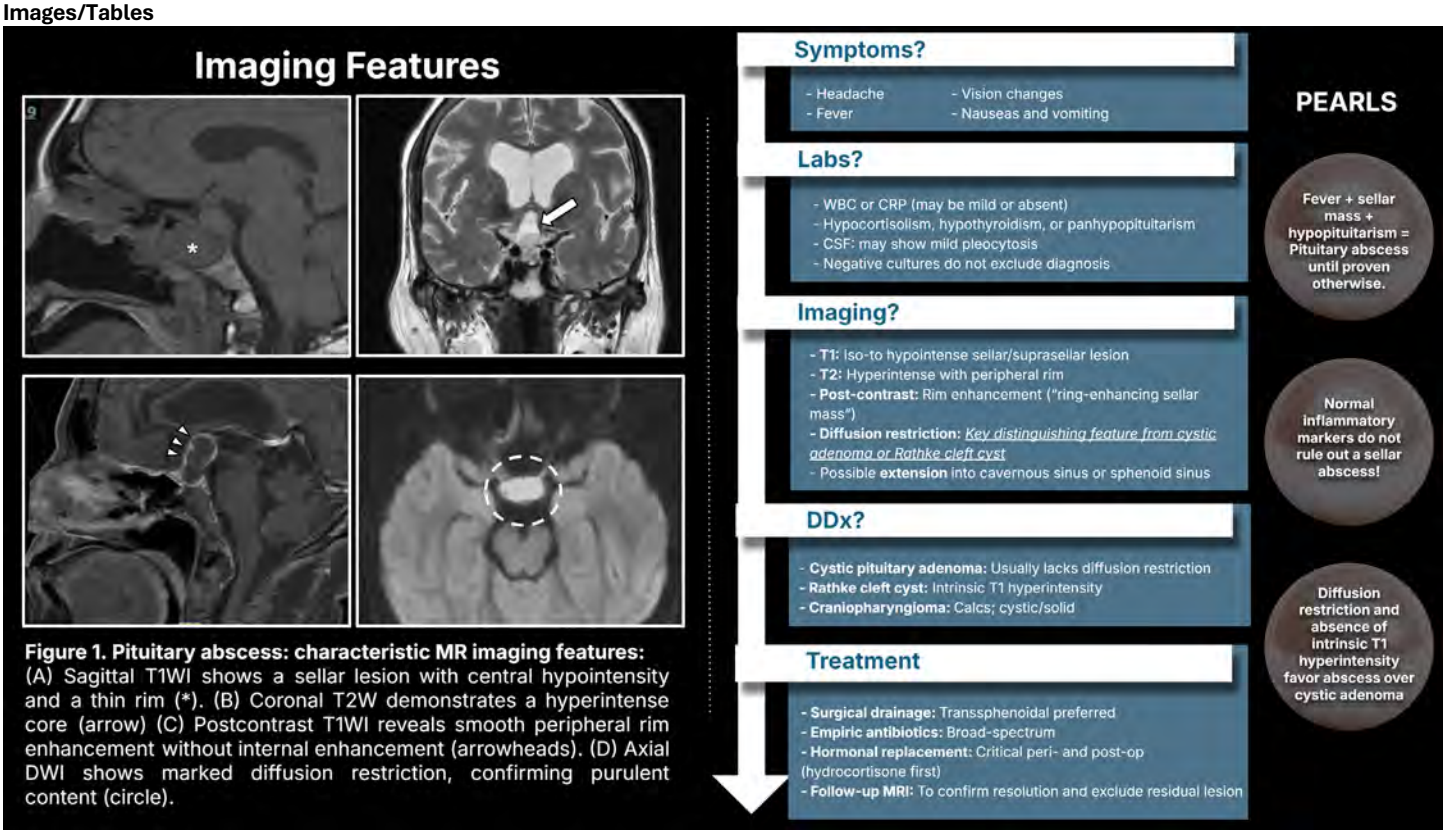

Figure 1. Pituitary abscess: characteristic MR imaging features: (A) Sagittal T1WI shows a sellar lesion with central hypointensity and a thin rim (*). (B) Coronal T2W demonstrates a hyperintense core (arrow) (C) Postcontrast T1WI reveals smooth peripheral rim enhancement without internal enhancement (arrowheads). (D) Axial DWI shows marked diffusion restriction, confirming purulent content (circle).

1153 From Meninges to Parenchyma: Imaging Features of CNS Cryptococcal Infection

Roshun Sankaran MD, Mona Shahriari MD
UCSD, San Diego, CA, USA

Summary & Objectives

Summary:
Cryptococcal infection typically results from hematogenous spread from the lungs. C. neoformans primarily affects immunocompromised individuals, including those with HIV/AIDS, and organ transplants. In contrast, C. gattii primarily affects immunocompetent individuals. Clinically, there are few differences between C. neoformans and C. gattii infections, with the most common symptoms including headache, low-grade fever, meningism, altered mental status, and nausea. Focal neurologic deficits and fever are observed more frequently in HIV-negative patients.
Objectives:
Recognize imaging features of CNS cryptococcal infection.
Identify characteristic imaging patterns, including basal meningeal enhancement, gelatinous pseudocysts, and cryptococcomas.
Understand MRI's role in detecting complications such as hydrocephalus, ventriculitis, and infarction.

Purpose

To provide a comprehensive, case-based review of CNS cryptococcal infection imaging, highlighting characteristic MRI findings, and teaching points, thereby improving diagnostic accuracy for radiologists.

Materials & Methods

Retrospective review of MRI studies of patients with confirmed CNS cryptococcal infection (via CSF analysis or biopsy) at a tertiary care center.

Results & Conclusion

Imaging Findings:
Meningoencephalitis: Basal leptomeningeal enhancement and meningeal thickening.
Intraventricular or intraparenchymal cryptococcomas.
Dilated perivascular spaces (gelatinous pseudocysts) in basal ganglia/thalami.
Communicating or non-communicating hydrocephalus (most common but least specific).
Ventriculitis with ependymal enhancement.
CNS cryptococcal infection demonstrates a wide spectrum of imaging findings on MRI, from subtle meningeal enhancement to parenchymal cryptococcomas and ventricular involvement. Recognition of characteristic patterns, especially dilated perivascular spaces and basal meningeal enhancement, is essential for early diagnosis and management. This exhibit provides radiologists with practical imaging clues and case-based examples to improve diagnostic confidence and patient outcomes.

Images/Tables

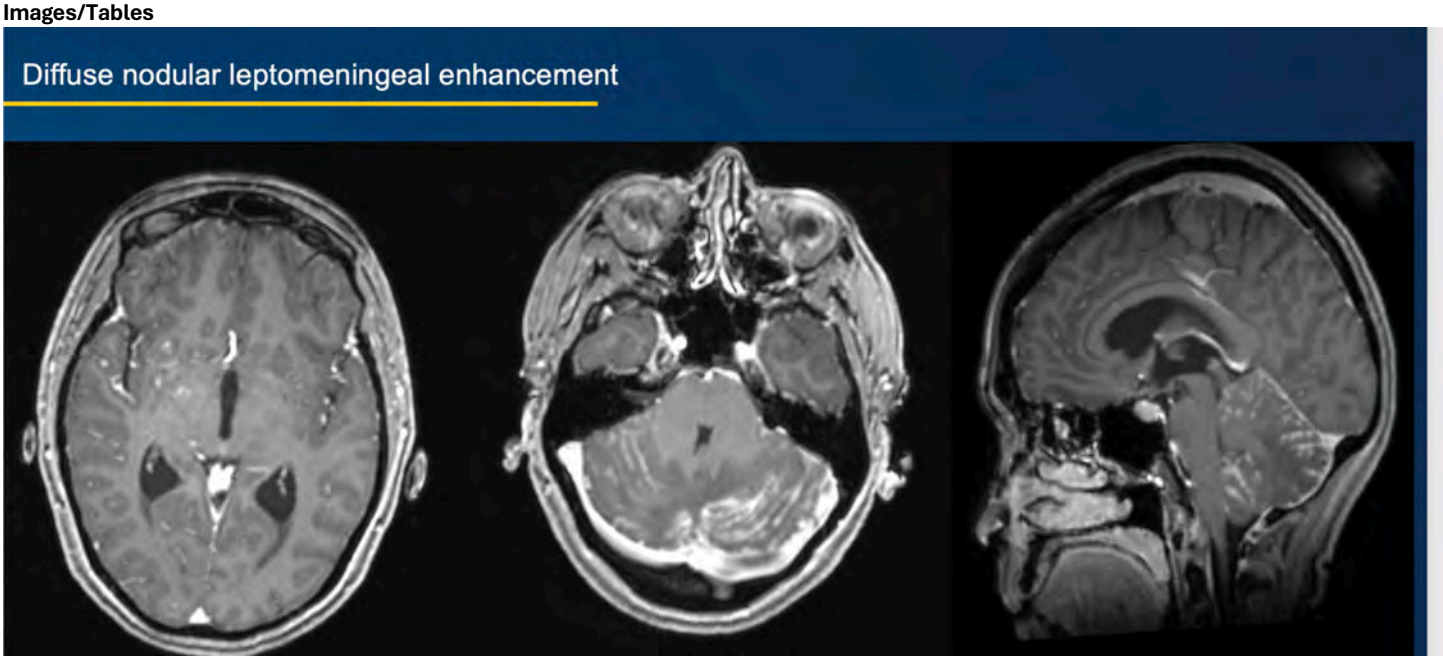

1212 To evaluate the diagnostic yield and clinical impact of dedicated cranial nerve imaging performed from the emergency department (ED).

Emmanuel Ansong MD, Karen Buch MD, William Mehan MD
Massachusetts General Hospital, Boston, MA, USA

Summary & Objectives

This single-institution, IRB-approved retrospective study evaluated 262 cranial nerve MRIs performed from the ED between 2020–2025 (164 IAC, 98 trigeminal). IAC MRIs yielded 25.0% positive findings, most commonly facial nerve enhancement or vestibular schwannoma, with 31.7% of positive cases resulting in hospital admission. Trigeminal MRIs were positive in 17.3%, including enhancement or vascular deformity of CN5, with 52.9% of positive cases resulting in hospital admission. Neurology was consulted in most positive cases (95.1% IAC, 82.4% trigeminal), while ENT involvement was limited (24.4% IAC, 0% Trigeminal). Dedicated cranial nerve MRI from the ED demonstrates moderate diagnostic yield, with most positive results corresponding to diagnoses that can be made clinically. Findings suggest opportunities to refine imaging indications and consultation pathways to optimize ED utilization and guide which patients may be managed as outpatients.

Purpose

To evaluate the diagnostic yield and clinical impact of dedicated cranial nerve imaging performed from the emergency department (ED).

Materials & Methods

This was a retrospective, IRB approved study performed at a single-institution. 262 cranial nerve MRI studies were performed in the ED between 2020-2025, including 164 IAC and 98 trigeminal nerve protocols. Radiology reports were reviewed for positive findings such as masses, abnormal enhancement, vascular lesions, etc. Clinical management including consultation rates for these ED cases from neurology and otolaryngology (ENT) were recorded as well as patient disposition (admission to inpatient service vs discharge with outpatient follow-up).

Results & Conclusion

Of 164 IAC MRIs, 41 (25.0%) demonstrated positive findings. Twenty-one showed abnormal facial nerve enhancement with final diagnoses of Bell's palsy or Ramsay Hunt syndrome, and 12 demonstrated vestibular schwannoma. Neurology was consulted in 39 of 41 positive IAC cases (95.1%), and ENT in 10 (24.4%). Thirteen of the positive IAC imaging cases (31.7%) resulted in inpatient admission. Among 98 trigeminal MRIs, 17 (17.3%) were positive. Five patients were ultimately diagnosed with Bell's palsy, two with Ramsay Hunt syndrome, and six with trigeminal neuralgia associated with CN V enhancement or vessel-related deformity. Neurology was consulted in 14 of 17 positive trigeminal imaging cases (82.4%), while none involved ENT consultation. Nine of the positive trigeminal MRI cases (52.9%) resulted in inpatient admission.

Advanced IAC and trigeminal MRI studies from the ED yielded positive findings in a substantial proportion of cases, with most resulting in Neurology consultation but few involving ENT. Most positive interpretations were related to an ultimate diagnosis of Bell's Palsy or Ramsay Hunt syndrome, both of which are diagnoses that can be made clinically, underscoring the need for refined imaging indications and standardized consultation pathways to optimize utilization and follow-up of cranial nerve MRI in the ED setting. Among the positive cases, approximately one third and one half of patients receiving advanced IAC and trigeminal MRI respectively were subsequently admitted, indicating that the imaging portion of the work-up for a subset of patients may reasonably be completed as an outpatient, if at all.

Images/Tables